This document was too large to scan as a single document; therefore, it has been divided into smaller sections.

Section 2 of 2

Document Information			
Document #	HNF-2193	Revision	0
Title	FLAMMABLE GAS DST EXPERT ELICITATION PRESENTATIONS [PART A & PART B]		
Date	04/17/98		
Originator	BRATZEL DR	Originator Co.	DESH
Recipient		Recipient Co.	
References	EDT-619962		
Keywords	BUOYANT DISPLACEMENT,DEFLAGRATIONS,DETONATIONS, TOXIC EXPOSURES,RADIOLOGICAL EXPOSURES, DOSE CONSEQUENCES		
Projects			
Other Information			

FLAMMABLE GAS DOUBLE SHELL TANK EXPERT ELICITATION PRESENTATIONS

Part B

David R. Bratzel
DUKE ENGINEERING SERVICES HANFORD

Donald J. Hammervold
Aurora B. Rau
FLUOR DANIEL NORTHWEST

April 1998

For the U.S. Department of Energy
Contract

This page intentionally left blank.

TABLE OF CONTENTS

This page intentionally left blank.

1.0 INTRODUCTION

This document is a compilation of presentation packages and white papers for the Flammable Gas Double Shell Tank Expert Elicitation Workshop #2. For each presentation given by the different authors, a separate section was developed.

The purpose for issuing these workshop presentation packages and white papers as a supporting document is to provide traceablity and a Quality Assurance record for future reference to these packages.

The following personnel were attendees to this workshop which was held on February 9 - 13, 1998, in the Ice Harbor and McNary Room at the Double Tree Hotel in Richland, Washington:

Expert Panelists

Stephen Agnew	Los Alamos National Laboratory
Edward Beahm	Oak Ridge National Laboratory
Paul d'Entremont	Westinghouse Savannah River Company
Clay Easterly	Oak Ridge National Laboratory
Michael Epstein	Fauske & Associates, Inc.
Phillip Gauglitz	Pacific Northwest National Laboratory
Jerry Havens	Department of Chemical Engineering - University of Arkansas
Mujid Kazimi	Department of Nuclear Engineering - Massachussets Institute of Technology
Nick Kirch	Lockheed Martin Hanford Company
Glenn Paulson	Paulson and Cooper, Inc.
Arlin Postma	G&P Consulting
Wallace Schulz	W2S Co., Inc.
Charles Stewart	Pacific Northwest National Laboratory
Kelly Thomas	Westinghouse Savannah River Company
Michael Yost	Department of Environmental Health - University of Washington

Other Workshop Participants

Thomas Eppel	Decision Insights, Inc.
Don Hammervold	Fluor Daniel Northwest
Richard John	Decision Insights, Inc.
Paul McConnell	Sandia National Laboratory
Chris Olson	Sandia National Laboratory
Scott Slezak	Sandia National Laboratory
Detlof von Winterfeldt	Decision Insights, Inc.
Richard Harrington	Lockheed Martin Hanford Corp.
David Bratzel	DE&S Hanford, Inc.
Jerry Johnson	DE&S Hanford, Inc.
Mike Grigsby	G&P Consulting
Jonathan Young	Management Strategies Inc.
Blaine Barton	Lockheed Martin Hanford Corp.

Agenda
Gas Release Event Safety Analysis

EXPERTS' PANEL WORKSHOP #2
February 9 - 13, 1998

DoubleTree Hotel Richland - Hanford House
Richland Washington

Monday, February 9 **Technical Moderator: Chris Olson / SNL**
Facilitator: Richard Harrington / PHMC Team

7:30 **Opening Remarks, Agenda Overview, Quality Assurance**
- Chris Olson / SNL

8:00 **Topic: Gas Generation and Void Fraction Predictions**
- 20 minutes: Presentation: Chuck Stewart / PNNL
- 20 minutes: Questions & Answers
- 20 minutes: Discussion on Implications for Analysis Framework

9:00 **Topic: Organic Content in Tanks**
- 20 minutes: Presentation: Steve Agnew / LANL
- 20 minutes: Questions & Answers
- 20 minutes: Discussion on Implications for Analysis Framework

10:00 **Break**

10:15 **Topic: Organic Aging**
- 20 minutes: Presentation: Leon Stock / PHMC consultant
- 20 minutes: Questions & Answers
- 20 minutes: Discussion on Implications for Analysis Framework

11:15 **Topic: Safety Analysis Approach and Results**
- 20 minutes: Presentation: Jon Young/ PHMC Team
- 20 minutes: Questions & Answers
- 10 minutes: Discussion on Implications for Analysis Framework

12:05 **Working Lunch**

12:35 ***Analysis tool (SST version)*: demonstration and discussion (Executive Boardroom)**
- Steve Humphreys / SNL

1:05 **Panel Caucus on Analysis Framework**

Project Teams (PHMC Team, SNL) Caucus (Executive Boardroom)

Tuesday, February 10 Technical Moderator: Scott Slezak / SNL
Facilitator: Richard Harrington / PHMC Team

7:30 **Status, Action Items**
Discussion of Analysis Framework and Previous Day's Topics

8:00 **Topic: Combustion-related Phenomena**
- 20 minutes: Presentation: Scott Slezak / SNL
- 20 minutes: Questions & Answers
- 20 minutes: Discussion on Implications for Analysis Framework

9:00 **Topic: Headspace Ventilation Modeling**
- 20 minutes: Presentation: Zen Antoniak / PNNL
- 20 minutes: Questions & Answers
- 10 minutes: Discussion on Implications for Analysis Framework

9:50 **Break**

10:00 **Topic: Headspace Ventilation Engineering**
- 20 minutes: Presentation: James Kriskovich / PHMC Team
- 20 minutes: Questions & Answers
- 10 minutes: Discussion on Implications for Analysis Framework

10:50 **Topic: DST Dome Response to Overpressure**
- 20 minutes: Presentation: TBD / PHMC Team
- 20 minutes: Questions & Answers
- 20 minutes: Discussion on Implications for Analysis Framework

11:50 **Working Lunch**

12:20 ***Analysis tool (SST version)*: demonstration and discussion (Executive Boardroom)**
- Steve Humphreys / SNL

12:50 **Panel Caucus on Analysis Framework**

Project Teams (PHMC Team, SNL) Caucus (Executive Boardroom)

Wednesday, February 11 **Technical Moderator: Chris Olson / SNL**
Facilitator: Richard Harrington / PHMC Team

7:30	**Status, Action Items** **Discussion of Analysis Framework and Previous Day's Topics**		
8:00	**Topic: Respirable Material Release**		
	•	20 minutes:	Presentation: Fred Gelbard / SNL
	•	20 minutes:	Questions & Answers
	•	20 minutes:	Discussion on Implications for Analysis Framework
9:00	**Topic: NH_3 Model Reprised**		
	•	20 minutes:	Presentation: Wu-Ching Cheng / SNL
	•	20 minutes:	Questions & Answers
	•	20 minutes:	Discussion on Implications for Analysis Framework
10:00	**Break**		
10:10	**Topic: In-equipment Burns (Being replaced by Epstein's presentation for tomorrow)**		
	•	20 minutes:	Presentation: Scott Slezak / SNL
	•	20 minutes:	Questions & Answers
	•	10 minutes:	Discussion on Implications for Analysis Framework
11:00	**Topic: Verification & Validation Results**		
	•	20 minutes:	Presentation: Fred Gelbard / SNL
	•	20 minutes:	Questions & Answers
	•	20 minutes:	Discussion on Implications for Analysis Framework
12:00	**Working Lunch**		
12:30	***Analysis tool (SST version)*: demonstration and discussion (Executive Boardroom)** - Steve Humphreys / SNL		
1:00	**Panel Caucus on Analysis Framework**		
	Project Teams (PHMC Team, SNL) Caucus (Executive Boardroom)		
6:00	**Group Dinner (No group dinner)**		

Thursday, February 12 **Technical Moderator: Scott Slezak / SNL**
Facilitator: Chris Olson / SNL

7:30 **Status, Action Items**
Discussion of Analysis Framework and Previous Day's Topics

8:00 **Topic: Seismic Response of DST Waste**
- 20 minutes: Presentation: Chuck Stewart / PNNL
- 15 minutes: Questions & Answers
- 15 minutes: Discussion on Implications for Analysis Framework

8:50 **Topic: Combustion Modeling for Plumes and Strata (presented yesterday)**
- 20 minutes: Presentation: Mike Epstein / Fauske & Assoc.
- 20 minutes: Questions & Answers
- 20 minutes: Discussion of Implications for Analysis Framework

9:50 **Break**

10:00 **Topic: Finalization of Analysis Framework and Elicitation Structure (no handout)**
- 30 minutes: Presentation: Scott Slezak / SNL
- 30 minutes: Questions & Answers
- 30 minutes: Discussion on Implications for Analysis Framework

11:30 **Topic: Elicitations - the Graduate-Level Course**
- 30 minutes: Presentation: D. von Winterfeldt / Decision Insights
- 15 minutes: Questions & Answers

12:15 **Working Lunch**

12:45 ***Analysis tool (SST version)*: demonstration and discussion (Executive Boardroom)**
- Steve Humphreys / SNL

12:55 **Panel Caucus on Analysis Framework**

Project Teams (PHMC Team, SNL) Caucus (Executive Boardroom)

Friday, February 13 **Technical Moderator: Chris Olson / SNL**
Facilitator: Scott Slezak / SNL

7:30	**Status, Action Items** **Discussion of Analysis Framework**
8:00	**Panel Caucus** Document Panel Consensus Positions and Open Issues Quality Assurance Issues
10:30	**Panel Report on Analysis Framework and Elicitation Structure**
11:15	**Assignments for Elicitations and Rationale Reports**
11:45	**Working Lunch: Panel Caucus on Open Issues**
12:45	**Report of Panel on Open Issues**
1:00	**Adjourn**

PD 4 - 1
Procedure for Elicitation Rationale Reports and
Expert Panelists' Elicitation Verification

1.0 Purpose and Scope

This procedure is provided to expert panelists participating in the Stage II Gas Release Event Safety Analysis project (here after in this procedure identified as "the project"). This Procedure is to be used by expert panelists for preparation of their Stage II *Expert Elicitation Rationale Summary Reports*. The Stage II Expert Elicitation Rationale Summary Reports are Quality Documents so panelist compliance with this Procedure is required.

In addition to describing the procedures for preparing the Stage II Expert Elicitation Rationale Summary Reports, this Procedure describes the process by which each expert panelist shall review the report prepared by the Elicitor on the individual panelist's elicitation. Also described is the process for providing explicit feedback to Sandia National Laboratories Methodology for Flammable Gas Risk Assessment in Double-shell Tanks project staff when queried regarding aspects of the Stage II Expert Elicitation Rationale Summary Reports or the Elicitors' report.

This procedure also describes the process by which the panel endorses and approves the final version of the Analysis Framework on the basis of which the experts shall be elicited.

2.0 References

None

3.0 Requirements

3.1 Stage II Expert Elicitation Rationale Summary Reports

The following format shall be implemented in preparing the various sections of the Stage II Expert Elicitation Rationale Summary Reports ("the report").

- Title Page: The Title Page shall include the phrase "Stage II Gas Release Event Safety Analysis Project Expert Elicitation Rationale Summary Report", the expert's name and organization, date of elicitation, and date of report.

- Table of Contents: The report shall include a Table of Contents. The pages of the report shall be numbered.

- Introduction: An Introduction shall be included which shall identify the elicitation process (Elicitor, date) for the panelist. The Introduction should include any general comments which the panelist wishes to make.

- Elicitation Parameter Rationales: For each parameter to which the panelist was elicited, a separate section within the report shall be included. The title of each Elicitation Parameter Rationale section in the Stage II Expert Elicitation Rationale Summary Report shall correspond to the title of the elicited parameter. Each Elicitation Parameter Rationale section shall provide a discussion of the probability distribution response provided at the time of the elicitation, changes subsequently made after the formal elicitation to that response (if any), and a detailed rationale by which the elicited response was derived. Included within each Elicitation Parameter Rationale section shall be subsections discussing conditioning factors, assumptions, references, and the elicited probability distributions for the parameter in table format. References employed in arriving at the elicited response shall be identified and shall be provided in both the section of the report on the particular elicited parameter and in a section of the report which collates all References. All referenced materials shall be in either the open technical literature or shall have received clearance for public document distribution.

- Each table shall be numbered with an arabic numeral and shall be given a title that is complete and descriptive. The table number and title shall be above the body of the table. In column headings, first include the quantity tabulated followed by a comma and the units. Do not use powers of 10 in column headings. Use notation such as "X10^6" for numbers to be expressed in powers of 10 within the body of the table. Each entry in the tables shall be specifically entered: do not refer to values in other tables or use multipliers for values of other entries in the table.

- References: References shall be provided in each Elicitation Parameter Rationale section and all of the references provided throughout the report shall be listed in a separate Reference section of the report.

Panelists shall prepare for each elicitation session by organizing their notes and references. Panelists may prepare summary notes prior to elicitation sessions to assist them in accessing the appropriate notes and references efficiently. These summary notes may be included in the Rationale Summary Report. Each panelist may obtain a printed version of the data and narrative recorded by the Elicitor at the end of the elicitation session. The Stage II Expert Elicitation Rationale Summary Reports are due at Sandia National Laboratories no later than two weeks following the date of the elicitation. Either hardcopy or electronic format is acceptable.

Preferred word-processing medium is WordPerfect® Times New Roman 12-point font format for the text is preferred.

3.2 Elicitors' Report / Elicitation Feedback

The Elicitors shall prepare a report for each set of elicited responses from each of the panelists. This report shall include the probability distributions provided by the panelists at the time of elicitation. These reports are due at Sandia National Laboratories no later than two weeks after the final panelist elicitation. The probability distributions for each of the elicited parameters shall be transmitted to Sandia National Laboratories in EXCEL® Version 7.0.

The Elicitor's report for each panelist shall subsequently be forwarded upon receipt by Sandia National Laboratories to the corresponding panelist. The panelist shall be requested to review the Elicitor's report to determine the accuracy of the information contained, particularly the probability distributions. The panelist is required to either 1) confirm the accuracy of the information in the Elicitor's report, 2) identify any discrepancies and provide the correct information, or 3) change any response originally provided to the Elicitor at the time of the elicitation. The review of the Elicitor's report shall be conveyed to Sandia National Laboratories within one week of receipt by the panelist. The response to the Elicitors' Report review may be transmitted by hard-copy or electronically. These responses shall be Quality Documents.

Subsequently, as Sandia National Laboratories staff review both the sets of Elicitor's reports and the Stage II Expert Elicitation Rationale Summary Reports, questions may arise to which the panelists shall be asked for clarification. Both the queries and the panelist's responses shall be documented. Hard-copies of electronic or written versions of these interchanges shall be Quality Documents.

3.3 Endorsement of Stage II Analysis Framework

The review of the Analysis Framework, changes to the Analysis Framework, and other consensus decisions reached by the expert panel are to be documented in writing, as well as in the voice recordings of the workshop meetings. Any changes to the Analysis Framework, as presented in project documents and workshop presentations, are to be documented on Decision Record forms. The record forms are to be signed and dated by the panel leader, the panel caucus facilitator, and the workshop meeting moderator. The Decision Records will be distributed to each panelist within one week of the end of the panel group sessions. The panel shall document on the Decision Record form any application guidelines and caveats that the panel members believe should be recorded to prevent misuse of the Analysis Framework. Provisions are to be made for documenting dissenting minority opinions to decisions if the dissenting panel members

*****
Excel is a trademark of Microsoft Corporation.

wish to document their differences of opinion. The review of the Analysis Framework is to be documented in the form of decision records that list the specific submodels, equations, or discussions in the Analysis Framework document or presentation slides that were discussed and agreed to by the panel. Other consensus decisions to be recorded include (1) agreements that specific phenomena are not risk-significant enough to include in the Analysis Framework, (2) that within the uncertainties and the current state of knowledge there is no basis for distinguishing between different potential elicitation parameters or different potential conditioning cases for a given elicitation parameter, and (3) any decision or consensus position reached by the panel that in the view of the project team warrants permanent documentation.

4.0 Records

Relevant items described in this procedure shall be Quality Documents.

5.0 Attachments

Analysis Framework Decision Record form.

Approvals:

Chris Olson, SNL Project Manager — Date 2-5-98

Larry Bustard, SNL QA Manager — Date 2/5/98

Stage II Gas Release Event Safety Analysis Project
Analysis Framework Decision Record

Analysis Framework issue:

Panel Comments:

Approvals:

Panel Leader	Date
Panel Caucus Facilitator	Date
Workshop Moderator	Date

The Rationale Reports for SSTs

- Diversity of styles
- Common feature: engagement and effort
- Range of references used and excluded
- Based on data and materials from Workshops
- Not afraid to make explicit judgments

Goal for DSTs: Uniform high quality and timely delivery

Things that enhance the quality of Rationale Reports

- Describe understanding of terms used
- Explicit description of reasoning
- Explicit description of judgment
- Explicit description of "best available" and analogies
- Clear citation of sources used
- Clear discussion of sources not used
- Ties to relevant data from Hanford and elsewhere
- Analysis used to reach conclusions
- Brevity without sacrifice
- Volume without useless repetition

Some Suggestions for Rationale Reports

- Outline major points and secure reference material before elicitation
- Leave elicitation session with printed copy of Elicitor's narrative and numbers
- Schedule time in advance to complete report promptly after elicitation session
- Use time-space-resources available at Richland during Week #3
- Adhere to QA procedure when preparing reports

A Simple Predictive Gas Retention Model for Hanford Waste Tanks

Perry Meyer, Del Lessor, Chuck Stewart

PNNL

Expert Panel Elicitation Workshop #2,
February 9-12, 1998,
Richland, Washington

A Simple Predictive Model for Gas Retention in Hanford Waste Tanks

A model is needed to predict how much gas waste can store in order to determine whether or not a buoyant displacement gas release is possible. A simple model has been developed for the steady state void profile as a function of waste layering, densities, gas generation rate, and temperature. The model is based on the following major assumptions:

- The void profile results from a balance between gas generation and steady gas release.
- Gas release is solely by slow bubble migration that qualitatively obeys Stokes Law
- The waste viscosity (determining bubble rise velocity) increases linearly with waste depth from zero at the top of the nonconvective layer and the rate of increase (slope) is the same for all tanks.

The latter assumption is consistent with ball rheometer measurements on five of the six double-shell tanks (DSTs) that are known to experience buoyant displacements.

The general form of the model is described by gas mass continuity and bubble number continuity along with equations for the bubble velocity and the gas state. The gas mass continuity equation is:

$$\frac{d(mu)}{dz} = G(z) \tag{1}$$

where m is the number of moles of gas per unit volume (mol/m^3) and G is the volumetric gas generation rate (mol/m^3-day). The bubble number continuity equation is:

$$\frac{d(nu)}{dz} = N(z) \tag{2}$$

where n is the number of bubbles per unit volume (#/m^3) and N is the volumetric bubble nucleation rate (#/m^3-day). The ideal gas equation of state is expressed as:

$$(m/n) = p(z)V_B(z)/RT(z) \tag{3}$$

where p is the pressure (Pa), V_B is the average bubble volume, R is the gas constant (8314 J/kg-K), and T is the temperature (K). The bubble velocity, u, is computed by a modified version of Stokes law as follows:

$$u(z) = C\frac{\rho_S V_B^{2/3}}{\mu(z)} \tag{4}$$

where ρ_S is the nonconvective layer density and μ is the viscosity.

Assuming the nucleation rate and gas generation rates are uniform and neglecting spacial variation of pressure and temperature (these have shown to be negligible), the solution of Eqs. (1) through (4) yields the following equation for the void fraction profile:

$$\alpha(\eta) = \frac{C}{\rho_S}\left(\frac{RT}{p}\right)^{1/3} H^2(1-\eta)\left[G\eta + \frac{\alpha_0\rho_S}{CH^2}\left(\frac{p}{RT}\right)\right]^{1/3}\left[V_0 N\eta + \frac{\alpha_0\rho_S}{CH^2}\right]^{2/3} \quad (5)$$

where η=z/H, H is the nonconvective layer height, and α_0 and V_0 are the initial void fraction and bubble volume at z=0, respectively.

There are two important bounding limits of Eq. (5). 1) If the bubble nucleation rate is zero, bubbles flow in at the lower boundary and grow due to gas generation; 2) On the other hand, if the nucleation rate is set to a constant and no bubbles are allowed to enter at the lower boundary, gas generation forms new bubbles and the average bubble volume remains constant. The N=0 model produces a void profile with a maximum at η=0.25 and the N=Const. model produces an axially symmetric profile with a maximum at η=0.5.

If the integral of the void fraction profile from the top of the nonconvective layer becomes equal to the neutral buoyancy void fraction at some elevation, all of the waste down to that elevation can rise to the surface and release a fraction of the gas it contains. This condition occurs for the N=0 model when the maximum void fraction is 1.51 times the neutral buoyancy void fraction and almost the entire nonconvective layer is buoyant. For the N=Const. model, buoyancy occurs when the maximum is 4/3 the neutral buoyancy void fraction but only 75% of the nonconvective layer is buoyant.

The model is assessed for a number of tanks representing the range of conditions in existing DSTs. With the leading constant, C in the two limiting cases of Eq. (5) adjusted so that all six burping DSTs are predicted to be unstable, both limits clearly predict that, with the exception of AN-107, only the six burping tanks are unstable. The marginal result for AN-107 may be the result of either a high gas generation rate or uncertainty in the waste densities. The details of the tank data and results are given in the presentation.

A Simple Predictive Gas Retention Model for Hanford Waste Tanks

Perry Meyer, Del Lessor, Chuck Stewart
PNNL

Expert Panel Elicitation Workshop #2,
February 9-12, 1998,
Richland, Washington

Basis of Model

- **Gas generated in sludge forms small bubbles**
- **Bubbles migrate (rise) very slowly (~1mm/day)**
- **Balance between generation & migration produces void profile**
- **Void profiles evolve in time**
- **GRE occurs in a layer when average void > neutral buoyant void**
- **Consider steady state profiles to see if burpers can be distinguished from non burpers**

Governing Equations

Conservation of moles

$m_t + (mu)_z = G(z)$

Conservation of bubbles

$n_t + (nu)_z = N(z)$

Bubble rise model

$u = u(V_b(z), \mu(z))$

State

$m/n = p(z)V_b(z)/RT(z)$

Definition of void

$\alpha = n(z)V_b(z)$

m = moles/m^3 sludge
n = #bubbles/ m^3 sludge
G = gas generation rate (moles/m^3 sludge/day)
N = bubble nucleation rate (#/m^3 sludge/day)
u = bubble rise velocity
V_b = average bubble volume
p = average sludge pressure
T = average sludge temperature
α = retained gas void fraction

Bubble Rise Model

Stokes Law

$$u = c\frac{\rho_s V_b^{2/3}}{\mu(z)}$$

Assume linear viscosity variation

$\mu(z) = b(H - z)$

Assume all tanks have same b

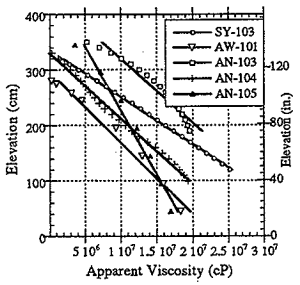

Solution

- **Steady state conditions**
- **Constant gas generation rate**
- **General nucleation rate**
- **Neglect pressure & temperature variation**

$$\alpha(\eta) = \frac{C}{\rho_s}\left(\frac{RT}{p}\right)^{1/3} H^2(1-\eta)\left[G\eta + \frac{\alpha_0\rho_s}{CH^2}\left(\frac{p}{RT}\right)\right]^{1/3}$$

$$\eta = z/H \qquad \times \left[V_0\int_0^{\eta} N d\eta + \frac{\alpha_0\rho_s}{CH^2}\right]^{2/3}$$

Two Important Limits

- **N = 0**
  - **Finite size bubbles inflow at z = 0**
  - **No additional bubble nucleation**
  - **Bubbles grow in size due to gas generation**
- **$N = N_0$**
  - **Bubbles begin to form at z = 0**
  - **Average bubble volume remains constant**
  - **New bubbles form due to gas generation**
- **These two limits bound more general cases where N = N(z)**

Limits, cont.

- **N = 0**

$$\alpha(\eta) = C\left(\frac{GT}{\rho_s p}\right)^{1/3} H^{2/3}\eta^{1/3}(1-\eta)$$

$$\alpha_m \text{ @ } \eta_m = 0.25$$

- **$N = N_0$**

$$\alpha(\eta) = \frac{C}{\rho_s}\left(\frac{GT}{p}\right)^{1/3} H^2\eta(1-\eta)$$

$$\alpha_m \text{ @ } \eta_m = 0.5$$

Buoyancy Condition

$$\int_{\eta_c}^{1} \alpha(\eta)d\eta = \alpha_{NB}(1-\eta_c)$$

η_c defined by $\alpha(\eta_c) \equiv \alpha_{NB}$

If $\alpha(\eta)$ known, integral gives relation between α_m and α_{NB}

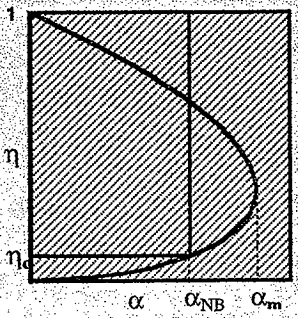

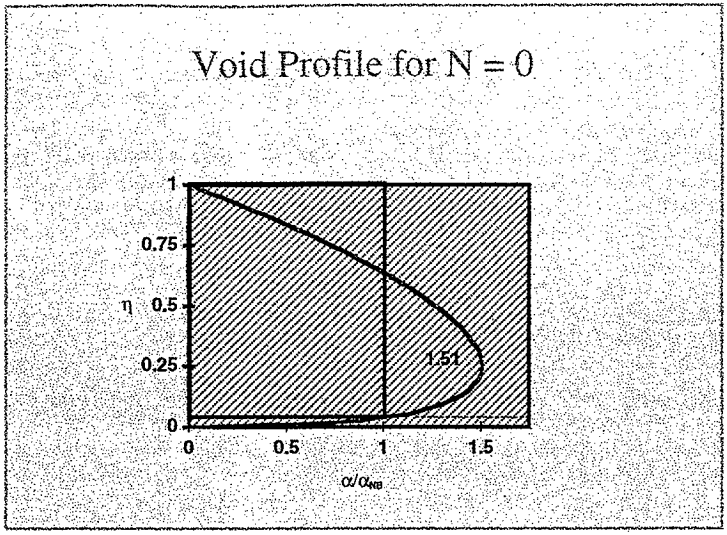
Void Profile for N = 0
1
0.75
η 0.5
0.25
0
1.51
0
0.5
1
1.5
α/α_NB

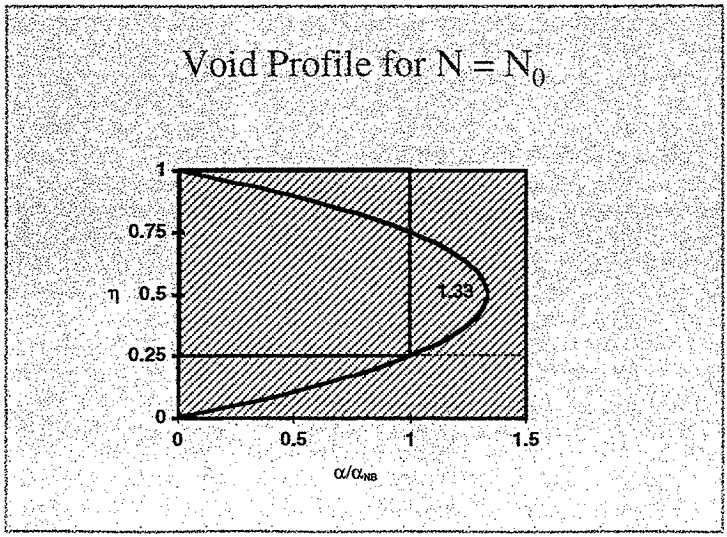
Void Profile for N = N0
1
0.75
η 0.5
0.25
0
1.33
0
0.5
1
1.5
α/α_NB

Applying the Model

- **Adjust leading constant to assure all 5 burping DST's have unstable void profiles**

  N = 0: $\alpha_m/\alpha_{NB} > 1.33$

  N = N_0: $\alpha_m/\alpha_{NB} > 1.51$

- **Apply model to known non-burpers using best available data as inputs**

Model Input Data

Tank	Gdot (mol/day/m3)	Layer height (m) NCL	Layer height (m) CL	Density (kg/m3) NCL	Density (kg/m3) CL	Temp. (K)	Pressure (atm)	
SY101	[illegible]	[illegible]	[illegible]	[illegible]	[illegible]	[illegible]	[illegible]	Burping DSTs
SY103	[illegible]	[illegible]	[illegible]	[illegible]	[illegible]	[illegible]	[illegible]	
AN105	[illegible]	[illegible]	[illegible]	[illegible]	[illegible]	[illegible]	[illegible]	
AN104	[illegible]	5.2	4.2	1590	[illegible]	[illegible]	[illegible]	
AN103	[illegible]	[illegible]	[illegible]	[illegible]	[illegible]	[illegible]	[illegible]	
AW101	[illegible]	[illegible]	[illegible]	[illegible]	[illegible]	[illegible]	[illegible]	
AN107	1.6E-5	2.3	7.4	1540	1357	308	2.1	Hot, deep NCL
C106	2.1E-5	1.8	0.5	1550	1170	355	1.2	
AZ101	1.3E-5	0.3	7.9	1490	1187	345	1.9	Hot, thin NCL
AZ102	1.1E-5	0.9	7.4	1490	1100	355	1.8	
AY102	6.7E-6	0.5	7.4	1400	990	310	1.7	
AW103	1.5E-6	3.4	1.4	1489	1011	303	1.3	Cold, deep NCL
AW104	4.2E-7	2.7	7.7	1460	1038	304	1.9	

All pressures computed from layer heights and densities. Densities (except SY101) averaged from latest TCD

SY101: data and densities from Reynolds (1993)

Burping DST's (exc. SY101): data from PNNL-11536

C106 & AY102: data from W320 Project Process Control Plan

Other tanks: waste levels from Hanlon (1997)

Gas Generation Rates

Tank	Waste data			Gas generation rate			
	Level (m)	Volume (m3)	Hydrogen fraction	Hydrogen (m3/day)	Total (m3/day-m3)	Total (mol/day-m3)	
SY101	[illegible]	[illegible]	[illegible]	[illegible]	[illegible]	[illegible]	Burping DSTs
SY103	[illegible]	[illegible]	0.57	[illegible]	[illegible]	[illegible]	
AN103	[illegible]	[illegible]	[illegible]	[illegible]	[illegible]	[illegible]	
AN104	[illegible]	[illegible]	[illegible]	[illegible]	[illegible]	[illegible]	
AN105	[illegible]	[illegible]	0.61	[illegible]	[illegible]	[illegible]	
AW101	[illegible]	[illegible]	0.31	[illegible]	[illegible]	[illegible]	
AN107	9.72	3989	0.8	1.20	3.8E-4	1.6E-5	Hot, deep NCL
C106	1.80	739	0.5	0.18	4.9E-4	2.1E-5	
AZ101	8.18	3357	0.8	0.82	3.1E-4	1.3E-5	Hot, thin NCL
AZ102	8.25	3386	0.8	0.70	2.6E-4	1.1E-5	
AY102	7.67	3148	0.8	0.40	1.6E-4	6.7E-6	
AW103	4.74	1945	0.8	0.05	3.5E-5	1.5E-6	Cold, deep NCL
AW104	10.32	4236	0.8	0.03	1.0E-5	4.2E-7	

Burping DST's: data from PNNL-11536, generation from Wilkins et al. (1997)

C106 & AY102: data and generation from W320 Project Process Control Plan

Other tanks: generation from Hu (1997), hydrogen fraction assumed 0.8, waste level from Hanlon (1997)

Results

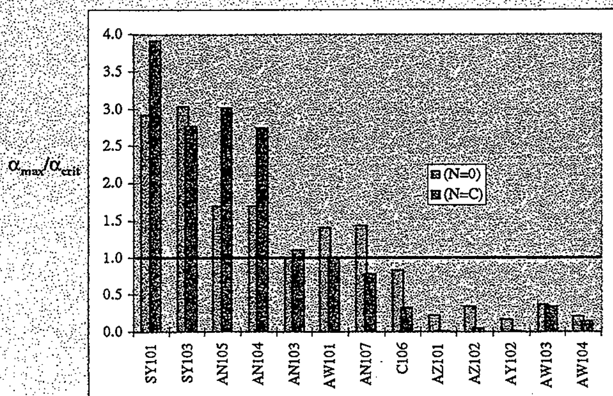

Results (tabulated)

Tank	Void fraction			Max./NB		Max./Crit.	
	NB	Max. (N=0)	Max. (N=C)	(N=0)	(N=C)	(N=0)	(N=C)
SY101	0.12	0.32	0.21	2.6	1.8	2.5	1.7
SY103	0.05	0.27	0.16	4.6	3.1	3.6	2.4
AZ101	0.18	0.46	0.40	2.6	2.2	1.7	1.5
AN103	0.12	0.31	0.25	2.6	2.1	1.7	1.4
AN105	0.18	0.34	0.23	1.9	1.3	1.6	1.1
AW101	0.10	0.22	0.14	2.1	1.4	1.4	1.0
AN107	0.12	0.26	0.13	2.2	1.1	1.4	0.8
C106	0.25	0.31	0.11	1.3	0.4	0.8	0.3
AZ101	0.20	0.07	0.00	0.4	0.0	0.2	0.0
AZ102	0.26	0.13	0.02	0.5	0.1	0.3	0.1
AY102	0.29	0.08	0.01	0.3	0.0	0.2	0.0
AW103	0.32	0.18	0.15	0.6	0.5	0.4	0.3
AW104	0.29	0.09	0.06	0.3	0.2	0.2	0.1

A Buoyant Displacement Criterion

N = 0

$$8.7\frac{\rho_s^{2/3}}{\rho_s-\rho_L}\left(\frac{MT}{p}\right)^{1/3} H^{2/3} > 1$$

$N = N_0$

$$\frac{210}{\rho_s-\rho_L}\left(\frac{MT}{p}\right)^{1/3} H^{2} > 1$$

History of Organic Carbon in Hanford HLW Tanks

Feb. 8, 1998
Flammable Gas Safety Analysis
DoubleTree Inn, Richland, WA

Stephen F. Agnew, project leader
505-665-1764 ph
505-667-0851 fa
sfagnew@lanl.gov e-mail
Robert Corbin
Tomasita Duran
Kenneth Jurgensen
John FitzPatrick
Bonnie Young
James Boyer
Theodore Ortiz

Chemical Science and Technology Division
Los Alamos National Laboratory
Los Alamos, NM 87545

Overview of Strategy

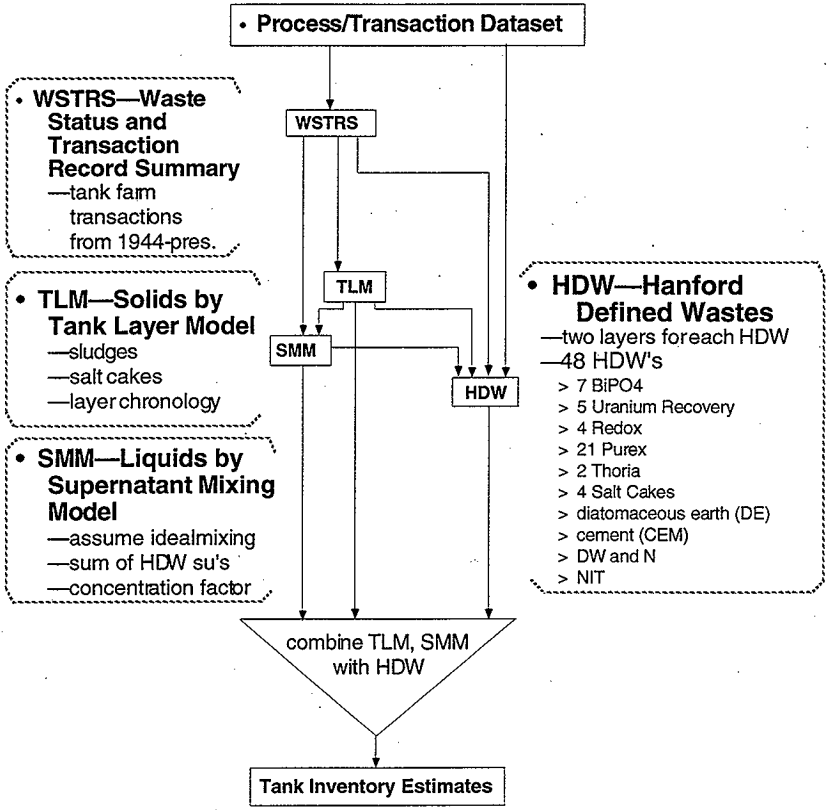

Los Alamos
NATIONAL LABORATORY

Overview of Strategy

■ Inventory calculation

$$\mathbf{tank}_i = \frac{\sum_j \mathrm{tlm}_{ij}\mathbf{hdw}_j^{sl}}{\mathrm{slVol}_i} + \frac{\sum_j \mathrm{smm}_{ij}\mathbf{hdw}_j^{su}}{\mathrm{suVol}_i}$$

where...

- $\mathbf{tank}_i$ = composition vector for tank i
- $\mathbf{hdw}_j^{sl}$ = composition vector for HDW sludge j
- $\mathbf{hdw}_j^{su}$ = composition vector for HDW supernatant j
- tlm_{ij} = kgal of hdw sludge j for tank i
- smm_{ij} = kgal of hdw supernatant j for tank i
- slVol_i = sludge kgal for tank i
- suVol_i = supernatant concentrate kgal for tank i.

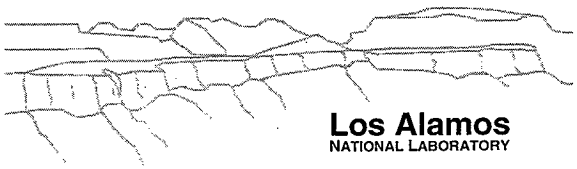

History of Organic Carbon at Hanford

- **Found three major classes of organic waste**
  - organic concentrates
    - highly blended and widely distributed
  - organic sludges
    - solids from original organic waste
    - usually high Sr-90 residues as well
  - surface residual organic remnants
    - highest potential concentrations
    - highly uncertain amounts

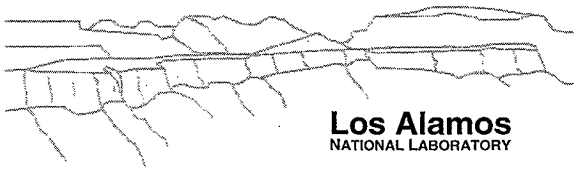

Los Alamos
NATIONAL LABORATORY

History of Organic Carbon at Hanford

- **Used HDW model Rev. 3 estimates**
  - updated evaporator blending with logbook dataset
- **Organic complexants have two main sources**
  - Purex solvent extraction
    - —TBP (as DBP, MBP, butanol)
    - —NPH residues
  - B Plant strontium extraction
    - —EDTA, HEDTA
    - —glycolate, citrate
- **Organic carbon is pervasive in concentrate**
  - evidently, gas retention highly correlated with organic complexants

History of Organic Carbon at Hanford

- **Funded by TWRS Characterization Program**
  - use best historical information on transaction and process histories for the purposes of predicting organic carbon in tanks.
- **21 of 24 H_2 W.L. tanks (88%) above 0.64 wt% TOC by HDW estimate**
  - nine tanks also meet criterion
    - —SST's A-103, S-101, S-103, S-107, TX-102, TX-111, U-102
    - —DST's AP-102, AP-105
  - three H_2 W.L. tanks below criterion
    - —S-111 (on edge), S-112, and SX-101
- **12 of 20 organic W.L. tanks above same threshold (60%).**

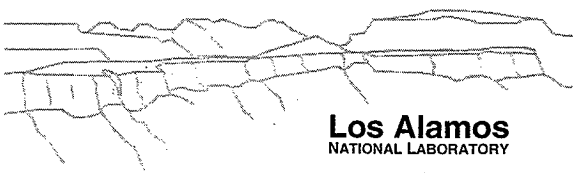

Table 3. Tank Concentrates Sorted by Decreasing TOC (no aging or evaporator degradation) with TOC > 0.64 wt%.

tank	total (kgal)	TLM (kgal)	SMM (kgal)	Dens. g/cc	TOC wt% now	radiolytic heat kW	W.L. or other
C-103	195	62.0	133	1.13	1.72	7.9	org.
AN-102	1,090	0.0	1,090	1.71	1.53	9.5	CC
AN-107	1,063	0.0	1,063	1.54	1.46	6.7	CC
AN-105	1,130	0.0	1,130	1.85	1.38	11.0	H2
A-102	41	3.0	38	1.49	1.37	0.9	
AX-101	748	13.0	735	1.49	1.35	8.8	H2
A-103	371	3.0	368	1.48	1.33	3.1	prop. H2
A-101	953	3.0	950	1.45	1.23	6.0	H2, org.
AY-101	881	33.0	848	1.16	1.22	14.1	DC, prop. H2
AX-103	112	14.0	98	1.45	1.20	5.6	H2
AX-102	39	6.0	33	1.53	1.18	4.1	org.
A-106	125	50.0	75	1.56	1.16	13.1	
AW-101	1,139	61.0	1,078	1.67	1.14	9.2	H2
SY-101	1,100	0.0	1,100	1.70	1.14	9.7	H2
U-106	226	26.0	200	1.66	1.13	1.6	org., prop. H2
U-109	463	48.0	415	1.71	1.13	3.7	H2
C-104	295	290.0	5	1.31	1.08	8.5	

Table 3 column descriptions.

tank	Hanford tank designation.
total (kgal)	Total inventory of waste in tank in kgal.
TLM (kgal)	Inventory of TLM solids for tank in kgal.
SMM (kgal)	Inventory of SMM concentrate in tank in kgal. Sum of TLM and SMM volumes equals total tank inventory.
Dens. g/cc	Average density of SMM concentrate (does not include TLM).
TOC wt% now	Average TOC for SMM concentrate (does not include TLM).
radiolytic heat kW	Heat of tank waste due to Sr-90 and Cs-137 present as per HDW Model calculations (includes both TLM and SMM).
W.L. or other	Indicates if a tank is on a watch list (H2, org., FeCN, or heat) or if it contains high organic carbon (CC, DC).

Table 8. Organic degradation by in-tank aging and/or evaporator destruction scenarios, sorted by decreasing TOC (complete table in App. A).

WSTRS Rev. 3	undegraded TOC wt%	Aging Remnant	80% T2 Degradation	20% A and S Degradation	radiolytic heat kW	organic heat kW	% organic heat of total	total gas prod. std. cu. ft./yr	equiv. slurry growth rate in./mo.
C-103	1.72	0.91	1.00	0.96	7.9	0.1	0.8	1,818	0.4
AN-102	1.53	0.63	0.93	0.60	9.5	2.3	19.7	70,675	8.7
AN-107	1.46	0.71	0.95	0.70	6.7	1.6	19.6	49,790	6.5
AN-105	1.38	0.60	0.90	0.56	11.0	2.5	18.5	77,556	9.0
A-102	1.37	0.72	0.93	0.65	0.9	0.1	5.6	1,610	0.4
AX-101	1.35	0.72	0.93	0.67	8.8	1.0	10.1	30,924	4.7
A-103	1.33	0.73	0.93	0.65	3.1	0.5	13.2	14,795	2.7
A-101	1.23	0.74	0.92	0.66	6.0	1.1	15.1	34,323	4.8
AY-101	1.22	0.91	0.99	0.96	14.1	0.3	2.0	9,395	1.5
AX-103	1.20	0.75	0.92	0.70	5.6	0.1	1.9	3,381	0.7

Table 8 Column Descriptions.

tank	Hanford tank designation.
TOC wt% now	Average TOC for SMM concentrate (i.e. does not include TLM).
Aging Remnant	Multiply TOC column by this column to apply aging with parameters shown in Table 2.
80% T2 Degradation	Multiply TOC column by this column to apply model for 80% degradation of organic carbon for every pass through T evaporator.
20% A and S Degradation	Multiply TOC column by this column to apply model for 20% degradation of organic carbon for every pass through either A or S evaporators.
radiolytic heat kW	Calculated based on HDW Cs-137 and Sr-90 estimated inventories. The TLM and SMM inventories are included.
organic heat kW	Heat production as a result of organic degradation using one carbon oxidation shown in text.
%organic heat of total	Per cent of total estimated heat that is due to organic degradation.
total gas prod. std. cu.ft./yr.	Gas production from both organic degradation and radiolysis with parameters shown in Table 2.
Index Now	Residual oganic index, numbers above one represent potential hazards if waste should dry out. See text for details.

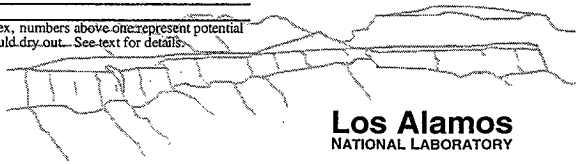

Los Alamos
NATIONAL LABORATORY

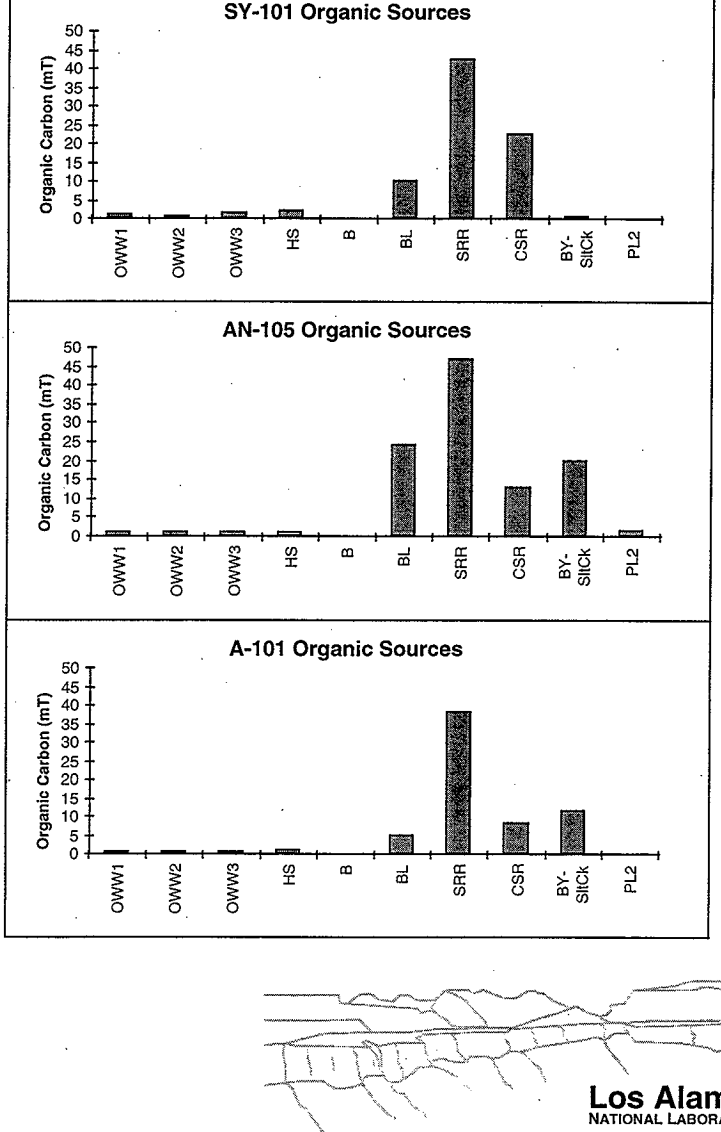
SY-101 Organic Sources
Organic Carbon (mT)
50
45
40
35
30
25
20
15
10
5
0
OWW1
OWW2
OWW3
HS
B
BL
SRR
CSR
BY-SlICk
PL2
AN-105 Organic Sources
Organic Carbon (mT)
50
45
40
35
30
25
20
15
10
5
0
OWW1
OWW2
OWW3
HS
B
BL
SRR
CSR
BY-SlICk
PL2
A-101 Organic Sources
Organic Carbon (mT)
50
45
40
35
30
25
20
15
10
5
0
OWW1
OWW2
OWW3
HS
B
BL
SRR
CSR
BY-SlICk
PL2

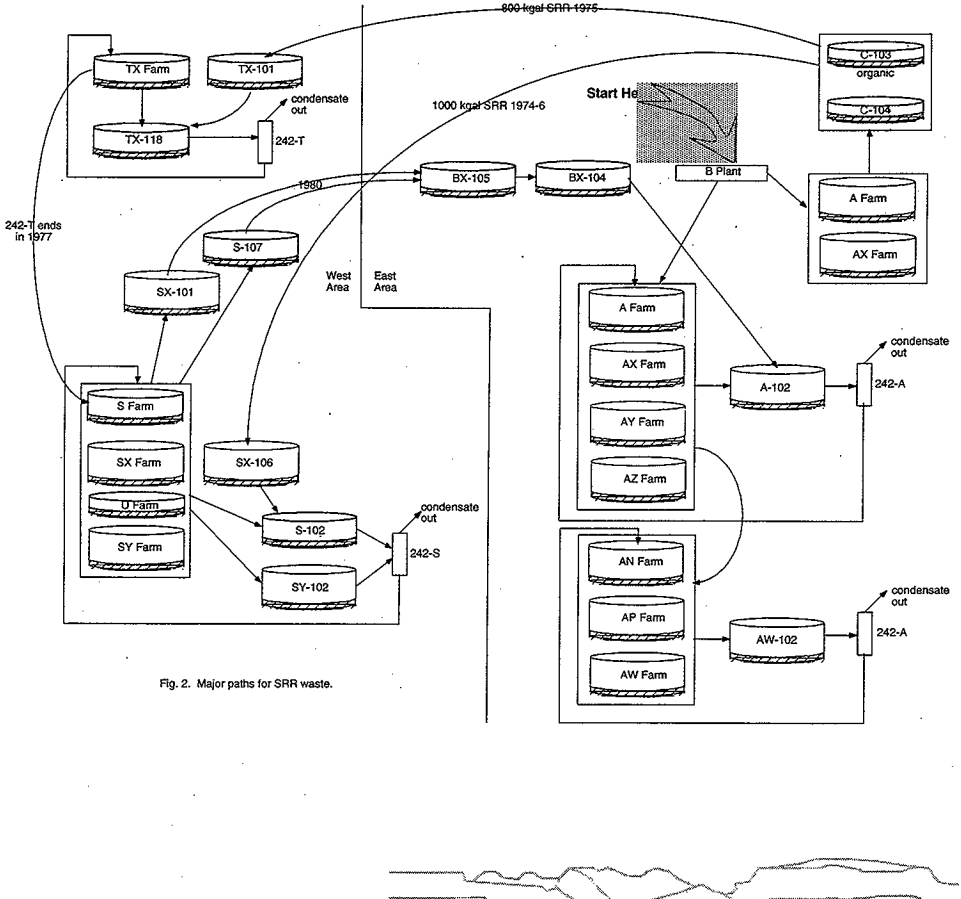

Fig. 2. Major paths for SRR waste.

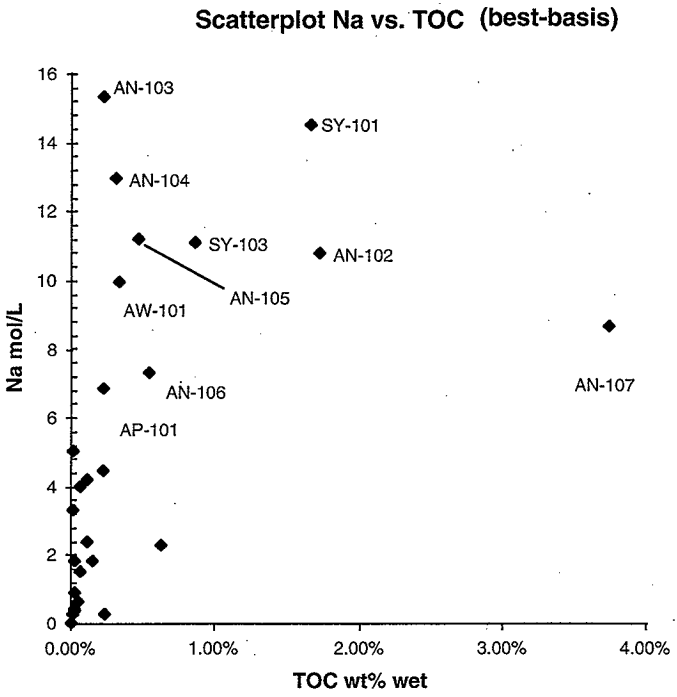
Scatterplot Na vs. TOC (best-basis)
Na mol/L
TOC wt% wet
16
14
12
10
8
6
4
2
0
0.00%
1.00%
2.00%
3.00%
4.00%
AN-103
SY-101
AN-104
SY-103
AN-102
AN-105
AW-101
AN-107
AN-106
AP-101

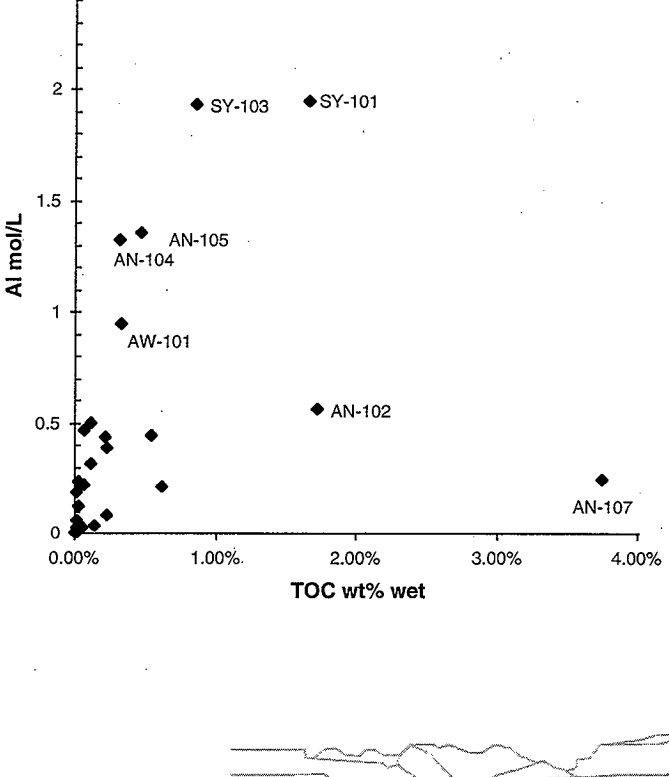

Los Alamos
NATIONAL LABORATORY

Comparisons of HDW and Assay Estimates

- **Scatter plots of assay vs. HDW estimates**
  - correlation coefficient shows extent of linear correlation between assay and model
    - —1 is perfect, 0 is random, -1 is orthogonal.
    - —Na correlation coeff. = 0.83
    - —Na correlation for assay vs. volume = 0.59
    - —one measure of HDW model validity is significant increase in correlation.
  - ratio of assay / HDW inventories= 1.02.
    - —shows average Na inventories within 2%
  - 65 tanks, 39% of Na site inventory.

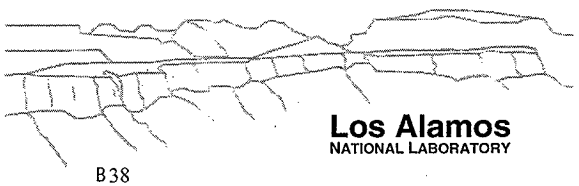

Los Alamos
NATIONAL LABORATORY

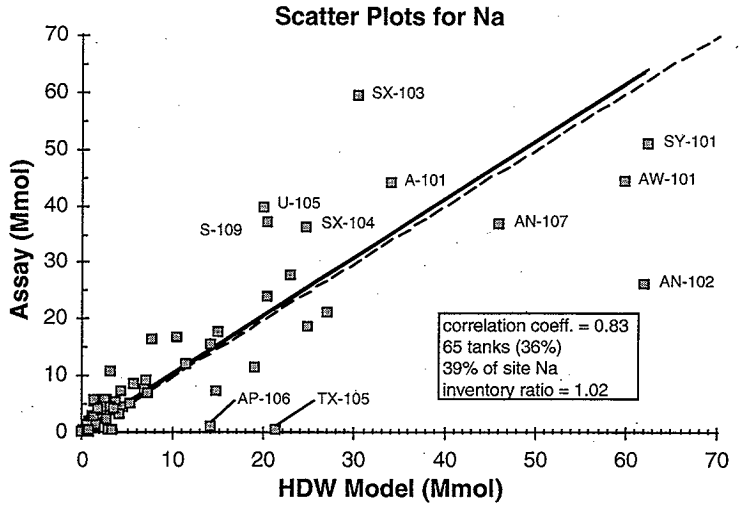
Scatter Plots for Na
Assay (Mmol)
HDW Model (Mmol)
SX-103
SY-101
A-101
AW-101
U-105
S-109
SX-104
AN-107
AN-102
AP-106
TX-105
correlation coeff. = 0.83
65 tanks (36%)
39% of site Na
inventory ratio = 1.02

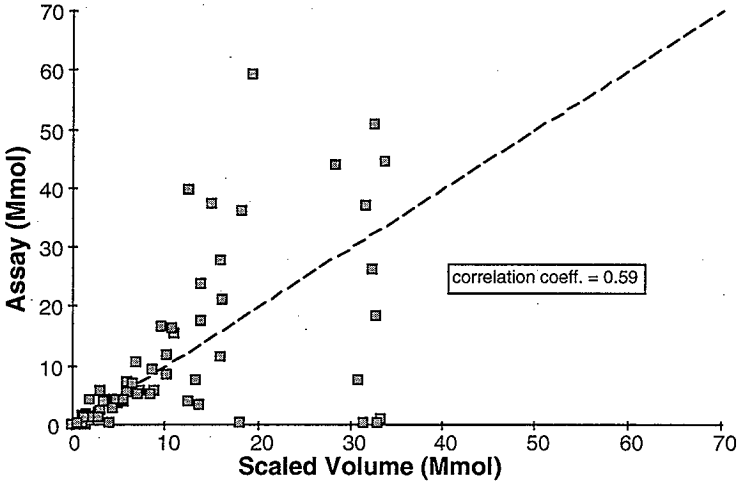
Assay (Mmol)
Scaled Volume (Mmol)
correlation coeff. = 0.59

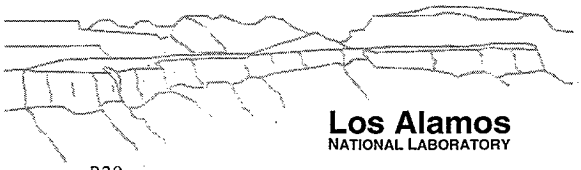
Los Alamos
NATIONAL LABORATORY

Scatter Plots for Al

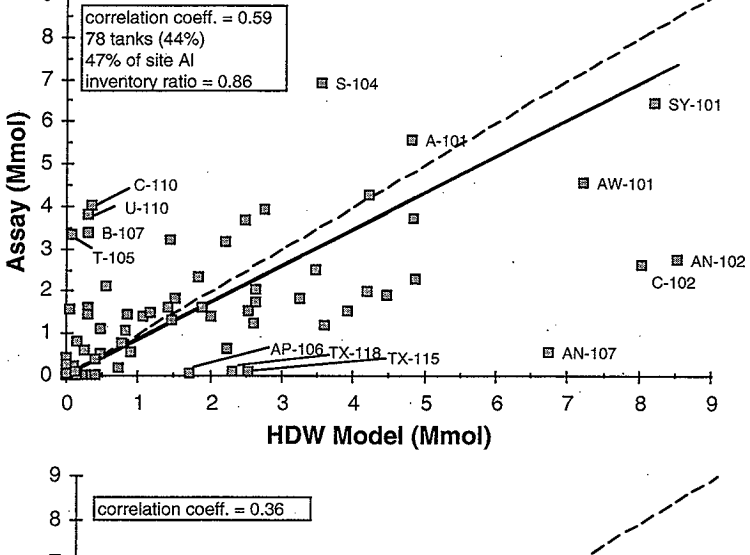

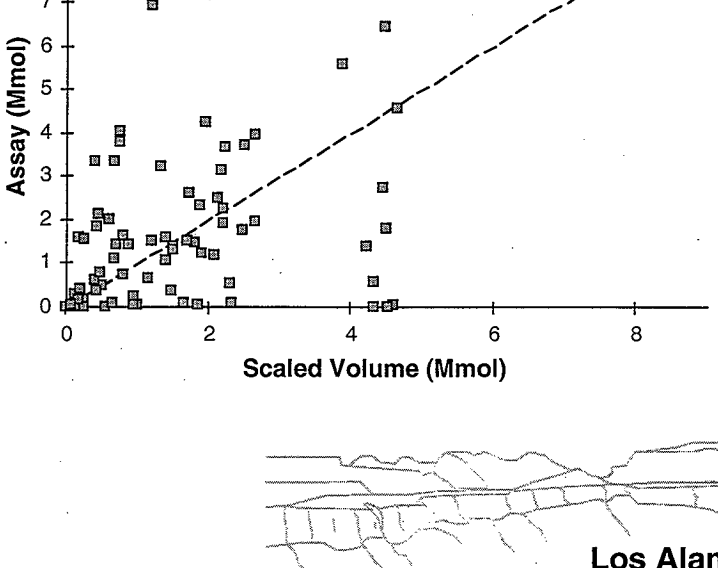

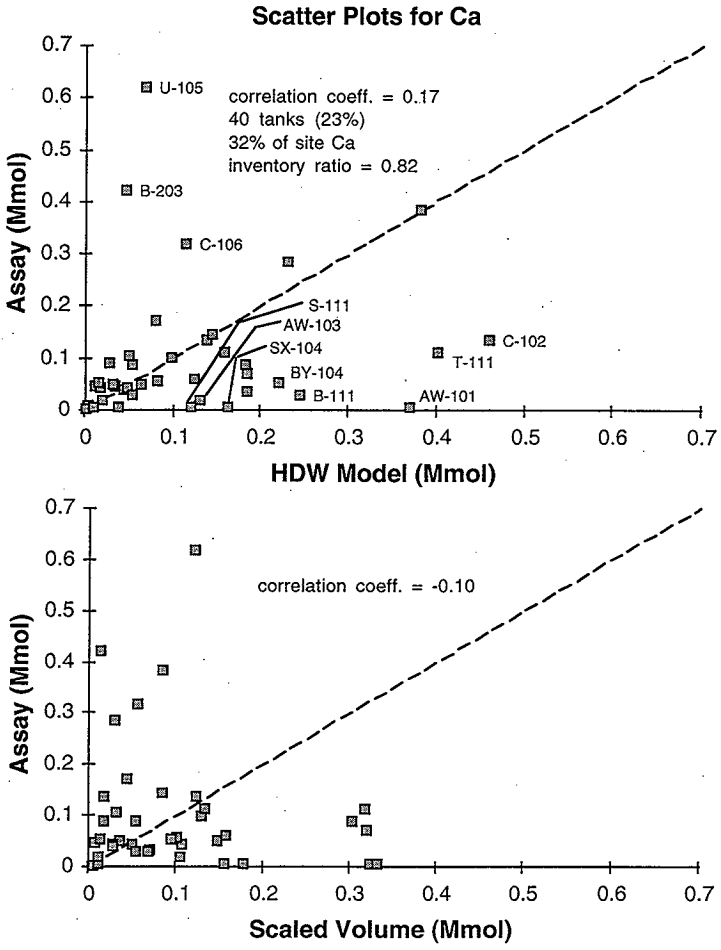
Scatter Plots for Ca
Assay (Mmol)
HDW Model (Mmol)
correlation coeff. = 0.17
40 tanks (23%)
32% of site Ca
inventory ratio = 0.82
U-105
B-203
C-106
S-111
AW-103
SX-104
BY-104
B-111
AW-101
C-102
T-111
correlation coeff. = -0.10
Scaled Volume (Mmol)
0
0.1
0.2
0.3
0.4
0.5
0.6
0.7

References

History of Organic Carbon

- Agnew, S.F.; Corbin, R.A.; Boyer, J.; Duran, T.B.; Jurgensen, K.A.; Ortiz, T.P.; Young, B.L. "History of Organic Carbon in Hanford HLW Tanks: HDW Model Rev. 3," LA-UR-96-989, March 1996.

HDW Model

- Agnew, S.F.; Boyer, J.; Corbin, R.A.; Duran, T.B.; FitzPatrick, J.R.; Jurgensen, K.A.; Ortiz, T.P.; Young, B.L. "Hanford Tank Chemical and Radionuclide Inventories: HDW Model Rev. 4," LA-UR-96-3860, January 1997.

Best-Basis Inventory

- Kupfer, M.J.; Boldt, A.L; Higley, B.A.; Lambert, S.L.; Orme, R.M.; Place, D.E.; Shelton, L.W.; Watrous, R.A.; Borsheim, G.L.; Colton, N.G.; LeClair, M.D.; Schulz, W.W.; Hedengren, D.C.; Winward, R.T. "Standard Inventories of Chemicals and Radionuclides in Hanford Site Tank Wastes," (Inventory F) WHC-SD-WM-TI-740, September 1997

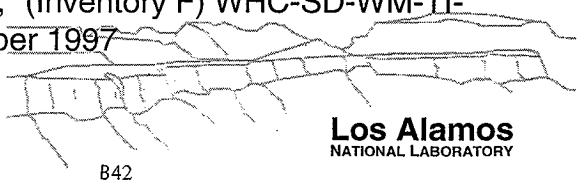

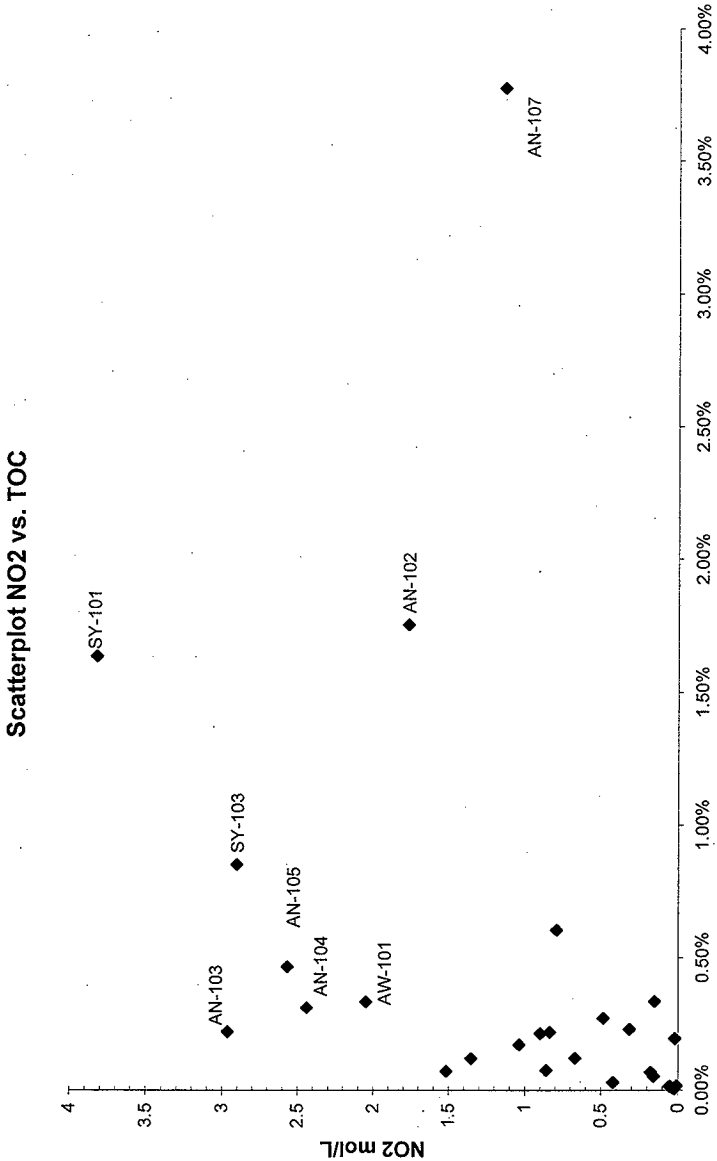
Scatterplot NO2 vs. TOC
NO2 mol/L
TOC wt% wet
SY-101
SY-103
AN-105
AN-104
AN-103
AW-101
AN-102
AN-107
4
3.5
3
2.5
2
1.5
1
0.5
0
0.00%
0.50%
1.00%
1.50%
2.00%
2.50%
3.00%
3.50%
4.00%


Scatterplot NO3 vs. TOC
NO3 mol/L
TOC wt% wet
AN-107
AN-102
SY-101
SY-103
AN-105
AN-104
AW-101
AN-103
AP-105
0
0.5
1
1.5
2
2.5
3
3.5
4
0.00%
0.50%
1.00%
1.50%
2.00%
2.50%
3.00%
3.50%
4.00%


Scatterplot CO3 vs. TOC
CO3 mol/L
TOC wt% wet
1.4
1.2
1
0.8
0.6
0.4
0.2
0
0.00%
0.50%
1.00%
1.50%
2.00%
2.50%
3.00%
3.50%
4.00%
AN-107
AN-102
SY-101
AN-104
AN-105
AY-101
SY-103
AZ-102
AZ-101
AN-103
AW-101

Evaporator Transaction Schematic

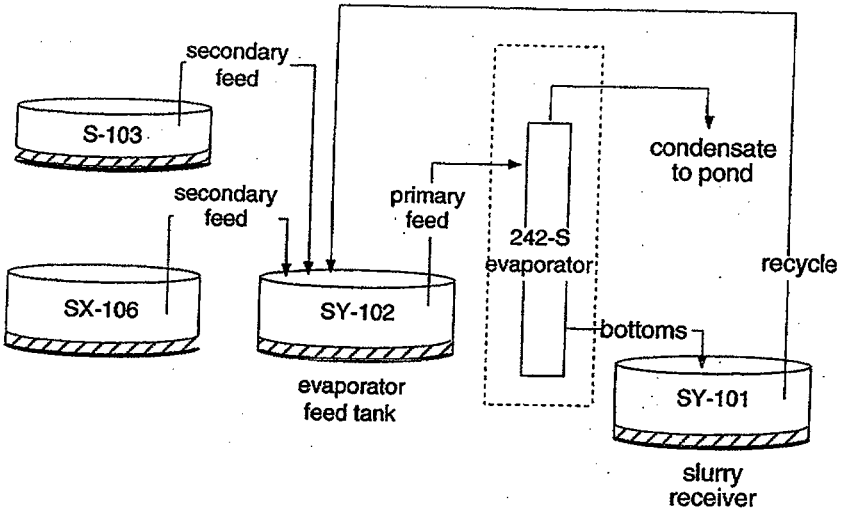

Fig. 1. Schematic showing complexity of evaporator operations.

Fig. 2. Major paths for SRR waste.

SY-101 Waste Composition

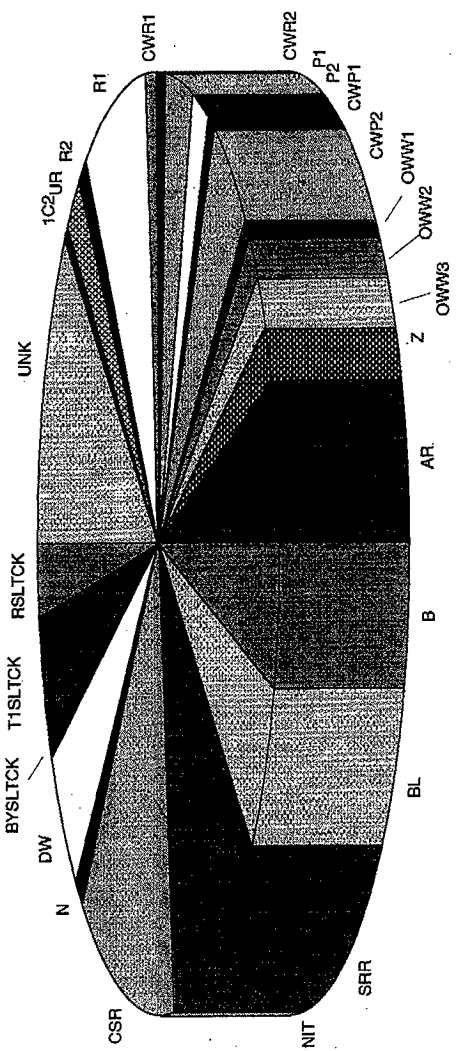

SRR Waste Distribution

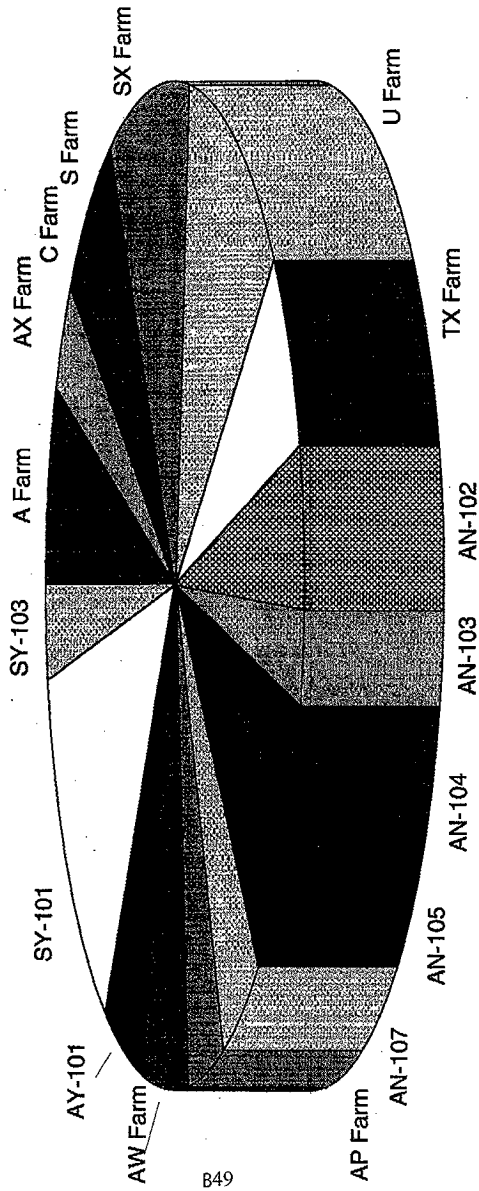

AW-101 SMM Composition

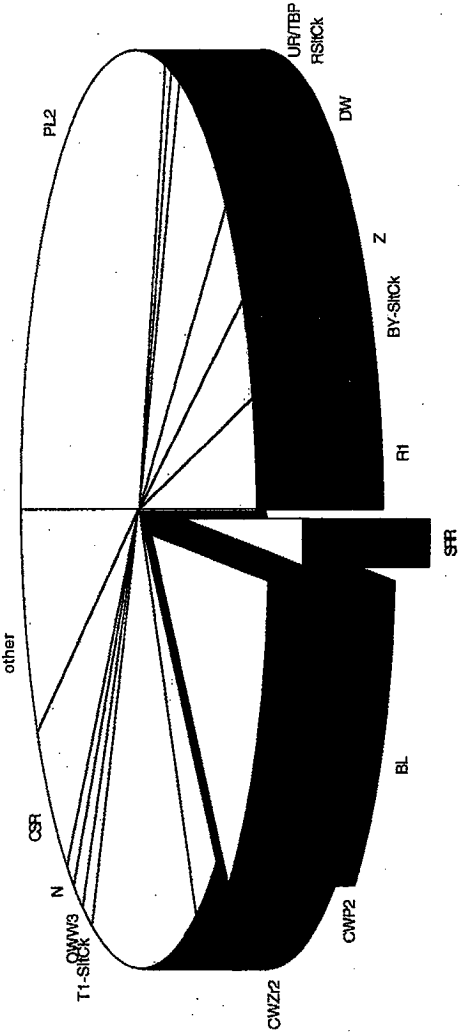

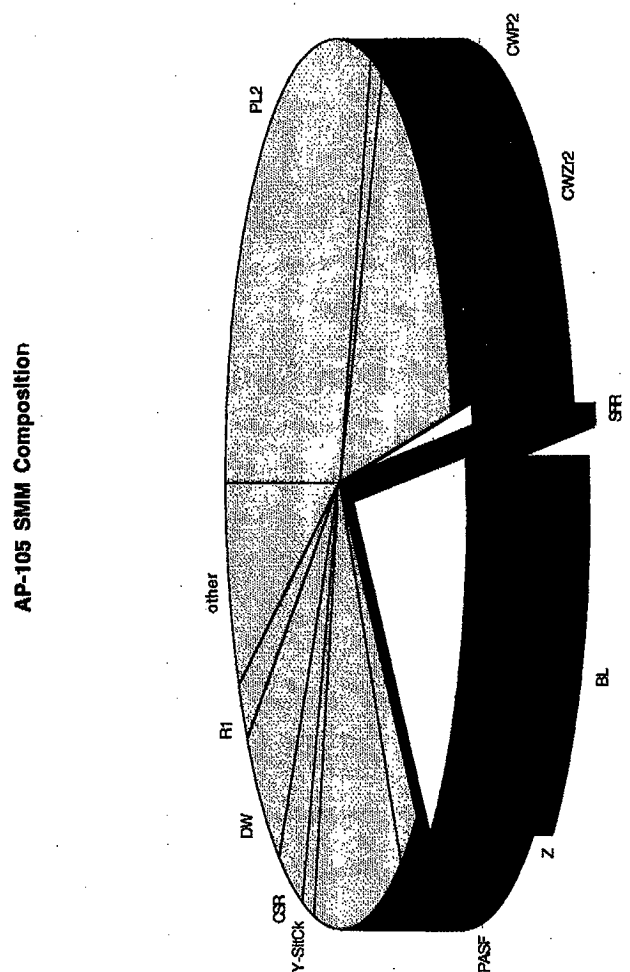
AP-105 SMM Composition
PL2
CWP2
CWZr2
SRR
other
R1
DW
BL
Z
QSR
BY-StlCk
PASF

AN-105 SMM Composition
BY-SltCk
CWF2
DW
N
other
CSR
PL2
R2
CWR1
AR
CWW3
UR/TBP
RSltCk
P1
BL
SRR
T1-SltCk
CWF2
Z
R1

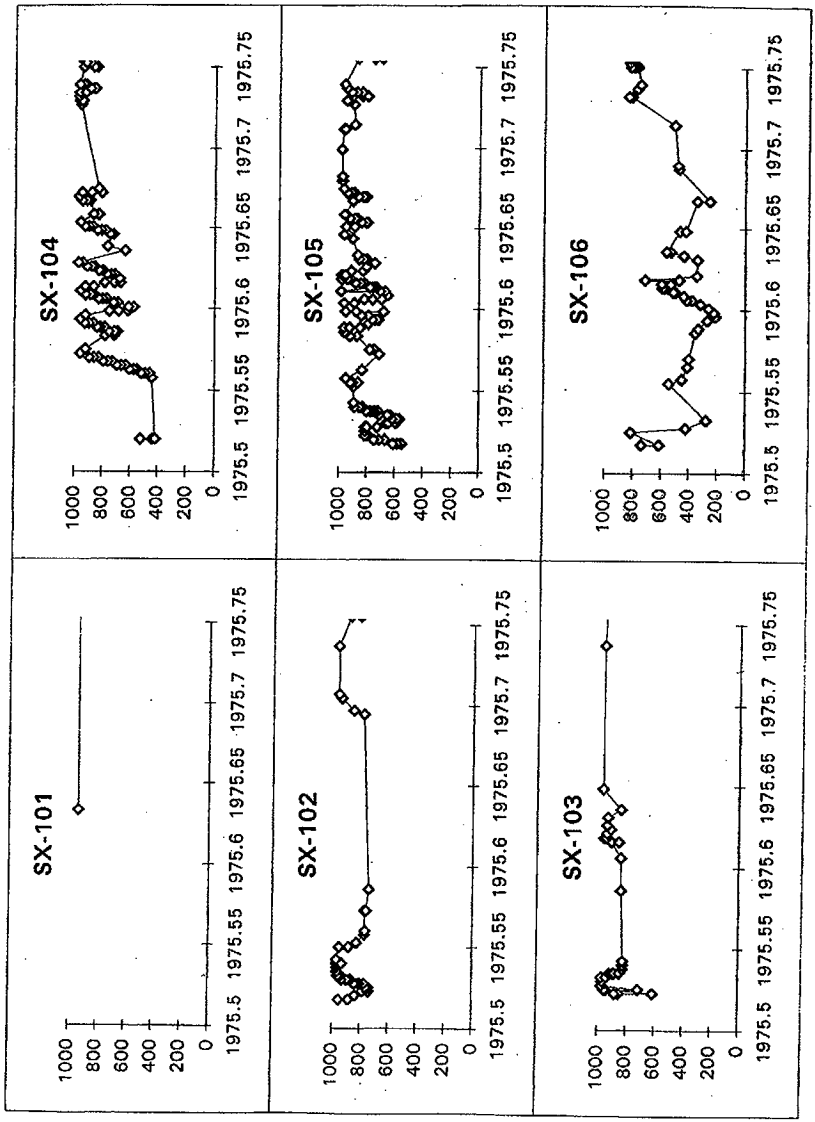
1975 qtr. 3
SX-101
SX-102
SX-103
SX-104
SX-105
SX-106
1000
800
600
400
200
0
1975.5
1975.55
1975.6
1975.65
1975.7
1975.75

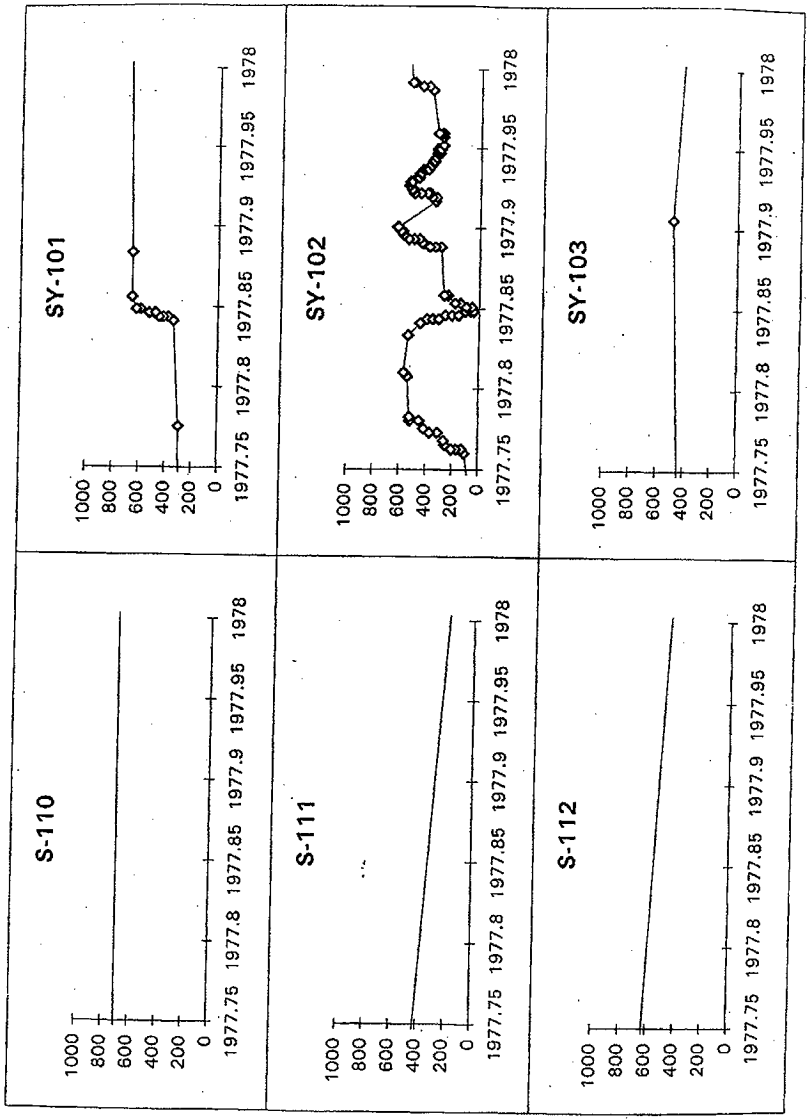
1977 qtr. 4
S-110
S-111
S-112
SY-101
SY-102
SY-103
1000
800
600
400
200
0
1977.75
1977.8
1977.85
1977.9
1977.95
1978

Organic Carbon Oxidation and Gas Formation

Leon M. Stock
February 9, 1998

Aging by Organic Carbon Oxidation

Direct Lines of Evidence

Tank Waste Analysis

- Original organic constituents are oxidized
- Chelator remnants, oxalate, formate
- Gases produced

Targeted Laboratory Experiments

- Verify inferences of tank waste analysis
- Nitrogen gases derived from nitrite ion
- Hydrogen in dihydrogen derived from organic constituents

Consequences

- Reduction in organic fuel content
- Formation of flammable gases

Tank Waste Analysis

Speciation of Organic Compounds in Waste

Composition of SY-103, wt % carbon in organic constituents

Original Anions	Now	Then	New Anion	Now
Citrate	0.16	0.35	IDA	0.22
Glycolate	0.00	0.47	NTA	0.07
HEDTA	0.00	0.67	Formate	0.40
EDTA	0.17	0.36	Oxalate	1.0
			Carbonate	

Comparable observations for approximately 20 other DST and SST

Oxalate ion contents of an additional array of tanks

Original constituents have been significantly oxidized

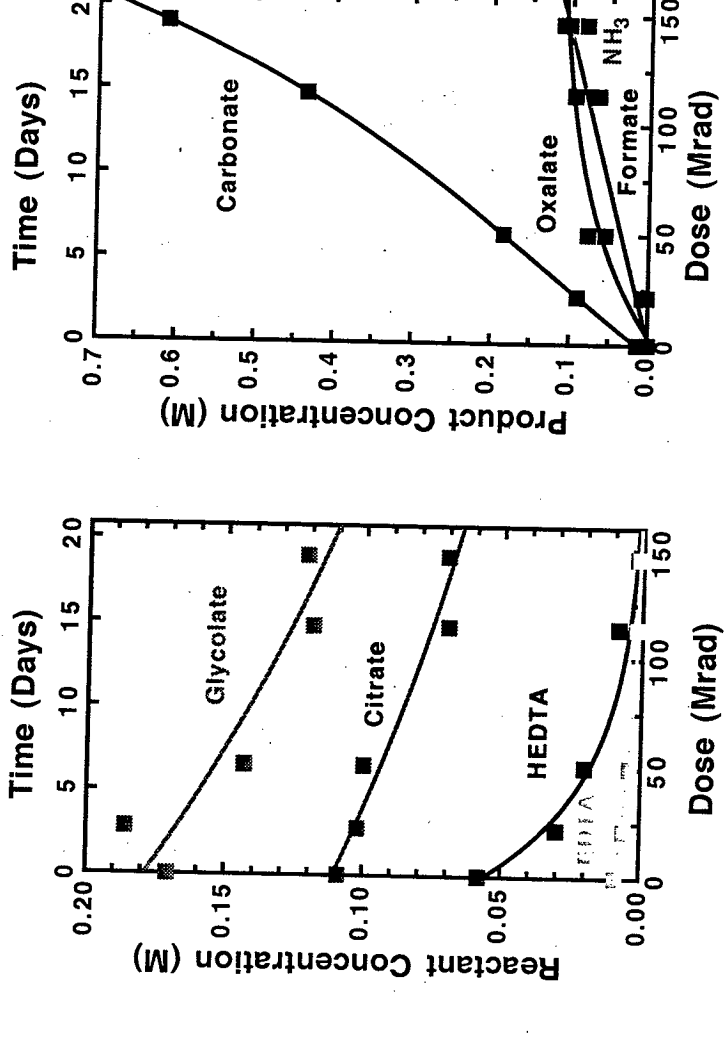
90 °C Radiolytic Aging Results
Time (Days)
Reactant Concentration (M)
Glycolate
Citrate
HEDTA
Dose (Mrad)
Time (Days)
Product Concentration (M)
Carbonate
Oxalate
Formate
NH_3
Dose (Mrad)

Oxidation Reduces the Fuel Content

Combustion of acetate yields about 4 fold more heat than combustion of oxalate ion

The Enthalpy of Mixtures of Sodium Acetate and Sodium Oxalate

Total Organic Carbon Wt %	Carbon As Oxalate Ion, %	Energy J/ g
3.0	0.0	1044
4.0	13.4	1044
5.0	34.0	1044
6.0	48.0	1044
7.0	59.0	1044

TOC is not an adequate measurement of the energy content

The Dynamic Organic Oxidation Cascade

Radiolysis of water (H, OH, electrons)
Radiolysis of nitrate and nitrite ions (NO_3 dianion, NO and NO_2)

Hydrogen Atom Abstraction and Radical Recombination

$$R_2NCH_2CO_2^- + \text{Radical} \longrightarrow R_2NCHCO_2^- + \text{RadicalH}$$

$$R_2NCHCO_2^- + OH \longrightarrow \underset{\text{Unstable}}{R_2NCH(OH)CO_2^-}$$

Electron Abstraction and Decarboxylation

$$R_2NCH_2CO_2^- + \text{Radical} \longrightarrow R_2N^+CH_2CO_2^- + \text{Radical Anion}$$

$$R_2N^+CH_2CO_2^- \longrightarrow \underset{\text{Unstable}}{R_2N^+{=}CH_2} + CO_2^-$$

Spontaneous transformations follow these initiation reactions

The Dynamic Gas Formation Cascade

Reduction of Nitrogen Constituents Coupled to Organic Oxidation

NO_2 NO_2^- NO $\underline{NO^-}$ N_2O N_2 $\underline{NH_2OH}$ NH_3 H_2

Nitrogen and Nitrous Oxide

From nitrite ion via hydroxylamine

From nitrite ion via nitroxyl anion

Ammonia

From HEDTA and EDTA via oxidation and hydrolysis

From nitrite ion via hydroxylamine

From nitrite ion via nitriles and cyanates

The Dynamic Hydrogen Rich Gas Cascade

Originate from Reactive Intermediate Oxidation Products

Tightly Coupled with Organic Carbon Oxidation

Hydrogen

Hydrogen atom abstraction

From formaldehyde and other aldehydes

Methane, Ethane, Propane

From acetate ion

From NPH

From TBP and butanol

Principal Factors Governing Oxidative Aging and Gas Formation

Radical Processes

- Radiolytic Dose
  - Nitrite and Nitrate Ion Concentration
- Thermal
  - Temperature
  - Nitrite Ion

Ionic Processes

- Temperature
- Reagent Concentration
  - Hydroxide Ion
  - Nitrite Ion
  - Aluminate Ion

Temperature independent radiolytic processes predominate

Gas Formation and Organic Content

Hydrogen: G values in molecules per 100 ev

Reaction System	G
Water at pH 13	0.4
with $NaNO_2$ and $NaNO_3$	0.03
with organic compounds	0.03 + 0.013[CH]

Deviations from linear relationship arise because C-H bond reactivity depends on structure.

Nitrous Oxide	G
with citrate	0.05
with IDA	0.7

Hydrogen Generation Rate

Principal Factors

- Radiation Dose
- Temperature
- Hydroxide, aluminate , and nitrite ion concentrations

Initial Approach of PNNL Team

- Measure hydrogen generation rate for reference tank
  - Measure temperature dependence for this tank
  - Establish Arrhenius rate law for this tank
- Use rate law for reference tank to calculate rates for others

  Rate(Tank A) = Rate(Reference) x Factor Ratios

Ongoing Approach

- Measure gas generation rates for different tanks with different compositional features to evaluate factors governing gas generation more broadly

The Influence of Oxygen

Thermal and Radiolytic Reactions

- Results from several investigators
- Rate of hydrogen formation increases
- Rate of nitrogen and nitrous oxide formation decreases
- Reaction products are more oxidized, oxalate rather than formate
- Rate of disappearance of organic compound may decrease

Explanation

- Interception of intermediates: O_2 oxidizes NO^- to NO_3^-
- O_2 promotes hydrogen formation from aldehydes

Assessments of Aging Rate

Empirical observations revealed that the cyanide tank problem was not converted into a formate (organic) tank problem

Experimental work showed that formate ion decomposed to carbonate under storage conditions

Formate is formed and decomposed during work with simulants

Formate reacts with nitrogen dioxide with a second order rate constant of approximately 3 liters per mole per second

Formate ion would decompose at perceptible rate in waste even at very low steady state concentrations of NO_2

G for NO_2 formation in solutions of sodium nitrite is about 6

Targeted work confirms formate ion decomposes in waste environment

Assessment of Aging Rate

Relative Rates of Consumption of Waste Constituents

Constituent	Camaioni Observations
HEDTA	(9)
EDTA	5
Formate	1
Glycolate	6
Acetate	0.7
Citrate	0.6

Modest differences between the organic constituents

Equivalence Between Gas Formation and Carbon Oxidation

Jim Person has measured gas formation rates and used chemical equivalency to determine the number of electrons transferred per unit time. Knowledge of the present composition of the waste, the required number of chemical equivalents to achieve a particular end state, for example oxalate or carbonate, and the number of electrons that need to be transferred to reach the oxidation end state enable estimates of the persistence of organic carbon and gas formation.

Some Considerations

$(N_2 + N_2O + NH_3) / H_2$ is greater than 1

Electron consumption for NH_3 N_2 N_2O H_2

Selection of family of oxidants, OH and NO_2 etc.

Projection

Application of the analysis to waste with 5 % TOC in the form of glycolate ion in a million gallon DST that is now producing 300 moles/day of gas indicates that decades would be required to convert the organic carbon into oxalate ion.

Summary

Observational Elements

Analysis of waste
Speciation of waste
Radiolysis of simulants and wastes
Measurements of gas formation rates
Interpretative chemical models

Conclusions

Tank wastes are dynamic chemical reaction systems that convert the organic components into more oxidized substances and produce gaseous reduction products in closely coupled processes

Although the organic fuel value has already decreased significantly and will continue to decrease, the remaining organic remnants will continue to produce gas for many years

Safety Analysis Approach and Results

(SST Flammable Gas Accident Authorization Basis Amendment)

February 9, 1998

Presented by: Jon Young

The Safety Analysis for Flammable Gas Accidents Uses Analysis Tool (AT)

- Produce AB Amendment for SSTs
  - Identify risk management strategy (e.g. controls)
  - Close the flammable gas USQ for SSTs
- Analyze three areas:
  - GRE risk
  - Steady state risk
  - Ex-tank region risk

The Safety Analysis for Flammable Gas Accidents Uses Analysis Tool (AT)

- Analysis approach:
  - Select representative tanks for detailed analysis
  - Use AT to support safety analysis in three areas
  - Assess impact of control strategies on risk
  - Compare results to risk evaluation guidelines
  - Use TWRS AB control selection process

AT used to Address Various Flammable Gas Accident Analysis

- GRE safety analysis uses AT results to assess risk
  - No controls case
  - Potential control strategies
- Steady state gas release case uses AT distribution for analysis
  - Plume behavior based on well mixed case
  - AT distributions used in simulation
    - ignition frequency
    - material suspended/released
    - tank failure pressures

AT used to Address Various Flammable Gas Accident Analysis

- Ex-tank analysis uses intermediate AT results for in-tank conditions
  - Headspace conditions
    - Gas volumes
    - Gas compositions
    - Time at risk
    - Distributions used in simulation

Three Tanks are Selected for GRE Control Analysis

- Tanks selected based on analysis (no-control case)
- Selection examined a number of potentially risk significant factors
  - Facility group
  - Pumping status
  - Source term
  - Fill factor (total tank volume/waste volume)
  - Dose consequences
  - Frequency
  - Fraction of deflagrations (hit density)

Three Tanks are Selected for GRE Control Analysis

- Fill factor is the most dominant factor
- Three tanks selected are:
  - TX-112 high fill factor (>0.5)
  - SX-103 medium fill factor (0.3 - 0.5)
  - TX-102 low fill factor (<0.3)

Control Selection Process

- Analysis of various control strategies under way:
  - No controls
  - Current controls
  - Perfect ignition controls
  - Robust HEPA filters
  - Active ventilation
  - Inerting
  - Ignition control set changes
  - Lightning controls

Control Selection Process

- Studies of specific tanks planned (e.g. A-101, C-106)
- Sensitivity studies planned to support control selection rationale and understanding of AT results
  - Parameters with most significant risk impact
  - Alternative tank groupings
  - Different perspectives on flammable gas accident phenomena

Results

- Scatter plots
  - All sizes, all TDS, all sources
  - Decompositions
- Cross hairs
  - TDS
  - GRE size

Refined Safety Analysis Methodology for
Flammable Gas Risk Assessment in Hanford Site Tanks

Combustion Related Phenomena: Impact on the Analysis Framework

February 11, 1998

Scott E. Slezak

Topics

- Flame propagation through small openings.
- Detonation behavior--cell size correlations to deflagration-to-detonation transitions and detonation propagation.
- Impact of limited data on AF modeling of potential for detonations--a bounding solution.
- Impact of burn and detonation behavior on potential for burns or detonations in waste.

Flame Propagation in Porous Media

- Maximum (or Minimum) Experimental Safe Gap (MESG) is largest opening through which a flame cannot propagate; typically ideal mixtures.
- Minimum gap for propagation increases as mixture becomes richer or leaner.
- MESG for most hydrocarbons ~0.75 mm (0.030"); MESG for H_2 = 0.076 mm (0.003)
- Presence of N_2O could reduce MESG slightly.
- Flame propagation in fine-pore media requires continuous pores with mean diameter > MESG.

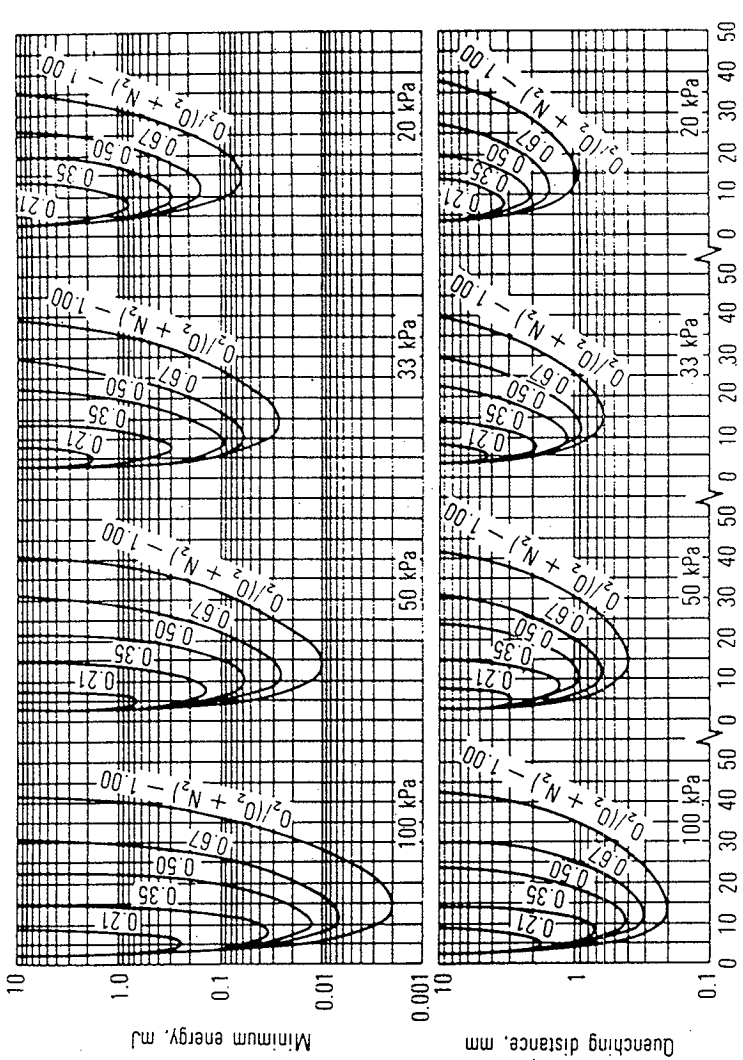

Figure 12-11 Effect of pressure, nitrogen dilution, and equivalence ratio on propane-oxygen flat-plate quenching distances and spark minimum-ignition energies. *(With permission from B. Lewis and G. von Elbe, Combustion Flames and Explosions of Gases, 2d ed., Academic, New York, 1961.)*

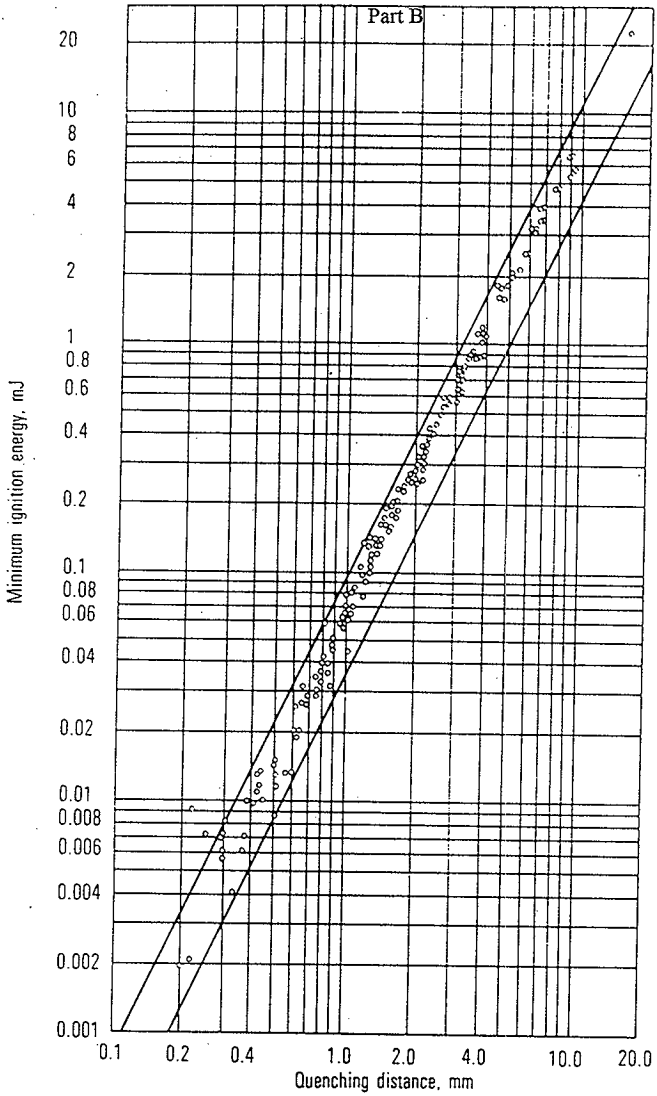

Figure 12-12 The relation between flat-plate quenching and spark minimum-ignition energies for a number of hydrocarbon–air mixtures. *(With permission from B. Lewis and G. von Elbe, Combustion Flames and Explosions of Gases, 1st ed., Academic, New York, 1951.)*

Detonation Cell Size (λ) Correlations

- Detonation cell sizes vary with fuel/oxidizer ratio like do minimum ignition energy and quench gap.
- Detonation propagation and burn to detonation transitions are precluded in pipes and porous media if $\lambda >$ ~ 1/3 to 3 times diameter (uncertainty due to inexactness of λ measurements).
- Detonation propagation from pipe into larger region precluded if pipe diameter < ~10 λ.
- Minimum λ for H_2-Air ~ 14 mm. Minimum λ for H_2-N_2O with no diluent ~ 2 mm.

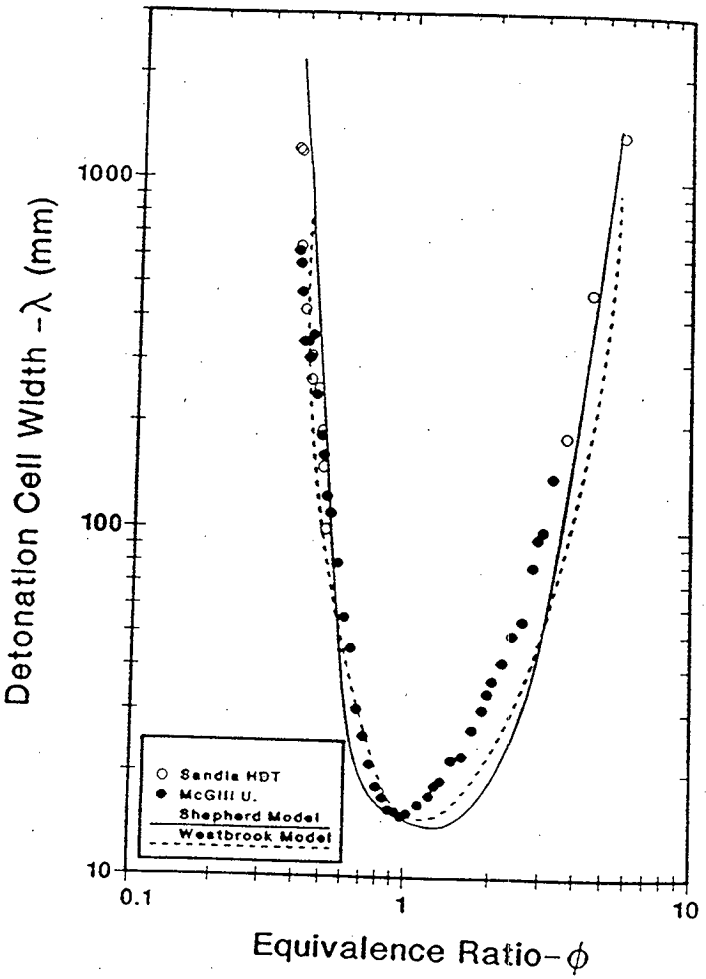

Figure 4-2. Detonation Cell Width vs. Equivalence Ratio for Test Series #1. (H_2-Air at P=1 atm, T=20°C)

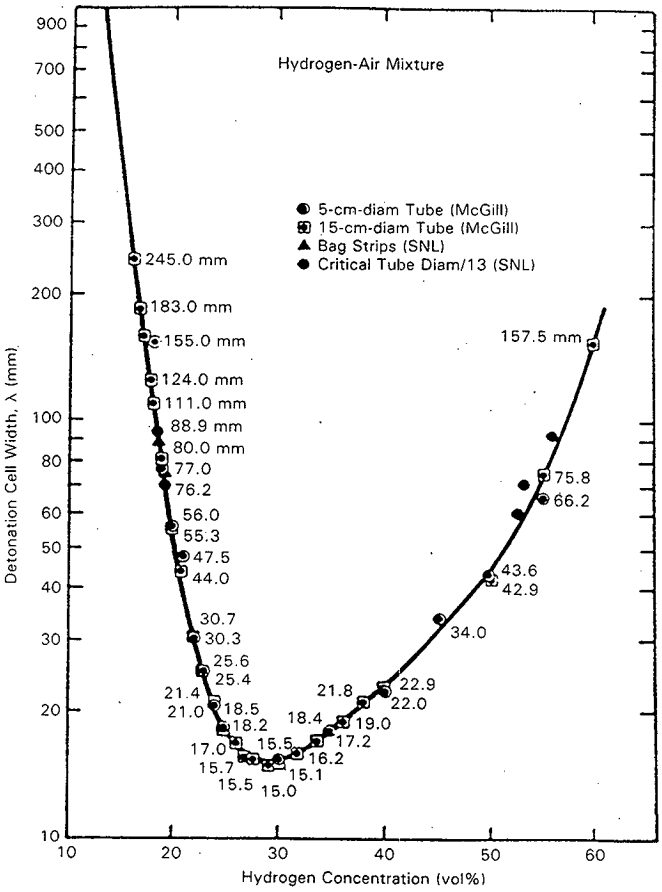

Fig. 3. Measured values (McGill University and SNL) of the detonation cell width λ as a function of hydrogen concentration.

II.C. Influence of Diluents and Thermodynamic Variables on the Propagation of Detonations

Until a few years ago, most experiments on detonations were conducted in small tubes a few centimetres in diameter. To determine the effects of initial temperature, pressure, and the presence of inert diluents on the sensitivity of fuel-air mixtures, a large heated tube must be used. Figure 6 shows a schematic of the HDT facility, which was recently constructed at Sandia National Laboratories (SNL). Its 43-cm i.d. and capability of operating at temperatures above 100°C make it a unique facility. In addition to measuring detonation speeds by means of pressure transducers that record times of arrival of the detonation wave, large smoked foils (3.7 m long × 1.2 m wide) are

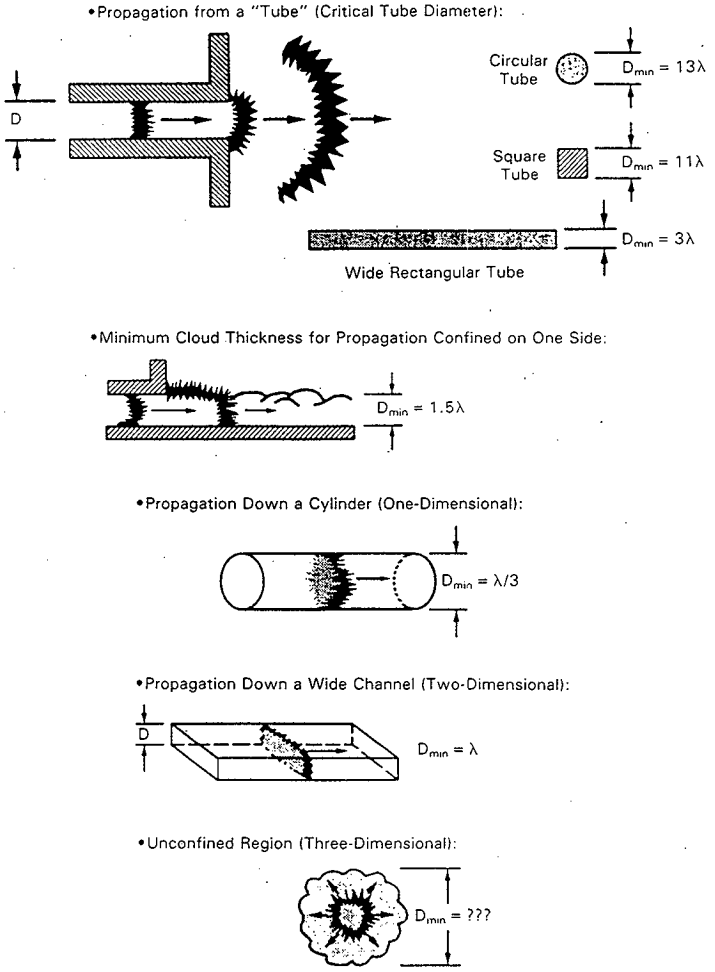

Fig. 4. Schematic illustration of the developing empirical understanding of the effects of geometry and scale on detonation propagation.

employed for directly recording the detonation cell structure, from which λ can be measured, as seen in Fig. 7.

Experimental conditions are selected to simulate possible nuclear reactor accidents; i.e., a test begins with 1 atm of air to which hydrogen and steam are added, with the concomitant increase in temperature and pressure before ignition. In these experiments, we

CalTech Detonation Cell Size Findings

- Prof. Joe Shepherd & students measured λ for H_2-N_2O-NH_3-CH_4-O_2-N_2 mixtures.
- Insufficient data for accurately predicting cell sizes for large number of possible AT mixtures.
- ZND code to predict λ is not suitably calibrated or practical in Monte Carlo-type application.
- Solution: apply λ vs. equiv. ratio curve fit to H_2-Air data to H_2-[Air+N_2O]; shift curve $\downarrow$ to λ_{min}= 2 mm @ 0% added N_2, shift min $\uparrow$ to fit diluent data.
- Adjusted curve conservative with $\lambda_{curve\ fit} \leq \lambda_{data}$.

Detonations in Headspace

- Sherman & Berman classification based on gas mixture sensitivity and geometric configuration ranks potential for DDT in headspace unlikely to highly unlikely or impossible.
- Most credible scenario: DDT in gases flowing out ventilation duct propagates back to headspace.
- Propagation from duct into headspace requires $\lambda \leq$ (duct diameter)/10.
- Will assume DDT if ventilation duct diameter is greater than $10\lambda_{\text{curve fit}}$.

Detonations in Equipment

- Large length to inside diameter ratios + sealed end(s) + interior obstacles in some equipment makes geometry highly favorable to DDT inside MITs, LOWs, TC trees, etc.
- Will assume DDT if equipment diameter is greater than $\lambda_{curve\ fit}$.

Burns or Detonations in Waste

- Minimum connected pore diameter > ~ 1 mm required for propagating detonations in waste.
- Minimum connected pore diameter > ~ 0.01 mm required for propagating burns in waste.
- Diffusion out of connected pores so fast relative to gas generation rate that highly unlikely to ever even reach LFL.
- Unconnected bubbles may exceed LFL, but unfavorable to propagating burn in waste.
- Ignition source for waste burns unlikely.

Conclusions

- Deflagrations and detonations within porous waste are highly unlikely and not significant risk.
- Potential for deflagration to detonation transition behavior in equipment or headspace can be conservatively approximated with modified fit of experimental data.

References

Roger Strehlow, "Combustion Fundamentals", McGraw-Hill, 1984

Marshall Berman, "A Critical Review of Recent Large-Scale Experiments on H_2-Air Detonations", *Nuclear Science and Engineering*, Vol. 93, pp. 321-347, 1986.

Sheldon Tieszen, Martin Sherman, William Benedick and Marshall Berman, "Detonability of H_2-Air-Diluent Mixtures", NUREG/CR-4905 (SAND85-1263), June 1987, Sandia National Laboratories, Albuquerque, NM.

Raza Akbar, Michael Kaneshige, Eric Schultz and Joseph Shepherd, "Detonations in H_2-N_2O-CH_4-NH_3-O_2-N_2 Mixtures", Explosion Dynamics Laboratory Report FM97-3, July 24, 1997, California Institute of Technology, Pasadena, CA.

Ulrich Pfahl and Joseph Shepherd, "Flammability, Ignition Energy and Flame Speeds in NH_3-H_2-CH_4-N_2O-O_2-N_2 Mixtures", Explosion Dynamics Laboratory Report FM97-4R1, July 15, 1997, California Institute of Technology, Pasadena, CA

Aristidis Makris, "The Propagation of Gaseous Detonations in Porous Media, Ph.D. Thesis, September, 1993, McGill University, Toronto, Canada

A. V. Pinaev and G. A. Lyamin, "Fundamental Laws Governing Subsonic and Detonating Gas Combustion in Inert Porous Media", translated from *Fizika Goreniya I Vzryva*, Vol. 25, No. 4, pp. 75-85, July-August, 1989 (reprinted in English as *Combustion, Explosion and Shock Wave*)

G. A. Lyamin and A. V. Pinaev, "Combustion Regimes for Gases in an Inert Porous Media", translated from *Fizika Goreniya I Vzryva*, Vol. 22, No. 5, pp. 64-70, September-October, 1986 (reprinted in English as *Combustion, Explosion and Shock Wave*)

Martin P. Sherman and Marshall Berman, "The Possibility of Local Detonations During Degraded-Core Accidents in the Bellefonte Nuclear Power Plant, *Nuclear Technology*, Vol. 81, pg. 63, 1988

Martin P. Sherman, Sheldon R. Tieszen and William B. Benedick, "The Effect of Obstacles and Transverse Venting on Flame Acceleration and Transition to Detonation for Hydrogen-Air Mixtures at Large Scale, NUREG/CR-5275, April 1989, Sandia National Laboratories, Albuquerque, NM.

F. E. Scott, R. W. Van Dolah and M. G. Zabetakis, "The Flammability Characteristics of the System H_2-NO-N_2O-Air",

wrkshp2–SS–2/11/98

slide 14

COMBUSTION FUNDAMENTALS

Roger A. Strehlow

Professor of Aeronautical and Astronautical Engineering
University of Illinois at Urbana-Champaign

McGraw-Hill Book Company

New York St. Louis San Francisco Auckland Bogotá Hamburg
Johannesburg London Madrid Mexico Montreal New Delhi
Panama Paris São Paulo Singapore Sydney Tokyo Toronto

based on the flow velocity and kinetic rate at the hottest point in the flame. They found that a plot of T vs. Da_I had the same general shape as the curve that we derived earlier for η vs. Da_I for the well-stirred reactor (Fig. 6-12*b*). They also found that Da_I could not be determined a priori. Over a large range of Da_I, three temperatures were predicted for the same value of Da_I and the uppermost of these corresponded to the diffusion flame solution. Referring to Fig. 6-12*b* they also observed a broad minimum in Da_I at relatively high temperature, which corresponded to extinction of the diffusion flame, and a sharp maximum at very low temperature. As was stated in Chap. 6, this lower branch is not physically real because the Arrhenius-rate expression is incorrect at these low temperatures. More recently Linan[3] has completed a comprehensive analysis of diffusion flame extinction.

The striking similarity of the behavior of the Damköhler number and the similar way that extinction is predicted for two markedly different exothermic flows leads us to a rather general conclusion. Namely, whenever a flow time can be adjusted independently of the chemical reaction rate in a highly exothermic, highly temperature-dependent reactive-flow situation, an examination of the behavior of the local Damköhler number should allow the prediction of extinction. We also note that another general conclusion is that even though extinction of inherently hot or high-temperature systems can be predicted using this approach, absolute compositional limits such as those tabulated in Table 12-1 cannot. These instead appear to be related to innate changes in the chemistry of the combustion process, i.e., a shift in the balance between chain-branching and recombination reactions. Finally we note that for flame-sheet theories $Da_I = \infty$ under all circumstances and thus extinction behavior cannot be discussed in the framework of a flame-sheet theory.

12-3 FLAMMABILITY LIMITS AND EXTINCTION IN PREMIXED GASES

Virtually every fuel–oxidizer combination will support premixed flame propagation only when the fuel concentration is within a certain range, bounded by some upper and lower limit concentration. Outside of this range a flame will not propagate a long distance from an ignition source. From a safety standpoint, where the oxidizer is air, the most important of these limits is the lean or lower flammability limit, LFL, or the lean or lower explosion limit, LEL (these terms are used interchangeably). The upper flammability limit, UFL, or upper explosion limit, UEL, can be important under certain circumstances, but they are usually not important from a safety standpoint because dilution with more air can cause a rich nonflammable mixture to become flammable.

The U.S. Bureau of Mines in Pittsburgh, Pennsylvania, has identified one particular technique for determining flammability limits as being their

3. A. Linan, *Acta Astronautica*, 1:1007–1039 (1974).

"standard" technique.[4] In this technique a 51 mm internal diameter tube 1.5 m long is mounted vertically and closed at the upper end with the bottom end open to the atmosphere. The gaseous mixture to be tested for flammability is placed in the tube and ignited at the lower (open) end. If a flame propagates the entire length of the tube to the upper end, the mixture is said to be flammable. If the flame extinguishes somewhere in the tube during propagation, the mixture is said to be nonflammable. The choice of this technique as a standard is the result of a considerable amount of research. Specifically, it is known that upward propagation in a tube of this type exhibits wider limits of flammability than downward propagation. In fact, if one places a mixture whose composition is between that of the measured upward and downward propagation limits in a large vessel, and ignites it at the center, one finds that the flame propagates to the top of the vessel and burns only a portion of the material in the vessel before extinguishing, leaving a fair portion of the fuel–air mixture unburned. In other research, it has been found that as the tube becomes smaller the combustible range becomes narrower until one reaches the quenching diameter. At that point there is no mixture of that fuel with air which will propagate a flame through the tube. Fifty-one millimeters was chosen as the diameter for the standard tube because this is the diameter at which a further increase in tube diameter causes only a slight change in the limits. Some typical limits are tabulated in Table 12-2.

The initial pressure and temperature of the mixture affects the flammability limits somewhat. Increasing the temperature always widens the limits because it causes the flame temperature to increase. Increasing the pressure has little effect on the lower or lean limit but causes the upper limit to increase.

The addition of inert gases or inhibitors to the mixture causes the limits to narrow and eventually with sufficient added inert all fuel–air mixtures are nonflammable. This is shown for methane and a general higher hydrocarbon (C_nH_{2n+2}; $n > 5$) in Figure 12-4. In general the addition of an inert such as He, N_2, H_2O, or CO_2 to the mixture narrows the limits because such mixtures have a lower flame temperature than the original fuel–air mixture. However inhibitors such as CCl_4 and CH_3Br tend to act as radical scavengers and thus alter the chemistry in the flame. It is interesting to note that methyl bromide can burn in air but it still acts as an inhibitor in rich methane flames. The dashed lines in Figure 12-4*a* represent the flammable range for CH_4–CH_3Br–air mixtures that lie outside the normal lean limit of CH_4–air mixtures. It is also interesting to note that the limit curves for methane–air–inert mixtures peak at approximately the stoichiometric line but gradually shift toward the carbon monoxide–hydrogen stoichiometric line as the number of carbons in the aliphatic chain increases. At C_5 and above the shift is essentially complete and the

4. H. F. Coward and G. W. Jones, *Limits of Flammability of Gases and Vapors*, Bureau of Mines Bulletin 503, 155 pp. (1952), also M. G. Zabetakis, *Flammability Characteristics of Combustible Gases and Vapors*, Bureau of Mines Bulletin 627, 121 pp. (1965).

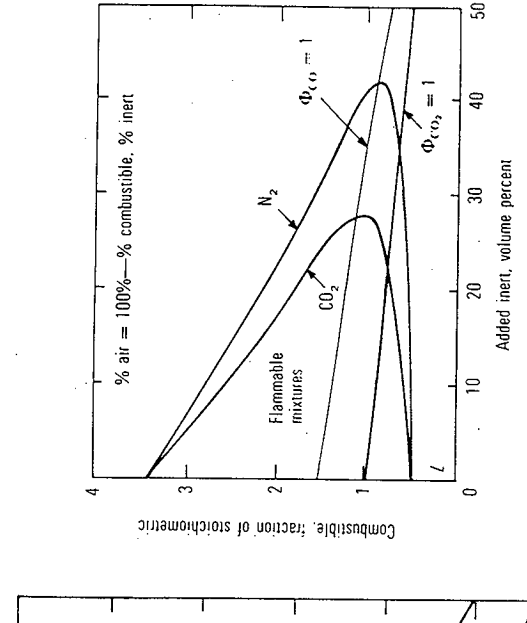

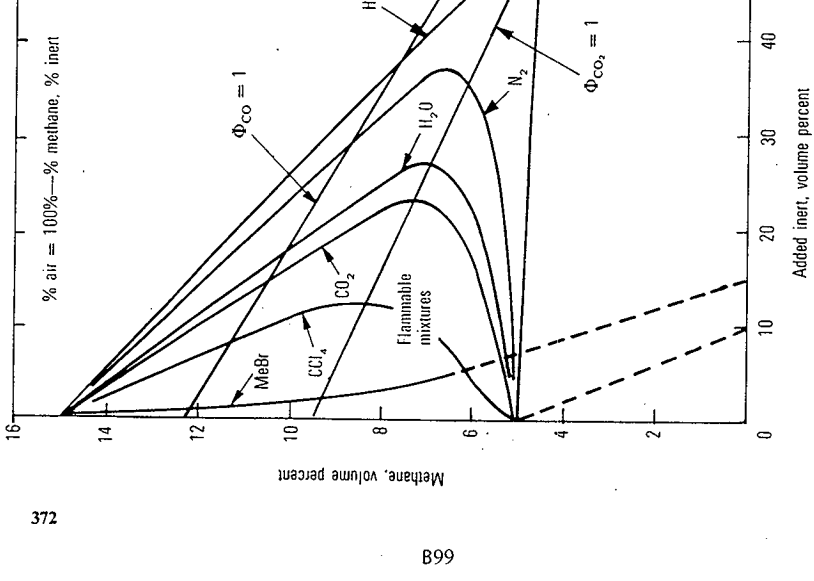

Figure 12-4 The effect of inerts and inhibitors on the flammability limits of methane and alkanes. *(Adapted, with permission, from M. G. Zabetakis, Flammability Characteristics of Combustible Gases and Vapors, U.S. Bureau of Mines Bulletin 627 (1965).)*

Table 12-2 Flammability limits of some common fuel–oxidizer mixtures (in mole %)‡

Fuel	Oxidizer	Lean limit	Rich limit
Hydrogen	Air	4.0	75.0
Carbon monoxide (moist at 18°C)	Air	12.5	74.0
Ammonia	Air	15.0	28.0
Cyanogen	Air	6.6	—
Methane	Air	5.0	15.0
Ethane	Air	3.0	12.4
Propane	Air	2.1	9.5
Butane	Air	1.8	8.4
Ethylene	Air	2.7	36.0
Acetylene	Air	2.5	100.0
Benzene	Air	1.3	7.9
Methyl alcohol	Air	6.7	36.0
Ethyl alcohol	Air	3.2	19.0
Diethyl ether	Air	1.9	36.0
Carbon disulphide	Air	1.3	50.0
Hydrogen	Oxygen	4.0	95.0

‡ Data taken from M. G. Zabetakis, *Flammability Characteristics of Combustible Gases and Vapors*, U.S. Department of Mines Bulletin 627 (1965) with permission.

limit behaviors for all higher hydrocarbons are similar enough to be plotted on one graph, Fig. 12-4*b*.

The excess enthalpy burner discussed theoretically in Sec. 8-4 allows one to stabilize a flame in ultralean mixtures which would ordinarily not support a propagating flame. Recently Kotani and Takeno[5] have stabilized such flames in a 50 mm circular burner that contained a close packed bundle of 1 mm o.d., 0.6 mm i.d., 30 mm long ceramic tubes. This burner block was well shielded from losses to make it as "adiabatic" as possible. The resulting stability diagram is shown in Fig. 12-5. Note that all types of burner behavior predicted by the theory were observed and that the lean limit was reduced to an equivalence ratio of 0.3 from its usual value of about 0.5.

In 1898 Le Châtelier and Boudouard[6] proposed a rule for determining the lean limit of a mixture of two combustible gases, from the known lean limits of the constituent species in the mixture. If we call LFL_m the volume percent of the fuel mixture at the lean limit and $LFL_1, LFL_2, \ldots, LFL_n$ the volume percent lean flammability limits of the n constituent fuels and $x_1, x_2, \ldots, x_n$ the

5. Y. Kotani and T. Takeno, An Experimental Study on Stability and Combustion Characteristics of an Excess Enthalpy Flame, *Nineteenth Symposium (International) on Combustion*, The Combustion Institute, Pittsburgh, Pa., p. 1503, (1983).

6. H. Le Châtelier and O. Boudouard, *Compt Rend.* 126: 1344–1347, 1898.

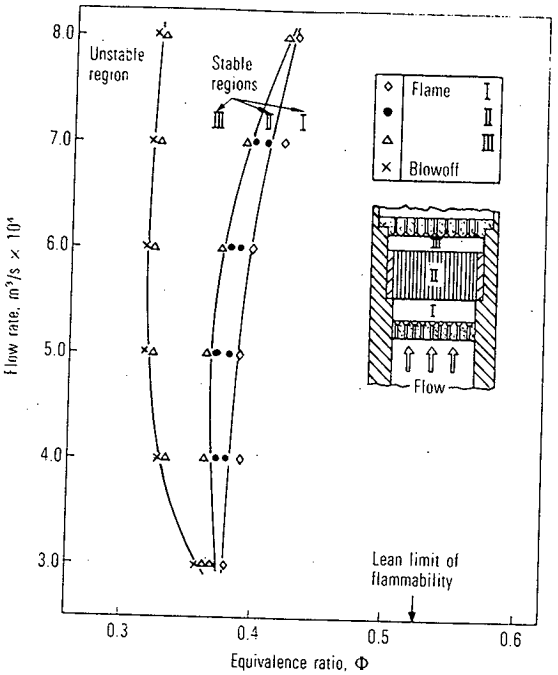

Figure 12-5 Stability diagram for an excess enthalpy flame holder. Fuel is methane. *(Adapted from Ref. 5, with permission.)*

mole fractions of each constituent fuel in the fuel mixture, a generalized form of Le Châtelier's rule is given by the formula

$$\mathrm{LFL}_m = \frac{1}{x_1/\mathrm{LFL}_1 + x_2/\mathrm{LFL}_2 + \cdots + x_n/\mathrm{LFL}_n} \tag{12-1}$$

If the fuel contains an inert diluent such as nitrogen or carbon dioxide the lean limit can still be calculated by not including the inert in Eq. (12-1). For example the lean limit for methane in air is 5 percent. If methane is diluted with an inert and this mixture is used as a fuel the lean limit for this mixture would be

$$\mathrm{LFL}_m = \frac{1.0}{x_1/5 + 0} = \frac{5}{x_1}$$

where x_1 is the mole fraction of CH_4 in the fuel mixture. The Le Châtelier formula works quite well if the fuel mixture contains hydrogen, carbon monoxide, or ordinary hydrocarbons. It does not work well for unusual compounds such as carbon disulfide, or when inhibiters are present.

One empirical observation[7] is that for many hydrocarbon–air mixtures, the lean limit volume percent of fuel multiplied by its heating value in kilojoules per mole is approximately 4.34×10^3. This means, of course, that the flame temperature has approximately the same value at extinction for all hydrocarbon fuels. This result is similar to that obtained for diffusion flames (see Table 12-1).

The flammability limit is thought to be caused by flame extinction due to a combination of heat loss from the flame, flame stretch, and/or spontaneous flame instabilities. Furthermore, all of these effects are complicated by the fact that the flame temperature of limit flames is so low that the competition between the hydrogen atom chain-branching and chain-breaking reactions mentioned in Secs. 6-10 and 8-5 occurs at a location very close to the hot reaction zone.

Unfortunately, there is no adequate theory for flammability limits. In essence, all the extant theories have so simplified the problem that the actual physical processes that occur at extinction are no longer modeled properly. As an example, take the heat-loss theory of Spalding.[8] He modeled the flame as a one-dimensional flame and removed heat from the hot gases while retaining the one-dimensionality of the flame. He removed heat at a fixed rate per unit length of gas column downstream of the flame front and found that there is a maximum value for this quantity above which one can no longer find a solution to the equations that were formulated. This critical maximum quantity of heat removal per unit length was then considered to be the condition for flame extinction. However, when large amounts of heat are removed from this flame the burning velocity drops and the flame thickness increases markedly. Under these conditions, even though the heat abstracted per unit length along the flame goes through a maximum, the total heat that is abstracted from the flame increases monotonically. Furthermore, since one can calculate the structure of a flame using nonsteady one-dimensional flame equations and full kinetics for compositions considerably leaner than the observed lean limit composition, it appears that one-dimensional theories for flame extinction, even with heat loss, are not adequate.

Experimentally it is found that different mechanisms of extinction are operative in different geometries. Tsuji and Yamaoka,[9] have recently studied the extinction of two opposed premixed flames using the type IV burner of Fig. 7-6. In this experiment they pass the same fuel–air mixture through the porous cylindrical holder and up the duct. When ignition is effected two opposed premixed flames appear as shown in Fig. 12-6. These have the property that they are separated by a stagnation-point region which is exactly adiabatic. As the compositions of the two mixtures approach either the lean- or the rich-limit

7. F. T. Bodurtha, *Industrial Explosion Prevention and Protection*, McGraw-Hill (1980).
8. D. B. Spalding, *Proc. R. Soc. London*, A240:83 (1957).
9. H. Tsuji and I. Yamaoka, "Structure and Extinction of Near Limit Flames in a Stagnation Flow," *Nineteenth Symposium (International) on Combustion*, The Combustion Institute, Pittsburgh, Pa., p. 1533, (1983).

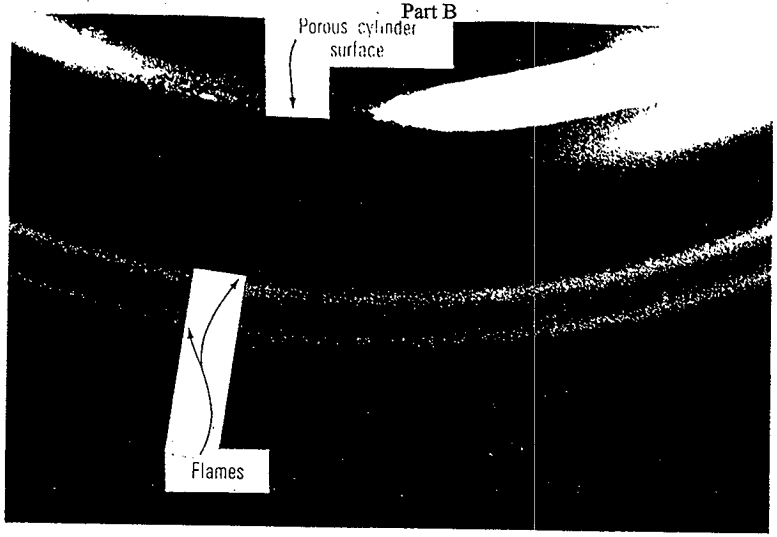

(*a*)

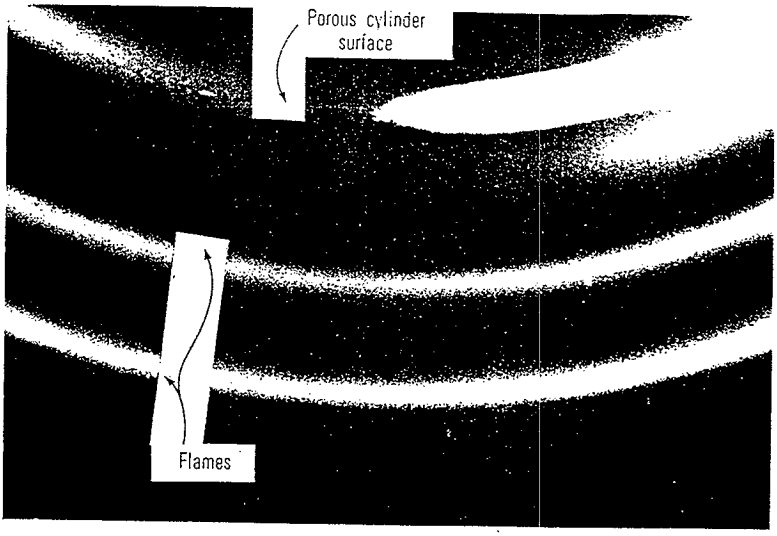

(*b*)

Figure 12-6 Visible light photograph of counterflow, premixed, twin flames established in the forward stagnation region of a porous cylinder. (*a*) Lean methane-air flames near the limit $\Phi = 0.53$. (*b*) Rich methane-air flames near the limit $\Phi = 1.58$. Notice how close the lean flames approach each other when compared to the rich flames. *(Courtesy Prof. H. Tsuji, University of Tokyo, from Ref. 8, with permission.)*

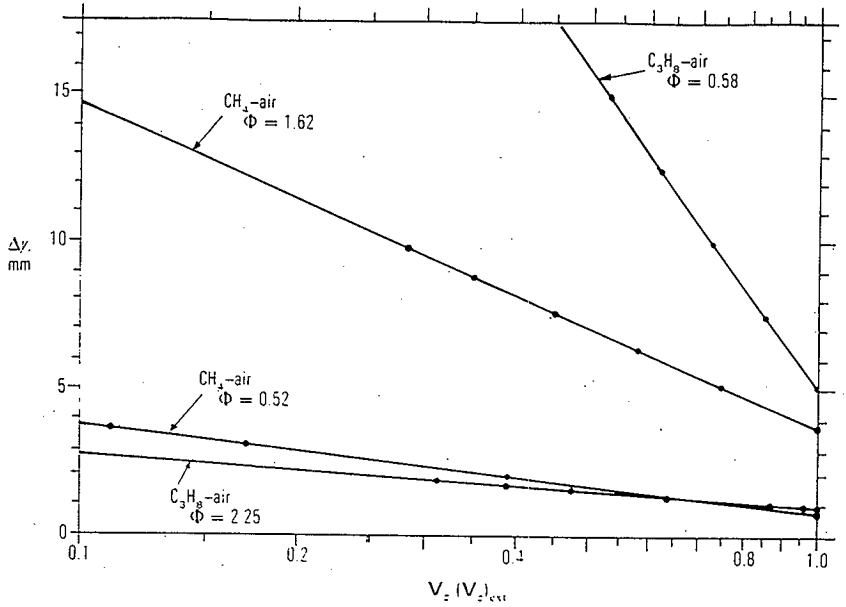

Figure 12-7 The separation distance between the two luminous zones of opposed premixed flames. *(Adapted from Ref. 8, with permission.)*

composition the flames approach each other. Both of the flames are stretched because of the nature of stagnation-point flow and eventually at some critical lean or rich composition the flames blow out. Experimentally it is observed that near the limit rich methane or lean propane flames stand quite some distance apart while lean methane or rich propane flames approach each other very closely. This is shown in Fig. 12-7, which is a plot of the distance between the two luminous zones at the centerline of the flow as a function of the relative blowing rate divided by the blowing rate at extinction.

Their study of the temperature profiles and composition of the gases at the stagnation point for a flame pair that is near extinction shows that the temperature is high and the chemical reactions are going to completion for the rich methane and lean propane flames and that the temperature is low and the chemical reactions are not going to completion for the lean methane and rich propane flames. This is shown in Fig. 12-8. This means that the mechanism of extinction is strongly dependent on the effective Lewis number of the deficient species. If the Lewis number is less than unity, as it is for a lean methane or rich propane flame, the flame extinguishes because the rate of stretch is so large that the chemical reactions cannot go to completion. However if it is greater than unity, as it is in a rich methane or lean propane flame, extinguishment is

not caused by the chemical reactions being incomplete but instead must be caused by a true stretch mechanism. We note that at the extinction limit for a rich methane or lean propane flame, stretch will cause a local reduction of the deficient species, i.e., at the centerline the local propane concentration will drop because of stretch in a propane–air flame and the local oxygen concentration will drop because of stretch in a methane–air flame.

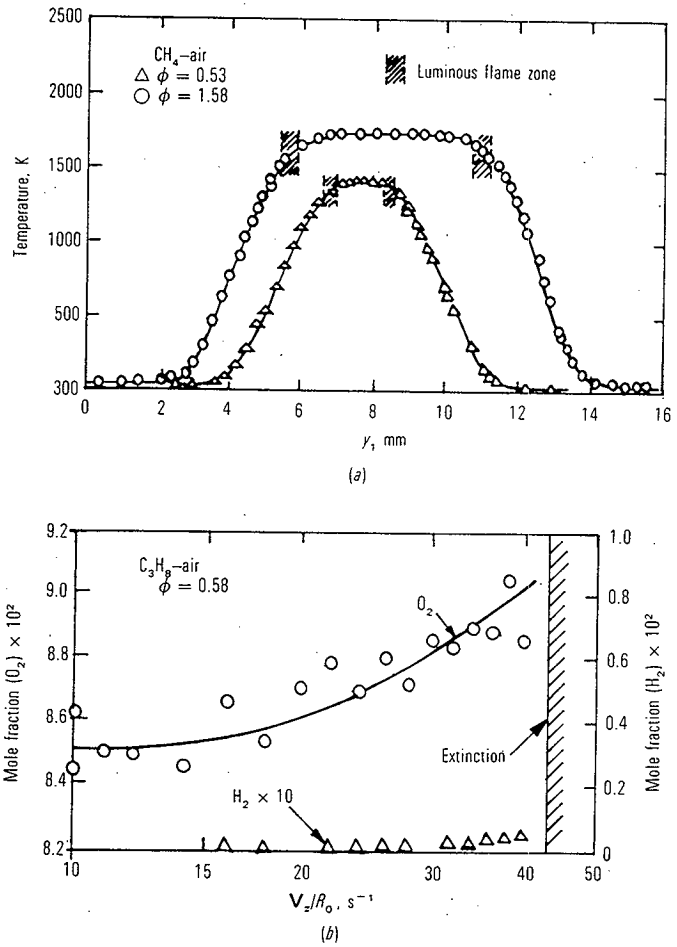

Figure 12-8 Temperature profiles and centerline concentrations for flames near extinction. *(From Ref. 8, with permission.)*

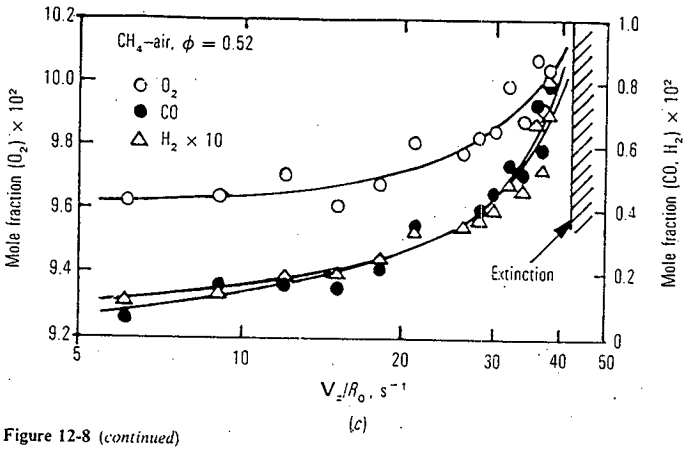

(*c*)

Figure 12-8 (*continued*)

Experiments using a standard flammability tube at one g and zero g have shown that the upward propagating flame and the zero g flames have a flame-cap shape that is controlled primarily by inviscid flow behavior ahead of the flame (see Fig. 10-8) and that the rate of propagation through the tube is determined by bouyancy forces.[10] Thus the length of the flame skirt for an upward propagating flame is related primarily to the speed at which the flame propagates through the tube, because the normal burning velocity is not affected by buoyancy.

In an upward propagating flame extinguishment occurs first at the center of the flame where it is held (see Sec. 10-4) and then propagates over the remainder of the flame.[11] A calculation based on the observed flame shape using potential flow theory indicates that stretch is indeed maximum at the holding point of this flame and therefore that extinguishment should start there.

The downward propagating flame in a standard flammability tube is markedly affected by gravity. Photographs of this flame taken with an image intensifier are shown in Fig. 12-9. The flame is almost flat but has a cellular structure, and it does not propagate uniformly down the tube but sort of oscillates as it propagates. At incipient extinguishment the flame recedes from the walls, and heat loss to the walls cools the gas in the neighborhood of the walls. At this time differential buoyancy of the central hot column and the surrounding cooler

10. R. A. Strehlow and D. Reuss, "Flammability Limits in a Standard Tube," *Combustion Experiments in a Zero Gravity Laboratory*, ed. T. H. Cochran, *Prog. Astronaut. Aeronaut.*, AIAA, 73:61–90 (1981).

11. J. Jarosinski, R. A. Strehlow, and A. Azarbarzin, "The Mechanism of Lean Limit Extinguishment of an Upward and Downward Propagating Flame in a Standard Flammability Tube," *Nineteenth Symposium (International) on Combustion*, The Combustion Institute, Pittsburgh, Pa., p. 1549 (1983).

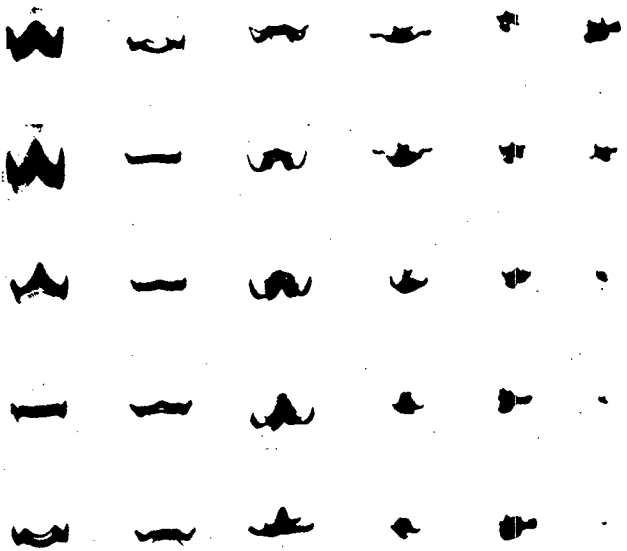

Figure 12-9 Extinction of a downward propagating lean limit methane–air flame in a standard 51 mm flammability tube. Propagation from the top open end toward the bottom closed end. Time increases from top to bottom and then from left to right. Fifty-five frames per second. Except for the last three frames, every third frame is shown. *(Adapted from A. Azarbarzin, A Study of Flame Extinction in a Vertical Flammability Tube. M.S. Thesis, University of Illinois at Urbana-Champaign, 50 pp. (1981).)*

annular space causes the cooler product gases to travel ahead of the flame and the small flame kernel that is left actually rises just prior to complete extinction. Thus extinction of a downward propagating flame is actually caused by a very complex sequence of events.

Chan and T'ien[12] have observed that a wick-held diffusion flame in a large vessel whose oxygen is slowly being depleted eventually takes the shape of a small blue hemispherical cap over the wick. At incipient extinguishment they observed that the flame's edge oscillates in and out symmetrically around the centerline with no apparent motion of the central region. Then, after a few oscillations a final oscillation causes complete extinguishment of the flame.

12. W. Y. Chan and J. S. T'ien, *Combust. Sci. Tech.*, **18**: 139–143 (1978).

12-4 MINIMUM IGNITION ENERGY AND QUENCHING DISTANCE

The minimum ignition energy is the smallest quantity of energy that must be added to a system to start flame propagation. Its value is quite dependent on the local rate and method of heat addition, and on the geometry of the heat source. Quenching distance is defined as the largest channel dimension that will just stop a flame from propagating through the channel if there is no large pressure drop along the channel. Values of the quenching distance are dependent on experimental geometry.

Combustible mixtures may be exploded "homogeneously" in "vessel" experiments like those discussed in Chap. 6, or they may be ignited by rapid heat addition at a localized region in the gas. In the latter case, successful ignition leads to the propagation of either a flame or a detonation. As the total quantity of energy is reduced for any one ignition technique, direct detonation ceases to occur, if it did at all (see the next chapter for a discussion of detonation initiation), and flames are observed to propagate from the source. Further reduction of the total quantity of energy that is added to the fluid continues to produce ordinary flame propagation until the minimum ignition energy for that source configuration is reached. At this point only a small quantity of the combustible gas is converted to products and the energy is dissipated harmlessly by thermal conduction.

A multitude of different energy sources and source configurations have been used to study flame ignition experimentally. However, an ordinary capacitor discharge spark has consistently yielded the lowest ignition energy for any specific combustible mixture. For an experimental determination of an ignition energy, high-performance (usually air-gap) condensers are used so that the majority of the stored energy will appear in the spark gap. The stored energy may be calculated using the equation $E = CV^2/2$, where C is the capacity of the condenser and V the voltage just before the spark is passed through the gas. The spark must always be produced by a spontaneous breakdown of the gap because an electronic firing circuit or a trigger electrode would either obviate the measurement of spark energy or grossly change the geometry of the ignition source. It has been found experimentally that for this type of spontaneous spark up to 95 percent of the stored energy appears in the hot kernel of gas in less than 10^{-5} s. The losses are thought to be due primarily to heat conduction to the electrodes. Since the total stored energy can be varied by changing either the capacity or the voltage, the electrode spacing (which is proportional to the voltage at breakdown) may be varied as an independent parameter. Two problems now arise: If the electrode spacing is too small, the electrodes will interfere with the propagation of the incipient flame and the apparent ignition energy will increase. If, however, the spacing is too large, the source geometry will become essentially cylindrical and the ignition energy will again increase because the area of the incipient flame is greatly increased in this geometry. This condition is shown schematically in Fig. 12-10. The fact that the increase

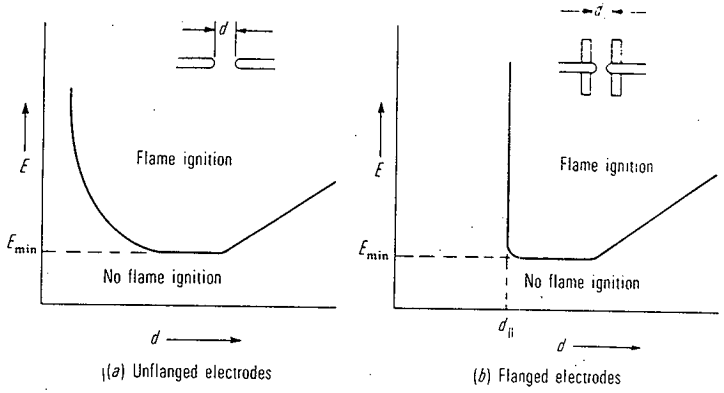

Figure 12-10 Quenching distance and minimum-ignition-energy measurement using a capacitor spark.

in minimum ignition energy is due to quenching at small electrode spacings may be confirmed by using electrodes flanged with electrically insulating material. Figure 12-10 shows the effect of electrode flanging on the ignition energy at small separations. Note that below a certain spacing, as the spacing is reduced the spark energy required to ignite the bulk of the gas sample rises very much more rapidly with flanged tips. This critical flange spacing is defined as the flat-plate quenching distance of the flame. Therefore this simple experiment may be used to determine the flat-plate quenching distance and the minimum ignition energy for spherical geometry, and may also be used to evaluate whether the ignition source is essentially spherical or cylindrical. The latter piece of information is obtained by determining the effect of electrode separation on E_{min} at large separations.

Quenching distances may also be measured by quickly stopping the flow through a tube of the desired geometry when a flame is seated on the exit of the tube. If the flame flashes down the tube, the minimum dimensions are above the quenching distance for that mixture. Quenching distances that have been measured between two flat plates using this technique agree quite well with the quenching distances measured using the flanged electrodes in the spark-ignition experiment described above. Parallel-plate quenching distances and minimum ignition energies determined by the spark method for propane, oxygen, and nitrogen mixtures at various initial pressures are given in Fig. 12-11. It should be noted that, in general, minimum ignition energies are extremely small—in some cases, corresponding to the passage of a barely audible spark through the mixture. In fact, it is well known that static electric sparks can cause the ignition of many explosive mixtures.

The relation between the characteristic quenching distance and the geometry of the quenching tube has been developed theoretically and confirmed

experimentally in a number of instances. The theory can be based on the assumption either that (1) wall capture of reactive species, or (2) heat transfer to the wall controls the quenching. Both these approaches yield the same theoretical relations relative to geometry effects, because of the similarity between diffusion and thermal conduction. Quenching measurements for a variety of geometries show quite good relative agreement ($\pm 10\%$) with the theoretical predictions for a number of hydrocarbon systems. The theory predicts that the circular tube quenching diameter should be related to the parallel plate quenching distance by the equation

$$d_{\parallel} = 0.65 d_0$$

Experimentally, one may show that the quenching distance is simply related to the pressure. This is because it is related to the preheat zone thickness of the flame. Also it is related to the minimum ignition energy of the system for virtually all hydrocarbon–air flames, through the equation $E_{\min} = 0.06 d_{\parallel}^2$ (see Fig. 12-12) where $E_{\min}$ has units of millijoules and d is measured in millimeters.

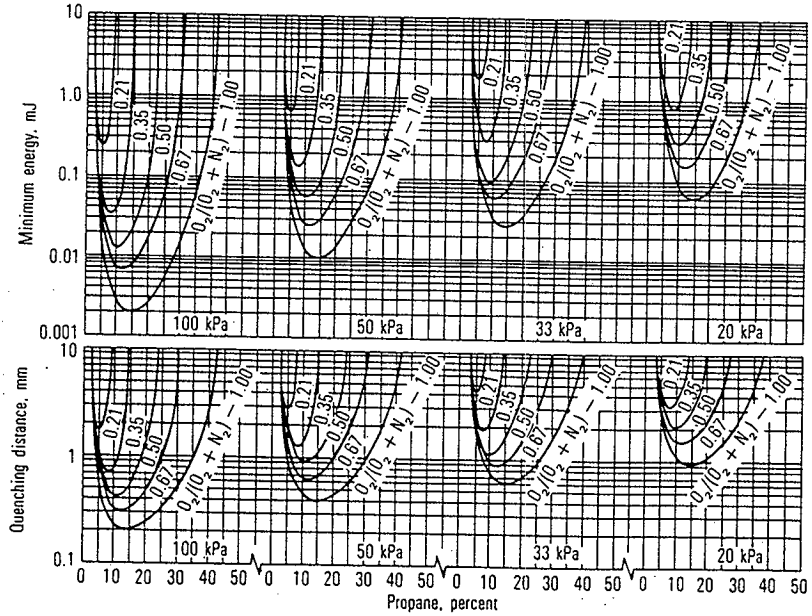

Figure 12-11 Effect of pressure, nitrogen dilution, and equivalence ratio on propane–oxygen flat-plate quenching distances and spark minimum-ignition energies. *(With permission from B. Lewis and G. von Elbe, Combustion Flames and Explosions of Gases, 2d ed., Academic, New York, 1961.)*

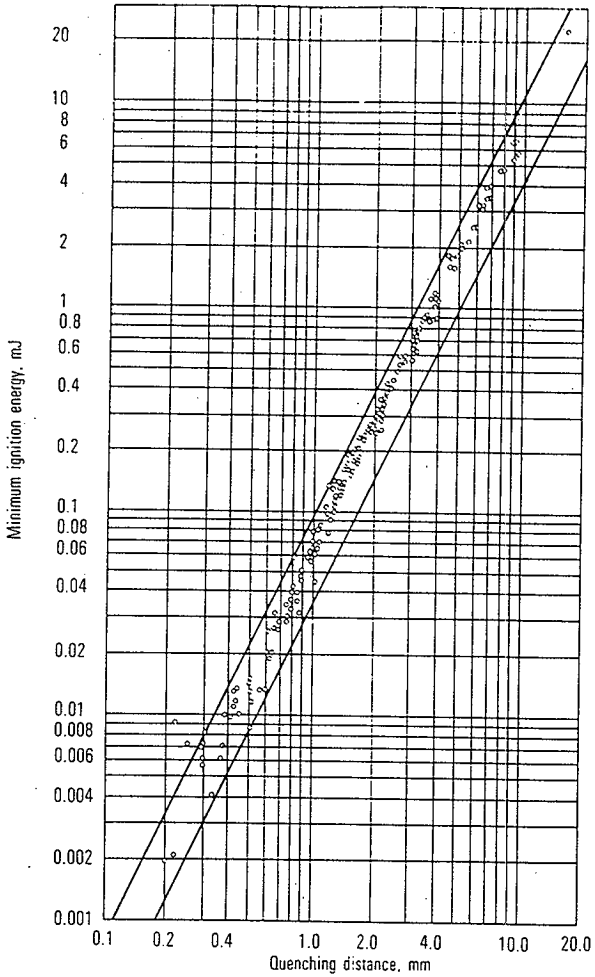

Figure 12-12 The relation between flat-plate quenching and spark minimum-ignition energies for a number of hydrocarbon–air mixtures. *(With permission from B. Lewis and G. von Elbe, Combustion Flames and Explosions of Gases, 1st ed., Academic, New York, 1951.)*

Figure 12-13 Effect of change in ignition energy upon flame propagation. Times are in microseconds. *(Courtesy H. Lowell Olsen, Applied Physics Laboratory, Silver Spring, Md. Originally in AGARD, Selected Combustion Problems, II, Butterworth, London, 1956.) (With permission.)*

Read down:

	Gas	$\frac{1}{2}CV^2$
	Air only	1.33 mJ
Subcritical energy	Propane–Air	1.14 mJ
Supercritical energy	Propane–Air	1.23 mJ

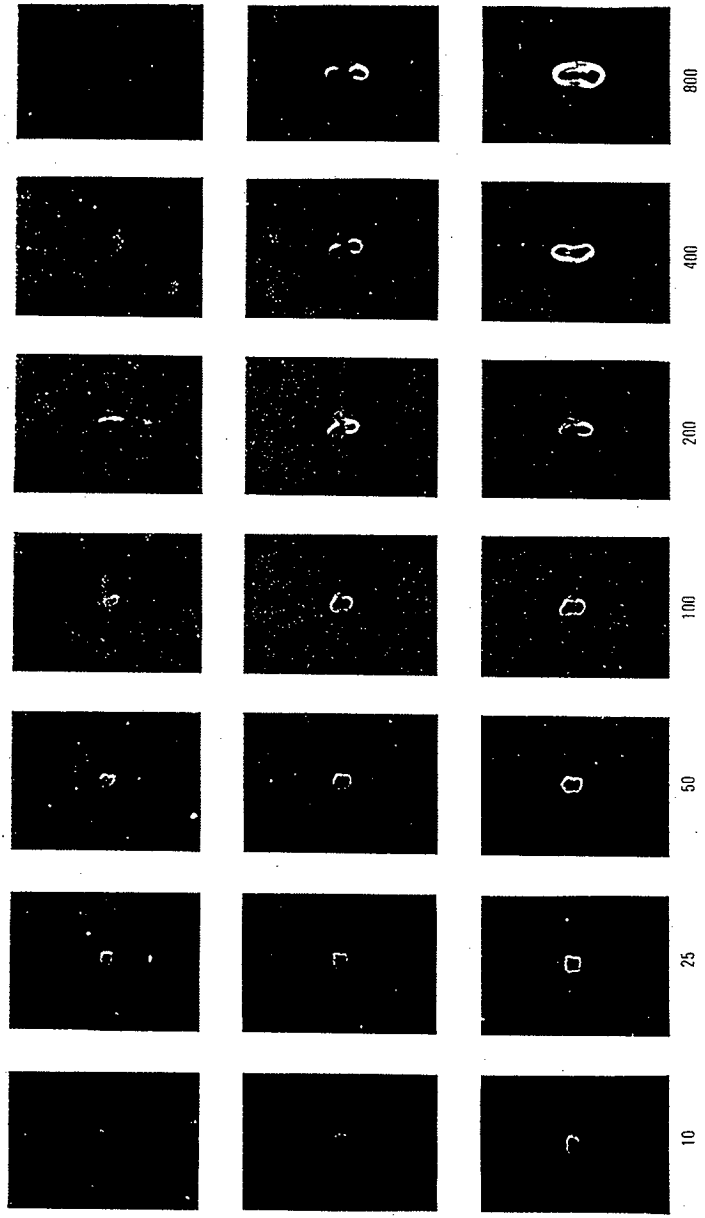
800
400
200
100
50
25
10

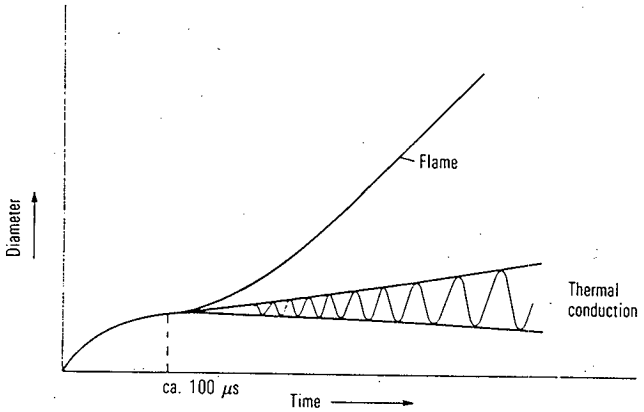

Figure 12-14 Schematic diagram of the decay or growth behavior of an ignition kernel (incipient flame ball) near the threshold value of energy for ignition of a propagating flame.

We will now look at the details of incipient growth from a small spark. Figure 12-13 contains repetitive schlieren photographs illustrating the appearance of the hot kernel of gas for an inert mixture and for a reactive mixture with both a subcritical and supercritical energy addition. In the reactive case, the spark kernel initially contains temperatures well above the ignition temperature of the mixture, and an incipient flame is seen to form. This behavior should be contrasted with the inert case where the initially high gradient simply flattens with time and eventually disappears. However, as the two reactive cases show, the formation of an incipient flame does not ensure subsequent propagation. At some point, well after spark passage (ca. 100 μs in Fig. 12-13) the incipient flame becomes a true flame in the supercritical case and starts to decay by thermal conduction in the subcritical case. This behavior is shown schematically in Fig. 12-14.

Ignition and quenching are difficult to discuss theoretically and complete theories are not as yet available. However, Rosen[13] has justified Lewis and von Elbe's[14] empirical relation for a plane source (i.e., one-dimensional) minimum ignition energy by applying the nonsteady equations to a simple first-order $A \rightarrow B$ flame with $\mathrm{Le} = 1$, similar to the steady flame discussed in Sec. 8-3. He assumed that heat was added in a very short time at an infinite flat plane in the mixture, and determined that the critical quantity of heat addition to cause

13. G. Rosen, *J. Chem. Phys.*, **30**:298 (1959).
14. B. Lewis and G. von Elbe, *Combustion Flames and Explosion of Gases*, 2d ed., Academic, New York, 1961.

flame propagation is related to the steady-flame properties by the equation

$$E_{\min} \simeq \frac{\kappa_u q}{(C_p/M)S_u} = \frac{\kappa_u}{S_u}(T_b - T_u) \tag{12-2}$$

where $E_{\min}$ has units of joules per square meter and $q = (C_p/M)(T_b - T_u)$, the heat of reaction at constant pressure in joules per kilogram. We note that q is defined as an enthalpy, while $E_{\min}$ is an energy. However, this equation is correct because the energy added to the system appears as an enthalpy in the system, since the process is taking place at constant pressure.

We note that when we substitute Eq. (8-7) from elementary flame theory into Eq. (12-2) we obtain the relationship

$$E_{\min} \simeq \eta_0 \rho_u c_p (T_b - T_u) \tag{12-3}$$

In Eq. (12-3) one should really use a variable density and not ρ_u. This would make the right-hand side of this equation smaller. This, plus the experiments on ignition delay described above show, in at least an approximate way, that one must add enough energy to the system to form a preheat zone before propagation will occur.

In addition, Aly and Hermance[15] have presented a two-dimensional theory for parallel plate or circular tube quenching using either overall first- or second-order kinetics with an Arrhenius temperature dependence to simulate a stoichiometric propane–air flame. They also allowed the Lewis number to range from one to infinity and neglected transverse diffusion of reactants. They justify this because, as Fig. 12-15*c* shows, there is quite a thick cool region near the wall where chemistry is not occurring. Figures 12-15*a* and *b* show the centerline longitudinal and the transverse structure of such a flame.

The authors also investigated the effect of varying the Lewis number. These results are shown in Fig. 12-16. Note from Fig. 12-16*a* that the "adiabatic" flame speed increases as the Lewis number goes from $1 \rightarrow \infty$, just as it did for the Friedman and Burke flame with simple Arrhenius kinetics. Also note that the theoretically determined quenching distance drops and that the Peclet number defined as

$$\mathrm{Pe} = \frac{\rho_u c_{pu} S_u d_{\parallel}}{\kappa_u} \tag{12-4}$$

is independent of the Lewis number. In this equation $d_{\parallel}$ is the parallel plate quenching distance. This means that in this two-dimensional flame, quenching is determined by the competition of the rate of flame propagation (or rate of heat generation) and rate of heat loss to the walls by thermal conduction. Also note that the maximum temperature of the centerline flame at incipient extinction is about 2100 K, that is, about 300 kelvins less than the "adiabatic" flame temperature in a 50 mm tube.

15. S. L. Aly and C. E. Hermance, *Combust. Flame*, 40:173–185 (1981).

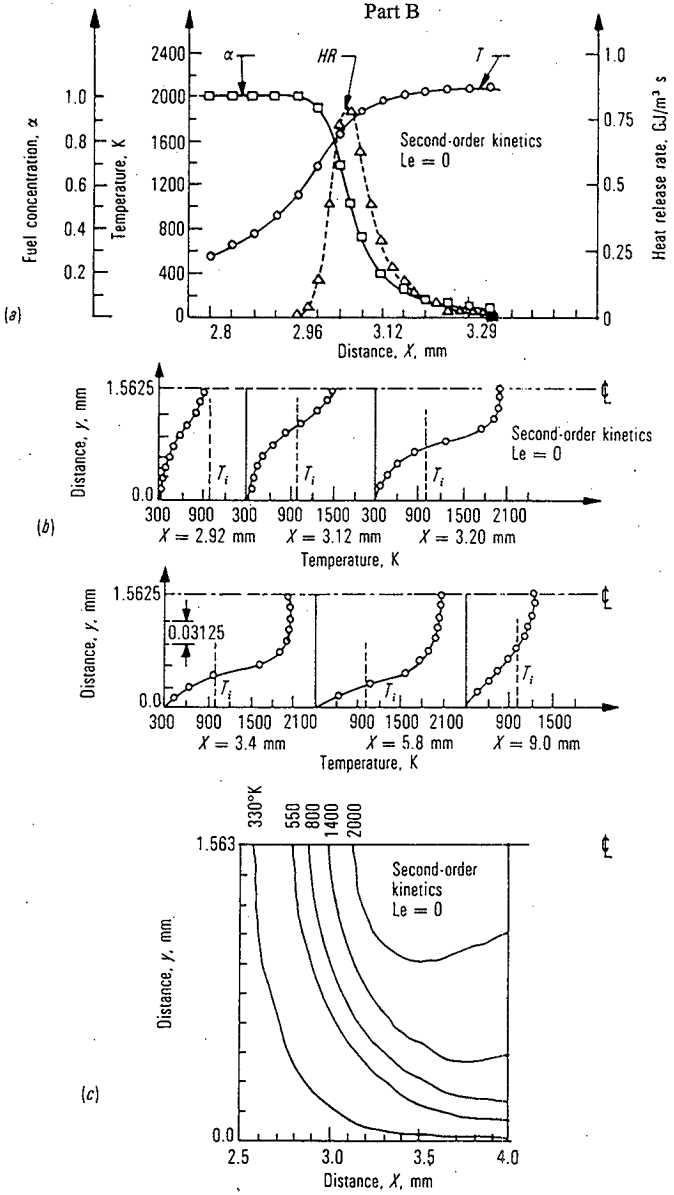

Figure 12-15 Longitudinal (*a*), transverse (*b*), and isothermic (*c*) structures of the flame at the quenching limit; second-order kinetics. *(Ref. 14, with permission.)*

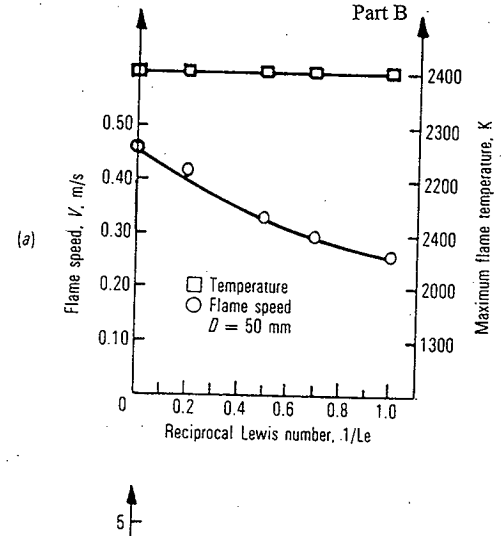

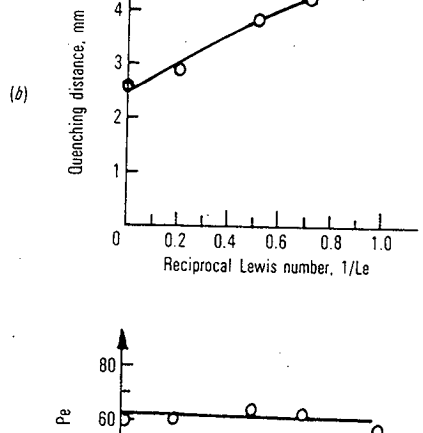

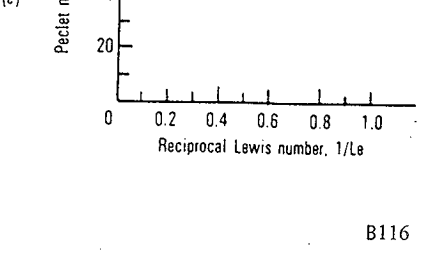

Figure 12-16 Temperature and flame speed (*a*), quenching distance (*b*), and Peclet number (*c*) dependence on Lewis number; first-order kinetics, all calculated for a 50 mm diameter tube. *(Ref. 14, with permission.)*

A different problem arises during spherical ignition. The incipient flame is always a stretched flame in the Karlovitz sense (see Sec. 10-3) because its area increases at an ever-increasing rate while its radius of curvature decreases. Using the same assumptions as were used in Sec. 10-3 one finds that the nondimensional stretch or the Karlovitz number for such a flame is given by the expression

$$K = 4 \frac{\eta_0}{d} \frac{\rho_u}{\rho_b} \tag{12-5}$$

As a result of this stretch, preferential diffusion of the lighter species, either fuel or oxygen, toward the ignition region causes two unique effects to occur. In the first place preferential diffusion alters the equivalence ratio in the incipient preheat zone by enriching the concentration of the lighter species there. This causes a shift in the equivalence ratio for the lowest minimum ignition energy as shown in Fig. 12-17. This is a plot of minimum ignition energy vs. composi-

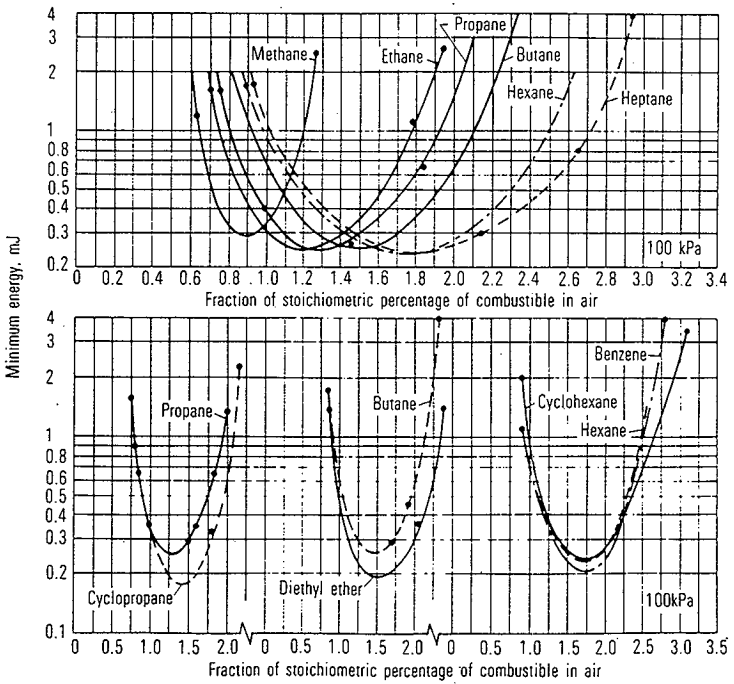

Figure 12-17 Minimum ignition energy vs. equivalence ratio for various fuel–air mixtures showing the effects of preferential diffusion. *(With permission from B. Lewis and G. von Elbe, Combustion Flames and Explosions in Gases, 2d ed., Academic, New York, 1961.)*

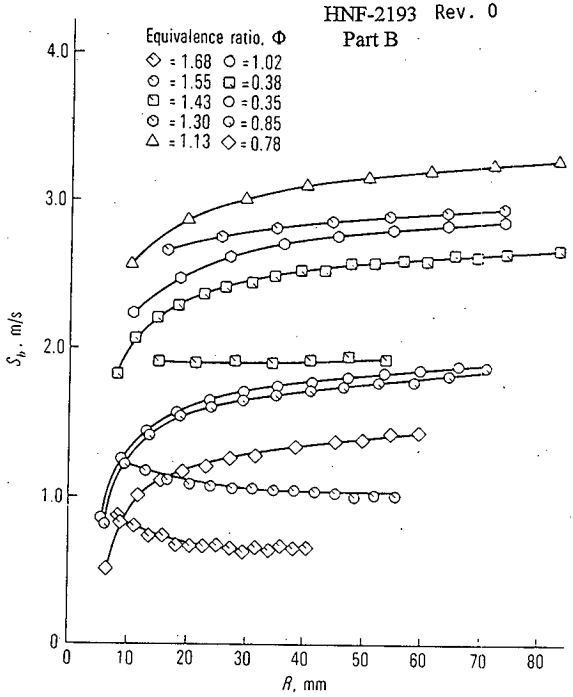

Figure 12-18 Space velocity S_b vs. radius for a laminar flame ball in propane–air mixtures.

tion for various fuels in air. Since from the elementary theory one would expect the minimum ignition energy to occur at the maximum burning velocity of these mixtures, these curves should all show a minimum in the neighborhood of $\Phi = 1.1$ (the approximate equivalence ratio for the maximum laminar burning velocity for all these systems). Notice that for methane, which is lighter than oxygen, Φ_{min} is 0.8, while for those fuels whose diffusivity is less than oxygen Φ_{min} is always greater than one and increases as the molecular weight of the fuel increases. Thus, the larger the difference in relative diffusivity, the larger the deviation of Φ_{min} from stoichiometric.

Another way that preferential diffusion plays an important role in early flame behavior is its effect on the burning velocity of an outwardly propagating flame. For example as shown in Fig. 12-18, in propane–air mixtures (i.e., for a heavy fuel and light oxidizer mixture), rich mixtures exhibit a higher space velocity at small radii while lean mixtures show a lower space velocity at small radii. In all cases the space velocity of the flame relaxes to the theoretically expected laminar space velocity after a few centimeters of flame travel. The effect is somewhat masked by two additional effects which cannot be easily

discussed quantitatively: (1) the slow relaxation of the burned products to the equilibrium composition adds a slow initial increase in velocity to the experimental curves, and (2) any excess ignition energy at the spark source can cause a higher propagation velocity of the early flame. However, the preferential diffusion effect is the only effect which shifts sign as the equivalence ratio passes through unity and is therefore quite definitely operating in this system.

Recently Frankel and Sivashinsky[16] have verified, using a large activation asymptotic analysis with the Lewis number defined for the deficient species, that rich and lean propane–air flames should exhibit the behavior shown in Fig. 12-18.

12-5 HOT SURFACE OR HOT GAS IGNITION: THE AUTOIGNITION TEMPERATURE AND THE MINIMUM EXPERIMENTAL SAFE GAP

There have been many attempts to study the ignition process using either a heated gas stream as an igniter, passing the combustible mixture over a heated surface, or injecting heated spheres into the mixture. These are all quite complex aerodynamically and therefore will not be discussed in this text. There are however two standardized ignition techniques which are important from the point of view of combustion safety that will be discussed here. These are the measurement of the autoignition temperature and the minimum experimental safe gap.

For gases, the autoignition temperature is the lowest vessel temperature at which any mixture of that fuel and air will explode. For liquid fuels the autoignition temperature is the temperature of a specified flask that contains air below which a flash of light will not be seen after a specified amount of liquid fuel is dropped into the flask. The autoignition temperature yields an imperfect indication of the maximum surface temperatures that can be tolerated in an environment where that liquid or gas may be handled in bulk.

The minimum experimental safe gap is also a safety-related combustion property. It is based on the fact that it is very expensive either to purge electrical switch boxes or motor housings or to attempt to make them completely air tight. Therefore when electrical devices are to be used in the presence of combustible vapors or gases the electrical boxes must be constructed to meet two requirements. These are: (1) the box should be strong enough to be able to stand an internal explosion without rupturing and (2) openings to the outside should be small enough so that escaping combustion products will not cause ignition of the surrounding flammable vapors or gases.

Studies of the ignition of a combustible mixture by hot product gases escaping from a vessel through a long slot have shown that for a sufficiently wide

16. M. L. Frankel and G. I. Sivashinsky, "On Effects Due to Thermal Expansion and Lewis Number in Spherical Flame Propagation," *Combust. Sci. Tech.*, **31**:131 (1983).

slot width, a flame simply propagates through the slot into the surrounding combustible mixture. However when the slot width becomes somewhat less than the ordinary parallel plate quenching distance, a flame no longer propagates through the slot but the hot gases that escape cause a slightly delayed ignition of the surrounding combustible mixture. Schlieren observations of this process have shown that ignition occurs some distance from the slot in the turbulent mixing region and that initially the ignition is a volumetric "explosion" which subsequently ignites a flame front which propagates away from the "exploded" turbulent mixing region. It has also been found that there is a critical slot width below which ignition of the surrounding gas no longer occurs. This critical width is called minimum experimental safe gap (MESG). For most hydrocarbons it is approximately $d_{\|}/2$.

12-6 FLASH POINT

Liquid fuels all exhibit an equilibrium vapor pressure which is dependent on the temperature of the fuel. As the temperature of the fuel is raised from some low value to some high value the equilibrium vapor pressure increases monotonically. If a mixture of this equilibrium fuel vapor with air contains less fuel vapor than required for lean limit combustion the liquid is said to be below its lower flash-point temperature. Above this temperature, as the liquid temperature is increased its equilibrium vapor pressure increases to the point where the vapor-air mixture contains so much fuel vapor that it is above the upper flammable limit for that fuel. Under these circumstances the liquid is said to be above its upper flash-point temperature.

In actual practice, the lower and upper flash-point temperatures are measured in any of a number of standardized pieces of apparatus. By far the most accurate measurements are obtained using equilibrium or closed-cup techniques. In these techniques the liquid is placed in a loosely closed container in a thermostat bath and is held at some temperature until the vapor space in the container holds fuel vapor which is in equilibrium with the liquid at that temperature. Then a part of the top of the container is opened and a flame from a torch is swept across the opening. If the flame "flashes" into the vapor space the thermostat temperature is between the lower and upper flash points. The test is then repeated at different temperatures until both the lower and upper flash points are found. A flame is used as a strong igniter that is easily available. Note that since the flame is applied to the top of the container the measured flash point corresponds to the limit for downward propagation of the flame.

There are other "approved" techniques for measuring the flash point. One set of these uses an "open cup." Here the fuel is heated in a cup which is open at the top and the high vapor density of the fuel is expected to stop the fuel vapors from escaping before the flame is applied. This is obviously less satisfactory than the closed-cup "equilibrium" technique described above.

Tank Headspace Mixing

Z. I. Antoniak
Fluid Dynamics Group
PNNL

Presented at

SCOPE Meeting

February 10, 1998

Evidence Supporting Headspace Mixing/Uniformity

- Physics (mechanisms captured in modeling)
  - Large, unobstructed space
  - Heated at bottom (by waste heat generation)
  - Ventilation (active or passive) has minor effect
- Measurements
  - SHMS data in tank 241-SY-101
  - Single-shell tank measurements (tracer and other gases)
- Modeling
  - Hydrogen plume releases
  - Ventilation effects
  - Tracer gas release concentrations

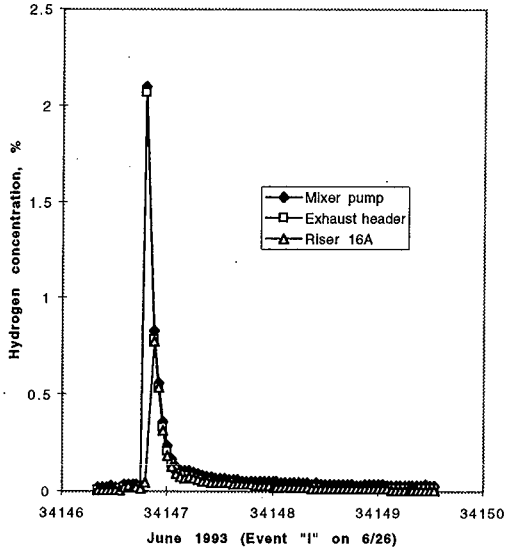

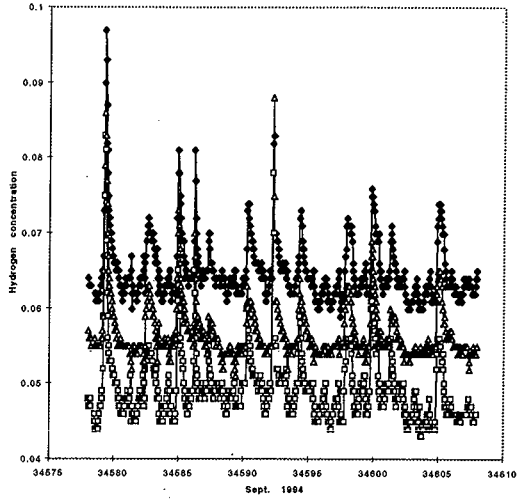

Whittaker Cell Hydrogen Concentration Measurements in 101-SY

Gas Concentration Measurements in Tank Domes

- Headspace homogeneity addressed (PNNL-11640)
  - Measured in 3 cool single-shell tanks (B-103, TY-103, U-112)
  - Samples taken at two risers, at 3 elevations, in the fall
  - Concluded that headspaces are essentially homogeneous
- Tracer gas release and monitoring (PNNL-11683)
  - He and SF6 in a number of single-shell tanks
  - Concentrations in tank S-102 indicate ~ complete mixing in < 1 hour
  - Concentrations in other tanks appear to corroborate this (meas. > 1 day)
- Seasonal variation in headspace gas concentrations (PNNL-11667)
  - Variation found to be small

Typical Simulation Showing Rapid Mixing

Hydrogen Concentrations Computed by TEMPEST at Vent of SST S-108 due to Release of Gas (~680 ft3/ 2 min) Containing 50% Hydrogen/50% Air by Volume (Tank S-108 is Passively Ventilated), with/without an Initial Established Flow Field.

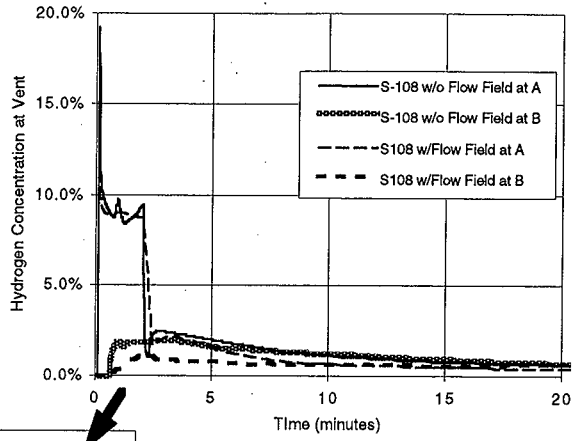

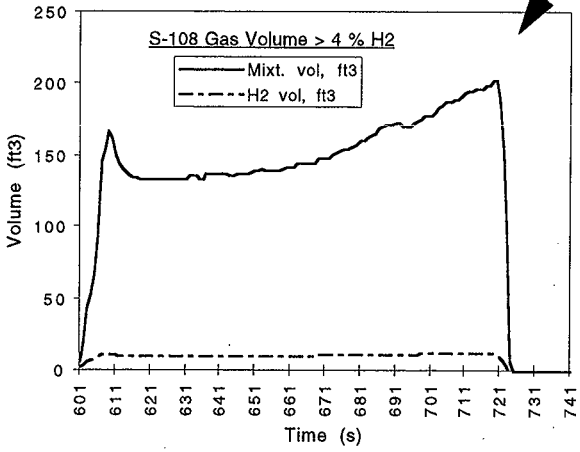

Mixture and Hydrogen Volumes in a Plume that is > 4 % Hydrogen; Case with Established Flow in an Unventilated SST (release at point A, near).

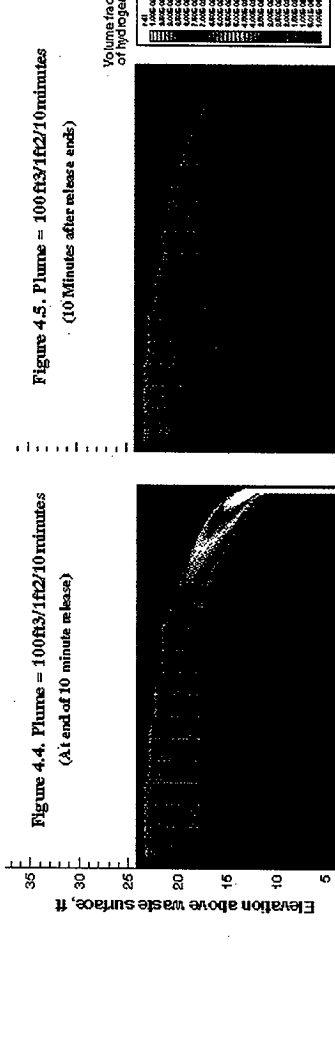

Figure 4.4. Plume = 100ft3/1ft2/10minutes
(At end of 10 minute release)

Figure 4.5. Plume = 100 ft3/1ft2/10minutes
(10 Minutes after release ends)

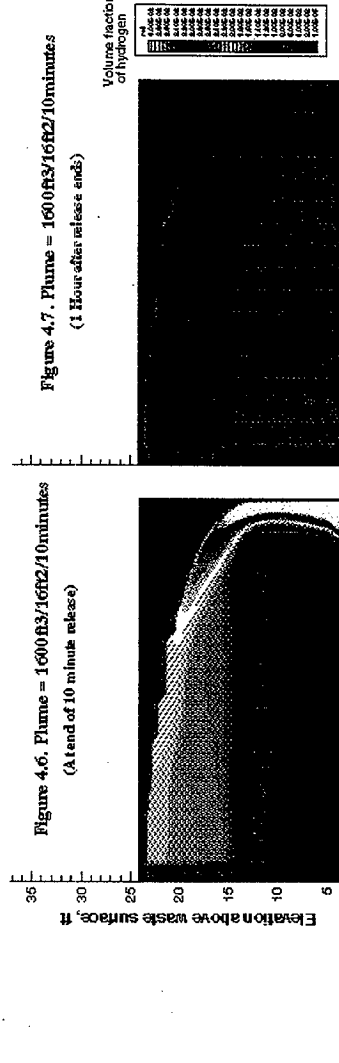

Figure 4.6. Plume = 1600ft3/16ft2/10minutes
(At end of 10 minute release)

Figure 4.7. Plume = 1600ft3/16ft2/10minutes
(1 Hour after release ends)

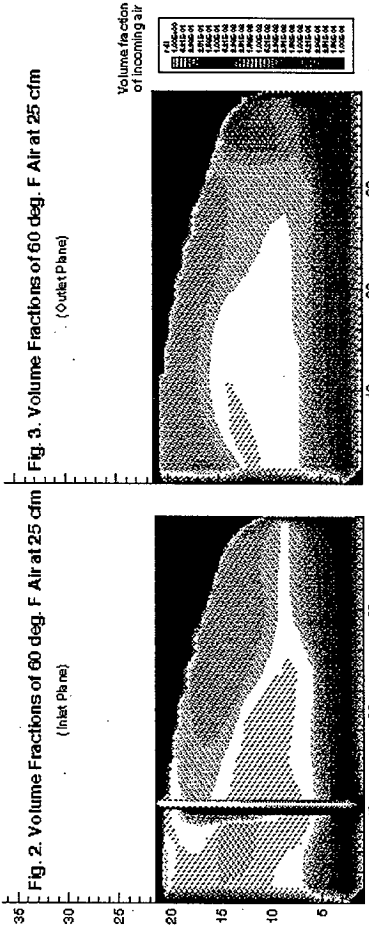
Fig. 2. Volume Fractions of 60 deg. F Air at 25 cfm
(Inlet Plane)
Elevation above waste surface, ft
Radius, ft

Fig. 3. Volume Fractions of 60 deg. F Air at 25 cfm
(Outlet Plane)
Volume fraction of incoming air
Radius, ft

Fig. 4. Volume Fractions of 79 deg. F Air at 25 cfm
(Inlet Plane)
Elevation above waste surface, ft
Radius, ft

Fig. 5. Volume Fractions of 79 deg. F Air at 25 cfm
(Outlet Plane)
Volume fraction of incoming air
Radius, ft

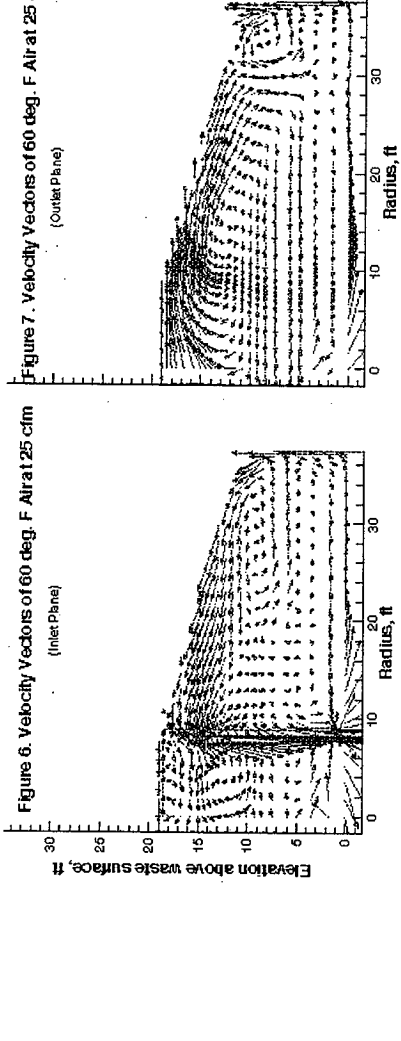
Figure 6. Velocity Vectors of 60 deg. F Air at 25 cfm
(Inlet Plane)
Figure 7. Velocity Vectors of 60 deg. F Air at 25 cfm
(Outlet Plane)
Elevation above waste surface, ft
Radius, ft
0
5
10
15
20
25
30

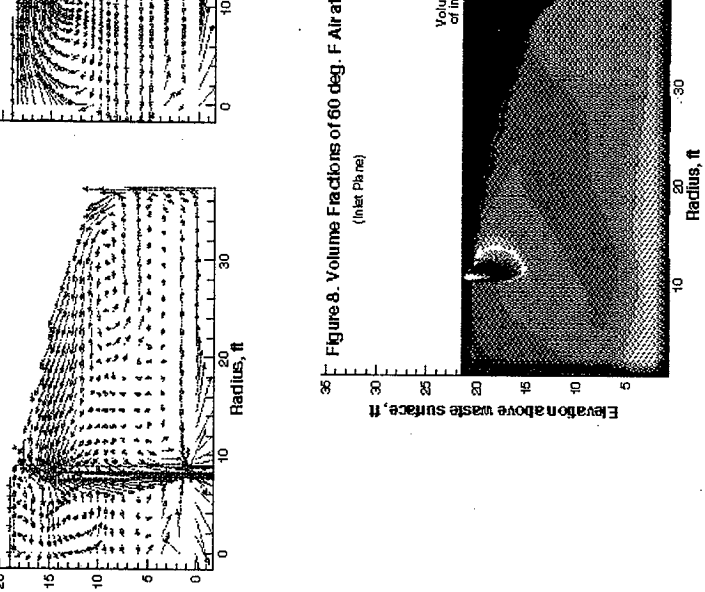
Figure 8. Volume Fractions of 60 deg. F Air at 5 cfm
(Inlet Plane)
Volume fraction of incoming air
Elevation above waste surface, ft
Radius, ft
5
10
15
20
25
30
35

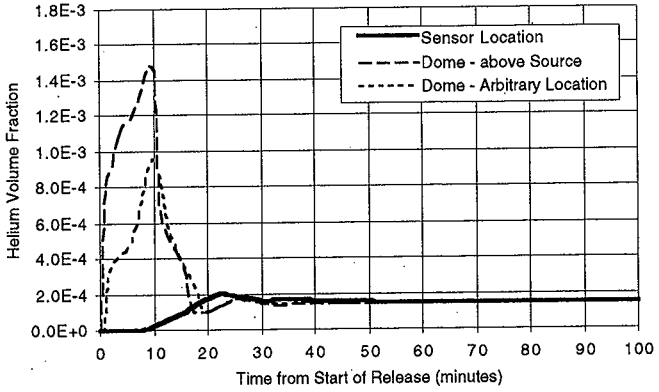

Simulated Helium Volume Concentrations in (65,120 ft3) Head Space of Tank 241-S-102 Due to 10-Minute Release of 10 ft3 of Helium Gas (80°F/78°F Crust/Dome Temperatures

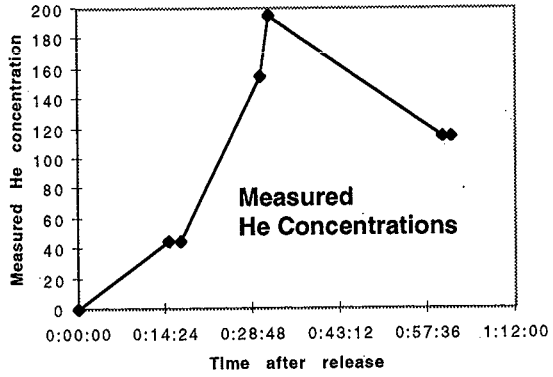

Conclusions

Although the evidence is circumstantial, it is compelling, and it consistently supports the propositions that:

- Headspaces are homogeneous, irrespective of tank type and condition
  - Neither measurements nor calculations indicate the presence of stratification, except for a brief period following a gas release
- Any gases released from the waste mix rapidly with the existing dome atmosphere
  - Gas releases are typically both turbulent and buoyant, which promotes mixing
- It is highly unlikely that any substantial "short-circuiting" of vent flow occurs
  - Inflow has sufficient momentum to penetrate deep into domespace and mix, precluding direct outflow

Tank Headspace Mixing

Z. I. Antoniak, PNNL
2/10/98

A considerable body of data exists on Hanford waste tanks to support the contention that their headspaces are well-mixed. The single exception to this well-mixed condition is during and briefly after a plume-type of gas release from the waste into the headspace. Multiple dispersion mechanisms are active in the headspace and serve to rapidly mix any released gas plume with the surrounding dome atmosphere. The chief mechanism promoting mixing is natural convection, driven by the temperature difference between the relatively warm waste and the cooler surroundings. Natural convection also assists in quickly entraining any air inflow, whether passive or active, into the dome atmosphere.

Measurements of gas concentrations in headspaces have consistently shown the headspaces to be generally homogeneous, with swift reversion to homogeneity after a gas release. Computer simulations of headspace hydrodynamics have also shown this to be the case; these simulations have furthered understanding of the relevant dispersion mechanisms.

Dispersion of a plume into its surroundings is a complex mixing process that occurs on several scales. On the microscale, mixing takes place by diffusion due to the random motion of both solute and solvent molecules. Much more rapid local mixing is a product of turbulence that may exist in the steady-state convective flow in the headspace or that may be generated by a bouyant plume as it rises. Finally, dispersion on the scale of the headspace dimensions occurs by thermal convection which prevents formation and persistence of stratified layers that might remain flammable. The latter mechanism dominates the plume dispersion process.

Thermal convection is driven by the heat generated in the waste. The waste temperature is higher than the headspace which is in turn higher than the tank walls. The air next to the waste is heated and rises to the tank dome where it cools and sinks. This establishes large-scale convective cells that keep the headspace atmosphere nearly isothermal.

Most SSTs have relatively cool waste so that the dome atmosphere is only somewhat above average ambient temperature. Past modeling and flow visualization studies that varied the ΔT between the waste surface and the dome atmosphere indicated that, even for the smallest ΔT (= 0.9°C [2°F]) examined, convective velocities were on the order of tenths of a foot per second. Such velocities are enough to rapidly disperse any stratified layer of hydrogen that tends to form during the release; i.e., a tank headspace becomes fully mixed within about an hour after the cessation of a hydrogen plume release.

Ventilation or inter-tank flow through cascade lines is a separate effect not directly related to plume dispersion inside the headspace. It can only assist dispersion to the extent that it influences the existing circulation within the headspace. The most important effect of ventilation is simply to dilute the hydrogen concentration in the headspace by removing it and replacing it with air at some rate. Typical passive ventilation rates are less than ~20 cfm which requires ~3 days to replace a headspace volume of 80,000 ft^3. A typical active ventilation system running at 200 cfm replaces the headspace volume in ~7 hours.

VENTILATION FOR FLAMMABLE GAS

Jim Kriskovich
Lockheed Martin Hanford Corporation
February 10, 1998

Tank Ventilation

Provides the safety function of flow used to remove flammable gas from dome space.

Configuration

- **Infiltration methods**
- **Positive pressure release paths**
- **Discharge configuration**
- **System configurations**
- **Flow rates through each dome**
- **Re-circulation configuration**

Configuration of DST Ventilation Systems

DST Tanks: All 28 DST Tanks are actively ventilated.

- Infiltration method
  - All double shell tanks, except AP farm and AY & AZ (until W-030), rely on inlet filters.
- Positive pressure release paths
  - AP farm and AY & AZ (until W-030).
  - AN, AW and SY inlet filter arrangement. Steps taken to seal the other openings (i.e., pump pit cover blocks)
  - Process piping in all tanks
- Discharge configuration
  - All tanks are ventilated to a common header, which leads to the main vent train. The common header is where the first mixing point occurs.

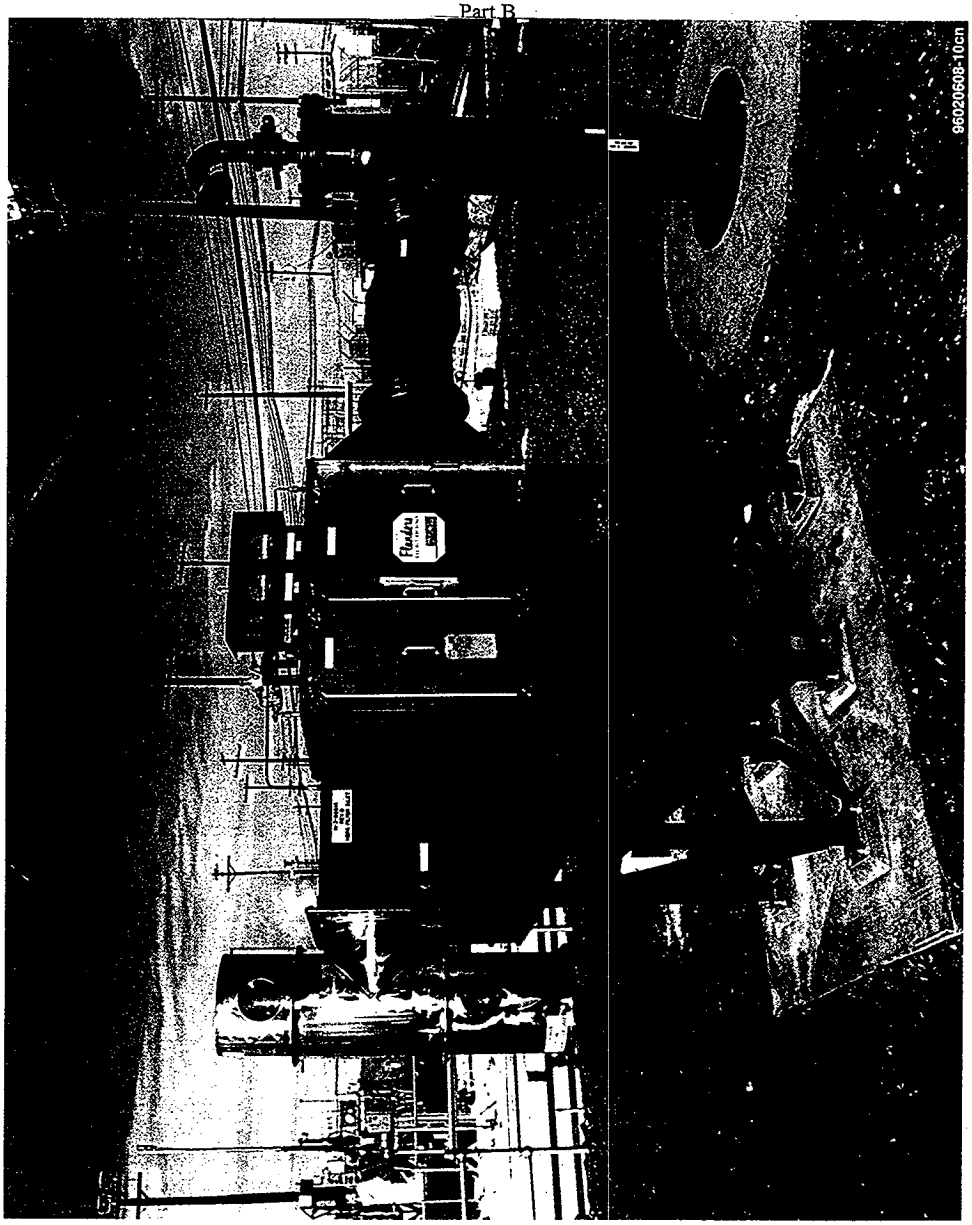
960206D8-10cn

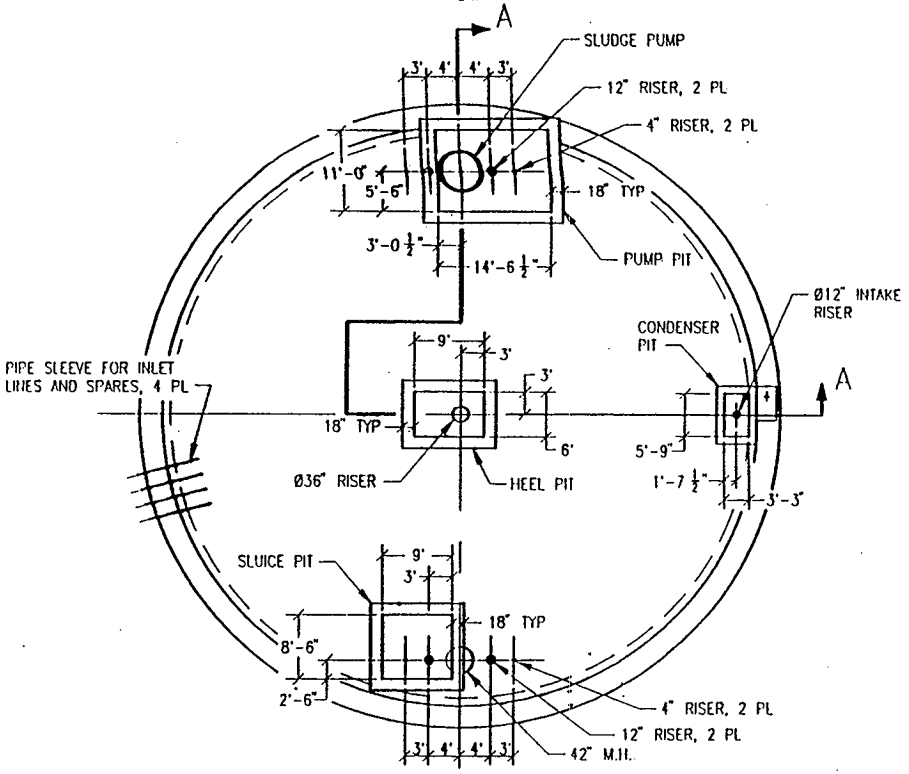

241-C-106
PLAN

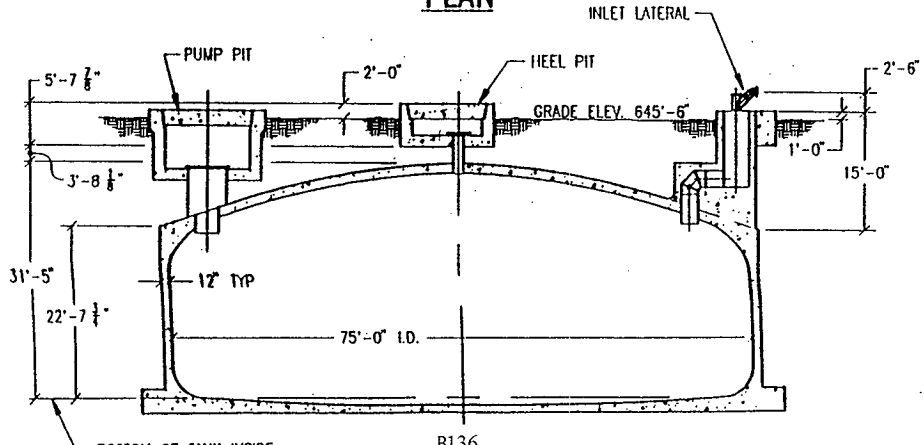

Configuration of DST Ventilation Systems

- Filter train
  - De-mister
  - Heater
  - Pre-filter
  - HEPA filters (2 in series)
  - Fan
  - Stack

241-AP K-2 System

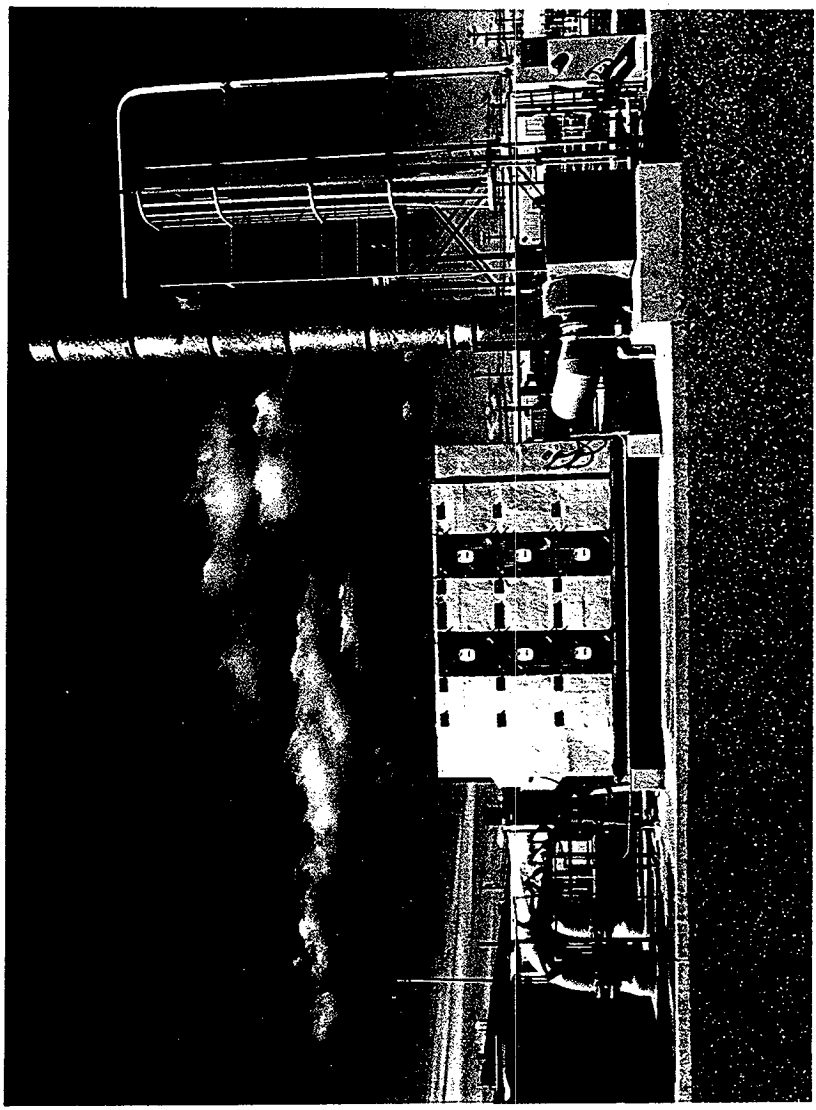

1/23/93

Configuration of DST Ventilation Systems

Flow Rates

- AN: Range from 50 to 120 cfm/tank, inlet filter flow control orifice plate.
- AP: Range from 50 to 120 cfm/tank. Not currently being measured
- AW: Range from 50 to 120 cfm/tank, inlet filter flow control orifice plate.
- AY & AZ: Ranges from approximately 500 to 650 cfm. Can not measure.
- SY: 101 between 300 and 450 cfm, 102 and 103 make up difference to reach approximately 1000 cfm

Configuration of SST Ventilation Systems

Single Shell Tanks: Only 15 are actively ventilated. These include 241-C-105 & 106, 241-SX-101, -102, -103, -104, -105, -106, -107, -108, -109, -110, -111, -112, & -114

- Infiltration Method
  - All actively ventilated SSTs rely on inlet filters for infiltration and pressure control.
- Positive pressure release paths
  - C and SX release paths are through inlet filter arrangement. Also could include pump pit cover blocks.
  - Process piping in all tanks

Configuration of SST Ventilation Systems

- Discharge Configuration

  - C - 105 & 106 are discharged individually and tie into a common header, which leads to the main vent train. The common header is where the first mixing point occurs

  - SX - The lower numbered actively ventilated tanks are routed through SX - 109. The other SX tanks are routed to a common header. The common header is where the first mixing point occurs.

Configuration of SST Ventilation Systems

- Filter Train
  - Heater
  - Pre-filter
  - HEPA Filters (back to back, not truly independent)
  - Fan
  - Stack

Configuration of SST Ventilation Systems

- Flow Rates
  - C-105: Ranges from 275 to 325 cfm/tank.
  - C-106: Ranges from 1150 to 1250 cfm/tank.
  - SX Tanks: Range from 50 to 120 cfm/tank. Can not be measured.
- Recirculation Configuration

- Used to help cool waste and lower emissions.

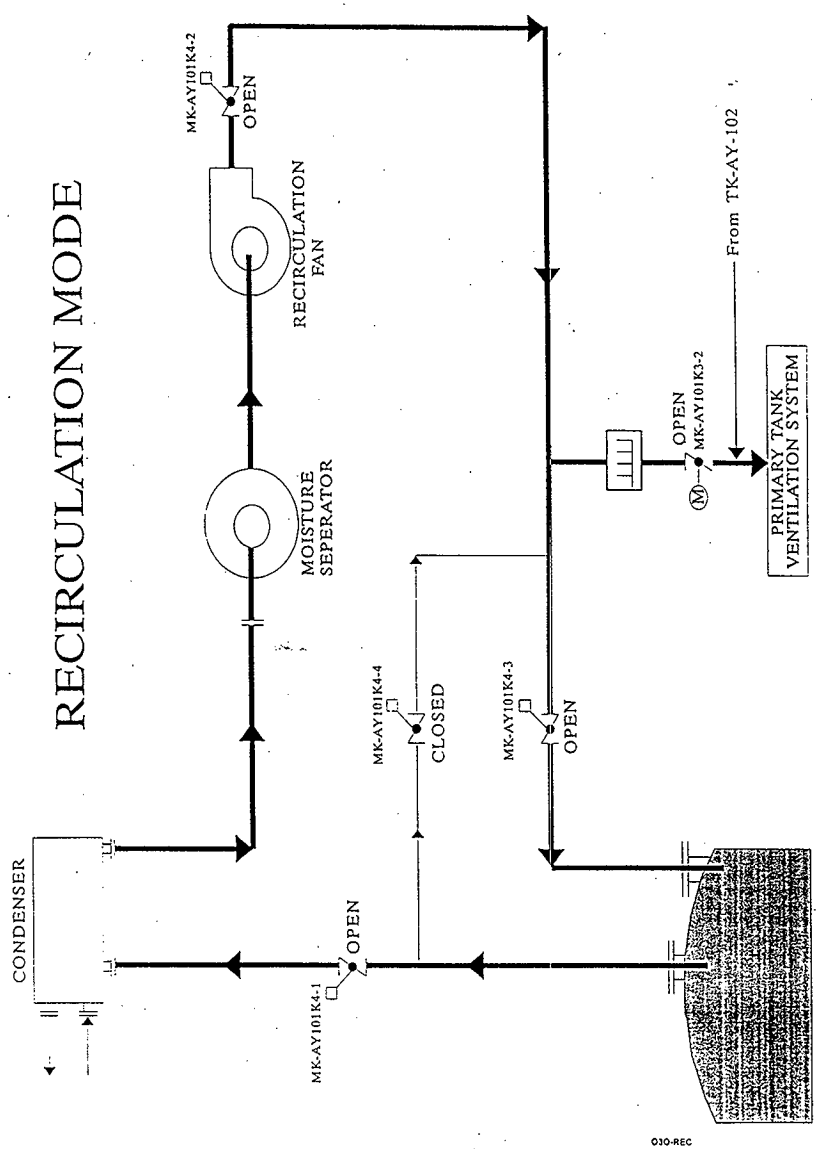
RECIRCULATION MODE
CONDENSER
MK-AY101K4-1
OPEN
MOISTURE SEPERATOR
MK-AY101K4-4
CLOSED
MK-AY101K4-3
OPEN
MK-AY101K4-2
OPEN
RECIRCULATION FAN
OPEN
MK-AY101K3-2
From TK-AY-102
PRIMARY TANK VENTILATION SYSTEM
030-REC

Conclusions

- Controlled infiltration method in majority of facilities.
- Tank pressurization paths dependent on tank configuration
- No minimum flow rate requirements.
- Mixing point prior to all ventilation trains. Therefore, there are no controls for ventilation trains.
- No minimum flow rate requirements.
- Recirculation method could provide additional mixing.

Gas Release Event Safety Analysis
EXPERTS' PANEL WORKSHOP #2

DST Dome Response to Overpressure

L. J. Julyk
Fluor Daniel Northwest

February 10, 1998

OBJECTIVE

Provide some "insight" as to how the tanks respond structurally to a postulated flammable gas deflagration, i.e., describe "expected" failure modes and "estimated" failure pressures.

CONSTRUCTION DETAILS AND CURRENT CONDITION

	SST (100-Series SSTs - 133 tanks)	DST (28 tanks)
Concrete Vault		
Concrete compressive strength (ksi)	3	3 (AY & AZ - 4 tanks) 4.5 (SY - 3 tanks) 5 (AN, AW, & AP 21 tanks)
Rebar yield strength (ksi)	40	60
Connection to foundation	Attached	Not attached
Soil overburden depth at dome apex (ft)	6 to 10	7 to 8

	SST (100-Series SSTs - 133 tanks)	DST (28 tanks)
Steel Liner		
Yield strength (ksi)	24 -33	32 (AY & AZ) 35 (SY) 50 (AN, AW, & AP)
Primary	Does not extend into dome Not anchored to concrete Not post-weld stress relieved	Free standing tank Anchored to dome Post-weld stress relieved Potential stress/strain concentrations at thickness transitions, riser-liner interfaces, and anchor locations
Secondary	None	Anchored to concrete side wall and dome haunch Transitions with primary tank at dome haunch 30 in. annulus space between primary and secondary Not post-weld stress relieved

	SST (100-Series SSTs - 133 tanks)	DST (28 tanks)
Current structural condition		
Built	1943 to 1964 exceed original design life	1968 to 1986 within original design life
High temperature exposure	More likely (degraded concrete strength and modulus)	Less likely
Leakers	68 known or expected	None
Interim stabilized *	106	Active

* Less than 50 kgal of drainable interstitial liquids and less than 5 kgal of supernatant liquid.

TYPICAL MGAL TANK GEOMETRIES

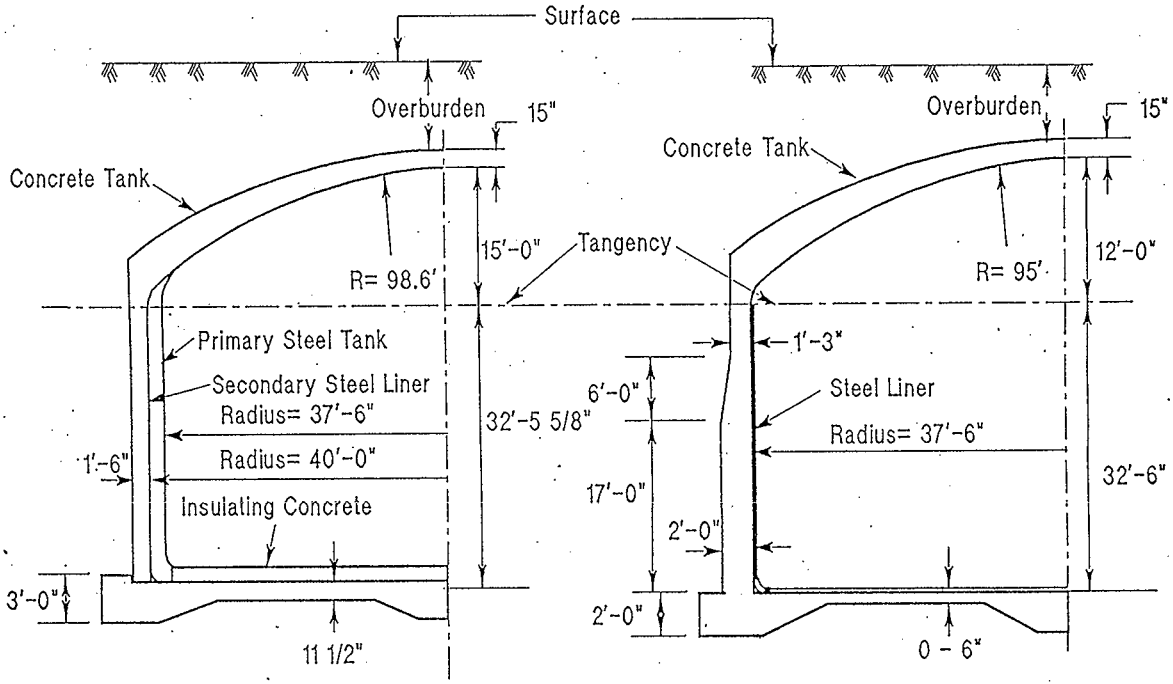

Double-Shell Tank **Single-Shell Tank**

PRESSURE TRANSIENT CHARACTERISTICS

Function of available volume and composition of released gas

Only DST SY-101 has been found to previously release sufficient quantities and concentrations of hydrogen and other gases greater than the lower flammability limit (3.5% H_2) during periodic episodic release events.

- Peak pressure
- Pressurization rate - fairly rapid (310 psia/s)
- Duration of pressure pulse (10 s) - relatively quick rise (0.2 s)
- Magnitude and duration of heat generation - adds little overall thermal energy to tank
- Rate and magnitude of depressurization - vacuum from cooldown
- Magnitude of pre- and post-leakage paths

BURN ANALYSIS FOR TANK SY-101

LANL HMS/TRAC burn analysis of gas release volume for Tank SY-101 with 66 percent of fully open 42-inch diameter vent-flow area from multi-port riser (MPR)

Gas Volume (ft^3)	Waste Level (in.)	Pressure	
		Rate (psi/s)	Peak (psig)
8,650	398	312	43.4
9,230	398	325	45.3

LANL PRESSURE TRANSIENT FOR SY-101

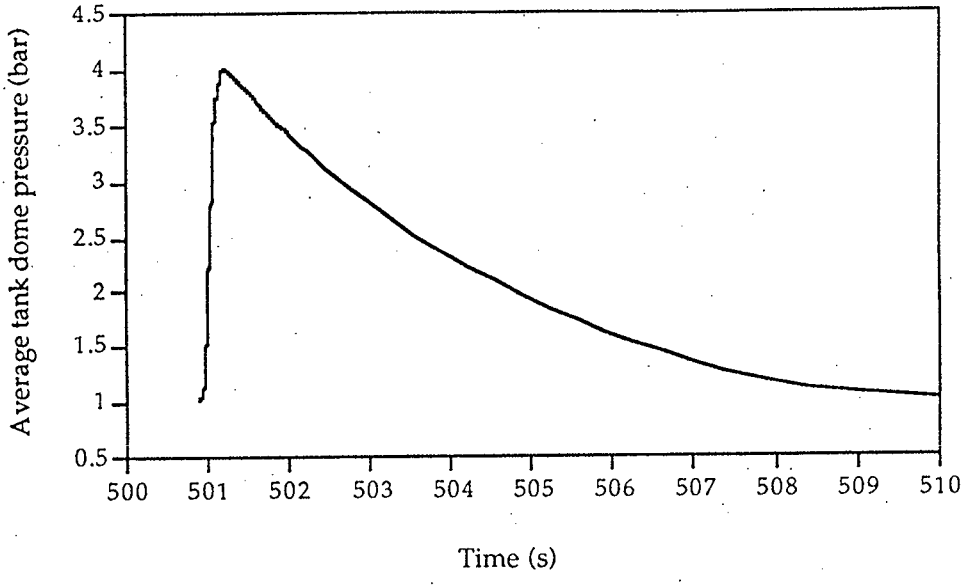

Tank 101-SY pressure history for a 245-m^3 (8650-ft^3) release.

DELPHI PANEL EVALUATION SUMMARY

SSTs

- Failure pressure: 11 - 14 psig (based on static analysis)
- Expected failure mode:

  Slow pressure transient

  - Extensive cracking of the upper wall and dome as failure pressure is approached.
  - Unfiltered release would take place through open risers, including lifting of cover blocks.
  - When pressure exceeds 11 - 14 psig additional filtered release of gases through dome cracks and soil overburden would occur limiting the peak pressure.
  - Dome uplift velocity imparting energy to soil cover is reduced by restraint of concrete vault to foundation base slab and leakage through concrete cracks.

SSTs (continued)

- Post-event spalling of concrete inside dome space.
- Post-event tank vacuum from cooldown of gases not expected to collapse the dome.
- Catastrophic dome collapse is not expected.

Rapid pressurization transients (flammable gas burn)

- Pressure may not have time to vent through cracks.
- Center region of dome (2 to 20 ft radius near meridional rebar over lap) could blow out along with soil overburden due to bond failure and large plastic deformations in steel reinforcement.
- Fall back of debris would be limited to ejected dome material and soil adjacent to the failed portion of the dome.
- Catastrophic dome collapse is not expected.

DSTs

- Primary tank changes the failure mode and failure pressure
- Failure pressure: 55 - 60 psig for pressurization phase
- Expected failure mode:
  - Primary tank will bulge, lifting the entire concrete tank dome and side walls from foundation base slab.
  - Unfiltered release would take place through open risers, including lifting of cover blocks.

Above pressurization failure pressure

- Failure of primary liner most likely along the transition weld at 6 ft radius of dome (stress/strain concentration) may cause a rapid "can-opener" partial opening of a flap in the tank dome.
- Energy of the high pressure gases at failure would likely blow out part of the concrete and soil above the 6 ft radius.
- Fall back of debris would be limited to ejected dome material and soil adjacent to the failed portion of the dome.

DSTs (continued)

- Catastrophic dome collapse is not expected.

Between about 44 psig and pressurization failure pressure

- Dome uplift velocity may be sufficient to cause soil cover separation of soil.

- Soil reimpaction - energy imparted to soil may exceed weakened capacity of dome rebar to absorb on soil reimpaction.

- Extensive damage to dome expected but catastrophic dome collapse not expected

- Fall in of debris is expected to be limited by remaining rebar net and primary liner - splash through of debris not expected or minimized.

- Post-event tank vacuum from cooldown would likely lead to additional sagging of dome.

At lower pressures

- Tank would be damaged but should maintain gross structural integrity

- Tank vacuum from cooldown is not expected to collapse the dome.

BURN AND STRUCTURAL RESPONSE ANALYSIS FOR TANK SY-101

LANL HMS/TRAC burn analysis of gas release volume for Tank SY-101 with 66 percent of fully open 42-inch diameter vent-flow area from multi-port riser (MPR)

Gas Volume (ft^3)	Waste Level (in.)	Pressure		Dome Response	
		Rate (psi/s)	Peak (psig)	Maximum Uplift (in.)	Peak Velocity (in/s)
8,650	398	312	43.4	12.0	50
9,230	398	325	45.3	14.5	65 *

* Exceeds critical dome velocity (estimated at 54.5 in/s) that would cause complete soil separation and subsequent failure of tank dome from soil reimpaction on basis of limiting kinetic energy at impact to the strain energy of the hoop rebar in the haunch region.

CAVEAT EMPTOR

- The estimation of "failure" pressures and "post-failure behavior" for a dynamic pressurization event in an underground reinforced concrete tank is difficult at best.

- The DELPHI results were guided by limited analyses and reinforced concrete failure test data that may or may not be directly applicable to the Hanford Tanks.

  - The only supporting "dynamic analysis" was for Tank SY-101. SST analyses have been static.

  - The test data are of qualitative interest - based on quasi-static pressurization of containment type vessels (Sandia Containment Failure Experiment) or on high pressure static and dynamic tests of unreinforced and reinforced concrete slabs (Army Corps of Engineering Data).

CAVEAT EMPTOR (continued)

- The Sandia containment test does support the initiation of failure at stiff discontinuities in the containment steel liner anchored to the concrete vault - similar to the primary tank dome discontinuities at thickness transition and riser-liner interface leading to the described "can-opener" type failure in the dome.

- The Army data supports the "blow-out" type failure of the concrete in SSTs and the retention of the concrete debris by the reinforcement net.

- However, the test data does not address the ability of the tank to continue to support the soil load in the post failure condition of the tank structure.

- The effect of venting through concrete cracks and soil to mitigate the peak pressure experienced in a SST had not been quantified.

- Although catastrophic dome collapse was not considered a likely failure mode, it can not be strictly ruled out either.

ARMY TESTS DATA

Reinforced Concrete Slab Local "Blow-Out" Type Failure
from Over-Pressurization with Air

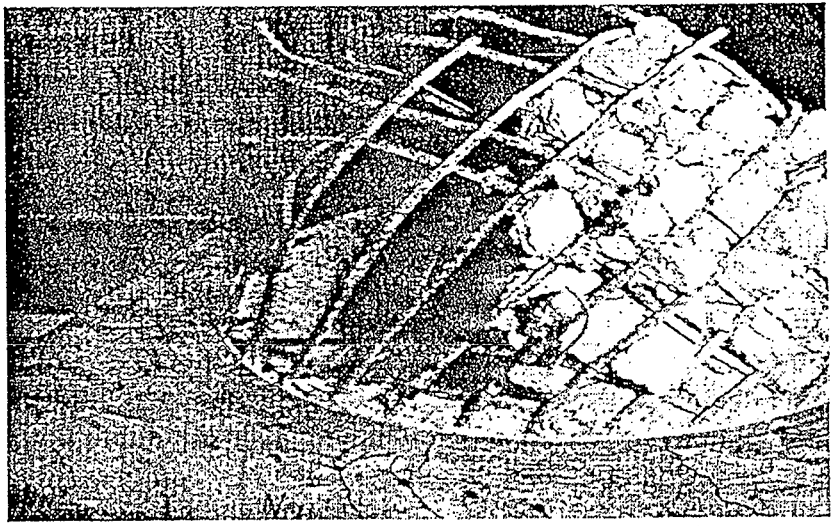

Note concrete retention by reinforcement net

Elicitation Parameters

1. ~~Maximum Achievable Void Fraction.~~
   obviated by $\rho_{net} < 1.41$, Meyer/Lessor/Stewart and TOC + Na/Al/NO_2 criteria.

2. ~~Efficiency of local release from nc layer when hydraulically, pneumatically or mechanically disrupted.~~
   obviated by panel specification that this is an engineering design requirement.

3. ~~Characteristic time for surface renewal.~~
   obviated by panel specification to make τ_{renew} proportional to $\tau_{release}$.

4. ~~Surface area disrupted by GRE or intrusive activity.~~
   obviated by panel specification to conservatively use area = A_{tank}.

5. Mass of material released from a DST.
   - 5a. Burn insufficient to fail HEPA
   - 5b. Burn with HEPA failure but no dome failure
   - 5c. Detonation with HEPA failure but no dome failure
   - 5d. Burn with dome failure
   - 5e. Detonation with dome failure

6. Probability of BD GRE-induced ignition source.
   - 6a. Small efficiency BD GRE
   - 6b. Medium efficiency BD GRE
   - 6c. Large efficiency BD GRE

7. Duration of a BD GRE
   - 7a. Small efficiency BD GRE
   - 7b. Medium efficiency BD GRE
   - 7c. Large efficiency BD GRE

8. Probability of an earthquake-induced GRE

8aa. Small efficiency GRE, 100-year quake, thick liquid layer DST
8ab. Medium efficiency GRE, 100-year quake, thick liquid layer DST
8ac. Large efficiency GRE, 100-year quake, thick liquid layer DST
8ad. Small efficiency GRE, 1,000-year quake, thick liquid layer DST
8ae. Medium efficiency GRE, 1,000-year quake, thick liquid layer DST
8af. Large efficiency GRE, 1,000-year quake, thick liquid layer DST
8ag. Small efficiency GRE, 10,000-year quake, thick liquid layer DST
8ah. Medium efficiency GRE, 10,000-year quake, thick liquid layer DST
8ai. Large efficiency GRE, 10,000-year quake, thick liquid layer DST
8ba. Small efficiency GRE, 100-year quake, FG2, pumped SST
8bb. Medium efficiency GRE, 100-year quake, FG2, pumped SST
8bc. Large efficiency GRE, 100-year quake, FG2, pumped SST
8bd. Small efficiency GRE, 1,000-year quake, FG2, pumped SST
8be. Medium efficiency GRE, 1,000-year quake, FG2, pumped SST
8bf. Large efficiency GRE, 1,000-year quake, FG2, pumped SST
8bg. Small efficiency GRE, 10,000-year quake, FG2, pumped SST
8bh. Medium efficiency GRE, 10,000-year quake, FG2, pumped SST
8bi. Large efficiency GRE, 10,000-year quake, FG2, pumped SST
8bj. Small efficiency GRE, 100-year quake, FG3, pumped SST
8bk. Medium efficiency GRE, 100-year quake, FG3, pumped SST
8bl. Large efficiency GRE, 100-year quake, FG3, pumped SST
8bm. Small efficiency GRE, 1,000-year quake, FG3, pumped SST
8bn. Medium efficiency GRE, 1,000-year quake, FG3, pumped SST
8bo. Large efficiency GRE, 1,000-year quake, FG3, pumped SST
8bp. Small efficiency GRE, 10,000-year quake, FG3, pumped SST
8bq. Medium efficiency GRE, 10,000-year quake, FG3, pumped SST
8br. Large efficiency GRE, 10,000-year quake, FG3, pumped SST
8ca. Small efficiency GRE, 100-year quake, FG2, unpumped SST
8cb. Medium efficiency GRE, 100-year quake, FG2, unpumped SST
8cc. Large efficiency GRE, 100-year quake, FG2, unpumped SST
8cd. Small efficiency GRE, 1,000-year quake, FG2, unpumped SST
8ce. Medium efficiency GRE, 1,000-year quake, FG2, unpumped SST
8cf. Large efficiency GRE, 1,000-year quake, FG2, unpumped SST
8cg. Small efficiency GRE, 10,000-year quake, FG2, unpumped SST
8ch. Medium efficiency GRE, 10,000-year quake, FG2, unpumped SST
8ci. Large efficiency GRE, 10,000-year quake, FG2, unpumped SST
8cj. Small efficiency GRE, 100-year quake, FG3, unpumped SST
8ck. Medium efficiency GRE, 100-year quake, FG3, unpumped SST
8cl. Large efficiency GRE, 100-year quake, FG3, unpumped SST
8cm. Small efficiency GRE, 1,000-year quake, FG3, unpumped SST
8cn. Medium efficiency GRE, 1,000-year quake, FG3, unpumped SST
8co. Large efficiency GRE, 1,000-year quake, FG3, unpumped SST
8cp. Small efficiency GRE, 10,000-year quake, FG3, unpumped SST
8cq. Medium efficiency GRE, 10,000-year quake, FG3, unpumped SST
8cr. Large efficiency GRE, 10,000-year quake, FG3, unpumped SST

9. Probability of an earthquake-induced ignition source.

9a. 100-year earthquake, thick liquid layer present
9b. 1,000-year earthquake, thick liquid layer present
9c. 10,000-year earthquake, thick liquid layer present

Key issues for seismic parameters:

- When is the liquid layer "thick"?
  liquid thickness > X? (X = absolute thickness, e.g. 1 m)
  liquid thickness divided by total waste depth < Y?
  (Y = fraction of waste height that is liquid, e.g. 10%)
- Does a tank that exhibits BD GREs have the same probability of seismic-induced GREs as a tank with a thick liquid layer but does not exhibit BD GREs, given that the earthquake magnitude and GRE efficiency is the same?
- For tanks with a thin liquid layer, do FG1 DSTs, FG2 DSTs, and unpumped FG2 SSTs have equivalent probabilities for seismic-induced GREs of equal release efficiency given the same earthquake magnitude?

Potential new parameters?

10. **Fraction of gas released from solids layer by steady-state mechanisms, $F_{ss\ rel}$.**
    - 10a. Tank at risk for BD GREs
    - 10b. Tank not at risk for BD GREs; thick liquid layer present
    - 10c. Saturated waste
    - 10d. Pumped waste

    Other potential conditioning factors:
    sludge, saltcake, FG2/FG3, [TOC], [Al], [Na], [NO_2]

    Gas generation in liquid layer already assumed steady state release.

11. **Frequency of spontaneous GREs by mechanisms other than BD when thick liquid layer is present but BD GREs are precluded.**
    - 11a. Small release efficiency
    - 11b. Medium release efficiency
    - 11c. Large release efficiency

    Other potential approach: absolute frequency of small releases + relative frequency of medium + relative frequency of large

    Other potential conditioning factors:
    sludge, saltcake, FG2/FG3, [TOC], [Al], [Na], [NO_2]

    Amount of release for each efficiency is determined by conservation of gas:
    $\sum$(release efficiency x volume retained gas x frequency of release)
    = (1-$F_{ss\ rel}$) x total gas generation in solids layer

Potential Sources of Significant Conservatism In AF for SSTs

No Steady-State Gas Release, only GREs

Void Fraction

Frequency of Induced Release for each release efficiency

Frequency of Spontaneous Release Efficiency

Probability of GRE-induced Ignition Source

99.5% Meteorology

Duration of Stratified Layer Time at Risk

Release Gas Concentration in Stratified Layer (centerline vs. average plume concentration when plume reaches dome)

Mass Suspended

Respirable Fraction of Mass Suspended

No Source Material Deposition or Splashback

No Overburden Filtration

ULDs Versus Actual Tank Inventories

Evidence of Conservatism in AF for SSTs

Mass Balance on Gas Generation & Release

Void Fraction Distribution Tails

Deflagration Release Frequency Mismatch to Historical Observations

Respirable Fraction Compared to Experiments and Experience

ULDs Versus Actual Tank Inventories

Mass Balance on Gas Generation & Release

Representative Tank TX-112

649,000 gal waste (~6.0 m depth, ~2460 m^3)

Calc Note 116 estimates 9.45×10^{-4} ft^3/min (14.07 m^3/yr)

50th Percentile Void Fraction (FG2 unpumped) ~12%
x 2460 m^3 waste x 1.5 atm avg pressure = ~440 m^3 retained

50th Percentile Release Frequencies:
small ~ 1/yr, medium ~ 1/150 yr, large ~ 1/100,000 yr.

Small ~ 2% efficient release, Medium ~ 10%, Large ~ 35%:
annual release = 0.02 x 440 m^3 x 1/yr
+ 0.10 x 440 m^3 x 1/150 yr
+ 0.35 x 440 m^3 x 1/100,000 yr
= 9.095 m^3/yr

90th Percentile Void Fraction ~ 28.5%
x 2460 m^3 waste x 1.22 atm avg press = ~ 850 m^3 retained

90th Percentile Release Frequencies:
small ~ 7/yr, medium ~ 1/5 yr, large ~ 1/500 yr

annual release = 0.02 x 850 m^3 x 7/yr
+ 0.10 x 850 m^3 x 1/5 yr
+ 0.35 x 850 m^3 x 1/500 yr
= 119.0 + 17.0 + 0.595 = 136.6 m^3/yr

Mass Balance on Gas Generation & Release (Cont.)

stimated tank gas generation rate = 14.07 m^3/yr

as per small release = 0.02 x 850 m^3 = 17.0 m^3/rel
nedium = 0.10 x 850 m^3 = 85.0 m^3/rel
arge = 0.35 x 850 m^3 = 297.5 m^3/rel

small = 17.0 m^3/rel x 7 rel/yr = 119.0 m^3/yr
medium = 85.0 m^3/rel x 1/5 yr = 17.0 m^3/yr
arge = 297.5 m^3/yr x 1/500 yr = 0.595 m^3/yr

gas gen rate from $\sum$(efficiency x volume x *f*) = 136.6 m^3/yr

small = 119.0 m^3/yr / 136.6 m^3/yr = 87.119% of gas release
medium = 17.0 m^3/yr / 136.6 m^3/yr = 12.446%
large = 0.595 m^3/yr / 136.6 m^3/yr = 0.435%

small = 87.119% x 14.07 m^3/yr = 12.26 m^3/yr
medium = 12.446% x 14.07 m^3/yr = 1.752 m^3/yr
large = 0.435% x 14.07 m^3/yr = 0.0613 m^3/yr

OPTION 1: Adjust release <u>amounts</u> to match gas generation
small = 12.26 m^3/yr / 7 release/yr = 1.75 m^3/release
medium = 1.752 m^3/yr / 1 release/5 yr = 8.76 m^3/release
large = 0.0613 m^3/yr / 1 release/500 yr = 30.65 m^3/release

OPTION 2: Adjust release <u>frequencies</u> to match gas generation
small = 12.26 m^3/yr / 17.0 m^3/rel = 1 rel/1.39 yr
medium = 1.752 m^3/yr / 85.0 m^3/rel = 1 rel/48.5 yr
large = 0.0613 m^3/yr / 297.5 m^3/rel = 1 rel/4853 yr

Adjusting amounts or frequencies to match total gas generation if

$$\sum(\text{efficiency} \times \text{volume} \times f) > \text{estimated gas generation}$$

results in zero steady state release.

Recommendation: the fraction of gas generated that is released by steady state mechanisms, $F_{ss\ rel}$, should be estimated and the GRE amounts or frequencies adjusted to:

$$\sum(\text{efficiency} \times \text{volume} \times f) = (1-F_{ss\ rel}) \times \text{est. gas generation}$$

Elicitation Parameters

5A. Mass of transportable material suspended/released from a DST.

5Aa. Total mass of transportable waste suspended in DST headspace by burn insufficient to fail HEPA

5Ab. Total mass of transportable waste suspended in DST headspace by burn < 20 psig with HEPA failure

5Ac. Total mass of transportable waste suspended in DST headspace by burn > 20 psig but no dome failure

5Ad. Total mass of transportable waste released from DST by burn that causes dome failure

5Ae. Total mass of transportable waste released from DST by detonation that causes dome failure

5B. Mass of respirable material suspended/released from a DST.

5Ba. Total mass of respirable waste suspended in DST headspace by burn insufficient to fail HEPA

5Bb. Total mass of respirable waste suspended in DST headspace by burn < 20 psig with HEPA failure

5Bc. Total mass of respirable waste suspended in DST headspace by burn > 20 psig but no dome failure

5Bd. Total mass of respirable waste released from DST by burn that causes dome failure

5Be. Total mass of respirable waste released from DST by detonation that causes dome failure

6. Probability of BD GRE-induced ignition source.

6a. Small efficiency BD GRE

6b. Medium efficiency BD GRE

6c. Large efficiency BD GRE

7. Duration of a BD GRE (time to ~95% of peak headspace concentration).

7a. Small efficiency BD GRE

7b. Medium efficiency BD GRE

7c. Large efficiency BD GRE

8. Probability of an earthquake-induced GRE

8aa. Small efficiency GRE, 100-year quake, thick liquid layer DST
8ab. Medium efficiency GRE, 100-year quake, thick liquid layer DST
8ac. Large efficiency GRE, 100-year quake, thick liquid layer DST
8ad. Small efficiency GRE, 1,000-year quake, thick liquid layer DST
8ae. Medium efficiency GRE, 1,000-year quake, thick liquid layer DST
8af. Large efficiency GRE, 1,000-year quake, thick liquid layer DST
8ag. Small efficiency GRE, 10,000-year quake, thick liquid layer DST
8ah. Medium efficiency GRE, 10,000-year quake, thick liquid layer DST
8ai. Large efficiency GRE, 10,000-year quake, thick liquid layer DST

8ba. Small efficiency GRE, 100-year quake, FG2, pumped SST
8bb. Medium efficiency GRE, 100-year quake, FG2, pumped SST
8bc. Large efficiency GRE, 100-year quake, FG2, pumped SST
8bd. Small efficiency GRE, 1,000-year quake, FG2, pumped SST
8be. Medium efficiency GRE, 1,000-year quake, FG2, pumped SST
8bf. Large efficiency GRE, 1,000-year quake, FG2, pumped SST
8bg. Small efficiency GRE, 10,000-year quake, FG2, pumped SST
8bh. Medium efficiency GRE, 10,000-year quake, FG2, pumped SST
8bi. Large efficiency GRE, 10,000-year quake, FG2, pumped SST
8bj. Small efficiency GRE, 100-year quake, FG3, pumped SST
8bk. Medium efficiency GRE, 100-year quake, FG3, pumped SST
8bl. Large efficiency GRE, 100-year quake, FG3, pumped SST
8bm. Small efficiency GRE, 1,000-year quake, FG3, pumped SST
8bn. Medium efficiency GRE, 1,000-year quake, FG3, pumped SST
8bo. Large efficiency GRE, 1,000-year quake, FG3, pumped SST
8bp. Small efficiency GRE, 10,000-year quake, FG3, pumped SST
8bq. Medium efficiency GRE, 10,000-year quake, FG3, pumped SST
8br. Large efficiency GRE, 10,000-year quake, FG3, pumped SST
8ca. Small efficiency GRE, 100-year quake, FG2, unpumped SST
8cb. Medium efficiency GRE, 100-year quake, FG2, unpumped SST
8cc. Large efficiency GRE, 100-year quake, FG2, unpumped SST
8cd. Small efficiency GRE, 1,000-year quake, FG2, unpumped SST
8ce. Medium efficiency GRE, 1,000-year quake, FG2, unpumped SST
8cf. Large efficiency GRE, 1,000-year quake, FG2, unpumped SST
8cg. Small efficiency GRE, 10,000-year quake, FG2, unpumped SST
8ch. Medium efficiency GRE, 10,000-year quake, FG2, unpumped SST
8ci. Large efficiency GRE, 10,000-year quake, FG2, unpumped SST
8cj. Small efficiency GRE, 100-year quake, FG3, unpumped SST
8ck. Medium efficiency GRE, 100-year quake, FG3, unpumped SST
8cl. Large efficiency GRE, 100-year quake, FG3, unpumped SST
8cm. Small efficiency GRE, 1,000-year quake, FG3, unpumped SST
8cn. Medium efficiency GRE, 1,000-year quake, FG3, unpumped SST
8co. Large efficiency GRE, 1,000-year quake, FG3, unpumped SST
8cp. Small efficiency GRE, 10,000-year quake, FG3, unpumped SST
8cq. Medium efficiency GRE, 10,000-year quake, FG3, unpumped SST
8cr. Large efficiency GRE, 10,000-year quake, FG3, unpumped SST

9. **Probability of an earthquake-induced ignition source in a DST.**
   - 9a. 100-year earthquake
   - 9b. 1,000-year earthquake
   - 9c. 10,000-year earthquake

11. **Frequency of spontaneous GREs in DSTs when thick liquid layer is present but criteria for potential BD GREs are not met.**
   - 11a. Small efficiency release
   - 11b. Medium efficiency release
   - 11c. Large efficiency release

- When is the liquid layer "thick"?
  liquid thickness > 1 meter
- For DSTs with liquid layer < 1 m, use unpumped FG2 SST probabilities for seismic-induced GREs

Refined Safety Analysis Methodology for
Flammable Gas Risk Assessment in Hanford Site Tanks

Respirable Material Release

February 11, 1998

Fred Gelbard & John Brockmann

OBJECTIVE: Quantify Effects on Respirable Material Release

- **Aerosolization**
  - Previously elicited respirable mass suspended (SSTs concrete dome, DSTs steel dome)
  - convective entrainment (data for dry powders)
  - smash and splash (data for glass rods)
- **All DSTs have active ventilation**
  - without dome collapse, for SSTs previously used pressure drop to release suspended aerosol
- **Washout by debris falling and collecting suspended aerosol**
- **Filtration by flow through overburden**

Respirable Fraction in SY101

Height (inches)	Percent Mass Less than 10 μm in diameter
372.5	70
277.5	95
182.5	75
144.5	100
68.5	90
11.5	55
Average	81

Herting et al., 1992, WHC-SD-WM-DTR-026.

"There is a minor tendency for volume to concentrate about the 4 to 6-μm range" p. 6-4.

Particle Removal by Falling Debris

Efficiency = fraction of aerosol removed from swept volume of a falling particle

Stokes Number = Stk = $\frac{\text{stopping distance of a particle}}{\text{characteristic dimension of obstacle}}$

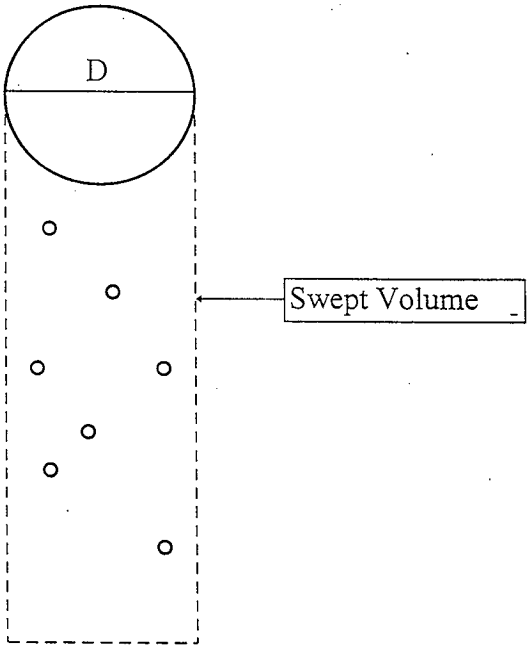

Particle Collection by Falling Debris

Plot on next page taken from M. J. Matterson and M. B. Prince, Aerosol Science and Technology, 12:745 (1990)

- Stokes Number = Stk = $[v\rho_{part}d_p^2]/[9\mu D]$
- Effective Stokes Number = Stk_{eff} = $1.22(Stk)(Re_p)^{-0.22}$
- Particle Reynolds Number = $Re_p = vd_p\rho_{gas}/\mu$
- d_p = aerosol particle diameter
- D = collecting particle diameter

Matterson and Prince (1990)

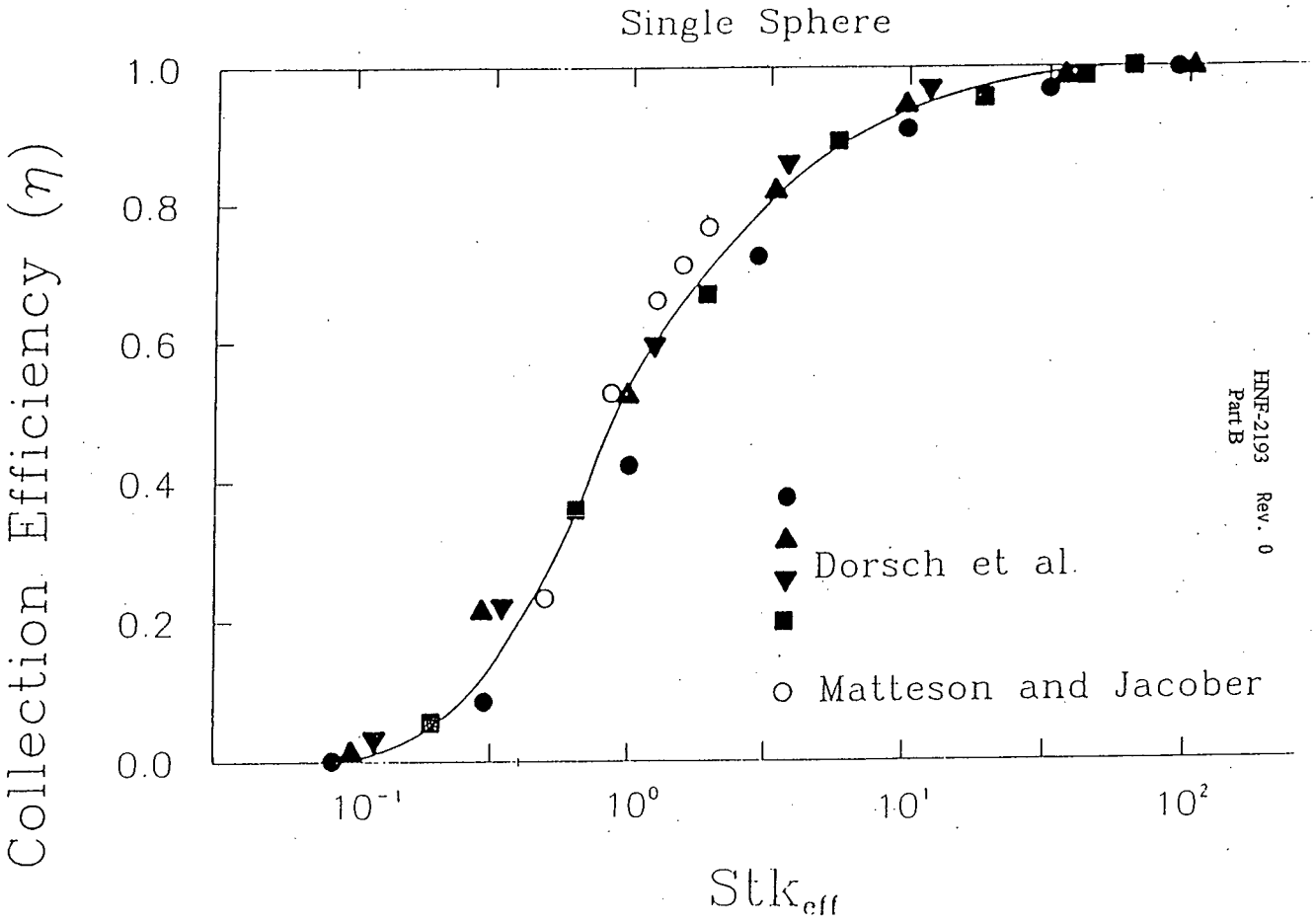

Collection Efficiency

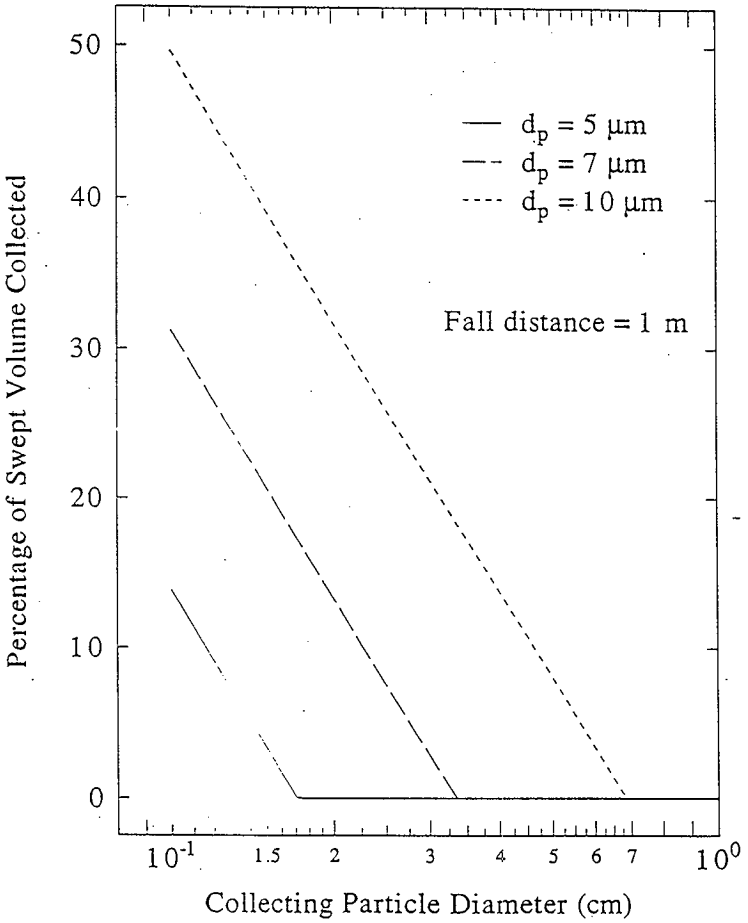

Collection Efficiency
(Powers and Burson, 1992, SAND92-2689)

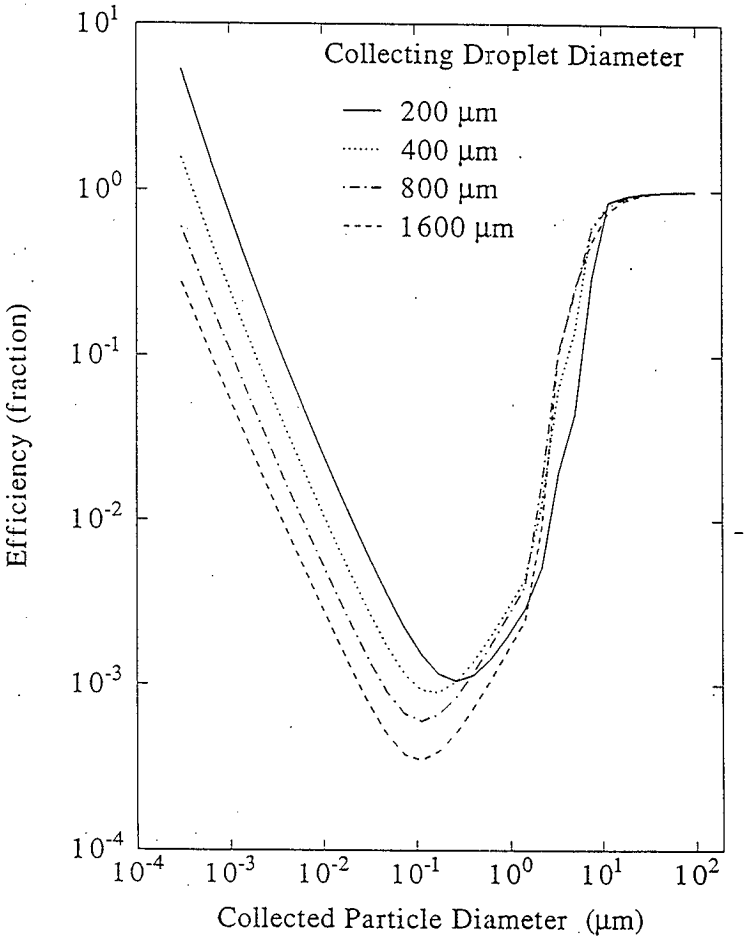

Gravel Filtration Correlations

- **Assumptions:**
  - Fixed bed of uniform spheres (i.e. no channels)
  - Steady flow
  - 8 ft of overburden
  - 40 psi pressure differential
  - Reference: Otani, Y., C. Kanaoka, and H. Emi, "Experimental Study of Aerosol Filtration by Granualr Bed Over a Wide Range of Reynolds Numbers" Aerosol Science and Technology, 10:463-474 (1989).
- **18 Feet Engineered Gravel Gertie Explosion Test: Respirable Release Fraction 0.5%**

Penetration Efficiency
(8 ft thick, 35% porosity, 40 psi pressure differential)

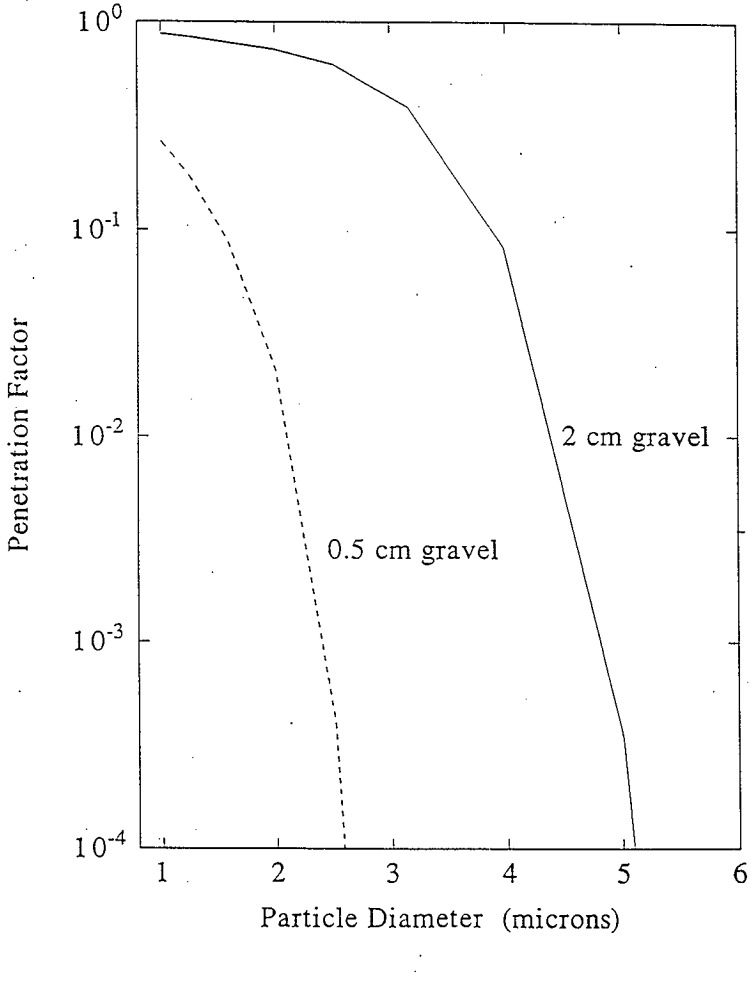

Summary

- Collection efficiency correlations available for washout by debris falling through aerosol cloud.
- For 8 ft of dirt that remains intact, correlation available for estimating penetration factor.
- Proposing that 80% of suspended mass is respirable based on particle size analysis.
- Data appended for convective entrainment of dry powders

Convective Entrainment Data
Dry Powders

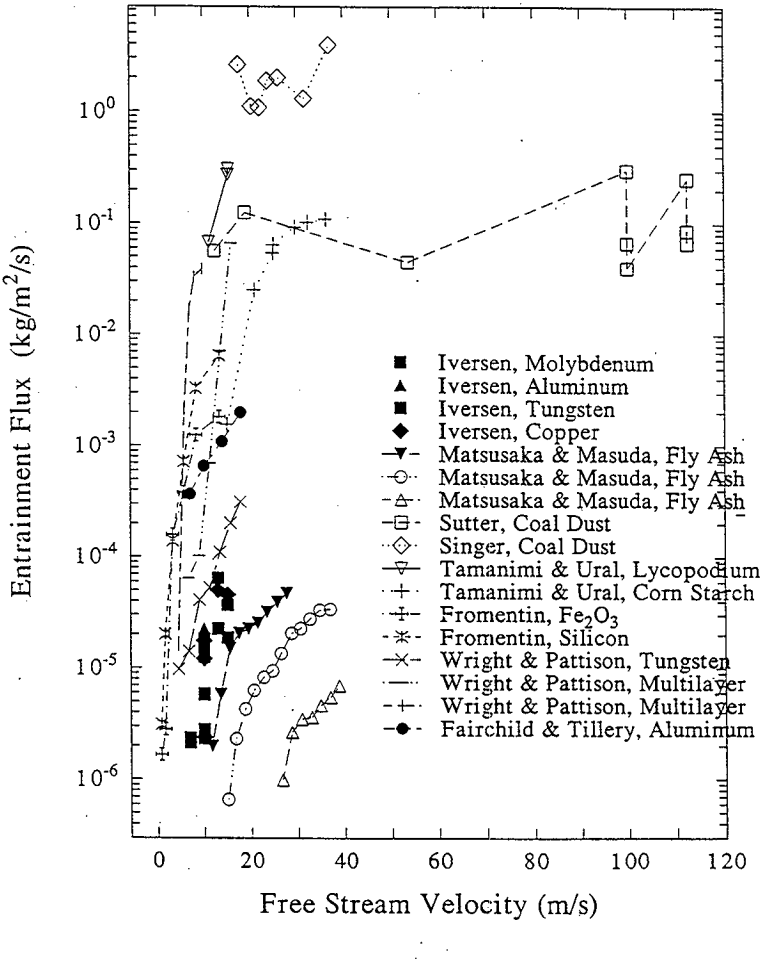

Summary Table

Investigator	Affiliation	Flow	Material	Deposit	Particle size	Remarks
Iversen[1]	Iowa State University (work performed at LANL)	Steady	Aluminum	Monolayer	3.3 and 4.6 μm	Velocities from about 7 to 15 m/sec and acceleration from about 1 to 4 m/sec^2
		Steady	Molybdenum	Monolayer	5.1 to 15 μm	
		Steady	Tungsten	Monolayer	8.4 μm	
		Steady	Copper	Monolayer	< 10 μm	
Matsusaka & Masuda[2]	Kyoto University	Steady	Fly Ash	Multilayer (flush)	3 μm	Velocity = 11 to 28 m/sec Acceleration = 0.6 m/sec^2
		Steady	Fly Ash	Multilayer (flush)	3 μm	Velocity = 15 to 39 m/sec Acceleration = 0.1 m/sec^2
		Steady	Fly Ash	Multilayer (flush)	3 μm	Velocity = 27 to 39 m/sec Acceleration = 0.01 m/sec^2
Singer et al.[3]	U. S. Bureau of Mines	Steady	Coal Dust	Multilayer (protruding)	< 14 μm	Velocity = 17 to 37 m/sec
Sutter.[4] (Singer et al.)	PNL	Air Blast	Coal Dust	Multilayer (protruding)	< 14 μm	Instantaneous velocities from 12 to 112 m/sec
Tamanini & Ural[5]	FMRC	Air Blast	Lycopodium	Monolayer	28 μm	Peak Velocity = 11 to 15 m/sec
		Air Blast	Corn Starch	Monolayer	12 μm	Peak Velocity = 15 to 36 m/sec
Fromentin[6]	Paul Scherrer Inst.	Steady	Si	Multilayer (slightly protruding)	2.8 μm	Velocity = 0.7 to 13 m/sec
		Steady	Fe2O3	Multilayer (slightly protruding)	~ 1 μm	Velocity = 0.7 to 13 m/sec
Fairchild & Tillery[7]	LANL	Steady	Aluminum	Monolayer	8.7 μm	Velocity = 7 to 18 m/sec
Wright & Pattison[8]	ORNL	Steady	Tungsten	Monolayer	0.5 μm	Velocity = 4.5 to 18 m/sec
		Steady	Tungsten	Multilayer (slightly protruding)	0.5 μm	Velocity = 7 to 16 m/sec
		Steady	Tungsten	Multilayer (slightly protruding)	10 μm	Velocity = 4.5 to 10 m/sec

Smash & Splash

To determine aerosolization from dome collapse

Experiments for smashing glasses and ceramic materials against a hard surface correlated with

$$V_{respirable} = 2 \times 10^{-10} [E_{impact}(J)/Volume] Volume$$

$$10^6 \text{ J/m}^3 < [E_{impact}(J)/Volume] < 10^7 \text{ J/m}^3$$

(MacDougall, Scully and Tillerson, SAND84-2641, 1987)

To apply, need kinetic energy of falling debris and volume of waste impacted.

Gravel Gertie Filtration

To determine venting filtration through overburden

Luna, Sandoval, Taylor, Grandjean, and Newton, SAND83-0840, 1984

Gravel Gertie	Hanford
• Gravel depth about 18 feet (gravel size 1- 3 inches)	8 feet of dirt with inches of gravel
• Gravel supported by wire mesh to allow venting	Concrete dome may inhibit venting
• Measured respirable release fraction $5.1 \times 10^{-3} \pm 4.0 \times 10^{-3}$	

Proposed Analysis Framework for Ammonia Release During Buoyant Displacement GREs and Waste Intrusive Activities - Part II

February 11, 1998

Wu-Ching Cheng

Outline

- Clarification of Mass Transfer Resistance in Gas Phase
- Sensitivity of Model to Ammonia Concentration in the Waste
- Application of Model to Waste Transfers

Mass Transfer Resistance in Gas Phase

- Overall resistance as sum of liquid and vapor phase resistances:

  $$1/h = 1/h_L + HRT/h_g$$

- Chilton-Colburn Analogy:

  $$Nu/Pr^n = Sh/Sc^n$$

- Correlation for Natural (Thermal) Convection

  $Nu/Pr^{1/3} = 0.15\ Gr^{1/3}$ $\qquad$ $Sh/Sc^{1/3} = 0.15\ Gr^{1/3}$

Mass Transfer Resistance in Gas Phase (continued)

Parameters

- μ= 0.017 cp = 1.7 x 10^{-5} kg/m-s
- ρ = (P/RT) (MW) = 1.17 kg/m3
- C_p = 0.25 cal/g-^{0}C = 1050 J/kg-^{0}C
- k = 0.0265 W-m/m^2 - ^{0}C
- D_g = 2.5 x 10^{-5} m^2/s
- $\beta = 1/V(dV/dT)_p = (1/V)(nR/P)$ = 3.3 x 10^{-3} K^{-1}
- L_c = area/perimeter = $\pi r^2/2\pi r = r/2$ = 11.4 m for the tank
- Sc = $\mu/\rho D_g = 0.581$
- Gr = $(g\ \beta\ \rho^2\ L_c^3\ \Delta T) / \mu^2 = 2.27 \times 10^{11}$
- ΔT = 1 ^{0}C
- Pr = $\mu Cp/k$ = 0.674
- HRT = 99.5

Mass Transfer Resistance in Gas Phase (continued)

Results

- $h_g = 1.66 \times 10^{-3}$ m/s
- Gas Phase Resistance $HRT/h_g = 6.0 \times 10^4$ s/m
- Liquid Phase Resistance $1/h_L = 8.3 \times 10^5$ s/m
  (for $\tau_{renew} = 2000$ s)
- Gas Phase Resistance/Liq. Phase Resistance = 0.072

Conclusion

- Gas phase resistance is small compared with liquid phase resistance.

Ammonia Release During Transfers

Model as Three Parts

- Falling waste column
- Turbulent waste surface
- Secondary disturbance region

For Each Region, Develop h_L and h_g
Then $1/h = 1/h_L + HRT/h_g$

Note: For m and T, use the larger of either the transferred or receiving waste for Turbulent and Secondary regions

Falling Waste Column

- "Fresh" waste is exposed
- Effective mass transfer area

  $A = f_1 A_{column}$ (suggest $f_1 = 10$)
- Liq. film coeff. is ave. over L

  $t_{fall} = (1/g)[(u_0^2+2gL)^{0.5} - U_0]$

  $h_L=(1/L)(D_L/4\phi)^{0.5}(2U_0 t_{fall}^{1/2} + 2/3\ g t_{fall}^{3/2})$
- **Vapor film coefficient by Chilton-Colburn analogy for flat plate**

  $h_g=0.664(D_g/d_{pipe})Re^{1/2} Sc^{1/3}$

Turbulent Waste Surface

- $d_T = f_2\, d_{pipe}$ suggest $f_2 = 10$
- Gas film coefficient

  Use same as for falling waste
- Liquid film coefficient

  Suggest $\tau_{renew} = d_T/U_{max}$

  then $h_L = (D_L/\tau_{renew})^{0.5}$

Parameters

Waste falling in air

f1= 10
density=1.18 kg/m3
viscosity=1.98E-05 kg/m-s
dpipe= 0.15 m
A= 23.93 m2
DL= 2.90E-09m2/s
Dg= 2.50E-05m2/s
Sc= 0.67 gas phase
L= 5 m
U0= 0.70 m/s
tfall= 0.94 s
Re=7.36E+04 gas phase
hg= 2.6E-02 m2/s
HRT= 1.00E+02
hL= 2.3E-05 m2/s
h=2.09E-05 m2/s

Turbulent

f2= 10
A= 1.823m2
Umax= 9.9 m/s
trenew= 0.154 s
hl=1.4E-04 m2/s
hg= 2.6E-02 m2/s
h= 9.0E-05m2/s

Secondary

f3= 30
A= 16.4
hg=1.70E-03 m2/s
h=1.7.E-05 m2/s

Region of Secondary Disturbance

- $d_{SD} = f_3 d_{pipe}$ (suggest $f_3 = 30$)
- h_L is difficult to model because of wave actions
- Assume mass transfer is gas phase limited and obtain h_g by natural convection relationship
- This gives a conservative result if liquid phase transfer is slower than gas phase transfer

Results

Release Rate, mole/s

Tank	m	column	turbulent	secondary	total	GRE
SY-101	360	0.18	3.0E-05	0.10	0.28	0.56
SY-103	360	0.18	3.0E-05	0.10	0.28	0.039
AN-105	4.2	2.1E-03	3.4E-07	1.2E-03	3.3E-03	6.4E-04

Note: m is in g-mole/m3

Conclusions

- Inclusion of gas-phase resistance with best estimate waste ammonia concentrations results in good agreement with GRE data
- Model calculations for transfers indicate release rates are in same order or greater than releases during GREs

Experimental and Theoretical Turbulent Diffusion Modeling of Global Light Gas Releases in a Tank Headspace

M. Epstein
and
J. P. Burelbach
Fauske & Associates, Inc.
Burr Ridge, Illinois

Presented at:
Gas Release Event Safety Analysis
Stage II Experts' Panel Elicitation Workshop #2

Richland, Washington

February 9-13, 1998

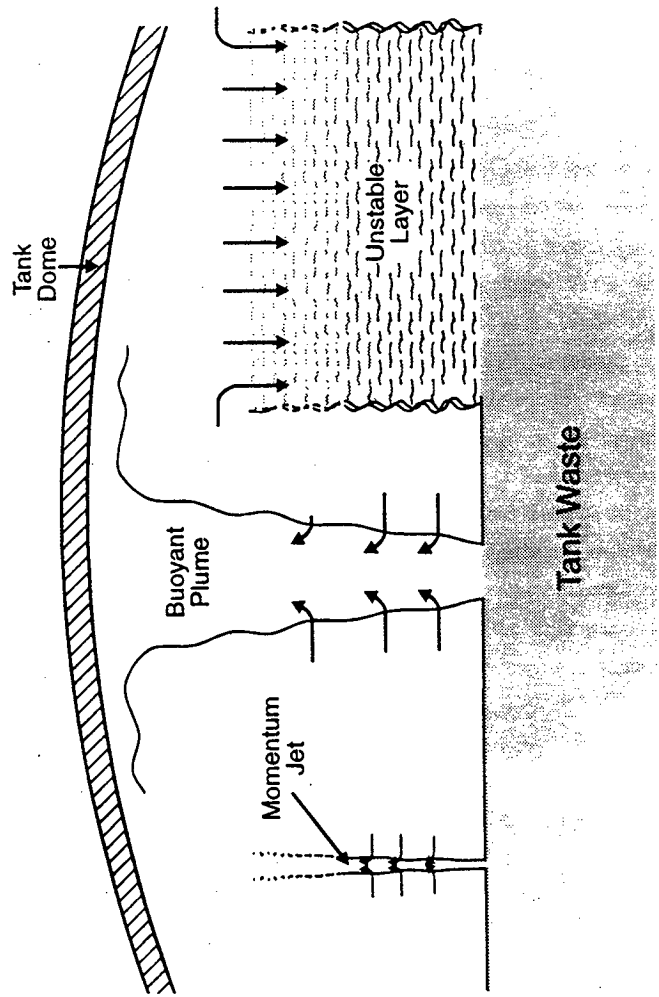

Figure 1-1 Light gas release regimes.

Problem Statement

1. **Consider global gas release events (GREs) characterized by release over a large fraction of the waste surface and by fairly uniform headspace concentration except early in time near the waste surface.**

2. **GRE is usually not of sufficient size to achieve the lower flammability limit (LFL) in the headspace as a whole; however,**

3. **the released gas concentration will exceed its LFL during the GRE in the transient concentration boundary layer just above the waste surface.**

4. **Can flammable gas concentrations in the boundary layer increase to levels that could threaten the tank dome?**

Gravitational Mixing Diffusion Coefficient
(Baird & Rice, 1975)

$$\dot{m}''(z,t) = -\rho D_T \frac{\partial Y}{\partial z}$$

$\dot{m}''$ = upward mass flux of light fluid

Y = mass fraction of light fluid

ρ = mixture density

z = vertical distance above release surface

$$D_T = \ell^2 \left(\frac{g}{\rho} \frac{\partial \rho}{\partial z} \right)^{1/2}$$

ℓ = characteristic mixing length

Previous Work on Gravitational Mixing in High-Aspect Ratio Tubes

Baird & Rice, 1975

Gardner, 1977

Epstein, 1988

Baird & Ramo Rao, 1991

Holmes et al., 1991

Baird et al., 1992

$\ell \simeq 0.65\ D$ **(D = tube diameter)**

Question: **What is ℓ for mixing layers that are broader than they are tall?**

Diffusion Theory for Dilute Solutions

$$D_T = \ell^2 \left(gk \frac{\partial Y}{\partial z} \right)^{1/2}$$

$$k = \begin{cases} 0.64 & \text{Brine/Water} \\ -\left(\frac{M_H}{M_L} - 1 \right) & \text{Heavy gas/Light gas (GRE)} \end{cases}$$

Species Conservation Equation:

$$\frac{\partial Y}{\partial t} = (gk)^{1/2} \frac{\partial}{\partial t} \left[\ell^2 \left(\pm \frac{\partial Y}{\partial z} \right)^{3/2} \right]$$

Boundary condition at release (waste) surface (i.e. at z = 0)

$$(gK)^{1/2} \left[\ell^2 \left(\pm \frac{\partial Y}{\partial z} \right)^{3/2} \right] = \begin{cases} u_0 Y_0 & \text{Brine/Water} \\ u_0 M_L / M_H & \text{Heavy gas/Light gas} \end{cases}$$

Y_0 = initial solute (salt) mass fraction
u_0 = light fluid release (injection) velocity
M = molecular weight

Potential Natural Length Scales for ℓ

$\ell = \ell_0$ = constant

$\ell = \alpha u_0 t$

$\ell = \beta\delta$ (see note)

α,β = empirical constants to be determined by experiment

δ = instantaneous vertical height (thickness) of mixing layer

Note: Similar length scale used in application of Prandtl's mixing length model to momentum transport in jets or wakes.

Asymptotic Similarity Solution to Diffusion Equation for Brine/Water System and $\ell = \beta\delta$

Mixing length thickness:

$$\delta(t) = 9.94\ \beta^2\ (gku_0Y_0)^{1/2}\ t^{3/2}$$

Solute (salt) mass fraction

$$Y(z,t) = Y_0 - \frac{0.216}{\beta^2}\left(\frac{u_0Y_0}{gkt}\right)^{1/2} f(\xi)$$

$$\xi = \frac{0.216\ z}{\beta^2\ (gku_0Y_0t^3)^{1/2}}$$

1. **Complete solution with molecular diffusion and forced convection converges to asymptotic solution in less than 0.5 sec.**

2. **β can be determined by measuring mixing length and/or solute mass fraction.**

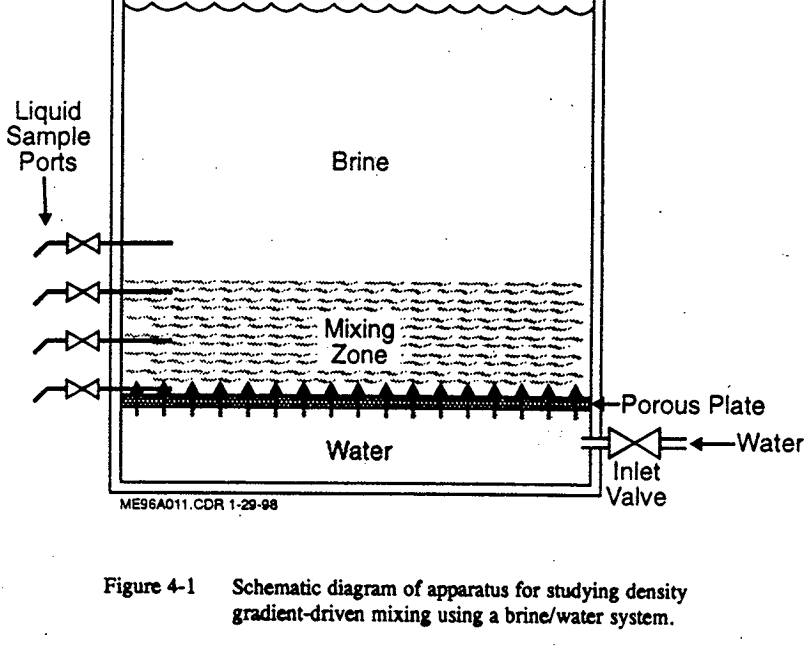

Figure 4-1 Schematic diagram of apparatus for studying density gradient-driven mixing using a brine/water system.

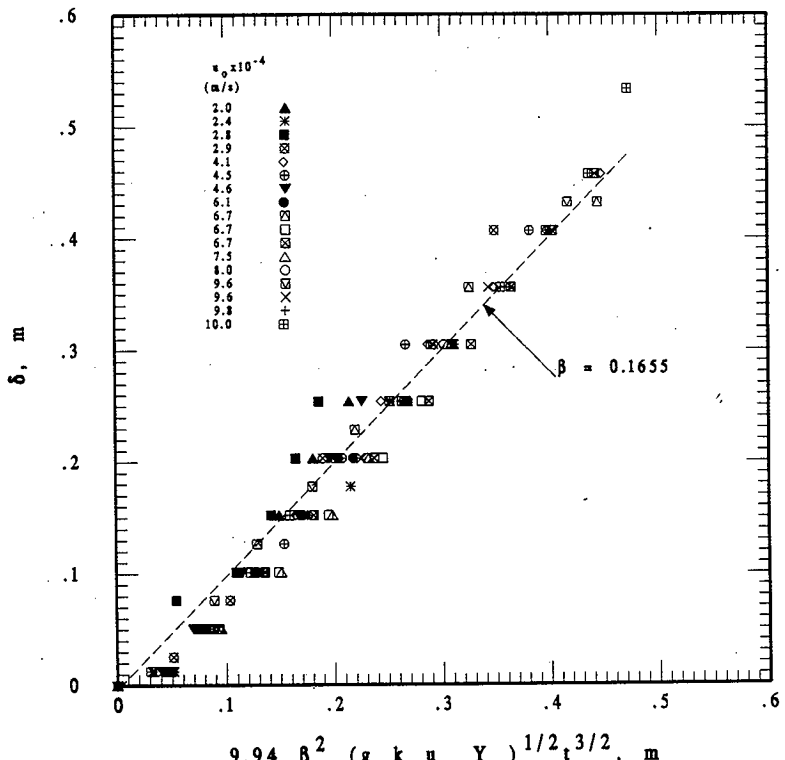
$u_o \times 10^{-4}$ (m/s)
2.0
2.4
2.8
2.9
4.1
4.5
4.6
6.1
6.7
6.7
6.7
7.5
8.0
9.6
9.6
9.8
10.0
β = 0.1655
δ, m
0
.1
.2
.3
.4
.5
.6
9.94 β² (g k u_o Y_o)^1/2 t^3/2, m

Asymptotic Similarity Solution to Diffusion Equation for GRE

Mixing length thickness:

$$\delta(t) = 9.94\ \beta^2\ [g\ u_0\ (1 - M_L/M_H)\ t^3]^{1/2}$$

Released gas mass fraction at waste surface

$$Y(0,t) = \frac{0.303}{\beta^2}\left[\frac{(M_L/M_H)\ u_0}{g(M_H/M_L - 1)\ t}\right]^{1/2}$$

Approximate released gas mass fraction distribution in mixing layer

$$Y(z,t) = Y(0,t)\left[1 - \frac{z}{\delta(t)}\right]^2$$

Mass of flammable gas within layer:

$$m_f = A_{rel}\ \rho \int_0^{z_{LFL}(t)} Y(z,t)\ dz = \frac{A_{rel}}{3}\ \rho\ Y(0,t)\ \delta(t)\left[1 - \left(1 - \frac{z_{LFL}}{\delta}\right)^3\right]$$

Z_{LFL} = instantaneous vertical distance to lower flammability plane

A_{rel} = release area

Example

GRE: 60 m^3 of H_2 gas released over 2 min through A_{rel} = 100 m^2 of waste surface (u_0 = 5 mm s^{-1}).

Predictions:

$v_{H_2,max}$ = 3.48 m^3 (5.8% of total H_2 released)

t_{max} = 16.5 s

$\delta(t_{max})$ = 4.11 m

$z_{LFL}(t_{max})$ = 0.7 m

$\bar{Y}_{H_2}(t_{max})$ = 3.49 x 10^{-3} (20% above LFL)

$\Delta P_{comb.}$ = 3.3 psi (stoichiometric)

$\Delta P_{comb.}$ = 1.3 psi (incomplete combustion)

Conclusion

Flammable gas buildup in the boundary layer above the waste surface to levels that could threaten the tank wall is unlikely.

TENTATIVE CRITERION FOR PLUME/MIXING LAYER TRANSITION

Mole fraction of light (released) gas at waste surface as a function of height $\delta(t)$ of mixing zone:

$$x[0,\delta(t)] = x_s = \frac{0.652}{\beta^{4/3}} \left[\frac{u_o^2}{g\ (1 - M_L/M_H)\ \delta} \right]^{1/3}$$

Region just above waste purged of headspace air if $x_s \simeq 1.0$. Thus the critical purging velocity is

$$u_o = 0.055 \left[g\delta\ (1 - M_L/M_H) \right]^{1/2}$$

What is δ?

TENTATIVE CRITERION FOR PLUME/MIXING LAYER TRANSITION (Continued)

Compare with flooding correlation of Epstein & Kenton (1989)

$$u_o = 0.24 \left[gD\ (1 - M_L/M_H)\right]^{1/2}$$

D = diameter of release area.

Recommendation:

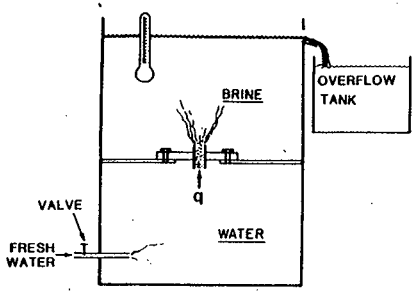

Fig. 3 Schematic diagram of the apparatus for the determination of the flooding flow rate at steady state by water injection

Plume behavior anticipated if

$$u_o \geq 0.055 \left[g\delta\ (1 - M_L/M_H)\right]^{1/2}$$

$$\delta = D \quad , \quad D \leq H$$

Otherwise $\delta = H$

TENTATIVE CRITERION FOR PLUME/MIXING LAYER TRANSITION (Continued)

As vertical distance above release area increases the unstable layer may become plume-like.

Air entrained by mixing (unstable) layer ($u\ell$)

$$Q_{u\ell} = 0.65\, A_{rel} \left[g\, u_o\, (1 - M_L/M_H)\, z\right]^{1/3}$$

Air entrained by plume ($p\ell$)

$$Q_{p\ell} = 0.15 \left[A_{rel}\, u_o\, g\, (M_H/M_L - 1)\, z^5\right]^{1/3}$$

Unstable layer transitions to plume at height z_{tr} where $Q_{p\ell} \simeq Q_{u\ell}$:

$$z_{tr} \simeq 3.0 \left(\frac{M_L}{M_H}\right)^{1/4} A_{rel}^{1/2}$$

Example: $M_L = 2.0$ $M_H = 29.0$

$A_{rel} = 1.0\ m^2$ $z_{tr} = 1.5\ m$

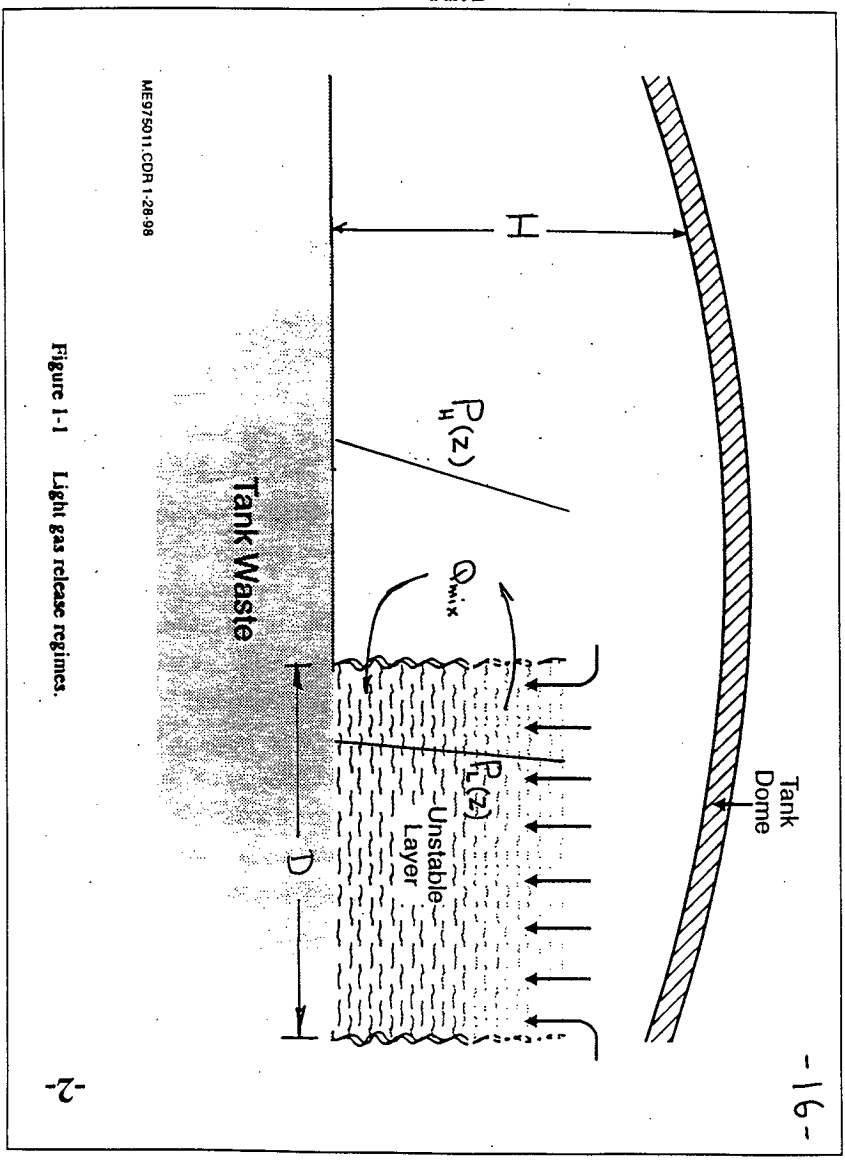

Figure 1-1 Light gas release regimes.

HEADSPACE AIR/UNSTABLE LAYER MIXING TIME

$$Q_{mix} \simeq D \sqrt{\left(\frac{M_H - M_L}{M_H + M_L}\right) g H^3}$$

$$t_{mix} = \frac{V_{HS}}{Q_{mix}}$$

Example:

$M_H = 29 \quad M_L = 25 \quad H = 5\,m \quad D = 10\,m$

$$Q_{mix} \simeq 95\ m^3/s$$

$$t_{mix} = \frac{2000\ m^3}{95\ m^3/s} = 21\ s$$

Refined Safety Analysis Methodology for
Flammable Gas Risk Assessment in Hanford Site Tanks

Verification & Validation Results

February 11, 1998

Fred Gelbard & Wu-Ching Cheng

Comparing Analysis Framework to Data and Other Models

- **Data Comparisons**
  - Void Fraction by barometric pressure variations and retained gas sampling.
  - Peak H_2 concentrations during a gas release event.
  - H_2 release rates during salt well pumping.
- **Model Comparisons**
  - H_2 release rates during salt well pumping.
  - Plume model calculations for time-at-risk (i.e. H_2 concentration above lower flammability limit).
  - Respirable mass suspended and released.

Void Fraction Comparison

- Elicited void fraction for the 5%, 50% and 95% confidence limits are 0.01, 0.12, and 0.32, respectively, for Facility Group 2.
- Average void fraction calculated from Whitney et al. (1997) is 0.09 (except TX-102) [void fraction = -(P/L)dL/dP]

Tank	dL/dP in/in Hg	Depth inch	Gas Pressure inch Hg	Supernate gal	Waste Vol. gal	Void Fraction
BX-104	-0.07	36	31.9	3,000	99,000	0.06
BX-107	-0.1	125	36.8	1,000	345,000	0.03
S-103	-0.39	90	34.9	17,000	248,000	0.15
S-106	-0.89	174	39.5	4,000	479,000	0.20
S-107	-0.13	136	37.4	14,000	376,000	0.04
S-111	-0.71	216	41.8	10,000	596,000	0.14
SX-106	-0.4	195	40.6	61,000	538,000	0.08
TX-102	-1.79	79	34.2	0	217,000	0.78
TX-103	-0.14	57	33.1	0	157,000	0.08
U-103	-0.47	170	39.2	13,000	468,000	0.11
U-105	-0.36	151	38.3	37,000	418,000	0.09
U-106	-0.08	82	34.4	15,000	226,000	0.03
U-107	-0.3	147	38.0	31,000	406,000	0.08
U-109	-0.38	168	39.1	19,000	463,000	0.09

wrkshp2–FG–2/98

slide 3

Void Fraction from Retained Gas Sampling

Tank	Average Void Fraction	Reference
U103	0.20	Mahoney et al. 1997
S106	0.10	Mahoney et al. 1997
BY109	0.09	Mahoney et al. 1997
A101	0.142	Shekarriz, A. et al., 1997

Mahoney, L. A., Z. I. Antoniak, and J. M. Bates, 1997, PNNL-11777

Shekarriz, A., et al, 1997, PNNL-11450.

Void Fraction
Comparing Elicited and Tank Data

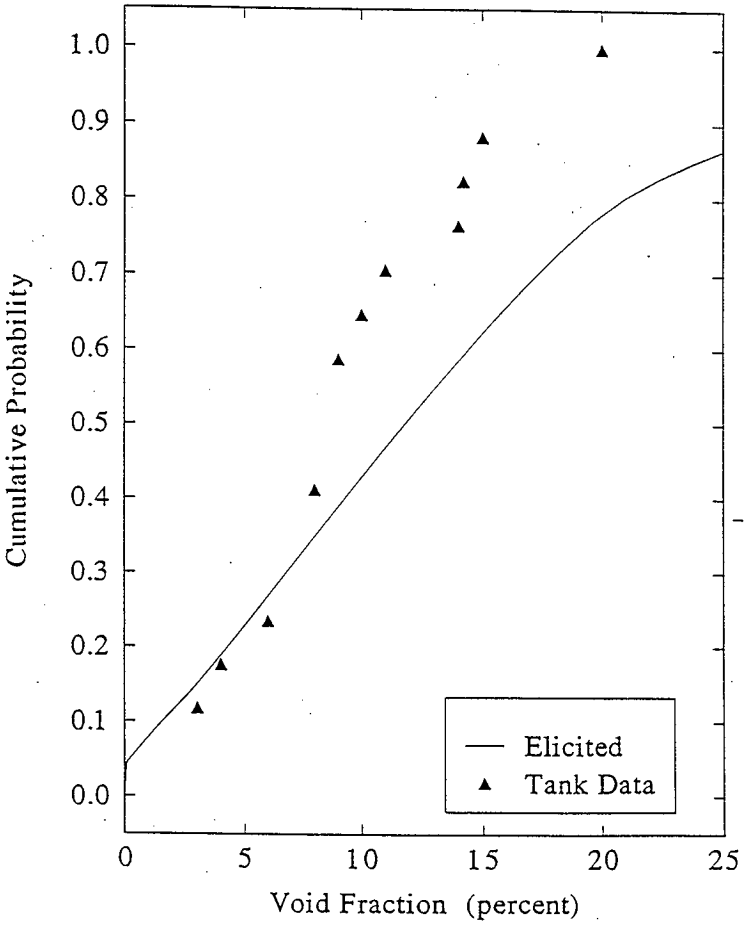

Peak GRE Hydrogen Concentrations

Amount of Gas Released from GREs in Single Shell Tanks [after Wilkins et al. (1997)]

Tank	GRE Date	Pre-GRE H_2 conc (ppm)	Vent rate (m^3/min)	H_2 released (m^3)	Peak H_2 measure (ppm)	Peak H_2 AF-calc (ppm)
S-111	12/11/95	470	0.11	1.0	1,270	3,603
U-103	12/12/95	110	0.057	0.5	1,080	2,636
	2/20/96	600	0.31	0.2	990	2,117
U-105	12/11/95	210	0.25	1.3	740	1,412
	2/7/96	50	0.14	0.4	540	1,495
	2/20/96	90	0.14	0.4	460	1,524
U-107	12/11/95	0	0.13	0.7	640	1,108
	2/20/96	50	0.085	0.1	370	1,205
U-108*	12/12/95	270	0.085	0.7	1,000	1,743
U-109	12/12/95	1,480	0.056	0.4	2,190	3,361
	2/20/96	660	0.056	0.5	1,390	2,628

*Elicited void fraction used for U-108

wrkshp2–FG–2/98

slide 6

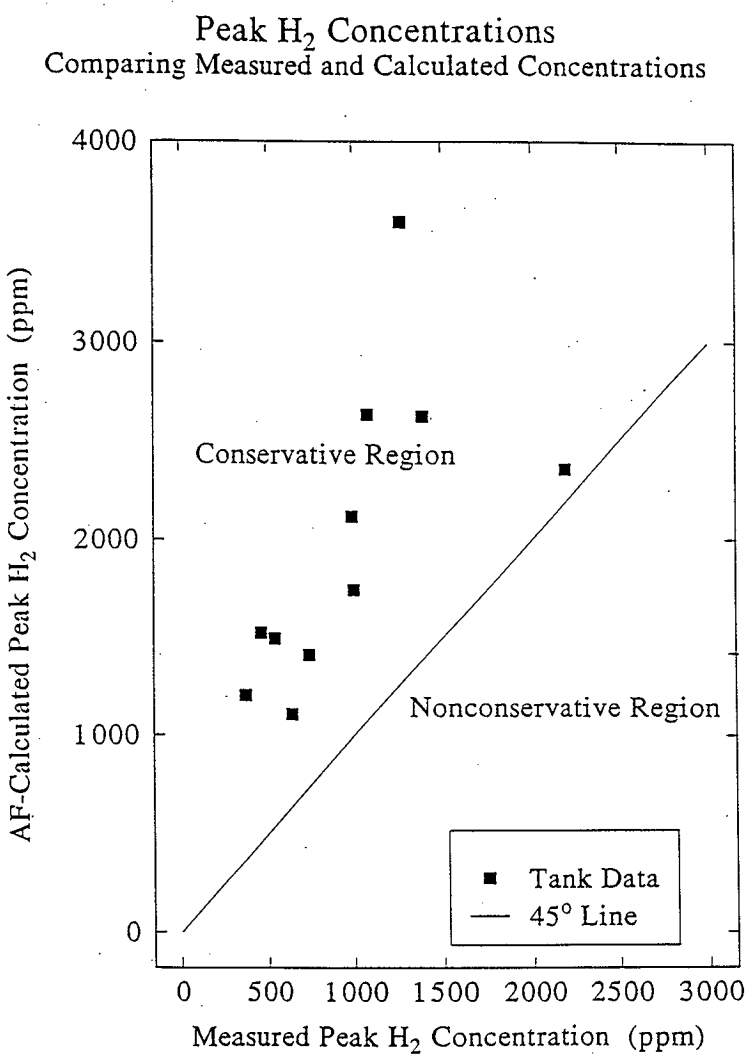
Peak H_2 Concentrations
Comparing Measured and Calculated Concentrations
AF-Calculated Peak H_2 Concentration (ppm)
4000
3000
2000
1000
0
Conservative Region
Nonconservative Region
Tank Data
45° Line
0
500
1000
1500
2000
2500
3000
Measured Peak H_2 Concentration (ppm)

H2 Release Rates During Salt Well Pumping

Tank	Pump Rate gpm (Data)	Headspace H2 Concen. ppmv (Data)	H2 Release moles/min (Data)	H2 Release mole/min (AF model)
S-108	0.19	103	6.0E-04	1.1E-03
T-104	0.4	246	1.4E-03	2.3E-03
BY-103	0.12	200	1.2E-03	6.8E-04
BY-106	0.42	200	1.2E-03	2.4E-03
BY-109	0.106	200	1.2E-03	4.7E-04*
S-110	0.236	200	1.2E-03	1.3E-03

*Void Fraction from RGS data

H_2 Release Rates (Salt Well Pumping)
(Data and Model)

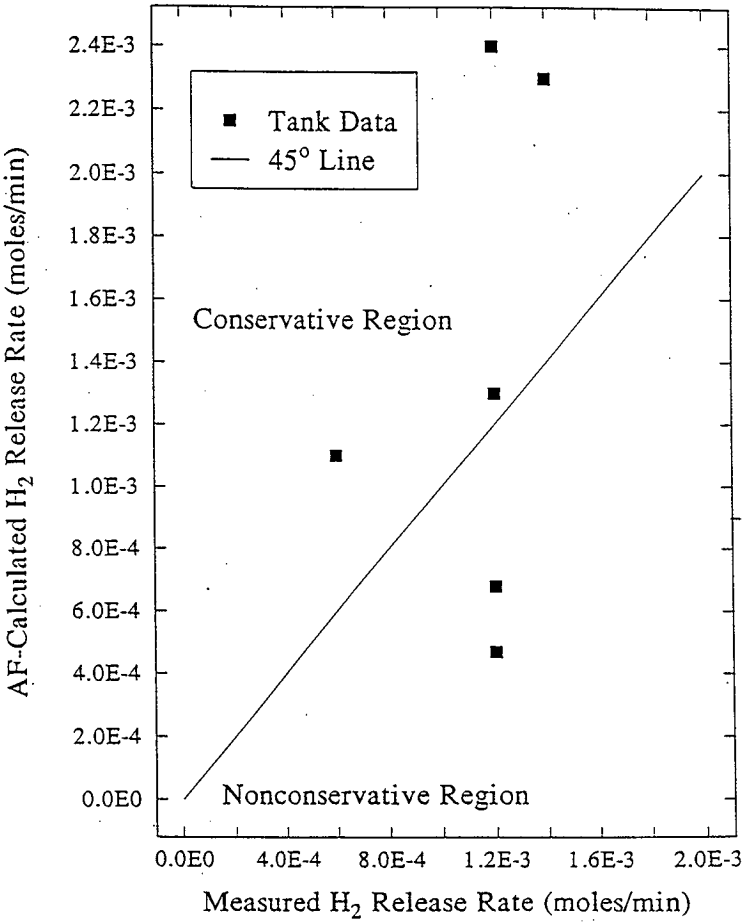

Comparing Models for H2 Release Rates by Salt Well Pumping

Tank	Liquid Pump Rate (gpm)	LANL Model (scfm)	AF Model (scfm)
A-101	5	0.070	0.130
A-101	1	0.010	0.087
A-101	5	0.070	0.130
A-101	5	0.070	0.130
A-101	1	0.010	0.087
A-101	5	0.070	0.130
S-109	5	1.14	0.054
S-109	1	0.3	0.011
S-109	0.5	0.19	0.006
S-109	0.2	0.13	0.003
SX-103	5	0.99	0.119
SX-103	1	0.27	0.034
SX-103	0.5	0.18	0.023
SX-103	0.2	0.13	0.017
BY-105	5	0.76	0.069
BY-105	1	0.23	0.026
BY-105	0.5	0.13	0.021
BY-105	0.2	0.12	0.018
S-102	5	0.75	0.110
S-102	1	0.23	0.067
S-102	0.5	0.16	0.062
S-102	0.2	0.12	0.059

Plume Model Comparison

- The Analysis Framework Plume Model predicts a conservative time-at-risk compared to the detailed discretized models computed either with the TEMPEST or FLUENT/UNS codes.

GRE (ft^3)	H_2 Conc. (%)	Duration (min)	Headspace (ft^3)	Vent Rate	t_{risk} (code) (min)	t_{risk} (AF) (min)
100	40	10	80,000	passive	10	10.03
400	40	10	80,000	passive	10	10.03
1600	40	10	80,000	passive	10	10.04
6400	40	10	80,000	passive	133	6460
6400	40	100	80,000	passive	10	100
1000	50	10	52,000	unvented	10.05	62.09
1000	50	2	52,000	unvented	2.4	44.50
1000	50	2	52,000	200 cfm	2.12	38.55
1000	50	1	52,000	200 cfm	1.25	39.22
2250	50	2	52,000	200 cfm	2.27	123
5000	50	10	52,000	500 cfm	7.22	105

wrkshp2–FG–2/98

slide 9

H_2 Release Rates (Salt Well Pumping)
(DRAIN Code and AF-Model)

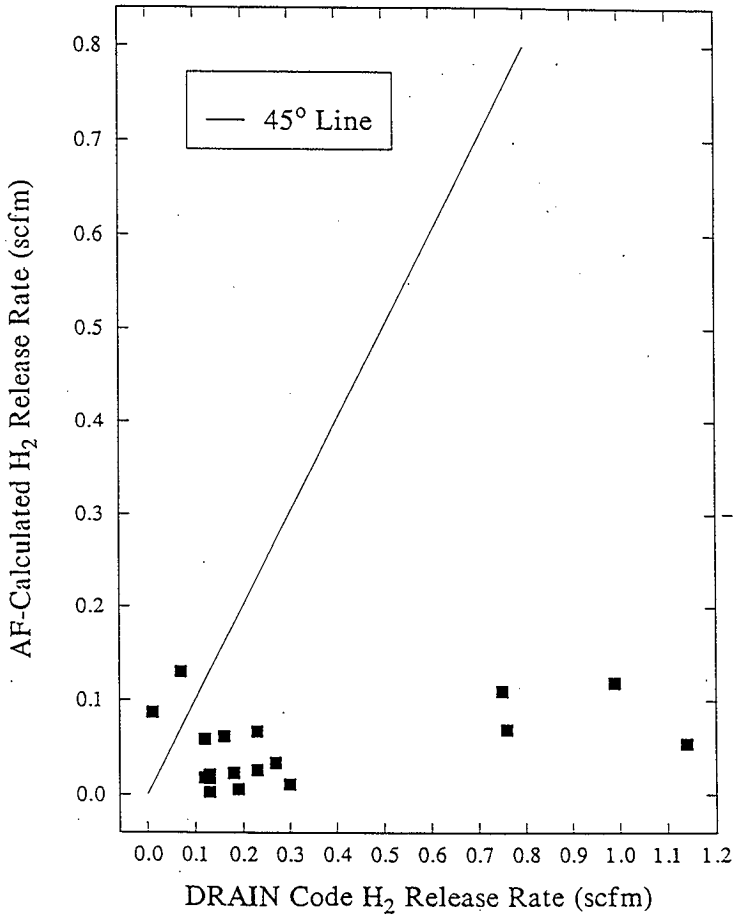

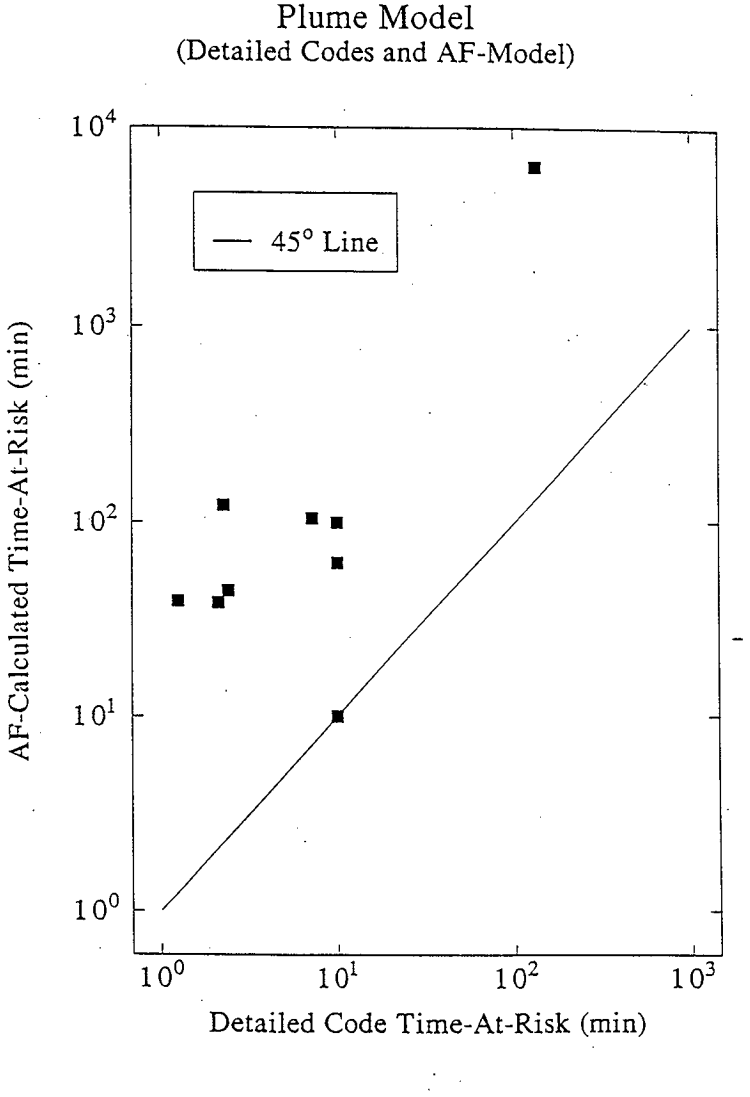
Plume Model
(Detailed Codes and AF-Model)
45° Line
AF-Calculated Time-At-Risk (min)
Detailed Code Time-At-Risk (min)
10^0
10^1
10^2
10^3
10^4

Respirable Aerosol Comparison

	Analysis Confidence Limits				
Damage State	5% (kg)	50% (kg)	95% (kg)	Delphi Panel (kg)	LANL (kg)
No Dome Damage	4E-5	.025	83	0.0063 suspended 0.0049 released	3.8 released
Dome Cracks	6E-4	0.55	83	4.2 suspended 0.02 released	not provided separately
Dome Collapse	0.07	5.5	475	not credible	100 released

wrkshp2–FG–2/98
slide 10

Summary of Comparisons with Measurements

- Average void fractions of 0.09 for barometric pressure measurements, and 0.13 for retained gas sampling measurements are between the 5% and 95% confidence limits of the Analysis Framework.
- Analysis Framework peak gas release event H_2 concentrations is conservative compared to measurements.
- During salt well pumping, H2 release rates calculated by the Analysis Framework divided by the measured rates is in the range of 2 to 0.4.

Summary of Comparisons with Other Models

- During salt well pumping, H2 release rates calculated by the Analysis Framework divided by the rates calculated by the DRAIN code is in the range of 8.3 to 0.02.
- Analysis Framework plume model predictions of the time-at-risk are conservative compared to TEMPEST and FLUENT/UNS calculations.
- Elicited respirable aerosol suspended encompasses Delphi Panel and LANL estimates for the 5%-to-95% confidence limits.

Seismic Response of DST Waste

Chuck Stewart **PNNL**

Part of the baseline risk of storing radioactive waste is the potential for retained gas to be released during the waste disturbance caused by a major earthquake. Waste mobilization during a 1000-year Design Basis Earthquake has been investigated via transient simulations with displacement boundary conditions using the ANSYS structural analysis code. Results are reported in Reid & Diebler (1997). Prior work is summarized in Stewart et al. (1996).

Four different waste configurations and several parametric cases were modeled to represent both single-shell tanks (SST) and double-shell tanks (DST). For SSTs a homogeneous solid waste with two depths and two yield stresses were modeled along with a special case representing the solid-over-liquid configuration of A-101. "Typical" DSTs were represented by a liquid-over-solid configuration with two depths and yield stresses. The total waste depth was divided equally between liquid and solid. A solid-over-liquid-over-solid waste was also modeled to represent tanks with a thick floating solids layer, specifically AN-103.

The simulations estimated the volume of the waste mobilized under the following assumptions:

- Waste is homogeneous except for distinction between liquid and solid layers
- Stress-strain behavior modeled as elastic to 5% strain then perfectly plastic (constant stress) to 100% strain at which point the material is considered "mobilized"
- Mobilized waste can release gas (though gas release was not specifically quantified)
- Perfect coupling assumed between soil and tank, effect of double-shell neglected

The details of finite element modeling and parameter values used are given in Reid & Deibler (1997). For a discussion of the seismicity of the Hanford area, refer to the presentation by Alan Rohay, PNNL, to the SCOPE Workshop #2, April 28-May 2, 1997.

All of the simulations quickly developed localized regions exceeding 100% strain. This stretched the capabilities of the ANSYS code. In hindsight, the phenomena might have been better modeled with fluid dynamics than with structural mechanics. However, the basic waste behavior revealed by the results gives some clear insights as to the potential effects of a severe earthquake. In summary:

- A large fraction of the seismic energy is dissipated in surface waves whose maximum amplitude is in the central region of the tank
- A liquid layer strongly amplifies the effect of the surface waves on the solids layer
- As a consequence, most of the solid waste in a DST is mobilized

Assuming 100% of the solids are mobilized and able to release gas, on the order of 50% of the total gas inventory might be released in the 1000-year earthquake studied. This release fraction is based on actual release fractions in the large, violent rollovers in SY-101 and from buoyancy considerations (see Meyer et al. 1997).

There is not sufficient data to extrapolate these results to more or less-severe earthquakes other than to say that a 10,000-year earthquake would probably not release much more than 50% of the gas and a 100-year earthquake would probably release somewhat less than 50% of the retained gas. Removing the liquid layer would tend to convert the DST waste to resemble an SST.

*****
ANSYS is a trademarked proprietary code, but a user's license is commercially available from Swanson Analysis Systems, Inc., Houston, PA.

In the absence of the surface wave amplification caused by the liquid, relatively little of the total waste is mobilized and relatively little of the total gas is released (Reid & Diebler 1997).

References

Reid HC and JE Deibler. 1997. *Seismic Event-Induced Waste Response and Gas Mobilization Predictions for Typical Hanford Waste Tank Configurations.* PNNL-11668, Pacific Northwest National Laboratory, Richland, Washington.

Meyer PA, ME Brewster, SA Bryan, G Chen, LR Pedersen, CW Stewart and G Terrones. 1997. *Gas Retention and Release Behavior in Hanford Double-Shell Waste Tanks.* PNNL-11536, Rev. 1, Pacific Northwest National Laboratory, Richland, Washington.

Stewart CW, ME Brewster, PA Gauglitz, LA Mahoney, PA Meyer, KP Recknagle and HC Reid. 1996. *Gas Retention and Release Behavior in Hanford Single-Shell Waste Tanks.* PNNL-11391, Pacific Northwest National Laboratory, Richland, Washington.

Seismic Response of DST Waste

Chuck Stewart
PNNL

Expert Panel Elicitation Workshop #1,
January 19-23, 1998,
Richland, Washington.

Seismic Response of DST Waste

- **Effect of 1000-year Design Basis Earthquake on SST and DST waste**
- **Based on transient simulations with displacements at tank walls (ANSYS)**
- **Elastic-perfectly plastic material**
- **"Mobilized" waste can release gas (based on strain energy density)**
- **Large gas releases can be expected from DSTs during severe earthquakes**

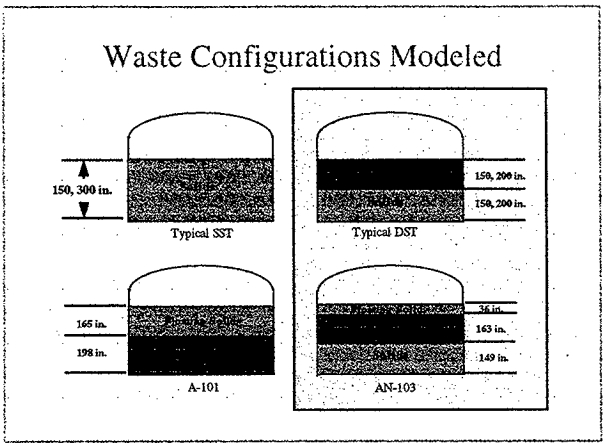
Waste Configurations Modeled
150, 300 in.
Typical SST
150, 200 in.
150, 200 in.
Typical DST
165 in.
198 in.
A-101
36 in.
163 in.
149 in.
AN-103

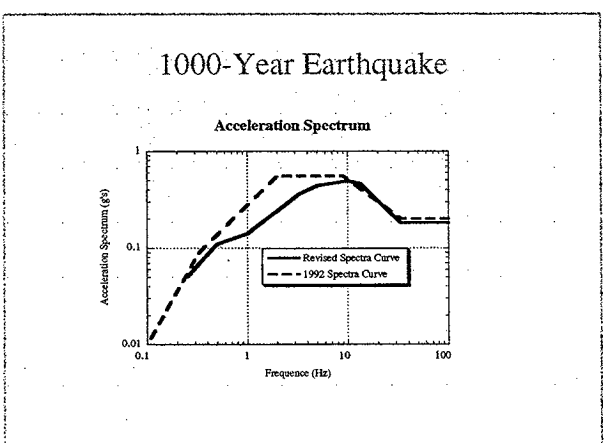
1000-Year Earthquake
Acceleration Spectrum
Acceleration Spectrum (g's)
1
0.1
0.01
0.1
1
10
100
Frequence (Hz)
Revised Spectra Curve
1992 Spectra Curve

Historical Seismicity of Columbia Plateau
1850 – March 23, 1969

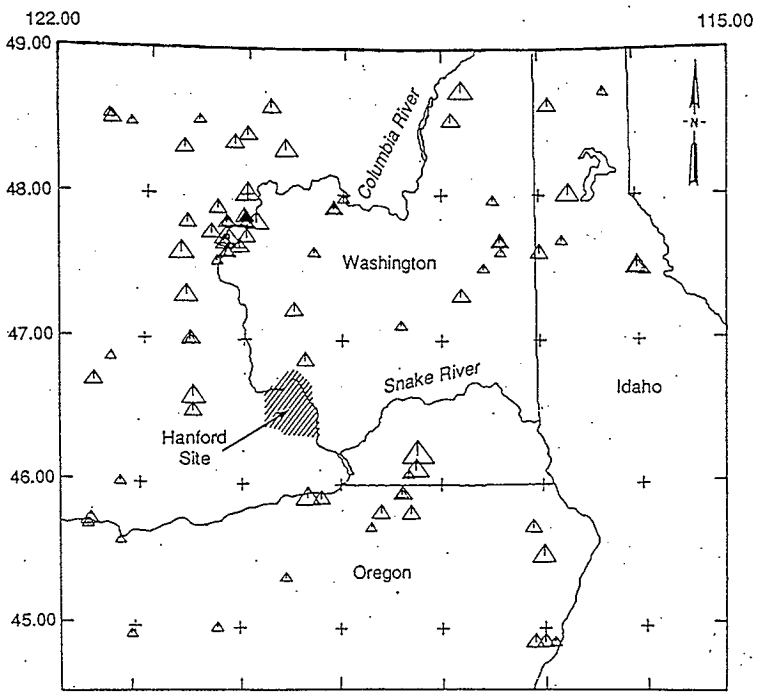

Recent Seismicity of the Columbia Platuea
March 23, 1969 - 1989

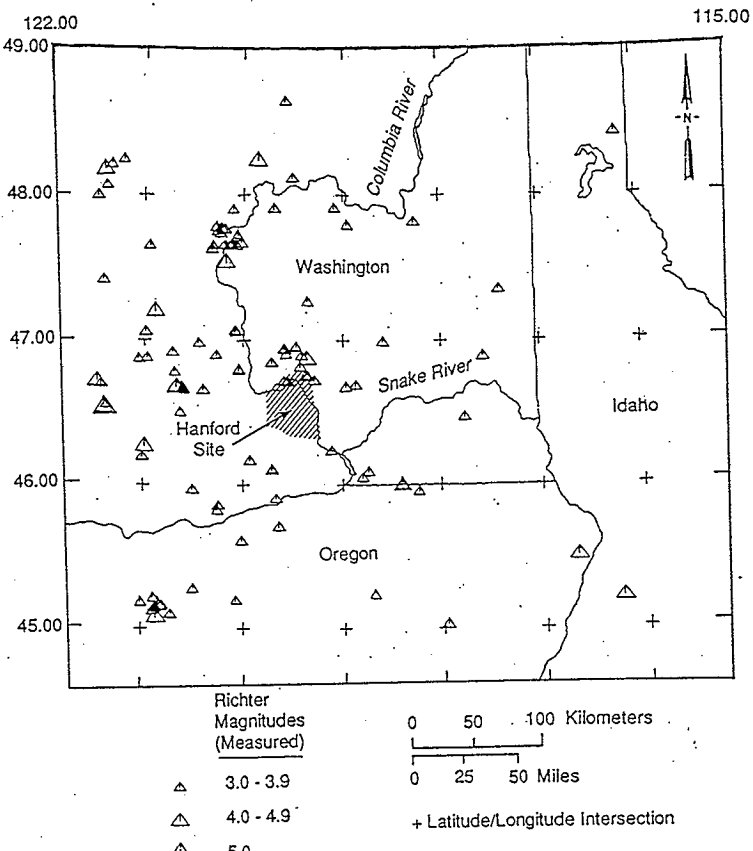

Displacement History

Vertical Displacement

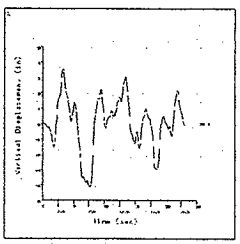

Horizontal Displacement

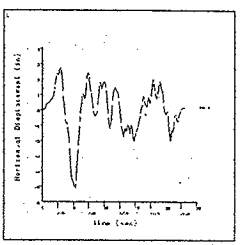

Waste Material Properties

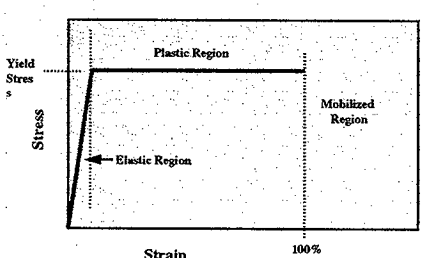

Simulation Results

- **A large portion of seismic energy is dissipated in surface waves**
- **The liquid layer amplifies the effect of waves on the solids layer**
- **Consequence: Most of the solid waste is mobilized**

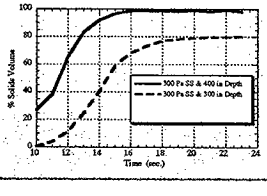

Strain Distribution in Solids

Map of Peak Strains

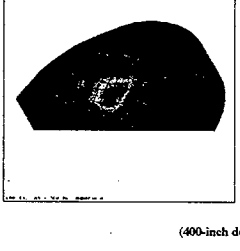

Map of Peak Strain Energy Density

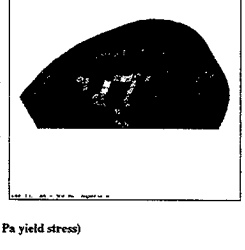

(400-inch depth, 300 Pa yield stress)

Summary of Results

Waste Configuration	Solid Yield Stress (Pa)	Solids Depth (in.)	Liquid Depth (in.)	Total Waste Depth (in.)	Volume Mobilized (%)
Homogeneous (SST)	300	150	0	150	5
	300	300	0	300	13
(A-101)	300	165	198	363	68
Liquid-over-Solid (DST)	300	150	150	300	98
	300	200	200	400	80
(AN-103)	200	36:149	163	348	~100

Gas releases ~50% of retained volume may be possible.

Extrapolation?

- **Other earthquakes?**
  - **10,000-year: still ~50% gas release**
  - **100-year: probably < 50% gas release**
- **Removal of supernate?**
  - **probably converts to SST pattern - little gas release**

ADVANCED ELICITATION TOPICS

Detlof von Winterfeldt

Decision Insights, Inc.

February 12, 1998

PURPOSE OF THE ELICITATION:

- **Review the rationale for your probability judgments**
- **Help you create a defensible representation of probability judgments**
- **Create a fit of your probability distribution**
- **Provide a rational for the fitted probability distribution**

WHAT WILL WE DO IN THE ELICITATION?

1. **One on one elicitation**

2. **Start with a variable of conditioning case that you have the most data for.**

3. **Elicitator checks fractiles, pushes a little on upper bounds and lower bounds, and checks for consistency.**

4. **Elicitator fits probability distribution using computer program, records reasoning for shape.**

5. **Elicitator prints out results for review.**

WHAT SHOULD YOU BRING TO THE ELICITATION?

For each elicitation variable that you chose and for each case:

1. **Minimum: 5^{th}, 50^{th}, and 95^{th} fractiles of the cumulative probability distribution**

2. **Desired: Lower and upper bounds**

3. **Explicit justification of at least three points identified in 1) and 2) using referenceable materials**

4. **Logic to extrapolate or interpolate between cases**

pg#1a

SCOPE: Probability Elicitation Protocol

Date: 5/20/97
Expert: Phil Gauglitz
Analyst: Detlof von Winterfeldt
Variable: #1: Void Fraction
Units: Percentage
Conditions: Case 1: II w/o SWP

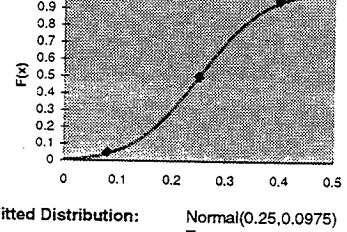

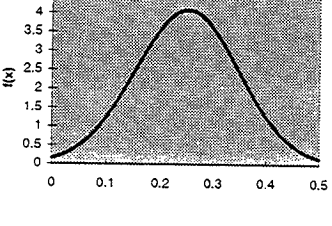

Fitted Distribution: Normal(0.25,0.0975)
Truncate at 0!

General Comments:
- S106, U103, S102
- at higher end of void fraction
- risk significant tanks
- see reference 2.1 in expert's write up

Specific Comments about Fractiles:

x	F(x)	Rationale
0.25	0.5	* U103 = max 37%, av=10% * A101 = 12-18%, lower gas fraction * S106 = barom. pressure suggests 38%(mid 20s, low 30s) * S102 = 19% (barom. pressure) * Lab studies up to 50%
0.08	0.05	* between 5 and 8% * 2 tanks measured at 15% * use half of this
0.4	0.95	* Lab studies up to 50% * experiments create bubbles too rapidly, overpredicts ret. gas * locally may exceed, but not on average

pg#1b

SCOPE: Probability Elicitation Protocol

Date: 5/20/97
Expert: Phil Gauglitz
Analyst: Detlof von Winterfeldt
Variable: #1: Void Fraction
Units: Percentage
Conditions: Case 1: II w SWP

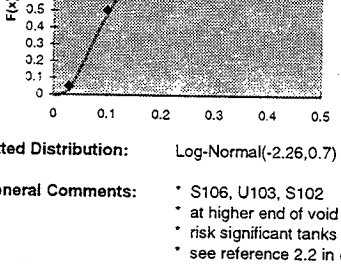

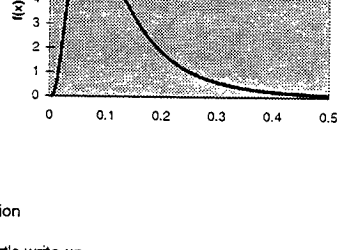

Fitted Distribution: Log-Normal(-2.26,0.7)

General Comments:
* S106, U103, S102
* at higher end of void fraction
* risk significant tanks
* see reference 2.2 in expert's write up

Specific Comments about Fractiles:

x	F(x)	Rationale
		* SWP releases gas, but limits to efficiency
		* reduced by half
0.1	0.5	* still a chance of one tank in 20 with properties to limit escape of gas
0.03	0.05	* half of w/ SWP
0.35	0.95	* Still some chance of retaining gas

WHAT WILL WE DO AFTER THE ELICITATION?

1. **DII will review the individual probability distributions and contact experts if there are any problems.**

2. **The fitted distributions will be averaged across experts.**

3. **Individual and averaged distributions will be shown to you for feedback.**

4. **The average distribution will be used in the Analysis Framework.**

1bChartAll

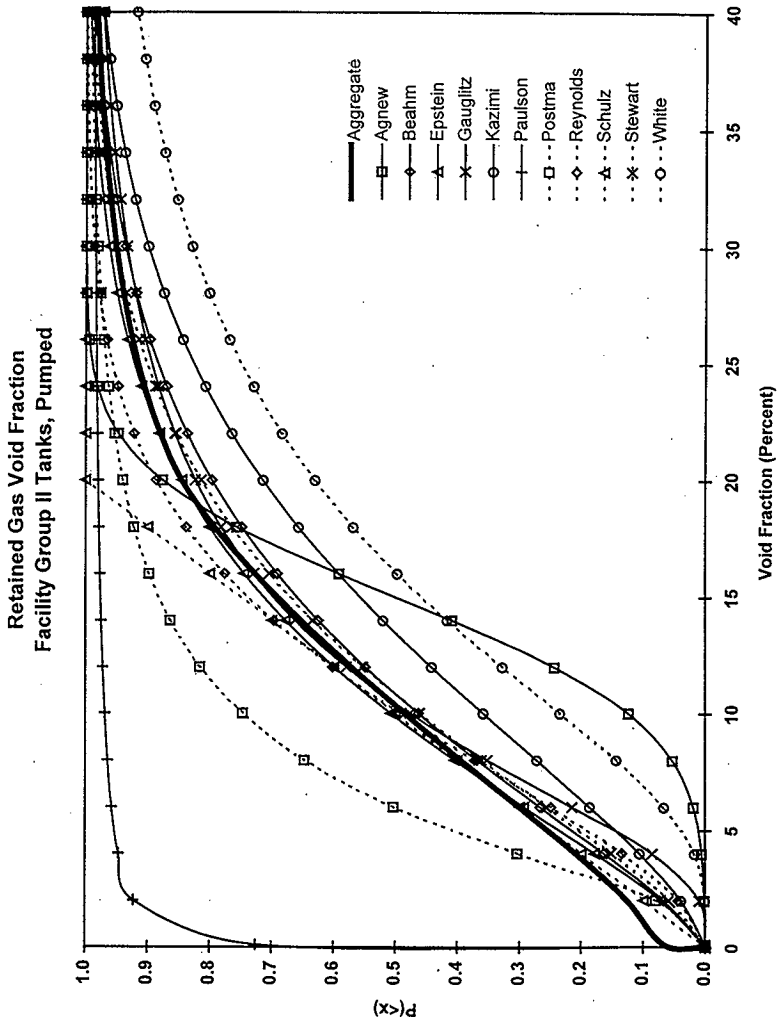
Retained Gas Void Fraction
Facility Group II Tanks, Pumped
P(<x)
Void Fraction (Percent)
Aggregate
Agnew
Beahm
Epstein
Gauglitz
Kazimi
Paulson
Postma
Reynolds
Schulz
Stewart
White
0.0
0.1
0.2
0.3
0.4
0.5
0.6
0.7
0.8
0.9
1.0
0
5
10
15
20
25
30
35
40

Experimental Study of Aerosol Filtration by the Granular Bed Over a Wide Range of Reynolds Numbers

Yoshio Otani,* Chikao Kanaoka, and Hitoshi Emi
Department of Chemical Engineering, Kanazawa University, 2-40-20 Kodatsuno, Kanazawa 920, Japan

The collection performance of granular bed filters consisting of uniform spheres with diameters of 0.5–2.0 mm was experimentally studied by using monodisperse aerosol particles ranging from 0.02 to 2 μm in diameter at superficial velocity from 0.4 to 120 cm/s. Based on the experimental data, prediction equations of collection efficiency due to individual mechanical collection mechanisms were obtained, elucidating the influence of the Reynolds number on the particle collection. Furthermore, by assuming the additivity of the individual mechanical collection efficiencies, a prediction equation applicable to the wide range of filtration conditions is proposed.

INTRODUCTION

The granular bed filter has a relatively high pressure drop compared to fiber bed filters but it is one of the few potential gas filtration media for high-temperature and high-pressure application. In predicting collection performance at a high temperature and a high pressure, the collection characteristics of the granular bed at standard temperature and pressure has to be well understood. Thus, the aim of the present study was to obtain a general expression of the collecitron efficiency of a clean granular bed.

Under ordinary conditions, aerosol particles are captured in the granular bed mainly by mechanical collection mechanisms, such as inertial impaction, Brownian diffusion, gravitational settling, and interception. There are a large number of theoretical studies. (e.g., Langmuir and Boldgett, 1946; Paretsky et al., 1971; Kanaoka et al., 1972; Tardos et al., 1978; Pendse and Tien, 1982; Gal et al., 1985) and experimental works (Ranz and Wong, 1952; May and Clifford, 1967; Kanaoka et al., 1973; Gebhart et al., 1973; Knettig and Beeckmans, 1974; Kennard and Meisen, 1979; D'Ottavio and Goren, 1983; Mann and Goren, 1984), but most of these studies were conducted focusing on one or two particular predominant collection mechanisms with the effect that the transitional regions of the mechanisms were not well understood. Furthermore, the effect of Reynolds number on particle collection has not been clarified in various mechanical mechanism control regimes.

In the present work, collection efficiencies of a clean granular bed were measured in a wide range of filtration conditions and prediction equations resulting from individual mechanisms were obtained taking account of the effect of Reynolds number. Additionally, assuming additivity of the efficiencies of individual mechanical collection mechanisms, a prediction equation covering transitional regions was obtained.

*To whom correspondence should be addressed.

Aerosol Science and Technology 10:463–474 (1989)

0278-6826/89/$3.50

EXPERIMENTAL APPARATUS AND PROCEDURE

The experimental setup is shown in Figure 1. For the simplification of particle collection phenomena, experiments were carried out in such a way that monodisperse particles were captured by the fixed bed of uniform spheres. The fixed bed was a 4- or 8-cm diameter iron tube in which granules were packed on a 32-mesh stainless steel screen. In order to avoid an electrostatic effect on the particle collection, the screen and the tube were electrically grounded. The packed granules were lead spheres with diameters of 1.2 and 2 mm and alumina particles with diameters of 0.5 and 1 mm.

Test aerosols used in the experiments were monodisperse NaCl and polystyrene latex (PSL) particles. The NaCl particles were obtained by classifying the polydisperse particles generated by a Collison atomizer with a differential mobility analyzer. The NaCl particles covered the size range from 0.02 to 0.3 μm. The uniform spheres of PSL particle were dispersed by the Collison atomizer from the suspension of the particles with the diameter between 0.5 and 2.02 μm. The test aerosols were neutralized by a radioactive source of ^{241}Am (about 90 μCi) before introducing them into the granular bed.

The aerosol concentrations upstream and downstream the granular bed were measured with a condensation nucleus counter (TSI Inc., model 3020) for the NaCl particles and a light scattering particle counter (Dan Inc., model PM-730) for the PSL particles.

The measurements of the collection efficiency of granular beds were carried out by changing test aerosol particle size from 0.02 to 2 μm and superficial filtration velocity from 0.4 to 120 cm/s. Test aerosol concentration was lower than 1×10^3 particles/cm^3 and packed granules were frequently washed so that the effect of already captured particles on the collection efficiency was negligi-

FIGURE 1. Experimental setup

TABLE 1. Experimental Conditions

Condition		Dimension
Packed granule diameter	d_g (mm)	0.5, 1.0 (alumina), 1.2, 2.0 (lead)
Packing density	α (--)	0.574–0.667
Bed diameter	D (cm)	4.0, 8.1
Bed depth	L (cm)	3.0–15.0
Test aerosol particle size	d_p (μm)	0.02, 0.03, 0.05, 0.1, 0.2, 0.3 (NaCl) 0.50, 0.81, 1.10, 1.86, 2.02 (PSL)
Particle density	ρ_p (g/cm^3)	2.16 (NaCl), 1.04 (PSL)
Superficial velocity	u_s (cm/s)	0.4–120

ble. The depth of the granular bed was varied from 3 to 15 cm in order to increase experimental accuracy by avoiding large pressure drop and extremely high or low penetration through the bed, since the log-penetration law was confirmed to hold for these beds. The experimental conditions are shown in Table 1.

EXPERIMENTAL RESULTS

Figure 2 shows the pressure drop of the granular bed measured by a pressure transducer. The pressure drops of the packed beds of different depths and different granule sizes are in good agreement with the lines predicted by Ergun's equation.

Figures 3 and 4 show the overall bed efficiency as a function of interstitial velocity for the NaCl particle and the PSL particle, respectively. As seen from Figure 3, the collection efficiency of NaCl particles with diameter smaller than 0.3 μm monotonically decreases with the filtration velocity, and increases as the particle size becomes small. This indicates that the control collection mechanism of the particles is Brownian diffusion. In Figure 4, for the PSL particles

FIGURE 2. Pressure drop of granular bed.

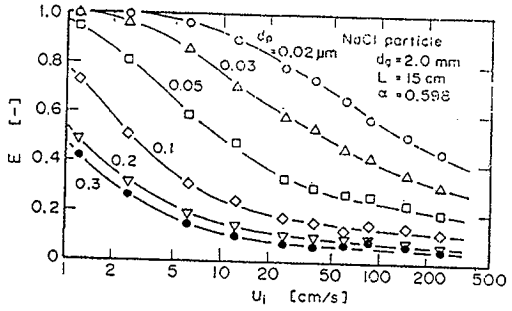

FIGURE 3. Overall bed efficiency of granular bed for NaCl particles with diameter smaller than 0.3 μm. The data for $u_i < 5$ cm/s were obtained for $L = 5$ cm and were converted by Eq. (1). The smooth change of the experimental lines at $u_i \sim 5$ cm/s indicates the consistency of Eq. (1).

with diameter larger than 0.5 μm, collection efficiency curves are concave against filtration velocity, and the minimum appears at a filtration velocity between 20 and 70 cm/s. Since the collection efficiency of the PSL particles becomes larger as the particle size increases, control mechanisms are inertial impaction at high velocity and gravitational settling at low velocity.

DISCUSSION

In order to discuss collection mechanisms in the granular bed, the total bed efficiency E is converted to the single-sphere efficiency by the following equation (Tardos et al., 1978):

$$\eta = -\frac{2}{3}\frac{1-\alpha}{\alpha}\frac{d_c}{L}\ln(1-E). \qquad (1)$$

The above equation is different from that used by D'Ottavio and Goren (1983) by a factor of $(1-\alpha)$. In general, $(1-\alpha)$ should be included if interstitial velocity is taken as a representative velocity of the system, whereas it should be excluded if the superficial velocity is used. There still remains some argument on the log-penetration expression for the granular bed so that one should be careful about which expression the experi-

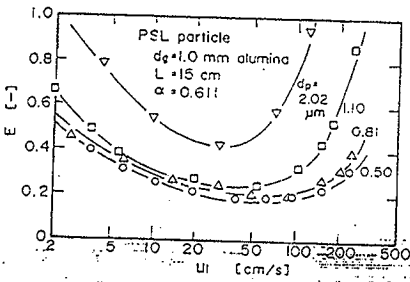

FIGURE 4. Overall bed efficiency of PSL particles with diameter larger than 0.5 μm.

mental single-sphere efficiency is reduced from the total bed efficiency. In the present work, the interstitial velocity is taken as the representative velocity, and thus Eq. (1) is used to calculate single sphere efficiencies.

In the absence of electrostatic effects, the single-sphere efficiency is a function of following dimensionless parameters:

$$\eta = \eta(Pe, G, Stk, R, Re, \alpha), \tag{2}$$

where Pe, G, Stk, and R are dimensionless parameters which are the measures of Brownian diffusion, gravitational settling, inertial impaction, and interception. Re and α are quantities related to flow and configuration of the granular bed. Provided that there are no interactions among the collection mechanisms, Eq. (2) may be rewritten as a sum of efficiencies due to individual mechanisms:

$$\begin{aligned}\eta &= \eta_{DGIR} = \eta_D + \eta_G + \eta_I + \eta_R \\ &= \eta_D(Pe, Re, \alpha) + \eta_G(G, Re, \alpha) \\ &\quad + \eta_I(Stk, Re, \alpha) + \eta_R(R, Re, \alpha).\end{aligned} \tag{3}$$

In the following sections, the single-sphere collection efficiency is discussed separately in the predominant regions of each collection mechanism.

Diffusion

The motion of fine particles with diameters smaller than several tenths of a micrometer is governed by Brownian diffusion.

In Figure 5, single-sphere collection efficiencies of NaCl particle with diameter smaller than 0.3 μm are plotted against $Sc = \nu/D_{BM}$ with Re as a parameter. The experimental lines connecting the data with a constant Re represent the dependence of η on particle size under a fixed-flow condition. It can be seen from the figure that the data with same Re but with different d_g and d_p (i.e., different R) lie on the same straight line, and the slope gradually changes from $-2/3$ to $-1/2$ with increasing Re. The deviation between the data and the empirical straight lines at $Sc = 1.19 \times 10^5$ may be attributed to the particle collection by other mechanisms. Therefore, in diffusion control regime, increase of Re reduces η at a constant Sc, and the dependence of η on Sc changes with Re.

The dependence of η on Re for a fixed Sc is clearly shown in Figure 6. For a constant Sc (i.e., constant particle size), η rapidly decreases with increasing Re in small Re region, but the decreasing rate of η become smaller and smaller as Re increases.

It has been theoretically shown that the single sphere efficiency is proportional to $Pe^{-2/3}$ for creeping flow ($Re \ll 1$; Levich, 1962) and $Pe^{-1/2}$ for potential flow ($Re \to \infty$; Chao, 1969). Since $Pe = ScRe$, it is expected from these theoretical works that η changes in proportion to $Sc^{-2/3}$ in a small Re region and $Sc^{-1/2}$ in a large Re region. Figure 5 indicates that there exists a transitional region between these two theoretical extreme cases and that the transition takes place at around $Re = 100$.

Through the experimental findings in Figures 5 and 6, in order to express functional dependence of η on both Re and Sc, the following form for diffusional efficiency is assumed:

$$\eta_D = A(Re) Sc^{f_1(Re)} Re^{f_2(Re)}, \tag{4}$$

$f_1(Re)$, which is equal to the slope of line shown in Figure 5, is plotted in Figure 7 against Re. As shown in the figure, the power of Sc, $f_1(Re)$, is a function that has asymptotes of $-2/3$ for $Re \to 0$ and $-1/2$ for $Re \to \infty$, and may be approximated by the following equation:

$$f_1(Re) = -\frac{2}{3} + \frac{Re^3}{6(Re^3 + 2.0 \times 10^5)}. \tag{5}$$

By plotting $\eta/Sc^{f_1(Re)}$ against Re, the remaining functions $A(Re)$ and $f_2(Re)$ are determined as follows:

$$\left.\begin{aligned} &A(Re) = 8.0,\ f_2(Re) = -\tfrac{1}{3} \\ &\quad \text{for } Re < 30 \\ &A(Re) = 40.0,\ f_2(Re) = -1.15 \\ &\quad \text{for } 30 \le Re < 100 \\ &A(Re) = 2.1,\ f_2(Re) = -\tfrac{1}{2} \\ &\quad \text{for } Re > 100 \end{aligned}\right\} \tag{6}$$

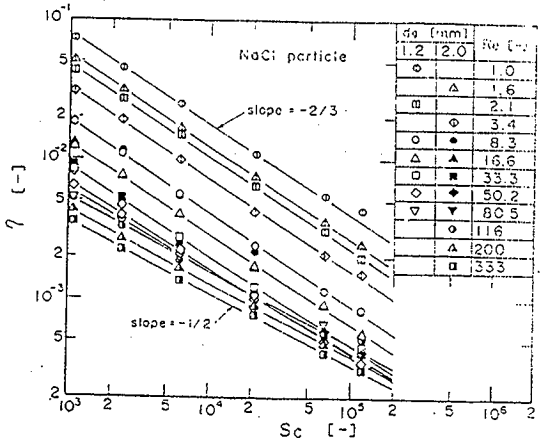

FIGURE 5. Single-sphere collection efficiency of fine NaCl particles as a function of Schmidt number.

FIGURE 6. Single-sphere collection efficiency of fine NaCl particles as a function of *Re*.

Eqs. (4)–(6) can be reduced to the following functions of *Pe* at the extremes of *Re*:

$$\eta_D = 8.0\, Pe^{-2/3} \quad \text{for } Re \to 0; \tag{7}$$

$$\eta_D = 2.1\, Pe^{-1/2} \quad \text{for } Re \to \infty. \tag{8}$$

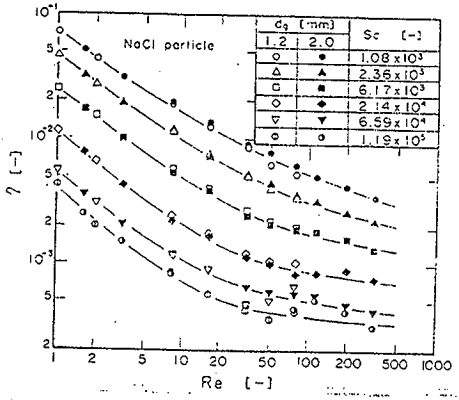

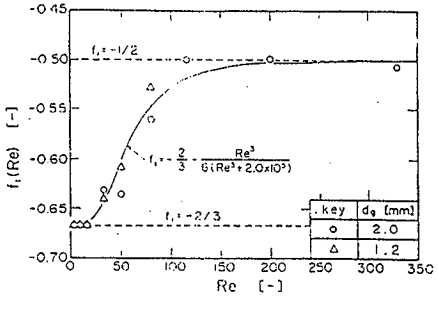

FIGURE 7. Change of the power of *Sc* with *Re*.

Experimental collection efficiencies are compared with those predicted by Eqs. (4)–(6) taking *Pe* on the abscissa in Figure 8. As seen in the figure, the predicted lines describe well all of our experimental data.

Very few data of the diffusional collection efficiencies at a high *Re* have been reported. The diffusional collection efficiencies predicted by Mann and Goren (1984) at $Re = 8.3$ and 330 are shown in Figure 8 by dashed lines. Their formula gives a close prediction at a low *Re*, but it underestimates our data at a high *Re*. Gebhart et al. (1973) measured the collection efficiencies of PSL particles with diameters of $d_p = 0.15$, 0.2, and 0.3 μm up to *Re* of about 50. All the data reported by them are in good agreement with our correlation equations.

FIGURE 8. Comparison of experimental single-sphere efficiency of fine NaCl particles with those predicted by Eqs. (4)–(6) (*solid lines*). The *dashed lines* are predicted by the Mann and Goren formula (1984) at $Re = 8.3$ and 330.

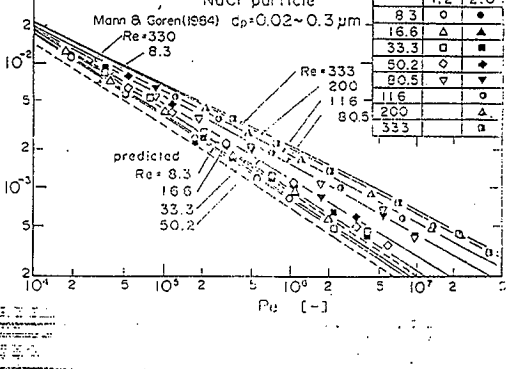

Gravitational Settling

For large particles at low velocity, gravitational settling becomes a predominant collection mechanism. The single-sphere efficiency due to gravitational settling has been theoretically derived by Tardos et al. (1980) and Lee (1980):

$$\eta_G = \frac{G}{1+G}. \qquad (9)$$

The single-sphere efficiency of large PSL particles with diameter larger than 0.5 μm is replotted in Figure 9 as a function of gravity parameter G. Although the data with different d_g and d_p have different trends in the small G region where gravity is not predominant, the data asymptotically approach the line predicted by Eq. (9). Therefore, in the gravitational control regime, Reynolds number does not affect collection efficiency and thus the efficiency is expressed by Eq. (9).

Inertial Impaction

For large particles at high velocity, the controlling collection mechanism is inertial impaction. Figure 10 shows the single-sphere efficiencies of PSL particles as a function of Stokes number. It is seen from the figure that the collection efficiency η is not a single value function of Stk and that, in the region where efficiency steeply rises, the experimental line connecting the data with the same interceptional parameter shifts to the left as R decreases. Since an increase of interception parameter generally gives rise to an increase of inertial efficiency, the contribution of R to η shown in Figure 10 seems contradictory. However, Stk is written in terms of Re and R as

$$Stk = \left(\frac{Cm\rho_p}{9\rho_f} \right) ReR^2. \qquad (10)$$

and, for a given aerosol of particles with diameter larger than 1 μm (Cm is nearly equal to unity and ρ_p and ρ_f are constant), Stk, Re, and R vary dependently in keeping the above relationship. For a packed bed of granules with diameter of millimeter order, interceptional effect is considered to be small so that, at a constant Stk, an decrease of R

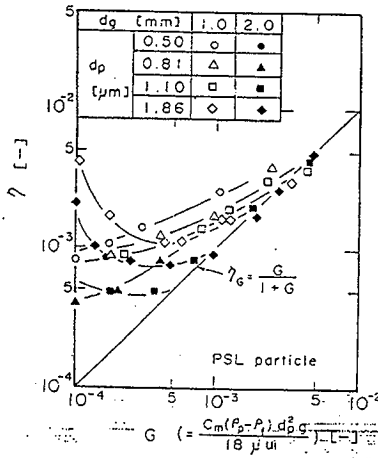

FIGURE 9. Single-sphere efficiency of large PSL particles as a function of gravity parameter, G.

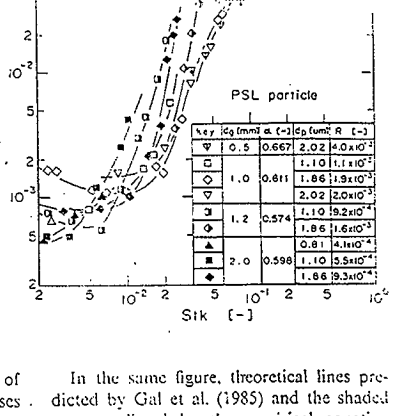

FIGURE 10. Single-sphere efficiency of large PSL particles at high velocities as a function of Stokes number, *Stk*.

has little effect on η, whereas an increase of Re resulting from the decrease of R raises collection efficiency, significantly. The same contribution of R to η was reported for fibrous filters and explained through numerical calculation (Yoshioka et al., 1969).

In order to take account the influence of Re in the inertial efficiency, effective Stokes numbers were proposed by D'Ottavio and Goren (1983) and Gal et al. (1985). Although the effective Stokes number proposed by the former is based on the hydrodynamical arguments, the following effective Stokes number based on the Ergun's equation proposed by the latter is adopted in the present work because it gives a better correlation to our experimental data:

$$Stk_{\text{eff}} = \left(1.0 + \frac{1.75Re(1-\alpha)}{150\alpha}\right) Stk. \qquad (11)$$

By using the above modified Stokes number, the single-sphere efficiencies are plotted in Figure 11. Although the data for $Stk_{\text{eff}} < 0.02$ show a different dependence on Stk_{eff}, the experimental data for $Stk_{\text{eff}} > 0.02$ may be correlated by the following equation:

$$\eta_I = \frac{Stk_{\text{eff}}^3}{1.4 \times 10^{-2} + Stk_{\text{eff}}^3}. \qquad (12)$$

In the same figure, theoretical lines predicted by Gal et al. (1985) and the shaded area predicted by the empirical equation proposed by D'Ottavio and Goren (1983) are shown for comparison. The present data show reasonable agreement with both previous works.

For a large solid particle at a high filtration velocity, bounce-off or reentrainment of particle may be significant. The decrease in the collection efficiency at $Stk_{\text{eff}} > 0.1$ is the indication of the phenomena. According to D'Ottavio and Goren (1983), the sticking efficiency of KHP (potassium biphthalate) particles on alumina and glass beads becomes less than unity at their defined effective kinetic energy larger than 10^{-11} J. They also reported that the threshold is not so sensitive to the granule material. For the data shown in Figure 11, the effective kinetic energies for 2.02- and 1.86-μm particles at the peak collection efficiency are 2.6×10^{-12} and 9.7×10^{-12} J, respectively. These values are fairly close to the threshold kinetic energy for KHP particle, showing that the bounce-off or the reentrainment of PSL particle may occur at the same effective kinetic energy as that of KHP particle. Incidentally, the region shown in Figure 11 with D'Ottavio and Goren's equation is based on the measurement with DOP particles. If the

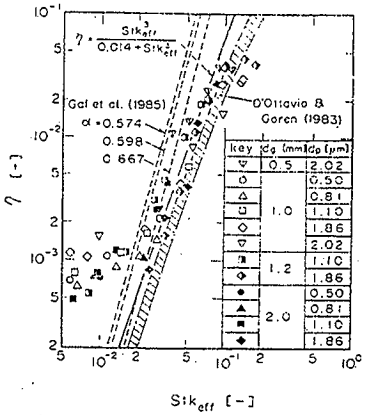

FIGURE 11. Inertial single-sphere efficiency as a function of effective Stokes number, Stk_{eff}.

bounce-off and reentrainment of the PSL particle were severe in our experimental condition, we would expect a lower efficiency than their prediction. Therefore, the effect of bounce-off and reentrainment seems small especially for the data for which the correlation equation of Eq. (12) was obtained.

Interception and All Mechanical Collection Mechanisms

In granular bed filtration, the effect of interception is usually small compared to the other mechanisms and it becomes relatively important only in the transitional regions of the other mechanical collection mechanisms. Thus, the interceptional efficiencies were obtained from the data of the PSL particles in the transitional regions as residues after subtracting the diffusional, gravitational, and inertial efficiencies calculated by Eqs. (4), (9), and (12) from the experimental efficiencies, according to the assumption of Eq. (3). The residual interception efficiencies are plotted in Figure 12 against R, using the same symbols for the data with nearly equal

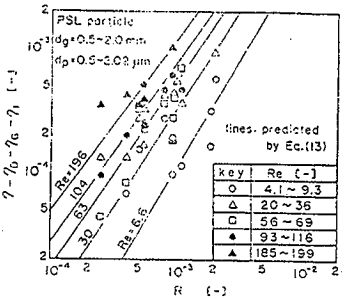

FIGURE 12. Comparison of residual efficiencies with those predicted by Eq. (13). The *solid lines* are predicted for the average Re of the data with the same symbol.

Re. Because the residual interception efficiencies are in the order of 10^{-4} and depend very much upon the other mechanical efficiency prediction equations, correlation by R and Re is not so good. However, it is seen from the figure that the residual efficiency

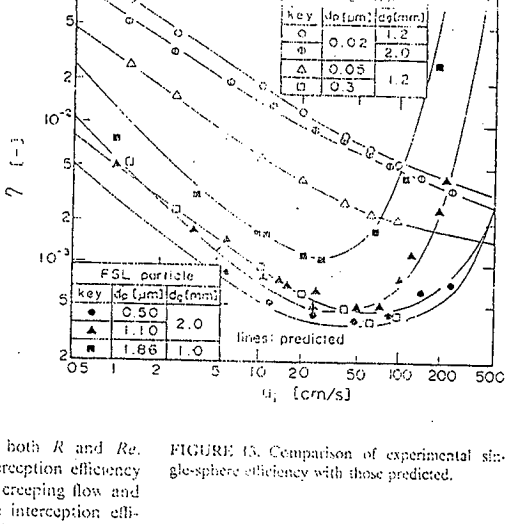

FIGURE 13. Comparison of experimental single-sphere efficiency with those predicted.

increases with increasing both R and Re. Referring to that the interception efficiency is proportional to R^2 for creeping flow and R for potential flow, the interception efficiency is approximated by the following equation:

$$\eta_R = 1.6R^{2-1.6/(R^{0.4}+1)}. \tag{13}$$

The predicted lines by Eq. (13) are compared with experimental data in Figure 12. Despite of the large scatter of the experimental data, the predicted lines describe the general trend of all experimental data well.

By using Eq. (3), the collection efficiency due to all the mechanical mechanisms can be predicted as a sum of the individual efficiencies. The predicted single-sphere efficiencies are compared with experimental efficiencies in Figure 13. It is seen that the prediction equation describes experimental data well over wide ranges of particle size and filtration velocity with fairly high accuracy even in the transitional regions of the collection mechanisms.

CONCLUSIONS

Through the experimental studies on the collection performance of granular bed filter, the prediction equations for each mechanical collection efficiency were obtained. Furthermore, an equation that can be applied in the wide range of filtration conditions was obtained by assuming the additivity of the individual mechanical efficiencies. The main conclusions obtained in the effect of Reynolds number on the collection efficiency are as follows:

1. In a diffusion control regime, Reynolds number gives rise to an increase in collection efficiency, and the power of Peclet number changes from $-2/3$ to $-1/2$ with increasing Re. The diffusional efficiency is well correlated by Eq. (4) as a function of Re and Sc.

2. In an inertial impaction regime, Reynolds number also raises collection efficiency. The dependence of the experimental efficiency on Reynolds number was described fairly well by the effective Stokes number proposed by Gal et al. (1985).

Subscripts

D	diffusion
G	gravitational settling
I	inertial impaction
R	interception

NOMENCLATURE

$A(Re)$, $f_1(Re)$ $f_2(Re)$	functions in Eq. (4)
Cm	slip correction factor
D	bed diameter
D_{BM}	Brownian diffusivity
d_g	granule diameter
d_p	particle diameter
E	overall bed efficiency
G	gravity parameter = $Cm\rho_p d_p^2 g/18\mu u_i$
g	acceleration of gravity
L	bed depth
P	penetration
ΔP	pressure drop
Pe	Peclet number = $u_i d_g/D_{BM}$
R	interception parameter = d_p/d_g
Re	Reynolds number = $\rho_f d_g u_i/\mu$
Sc	Schmidt number = ν/D_{BM}
Stk	Stokes number = $Cm\rho_p d_p^2 u_i/9\mu d_g$
Stk_{eff}	modified Stokes number defined by Eq. (11)
u_i	interstitial velocity
u_s	superficial velocity
α	packing density
η	single sphere collection efficiency
μ	dynamic viscosity of air
ν	kinematic viscosity of air
ρ_f	density of air
ρ_p	density of particle

REFERENCES

Chao, B. T. (1969). *J. Heat Transfer Trans. ASME* 91:273.

D'Ottavio, T., and Goren, S. L. (1984). *Aerosol Sci. Technol.* 3:91.

Gal, E., Tardos, G. I., and Pfeffer, R. (1985). *AIChE J.* 31:1093.

Gebhart, J., Roth, C., and Stahlhofen, W. (1973). *J. Aerosol Sci.* 4:355.

Kamaoka, C., Yoshioka, N., Iinoya, K., and Emi, H. (1972). *Kagaku Kougaku* 36:304.

Kennard, M. L., and Meisen, A. (1979). 2nd World Filtration Congr., pp. 229.

Knettig, P., and Beeckmans, J. M. (1974). *J. Aerosol. Sci.* 5:255.

Langmuir, I., and Blodgett, K. B. (1946). *Army Air Force Tech. Rep.* 5418.

Lee, K. W. (1983). *J. Aerosol Sci.* 12:79.

Levich, V. G. (1962). *Physicochemical Hydrodynamics*, Prentice-Hall, Englewood Cliffs, New Jersey.

Mann, L. A., and Goren, S. L. (1984). *Aerosol Sci. Technol.* 3:195.

May, K. R., and Clifford, R. (1967). *Ann. Occup. Hyg.* 10:83.

Paretsky, L., Theodore, L., Pfeffer, R., and Squires, A. M. (1971). *J. Air Pollut. Control Assoc.* 21:204.

Pendse, H., and Tien, C. (1982). *AIChE J.* 28:677.

Ranz, W. E., and Wong, J. B. (1952). *Ind. Eng. Chem.* 44:1371.

Tardos, G. I., Gonzal, N., and Gutfinger, C. (1978). *J. Air Pollut. Control Assoc.* 28:354.

Tardos, G. I., Yu, E., Pfeffer, R., and Squires, A. M. (1979). *J. Colloid Interface Sci.* 71:616.

Yoshioka, N., Emi, H., Matsumura, H., and Yasunami, H. (1969). *Kagaku Kogaku* 33:381.

Received 14 January 1987; revised and accepted 29 November 1987.

Particle Deposition in Wakes

Inertial and Coulombic Effects on Capture By Single and Multiple Spheres in Line

Michael J. Matteson* and Michael B. Prince
School of Chemical Engineering, Georgia Institute of Technology, Atlanta, GA 30332

Ten-micrometer dioctylphthalate droplets tagged with sodium fluorescein were collected on six metal spheres, 0.6 cm in diameter and arranged in a line parallel to the axis of flow. The particles carried negative charge in the range $0.9–1.7 \times 10^{-5}$ stC while the collectors were charged positively in the range 8.0–23.0 stC. The carrier stream velocities used were 600, 1200, 1500, 1800, and 2400 cm/s and spacings between targets of two through six diameters center-to-center were tested. Collection efficiencies for each target were determined by measuring the number of deposited particles, and the particle concentration in the air stream using fluorometric techniques.

An effective Coulombic attraction parameter $K_{\varepsilon_{eff}}$ was defined to take into account non-Stokesian drag during particle collection at high velocities. This term was combined with an effective Stokes number to provide the empirical relation, for single spherical targets: $\eta = 1.4[Stk_{eff} + (2K_{\varepsilon_{eff}})^{1/2}]$. A model is presented to describe the concentration distribution of particles in the wakes of multiple spherical targets, in-line. This model is based on the lateral turbulent transport of particles into the wake between targets. A correlation between the particle deposition of any trailing target, normalized to that of the leading target, and the modified Graetz number, $(n-1)^{1/3}(Gz)^{-1}$, where n is the rank of the target in the series and $Gz = 4(z/D)/Pe$, enables one to predict deposition on trailing targets.

INTRODUCTION

The application of electrically charged droplets to the removal of dusts from waste gas streams is a concept which has found recent application in electrostatic spray droplet scrubbers. In some cases these sprays are injected in conventional scrubbing towers, in others the charged droplets are introduced in venturi systems.

Several mechanisms combine to make such a particle-capture system so effective. Diffusion, impaction, interception, and electrostatic attraction are all at work, and have varying levels of influence, depending on the velocity and orientation of the encounter, and the charge-field intensity relationship.

In the flow of gases past spheres, streamlines begin to separate from the surface at Reynolds numbers (Re) around 20. The wake behind the sphere changes from convex to concave at about $Re = 35$. Vortices form and enlarge until, at $Re = 130$, oscillations appear. At Reynolds numbers around 270, large vortices periodically form and move downstream as a result of flow instabilities.

Since sprays developed in scrubbers consist of droplets moving at high Reynolds numbers and high droplet populations, it is likely that there are many droplet–vortex encounters in the wakes of droplets. Two basic encounters exist: vortex pairs exist behind droplets moving at $Re > 35$, and vortices released from these droplets at $Re > 270$ strike droplets traveling in their wake. A sphere 2 mm in diameter traveling at a terminal velocity of 550 cm/s has a vortex shedding frequency of 550 s^{-1}. Droplets smaller than 1 mm do not exhibit the vortex shedding (Strouhal number = 0) when mov-

*To whom correspondence should be addressed.

Aerosol Science and Technology 12:745–761 (1990)

0278-6826/90/$3.50

ing at terminal velocities, but would at velocities higher than terminal.

The scavenging mechanism of raindrops returns a great deal of the aerosol particles suspended in the atmosphere to the earth. Among the first to study the combined effects of various atmospheric scavenging mechanisms was Greenfield (1957). Whereas Greenfield considered Brownian diffusion, turbulent shear diffusion and inertial impaction (simply formulated), he did not account for the interaction of the forces. Slinn and Hales (1971) studied the effect of phoretic forces on aerosol scavenging by cloud droplets along with Brownian diffusion and inertial impaction. Their work also did not take into consideration the interaction of the forces. Fuchs (1964) developed a model analogous to that of Slinn and Hales model for the case of Brownian diffusion and electric forces.

The studies of Pilat (1975), Pilat and Prem (1976, 1977), Sparks and Pilat (1970) included the interaction of all the various effects neglected by the others. They computed the collection efficiency of drops based on a determination of particle trajectory around the drops. These studies assumed that potential flow around the sphere was applicable at Reynolds numbers < 264.

The potential flow model however, does not account for standing eddies at $Re > 20$ on the downstream side of the drop. Significant quantities of particles may undergo aft-side capture under these conditions (Grover et al., 1977; Grover, 1976; Grover and Beard, 1975; and Beard, 1974). Grover et al. (1977) and Wang et al. (1978) developed models to predict collection efficiencies combining all relevant forces. Herbert (1978) formulated a model describing the motion of aerosol particles affected by Brownian diffusion, inertial impaction, electric forces, and phoretic forces based on nonequilibrium thermodynamics. He concluded, however, that the best method of determining scavenging efficiencies were still the models developed by Grover et al. (1977) and Wang et al. (1978).

A theoretical estimation of the collection efficiency of aerosol particles on a sphere using inertia as the only mechanism of collection was developed by Langmuir and Blodgett (1946). Ranz and Wong (1952) developed a mathematical statement of the problem of impaction on flat plates, cylindrical collectors, and spherical collectors. They carried out limiting solutions to establish the nature and importance of the various impaction mechanisms. Kraemer and Johnstone (1955) developed models for the collection of aerosol particles via electrostatic forces on spheres, cylinders, and flat plates. They established that, for nonpolarized spheres the collection efficiency for oppositely charged particles, is $\eta = 4K_E$, where K_E is the attraction parameter which expresses the ratio between coulombic and drag forces on the particles.

Zebel (1968) studied the theoretical capture of small particles by relatively larger droplets falling in homogeneous electric fields oriented parallel to the direction of flow. He assumed Stokes flow ($Re \ll 1$) and considered diffusion within the boundary layer for various combinations of charge and field strength. Several possible particle trajectories were described. This work provided the theoretical basis for Kraemer and Johnstone's observations.

In the early to mid-1970s models were developed by George and Poehlein (1974) and Nielsen and Hill (1976a, 1976b) which predicted the collection efficiencies of micrometer-sized particles on charged, spherical collectors. Both workers considered inertial, viscous, gravity, electrostatic forces, and interception phenomena in their models. Chiu-Sen Wang et al. (1977) formulated a new theory for the deposition of solid particles on a collector taking into consideration dendrite and shadow formulation.

Goldschmid and Calvert (1963), studying inertial collection effects, showed experimentally that, at high collector Reynolds numbers ($1000 < Re < 8000$), particles 1 μm and smaller in diameter would collect primarily on the aft-side of the collector. Deryagin

(1972), using a jet method to experimentally determine the capture coefficient of aerosol particles on a sphere due to inertial deposition and van der Waals forces, concluded that with a steady-state vortical ring behind the sphere, there is deposition of particles on the trailing edge of the surface of the sphere. Beard (1974) found from his theoretical investigation that, even without electrostatic forces, wake capture occurs. Robig and Porstendorfer (1979) investigated the effect of flow regime on electrostatic collection at high Reynolds numbers and low Stokes number (1.5×10^{-3}). For $44 < Re < 3200$ they found, experimentally, no effect of flow field. They also found, experimentally, that from 50% to 60% of the particles collected on the aft-side. Nielsen and Hill (1976b) theoretically estimated the collection on the aft-side of a spherical collectors as a function of both Stokes number and K_E.

A comparison of the model developed by George (1974) with experimental data collected by Matteson (1978) revealed a large discrepancy in certain results. Nielsen and Hill found George's aft-side collection computation deficient; however, they also found their estimates to agree in order of magnitude.

Battler et al. (1982) showed that the developed wake has a definite influence on the overall collection efficiency of single charged spheres. They also found high rates of deposition on the aft-side where flow conditions are not adequately represented by potential flow theory. Their Reynolds numbers were in the range 40–400 with Stokes numbers on the order 10^{-4}–10^{-3}.

All of these earlier studies involved single spherical targets. In 1985, Jacober and Matteson determined collection efficiencies for arrays of one to six spheres (uncharged) in the Reynold's number (free stream) range 2400–12,000. Here it was clearly shown that the intertarget spacing had a strong influence on the collection of particles by successive targets when spaced at $x/d < 7$. Also, the presence of a concentration wake in which greater than free-stream concentrations were present at the edge of the velocity wake was indicated.

In a later study, Jacober and Matteson (1990) experimentally determined the eddy diffusion coefficients for momentum and concentration in the turbulent wake of single spheres. They found that the concentration profile in the wake was complicated by the superposition of particles penetrating the target with those entering the wake region by turbulent convection.

The goal of this work is to extend the investigation of multiple targets to include the enhancement in collection resulting from Coulombic attraction with inertial effects.

THEORY

Experimental evidence supports the theoretical description of the capture of particles in a high-velocity flow field as characterized by the Stokes number (Stk), which is the ratio of the stop distance of a particle to the target radius. The stop distance is the distance a particle will travel in a gravity-free environment and may be expressed as:

$$l_p = v_p \tau = v_p (v_t / g). \tag{1}$$

where τ is the relaxation time, v_t the particle terminal velocity, v_p the free-stream particle velocity, and g the gravitational acceleration. The Stokes number in the potential flow regime is defined as:

$$Stk = \frac{v_p d_p^2 \rho_p}{18 \mu_g r_c}, \tag{2}$$

where d_p is the particle diameter, ρ_p the particle density, μ_g the gas viscosity, and r_c the target radius.

However, for non-Stokesian particles the collection efficiency also depends on a Reynolds number based on particle diameter and free-stream velocity. The particle Reynolds number is defined as:

$$Re_p = \frac{d_p v_\infty \rho_g}{\mu_g}, \tag{3}$$

where v_∞ is the free-stream gas velocity.

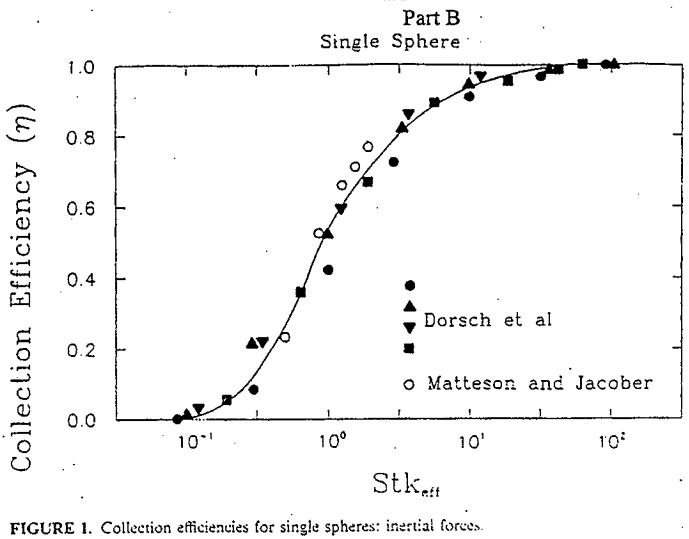

FIGURE 1. Collection efficiencies for single spheres: inertial forces.

For a potential flow field approximation to the fluid motion about a collector, the collision efficiencies of spherical and cylindrical targets have been calculated numerically as a function of both the Stokes and particle Reynolds numbers (Dorsch et al., 1955; Brun et al., 1955). From experimental results obtained in the limit of negligible Mach numbers, capture efficiencies plotted as a function of the Stokes number for both Stokesian and non-Stokesian particles produce curves that are qualitatively alike. Israel and Rosner (1983) developed a similarity parameter that would reduce the dependence of target capture efficiencies to a single combination of the Stokes and particle Reynolds numbers.

Termed the effective Stokes number, this parameter accounts for the fact that the drag on a particle may be non-Stokesian.

$$Stk_{\text{eff}} = \Psi Stk, \tag{4}$$

where

$$\Psi = \frac{24}{Re_p} \int_0^{Re_p} \frac{dRe}{C_D Re} = 1.22\, Re_p^{-0.32}. \tag{5}$$

Our results are compared in Figure 1 with those of Dorsch et al. (1955) for single collectors by plotting collection efficiency vs. effective Stokes number as determined by Eqs. (4) and (5).

Single Collectors: Electrostatic Forces

Particle capture is enhanced by applying opposing charges to the aerosol and collectors. The predominant dimensionless group used to characterize the relative electrostatic forces is the Coulombic attraction parameter K_E, and this is the ratio of the Coulombic force between the charged collecting body and the oppositely charged aerosol to the drag force tending to keep the aerosol particle within a

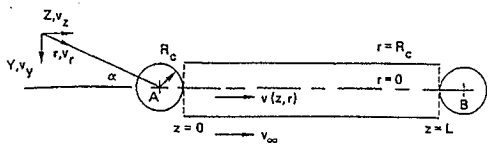

FIGURE 2. Particle–target orientation capture model.

streamline. For Stoke's drag this is:

$$K_E = \frac{F_{elec}}{F_{drag}} = \frac{Q_1 Q_2}{6\pi^2 d_p \mu_g v_\infty \epsilon_0 d_c^2}. \quad (6)$$

However, because the drag force may vary over a range of Reynolds numbers, K_E may take various forms.

Consider the trajectory of a particle approaching a collecting sphere at a distance z (Figure 2), where y is the vertical component of the particle's path. The description of the trajectory is facilitated by the geometric relations:

$$\begin{aligned} &a)\ y = r\sin\alpha \qquad b)\ v_y = v_r \sin\alpha \\ &c)\ v_y = v_z \frac{dy}{dz} \qquad d)\ r\,d\alpha = \sin\alpha\, dz \end{aligned} \quad (7)$$

Now the Coulombic force is equated to the drag force in the r direction and the relative velocity v_r becomes

$$v_r = \left\{ \frac{2Q_1 Q_2}{\pi^2 \epsilon_0 d_p^2 \rho_g C_D r^2} \right\}^{1/2}. \quad (8)$$

If the drag is Stokesian, the drag coefficient in the radial direction is $C_D = 24/Re_p$, and Eq. 8 may be rearranged with the aid of Eq. (7) to yield

$$y\,dy = \frac{Q_1 Q_2}{12\pi^2 d_p \mu_g v_z \epsilon_0} \sin\alpha\, d\alpha, \quad (9)$$

which may be integrated between the limits

$$y = y_i, \qquad \alpha = 0$$

$$y = 0, \qquad \alpha = \frac{\pi}{2}$$

to obtain

$$y_i^2 = \frac{Q_1 Q_2}{6\pi^2 d_p \mu_g v_\infty \epsilon_0}, \quad (10)$$

where v_∞ has been assumed $\approx v_z$.

The collection efficiency may then be defined as the ratio of particles removed from the area πy_i^2 to the target's cross-section $\pi d_c^2/4$

$$\eta = \frac{Q_1 Q_2}{3\pi^2 d_p \mu_g v_\infty \epsilon_0 d_c^2}. \quad (11)$$

This is $2K_E$ if the Coulombic force is taken at the surface of the collecting sphere.

Now if the drag is non-Stokesian the drag coefficient is other than $24Re_p^{-1}$, as with the range of velocities studied here, wherein $4.0 < Re_p < 16.0$, here the empirical expression for the drag coefficient is

$$C_D = 25.2\, Re_p^{-0.78}. \quad (12)$$

Inserting this in Eq. (8) and integrating, we get for the non-Stokesian case

$$Y_{NS}^2 = 2.13\left(\frac{2Q_1 Q_2}{25.2\pi^2 \epsilon_0 d_p^{1.22} \rho_g^{0.22} \mu_g^{0.78} v_\infty^{1.22}} \right), \quad (13)$$

such that

$$\frac{Y_{NS}^2}{Y^2} = 1.01\, Re_p^{0.22} = 1.06 \frac{C_D}{C_{D,NS}}, \quad (14)$$

but this is also

$$\frac{Y_{NS}^2}{Y^2} = \frac{K_{E,eff}}{K_E} = \phi, \quad (15)$$

so for the flow region $4.0 < Re_p < 16.0$

$$\phi = 1.01\, Re_p^{0.22}. \quad (16)$$

Now since we wish to test the effects of combined inertial and coulombic forces, a suitable parameter might be the sum of the two vertical distances, $l_p + Y$, the stop distance which represents the distance the particle's inertia will carry it, and the vertical distance travelled due to electrostatic forces, rationalized by the target radius:

$$\eta = \eta\left(\frac{l_p + Y}{R_c}\right)_{NS} = \eta\left(Stk_{eff} + \left(2K_{E_{eff}}\right)^{1/2}\right). \quad (17)$$

Multiple Targets: Spheres in Line

The influence of inertial forces on the collection of particles by spheres moving in a line parallel to the axis of flow has been studied by Jacober and Matteson (1985). In that work it was demonstrated that trailing spheres move in a concentration "shadow" where particles are concentrated in the wake boundary of the leading target. The particles in the wake are gradually transported, radially inward by convective diffusion, and the concentration distribution tends to smooth out several diameters downstream from the lead target.

A model describing this concentration distribution may be obtained by considering the cylindrical void between the lead sphere A and the trailing sphere B (Figure 2). The void between A and B is filled both by particles from A's boundary layer and by particles injected from the surrounding turbulent stream.

The equation of transport for a scalar quantity in an axisymmetric wake resulting from approximations like those considered for free turbulent shear flows may be written as (Jacober and Matteson, 1990):

$$\frac{\partial}{\partial z}\left(\frac{\Delta C_p}{C_{p\infty}}\right) = \frac{1}{r}\frac{\partial}{\partial r}\left(\frac{v_r' c_z'}{v_\infty C_{p\infty}}\right). \quad (18)$$

where z and r are the axial and radial coordinates, ΔC_p is the average particle concentration defect, $C_{p\infty}$ is the free-stream particle concentration and $v_r' c_z'$ is the product of the fluctuating components of velocity and concentration in the r and z directions, respectively.

Assuming that the turbulent transport of ΔC_p can be described by analogy to Fick's law, using a coefficient of diffusivity, ϵ_p, the following expression is put forward:

$$v_r' c_z' = \epsilon_p \left|\frac{\partial C_p}{\partial r}\right|, \quad (19)$$

where ϵ_p does not account for molecular effects.

If the ΔC_p profiles are also assumed to be similar in consecutive sections of the wake, a relation is obtained:

$$\frac{\Delta C_p}{\Delta C_{p\,max}} = \exp\left[\frac{v_\infty d}{3}\left(\frac{z}{d}\right)^{-1/3}\int\frac{\xi\, d\xi}{\epsilon_p}\right] \quad (20)$$

where $\xi = (r/d)/(z/d)^{1/3}$ and $\Delta C_{p\,max}$ represents the centerline defect.

In the simplest case, where ϵ_p is a function of $z^{-1/3}$ but is constant in the radial cross section, the Gaussian distribution is obtained:

$$\frac{\Delta C_p}{\Delta C_{p\,max}} = \exp\left[-\frac{\xi^2}{\beta_p}\right] \quad (21)$$

where $\beta_p = (6\epsilon_p / v_\infty d)(z/d)^{1/3}$.

The maximum concentration defect, $\Delta C_{p\,max}$ is still a function of z, varying according to $z^{-2/3}$. Solution of the particle flux balance about the sphere gives (Jacober and Matteson, 1990):

$$\frac{\Delta C_{p\,max}}{C_{p\infty}} = \alpha_p\left(\frac{z}{d}\right)^{-2/3}, \quad (22)$$

where $\alpha_p = (\eta/24)(v_\infty d/\epsilon_p)(z/d)^{-1/3}$ and η is the impaction efficiency of a sphere for particles.

So that

$$1 - \theta = \frac{\Delta C_p}{C_{p\infty}} = \alpha_p\left(\frac{z}{d}\right)^{-2/3}\exp\left(-\frac{\xi^2}{\beta_p}\right), \quad (23)$$

where $\theta = C_p / C_{p\infty}$, is the normalized particle concentration in the wake.

In order to evaluate θ from deposition data, we know that, on the first target,

$$\text{deposition}_1 = \eta_1 C_{p\infty} \pi r_c^2 v_\infty t,$$

and on subsequent targets, n

$$\text{dep}_n = \eta_n C_{pn} \pi r_c^2 v_n t,$$

so that

$$\frac{C_{pn}}{C_{p\infty}} = \frac{(\text{dep})_n}{(\text{dep})_1} \frac{v_\infty}{v_n} \frac{\eta_1}{\eta_n}.$$

Now since $\eta = \eta(Stk, K_E)$, for a given set of conditions, the greatest variation between targets in the capture efficiency is a result of the velocity deficit in the wake of the target, so we make the approximation

$$\frac{\eta_1}{\eta_n} \approx \frac{v_\infty}{v_n}$$

then

$$\frac{C_{pn}}{C_{p\infty}} = \frac{(\text{dep})_n}{(\text{dep})_1} \left(\frac{v_\infty}{v_n} \right)^2.$$

In order to account for the repeated encounters between particles and targets, the distance parameter must be made a function of n, the target rank. To do this we introduce the group $(n-1)^g$ where g is to be determined empirically. So now

$$1 - \theta = \alpha_p (n-1)^{-g} (z/d)^{-2/3} \exp\left(-\frac{\xi_n^2}{\beta_p} \right) \tag{24}$$

and

$$\xi_n = \frac{r/d}{(n-1)^g (z/d)^{1/3}}.$$

This reduces to

$$(1 - \theta)_{max} = \alpha_p (n-1)^{-g} (z/d)^{-2/3} \tag{25}$$

for the centerline or maximum defect. Substituting the value of α_p into Eq. (25)

$$(1 - \theta)_{max} = \frac{\eta_1}{2\pi} (n-1)^{-g} \frac{v_\infty d}{\epsilon_p} (z/d)^{-1} \tag{26}$$

or

$$(1 - \theta)_{max} = \frac{\eta_1 P_e}{24(n-1)^g (z/d)} = \frac{\eta_1}{24(n-1)^g (Gz)}, \tag{27}$$

where the dimensionless Peclet and Graetz numbers are defined:

$$P_e = \frac{v_\infty d}{\epsilon_p}, \quad Gz = \frac{(z/d)}{P_e}.$$

Further, since we are taking $C_{p\infty}$ as the constant concentration at the outer edge of the cylindrical void, then a correction must be made for the concentration wake which contains particles both from the free stream and those penetrating the leading target.

Let

$$\theta = \frac{C_{p_n}}{C_{p_\infty}} \frac{1}{(1 + P_1)},$$

where $P_1 = \eta_1^{-1}$. Now

$$\theta = \frac{(\text{dep})_n}{(\text{dep})_1} \left(\frac{v_\infty}{v_n} \right)^2 \frac{1}{(1 + P_1)}. \tag{28}$$

Velocity profiles behind spherical targets in series were determined by Jaeger and Matteson (1985) and the velocity deficit is found from the empirical expression:

$$1 - \frac{v_n}{v_\infty} = 0.38 \left(\frac{z}{d} \right)^{-2/3} (n-1)^{-1/3}. \tag{29}$$

EXPERIMENTAL ARRANGEMENT

The test aerosol was produced from a solution of 0.1 g of sodium fluorescein, 10 mL of dioctylphthalate (DOP), diluted to 1.0 L with 2-propanol. This solution was pumped through a vibrating orifice aerosol generator (Berglund-Liu model 350) with a 20-μm orifice to produce 10 ± 0.1-μm DOP droplets when dried. For schematic diagram, see Figure 3.

The aerosol stream meets and merges with the main air stream at the top of the drying tube. This other stream is supplied by an electric power blower (1 hp, 1 A) controlled

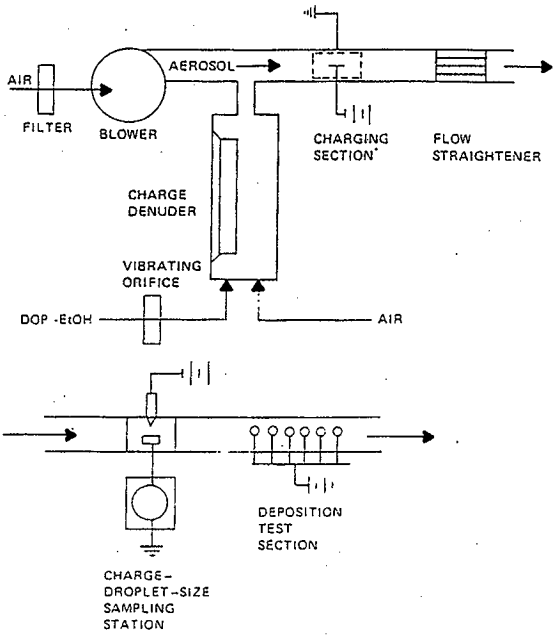

FIGURE 3. Experimental arrangement.

by a type 3PN1010 variable transformer (Staco Energy Products Co., Dayton, OH). The combined stream travels for 43 cm through 5.72-cm ID plexiglass tube before encountering the custom-made flow straightener of 97 tubes of 0.61 cm ID, 6.35 cm long. Velocities used were 600, 1200, 1500, 1800, and 2400 cm/s, which provided Stokes numbers of 0.6, 1.2, 1.52, 1.80, and 2.4.

The charging section consists of a 2.54-cm-long, 0.2-cm diameter steel rod sharpened on the upstream end, and held in the center of the collar by a 0.2-cm diameter steel rod. Surrounding the charging rod is a grounded coaxial cylindrical steel shell 5.08 cm ID and 6.35 cm long. Charging the collar is a Power Designs model 10K10 high-voltage DC power supply (Pacific Instruments Inc., Concord, CA). The spheres' positive voltage was maintained by a model 1150-1 high-voltage DC power supply (Beckman Instruments, Inc., Fullerton, CA). The aerosol became charged by passing through the corona between the rod and collar.

The aerosol then passes through a further 16.5 cm before encountering the first collection sphere. Trailing spheres are at varying distances downstream depending on the separations (2, 3, 4, 5, and 6 sphere diameters, center-to-center). The spheres themselves are

18K gold and 0.6-cm diameter. These are supported by 0.8-mm insulated wire.

The free-stream velocity was determined with a model 1210-20 hot wire anemometer with a model 1051-1 anemometer monitor supply (TSI, Inc., St. Paul, MN). The probe was placed at the approximate position of the first sphere.

Free-stream particle concentrations were monitored by sampling isokinetically with a Millipore RAWP 04700, 1.2-μm filter in-line. A model 110A fluorometer (Turner Designs, Mountain View, CA) was used to measure the amount of aerosol collected.

The charge per particle was found by grounding one sphere through a model 610A electrometer (Keithly Instruments, Inc., Cleveland, OH) to determine the total charge collected by the sphere. The Turner fluorometer was used to measure mass and hence the number of particles collected. Voltages were selected so as to maintain K_E at values of 0.1, 0.3, 0.5, 0.7, and 0.9. As velocity was increased to obtain greater Stokes numbers, the K_E was held constant by increasing the collector charge accordingly.

During an actual test, once the sphere had been exposed to aerosol for 60 min, the aerosol was discontinued, and both voltage sources and the blower were turned off. The spheres were removed and each was washed in 25 mL of absolute ethanol. The solutions of ethanol and dissolved particles were then analyzed using the fluorometer. The readings were then converted to concentrations and ultimately to efficiencies.

RESULTS AND DISCUSSION

The particle collection efficiencies for charged single spheres are shown in Figure 4 as a function of the parameter for dimensionless distance a particle deviates from a streamline. Efficiencies were determined from the experimental data by dividing the number of particles caught by the number exposed so that

$$\eta = \frac{\text{number particles deposited}}{\pi r_c^2 v_\infty \bar{C}_p t} \qquad (30)$$

where $\bar{C}_p$ is the average number concentra-

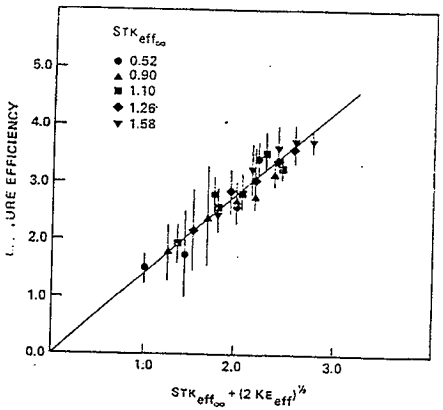

FIGURE 4. Collection efficiencies for single spheres: inertial and Coulombic forces.

tion of particles in the aerosol stream and t is the exposure time. In cases where there were multiple targets the efficiency for successive targets was based on the appropriately reduced number density.

Collection efficiencies for single targets increased linearly with $K_{E_{eff}}^{1/2}$, for fixed Stk_{eff}, to an upper value of 4.0 at the greatest Stk_{eff}, $K_{E_{eff}}$ values. This represents a cross-sectional area about four times that of the target. The correlation that best fit the data for collection by single spheres was:

$$\eta = 1.4\left[Stk_{eff} + (2K_{E_{eff}})^{1/2}\right]. \qquad (31)$$

Kraemer and Johnstone (1955), working at very low Stokes numbers ($\sim 10^{-5}$) found that $\eta = 4K_E$. This agrees with our theoretical development for capture by coulombic forces alone (Eq. 11) if instead of integrating over the front side of the target, we integrate over the entire surface area. However at high velocities, deposition tends to shift toward the front side of the sphere (Battler et al., 1982) and collection is a combined mechanism. For this reason we chose a parameter based on trajectory rather than a ratio of forces. The trajectory analysis is considerably simplified in ignoring the acceleration term in the motion equation, however the purpose is to arrive at a dimensionless distance characteristic of the particles departure from the flow field about the sphere and not to provide an exact description of the path followed. Nevertheless, the concept of additive inertial and electrostatic trajectories appears to be a useful parameter in predicting the capture efficiencies for single spherical targets.

Robig and Porstendorfer (1979) found the relationship $\eta = 4K_E$ to hold up to velocities of 12 m/s, but their Stokes numbers were on the order of 10^{-3}. Our tests however covered the range $0.52 < Stk_{eff} < 1.58$ and $0.05 < K_{E_{eff}} < 0.50$ and in the region there appeared a definite dependence of η on Stk_{eff}. The mathematical model of Nielson and Hill (1976) showed a negative dependency on Stk:

$$\left(\eta = \left[2(K_E)^{1/2} - 0.8Stk\right]^2\right)$$

for the region $0 < Stk < 0.3K_E$ and $1.5 < K_E < 10$. However, in the region of our tests, their predicted collection efficiencies are somewhat positively dependent on Stk, but yield values of one-third to one-half those we obtained experimentally.

A representation of the relative collection efficiencies of spheres as a function of their rank in line is shown in Figure 5. At 2-D spacing the second sphere collects only about a tenth of the particles trapped by the lead target, but this collection increases with each successive sphere until, at $Stk_{eff} = 0.52$ (600 cm/s) the rear target collects about the same as the initial sphere. This is a consequence of the relatively weak lateral mixing and low axial velocity in the void when targets are so closely spaced. Also, those spheres situated between two other spheres have greatly diminished Coulombic forces because of image charges. At higher velocities and close spacing ($Stk_{eff} = 1.58$, 2400 cm/s) the recovery is even weaker with the trailing sphere capturing only 25% that of the lead. Although intertarget velocities are somewhat greater this is more than offset by the reduction in lateral mixing.

Moving up to 6-D spacing, we see the improvement in collection by the lead target over 2-D spacing. This takes place because the initial sphere is relatively unaffected by image charging from the next target. The most dramatic change at 6-D over 2-D spacing is that there is little variation in collection according to target position in line and there is little difference in capture efficiency at the two different velocities. This would indicate that the targets are acting independently of one another both from an electrostatic and an inertial point of view.

In Figure 6 we compare the effects on collection of five different spacings of a six sphere ensemble with that of a single sphere, both systems at $Stk_{eff} = 1.10$. Capture effi-

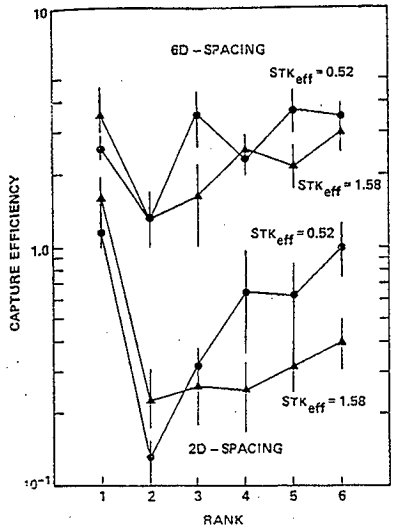

FIGURE 5. Effect of rank of target in line on collection of particles at 2-D and 6-D spacing and 600 and 2400 cm/s free-stream velocity, $\overline{K}_{E_{eff}} = 0.307$.

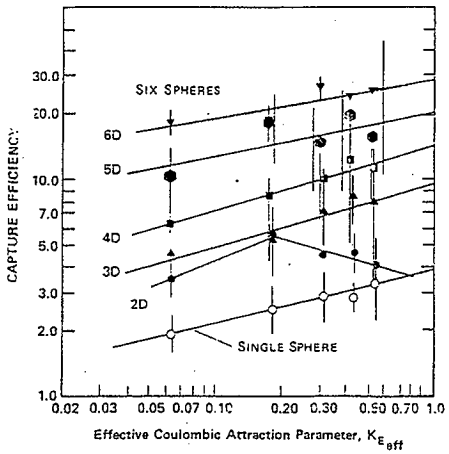

FIGURE 6. A comparison of collection by a single sphere with that of a six-sphere ensemble at various spacings. $Stk_{in} = 1.10$.

ciency is based on the cross section of the lead target. Generally, at this velocity, the same trend in improved collection with increasing Coulombic forces holds for the group of six targets as with a single sphere. However, at 2-D spacing for six spheres there is only a slight improvement over the collection by a single target. It is not until 6-D spacing is reached that the individual collection efficiency for each of six bodies exceeds that for a single body. This, again, is the result of image charging, poor intertarget penetration by particles and low intertarget velocities.

The effect of electrostatic forces at various fixed free-stream velocities on particle capture by multiple targets is best illustrated in Figure 7. In all cases we experienced maxima in collection at $K_E \approx 0.5$; further increases in charge on the collectors resulted in decreases in particle collection. This maximum was greatest at target Reynolds' numbers of 2400 and 4800 and least at 9600. One explanation for these maxima is that, as positive charge on the targets is increased, image charges increase in intensity in neighboring targets compressing the region of positive charge available for collection.

The overall effect may be to cause a polarization on each sphere where the forward region contains a compressed positive charge and the aft side a compressed negative charge. This would enhance collection on the forward stagnation region and reduce collection on the aft side of the targets and also in the regions between. This constriction of the region favoring deposition along with a reduction in particle concentration in the favored region may combine to produce the maxima shown in Figure 7.

The eddy diffusion coefficient for particle mass transfer, ϵ_p, is a function of both the scale of turbulence in the void region and the size of particles dispersed. Values of a

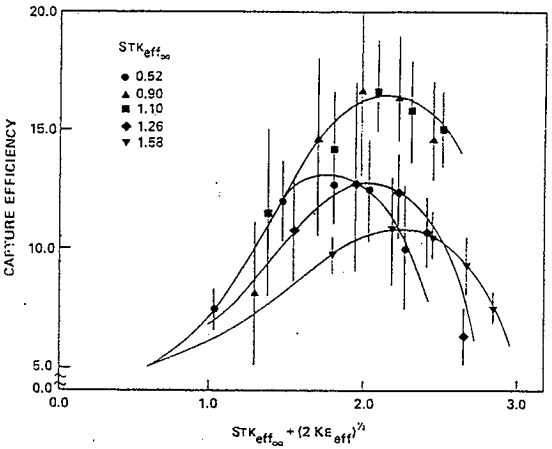

FIGURE 7. Collection efficiencies for six spheres in line: inertial and Coulombic forces. $L/D_c = 4$.

modified inverse Peclet number, $\epsilon_p/(v_\infty d)(z/d)^{1/3}$ were determined by Jacober and Matteson, 1990, for particle transport behind single spherical targets, and the variation of the ratio of eddy diffusion for momentum to that for particle mass transfer was correlated to the effective Stokes number

$$\epsilon_{m/\epsilon_p} = 2.2\,(\mathrm{Stk})^{0.2} \quad \text{and}$$

$$\frac{\epsilon_m}{v_\infty d}\left(\frac{z}{d}\right)^{1/3} = 0.0959.$$

These values of $\epsilon_p/(v_\infty d)(z/d)^{1/3}$ were constant for a given particle size and free-stream velocity and were used here in correlating the particle concentration profiles.

When multiple targets were tested, the target rank had to be taken into account along with spacing in the Graetz parameter. A best fit in correlating average particle concentration approaching a trailing target with target rank was obtained when the dimensionless distance term was multiplied by $(n-1)^{1/3}$ where n is the rank of the target.

The concentration data are plotted in Figure 8 with variables $(n-1)^{1/3}(z/d)^{2/3}$ for a given velocity and best fit the model based on centerline concentration (Eq. 25) in the region $0 < \theta < 0.7$ and $4(n-1)^{1/3}z/d/(\eta_1 P_e) < 1.0$. The intercept value of $1-\bar{\theta} = 0.33$ is obtained for an abcissa of 1.0 to yield $\alpha_p = \eta_1/12(v_\infty d/\epsilon_p)(z/d)^{-1/3}$, which is twice the value obtained from concentration profiles behind single targets. This may be a result of assuming that the concentration deposited on the targets are centerline values when in fact they are less.

The average value of the concentration facing a trailing target can be found from

$$\overline{\Delta C_p} = \frac{\int_0^{2\pi}\int_0^R \Delta C_p \Delta v\, r\, dr\, d\theta}{\int_0^{2\pi}\int_0^R \Delta v\, r\, dr\, d\theta}, \tag{32}$$

where

$$\Delta v = v_\infty \alpha_m \left(\frac{z}{d}\right)^{-2/3}(n-1)^{-1/3}\exp\left\{\frac{\xi^2}{\beta_m}\right\},$$

$$\beta_m = (6\epsilon_m/v_\infty d)(z/d)^{1/3},$$

$$\alpha_m = C_D(v_\infty d/48\epsilon_m)(z/d)^{-1/3} = \frac{C_D}{8\beta_m}.$$

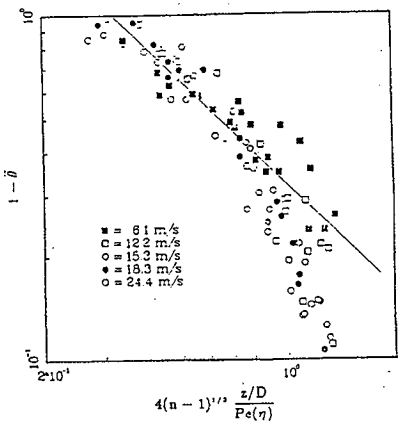

FIGURE 8. Mean particle concentrations in the wake of spherical targets, in line vs modified Graetz number.

The result of integrating Eq. (32) is

$$1-\bar{\theta}=\frac{\eta_1}{4}\left(\frac{z}{d}\right)^{-2/3}(n-1)^{-1/3}\frac{1}{(\beta_p+\beta_m)}\left\{\frac{1-\exp\left[-\frac{1}{4}\left(\frac{z}{d}\right)^{-2/3}(n-1)^{-1/3}\left(\frac{1}{\beta_p}+\frac{1}{\beta_m}\right)\right]}{1-\exp\left[-\frac{1}{4}\left(\frac{z}{d}\right)^{-2/3}(n-1)^{-1/3}\frac{1}{\beta_m}\right]}\right\} \tag{33}$$

Now the ratio $(1-\bar{\theta})/(1-\theta)_{max}$ is

$$\frac{\beta_p}{\beta_p+\beta_m}\left\{\frac{1-\exp\left[-\frac{1}{4}\left(\frac{z}{d}\right)^{-2/3}(n-1)^{-1/3}\left(\frac{1}{\beta_p}+\frac{1}{\beta_m}\right)\right]}{1-\exp\left[-\frac{1}{4}\left(\frac{z}{d}\right)^{-2/3}(n-1)^{-1/3}\left(\frac{1}{\beta_m}\right)\right]}\right\}, \tag{34}$$

which approaches 1.0 for large values of z/d, but in our tests is in the range of 0.65–0.90.

Another factor which may account for greater defects than predicted by Eq. 27 is that Peclet numbers determined by Jacober and Matteson (1990) were based on a model which applied similarity conditions in the wake at distances greater than five diameters. At closer distances one may expect a greater distance of interference from near wake effects.

Molecular scale (Brownian) diffusion may also occur but this is considered negligible compared to the turbulent or eddy diffusion considered here. For example if we compare

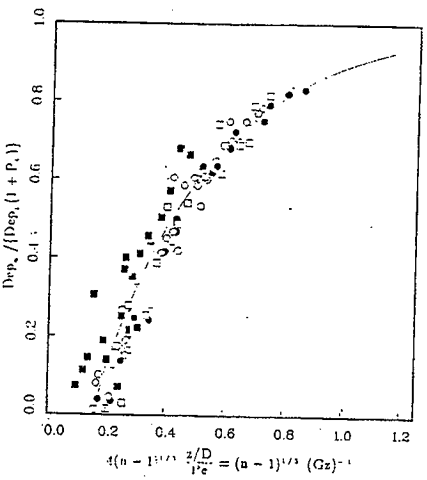

FIGURE 9. Particle deposition on trailing targets as a function of modified Graetz number. Solid line is best fit.

the Peclet number for molecular diffusion

$$P_e = \frac{dv_\infty}{D} \approx 10^{10},$$

where D is the diffusion coefficient of the particle due to thermal bombardment, with that for turbulent diffusion

$$P_e = \frac{dV_\infty}{\epsilon_p} \approx 72$$

at 6 m/s and $z/d = 5$, it is apparent that contributions to deposition based on thermal diffusion may be safely ignored.

The experimental data are again presented in Figure 9 in a form that lends itself to practical estimation of the deposition on trailing spheres. The ordinate of Figure 9 is the ratio of particles deposited on the nth target to that deposition on the first normalized to the value $(1 + P_1)$. The abscissa is now

$$(n-1)^{1/3}(Gz)^{-1}.$$

CONCLUSIONS

The capture of particles from air streams moving by single and multiple spherical targets has been evaluated at various levels of electrostatic charge in the non-Stokesian flow regime. An expression has been derived for the effective Coulombic attraction parameter which takes into account the non-Stokesian behavior of particles in the range $4.0 < Re_p < 16.0$, where

$$K_{E_{eff}} = \phi K_E \tag{15}$$

$$\phi = 1.01 Re_p^{-0.22} \tag{16}$$

This term has been combined with the effective Stokes number

$$Stk_{eff} = \psi Stk \tag{4}$$

$$\psi = 1.22 Re_p^{-0.22} \tag{5}$$

to describe capture efficiency by single, spherical targets charged opposite to the aerosol droplets

$$\eta = 1.4\left[Stk_{eff} + (2K_{E_{eff}})^{1/2}\right]. \tag{17}$$

Groups of spheres up to six in line were tested for collection efficiencies as a function of rank in line, spacing, and Coulombic and inertial parameters. It was demonstrated that, the concentration of particles in the wake of preceding targets estimated by measuring the deposition and velocity in those wakes, can be modeled using the similarity solution for the steady state transport of particles in the turbulent wake of single spheres as developed by Jacober and Matteson (1990).

The model is presented such that, if the free-stream concentration and velocity are known, then capture by the leading target can be obtained from the single target efficiency correlation (Eq. 17). Then deposition on succeeding targets can be obtained from an empirical curve relating deposition on the nth target to the dimensionless group $(n-1)^{1/3}(Gz)^{-1}$.

APPENDIX

An example will show how this data can be used to estimate deposition on an individual target. Let the particle size and density be 15.0 μm in diameter, and 1.0 g cm^{-3}, respectively; the free-stream velocity is 2400 cm s^{-1}; the targets are 0.6 cm in diameter and spaced $L/D = 5.0$ center-to-center; the free-stream concentration is 5.0 cm^{-3}. We wish to find the deposition on the fifth target after 10.0 min. The Coulombic attraction parameter $K_E = 0.10$.

It is first necessary to estimate Dep_1, the deposition on the lead target:

$$Dep_1 = \eta_1 (v_\infty C_{p\infty} A_1 t)$$

$$\eta = 1.4\left\{(Stk)_{eff} + (2K_{E_{eff}})^{1/2}\right\}$$

$$Stk = \frac{\tau v_\infty}{rc} = \frac{d_p^2 \rho_p}{18\mu} \frac{v_\infty}{rc}$$

$$= \frac{(2.25 \times 10^{-6})(1.0)(2400)}{18(1.8 \times 10^{-4})(0.3)} = 5.55$$

$$Stk_{eff} = 1.22(Re_p)^{-0.22} Stk$$
$$= 1.22\left(\frac{1.5\times10^{-3}(2400)}{0.15}\right)^{-0.22} \quad (5.55)$$
$$= 3.37$$
$$K_{E_{eff}} = 1.01(Re_p)^{-0.22}(K_E)$$
$$= 1.01(0.497)(0.1)$$
$$= 0.050$$
$$\eta_1 = 1.4\left[3.37 + ((2)(0.050))^{1/2}\right]$$
$$= 5.16.$$

Now it is necessary to estimate the value of the abscissa in Figure 9:

$$4(n-1)^{1/3}\frac{z/d}{P_e}$$
$$= 4(n-1)^{1/3}\left(\frac{\epsilon_p}{v_\infty d}\right)\left(\frac{z}{d}\right)^{1/3}\left(\frac{z}{d}\right)^{2/3}.$$

Values of the dimensionless eddy particle diffusion coefficient are obtained from Jacober and Matteson (1990):

$$\frac{\epsilon_m}{\epsilon_p} = 2.2(Stk_{eff})^{0.2}$$

and

$$\frac{\epsilon_m}{v_\infty d}\left(\frac{z}{d}\right)^{1.3} = 0.0959;$$

therefore

$$\frac{\epsilon_m}{\epsilon_p} = 2.2(3.37)^{0.2} = 2.81$$

and

$$\frac{\epsilon_p}{v_\infty d}\left(\frac{z}{d}\right)^{1.3} = \frac{0.0959}{2.81} = 0.0342.$$

Now, if $n = 5$ and $z/d = 5(n-1)^{1/3} = 1.59$, $(z/d)^{2/3} = 2.92$, and the abscissa for Figure 9 becomes: $4(1.59)(.0342)(2.92) = 0.635$. This yields a value for

$$\frac{Dep_5}{Dep_1(1+P_1)} = 0.72,$$

so

$$Dep_5 = (0.72)\eta_1(v_\infty C_\infty A_1 t)(1+P_1)$$
$$= (0.72)(5.16)(2400)(5.0)$$
$$\left(\frac{\pi(0.3)}{4}\right)^2(1800)(1.19)$$

$$Dep_5 = 6.75\times10^{\wedge} \text{ particles}$$

and

$$Dep_1 = 7.88\times10^6 \text{ particles.}$$

The authors wish to acknowledge partial support of this project by Environmental Protection Agency (EPA) grant R-812137-01. The contents do not necessarily reflect the views and policies of the EPA. Mention of commercially produced instruments and products does not constitute endorsement or recommendation for use by the EPA.

NOMENCLATURE

C_D	Particle drag coefficient (dimensionless)
C_{p_∞}	Particle number concentration (cm^{-3})
D_C, R_C	Collector diameter, radius (cm)
ϵ_p, ϵ_m	Eddy (particle, momentum) diffusion coefficient, ($cm^2 s^{-1}$)
d_p	Particle diameter (cm)
g	Acceleration due to gravity ($cm\ s^{-2}$)
Gz	Graetz number (dimensionless)
i	Subscript denoting interrarget conditions
K_E, $K_{E_{eff}}$	Coulombic attraction parameter, effective coulombic attraction parameter, defined in Eqs. (11) and (15), (dimensionless)
l_p	Stop distance (cm)
L	Spacing between spheres (cm)
n	Target rank
Q_1, Q_2	Particle, collector charge, (statcoulombs)
r, γ, z, α	Coordinates in particle trajectory defined in Figure 2, Eq. (7)
Re_p, Re_c	Reynolds number of particle, collector (dimensionless)
Stk	Stokes number, defined in Eq. 2 (dimensionless)
Stk_{eff}	Effective Stokes number, defined in Eqs. (4) and (5), (dimensionless)
Sc	Schmidt number $= \frac{\nu}{\epsilon_p}$
v_p, v_∞	Free stream particle, gas velocity ($cm\ s^{-1}$)
v_t	Terminal velocity of particle ($cm\ s^{-1}$)

v_r, v_y, v_z velocities in trajectory analyses, defined in Figure 2, Eq. (7)

ϵ_0 Permittivity of free space $= \frac{1}{4\pi}$ in cgs

η Particle capture efficiency, defined in Eq. (30), (dimensionless)

μ_g Carrier stream viscosity (g cm^{-1} s^{-1})

ρ_p, ρ_g particle, gas density (g cm^{-3})

ν kinematic viscosity (cm^2 s^{-1})

REFERENCES

Battler, J. R., Zhavoronkov, A. A., and Matteson, M. J. (1982). *J. Aerosol Sci.* 13:491–498.

Beard, K. V. (1974). *J. Atmos. Sci.* 31:1595–1603.

Brun, R. J., Lewis, W., Perkins, P. J., and Serafini, J. S. (1955). NACA TR 1215.

Deryagin, B. V. (1972). *Colloid J.* USSR (USA) 34:666–670.

Dorsch, R., Super, P., and Kadow, C. (1955). NACA TN 2587.

Fuchs, N. A. (1964). The Mechanics of Aerosols. Pergamon Press, Oxford.

George, H. F., and Poehlein, G. W. (1974). *Environ Sci. Technol.* 8:46–49.

Goldschmid, Y., and Calvert, S. (1963). *AIChE. J.* 9:352–358.

Graetz, L. (1883). *Ann. Phys.* 18:79–87.

Greenfield, S. (1957). *J. Met.* 14:115–125.

Grover, S. N. (1976). *Pure Appl. Geophys.* 114:509–539.

Grover, S. N., and Beard, K. V. (1975). *J. Atmos. Sci.* 32:2156–2165.

Grover, S. N., Pruppacher, H. R., and Hamielec, A. E. (1977). *J. Atmos. Sci.* 34:1655–1663.

Herbert, F. (1978). *J. Atmos. Sci.* 35:1744–1750.

Israel, R., and Rosner, D. E. (1983). *Aerosol Sci. Technol.* 2:45–51.

Jacobi, D. E., and Matteson, M. J. (1985). *Aerosol Sci. Technol.* 4:433–443.

Jacobi, D.E., and Matteson, M. J. (1990) *Aerosol Sci. Technol.* 12: in press.

Kraemer, H. F., and Johnstone, H. F. (1955). *Ind. Eng. Chem.* 47:2426–2434.

Langmuir, I., and Blodgett, K. (1946). U.S. Army TR 5418.

Matteson M. J. (1978). *The Collection of Aerosols by Charged Water Droplets.* Society of Chemical Industry Symposium on Deposition and Filtration of Particles. Loughborough University, September 6–8.

McAdams, W. H. (1954). *Heat Transmission.* McGraw-Hill, New York, p. 232.

Nielsen, K. A., and Hill, J. C. (1976a). *Ind. Eng. Chem. Fundam.* 15:149–156.

Nielsen, K. A. and Hill, J. C. (1976b). *Ind. Eng. Chem. Fundam.* 15:157–163.

Pilat, M. J. (1975). *J. Air Pollut. Control Assoc.* 25:176–178.

Pilat, M. J. and Prem, A. (1976). *Atmos. Environ.* 10:13–19.

Pilat, M. J. and Prem, A. (1977). *J. Air Pollut. Control Assoc.* 27:982–988.

Robig, G., and Porstendorfer, J (1979). *J. Colloid Interface Sci.* 69: 183–187.

Slinn, W. G. N. and Hales, J. M. (1971). *J. Atmos. Sci.* 28:1465–1471.

Sparks, L. E., and Pilat, M. J. (1970). *Atmos. Environ.* 4:651–660.

Ranz, W. E., and Wong, J. B. (1952). *Ind. Eng. Chem.* 44:1371–1381.

Walton, W. H., and Woolcock, A. (1960). *Aerodynamic Capture of Particles* (E. G. Richardson, ed.). Pergamon Press, New York, p. 129.

Wang, C. S., Beizaie, M., and Tien, C. (1977). *AIChEJ* 23:879–889.

Wang, P. K., Grover, S. N., and Pruppacher, H. R. (1978). *J. Atmos. Sci.* 35:1735–1743.

Zebel, G. (1968). *J. Colloid Interface Sci.* 27:294–304.

Received February 16, 1988; accepted October 20, 1988

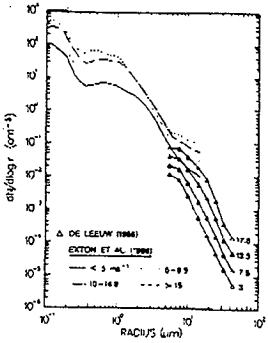

Fig. 3. Dependence of the particle size distribution on wind speed. Wind speed values are in $m\,s^{-1}$.

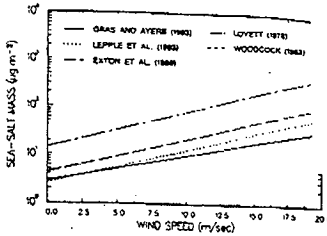

Fig. 4. Sea-salt mass concentration as a function of wind speed.

exhibited a relative minimum at 0.5 m for wind speeds below 5 $m\,s^{-1}$ and a maximum at a height of 1–2 m for winds in excess of 7 $m\,s^{-1}$.

Figure 3 shows the dependence of the particle size distribution on wind speed at a height of about 10 m, as measured by de Leeuw (1986) and Exton *et al.* (1986). The measurements of Exton *et al.* (1986) were made on a tower located on a beach of South Uist Island, the outer Hebrides, during periods when then the air trajectory was from the North Atlantic. The influence of surf-generated aerosol on the data of Exton *et al.*, if any, is not known. It is seen that wind speed has a strong influence on particle concentrations. The wind speed dependence of particle concentrations is a function of particle size and this is manifested by some change in the shape of the size distribution with increasing wind speed. In the giant particle size range, the data of de Leeuw (1986) indicate that the influence of wind speed is greatest for particles around 20–25 μm radius. The wind speed dependence of sea-salt particle concentrations and their vertical distribution in the surface layer is determined by the production rate of sea-salt particles as a function of wind speed, by the turbulent wind structure over waves and by gravitational and convective forces.

Figure 4 shows the dependence of sea-salt aerosol mass concentration on wind speed, as reported by several investigators. Each curve is a linear least squares fit of the expression $\ln\theta = b + aU$, where θ is the salt mass concentration and U is wind speed, to scatter plots of sea-salt mass vs wind speed. Sea-salt concentrations are determined either by computing the integrated volume from measurements of the particle size distribution or by measuring the sodium content of the salt solution extracted from aerosol samples. The individual scatter plots show that salt mass concentrations can vary by as an order of magnitude or more at a given wind speed. Factors contributing to this scatter include variations in wind speed history of the air mass (i.e. whether wind speeds are increasing or decreasing), variations in the stability structure of the marine boundary layer, variations in sea surface temperature which may affect viscosity and bubble production, and scavenging effects of precipitation.

Monahan *et al.* (1983, 1986) have combined the relationship between whitecap coverage and wind speed derived from shipboard photographic observations of the sea surface (Monahan, 1971; Toba and Chaen, 1973) with wave tank measurements of the sea-spray aerosol production rate per unit area of whitecap, to develop a model of the open-ocean sea-salt production rate, per unit area of sea surface, per increment of particle radius. The production rate in particles $m^{-2}\,s^{-1}\,\mu m^{-1}$ is given by

$$\frac{dF}{dr} = 1.373\,U^{3.41}\,r^{-3}(1+0.057\,r^{1.05})\,10^{1.19e^{-B^2}}$$

where U is the 10-m wind speed in $m\,s^{-1}$, $B = (0.38 - \log r)/0.65$, and r is particle radius in microns. Such a model is an important element in the development of a time-dependent model of the evolution of aerosol size distributions in the marine boundary layer.

4.3. *Mineral dust*

Mineral dust is a highly variable constituent of the marine aerosol. It is transported to the marine atmosphere from semiarid and desert regions when wind patterns are favorable. The coarse mode almost always contains a mineral dust component, but mean dust concentrations over most ocean areas including the North Atlantic, the tropical Pacific and the Southern Hemisphere oceans are typically less than 0.5 $\mu g\,m^{-3}$ and can be as low as 0.05 $\mu g\,m^{-3}$ (Prospero, 1979; Raemdonck *et al.*, 1986; Savoie *et al.*, 1987). However, high dust concentrations, sometimes exceeding the sea-salt concentration, can occur over certain ocean regions such as the tropical and equatorial North Atlantic Ocean, the northwest Indian

Temperature Information On Bouyant Displacements

The following table lists the bouyant displacement events detected in the burping tanks (less SY-101) since the Standard Hydrogen Monitoring Systems (SHMS) were installed. The last column indicates ~~that~~ whether a change was seen in the temperature profile after the "burp". The following graphs ~~are~~ show the temperature profiles for each event which shows the changes.

It should be remembered the temperature profile is measured at only two locations in each tank. If the "gob" does not move in the specific location of the HLT/thermocouple Tree no effect should be seen in the NC layer.

Conservation of energy would suggest that when the NC layer cools the C layer should warm. I haven't done detailed calculations around these to see how good the data fits.

The questions which this data may address are:

1) Do all the burping tanks experience bouyant displacement or is there some other mechanism?
   AW-101 is inconclusive on this point
2) How deep is the NC layer disturbed and does this give insight to the hardpan layer?

Tank	GRE Date	Temperature change?
SY-103	1/22/95	No
	3/1/95	Yes
	5/2/95	No
	8/23/95	No
	9/6/95	No
	12/3/95	Yes
	6/6/96	No
	7/14/96	Yes
	12/20/96	Yes
	11/27/97	Yes
	12/7/97	No
AW-101	10/1/94	No
	10/21/94	No
	11/27/94	No
	2/22/95	Yes
	5/8/95	No
	5/17/95	No
	7/8/95	No
	7/12/95	No
	8/2/95	No
	9/15/95	No
	9/22/95	No
	10/16/95	No
	12/12/95	No
	12/29/95	No
	2/5/96	No
	5/14/96	No
	6/5/96	No
AN-103	8/22/95	No
AN-104	11/6/94	No
	2/16/95	No

	8/3/95	No
	10/2/95	No
	10/5/95	No
	10/8/95	No
	5/3/96	Yes
	5/1/97	No
AN-105	8/21/95	Yes
	5/30/96	Yes
	4/5/97	No
	9/25/97	No
	12/31/97	No

Tank 241-AN-105
Temperature Profiles

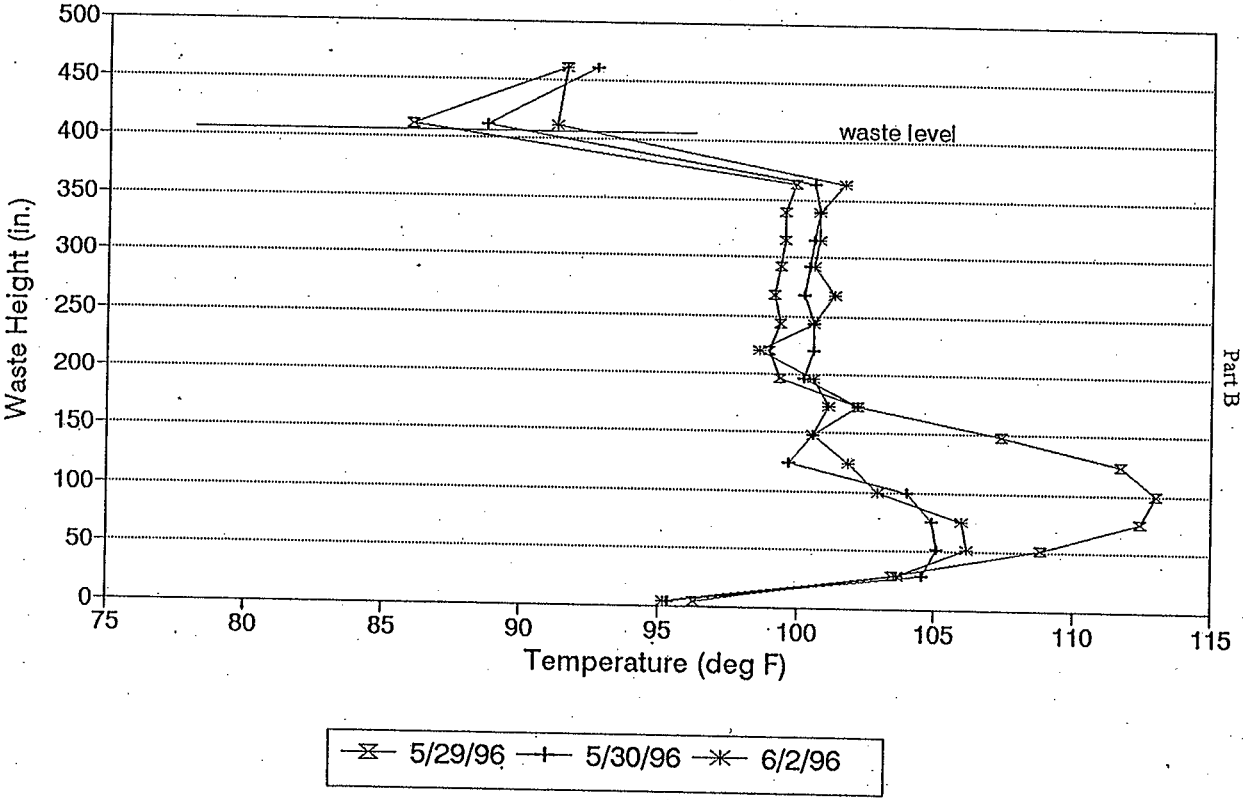

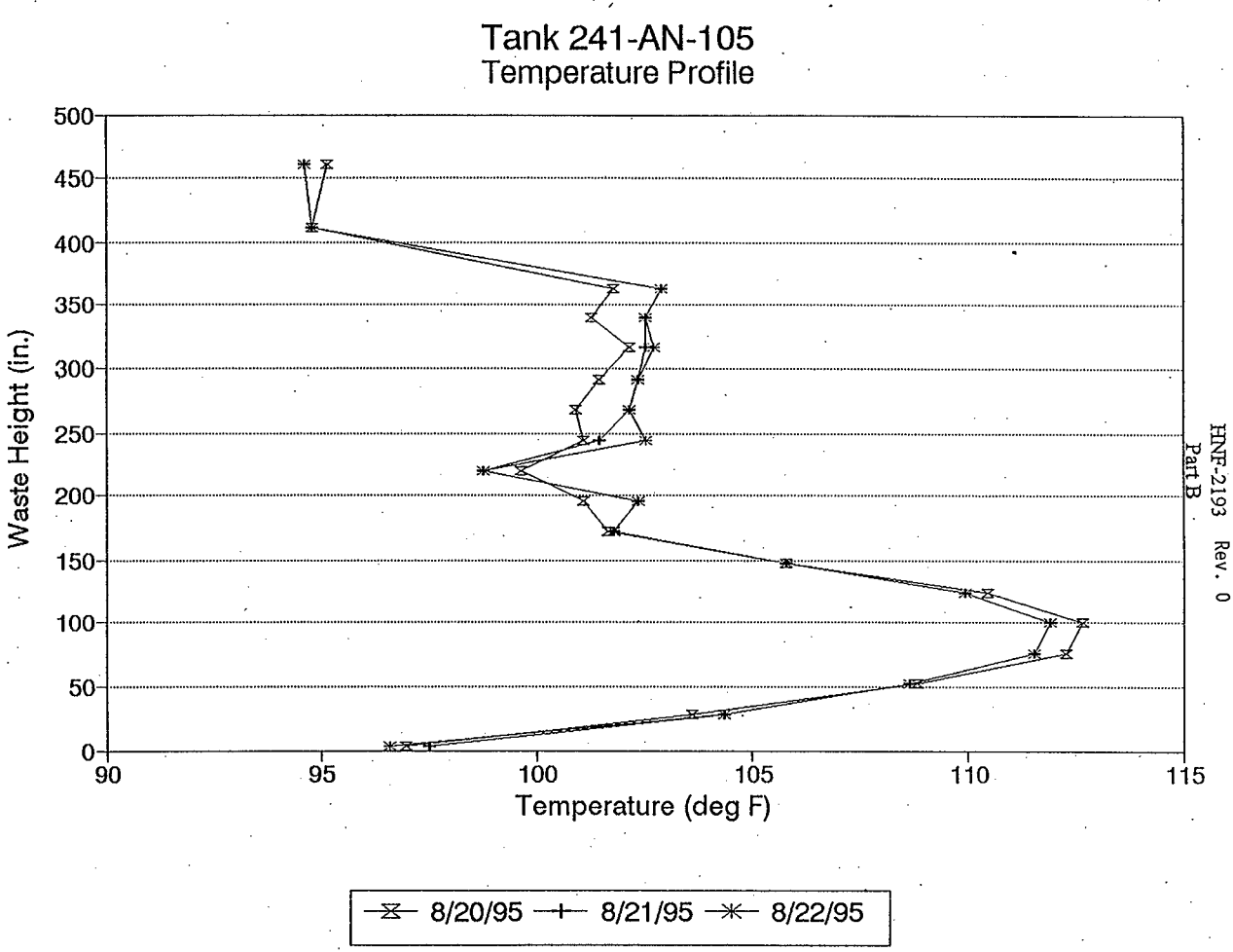
Tank 241-AN-105
Temperature Profile
Waste Height (in.)
500
450
400
350
300
250
200
150
100
50
0
90
95
100
105
110
115
Temperature (deg F)
8/20/95
8/21/95
8/22/95

Tank 241-AN-104
Temperature Profiles

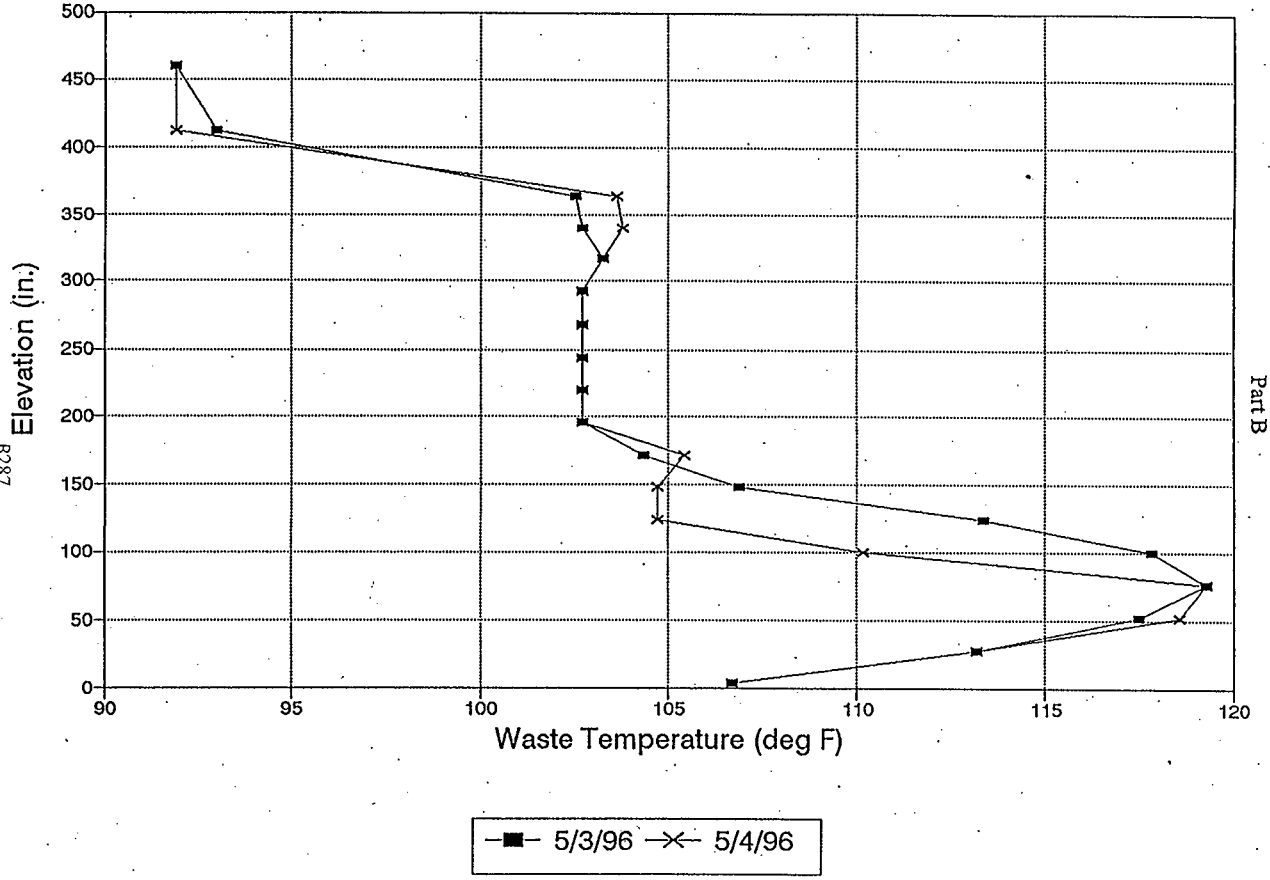

Tank 241-AW-101
Waste Temperatures

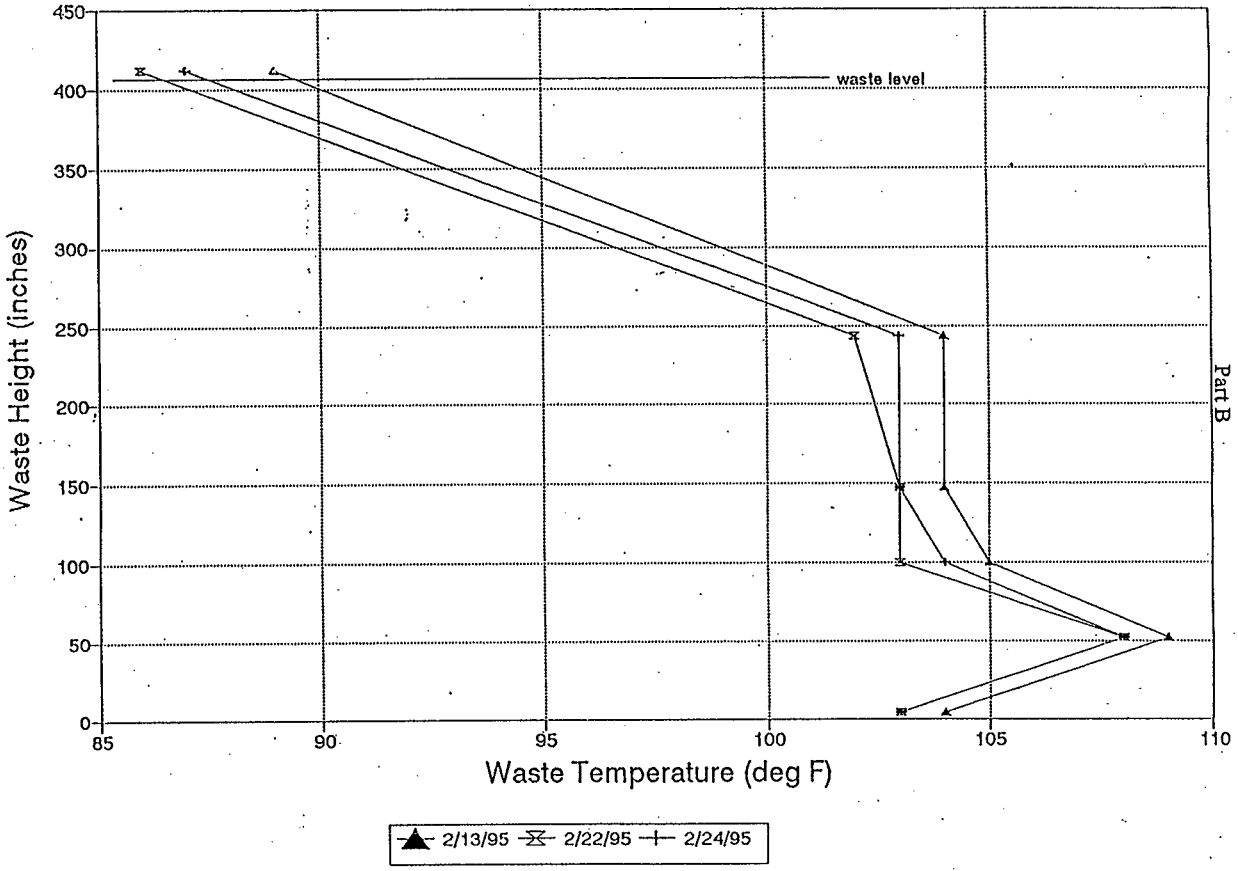

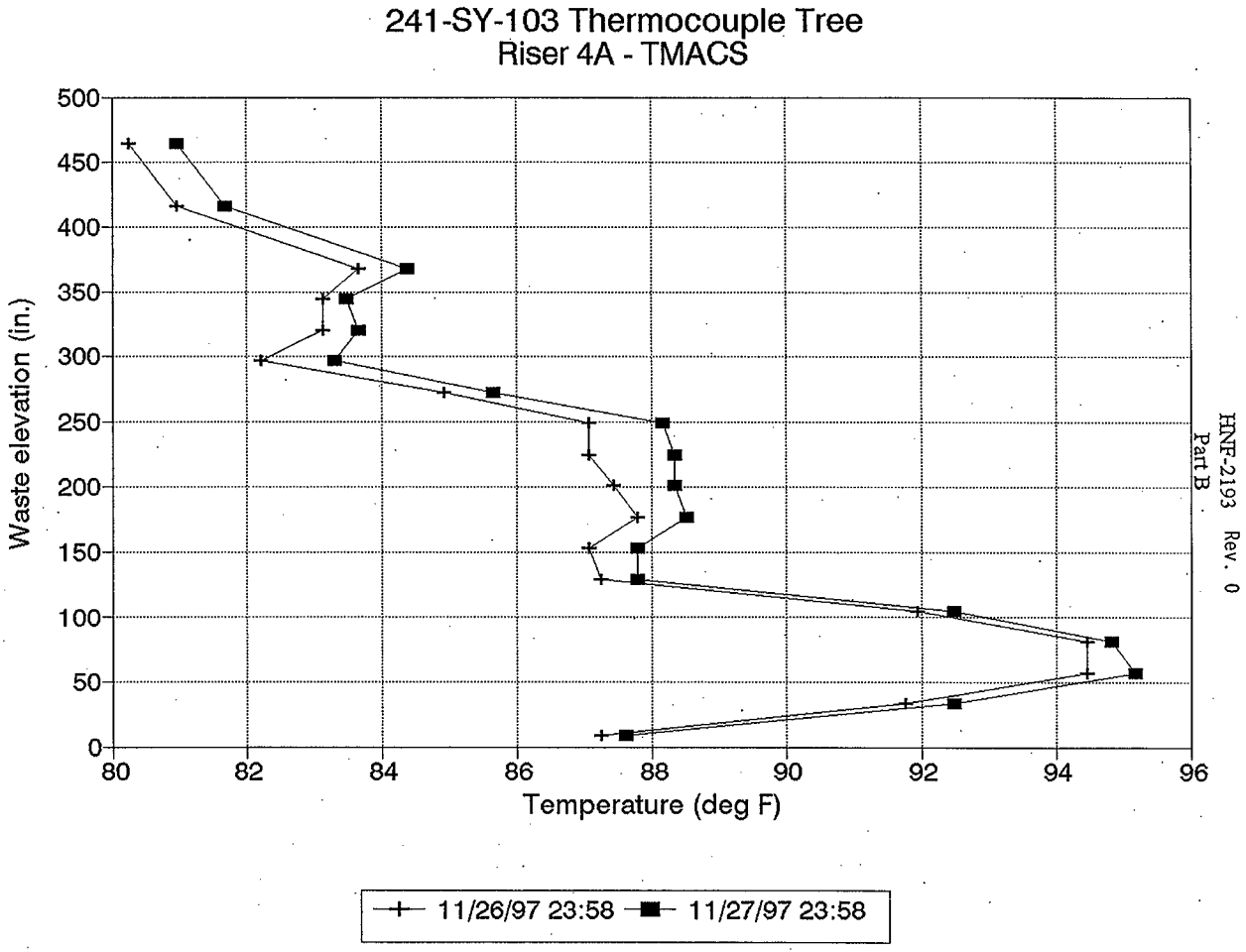
241-SY-103 Thermocouple Tree
Riser 4A - TMACS
Waste elevation (in.)
500
450
400
350
300
250
200
150
100
50
0
80
82
84
86
88
90
92
94
96
Temperature (deg F)
11/26/97 23:58
11/27/97 23:58

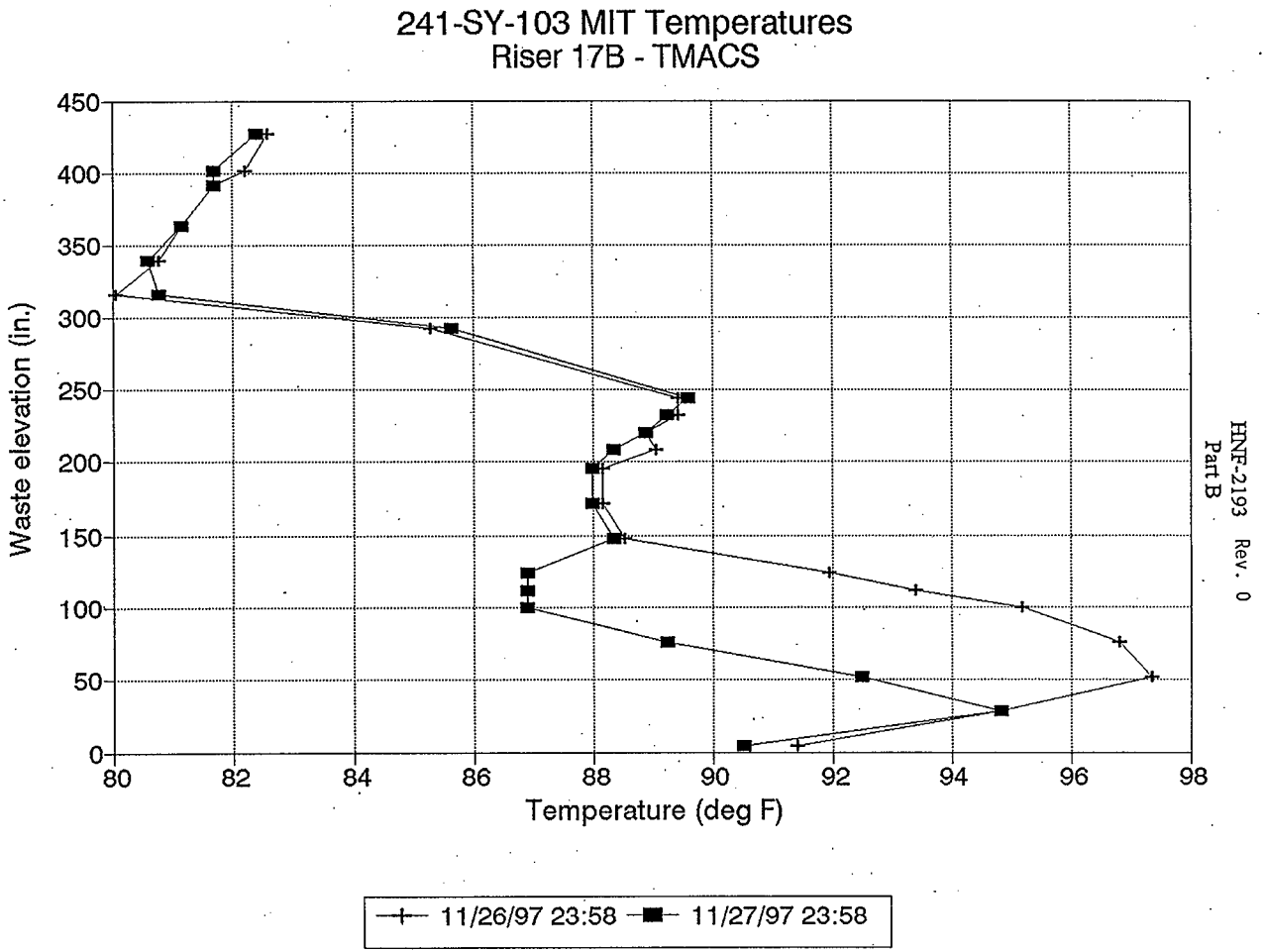
241-SY-103 MIT Temperatures
Riser 17B - TMACS
Waste elevation (in.)
450
400
350
300
250
200
150
100
50
0
80
82
84
86
88
90
92
94
96
98
Temperature (deg F)
11/26/97 23:58
11/27/97 23:58

Tank 241-SY-103
Waste Temperatures - Riser 4A
waste level : 272 in.
Elevation (in.)
Temperature (deg F)
450
400
350
300
250
200
150
100
50
0
78
80
82
84
86
88
90
92
94
96
98
3/1/95
3/3/95
3/7/95

Tank 241-SY-103
Waste Temperature - Riser 17B
waste level
Waste Temperature (deg F)
Elevation (in.)
2/28/95
3/3/95
3/5/95
100
95
90
85
80
75
450
400
350
300
250
200
150
100
50
0

UN 06 1996 (2) ENGINEERING DATA TRANSMITTAL

Page 1 of 1

1. EDT 610265

2. To: (Receiving Organization)	3. From: (Originating Organization)	4. Related EDT No.:
Distribution	Waste Tanks Process Engineering	N/A
5. Proj./Prog./Dept./Div.:	6. Cog. Engr.:	7. Purchase Order No.:
TWRS/74A10	S. D. Estey	N/A
8. Originator Remarks:		9. Equip./Component No.:
Transmitted for approval and release		N/A
		10. System/Bldg./Facility:
		N/A
11. Receiver Remarks:		12. Major Assm. Dwg. No.:
		N/A
		13. Permit/Permit Application No.:
		N/A
		14. Required Response Date:
		N/A

15. DATA TRANSMITTED

(A) Item No.	(B) Document/Drawing No.	(C) Sheet No.	(D) Rev. No.	(E) Title or Description of Data Transmitted	(F) Approval Desig-nator	(G) Reason for Trans-mittal	(H) Origi-nator Dispo-sition	(I) Receiv-er Dispo-sition
1	WHC-SD-WM-TI-755		0	An Analysis of Parameters Describing Gas Retention/Release Behavior in Double Shell Tank Waste	N/A	1,2	1	1

16. KEY

Approval Designator (F)	Reason for Transmittal (G)	Disposition (H) & (I)
E, S, Q, D or N/A (see WHC-CM-3-5, Sec.12.7)	1. Approval 4. Review 2. Release 5. Post-Review 3. Information 6. Dist. (Receipt Acknow. Required)	1. Approved 4. Reviewed no/comment 2. Approved w/comment 5. Reviewed w/comment 3. Disapproved w/comment 6. Receipt acknowledged

(G) Reason	(H) Disp.	17. SIGNATURE/DISTRIBUTION (See Approval Designator for required signatures) (J) Name (K) Signature (L) Date (M) MSIN	(J) Name (K) Signature (L) Date (M) MSIN	(G) Reason	(H) Disp.
1	1	Cog.Eng. S. D. Estey L. D. Estey 5/30/96 12:8	M.D. Guthrie 6/4/96	1	1
1	1	Cog. Mgr. W. B. Barton WB Barton 6/4/96			
		QA			
		Safety			
		Env.			

18.	19.	20.	21. DOE APPROVAL (if required) Ctrl. No.
S. D. Estey L. D. Estey 5/30/96 Signature of EDT Originator / Date	J. P. Harris 6-5-96 Authorized Representative for Receiving Organization / Date	W. B. Barton WB Barton 6/4/96 Cognizant Manager / Date	☐ Approved ☐ Approved w/comments ☐ Disapproved w/comments

)-7400-172-2 (04/94) GEF097

An Analysis of Parameters Describing Gas Retention/Release Behavior in Double Shell Tank Waste

S. D. Estey/M. D. Guthrie
WHC, Richland, WA 99352
U.S. Department of Energy Contract DE-AC06-87RL10930

EDT/ECN: 610265 UC: 2030
Org Code: 74A10 Charge Code: D2ME6
B&R Code: EW3130010 Total Pages: 25

Key Words: Gas Retention, Gas Release Event, Convective Waste, Non-Convective Waste, Depth, Specific Gravity

Abstract: This report documents a study to further define criteria associated with gas retention and subsequent release in double-shell tank (DST) waste. Each DST was analyzed to determine the compressibility of its waste contents by correlating changes in tank level with changes in atmospheric pressure. The compressibility of each DST's waste was then compared with two other parameters and two combinations of parameters describing the waste in the tank. These parameters/combinations were: (a) depth of non-convective waste; (b) specific gravity of convective waste; (c) the product "(a)x(b)"; (d) the difference "(a)/(b)". The data combination described in (c) is presented as the best correlation between analyzed parameters and DST gas release event (GRE) behavior.

Release Approval 6/6/96 Date

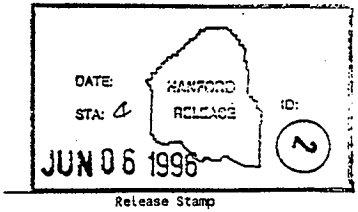

Release Stamp

Approved for Public Release

TABLE OF CONTENTS

LIST OF TABLES

LIST OF FIGURES

WHC-SD-WM-TI-755
Revision 0

1.0 SUMMARY

This report documents a task associated with the technical justifications which were specified as a condition of the Multi-Function Waste Tank Facility (MWTF) cancellation decision (Alumkal 1995; Sidpara 1995). The original task specification was titled "Validate 1.35 SpG", and was intended to refine the impacts of waste concentration limits on double-shell tank (DST) operational volume capacity. Schedule and budget limitations reduced the task to a brief survey and analysis of available waste tank data to see if additional justification could be demonstrated for the current waste concentration limits (Fowler, 1995a & 1995b), or to determine if some alternative analysis approach was appropriate. The results were originally communicated via internal memo (Estey & Guthrie 1995). This report presents the results in the supporting document format.

This effort resulted in the calculation of a theoretically objective measure of the relative magnitude of gas entrapment in each DST. This measure, (dL/dP), indicates the compressibility of DST waste, and, with certain assumptions, can be related to the amount of gas trapped in the waste. If gas were trapped in the DST waste, an increase in pressure on the gas (attributed to an increase of barometric pressure) would result in a decrease of waste volume or tank level. Therefore, to have any physical significance, tank waste with trapped gas must exhibit a dL/dP value which is negative. In addition, the most current measurements or best estimates of two DST waste quantities were obtained: 1) total thickness or depth of non-convective wastes in each DST, and 2) the density of the convective waste in each DST. With the depths, densities, and dL/dP values known for each of the DST, various combinations of these parameters were analyzed. This analysis presents evidence of new correlations of waste parameters and gas entrapment/release behavior of DST waste and suggests a new criteria which could be used as a waste concentration limit.

2.0 INTRODUCTION

Allowable dewatering of Hanford tank wastes is an important factor in determining reserve volume capacity of the double shell tank (DST) system (Awadalla 1995). Analysis in recent years suggested that unrestricted dewatering of wastes, while maximizing the available DST capacity, establishes conditions likely to cause undesirable gas retention within the waste (Reynolds 1994; Fowler 1995a & 1995b). The mechanisms by which tank waste retains gas are unknown, but the empirical property historically found to most closely correlate with gas retentive behavior is specific gravity (SpG) (Reynolds 1994). Most likely, other properties associated with high specific gravity waste (e.g, high waste viscosities caused by formation of large amounts or certain types of solids, saturated salt solutions, or formation of gelatinous aluminum compounds) actually cause the gas retention, but such mechanisms have not been established. Other specific gravity values (Hudson

1995) have been proposed as a limit describing waste gas retention behavior, but (Reynolds 1994) describes the current basis for the controlling criteria specified in (Fowler 1995a & 1995b).

The criteria (Fowler 1995a & 1995b) intended to prevent undesired gas retention in DST waste are stated as a phased approach. Any waste to be transferred into a DST must have a specific gravity equal to or less than 1.3, or additional analysis will be required to justify the transfer. If the specific gravity of the waste to be transferred is greater than 1.3, the weighted mean of the commingled waste must be determined. The interpretation is that the bulk specific gravity of the waste in the receiver tank, after receipt of the new waste, must be determined (estimated by calculation) if the waste to be added to the receiver tank has a specific gravity of greater than 1.3. If this weighted mean specific gravity is calculated at less than 1.41, the transfer will be allowed. If the weighted mean specific gravity is calculated at greater than or equal to 1.41, additional technical evaluation will be required to show that unsafe gas retention conditions will not occur in the receiver tank.

Although the criteria widely referred to as the "1.41 specific gravity limit" does not represent an absolute requirement for a waste transfer, practical considerations, such as the difficulty in demonstrating that a higher specific gravity won't create a problem, treat it as such. The issue of the suitability of the specific gravity limit continues to be questioned due to the lack of definition for the mechanism which relates specific gravity to gas retentive behavior (Fowler 1995b). Further, new information and relationships have recently come to light which were either not known or available when the initial work which developed the current waste specific gravity limits was performed. These considerations suggest that further investigation the limits associated with gas retention is warranted, particularly if conservation of DST operational volume is indicated.

3.0 DISCUSSION

3.1 Defining the Analysis Methodology

Due to the importance assigned to recent waste tank flammable gas analyses performed at the Hanford Site, use of a similar analysis was desired to determine if it might represent an objective measure of a tank's gas retention properties. If the analysis indicated that the amount of gas trapped within tank waste could correlate with some other descriptive measure of the waste contained within the tank, such as accurate estimates of a tank's solid (non-convective) waste volume or a liquid (non-convective) specific gravity, strong evidence of a relationship would be established. Therefore, this analysis looked as comparisons of calculated dL/dP values for a given tank with the nonconvective waste volume (depth), or a convective waste (liquid) specific gravity, or various combinations thereof.

This investigation focused on the relationships identified by and developed in recent tank waste analyses which suggests a quantitative measure of gas trapped within tank waste (Whitney 1995; Hodgson 1995a). The physical principles upon which these analyses were performed is repeated here. The logic reasoned that real changes in tank level caused by variations in atmospheric pressure, without interference from any additional factors, implies the presence of a compressible volume within the waste - i.e., a gas volume.

Such a relationship, a change in tank level with a change in barometric pressure (dL/dP), is a measure of the compressibility of the waste. When the volumes, specific gravities, and locations of the various physical forms of waste contained within the tank are known, the relationship between dL/dP and the amount of trapped gas can be derived from Boyle's Law or the Ideal Gas Law, when ideal behavior is assumed. This relationship is simply stated in the form:

$V = -A*P*dL/dP$ where,

V volume of gas trapped in tank waste at pressure P (e.g., ft^3)

A cross-sectional area of the tank (e.g., ft^2)

P pressure exerted on the volume of trapped gas (e.g., lb_f*ft^{-2})

dL/dP = measured change in tank level divided by a measured change in atmospheric pressure (slope, e.g, $lb_f^{-1}*ft^3$)

Only approximate estimates of V can be obtained in this manner because the true configuration of tank wastes and distribution of gas within the wastes is not known. However, the value yielded based on assumptions of the gas distribution may be useful for comparison purposes. This analysis did not attempt to determine volumes of gas trapped within a DST, but rather compares calculated dL/dP values to information already known about the DSTs.

In determining dL/dP values for the DSTs, this analysis took a simpler and more direct approach than the statistical barometric pressure/tank level analyses used in (Whitney 1995; Hodgson 1995a). In this analysis, dL/dP was determined by comparing tank level and atmospheric pressure data over a single, discrete time period. The intent was to create data comparisons which allow elimination of as many potential error terms as possible. This resulted in selectivity of the time intervals chosen, and the time intervals for any given DST may range from about one week to six months or more.

The major assumption of this analysis is that the effects of temperature changes and water evaporation can be factored out of the raw tank level data. Engineering judgement and knowledge of the latest tank conditions, along with visual interpretation of the tank level data, were used to select time intervals which were apparently not affected by the waste transfers, waste

additions, and water additions common in numerous DSTs. The combination of assumptions and selectivity of time interval used in the analysis increases the chances that the previously mentioned complicating factors are effectively eliminated from the analysis. The standard time interval used was 10/1/95 to 12/31/95. A different time interval was used if knowledge of one of the concerns mentioned previously ruled out use of the standard interval. An obvious example here was tank 101-SY, which was evaluated during what is considered to be a quiescent period between gas release events (GREs) in 1992. An advantage of the standard interval is that it included the time period around 12/12/95, which featured an extreme atmospheric pressure drop and subsequent rise accompanying a major storm system that passed over the Northwestern States.

All data relationships investigated were expressed in the form of dL/dP = f(non convective waste volume and/or liquid specific gravity). In these analyses, non convective waste volume and liquid specific gravity for each tank constitute the independent data/data sets, while the calculated values of dL/dP for each tank constitute the dependent data. Some other assumptions used in this analysis must be stated for the independent data. One is that, in the absence of a direct measurement, the sum of volumes of sludge, salt cake and crust were the equivalent of the volume of non-convective waste in a tank. The second is that a liquid specific gravity is synonymous to the specific gravity of the convective waste in the tank.

3.2 Development of the Dependent Data (dL/dP)

The general procedure to derive the value dL/dP started by obtaining tank level and barometric pressure data for the interval of concern (nominally 10/1/95 to 12/31/95). If investigation of the tank level behavior indicated an unstable history, additional level and pressure data would be investigated until a satisfactory time interval was identified. The term "unstable history" indicates that discrete and rapid step level changes were in evidence, indicating that the tank was experiencing a waste transfer or water addition. A "satisfactory time interval" exhibited no evidence of a waste transfer or water addition.

The level data for each DST was obtained through the personal computer surveillance analysis computer system (PC SACS) using manual Enraf, automatic Food-Instrument Corporation (FIC), or manual tape measurements, depending on which instrument was available for a given tank during the desired time period. The barometric pressure data was obtained from the weather station at 6 hour increments (2400, 0600, 1200, 1800) for all time periods in question. The level and pressure data were then placed in a spreadsheet to allow for comparison. The time at which level data was recorded was compared to the times of the available barometric pressure data. The specific barometric pressure readings selected for use were those recorded at the time most closely matching the estimated average time at which the level data was recorded. This selection was made based simply upon visual observation of the data as reported.

Next, a decision was made on whether the tank level data required detrending. Detrending is the term which describes the process of removing any additive trend in the level data, which in accordance with the analysis assumptions, would be due to waste temperature changes, water evaporation, or slow waste transfers/water additions. To determine is detrending was required, the data was graphed with the number of days plotted on the horizontal axis while the tank level data was plotted on the vertical axis. The plot was visually inspected. If the average tank level did not change over the time interval, the level data was not detrended. If the average tank level showed a trend over the time interval, it was an indication that waste temperature was changing and or water was evaporating from the waste, etc. If the level data indicated waste temperature changes or evaporation, the level data was detrended. If detrending was required, it was first performed by linear regression, with time as the independent variable and tank level as the dependent variable. In a few cases, the linearly regressed level data plot showed obvious non-linear behavior, and the level data was detrended again using a quadratic interpolating polynomial. In one extreme case (tank 101-AZ), the linearly detrended level data presented an evident S-curve and a cubic interpolating polynomial was used for its final detrending.

The linear or polynomial fits used for detrending the data were applied with the first tank level data point as the day zero (x=0) intercept on the tank level axis (y-axis) of the plot. The subsequent level data was detrended by subtracting the product of the slope(s) of the linear regression multiplied by the number of days which had elapsed from day 0 of the interval. If detrending was performed by a polynomial, each term of the polynomial was multiplied by the number of days raised to the power appropriate for the order of fit term. Figure 1 illustrates an example of these manipulations, showing a plot of days versus both raw and detrended level data for tanks 101-AZ and 104-AN.

The next step in the development of the dependent data was to remove the raw level data from the plots illustrated in Figure 1 where appropriate, and add the barometric pressure data on the secondary (right side) vertical axis. Obviously, if detrending was not performed on a set of tank level data, the raw level is still used. While these plots are not really needed to obtain the value of dL/dP, they permit visual observation of any correlations in the data. These plots were prepared for all the DSTs, but only in a few cases can a correlation be visually observed. Those correlations which were evident were from tanks with dL/dP values of the greatest magnitude. Examples of these plots for tanks 101-AZ and 104-AN are shown in Figure 2.

Finally, for each DST, another regression was performed on the tank level data, which may or may not have been detrended, and the barometric pressure data. In all cases, linear regression was performed, using barometric pressure as the independent variable and tank level as the dependent variable. This linear regression gave the best-fit straight line through what is essentially a scatter plot of the detrended level and pressure data. The slope of the best-fit line through the data corresponds to the desired value

dL/dP. An example of this, once again for tanks 101-AZ and 104-AN, is shown in Figure 3. To have any physical significance, the slope would have to be a negative value, which indicates a volume reduction upon a pressure increase. It can be seen in Figure 3 that tank 101-AZ exhibits a positive value for dL/dP. Only a few tanks exhibit positive values for dL/dP, and the magnitudes of those calculated positive slopes are, in general, small compared to the magnitudes of the calculated negative slopes. For example, no positive dL/dP slope was found to exceed 0.1 inches level/in mercury (Hg), whereas the magnitude of negative dL/dP slopes frequently exceeds a magnitude of 0.1 inches level/in Hg, reaching a magnitude of 0.85 for tank 101-SY.

Tables 1 and 2 summarize results from the development of the dL/dP data for each DST, and includes 95% confidence values for the dL/dP slopes determined in the final regression of the scatter-plot data shown in Figure 3.

Table 1

Determining dL/dP Values

Tank	Date of Initial Tank Level Observation	Number of Tank Level Observations	Method of Tank Level Measurement	Time Barometric Pressure Recorded
AN-101	12/12/95	19	Auto FIC	0600
AN-102	10/01/95	92	Auto FIC	0600
AN-103	10/23/95	80	Manual Enraf	1200
AN-104	10/11/95	80	Manual Enraf	1200
AN-105	09/01/95	116	Manual Enraf	1200
AN-106	11/01/95	50	Auto FIC	0600
AN-107	10/01/95	92	Auto FIC	0600
AP-101	10/01/95	92	Auto FIC	0600
AP-102	10/01/95	92	Auto FIC	0600
AP-103	12/01/95	21	Auto FIC	0600
AP-104	10/01/95	32	Auto FIC	0600
AP-105	01/01/95	236	Auto FIC	0600
AP-106	10/01/95	34	Auto FIC	0600
AP-107	10/01/95	92	Auto FIC	0600
AP-108	10/01/95	30	Auto FIC	0600
AW-101	10/01/95	92	Manual Enraf	1200
AW-102	05/02/95	15	Manual Tape	1200
AW-103	10/01/95	91	Manual Tape	1200
AW-104	10/01/95	91	Manual Tape	1200
AW-105	12/08/95	11	Manual Tape	1200
AW-106	10/01/95	91	Manual Tape	1200
AY-101	10/01/95	92	Manual Tape	1200
AY-102	11/15/95	30	Auto FIC	0600
AZ-101	06/22/95	113	Manual Enraf	1200
AZ-102	10/01/95	34	Auto FIC	0600
SY-101	05/01/92	123	Auto FIC	2400
SY-102	10/01/95	92	Manual Enraf	1200
SY-103	05/08/95	102	Manual Enraf	0600

Table 2

Determining dL/dP Values (continued)

Tank	Regression Polynomial used to Detrend Tank Level	Mean dL/dP values from linear regression of tank level and barometric pressure data	Standard Deviation	95% Confidence Interval on the Mean
AN-101	none	+7.3E-6	2.5E-4	±9.9E-5
AN-102	none	-0.0044	0.019	±0.0033
AN-103	none	-0.44	0.038	±0.0071
AN-104	linear	-0.17	0.024	±0.0045
AN-105	quadratic	-0.11	0.020	±0.0031
AN-106	none	+1.1E-11	1.6E-12	±3.8E-13
AN-107	none	+0.080	0.081	±0.014
AP-101	linear	+0.00038	0.017	±0.0030
AP-102	linear	-0.0070	0.014	±0.0024
AP-103	none	-6.6E-14	1.5E-14	±0.56E-14
AP-104	none	-6.3E-12	1.2E-12	±0.36E-12
AP-105	quadratic	-0.036	0.010	±0.0011
AP-106	none	-0.0027	0.00023	±0.000067
AP-107	linear	+0.018	0.023	±0.0040
AP-108	none	-0.0025	0.00012	±0.000037
AW-101	none	-0.25	0.024	±0.0042
AW-102	none	none	none	±0
AW-103	none	-0.067	0.018	±0.0031
AW-104	linear	-0.15	0.064	±0.011
AW-105	none	-0.054	0.015	±0.0081
AW-106	quadratic	-0.066	0.025	±0.0044
AY-101	linear	+0.021	0.072	±0.013
AY-102	linear	-0.040	0.035	±0.011
AZ-101	cubic	+0.029	0.039	±0.0061
AZ-102	quadratic	-0.011	0.026	±0.0075
SY-101	linear	-0.85	0.019	±0.028
SY-102	linear	-0.013	0.016	±0.0028
SY-103	quadratic	-0.13	0.016	±0.0026

Figure 1

Examples of Tank Level Detrending

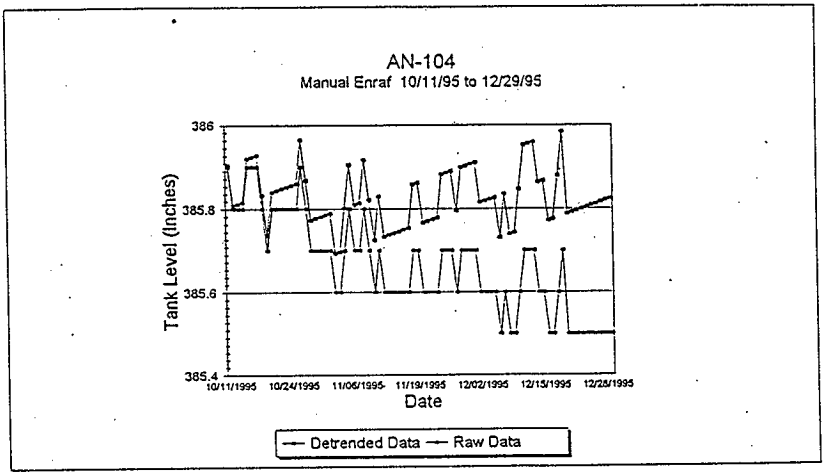

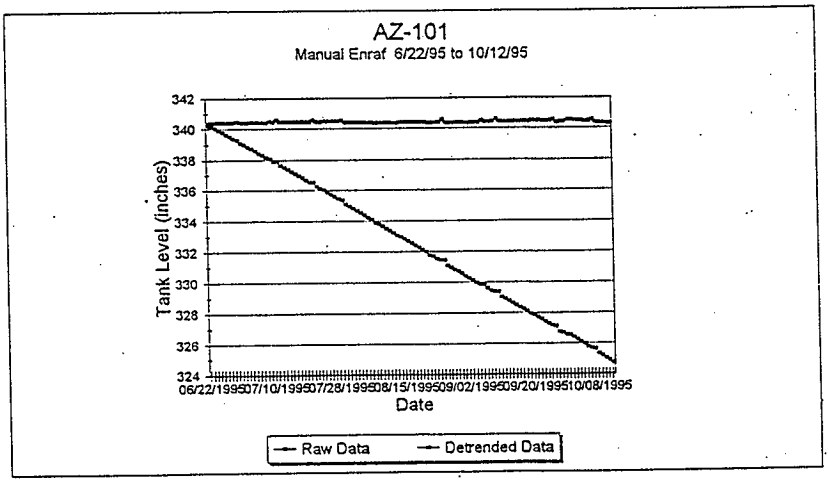

Figure 2

Chronological Plots of Tank Level and Barometric Pressure

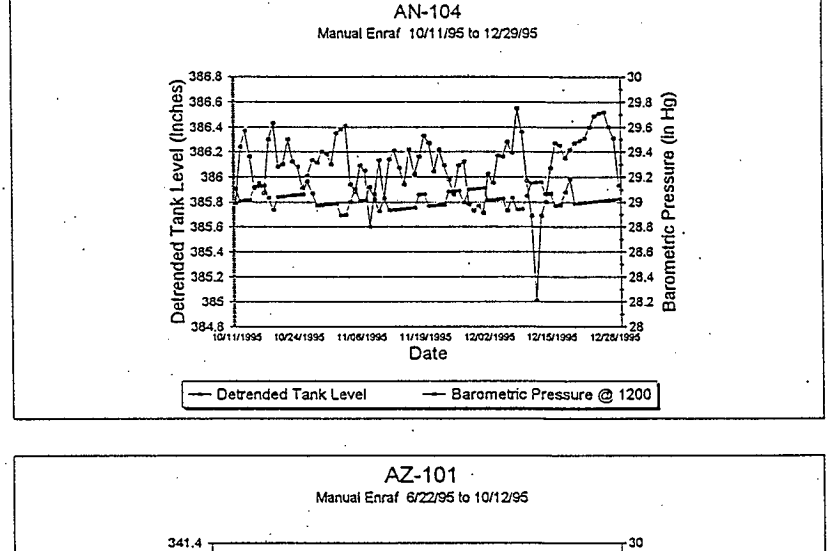

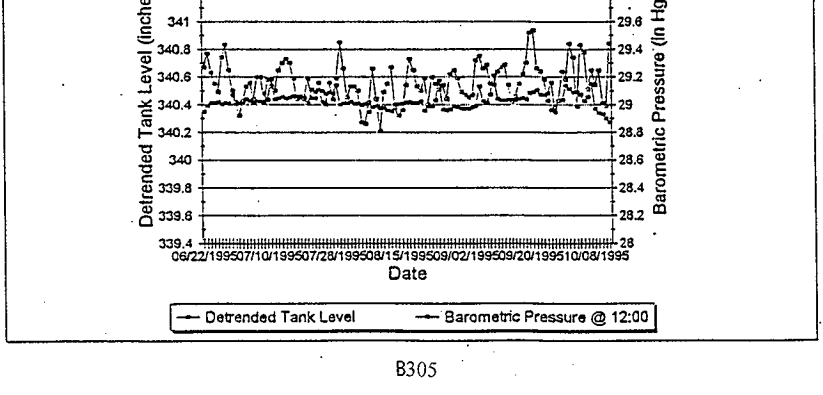

Figure 3

Examples of Tank Level - Barometric Pressure Linear Regression

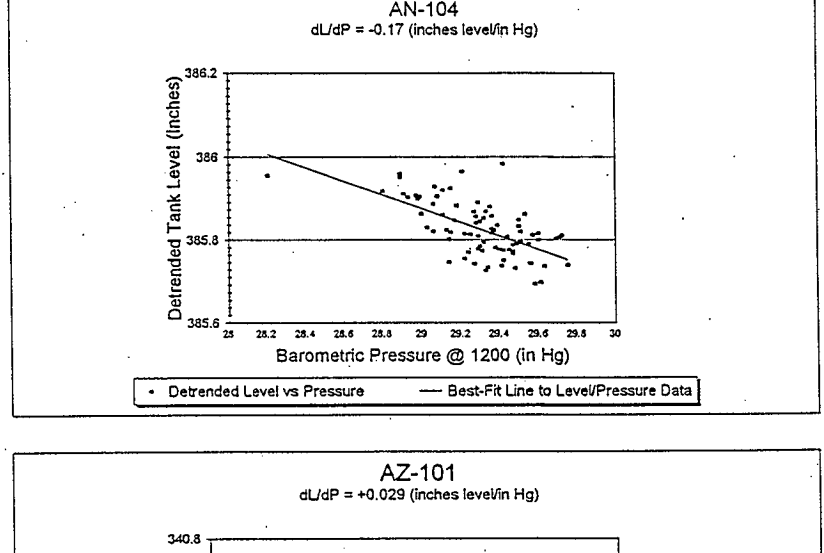

3.3 Identification of the Independent Data

The independent data used in this study was limited to estimates of the total volume of non-convective waste in a DST and the specific gravity of the convective waste in the DST. Tables 3 and 4 summarize the values identified for these two quantities and gives references for each of the values listed. These quantities are believed to represent the best engineering estimates of the current tank conditions.

3.4 Data Analysis

The final data set included the calculated dL/dP values for each of the DST's analyzed, along with a variety of combinations of the independent data identified for the tank. Data relations were investigated by correlating independent data (non-convective waste volumes and convective waste specific gravities), either singly or in combination, with the dependent data (dL/dP). As a result, limited data analysis was performed on four combinations of chosen data:

1. dL/dP vs Total Non-Convective Waste Depth
2. dL/dP vs Convective Waste SpG
3. dL/dP vs (Total Non-Convective Waste Depth*Convective Waste SpG)
4. dL/dP vs (Total Non-Convective Waste Depth/Convective Waste SpG)

A correlation of the form dL/dP vs (convective Waste SpG/Total Non-Convective Waste Depth) was ruled out because it is undefined for tanks without a non-convective waste volume and because it gave meaningless results for DSTs which did possess a volume of non-convective waste. Figures 4 - 7 show a graphical depiction of the correlations. Also shown in the Figures is a quadratic regression of the results which were plotted for each of the four cases. A quadratic fit was chosen because the data plot clearly exhibit non-linear behavior. In addition, this best-fit curve to the data was felt to offer some simple means to objectively compare one data combination to the other. One observation immediately evident is that Figure 5 indicates that the specific gravity of wastes in a DST must exceed 1.4 in order for the tank to exhibit GRE behavior. This is consistent with the existing waste compatibility criteria (Fowler 1995a & 1995b). From the data analysis, the following is noted:

Fig.	Data Combination	Regression Variance (R^2 Values)
4	1. dL/dP vs waste depth	0.87
5	2. dL/dP vs waste SpG	0.49
6	3. dL/dP vs depth*SpG	0.87
7	4. dL/dP vs depth/SpG	0.73

The variance of the regression, which is an indicator of the degree of correlation between the independent and dependent variables, indicates that dL/dP correlates more strongly, and to an equal degree, with non-convective waste depth and (non-convective waste depth*convective waste specific gravity) as the independent variables. However, it is felt that the correlation shown in Figure 6 (Data Combination 3, dL/dP vs waste depth*waste SpG) offers two key advantages over that shown in Figure 4 (Data Combination 1, dL/dP vs waste depth). These advantages are:

a. Figure 6 shows a clearly evident separation between those DSTs which have documented GRE behavior and those DSTs which do not. This separation is not at all evident in Figure 4.

b. Figure 6 exhibits a stronger (i.e., more linear) correlation if only DSTs with documented GRE behavior are considered.

WHC-SD-WM-TI-755
Revision 0

Table 3

Data Sources for Waste Depths and Specific Gravities

Tank	Sludge+Salt Cake Volume	Crust Volume	Liquid Density
AN-101	(Hanlon 1995)	estimated*	(Esch 1996)
AN-102	(Hanlon 1995)	estimated*	(Van Vleet 1993)
AN-103	estimated*	estimated*	(Guthrie 1996)
AN-104	estimated*	estimated*	(Guthrie 1996)
AN-105	estimated*	estimated*	(Guthrie 1996)
AN-106	(Hanlon 1995)	estimated*	(Dodd 1994)
AN-107	(Hanlon 1995)	estimated*	(Herting 1993)
AP-101	(Hanlon 1995)	estimated*	(Simpson 1994c)
AP-102	(Hanlon 1995)	estimated*	(Simspon 1994b)
AP-103	(Hanlon 1995)	estimated*	(Simpson 1994a)
AP-104	(Hanlon 1995)	estimated*	(Winters 1988)
AP-105	(Hanlon 1995)	estimated*	(Simpson 1994d)
AP-106	(Hanlon 1995)	estimated*	(Welsh 1994)
AP-107	(Hanlon 1995)	estimated*	(Miller 1995)
AP-108	(Hanlon 1995)	estimated*	(Jones 1994)
AW-101	estimated*	estimated*	(Guthrie 1996)
AW-102	(Hanlon 1995)	estimated*	(Guthrie 1996)
AW-103	(Hanlon 1995)	estimated*	(Hodgson 1995b)
AW-104	(Hanlon 1995)	estimated*	(Tusler 1995)
AW-105	(Hanlon 1995)	estimated*	(Jones 1994)
AW-106	(Hanlon 1995)	estimated*	(Guthrie 1996)
AY-101	(Hanlon 1995)	estimated*	(Van Vleet 1993)
AY-102	(Hanlon 1995)	estimated*	(Van Vleet 1993)
AZ-101	(Hanlon 1995)	estimated*	(Rollison 1994)
AZ-102	(Hanlon 1995)	estimated*	(Schreiber 1995)
SY-101	estimated*	estimated*	(Reynolds 1992)
SY-102	(Hanlon 1995)	estimated*	(Sutey 1995)
SY-103	estimated*	estimated*	(Wilkins 1995)

* quantity was determined by engineering judgement based on in-tank thermocouple tree temperature profiles or other process information

Table 4

Waste Depths and Specific Gravities used in Analysis

Tank	Sludge+Salt Cake Depth (inches)	Crust Depth (inches)	Liquid Density (g/cc)
AN-101	0	0	1.24
AN-102	32	0	1.39
AN-103	150	51	1.60
AN-104	180	55	1.46
AN-105	204	2	1.43
AN-106	6	0	1.19
AN-107	49	0	1.40
AP-101	0	0	0.99
AP-102	0	0	1.20
AP-103	0	0	1.00
AP-104	0	0	1.03
AP-105	56	0	1.33
AP-106	0	0	1.00
AP-107	0	0	1.01
AP-108	0	0	0.99
AW-101	125	51	1.54
AW-102	20	0	1.16
AW-103	132	0	1.04
AW-104	142	0	0.99
AW-105	108	0	1.01
AW-106	108	0	1.31
AY-101	30	0	1.09
AY-102	12	0	1.00
AZ-101	13	0	1.20
AZ-102	35	0	1.10
SY-101	220	47	1.49
SY-102	26	0	1.03
SY-103	140	24	1.47

Figure 4

Plot of dL/dP vs Non-Convective Waste Depth for DSTs

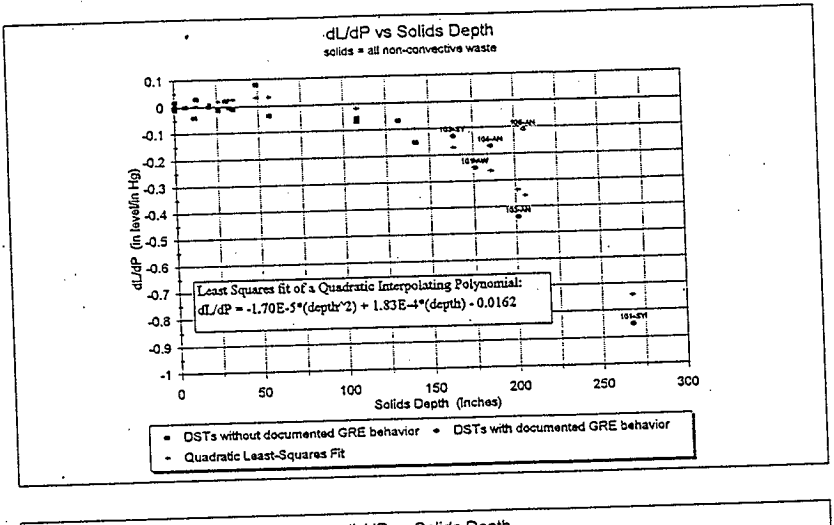

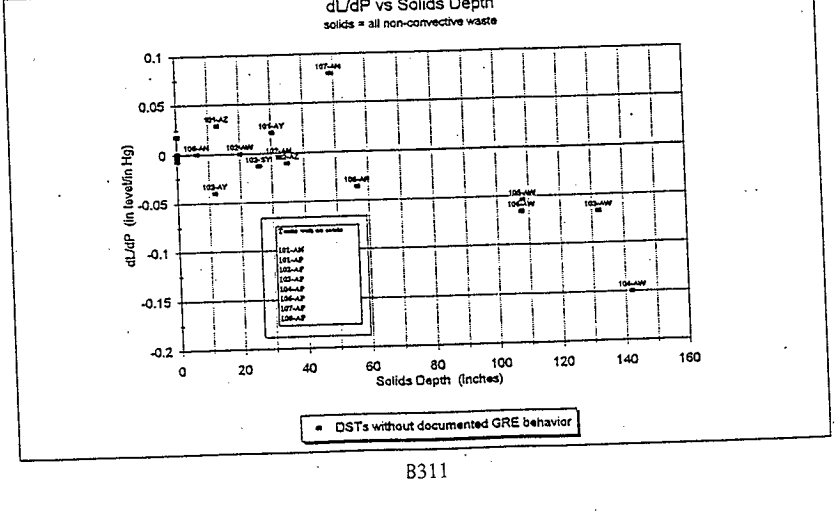

Figure 5

Plot of dL/dP vs Convective Waste Specific Gravity for DSTs

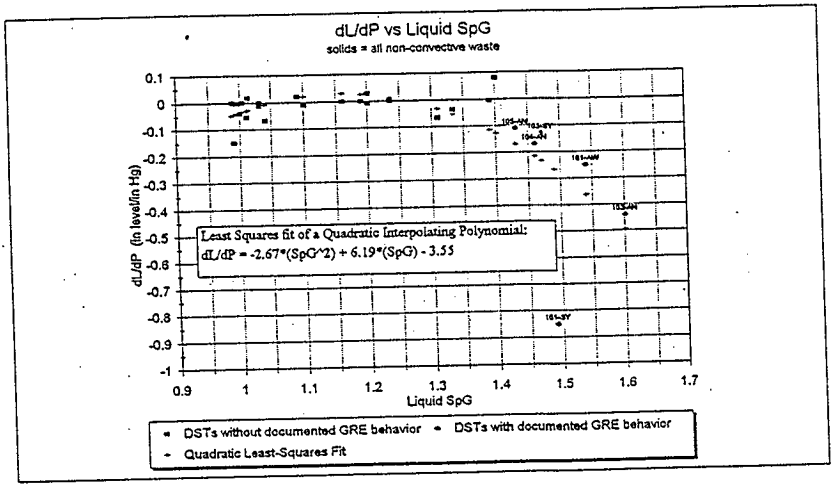

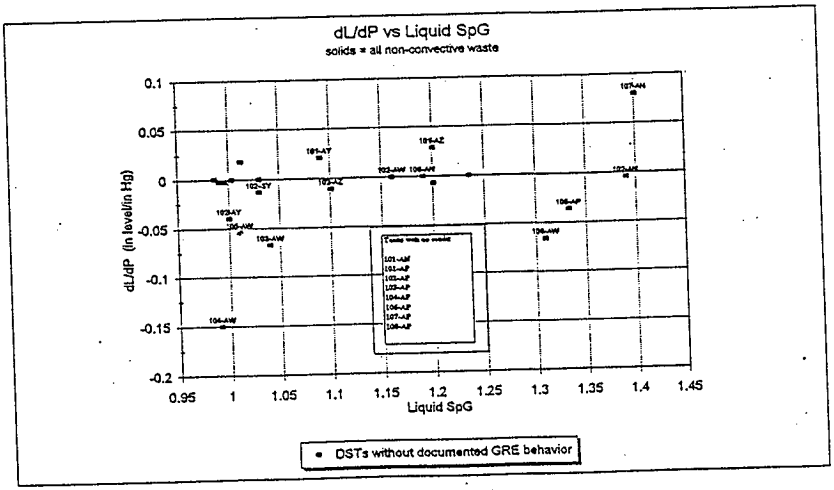

Figure 6

Plot of dL/dP vs Waste Depth*Waste Specific Gravity for DSTs

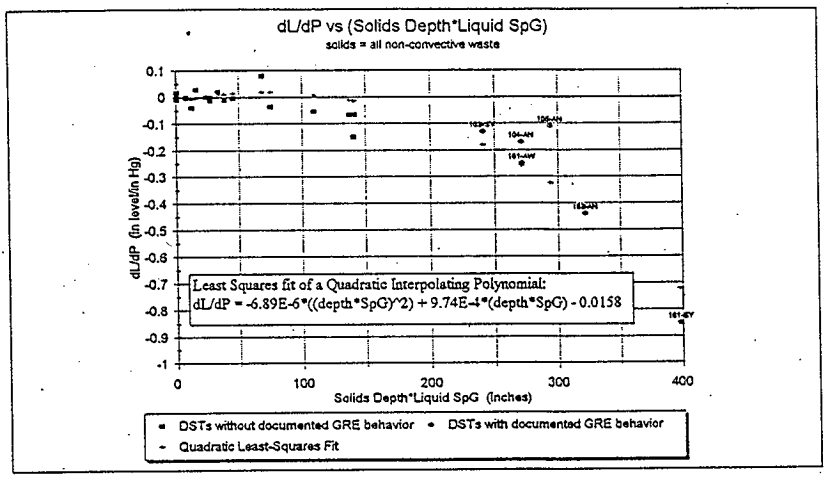

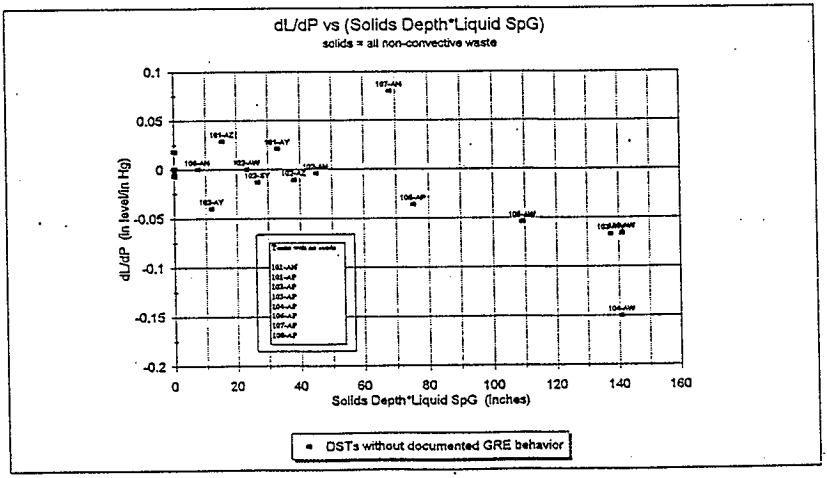

Figure 7

Plot of dL/dP vs Waste Depth/Waste Specific Gravity for DSTs

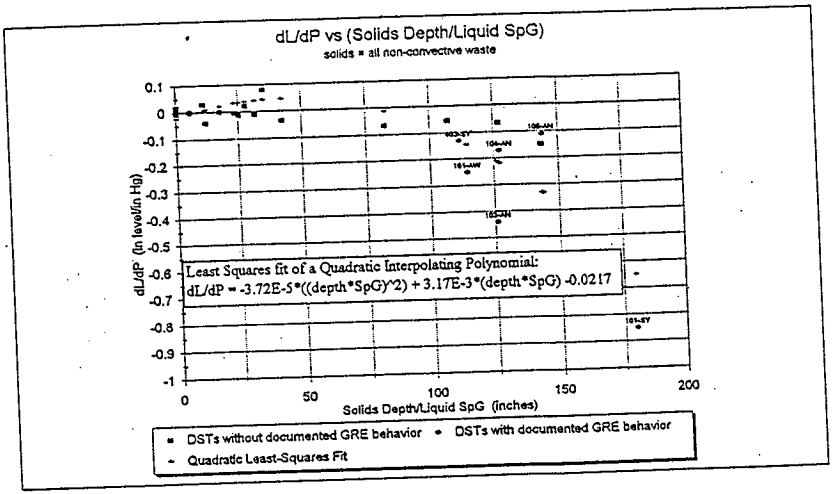

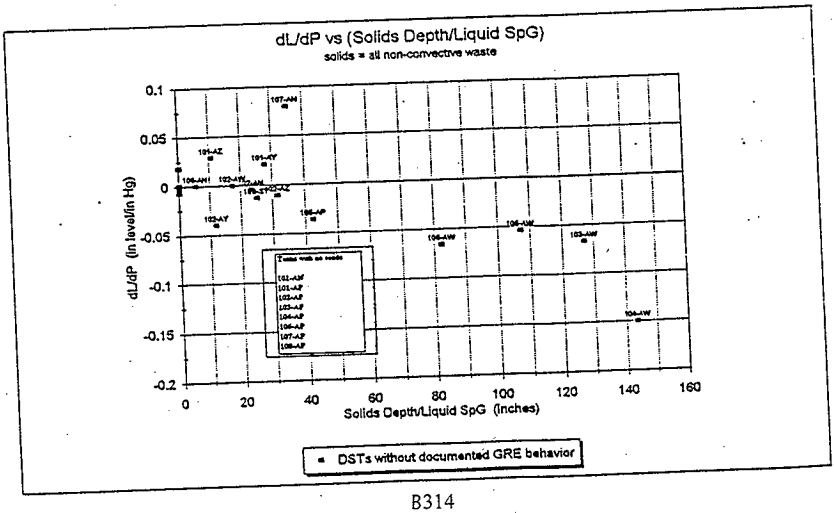

4.0 CONCLUSIONS AND RECOMMENDATIONS

The findings of this study were that the best correlation of the analyzed tank waste properties and the degree to which that waste may retain and release gas was determined by the product of the total solids (non-convective waste) volume or depth and the specific gravity of the liquid (convective waste) in contact with the solids. This makes some intuitive sense in that solids are the only waste form that can retain gas and the liquid specific gravity (assumed equivalent to the liquid occupying the solids pore volume) generally correlates with the viscosity of the liquid. The correlation of total solids depth to waste compressibility was also found to be significant, as could be expected from postulated waste tank gas retention mechanisms. However, depth of solids alone cannot differentiate why one tank with a given volume of solids exhibits GRE behavior while another tank with a similar solids volume does not. It appears that the specific gravity of the convective waste could be a key parameter describing why two tanks with the same total solids volume may exhibit dramatically different behaviors in terms of GRE.

The preferred correlation suggests that there are distinct differences between wastes in DSTs which are known to exhibit GRE behavior and waste in DSTs which are not. Although similar to the current waste specific gravity limits (Fowler 1995a & 1995b) in that they are based on empirical data, the results show that, to date, no episodic gas releases have been observed in DSTs where the total solids depth in inches multiplied by the specific gravity of the contacting liquid is less than 150 inches. A corresponding statement is that, to date, all DST s known to exhibit GRE behavior possess a value of the total solids depth in inches multiplied by the specific gravity of the contacting liquid of greater than 230 inches.

Based on these findings, practical considerations to be could be suggested for use when waste is transferred into a DST in the future. It is likely that when the total depth of well settled solids (inches) multiplied by the supernate specific gravity in a DST is less than 150 inches, the probability of a GRE of concern developing in the tank is low. Conversely, it is likely that when the total depth of well settled solids (inches) multiplied by the supernate specific gravity in a DST is greater than 230 inches, the probability of a GRE of concern developing in the tank is high.

5.0 REFERENCES

Alumkal, W. T., 1995, *MULTI-FUNCTION WASTE TANK FACILITY - DECISION PAPER*, (Letter 955011 to T. R. Sheridan, January 13), Westinghouse Hanford Company, Richland, Washington.

Awadalla, N. G., 1995, *MULTI-FUNCTION WASTE TANK FACILITY PHASE-OUT BASIS*, WHC-SD-W236A-ER-021, Rev. 2, Westinghouse Hanford Company, Richland, Washington.

Dodd, R. A., 1994, *242-A Evaporator Campaign 94-2 Waste Compatibility Assessment of Tank 241-AW-106 Waste With Waste Contained in Tank 241-AN-106* (Internal Memo 7CF10-025-094 to W. E. Ross, September 9), Westinghouse Hanford Company, Richland, Washington.

Esch, R. A., 1996, *Final Report for Tank 241-AN-101 Grab Samples 1AN-95-1 through 1-AN-95-7*, WHC-SD-WM-DP-148, Rev. 1, Westinghouse Hanford Company, Richland, Washington.

Estey, S. D. & M. D. Guthrie, 1996, *DATA ANALYSIS AND CRITERIA DEVELOPMENT TO PREVENT ACCUMULATION OF DST WASTE WITH UNACCEPTABLE GAS RETENTION BEHAVIOR* (Internal Memo 74A10-96-029 to N. G. Awadalla, March 29), Westinghouse Hanford Company, Richland, Washington.

Fowler, K. D., 1995a, *Tank Farm Waste Compatibility Program*, WHC-SD-WM-OSD-015, Rev. 1, Westinghouse Hanford Company, Richland, Washington.

Fowler, K. D., 1995b, *Data Quality Objectives For Tank Farm Waste Compatibility Program*, WHC-SD-WM-OSD-015, Rev. 1, Westinghouse Hanford Company, Richland, Washington.

Guthrie, M. D., 1996, *242-A Evaporator Campaign 95-1 Post-Run Document*, WHC-SD-WM-PE-055, Rev. 0, Westinghouse Hanford Company, Richland, Washington.

Hanlon, B. M., 1995, *Waste Tank Summary Report for Month Ending September 30*, WHC-EP-0182-90, Westinghouse Hanford Company, Richland, Washington.

Herting, D. L., 1993, *Tank 241-AN-107 Caustic Demand* (Internal Memo 12110-PCL93-042 to K. G. Carothers, May 13), Westinghouse Hanford Company, Richland, Washington.

Hodgson, K. M., 1995a, *Evaluation of Hanford Tanks for Trapped Gas*, WHC-SD-WM-ER-526, Rev. 0, Westinghouse Hanford Company, Richland, Washington.

Hodgson, K. M., 1995b, *Tank Characterization Report for Double Shell Tank 241-AW-103*, WHC-SD-WM-ER-455, Rev. 0, Westinghouse Hanford Company, Richland, Washington.

Hudson, J. D., G. S. Barney, P. R. Bredt, A. R. Felmy, D. L. Herting, A. P. Larrick, D. A. Reynolds, C. W. Stewart, D. S. Trent, 1995, *An Assessment of the Dilution Required to Mitigate Hanford Tank 241-SY-101*, PNL-10417/UC-510, Pacific Northwest National Laboratory, Richland, Washington.

Jones, J., 1994, *242-A Evaporator Campaign 95-1 Waste Compatibility Assessment of Tank 241-AW-105 Waste With Tank 241-AP-108 Waste* (Internal Memo 7CF10-055-094 to R. A. Dodd, November 15), Westinghouse Hanford Company, Richland, Washington.

Miller, G. L., 1995, *45-Day Safety Screening Report for Grab Samples from Tank 241-AP-107*, WHC-SD-WM-DP-098, Rev. 0A, Westinghouse Hanford Company, Richland, Washington.

Reynolds, D. A., 1994, *EVALUATION OF SPECIFIC GRAVITY VERSUS GAS RETENTION* (Internal Memo 7E310-94-024 to N. W. Kirch, June 20), Westinghouse Hanford Company, Richland, Washington.

Reynolds, D. A., 1992, *Tank 241-SY-101 Window C Core Sample Results and Interpretation*, WHC-EP-589, Westinghouse Hanford Company, Richland, Washington.

Rollison, M. D., 1994, *Results for 241-AZ-101 Grab Samples* (Internal Memo 75970-95-037 to J. M. Jones, September 11), Westinghouse Hanford Company, Richland, Washington.

Schreiber, R. D., 1995, *Tank Characterization Report for Double Shell Tank 241-AZ-102*, WHC-SD-WM-ER-411, Rev. 0, Westinghouse Hanford Company, Richland, Washington.

Sidpara, A. B., 1995, *EXPECTATIONS FOR THE TANK WASTE REMEDIATION SYSTEM (TWRS) MWTF WASTE MANAGEMENT ACTIONS ACTIVITIES*, (Letter 95-TOP-076 to President, WHC, June 1), Department of Energy, Richland Operations Office, Richland, Washington.

Simpson, B.C., 1994a, *Tank Characterization Report for Double Shell Tank 241-AP-103*, WHC-SD-WM-ER-359, Rev. 0, Westinghouse Hanford Company, Richland, Washington.

Simpson, B.C., 1994b, *Tank Characterization Report for Double Shell Tank 241-AP-102*, WHC-SD-WM-ER-358, Rev. 0, Westinghouse Hanford Company, Richland, Washington.

Simpson, B.C., 1994c, *Tank Characterization Report for Double Shell Tank 241-AP-101*, WHC-SD-WM-ER-357, Rev. 0, Westinghouse Hanford Company, Richland, Washington.

Simpson, B. C., 1994d, *Tank Characterization Report for Double Shell Tank 241-AP-105*, WHC-SD-WM-ER-360, Rev. 0, Westinghouse Hanford Company, Richland, Washington.

Sutey, M. J., 1995, *Waste Compatibility Assessment of Tank 241-AP-104 with Tank 241-SY-102* (Internal Memo 71729-95-008 to J. H. Wicks, March 24), Westinghouse Hanford Company, Richland, Washington.

Tusler, L. A., 1995, *Tank Characterization Report for Double Shell Tank 241-AW-104*, WHC-SD-WM-ER-453, Rev. 0, Westinghouse Hanford Company, Richland, Washington.

Van Vleet, R. J., 1993, *Radionuclide and Chemical Inventories for the Double Shell Tanks*, WHC-SD-WM-TI-543, Rev 1, Westinghouse Hanford Company, Richland, Washington.

Welsh, T. L., 1994, *Tank 241-AP-106 Characterization Results*, WHC-SD-WM-TRD-170, Rev. 0, Westinghouse Hanford Company, Richland, Washington.

Whitney, P., 1995, *Screening the Hanford Tanks for Trapped Gas*, PNL-10821/UC-510, Pacific Northwest National Laboratory, Richland, Washington.

Wilkins, N. E., 1995, *Tank 241-SY-103 Core Sample: Interpretation of Results*, WHC-SD-WM-TI-712, Rev. 0, Westinghouse Hanford Company, Richland, Washington.

Winters, W. I., 1988, *Analytical Results for 241-AP-104 Phosphate/Sulfate Wastes*, SD-RE-TI-212, Rev. 0, Westinghouse Hanford Company, Richland, Washington.

Westinghouse Hanford Company | Internal Memo

From: Waste Tanks Process Control 7E310-94-024
Phone: 373-3115 R2-11
Date: June 20, 1994
Subject: EVALUATION OF SPECIFIC GRAVITY VERSUS GAS RETENTION

To: N. W. Kirch R2-11

cc: N. A. Bostic R2-11 R. J. Nicklas R1-43
K. G. Carothers R1-51 R. C. Roal H5-27
R. A. Dodd R1-51 J. S. Schofield R1-51
G. D. Johnson R2-78 DAR File/LB

During development of the Data Quality Objective (DQO) for waste compatibility, waste characteristics and limits were identified which related to tank safety issues. A limit was desired that would allow tank operations without creation of an additional Flammable Gas Watch List (FGWL) tank. For the DQO, a limit of 1.41 specific gravity (SPG) was chosen. The DQO stated that exceeding the 1.41 SPG limit requires further technical evaluation of the potential for flammable gas accumulation in the waste. This memo provides information on the waste volume impact due to implementing a 1.41 SPG limit and on the basis for why the limit was chosen. The SPG limit was chosen because of the strong statistical correlation between SPG and FGWL. Although, there are other parameters that also influence whether a tank exhibits gas retention and release, no other single parameters distinguished between FGWL and non-FGWL tanks. Tank sampling and vapor monitoring from FGWL tanks other than 241-SY-101 may allow revision of the 1.41 SPG value.

1) What does the 1.41 SPG limit really do to waste volume projections?

There has been a rough estimate that the 1.41 SPG may increase the final storage volume by 25%. With double-shell tank (DST) space at a premium, the volume increase will need closer evaluation and alternatives to be pursued.

To see what practical effect the 1.41 SPG limit has, the following sample data from tank AW-102 was evaluated.

This composition was used for input to both PREDICT and ESP. (It should be pointed out that the version of PREDICT used is not the same one used by the Waste Volume Projections.) Both programs told essentially the same story. The waste in 102-AW may be evaporated about 90%. Very few solids are formed before the final evaporator pass by either model. Densities for the PREDICT run were calculated based on the equation from Herting's work[1]. ESP calculates the densities of the liquid. PREDICT would say that the 8 M OH rule is reached first with the density of 1.39. ESP would say that the

[1] D. A. Reynolds, D. L. Herting, "Solubilities of Sodium Nitrate, Sodium Nitrite, and Sodium Aluminate in Simulated Nuclear Waste," RHO-RE-ST-14P, 1984, Page 24.

density rule would be hit first with the OH at 6.8 M. PREDICT indicates a WVR of 91.2% and ESP would have a WVR of 90%. Essentially both models indicate the same thing. At least for this waste, the 1.41 SPG limit would have minimal impact on the evaporation.

Table 1
Composition of AW-102 from sample T-8435 taken in 1988

Component	Concentration Unit	Concentration
Al	moles/liter	2.48E-2
NO2	moles/liter	5.48E-2
NO3	moles/liter	3.16E-1
OH	moles/liter	6.69E-1
PO4	moles/liter	2.54E-3
SO4	moles/liter	1.16E-2
Cl	moles/liter	4.76E-3
CO3	moles/liter	4.83E-2
TOC	grams/liter	4.95E-1
F	moles/liter	3.34E-1
% H2O	percent	9.327E-1
Ca	moles/liter	3.97E-4
Mg	moles/liter	1.1E-4
B	moles/liter	5.76E-4
Cr	moles/liter	4.39E-4
Na	moles/liter	1.19
K	moles/liter	2.7E-1
NH3	moles/liter	5.9E-2
SPG		1.0371

2) Is the 1.41 SPG limit real or is there a better limit?

The basis for the 1.41 SPG limit came from a preliminary study. An attempt was made to estimate the densities of the waste in all the double-shell tanks. When the tanks were sorted by density, all the flammable watch list DSTs came to the top. All the flammable watch list tanks had SPG > 1.4. All the non-watch list DSTs had SPG < 1.4. It should be pointed out that all the tanks containing double shell slurry are on the watch list. All the tanks containing double shell slurry feed except one are on the watch list.

The one tank of DSSF not on the watch list (AP-105) was evaluated as a potential watch list tank at one time. That tank also is the lowest SPG of the DSSF tanks. There seems to be a close correlation between double-shell slurry, double-shell slurry feed tanks and the ability to retain gases.

A 1982 study[2] indicated that the slurry growth was related to viscosity and initial gas generation rate. In other words, the ability to trap gases was related to a trapping mechanism (viscosity) and a generation term. The 1982 study shows that hydroxide concentration, aluminum concentration, nitrite concentration, iron concentration, temperature, and terms relating to total organic carbon (TOC) were all important to gas generation. Our current understanding of gas generation would also include a radiation term. These variables became the items to focus on while looking for a new limit.

In 1988, a internal memo was released on viscosity[3]. During this study, no samples with a SPG of <1.35 had solids in the waste. Above 1.35 SPG, solids were usually present. It can be surmised that by the time the SPG reaches above 1.4, there is enough solids present to trap the gas that is formed in all tanks.

The most readily available source of information on these variables was the Van Vleet document[4]. This document provided the double shell tank characterization data for the Interim Safety Basis. Table 2 is the collection of the data from the Van Vleet document.

The information in Table 2 represents a tank average. When the analysis indicated both a liquid and a solid phase, the relative volumes of each were used to derive a volume weighted average which is shown in Table 2. The column labeled "Watch List" is the code for whether or not the tank is on the Flammable Gas Watch List. A 1 was assigned to nonwatch list tanks and a 2 was assigned a watch list tank. These assignments were totally arbitrary. Several tanks do not have any values listed. These tanks are full of dilute waste. Typically they contain mostly water from PUREX off gas scrubbing and other flushes. These tanks do not contribute to our understanding of a limit and so were not considered in the evaluation that follows.

Plots of the information in Table 2 quickly showed that iron and the radiation terms would not differentiate between FGWL and non FGWL tanks. Perhaps what this shows is that all of the tanks have enough iron and radiation to drive the gas generation reaction or these variables are not important to the reaction. In any case, they were dropped from consideration.

---

[2] Gale, L. A., "Summary of Slurry Growth Experiments -- 1982," SD-WM-TI-049, 1982.

[3] D. A. Reynolds to M. C. Teats, "Viscosity of Evaporator Slurries," IM 13314-88-105, June 30, 1988.

[4] Van Vleet, R. J., "Radionuclide and Chemical Inventories for the Double Shell Tanks," WHC-SD-WM-TI-543, Rev. 1, Aug. 1993.

Table 2
Database for Double Shell Tanks

Tank	Watch List	Density g/ml	TOC g/l	NO3 M	NO2 M	Na M	Al M	Fe M	OH M	Cs137 Bq	Sr90 Bq	Total Bq	Waste Type
AN-101	1	1.11	2.35	2.29	0.81	6.57	0.63		2.32	1.80e+16	1.60e+14	1.80e+16	DN
AN-102	1	1.40	3.37	3.61	1.32	10.40	0.56		0.20	6.10e+16	2.50e+16	8.60e+16	CC/SLUDGE
AN-103	2	1.60	7.36	2.58	3.00	14.61	2.13		5.74	9.80e+16	1.70e+15	1.00e+17	DSS
AN-104	2	1.46	3.83	2.72	1.87	7.85	1.81	0.00	4.00	8.20e+16	1.70e+14	8.30e+16	DSSF
AN-105	2	1.43	3.36	2.17	1.36	7.85	0.94		2.23	5.60e+16	3.50e+14	5.60e+16	DSSF
AN-106	1	1.20	5.28	1.28	0.73	5.22	0.39	0.00	0.71	6.20e+14	3.80e+16	3.90e+16	CP
AN-107	1		39.1	2.70	0.83	9.13	0.14	0.03	0.05	2.30e+16	5.50e+16	7.90e+16	CC
AP-101	1												DN
AP-102	1			0.00	0.00	0.54		0.00		7.40e+10	5.10e+09	1.00e+12	DN/CP
AP-103	1		0.42	0.00	0.03	0.08	0.00		0.19	5.60e+11	9.90e+11	1.90e+12	DN
AP-104	1	1.03	0.19	0.00		0.49	0.00	0.00		1.80e+09	1.00e+08	5.20e+10	DN
AP-105	1												DSSF
AP-106	1												DN
AP-107	1												DN
AP-108	1												DN
AW-101	2	1.54	2.46	3.46	2.21	10.00	1.03		5.07	7.90e+16	1.60e+14	7.90e+16	DSSF/SLUDGE
AW-102	1	1.16	1.23	0.91	0.23	2.63	0.14		1.27	8.70e+15	2.10e+13	8.80e+15	DN
AW-103	1	1.55				7.36	0.04	0.01				1.00e+14	NCRW

AW-104	1	1.41	4.67	2.73	1.41	10.60	0.87		3.10	1.30e+17	5.40e+15	1.30e+17	DN
AW-105	1	1.01	0.36	0.11	0.01	0.55	0.02		0.33				NCRW
AW-106	1	1.24	2.68	0.20	0.54	5.72	0.33		2.58	1.60e+16	1.70e+15	1.80e+16	DN/SLUDGE
AY-101	1	1.09	4.47	0.62	0.30	1.95	0.17		0.47	1.30e+16	1.20e+17	1.30e+17	SLUDGE/DC
AY-102	1	1.02	2.69	0.03	0.01	0.19	0.08	0.08			1.90e+17	1.90e+17	SLUDGE/DN
AZ-101	1	1.24	0.22	0.14	0.19	0.38	0.32	0.16		2.70e+17	1.70e+17	4.50e+17	NCAW
AZ-102	1	1.21	1.88	0.10	0.11	2.31	0.28	0.33		1.20e+17	4.10e+17	5.40e+17	NCAW
SY-101	2	1.55	24.93	2.90	3.79	13.82	1.84	0.01	2.35	7.70e+16	4.50e+15	1.90e+17	DSS/CC
SY-102	1	1.35		5.85	1.79	2.42	0.34	0.01	1.80	3.40e+15	1.20e+15	4.70e+15	PFP/DN
SY-103	2	1.52	44.11	2.68	2.80	11.91	2.14		1.56	1.50e+17	2.90e+14	1.50e+17	DSS/CC

OTES: AW-104 used an analysis of a 1984 sample. Since that time the tank has been emptied and filled 3 times. This is probably not a good representation of the waste currently in the tank.

The NCRW tanks (AW-103, AW-105) probably do not have the correct densities. A closer study of the densities would have both tanks close to 1.4. However, the information in the table was kept for the subsequent analysis.

The tanks were sorted into the watch list and nonwatch list groupings. A statistical technique called analysis of variance (ANOVAR) was used on those groupings. This technique looks at the averages and standard deviations to answer the question: "Could these averages both come from the same population?" If the answer is no, then the conclusion is that the two groupings (watch list and non-watch list) are different. This analysis showed that density, sodium concentration, aluminum concentration and hydroxide concentration had different populations for watch list versus non-watch list. In other words, the watch list tanks were significantly different from nonwatch list tanks for these variables. There were two variables, TOC and NO2, which the statistical test could not differentiate between watch list and nonwatch list tanks.

These two variables have been identified as being important in the gas generation reactions. Plots of watch list and non-watch list tanks are shown in Figure 1 and Figure 2. Both of these figure show that the watch list tanks tend to have larger values but the overlap between the data of the watch list and nonwatch list tanks is so great that TOC nor NO2 are useful as a criteria. Once again, this may be an indication that all tanks have sufficient TOC and NO2 to generate gas.

The variables which ANOVAR chose are not independent. As waste is concentrated, the density and the concentrations both increase in a related manner. Consequently, a limit on density (SPG) automatically sets limits on the concentrations of the other variables. Table 3 shows a correlation between the variables.

Table 3
Correlation Between Variables

	Density	NO2	Na	Al	OH
Density	1				
NO2	0.898	1			
Na	0.869	0.843	1		
Al	0.840	0.884	0.845	1	
OH	0.665	0.557	0.581	0.617	1

To see if the variables chosen by the ANOVAR may provide a better limit, a technique called forward and backward multiple linear regression was used. Each of the four variables that ANOVAR indicated as important (density, sodium, aluminum and hydroxide) were multiplied by each other to supply a term for interactions between the variables. The forward linear regression will then allow one variable or interaction at each step into the regression equation. In the forward linear regression, the variable that is most related to the dependent variable is first put into the equation. If there is still significant relationship with other variables, then an additional variable is put in. Stepping through this way allows the variables to show the relative importance. A similar method applies to backward regression. Backward

regression starts with all variables and interactions in the equation and then removes the least significant variable at each step. Finally, only the most important variable is left in the equation.

An equation is not supplied in this study. This is because the value for the dependent variable (watch list or not) was purely arbitrary. However, both the forward and the backward linear regression showed that the interaction "density times the aluminum" was the variable that had the largest correlation to whether or not a tank was on the watch list.

Figure 3 shows the density versus aluminum concentration plot. Notice that all of the watch list tanks fall above .9 M Al. All of the watch list tanks fall to the right of the 1.41 g/ml density. There are three other tanks identified above 1.41 g/ml. Note that the density and aluminum concentration of AW-104 are not believed to have accurate information in the database. The sample used in the database was a 1984 sample. Since that time, the tank has been emptied and filled several times. The other tanks fall in two categories -- complexed concentrate (AN-102) and neutralized coating removal waste (AW-103). Complexed concentrate waste was concentrated up to the point of making solids. Consequently, there is lots of organic in the tank, high density, etc. yet there is only a small solids layer to trap gas. The NCRW waste is also quite a different waste from other waste streams. There is little organic in the NCRW waste but there is large amounts of solids. However, the solids are of a different type from the solids produced in evaporator. These solids may not have the strength to retain gases.

It is also interesting to note that to make double-shell slurry or double-shell slurry feed, the waste is evaporated to the aluminate solubility boundary. The resulting waste may contain sodium aluminate. The resulting waste is certainly very dense.

Table 3 shows the density, aluminum and a column which has the aluminum and density multiplied together. The tank which has the density times the aluminum of 1.22 is tank AW-104 which has been mentioned before. There seems to be a clear change at about 1.3 on the density times aluminum.

Table 3
Density and Aluminum

Watch list	Density	Al	Density*Al
2	1.60	2.13	3.41
2	1.52	2.14	3.25
2	1.55	1.84	2.84
2	1.46	1.81	2.65
2	1.54	1.03	1.59
2	1.43	0.94	1.34
1	1.41	0.87	1.22
1	1.40	0.56	0.78
1	1.11	0.63	0.70
1	1.20	0.39	0.47
1	1.35	0.34	0.46
1	1.24	0.33	0.40
1	1.24	0.32	0.40
1	1.21	0.28	0.34
1	1.09	0.17	0.19
1	1.16	0.14	0.16
1	1.02	0.08	0.09
1	1.55	0.04	0.07
1	1.01	0.02	0.02
1	1.03	0.00	0.00
1		0.14	0.00
1		0.00	0.00

Conclusion:

After looking at many other variables, the density limit still seems to be the best limit to apply to prevent a flammable watch list tank. There are still some unanswered questions with this limit but density still remains a valid limit. The limit of 1.41 also still seems to be the appropriate limit.

It should be pointed out that the other variables have the potential for being involved with the gas generation or retention but these other variables do not provide a basis for setting a criteria.

While the density appears to represent the gas entrapment mechanism, the density limit is not meant to imply a mechanism. The 1.41 SPG limit is based on the total tank contents. This does not imply that the solids have a limit on density.

There seems to be at least two types of waste, complexed concentrate and neutralized cladding removal waste, which may approach or even exceed the 1.41 limit with out producing flammable watch list tanks. These waste types either produce no solids or else the solids are a different type solids than is formed in the evaporator. The double-shell slurry type waste seems to be the main problem of the double-shell flammable gas watch list tanks.

D. A. Reynolds

D. A. Reynolds, Engineer
Waste Tanks Process Control

mjg

Attachment

Figure 1
TOC

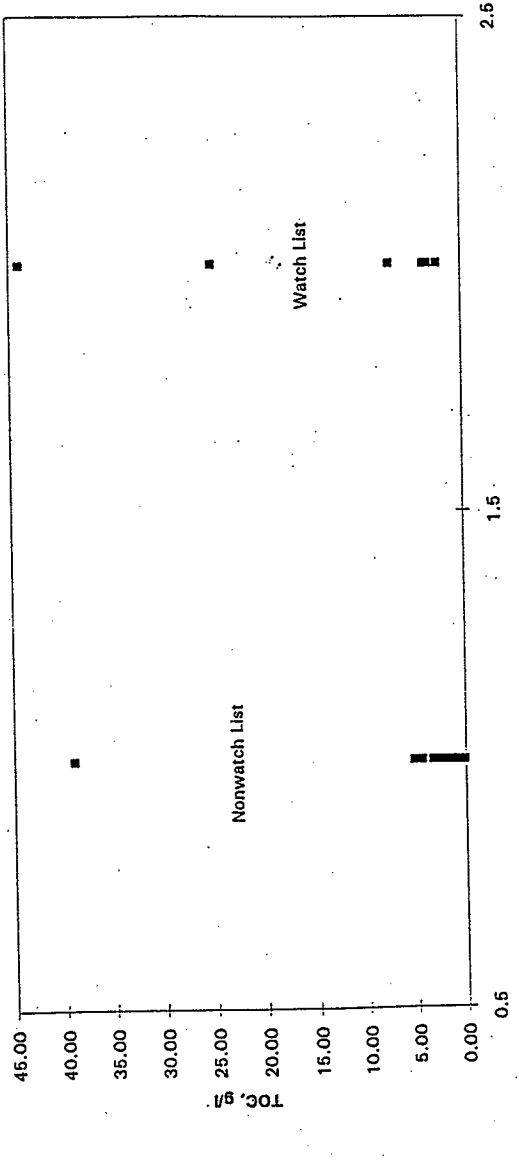
TOC, g/l
45.00
40.00
35.00
30.00
25.00
20.00
15.00
10.00
5.00
0.00
0.5
1.5
2.5
Watch List
Nonwatch List

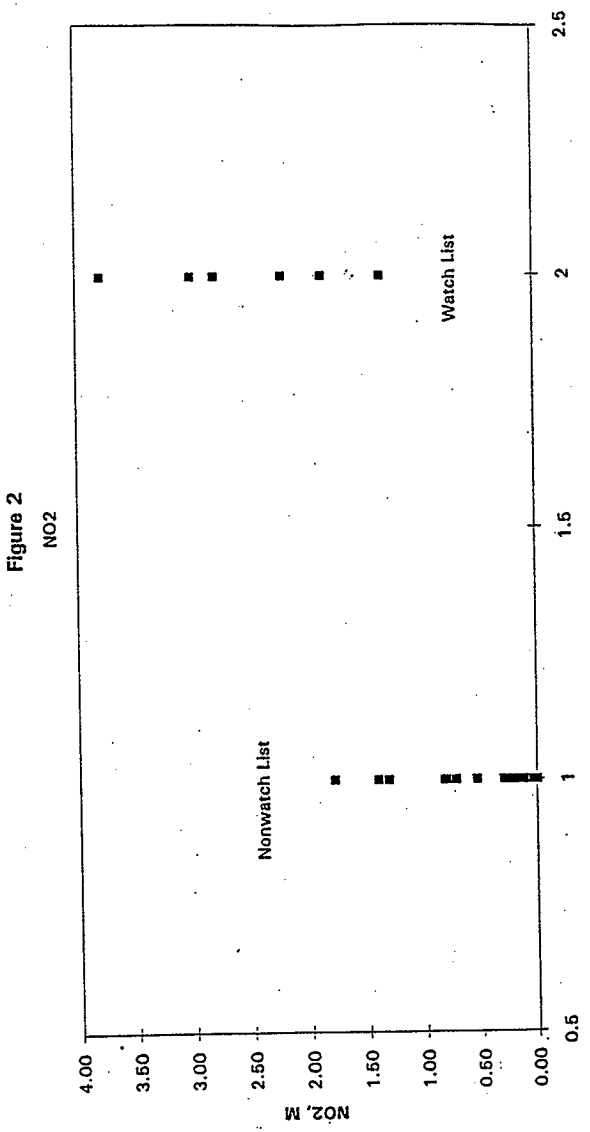
NO2
Watch List
Nonwatch List
NO2, M
4.00
3.50
3.00
2.50
2.00
1.50
1.00
0.50
0.00
2.5
2
1.5
1
0.5

Figure 2

Figure 3
Aluminum vs. Density

Key Issues

1. Does BD GRE behavior add to, replace, or add to but change releases from other GRE mechanisms? How do we quantify the combined effect on release behavior?

2. When are BD GREs precluded? (Potential criteria: max achievable α; organics; liquid layer thickness, bubble migration, potential energy, liquid density, liquid to nc density ratio, ...)

3. Is BD GRE analysis in AF adequate?

4. Are seismic-induced GREs affected by presence of liquid layer? By pumping status?

5. Are subsurface burns sufficiently risk-insignificant to neglect?

6. Is criteria adequate for when headspace and in-equipment detonations are precluded?

7. Do the physical parameters in the AF allow adequate assessment of the impact of controls on gas release behavior?

8. Is the modeling of NH_3 releases from BD GREs adequate? From waste transfers? Are NH_3 releases significant contributors to flammable gas risk? Is NH_3 modeling appropriate for assessing toxicological risk?

9. Is the material release from burns adequately modeled?

GAS RELEASE EVENT SAFETY ANALYSIS TOOL LIBRARY

1. Risk Analysis, Vol. 14, Nov. 5, 1994 — Workshop Proceedings: When and How Your Specify A probability Distribution When you Don't Know Much.

2. 9655781 Lockheed Martin — Flammable Gas Project: Memorandum of Understanding on the Strategy for Closure of the Flammable Gas Unreviewed Safety Question to meet Performance Agreements TWR1.3.2 and 1.3.6

3. American Institute of Chemical Engineers: — Symposium Series, Heat Transfer -- Pittsburgh 1987.

4. ANL-RE-92/2 — Effect of Viscosity on Seismic Response of Waste Storage Tanks, June 1992

5. CONF-660904, Volume 1 — Proceedings of the Ninth AEC Air Cleaning Conference - held in Boston, Massachusetts - 13 - 15, September 1966.

6. COO-4442-4 — Compilation and Analysis of Hydrogen Accident Reports, Final Technical Report, by Robert G. Zalosh and Thomas P. Short., October 1978

7. Guidelines for Safe Storage and Handling of Reactive Materials, American Inst. of Chemical Engineers

8. HNF-EP-0182-103 — Waste Tank Summary Report for Month Ending October 31, 1996

9. HNF-EP-0182-107 — Waste Tank Summary Report for Month Ending February, 28, 1997

10. HNF-EP-0182-113 — Waste Tank Summary Report for Month Ending August 31, 1997.

11. HNF-EP-0899-2 — The Solubilities of Significant Organic Compounds in HLW Tank Supernate Solutions - FY 1997 Progress Report

12. HNF-SD-WM-CN-116 — Calculaton Note: Hydrogen Generation Rates at Steady-State Flammable Gas Concentrations for Single Shell Tanks, September 1997.

GAS RELEASE EVENT SAFETY ANALYSIS TOOL LIBRARY

13. HNF-SD.CN-116, Rev. 0-A — Calculation Note: Hydrogen Generation Rates at Steady-State Flammable Gas Concentrations for Single Shell Tanks, September 1997.

14. HNF-SD-WM-CN-117, Rev.0 — Calculations of Hydrogen Release Rate at Steady State for Double-Shell Tanks, September 1997.

15. HNF-SD-WM-ES-410, Rev. 0 — Safety Controls Optimization by Performance Evaluation (SCOPE) Analysis Framework, August 1997

16. HNF-SD-WM-JCO-007, Rev. 1 — Flammable Gas/Slurry Growth Unreviewed Safety Question: Justification for Continued Operation for the Tank Farms at the Hanford Site.

17. WHC-SD-WM-TI-724, Rev. 0 — Methodology for Flammable Gas Evaluations, December 1995.

18. WHC-SD-WM-TI-724, Rev. 1 — Methodology for Flammable Gas Evaluations, June 1996

19. HNF-SD-WM-TI-797, Rev. 0 — Results of Vapor Space Monitoring of Flammable Gas Watch List Tanks, January 1997.

20. HNF-SD-WM-TI-806, Rev. 0 — Safety Controls Optimization by Performance Evaluation - Analysis Tool (SCOPE-AT) Pedigree Database for Hanford Tanks, September 1997

21. HNF-SP-1193, Rev. 2 — Flammable Gas Project Topical Report, January 1997.

22. HNF-SD-WM-ES-412, Rev. 0 — Safety Controls Optimization By Performance Evaluation (SCOPE) Expert Elicitation Results for Hanford Site Single-Shell Tanks - August 1997

23. IN TANK PHOTO COLLAGES of the 177 Waste Storage Tanks for the Hanford 200 Areas.

24. LA-UR-92-3196 — A Safety Assessment for Proposed Pump Mixing Operations to Mitigate Espsodic Gas Releases in Tank 241-SY-101: Hanford Site, Richland, Washington

GAS RELEASE EVENT SAFETY ANALYSIS TOOL LIBRARY

25. LA-UR-94-1323-TSA-6-94-R142 Bounding Gas Release Calculations of Flammable Gas Watch List Single-Shell Tanks.

26. LA-UR-94-2088-TSA-694-R120 Double-Shell Tank Bounding Analysis

27. LA-UR-95-1900, TSA-11-94-R110 Probabilistic Safety Assessment for Hanford High-Level Waste Tanks

28. LA-UR-95-4038 The Eleventh Workshop on Mathematical Problems in Industry, June 12-16, 1995.

29. LA-UR-97-2214 Data Reconcililiation Study of Tank 241-AW-101 at the Hanford Site, Los Alamos National Laboratory, Los Alamos, New Mexico

30. LA-UR-97-3916 Data Reconciliation Study of Tank 241-AN-105 at the Hanford Site, Los Alamos National Laboratory, Los Alamons, New Mexico

31. LA-UR-97-3954 Data Reconciliation Study of Tank 241-AN-104 at the Hanford Site, Los Alamos National Laboratory, Los Alamos, New Mexico

32. LA-UR-97-3955 Data Reconciliation Study of Tank 241-AN-103 at the Hanford Site, Los Alamos National Laboratory, Los Alamos, New Mexico

33. LA-UR-97-4021 Parameters to Consider Before Mixing Waste From Different Hanford Waste Tanks From A Flammable Gas Perspective, Fluor Daniel Northwest & Los Alamos National Laboratory, September 1997.

34. Los Alamos National Laboratory Interim Report: Flame Speed Scaling for Turbulent Reacting Flow

35. March 6, 1997, Rev. 1 Sandia National Laboratories
Safety Controls Optimization by Performance Evaluation (SCOPE) Proposed Analysis Framework for Scope Expert Panel Deliberations on Suitable Uncertainty Distribution Parameters

GAS RELEASE EVENT SAFETY ANALYSIS TOOL
LIBRARY

36. NUREG/CR-178 SAND80-0200 RX, AN Handbook of Human Reliability Analysis with Emphasis on Nuclear Power Plant Operations - Final Report

37. NUREG 1150 Methodology: Eliciting Expert Judgements to Predict the Outcomes of the FARO L-21 Experiment: by Thomas Eppel and Detlof von Winterfeldt. Final Report (Revised) January 29, 1997.

38. PNL-10091, UC-2030 Some Theories of Dissolved Gas Release from Tank 241-SY-101, September 1994.

39. PNL-10120, UC-510 Mechanisms of Gas Bubble Retention, September 1994.

40. PNL-10173 Ammonia in Simulated Hanford Double-Shell Tank Wastes: Solubility and Effects on Surface Tension, September 1994.

41. PNL-10198 The Effects of Heating and Dilution on the Rheological and Physical Properties of Tank 241-SY-101 Waste, Pacific National Laboratory, Richland, Washington

42. PNL-10417 An Assessment of the Dilution Required to Mitigate Hanford Tank 241-SY-101, February 1995

43. PNL-10681 The Behavior, Quantity, and Location of Undissolved Gas in Tank 241-SY-101, October 1995.

44. PNL-10682 In Situ Determination of Rheological Properties and Void Fraction in Hanford Waste Tank 241-SY-101, August 1995.

45. PNL-10740 Gas Bubble Retention and Its Effects on Waste Properties: Retention Mechanisms, Viscosity, and Tensile and Shear Strengths, August 1995

46. PNL-10773 Hanford Tank Clean up: A Guide to Understanding the Technical Issues, TWRS Technology Program Office, October 1994.

47. PNL-10821 Screening the Hanford Tanks for Trapped Gas, October 1995.

48. PNL-10865 In Situ Determination of Rheological Properties and Void Fraction: Hanford Waste Tank 241-SY-103, November 1995

GAS RELEASE EVENT SAFETY ANALYSIS TOOL
LIBRARY

49. PNL-8124, AD-940 Gas Generation and Retention in Tank 101-SY-101: A Summary of Laboratory Studies, Tank Data, and Information Needs, June 1992.

50. PNL-8880 Historical Trends in Tank 241-SY-101 Waste Temperatures and Levels, September 1993.

51. PNL-9423 Mitigation of Tank 241-SY-101 by Pump Mixing: Results of Testing Phases A and B, March 1994.

52. PNL-9959 Mitigation of Tank 241-SY-101 by Pump Mixing: Results of Full-Scale Testing, June 1994.

53. PNNL-11237 Evaluation of the Potential for Significant Ammonia Releases from Hanford Waste Tanks, July 1996.

54. PNNL-11296 In Situ Rheology and Gas Volume in Hanford Double-Shell Waste Tanks, September 1996.

55. PNNL-11297 Status and Integration of Studies of Gas Generation in Hanford Wastes, October 1996.

56. PNNL-11298 Mechanisms of Gas Bubble Retention and Release: Results for Hanford Waste Tanks 241-S-102 and 241-SY-103 and Single-Shell Tank Simulants, September 1996

57. PNNL-11310 Gas Release During Salt Well Pumping: Model Predictions and Comparisons to Laboratory Experiments, September 1996.

58. PNNL-11335 Summary of Tank Information Relating Salt Well Pumping to Flammable Gas Safety Issues, September 1996.

59. PNNL-11373 Flammable Gas Data Evaluation Progress Report, October 1996.

60. PNNL-11391 Gas Retention and Release Behavior in Hanford Single-Shell Waste Tanks, December 1996.

61. PNNL-11416 Mechanisms of Stability of Armored Bubbles: FY 1996 Final Report, December 1996

GAS RELEASE EVENT SAFETY ANALYSIS TOOL
LIBRARY

62. PNNL-11450, Rev. 1 Composition and Quantities of Retained Gas Measured in Hanford Waste Tanks 241-AW-101, A-101, AN-105, AN-104, and AN-103, March 1997.

63. PNNL-11536, Rev. 1 Gas Retention and Release Behavior in Hanford Double-Shell Waste Tanks, May 1997

64. PNNL-11600 Thermal and Radiolytic Gas Generation from Tank 241-S-102 Waste, July 1997.

65. PNNL-11621 Gas Release During Salt-Well Pumping: Model Predictions and Laboratory Validation Studies for Soluble and Insoluble Gases, August 1997.

66. PNNL-11639 Initial Parametric Study of the Flammability of Plume Releases in Hanford Waste Tanks, August 1997

67. PNNL-11642 Mechanisms of Gas Retention and Release: Experimental Results for Hanford Waste Tanks 241-AW-101 and 241-AN-103

68. PNNL-11668 Seismic Event-Induced Waste Response and Gas Mobilization Predictions for Typical Hanford Waste Tank Configurations

69. PNNL-11674 Ammonia Concentration Modeling Based on Retained Gas Sampler Data

70. PNNL-11693 Estimating Retained Gas Volumes in the Hanford Tanks using Waste Level Measurements, September 1997.

71. LA-UR-96-989 History of Organic Carbon in Hanford HLW Tanks: HDW Model Rev. 3.

72. PNNL-11737 Evaluation of Scaling Correlations for Mobilization of Double-Shell Tank Waste, September 1997.

73. HNF-2192 Flammable Gas Single Shell Tank Expert Elicitation Presentations (Part A)

74. HNF-2192 Flammable Gas Single Shell Tank Expert Elicitation Presentations (Part B)

75. HNF-2193 Flammable Gas Double Shell Tank Expert Elicitation Presentations (Part A)

GAS RELEASE EVENT SAFETY ANALYSIS TOOL
LIBRARY

76. HNF-2193 Flammable Gas Double Shell Tank Expert Elicitation Presentations (Part B)

77. SNL-SCOPE Project -- PQAP, Rev. 1 Safety-Controls Optimization by Performance Evaluation (SCOPE) Project, Project Quality Assurance Plan (PQAP) Sandia National Laboratories, October 1997.

78. Safety Controls Optimization by Performance Evaluation (SCOPE) Flammable Gas Expert Elicitation Results for Hanford Site Single-Shell Tanks - July 1997

    Sandia National Laboratories Safety-Controls Optimization by Performance Evaluation (SCOPE) Project, October 1997

79. Scope Concept Paper Safety-Controls Optimization by Performance Evaluation: A Systematic Approach for Safety-Related Decisions at the Hanford Tank Waste Remediation System. CONCEPT PAPER, August 1996.

80. Software Requirements Specification (SRS) (SCOPE-AT VERSION 1.0)

81. Summary of CRS Comments on Flammable Gas (First 25 Meetings, December 1993 - February 1997), 1st CRS Meeting (December 7 - 9, 1993)

82. TSA10-CN-WT-SA-TH-108, Dome Collapse Accident for Single-Shell Flammable Watch List Tanks

83. TWS96.3 Analysis of Visual Waste Observations for Single Shell Tanks, May 3, 1996.

84. TWSFG97.40 Preliminary Retained Gas Sampler Measurement Results for Hanford Waste Tank

85. Westinghouse Memo 12110PCL92-068 To. J.W. Lentsch, from J.C. Person, , Gas Retention Tests on 101-SY Tank Waste After Mixing, Westinghouse Hanford Company, Richland, Washington

GAS RELEASE EVENT SAFETY ANALYSIS TOOL
LIBRARY

86. Westinghouse Internal Memo 75210-906-006 Evidence of Release Events During Waste Intrusive Activities in Flammable Gas Watch List (FGWL) and Proposed FGWL Tanks.

87. WHC-EP-0182-102 Waste Tank Summary Report for Month Ending September 30, 1996.

88. WHC-EP-0628 Tank 101-SY Window E Core Sample: Interpretation of Results, January 26, 1993, Westinghouse Hanford Hompany, Richland, Washington

89. WHC-EP-0734, Rev. 1 Tank 241-C-103 Headspace Flammability, May 1994.

90. WHC-SD-TWR-RPT-002, Rev. 0 Structural Integrity & Potential Failure Modes of the Hanford HLW Tanks, September 1996.

91. WHC-SD-WM-CN-041, Rev. 0 Tank Farm Deflagration Rates Due to Various Ignition Sources

92. WHC-SD-WM-CN-116, Rev. 0 Calculation Note: Hydrogen Generation Rates at Steady-State Flammable Gas Concentrations for Single ShellTanks, June, 1997

93. WHC-SD-WM-DTR-045, Rev. 0 Effects of NaOH Dilution on Solution Concentrations in Tank 241-SY-101 Waste, January 1997

94. WHC-SD-WM-ER-411, Rev. 0A Tank Characterization Report for Double-Shell Tank 241-AZ-102, December 1995.

95. WHC-SD-WM-ER-515, Rev. 0 Waste Tank 241-SY-101 Dome Airspace & Ventilation System Response to a Flammable Gas Plume Burn, November 1995.

96. WHC-SD-WM-ER-526, Rev. 1 Evaluation of Hanford Tanks for Trapped Gas., March 1996

97. WHC-SD-WM-ER-526, Rev. 1 Evaluation of Hanford Tanks Trapped Gas, December 1996.

GAS RELEASE EVENT SAFETY ANALYSIS TOOL
LIBRARY

98. WHC-SD-WM-ER-526, Rev. 1A — Evaluation of Hanford Tanks for Trapped Gas, March 1996 and January 1997.

99. WHC-SD-WM-ER-526, Rev. 1C — Evaluation of Hanford Tanks for Trapped Gas, April 1997

100. WHC-SD-WM-ER-571, Rev. 0 — Evaluation of Hydrogen Release During Saltwell Pumping for Tanks T107 & S110 & S108, April 1996.

101. WHC-SD-WM-ER-576, Rev. 0 — Compilation of Hydrogen Data for 22 Single Shell Flammable Gas Watch List Tanks, May 1996.

102. WHC-SD-WM-ER-594, Rev. 0 — Evaluation of Recommendation for Addition of Tanks to the Flammable Gas Watch List, June 1996.

103. WHC-SD-WM-ES-219, Rev. 0 — Lab Flammability Studies of Mixtures of Hydrogen & Nitrous Oxide & Air, September 1992.

104. WHC-SD-WM-ES-362, Rev. 1 — Tank Farm Potential Ignition Sources, January 1996.

105. WHC-SD-WM-ES-387, Rev. 1 — Probability, Consequences, and Mitigation for Lightning Strikes to Hanford Site High-Level Waste Tanks, August 1996.

106. WHC-SD-WM-FHA-020, Rev. 0 — Fire Hazard Analysis for Tank Farms

107. WHC-SD-WM-PE-046, Rev. 0 — Evaluation of December 1991 TANK 101-SY Gas Release Event, April 1992.

108. WHC-SD-WM-RPT-281, Rev. 0 — Deflgration and Detonation Hazards in Hanford Tank Farm Facilities.

109. WHC-SD-WM-SAD-033, Rev. 2-A, Section I — Safety Assessment for Proposed Pump Mixing Operations to Mitigate Episodic Gas Releases in Tank 241-SY-101, Hanford Site, Richland, Washington

GAS RELEASE EVENT SAFETY ANALYSIS TOOL
LIBRARY

110. WHC-SD-WM-SAD-033, Rev. 2-A, Section II	Safety Assessment for Proposed Pump Mixing Operations to Mitigate Episodic Gas Releases in Tank 241-SY-101, Hanford Site, Richland, Washington
111. WHC-SD-WM-SAD-033, Rev. 2	Tank 241-SY-101 Mitigation Program, July 1996.
112. WHC-SD-WM-SAD-035, Rev. 0-A	A Safety Assessment for Rotary Mode Core Sampling in Flammable Gas Single Shell Tanks, Hanford Site, Richland, Washington
113. WHC-SD-WM-SAD-035, Rev. 0	A Safety Assessment for Saltwell Jet Pumping Operations in Tank 241-A-101: Hanford Site, Richland, Washington
114a. WHC-SD-WM-SAD-036, Rev. 0	Tank Farm Transition Projects (TFTP), November 1996.
114b. WHC-SD-WM-SAD-036,	A Safety Assessment forSalt-Well Pumping Operations in Tank 241-A-101: Hanford Site, Richland, WA.
115. WHC-SD-WM-SAR-061, Rev. 0	Tank 241-SY-103 Hazard Assessment, October 1993.
116. WHC-SD-WM-SARR-004, Rev. 1	Safety Basis for Activities in SST with Flammable Gas Concerns
117. WHC-SD-WM-SARR-016, Rev. 2	Tank Waste Compositions & Atmospheric Dispersion Coefficients for use in Safety Analysis Consequence Assessments, July 1996.
118. WHC-SD-WM-TI-513, Rev. 0	101-SY Window "C" Core Sample-Evaluation of the Chemical and Physical Properties, April 1992.
119. WHC-SD-WM-TI-724, Rev. 1	Methodology for Flammable Gas Evaluations, April 1996.

GAS RELEASE EVENT SAFETY ANALYSIS TOOL
LIBRARY

120. WHC-SD-WM-TI-753, Rev. 0	Summary of Flammable Gas Hazards and Potential Consequences in Tank Waste Remediation System Facilities at the Hanford Site, December
121. WHC-SD-WM-TRP-256, Rev. 0	Test Evaluation of Industrial Hygiene Hand Held Combustible Gas Monitor, May 1996
122. WHC-SP-1193, Rev. 0	Flammable Gas Program Topical Report, October 1996.
123. WHC-SP-1193, Rev. 1	Flammable Gas Program Topical Report
124. WHC-IP-0842, Rev. 0b	Authorization Basis Amendments and Annual Updates
125. Sandia Nat'l Lab	Software System Test Plan (SSTP) Gas Release Event Safety Analysis Tool (Resolve! Version 1)
126. HNF-SD-WM-ES-412, Rev. 0	Safety Controls Optimization By Performance Evaluation (SCOPE) Expert Elicitation Results for Hanford Site Single-Shell Tanks
127. FDH-9761360A R1	Contract Number DE-ACO6-96RL13200; Flammable Gas Project: Revised Review Comment Records for Closure of the Flammable Gas Unreveiwed Safety Questions for Single-Shell Tanks
128. FDH-9761064	Contract Number DE-ACO6-96RL13200; Flammable Gas Project: Revision of the Expert Elicitation Results for Hanford Site Single-Shell Tanks
129. FDS-9761360A R2	Contract Number DE-ACO6-96RL13200; Flammable Gas Project: Directed to Perform Data Correlation on Available Void Fraction Data with Respect to Tank Wastes Types

GAS RELEASE EVENT SAFETY ANALYSIS TOOL
LIBRARY

130. HNF-SD-WM-ES-410	Enhanced Safety Analysis methodology For Flammable Gas Risk Assessment In Hanford Site Tanks
131. PNL-10198	The Effects of Heating and Dilution On The Rheological and Physical Properties of Tank 241-SY-101 Waste
132. PNL-9062	Flammable Gas Safety Program Analytical Methods Development: FY 1993 Progress Report
133. PNL-10776	Flammable Gas Safety Program Organic Analysis and Analytical Methods Development: FY 1995 Progress Report
134. PNL-11307	Flammable Gas Safety Program: Actual Waste Organic Analysis: FY 1996 Progress Report
135. PNNL-11312	Organic Tanks Safety Program: FY 96 Waste Aging Studies
136. PNNL-11309	Organic Tanks Safety Program Advanced Organic Analysis: FY 1996 Progress Report
137. PNNL-11480	Speciation of Organic Carbon in Hanford Waste Tanks: Part I
138. Letter from Dan Meisel	Environmental Management Science Program (EMSP) Report FY-1997
139. PNNL-11640	Homogeneity of Passively Ventilated Waste Tanks
140. PNNL-11702, Rev. 1	Chemical Pathways for the Formation of Ammonia in Hanford Wastes.
141. PNL-11670	Organic Tanks Safety Program FY 97 Waste Aging Studies.

GAS RELEASE EVENT SAFETY ANALYSIS TOOL
LIBRARY

142. WHC-SD-TWR-RPT-003	DELPHI Expert Panel Evaluation of Hanford High Level Waste Tank Failure Modes and Release Quantities.
143. Presentation	Illustrative Examples from SST Elicitation Rationale Reports.
144. Information	Explosive Fragmentation.
145. 97-SCD-031	Flammable Gas Project - Safety Controls Optimization by Performance Evaluation (SCOPE) Flammable Gas Expert Elicitation Results for Hanford Site Single-Shell Tanks to Meet Performance Agreement TWR 1.3.2.
146. LMHC-9761360 R3	Subcontract Number 80232764-9-K001, Flammable Gas Project, Data Correlation Analysis Results.
147. Information	Solving the "Small-Medium-Larg" Problem.
148. Empty	

GAS RELEASE EVENT SAFETY ANALYSIS TOOL LIBRARY

149. HNF-SD-WM-TI-797	Results of Vapor Space Monitoring of Flammable Gas Watch List Tanks.
150. LA-UR-97-3955	Data Reconciliation Study of Tank 241-AN-103 at the Hanford Site.
151. HNF-1821	Gas Release Event Safety Analysis Tool Software Configuration Management Plan
152. PNNL-11638	Organic Tank Safety Project: Effect of Water Partial Pressure on the Equilibrium Water Content of Waste Samples from Hanford Tank 241-U-105
153. PNNL-11667	Seasonal Changes in the Composition of Passively Ventilated Waste Tank Headspace
154. HNF-2306, Rev. 0	Gas Release Event Safety Analysis Tool Resolve! Version 1.4 Software Requirements Specification (SRS) Revision 1.2
155. HNF-2307, Rev. 0	Gas Release Event Safety Analysis Tool Resolve! Version 1.4 Software Management Plan (SMP)
154. HNF-2308, Rev. 0	Gas Release Event Safety Analysis Tool Resolve! Version 1.4 Users Guide Revision: 1.0
154. HNF-2309, Rev. 0	Gas Release Event Safety Analysis Tool Resolve! Version 1.4 Software Design Description (SDD) Revision 1.2
154. HNF-23010, Rev. 0	Gas Release Event Safety Analysis Tool Resolve! Version 1.4 Software System Test Plan (SSTP) Revision 1

GAS RELEASE EVENT SAFETY ANALYSIS TOOL LIBRARY

This page intentionally left blank.

DISTRIBUTION SHEET

To	From	Page 1 of 1
Distribution	David R. Bratzel	Date 4/2/98
Project Title/Work Order		EDT No. 619962
Gas Release Event Safety Analysis Tool/2N160		ECN No. N/A

Name	MSIN	Text With All Attach.	Text Only	Attach./ Appendix Only	EDT/ECN Only
W. B. Barton	R2-12	X			
D. R. Bratzel (5)	S7-14	X			
M. J. Grigsby	S7-14	X			
D. J. Hammervold	B4-43	X			
R. K. Hampton	S7-40	X			
G. D. Johnson	S7-14	X			
A. B. Rau	B4-46	X			
J. Young	S7-14	X			
Central Files (2)	B1-07	X			
Sandia National Laboratories P.O. Box 5800 Albuquerque, NM 87185					
Chris E. Olson	87185-0715	X			
Scott E. Slezak	87185-0718	X			
U. S. Department of Energy, Richland Operations Office 99352					
K. Chen	S7-54	X			
C. A. Groendyke	S7-54	X			
Public Reading Room	H2-53	X			
RL Docket File (2)	A3-02	X			

This document was too large to scan as a single document; therefore, it has been divided into smaller sections.

Section 1 of 2

Document Information			
Document #	HNF-2193	Revision	0
Title	FLAMMABLE GAS DST EXPERT ELICITATION PRESENTATIONS [PART A & PART B]		
Date	04/17/98		
Originator	BRATZEL DR	Originator Co.	DESH
Recipient		Recipient Co.	
References	EDT-619962		
Keywords	BUOYANT DISPLACEMENT,DEFLAGRATIONS,DETONATIONS,TOXIC EXPOSURES,RADIOLOGICAL EXPOSURES,DOSE CONSEQUENCES		
Projects			
Other Information			

APR 17 1998
Station 15 (21)

ENGINEERING DATA TRANSMITTAL

1. EDT 619962

2. To: (Receiving Organization)	3. From: (Originating Organization)	4. Related EDT No.:
Safety Issue Resolution	Safety Issue Resolution, Flammable Gas Project	N/A
5. Proj./Prog./Dept./Div.:	6. Design Authority/ Design Agent/Cog. Engr.:	7. Purchase Order No.:
Flammable Gas Project	David R. Bratzel	N/A
8. Originator Remarks: This EDT transmits the release of the supporting document HNF-2193.		9. Equip./Component No.: N/A
		10. System/Bldg./Facility:
11. Receiver Remarks: Approval & release.	11A. Design Baseline Document? [ ] Yes [X] No	12. Major Assm. Dwg. No.: N/A
		13. Permit/Permit Application No.: N/A
		14. Required Response Date: N/A

15. DATA TRANSMITTED

(A) Item No.	(B) Document/Drawing No.	(C) Sheet No.	(D) Rev. No.	(E) Title or Description of Data Transmitted	(F) Approval Designator	(G) Reason for Transmittal	(H) Originator Disposition	(I) Receiver Disposition
1	HNF-2193	-	0	Flammable Gas Double Shell Tank Expert Elicitation Presentations (Part A and Part B)	NA	1,2	1	1

16. KEY

Approval Designator (F)	Reason for Transmittal (G)	Disposition (H) & (I)
E, S, Q, D or N/A (see WHC-CM-3-5, Sec.12.7)	1. Approval 2. Release 3. Information 4. Review 5. Post-Review 6. Dist. (Receipt Acknow. Required)	1. Approved 2. Approved w/comment 3. Disapproved w/comment 4. Reviewed no/comment 5. Reviewed w/comment 6. Receipt acknowledged

17. SIGNATURE/DISTRIBUTION
(See Approval Designator for required signatures)

(G) Reason	(H) Disp.	(J) Name (K) Signature (L) Date (M) MSIN	(G) Reason	(H) Disp.	(J) Name (K) Signature (L) Date (M) MSIN
		Design Authority N/A			
		Design Agent N/A			
1	1	Cog.Eng. D. R. Bratzel DRB 4/8/98 S7-14			
1	1	Cog. Mgr. R. J. Cash for RJC 4/8/98 S7-14			
		QA N/A			
		Safety N/A			
		Env. N/A			

18.	19.	20.	21. DOE APPROVAL (if required) Ctrl. No.
D. R. Bratzel DRB 4/8/98 Signature of EDT Originator / Date	R. J. Cash 4/8/98 Authorized Representative for Receiving Organization / Date	D. R. Bratzel DRB 4/8/98 Design Authority/ Cognizant Manager / Date	[ ] Approved [ ] Approved w/comments [ ] Disapproved w/comments

BD-7400-172-2 (05/96) GEF097

A-6000-135 (01/93) WEF067

BD-7400-172-1

Flammable Gas Double Shell Tank Expert Elicitation Presentations (Part A and Part B)

D. R. Bratzel
DE&S Hanford, Inc., Richland, WA 99352
U.S. Department of Energy Contract DE-AC06-96RL13200

EDT/ECN: 619962 UC:
Org Code: D4160000 Charge Code: N23CD
B&R Code: EW3120072 Total Pages: 781

Key Words: flammable gas, GRE's, buoyant displacement, deflagrations, detonations, toxic exposures, radiological exposures, dose consequences

Abstract: This document is a compilation of the presentation packages and white papers presented at the Flammable Gas Double Shell Expert Elicitation Workshops #1 and #2 held in January and February of 1998 at the Hanford DoubleTree Hotel in Richland, Washington.

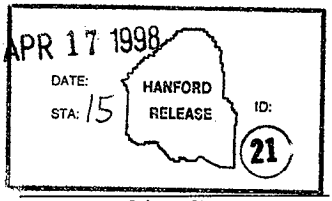

Karen L. Boland 4/17/98
Release Approval Date

Release Stamp

Approved for Public Release

FLAMMABLE GAS DOUBLE SHELL TANK EXPERT ELICITATION PRESENTATIONS

Part A

David R. Bratzel
DUKE ENGINEERING SERVICES HANFORD

Donald J. Hammervold
Aurora B. Rau
FLUOR DANIEL NORTHWEST

April 1998

For the U.S. Department of Energy
Contract

This page intentionally left blank.

TABLE OF CONTENTS

This page intentionally left blank.

1.0 INTRODUCTION

This document is a compilation of presentation packages and white papers for the Flammable Gas Double Shell Tank Expert Elicitation Workshop #1. For each presentation given by the different authors, a separate section was developed.

The purpose for issuing these workshop presentation packages and white papers as a supporting document is to provide traceablity and a Quality Assurance record for future reference to these packages.

The following personnel were attendees to this workshop which was held on January 19 - 23, 1998, in the Ice Harbor and McNary Rooms at the Double Tree Hotel in Richland, Washington:

Expert Panelists

Stephen Agnew	Los Alamos National Laboratory
Edward Beahm	Oak Ridge National Laboratory
Paul d'Entremont	Westinghouse Savannah River Company
Clay Easterly	Oak Ridge National Laboratory
Michael Epstein	Fauske & Associates, Inc.
Phillip Gauglitz	Pacific Northwest National Laboratory
Jerry Havens	Department of Chemical Engineering - University of Arkansas
Mujid Kazimi	Department of Nuclear Engineering - Massachussets Institute of Technology
Nick Kirch	Lockheed Martin Hanford Corp.
Glenn Paulson	Paulson and Cooper, Inc.
Arlin Postma	G&P Consulting
Wallace Schulz	W2S Co., Inc.
Charles Stewart	Pacific Northwest National Laboratory
Kelly Thomas	Westinghouse Savannah River Company
Michael Yost	Department of Environmental Health - University of Washington

Other Workshop Participants

Thomas Eppel	Decision Insights, Inc.
Don Hammervold	Fluor Daniel Northwest
Richard John	Decision Insights, Inc.
Paul McConnell	Sandia National Laboratory
Chris Olson	Sandia National Laboratory
Scott Slezak	Sandia National Laboratory
Detlof von Winterfeldt	Decision Insights, Inc.
Richard Harrington	Lockheed Martin Hanford Corp.
David Bratzel	DE&S Hanford, Inc.
Jerry Johnson	DE&S Hanford, Inc.
Mike Grigsby	G&P Consulting
Jonathan Young	Management Strategies Inc.
Blaine Barton	Lockheed Martin Hanford Corp.

Agenda

Gas Release Event Safety Analysis

STAGE II EXPERTS' PANEL ELICITATION WORKSHOP #1
January 19 - 23, 1998

DoubleTree Hotel Richland • Hanford House
802 George Washington Way
Richland Washington

Monday, January 19 - Moderator: Chris Olson / SNL

8:00	Welcome - Craig Groendyke / DOE/RL, Tom Geer / DESH
8:15	Opening Remarks - Chris Olson / SNL *INTRODUCTIONS; AGENDA OVERVIEW; MEETING LOGISTICS / RULES / BOUNDARIES; QUALITY ASSURANCE*
8:45	"RL Tier 2 Review Comment Resolution and Data Correlation Results" - Blaine Barton / LMHC
9:00	"Stage I Overview" - Scott Slezak / SNL
9:30	BREAK
9:45	*Resolve!* (the Analysis Tool) Demonstration- Steve Humphreys / SNL *VERSION 1.4 FOR SSTs*
10:30	"Status of DST Waste" - Kent Hodgson / LMHC *GENERAL REVIEW AND HISTORY OF DST WASTE TYPES;* *CURRENT TANK CONDITIONS AND OPERATIONS;* *COMPARISON OF DSTs AND SSTs;* *HARDWARE DIFFERENCES BETWEEN DSTs AND SSTs*

11:15	**"Future DST Operations" - Kent Hodgson / LMHC** *DISCUSSION OF POTENTIAL CONFIGURATIONS, ADDITIONS AND/OR OPERATIONS IN FUTURE WASTE TRANSFERRED FROM SSTs OR PRETREATED FOR VITRIFICATION PLANTS; REVIEW OF PRECLUDED OPERATIONS AND WASTE MIXING*
12:00	**WORKING LUNCH**
1:00	**"Introduction to Stage II Analysis Framework"** **- Fred Gelbard, Scott Slezak / SNL**
3:00	**Panel Caucus on Analysis Framework**
4:30	**Discussion of Analysis Framework** **Summary of Day's Topics / Q&A Session** **- Panelists & PHMC/SNL Teams**
5:00	**Adjourn / Project Teams (SNL, PHMC) Caucus**

Tuesday, January 20 - Moderator: SNL

8:00	**Status / Action Items Update**
8:15	**"Buoyant Displacement GRE History" - Chuck Stewart / PNNL** *GRE RELEASE HISTORIES IN DSTS; REVIEW OF OBSERVATIONS AND DATA ON BUOYANT DISPLACEMENT RELEASES* **"Overview of Field Data on Buoyant Displacement GREs"** *REVIEW OF CORE SAMPLE RHEOLOGY RESULTS, BALL RHEOMETER FINDINGS, VFI MEASUREMENTS, RGS RESULTS, ETC*
9:30	**"Buoyant Displacement Modeling" - Perry Meyer / PNNL** *SUMMARY OF ANALYTICAL MODELING AND EXPERIMENTAL TESTS ON BUOYANT DISPLACEMENT GRES; REVIEW OF GAS RETENTION AND RELEASE MECHANISMS*
10:30	**BREAK**

10:45	"Mixer Pump Operations" - Nick Kirch / LMHC *REVIEW OF INFORMATION ON EFFICIENCY OF GAS RELEASE BY 101SY; VOLUME OF WASTE AFFECTED; LABORATORY AND COMPUTER MODELING RESULTS*
11:45	WORKING LUNCH
12:45	"Gas Generation Rates, Retained Gas Composition Data, and Modeling" - Dan Reynolds / LMHC *DATA RELEVANT TO THE TOTAL GAS GENERATION RATES FOR EACH TANK AND THE H_2 GENERATION MODELING FOR DSTS AND SSTS. DATA AND MODELING FOR THE RETAINED GAS COMPOSITION. GIVEN A MODEL THAT NEEDS TOTAL GAS GENERATION RATE, AND THAT THE HU MODEL ONLY GIVES H_2 GENERATION RATE, THIS PRESENTATION ADDRESSES HOW WELL WE CAN RELATE THE TWO.*
1:45	"Proposed DST AF of Buoyant Displacement of GREs" - Fred Gelbard, Scott Slezak / SNL (Continuation of yesterday's presentation)
3:00	Panel Caucus on Analysis Framework
4:45	Discussion of Analysis Framework Summary of Day's Topics / Q&A Session - Panelists & PHMC/SNL Teams
5:15	Adjourn / Project Teams Caucus

Wednesday, January 21 - Moderator: SNL

8:00	Status / Action Items Update
8:15	Document Panel Consensus Positions and Open Issues
9:00	"Double-shelled Tank Intrusive Activity History" - Blaine Barton / LMHC *REVIEW OF HISTORY AND DESCRIPTION OF TANK INTRUSIVE ACTIVITIES; DATA INDICATION RELEASES DURING ACTIVITIES; DESCRIPTION OF ACTUAL AND POTENTIAL ACTIVITIES UNIQUE TO DSTS*

9:45	"NH_3 Release Data" - Blaine Barton / LMHC
	REVIEW OF NH_3 OBSERVATIONS ASSOCIATED WITH BUOYANT DISPLACEMENT GRES; DISCUSSION OF NH_3 RELEASE MECHANISMS FOR WASTE TRANSFER IN OR OUT OF TANKS
10:15	BREAK
10:30	"Proposed AF for NH_3 Release, Gas Composition, and Waste Intrusive Activity" - Wu-Ching Cheng / SNL
12:00	WORKING LUNCH
1:00	Panel Caucus on Analysis Framework
	Breakout Meeting: Project Teams (PHMC, SNL) Caucus with Observers and DOE/RL
3:30	Discussion of Analysis Framework Summary of Day's Topics / Q&A Session - Panelists & PHMC/SNL Teams
5:00	Adjourn
7:00	Group Dinner [tbd]

Thursday, January 22 - Moderator: SNL

8:00	Status / Action Items Update
8:15	"Control Strategies" - Mike Grigsby / G&P Consulting
9:00	"Review of Models and Analysis for Facility Group 1 Tanks" - Cetin Unal / LANL
	PHYSICAL PARAMETER CONSIDERATIONS IN GAS RELEASE MECHANISMS; REVIEW OF EXISTING MODELS
10:30	BREAK

10:45	"Evaluation of Mitigation Strategies in Facility Group 1 Double-shell Flammable Gas Tanks at Hanford Site" - Cetin Unal / LANL
11:45	"Controls Implementation in AF" - Scott Slezak / SNL
12:15	WORKING LUNCH
1:15	"Ex-tank vs. In-tank Ignition Sources" - Dave Smet / TWRS Equipment Engineering *REVIEW OF POSSIBLE EX-TANK AND IN-TANK IGNITION SOURCES; IMPLICATIONS OF IC SET 1 VS. SET 2 VS. PAST PRACTICES*
2:15	"Proposed AF for Mixing and Ex-tank Ignition Controls" - Scott Slezak / SNL (No handouts)
3:00	Panel Caucus on Analysis Framework
4:30	Discussion of Analysis Framework Summary of Day's Topics / Q&A Session - Panelists & PHMC/SNL Teams
5:00	Adjourn / Project Teams Caucus

Friday, January 23 - Moderator: Chris Olson / SNL

8:00	Status / Action Items Update
8:15	"Seismic Response of DST Waste" - Chuck Stewart / PNNL *REVIEW OF MODEL RESULTS AND IMPLICATIONS FOR RELEASES FROM WASTE WITH THICK SUPERNATE LAYER; DISCUSSION OF INFLUENCE OF PUMPED VS. UNPUMPED WASTE ON SEISMIC RESPONSE* (Scheduled for second workshop)
9:00	"Proposed AF on Seismic Response" - Scott Slezak (no handouts)
10:15	Document Panel Consensus Positions and Open Issues

11:00	**General Discussion of Panel Process / Feedback from Experts** **Plans for Workshop #2 (February 9 - 13, 1998) / Assignments**
11:30	**Adjourn**

Only expert panel members and the Panel Moderator shall be seated at the main table. Only the Panel Moderator and the panel members shall be allowed to speak or ask questions of guest speakers or to engage in panel discussions, except that the Panel Moderator may specifically recognize non-panel members for the purpose of efficiently covering necessary topics of discussion or for the purpose of efficiently conducting the meeting.

<Ver. 6.1 FINAL 1/15/98>

PD 4 - 1
Procedure for Elicitation Rationale Reports and
Expert Panelists' Elicitation Verification

1.0 Purpose and Scope

This procedure is provided to expert panelists participating in the Stage II Gas Release Event Safety Analysis project (here after in this procedure identified as "the project"). This Procedure is to be used by expert panelists for preparation of their Stage II *Expert Elicitation Rationale Summary Reports*. The Stage II Expert Elicitation Rationale Summary Reports are Quality Documents so panelist compliance with this Procedure is required.

In addition to describing the procedures for preparing the Stage II Expert Elicitation Rationale Summary Reports, this Procedure describes the process by which each expert panelist shall review the report prepared by the Elicitor on the individual panelist's elicitation. Also described is the process for providing explicit feedback to Sandia National Laboratories Methodology for Flammable Gas Risk Assessment in Double-shell Tanks project staff when queried regarding aspects of the Stage II Expert Elicitation Rationale Summary Reports or the Elicitors' report.

This procedure also describes the process by which the panel endorses and approves the final version of the Analysis Framework on the basis of which the experts shall be elicited.

2.0 References

None

3.0 Requirements

3.1 Stage II Expert Elicitation Rationale Summary Reports

The following format shall be implemented in preparing the various sections of the Stage II Expert Elicitation Rationale Summary Reports ("the report").

- Title Page: The Title Page shall include the phrase "Stage II Gas Release Event Safety Analysis Project Expert Elicitation Rationale Summary Report", the expert's name and organization, date of elicitation, and date of report.

- Table of Contents: The report shall include a Table of Contents. The pages of the report shall be numbered.

- Introduction: An Introduction shall be included which shall identify the elicitation process (Elicitor, date) for the panelist. The Introduction should include any general comments which the panelist wishes to make.

- Elicitation Parameter Rationales: For each parameter to which the panelist was elicited, a separate section within the report shall be included. The title of each Elicitation Parameter Rationale section in the Stage II Expert Elicitation Rationale Summary Report shall correspond to the title of the elicited parameter. Each Elicitation Parameter Rationale section shall provide a discussion of the probability distribution response provided at the time of the elicitation, changes subsequently made after the formal elicitation to that response (if any), and a detailed rationale by which the elicited response was derived. Included within each Elicitation Parameter Rationale section shall be subsections discussing conditioning factors, assumptions, references, and the elicited probability distributions for the parameter in table format. References employed in arriving at the elicited response shall be identified and shall be provided in both the section of the report on the particular elicited parameter and in a section of the report which collates all References. All referenced materials shall be in either the open technical literature or shall have received clearance for public document distribution.

- Each table shall be numbered with an arabic numeral and shall be given a title that is complete and descriptive. The table number and title shall be above the body of the table. In column headings, first include the quantity tabulated followed by a comma and the units. Do not use powers of 10 in column headings. Use notation such as "$X10^6$" for numbers to be expressed in powers of 10 within the body of the table. Each entry in the tables shall be specifically entered: do not refer to values in other tables or use multipliers for values of other entries in the table.

- References: References shall be provided in each Elicitation Parameter Rationale section and all of the references provided throughout the report shall be listed in a separate Reference section of the report.

Panelists shall prepare for each elicitation session by organizing their notes and references. Panelists may prepare summary notes prior to elicitation sessions to assist them in accessing the appropriate notes and references efficiently. These summary notes may be included in the Rationale Summary Report. Each panelist may obtain a printed version of the data and narrative recorded by the Elicitor at the end of the elicitation session. The Stage II Expert Elicitation Rationale Summary Reports are due at Sandia National Laboratories no later than two weeks following the date of the elicitation. Either hardcopy or electronic format is acceptable.

Preferred word-processing medium is WordPerfect® 5.2, Times New Roman 12-point font format for the text is preferred.

3.2 Elicitors' Report / Elicitation Feedback

The Elicitors shall prepare a report for each set of elicited responses from each of the panelists. This report shall include the probability distributions provided by the panelists at the time of elicitation. These reports are due at Sandia National Laboratories no later than two weeks after the final panelist elicitation. The probability distributions for each of the elicited parameters shall be transmitted to Sandia National Laboratories in EXCEL® Version 7.0.

The Elicitor's report for each panelist shall subsequently be forwarded upon receipt by Sandia National Laboratories to the corresponding panelist. The panelist shall be requested to review the Elicitor's report to determine the accuracy of the information contained, particularly the probability distributions. The panelist is required to either 1) confirm the accuracy of the information in the Elicitor's report, 2) identify any discrepancies and provide the correct information, or 3) change any response originally provided to the Elicitor at the time of the elicitation. The review of the Elicitor's report shall be conveyed to Sandia National Laboratories within one week of receipt by the panelist. The response to the Elicitors' Report review may be transmitted by hard-copy or electronically. These responses shall be Quality Documents.

Subsequently, as Sandia National Laboratories staff review both the sets of Elicitor's reports and the Stage II Expert Elicitation Rationale Summary Reports, questions may arise to which the panelists shall be asked for clarification. Both the queries and the panelist's responses shall be documented. Hard-copies of electronic or written versions of these interchanges shall be Quality Documents.

3.3 Endorsement of Stage II Analysis Framework

The review of the Analysis Framework, changes to the Analysis Framework, and other consensus decisions reached by the expert panel are to be documented in writing, as well as in the voice recordings of the workshop meetings. Any changes to the Analysis Framework, as presented in project documents and workshop presentations, are to be documented on Decision Record forms. The record forms are to be signed and dated by the panel leader, the panel caucus facilitator, and the workshop meeting moderator. The Decision Records will be distributed to each panelist within one week of the end of the panel group sessions. The panel shall document on the Decision Record form any application guidelines and caveats that the panel members believe should be recorded to prevent misuse of the Analysis Framework. Provisions are to be made for documenting dissenting minority opinions to decisions if the dissenting panel members

****
WordPerfect is a trademark of Corel Corporation.
EXCEL is a trademark of Microsoft Corporation.

wish to document their differences of opinion. The review of the Analysis Framework is to be documented in the form of decision records that list the specific submodels, equations, or discussions in the Analysis Framework document or presentation slides that were discussed and agreed to by the panel. Other consensus decisions to be recorded include (1) agreements that specific phenomena are not risk-significant enough to include in the Analysis Framework, (2) that within the uncertainties and the current state of knowledge there is no basis for distinguishing between different potential elicitation parameters or different potential conditioning cases for a given elicitation parameter, and (3) any decision or consensus position reached by the panel that in the view of the project team warrants permanent documentation.

4.0 Records

Relevant items described in this procedure shall be Quality Documents.

5.0 Attachments

Analysis Framework Decision Record form.

Approvals:

Chris Olson, SNL Project Manager — Date: 2-5-98

Larry Bustard, SNL QA Manager — Date: 2/5/98

Stage II Gas Release Event Safety Analysis Project
Analysis Framework Decision Record

Analysis Framework issue:

Panel Comments:

Approvals:

Panel Leader	Date
Panel Caucus Facilitator	Date
Workshop Moderator	Date

Introduction
Expert Panel Workshop #1
Double Shell Tanks

January 19, 1998

Chris Olson

Expert Panel Membership

- Same membership as the SST panel, except:
  - New members added: Kirch, Yost, d'Entremont
  - Former members lost: Grelecki, Reynolds, White
- Same qualification requirements
- New members participated in two-day miniworkshop in December 1997

Status of SST model

- Version 2.4 of Resolve!, the analysis tool, is in use in analysis of SST safety control options
- A few technical issues need to be revisited
- Analysis framework/analysis tool validation work is in progress
- Lessons learned will be applied in DST stage of project

Concept for DST Stage of Project

- Build on previous SST milestones wherever appropriate
- Incorporate new AF components to treat phenomena peculiar to DSTs
- Modify/update pedigreed database (PDB) to represent DSTs and remain compatible with AF
- Use expert elicitation to quantify uncertainty for parameters not in the PDB that are used in the AF
- Deliver distributed analysis tool application that can be accessed and run over the Web

Expert Panel Objectives

- **Review DST Analysis Framework and recommend final version to:**
  - **Accurately model flammable gas release and ignition phenomena**
  - **Support expert elicitation to quantify uncertainty for unknown parameter values**
  - **Provide structure to represent safety controls**
- **Provide individual elicitation distributions for conditioned parameters required by the Analysis Framework and unavailable in the Pedigreed Data Base**

Expert Panel Schedule

- 1st Workshop: 1/19/98-1/23/98: determine information needs and begin technical briefings and group discussion
- 2nd Workshop: 2/9/98-2/13/98: complete technical briefings and reach consensus on AF and elicitation structure
- 3rd Workshop: 3/9/98-3/13/98: additional group discussion as required and individual elicitations
- Rationale reports: due to Sandia by 3/27/98
- Review of final AF draft by 4/10/98

wrkshp1-CEO-1/98
slide 6

Agenda

- **Monday: 8:00AM-5:00PM**
  - Briefings #2.1.0-2.1.7
- **Tuesday: 8:00AM-5:15PM**
  - Briefings #2.1.8-2.1.13
- **Wednesday: 8:00AM-5:00PM**
  - Briefings #2.1.14-2.1.16
- **Thursday: 8:00AM-5:00PM**
  - Briefings #2.1.17-2.1.21
- **Friday: 8:00AM-11:30AM**
  - Briefings #2.1.22-2.1.23

Meeting Logistics

- Briefings and expert panel caucuses
- Document library
- Web page
- Sandia contacts:
  - Paul McConnell, 505.845.8361
  - Scott Slezak, 505.844.2050
  - Chris Olson, 505.845.8670
  - Steve Humphreys, 505.844.7223
- Wednesday night group dinner (?)

Meeting Rules and QA Elements

- **Workshop is for the expert panel:**
  - Briefings are open, moderated -- non-panel members may submit questions or observations to moderator; all sessions audio-recorded
  - Panel caucuses are closed, facilitated -- findings, questions, and consensus positions will be reported formally with assistance of facilitators
  - Elicitations are conducted individually by normative expert and reviewed by individual expert, by normative expert, and by Sandia project team members
  - Proceedings will be formally published as Hanford reports

Expert Elicitation Reports

- Specifications and quality assurance for expert elicitation reports
- Use of document library and expert workshop proceedings
- Use of expert judgment and synthesis of information

A Note About Project Terminology

- This project is part of a larger initiative to develop and apply a Refined Safety Analysis Methodology for Flammable Gas Risk Assessment in Hanford Site Tanks
- The acronym "SCOPE" will no longer be used, but it may appear in documents generated earlier in the project
- This project will generally be referred to as the "Gas Release Event Safety Analysis" project

RL Tier 2 Review Comment Resolution and Data Correlation Results

W. B. (Blaine) Barton
Lockheed Martin Hanford Co.
January 19, 1998

Introduction

- DOE conducts a three tier review process of all safety analysis related documents
- Overview of results of review and status of resolution of issues

Tier 1 Review

- Tier 1 is the Contractor internal review for technical accuracy

- Issues identified were:
  - Verification and validation
  - Adequacy of models, ammonia, and plume burn
  - How the products would be used

- Comments were resolved

Tier 2 Review

- DOE review of the technical adequacy of the work
  - Analysis framework
  - Elicitation results
  - Summary results
- Conducted by DOE Safety and independent reviewers
- One open comment remaining, data correlation study proposed

Data Correlation Study

- Phase 1 restricted to measured data
- Considered void fraction and GRE frequency as dependent variables
- Waste type, elevation, temperature, heat load, and pressure as independent variables
- Phase 2 to expand sample by using estimated void fraction from barometric response data

	Sample Elevation (in)	Sample-Elevation-to-Solids-Level Ratio	Hydrostatic Pressure (atm)	Temperature (deg F)	Waste Type Total Volume (kgal)	Heat Load (kW)	In Situ Void Fraction
Sample Elevation (in)	1						
Sample-Elevation-to Solids-Level Ratio	0.9109	1					
Hydrostatic Pressure (atm)	0.0889	0.1546	1				
Temperature (deg F)	-0.0707	-0.2415	0.0257	1			
Waste Type Total Volume (kgal)	0.6258	0.5712	0.1640	0.0915	1		
Heat Load (kW)	-0.0179	0.0670	-0.0169	0.2303	0.01466	1	
In Situ Void Fraction	**-0.3947**	**-0.4413**	**-0.0466**	**-0.0758**	**-0.30130**	**0.02539**	**1**

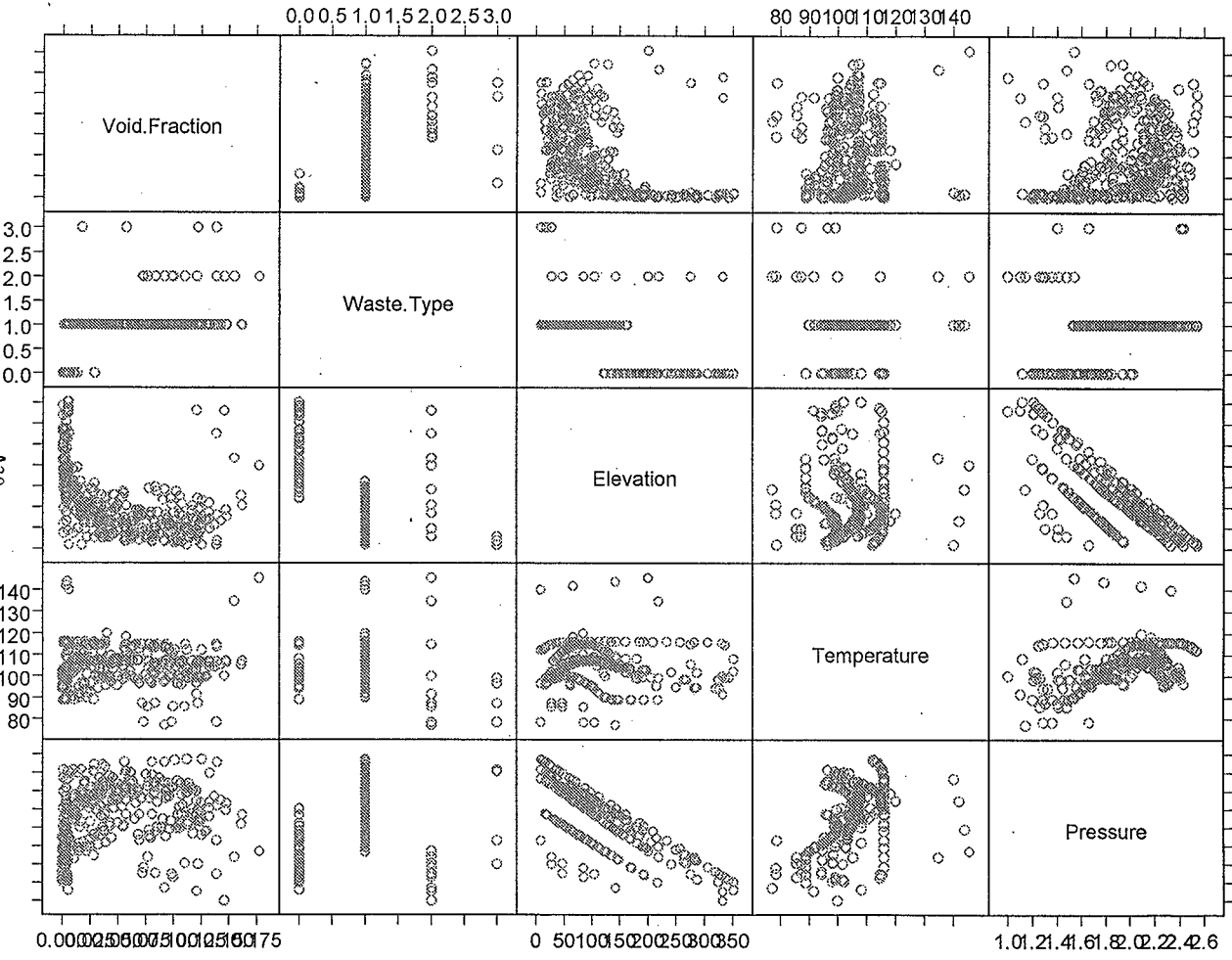
Void.Fraction
Waste.Type
Elevation
Temperature
Pressure

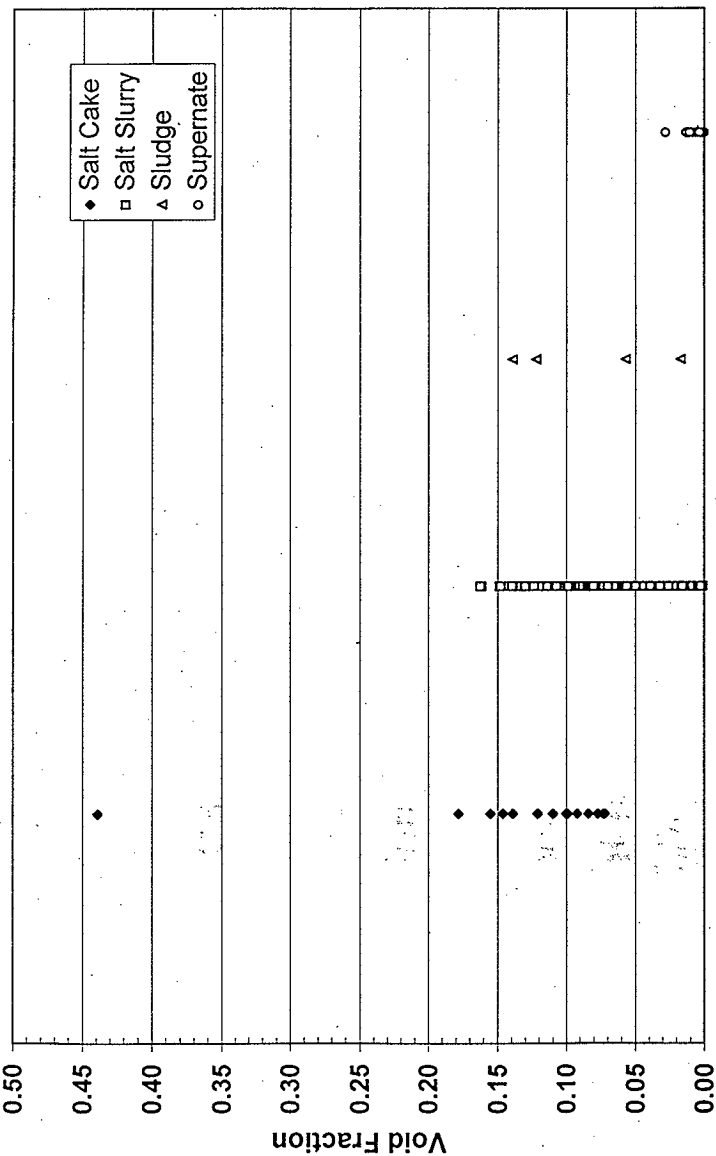

Figure 1. Waste Type Versus Void Fraction.

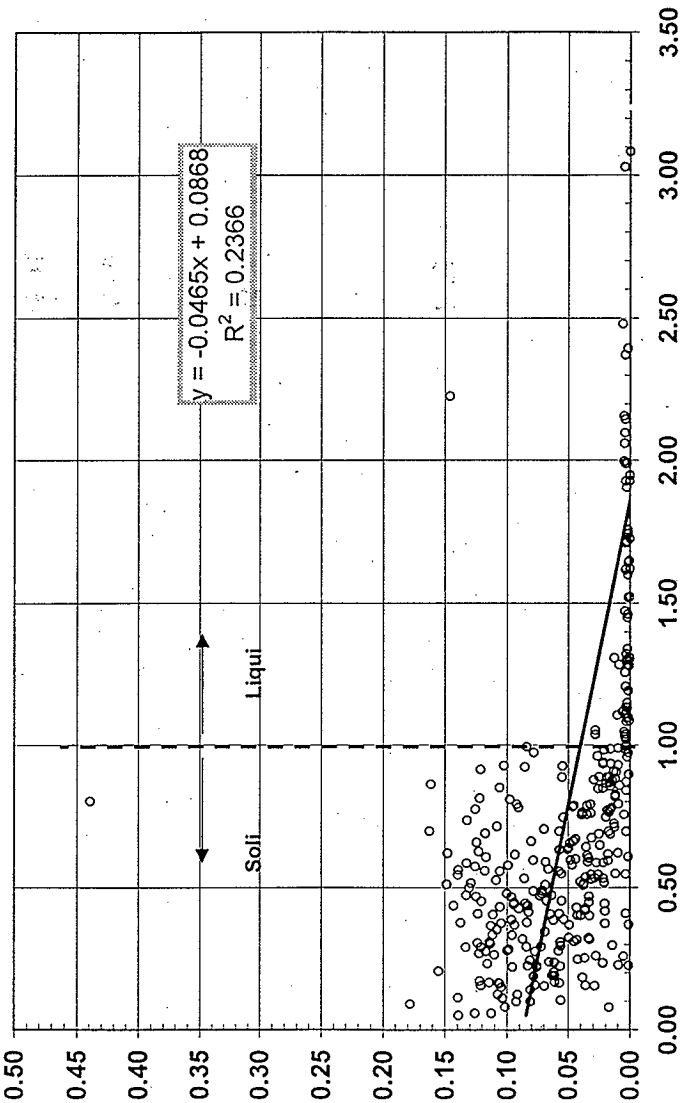

Figure 2. Sample-Elevation-to-Solids-Level Ratio Versus Void Fraction.

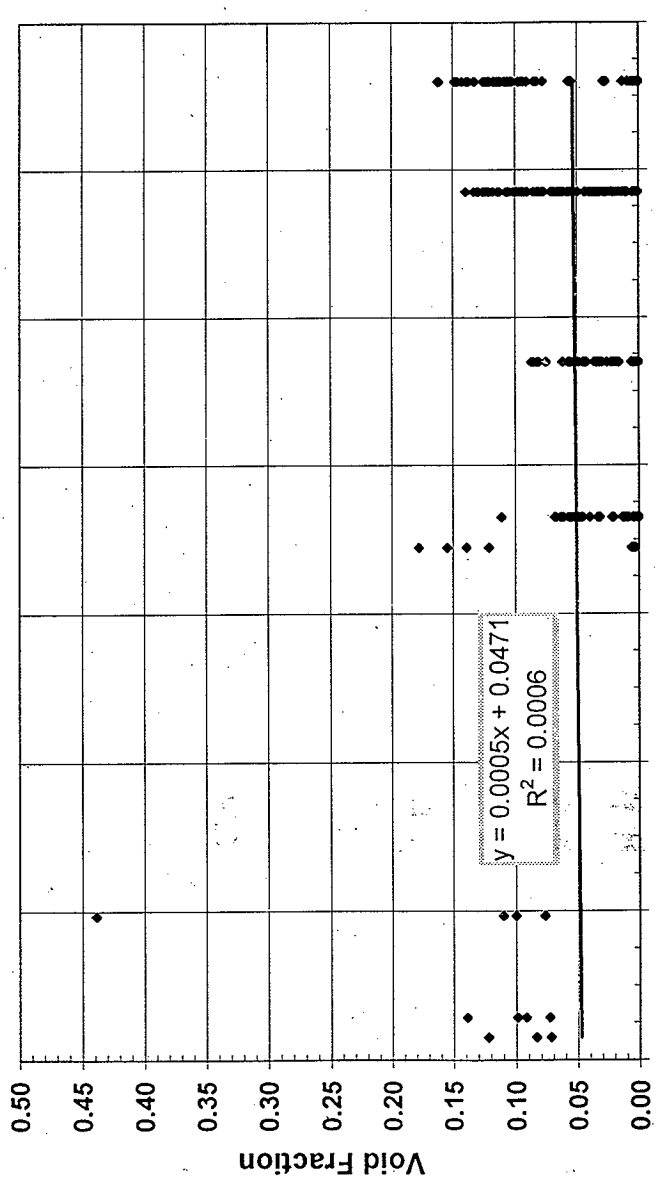

Figure 3. Heat Load Versus Void Fraction.

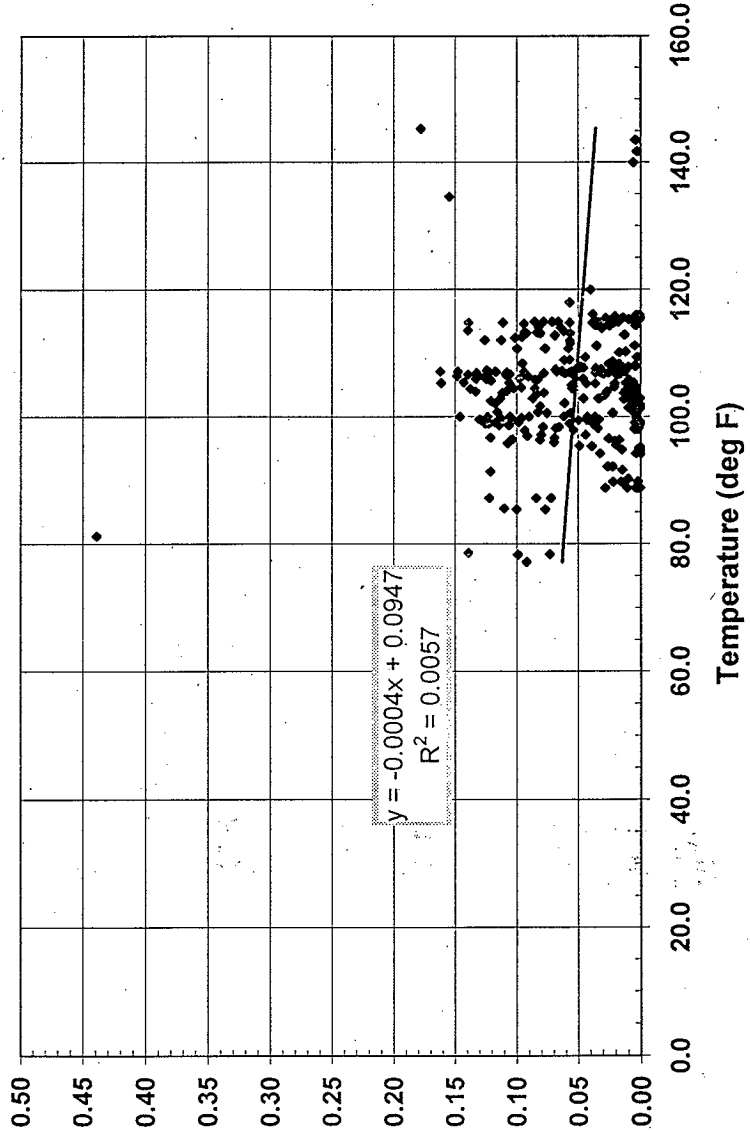

Figure 4. Temperature Versus Void Fraction.

	Sample Elevation (in)	Sample-Elevation-to-Solids-Level Ratio	Hydrostatic Pressure (atm)	Temperature (deg F)	Waste Type Total Volume (kgal)	Heat Load (kW)	GRE Frequency (events/year)
Sample Elevation (in)	1						
Sample-Elevation to-Solids-Level Ratio	0.9109	1					
Hydrostatic Pressure (atm)	0.0889	0.1546	1				
Temperature (deg F)	-0.0707	-0.2415	0.0257	1			
Waste Type Total Volume (kgal)	0.6258	0.5712	0.1640	0.0915	1		
Heat Load (kW)	-0.0179	0.0670	-0.0169	0.2303	0.01466	1	
GRE Frequency (events/year)	**-0.1642**	**-0.0127**	**0.0875**	**-0.2317**	**-0.30459**	**-0.15516**	**1**

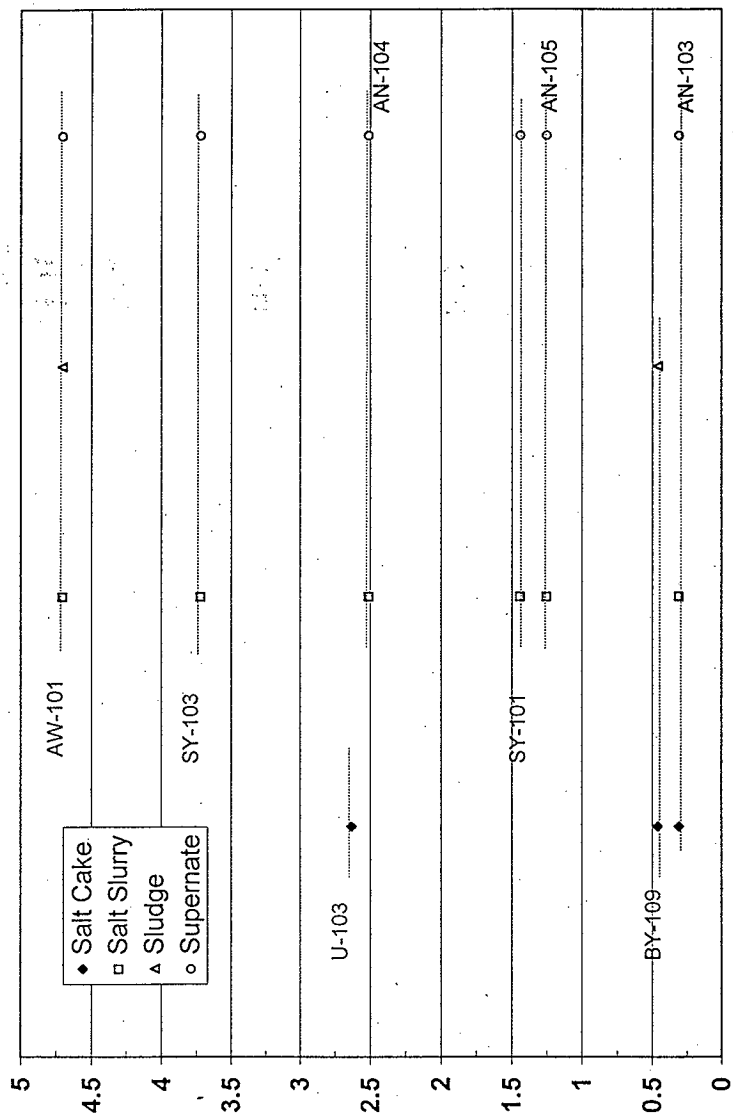

Figure 5. Waste Type Versus GRE Frequency.

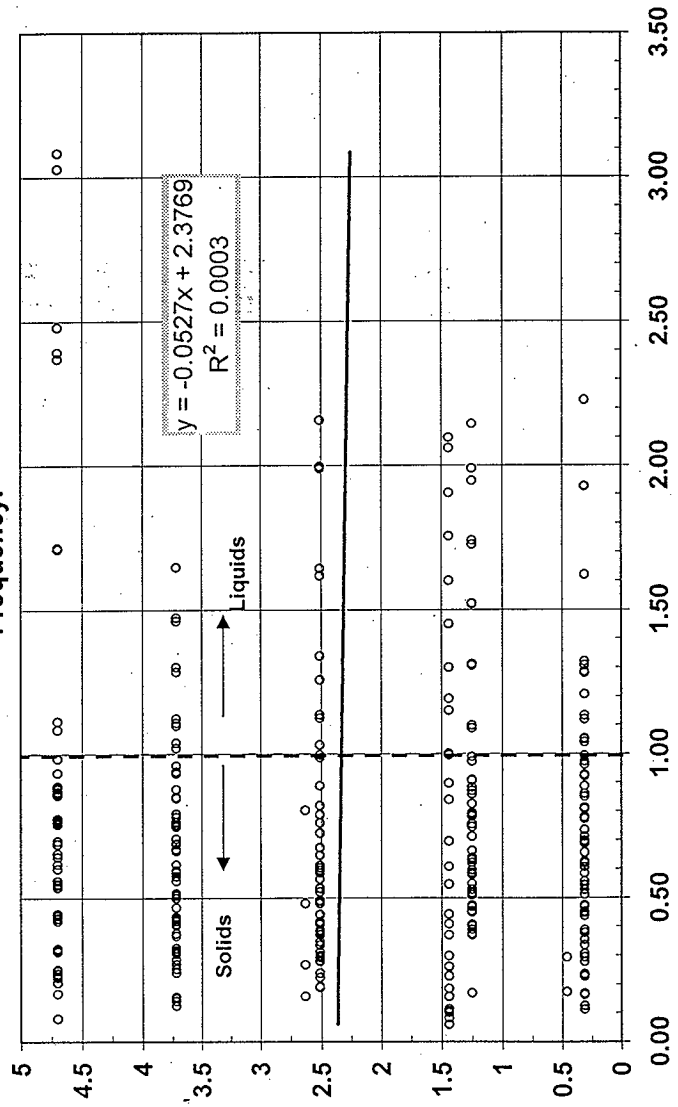

Figure 6. Sample Elevation to Solids Level Ratio Versus GRE Frequency.

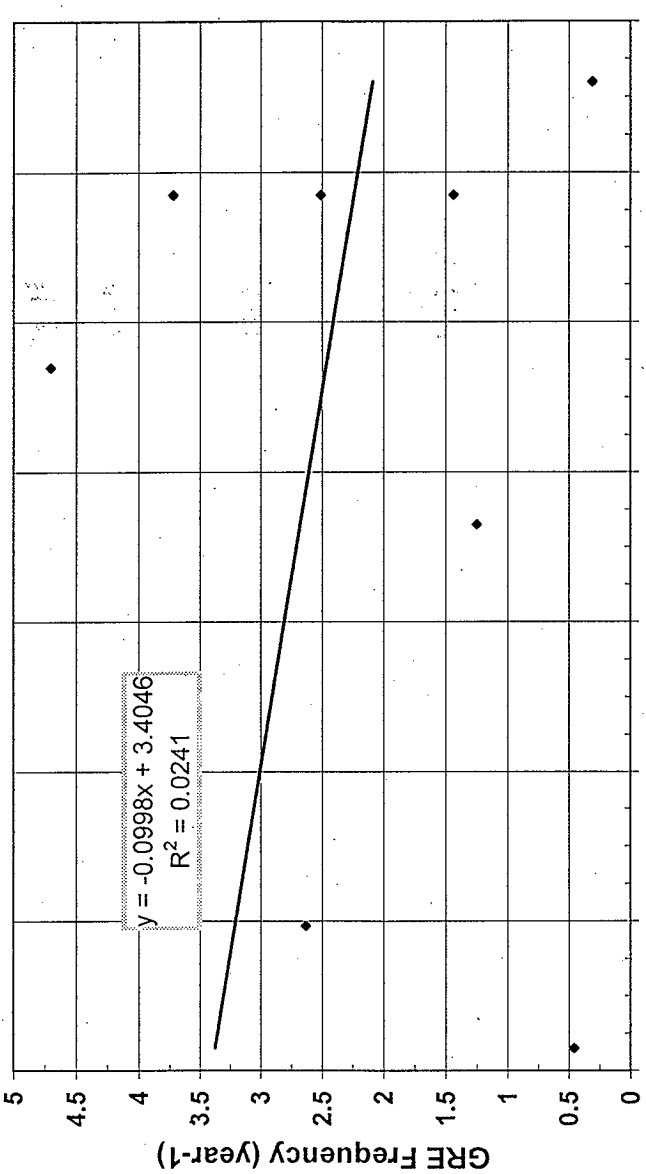

Figure 7. Heat Load Versus GRE Frequency.

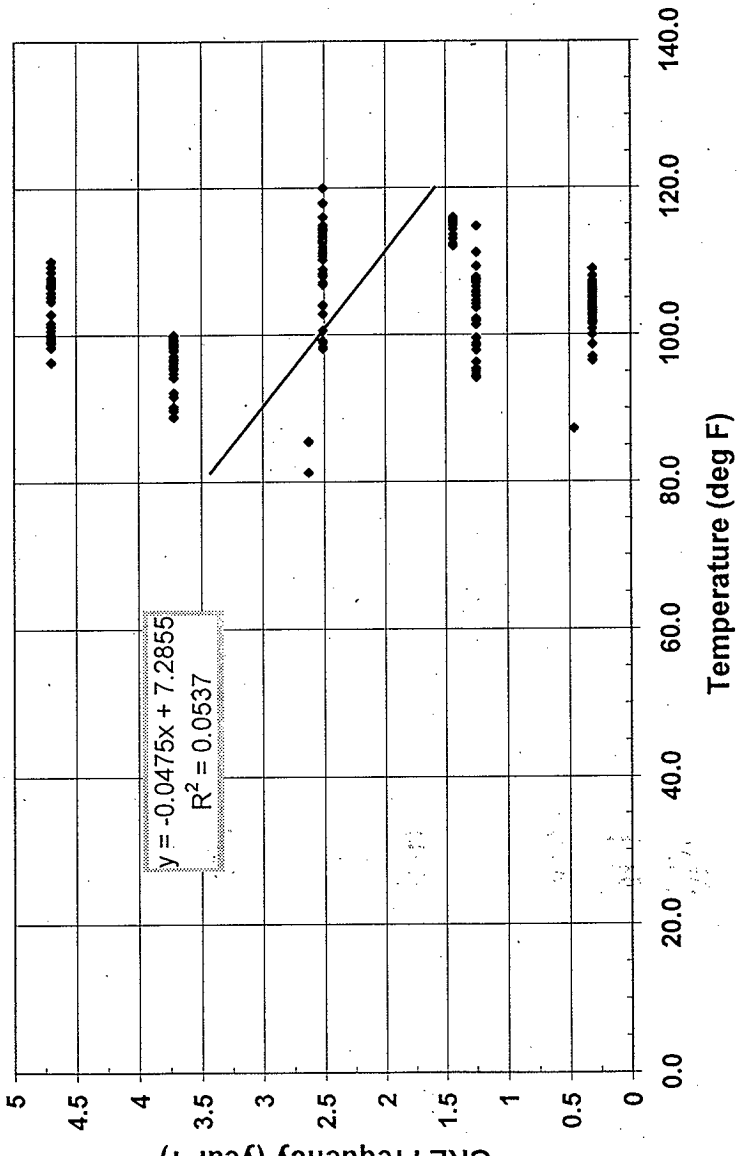

Figure 8. Temperature Versus GRE Frequency.

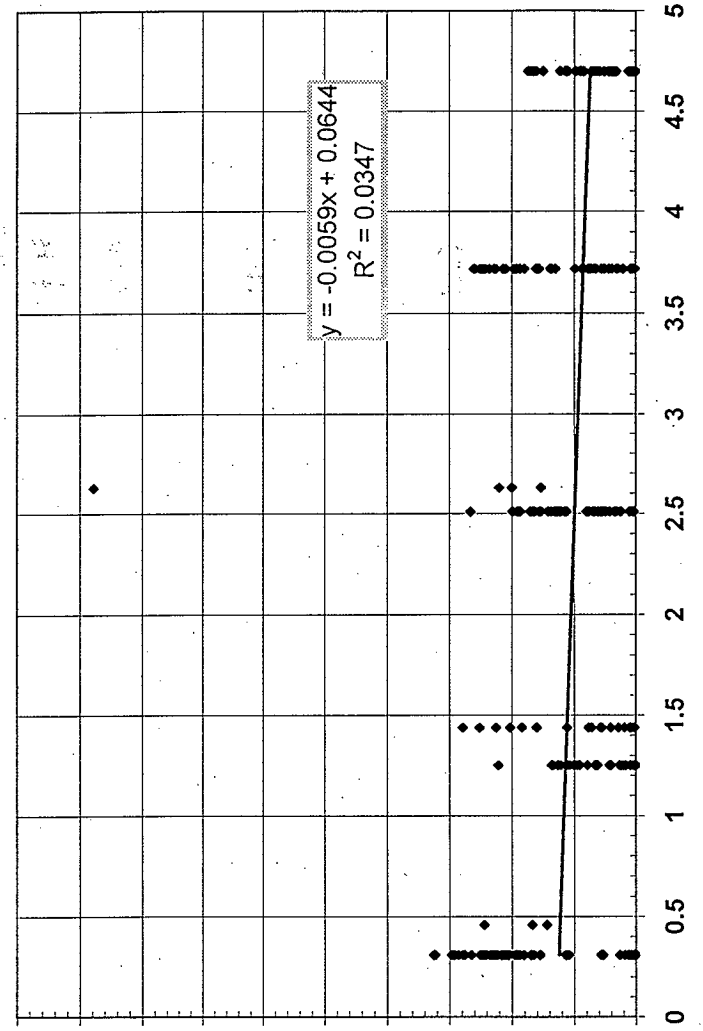

Figure 9. GRE Frequency Versus Void Fraction.

Planned Actions

- Complete Phase 2 data correlation study
- Complete validation and verification activities
- Improve documentation of expert panel guidance

Data Correlation Study Results

- No clear correlation was found in Phase 1
- Examples of results

Further Information

- RL Tier 2 comments and response are in the library
- The result of the Phase 1 study are in the library

Overview of Results for SSTs

January 19, 1998

Scott Slezak

OBJECTIVE: Review Model Status for SSTs.

- To know where we are going, we first need to know where we have been and we are.
- Overview of models for GRE release, combustion, waste material released, etc.
- Qualitative discussion of results of Analysis Framework calculations for SSTs by *Resolve!* software.

Retained Gas

- Undissolved flammable gas is contained within the void spaces in waste.
- Panel quantified void fraction uncertainty distributions conditioned on Facility Group and saltwell pumping status.
- H_2, N_2O, CH_4 determined from distributions developed from data in *Resolve!* database.
- Default NH_3 and N_2 distributions provided.
  - N_2 is normal distribution with median = 20%, σ = 7%.
  - NH_3 is Weibull distribution with median = 1.67, 90th percentile at 3.0, 98th percentile at 5.0.

WS1–SS–1/19/98-A
slide 3

Gas Release

- Flammable gas is released by GREs (Gas Release Events) that can be spontaneous or induced.
- Panel quantified uncertainty for frequency of spontaneous releases, and probability that an activity can induce a GRE.
- Uncertainty distributions conditioned on Facility Group, efficiency of release (small, medium, large), and extent of disturbance by waste-intrusive activity (local, global).

WS1–SS–1/19/98-A
slide 4

Gas Release (2)

- Efficiency, frequency, and rate of release are not independent.
- Therefore, uncertainty distributions for frequency, probability and duration conditioned on given efficiency of release (small, medium, large) to make analysis manageable for panel.

WS1–SS–1/19/98-A
slide 5

GRE Terminology

- Efficiency of release
  - Small (<5% of retained gas)
  - Medium (5% to 25% of retained gas)
  - Large (>25% of retained gas)
- Facility Group
  - FG-1 tanks: acknowledged with little or no controversy to be of the greatest concern with respect to the flammable gas hazard.
  - FG-2 tanks: postulated to have the potential for a large induced GRE but only a small spontaneous GRE.
  - FG-3 tanks: includes all of the remaining tanks not assigned to either Facility Groups 1 or 2.

WS1–SS–1/19/98-A
slide 6

Waste Disturbing Operations

- **Globally waste-disturbing operations**
  - Saltwell pumping
  - Large waste additions, removal, and transfers
  - Chemical additions (including large water additions)
  - (Earthquake)
- **Local waste-disturbing operations**
  - Lancing (<500 gallons of water total)
  - Waste Sampling
    - push or rotary mode core, auger, grab, void meter
  - Equipment (e.g. TC tree, LOW) installation or removal

WS1-SS-1/19/98-A
slide 7

Ammonia Release

- **Salt well pumping enhances both undissolved gas and ammonia release.**
  - Panel provided uncertainty distributions for volume of waste releasing undissolved gas per volume of liquid salt well pumped and rate of decay of release after pumping stops.
  - Panel provided uncertainty distributions for volumetric rate of NH_3 release during salt well pumping and rate of decay of release after pumping stops.
- **Ammonia releases that do not burn contribute to toxicological consequences.**

WS1-SS-1/19/98-A
slide 8

Plume Model

- Asymptotic plume rise model used to calculate plume dilution.
- If a combustible mixture reaches tank dome, stable stratified layer forms.
- Stratified layer dilutes by molecular diffusion and by ventilation.
- The following considered risk-insignificant:
  - Plume dilutes below LFL before reaching dome (too little gas).
  - Plume burns as stable diffusion flame (releases too irregular to support this model and rate is so slow that ventilation would limit pressure rise).

WS1–SS–1/19/98-A
slide 9

GRE Combustion Model

- Small efficiency GREs evaluated only for plume (and stratified layer) combustion behavior.
- Large efficiency GREs evaluated only for well-mixed headspace combustion behavior.
- Medium efficiency GREs evaluated for both plume and well-mixed combustion behaviors.
  - Panel provided uncertainty distributions for efficiency of stratified layer combustion and the fraction of medium GREs that are best described by the plume analysis.
  - (fraction) x frequency of release = frequency of plumes.
  - (1-fraction) x f_{rel} = frequency of well-mixed conditions.

WS1–SS–1/19/98-A
slide 10

Mass Release

- Panel provided uncertainty distributions for mass and respirable fraction of material suspended by a burn conditioned on:
  - burn fails HEPA but does not crack dome
  - burn cracks dome but does not cause gross failure
  - burn causes gross structural failure of dome
- Mass release computed from fraction of headspace gas vented by isentropic expansion.
- Dose consequences computed by unit liter dose analysis.

WS1–SS–1/19/98-A
slide 11

Ignition Frequencies

- Combustion frequency or probability is ≤ release frequency or probability.
- Not all releases have ignition sources; not all releases with ignition sources are flammable.
- Panel provided uncertainty distributions for:
  - frequency of random sources (not affected by controls)
  - probability of GRE, earthquake, and operation-induced ignition sources.
  - probability of ignition source conditioned on ignition controls in place (IC set 1, IC set 2, past practices).

WS1–SS–1/19/98-A
slide 12

Equipment Burns

- Panel provided uncertainty distributions for mole fraction of source gas in equipment conditioned on equipment purged or not.
- Panel provided uncertainty distributions for mass of material ejected from a burn in equipment conditioned on a deflagration or detonation and air or inert gas normally maintained in equipment.
- Analysis framework results not yet fully implemented in software.

WS1–SS–1/19/98-A
slide 13

Observations from Calculations

- The sensitivity analysis presented at 2nd SST workshop appears fully supported by *Resolve!*:
  - Waste volume is by far the single largest influence on computed risk.
  - For tank-specific evaluations with fixed waste volume, the primary sensitivities are:
    - frequency/probability of spontaneous/induced GRE.
    - retained gas fraction.
    - stratified layer combustion efficiency.
    - gas release efficiency.
    - mass of material suspended by combustion event.
  - Effect of gas composition is negligible.

WS1–SS–1/19/98-A
slide 14

Uncertainty Distribution Observations

- Span of uncertainty distributions wider than expected by many observers.
- Threshold behaviors (e.g., flammability limit, frequency categories in risk guidelines) make large ranges of some uncertainty distributions unimportant to computed results.
- In spite of uncertainty distributions that span several decades in value, results are very useful in assessing impact of flammability controls.
- No bias evident for "Hanfordites" vs. "outsiders".

WS1–SS–1/19/98-A
slide 15

Lessons Learned

- Mass of material *suspended* versus *released*.
  - splash-back and filtering effects not credited
- Time at risk in ex-tank intrusive regions.
- Interpretation of results.
  - scatter plots versus statistics
  - all results versus specific results
- Importance of intermediate calculations.
  - releases versus combustion events
  - dose consequences versus %LFL, peak pressure, etc.

WS1–SS–1/19/98-A
slide 16

Summary

- Software implementation of Analysis Framework for SSTs (*Resolve!*) is operating.
- Tank-specific and representative tank evaluations can be done.
- Results have provided insights to both safety analysis methods and operational safety.
- Users of *Resolve!* have provided valuable lessons for how to improve both the Analysis Framework and the interpretation of results.

WS1–SS–1/19/98-A
slide 17

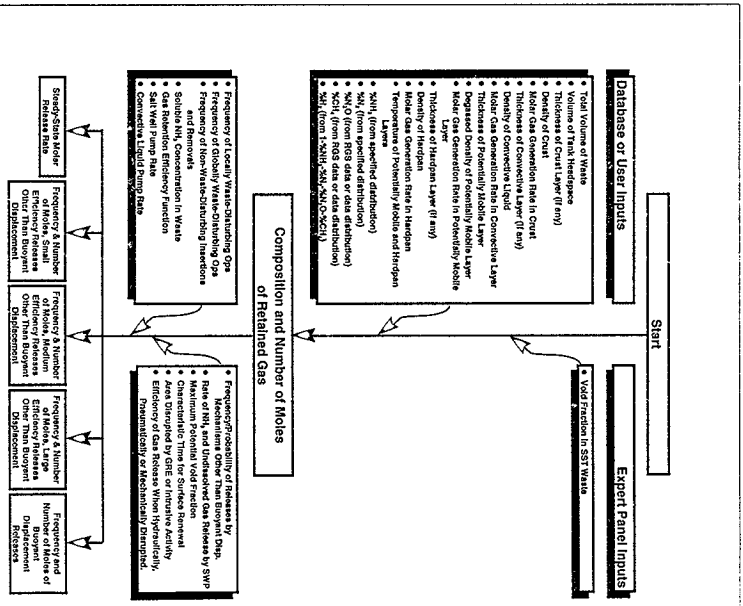

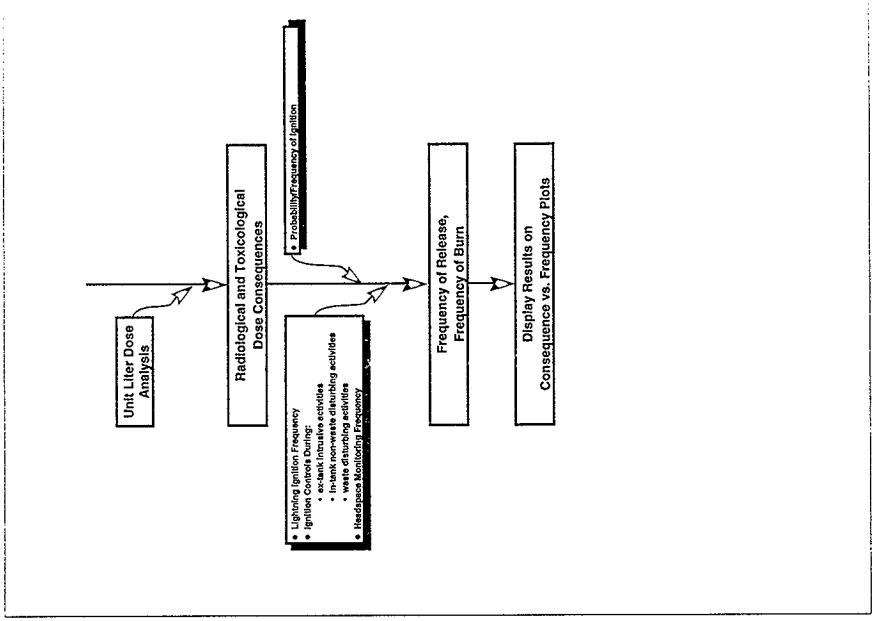
Unit Liter Dose Analysis
Radiological and Toxicological Dose Consequences
Probability/Frequency of Ignition
Lightning Ignition Frequency
Ignition Controls During:
ex-tank intrusive activities
in-tank non-waste disturbing activities
waste disturbing activities
Headspace Monitoring Frequency
Frequency of Release, Frequency of Burn
Display Results on Consequence vs. Frequency Plots

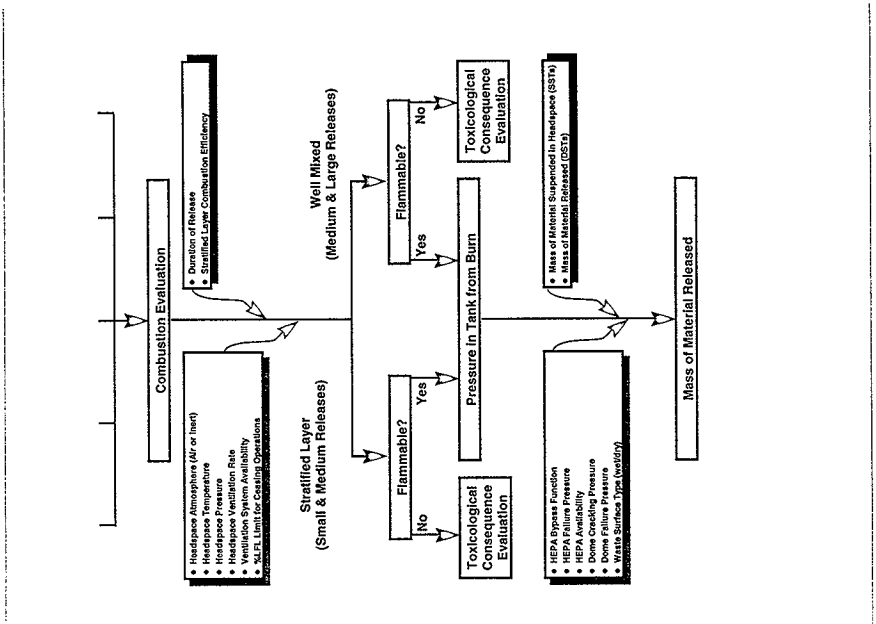
Combustion Evaluation
Duration of Release
Stratified Layer Combustion Efficiency
Headspace Atmosphere (Air or Inert)
Headspace Temperature
Headspace Pressure
Headspace Ventilation Rate
Ventilation System Availability
%LFL Limit for Ceasing Operations
Well Mixed
(Medium & Large Releases)
Stratified Layer
(Small & Medium Releases)
Flammable?
Yes
No
Toxicological Consequence Evaluation
Pressure in Tank from Burn
Flammable?
Yes
No
Toxicological Consequence Evaluation
Mass of Material Suspended in Headspace (S3Th)
Mass of Material Released (DS3Th)
HEPA Bypass Function
HEPA Failure Pressure
HEPA Availability
Dome Cracking Pressure
Dome Failure Pressure
Waste Surface Type (wet/dry)
Mass of Material Released

STATUS OF DOUBLE-SHELL TANK WASTE

Kent Hodgson

January 19, 1998

Gas Release Event Safety Analysis Workshop

Richland, Washington

Outline

- Double-Shell Tank Construction and History
- Double-Shell Tank Location
- Types of Waste in Double-Shell Tanks

Hanford High-level Waste Radioactive Underground Storage Tanks are Large

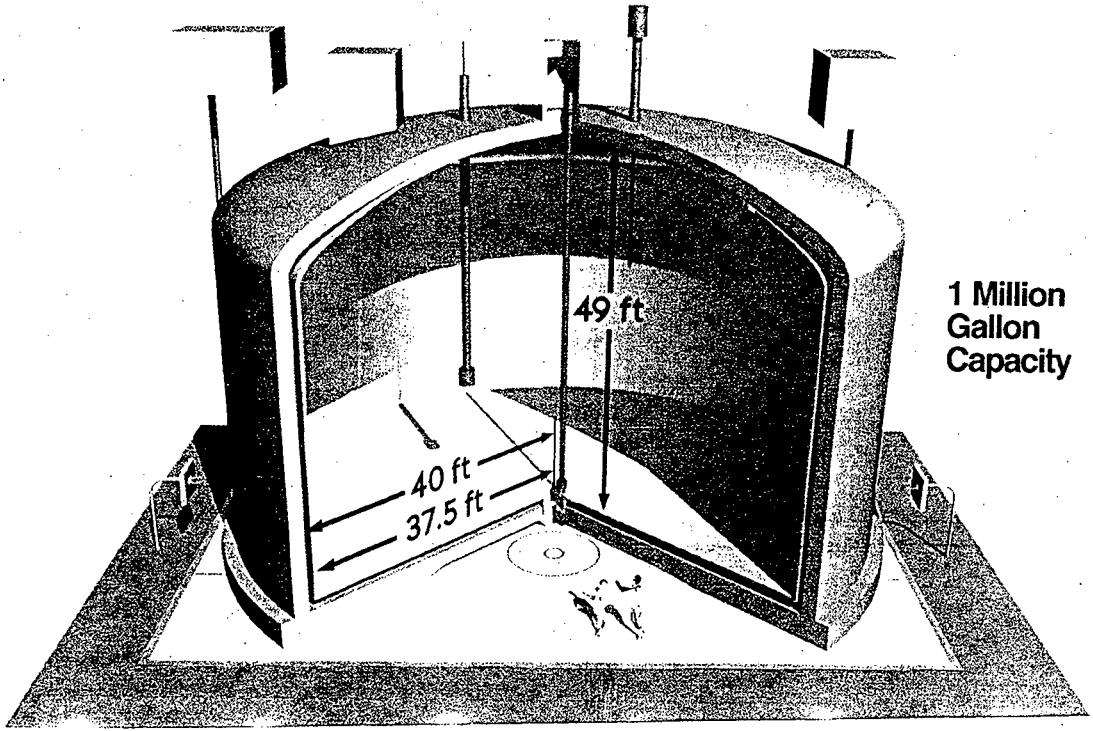

241-AY-102 Double-Shell Receiver Tank

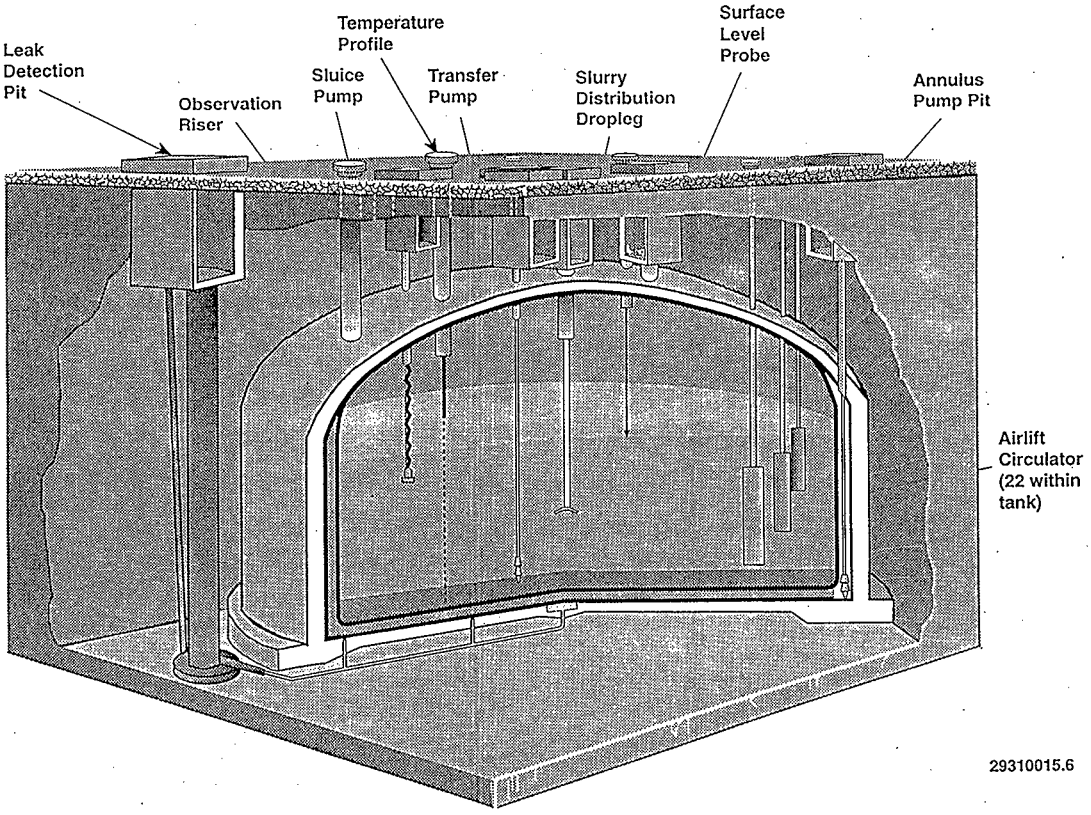

Outline

- Double-Shell Tank Construction and History
- Double-Shell Tank Location
- Types of Waste in Double-Shell Tanks

Double-Shell Tank Farm Under Construction

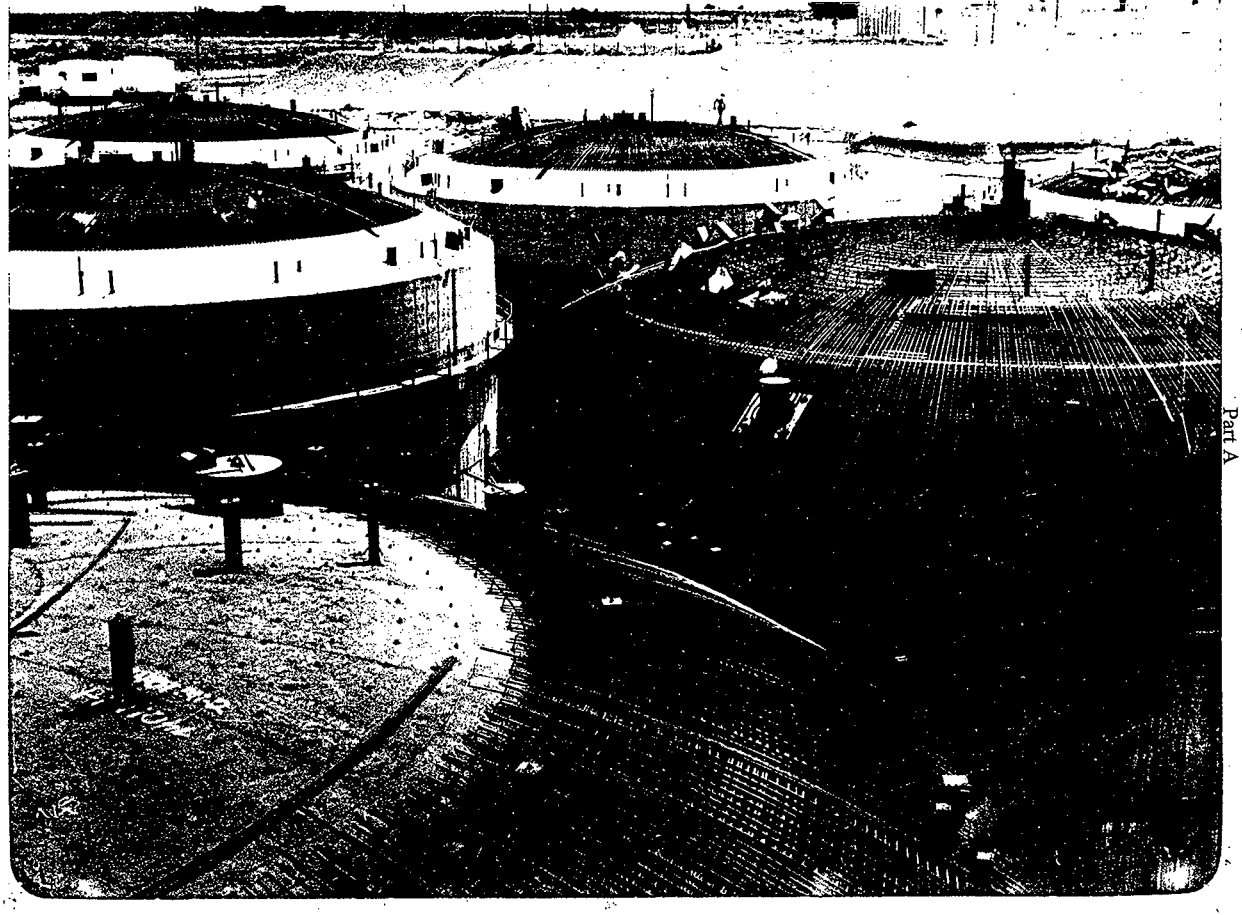

Jan Hanson

Double-Shell Tank Description

- **Construction:** 28 tanks of double-shell constructions –built between 1968 and 1986
- **Diameter:** 22.8 meters (75 feet) primary tank
  24.3 meters (80 feet) annulus tank
- **Capacity:** 3.8×10^6 liters
  (1,000,000 gallons)

C219A041191J.7

Double-Shell Tank Description (Cont)

- **Buried:** Beneath a minimum of 2.1 meters (7 feet) of soil cover
- **Located:** At least 45.5 meters (150 feet) above groundwater
- **Shell:** Reinforced concrete – 45.7 centimeters (18 inch) thick
- **Primary liner:** Carbon steel – 1.0 to 2.5 centimeters (3/8 to 1 inch) thick
- **Secondary liner:** Carbon steel – 1.0 to 1.3 centimeters (3/8 to 1/2 inch) thick

C219A041191J.8

Double-Shell Tank Description (Cont)

- **Double leachate:** 1st collection – annulus and associated pump-out system
  2nd collection – waffle grid in concrete and associated pump-out system

- **Currently storing:** Approximately 9×10^7 liters (24 million gallons) of sludge, saltcake, and liquid waste

C219A041191J.9

Double-Shell Tank Farm Generic Description

Type	Double-Shell
Constructed	1970-86
In Service	1971-86
Diameter	22.9m (75 ft)
Maximum Waste Depth	10.7m (35 ft) AY/AZ: 9.27m (30.4 ft)
Operating Capacity	4,320,000 L (1,140 kgal) AY/AX: 3,790,000 L
Bottom Shape	Flat
Ventilation	Operating Exhauster (Active)
Air lift circulators (each)	AY (22), AZ (22), AN-107(21), AW-102
Risers, total	59:AN (61:AN-101, 80:AN-107) 71:AP (72: AP-102) 59:AW 58:SY (59: SY-102)

Double-Shell Tank Farms

- 6 double-shell tank farms
  - 5 in 200 East Area
  - 1 in 200 West Area
- 28 double-shell tanks (DSTs)
  - Built between 1968 and 1986
  - In use since 1970
- No DST has leaked

C219A033192J.7

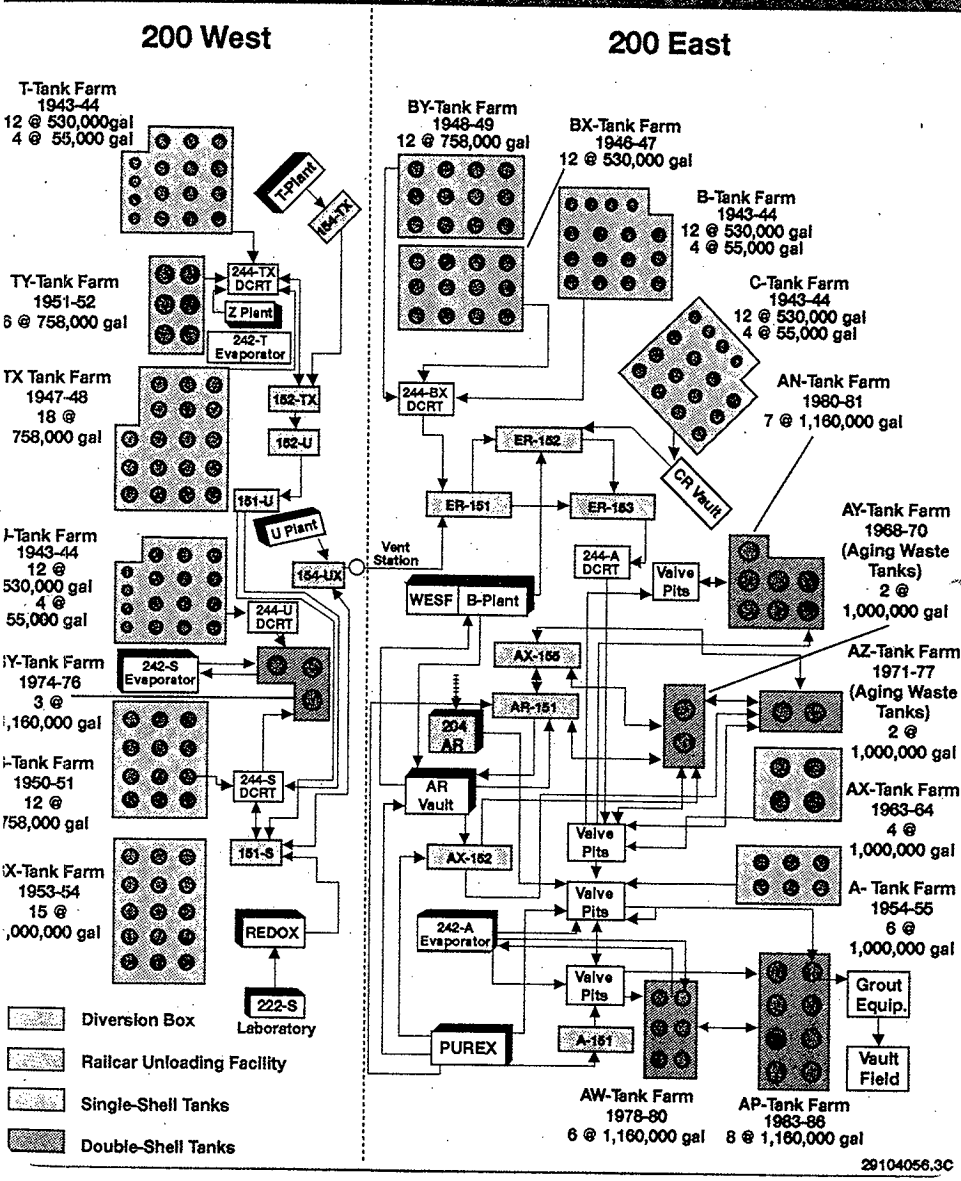
200 West
200 East
T-Tank Farm
1943-44
12 @ 530,000gal
4 @ 55,000 gal
T Plant
W-TX
TY-Tank Farm
1951-52
6 @ 758,000 gal
244-TX
DCRT
Z Plant
242-T
Evaporator
TX Tank Farm
1947-48
18 @
758,000 gal
152-TX
152-U
151-U
U Plant
I-Tank Farm
1943-44
12 @
530,000 gal
4 @
55,000 gal
154-UX
244-U
DCRT
SY-Tank Farm
1974-76
3 @
,160,000 gal
242-S
Evaporator
S-Tank Farm
1950-51
12 @
758,000 gal
244-S
DCRT
151-S
SX-Tank Farm
1953-54
15 @
,000,000 gal
REDOX
222-S
Laboratory
Diversion Box
Railcar Unloading Facility
Single-Shell Tanks
Double-Shell Tanks
BY-Tank Farm
1948-49
12 @ 758,000 gal
BX-Tank Farm
1946-47
12 @ 530,000 gal
B-Tank Farm
1943-44
12 @ 530,000 gal
4 @ 55,000 gal
C-Tank Farm
1943-44
12 @ 530,000 gal
4 @ 55,000 gal
AN-Tank Farm
1980-81
7 @ 1,160,000 gal
244-BX
DCRT
ER-152
ER-151
ER-153
CR Vault
Vent
Station
244-A
DCRT
Valve
Pits
WESF
B-Plant
AY-Tank Farm
1968-70
(Aging Waste
Tanks)
2 @
1,000,000 gal
AX-155
AR-151
AZ-Tank Farm
1971-77
(Aging Waste
Tanks)
2 @
1,000,000 gal
204
AR
AR
Vault
AX-Tank Farm
1963-64
4 @
1,000,000 gal
Valve
Pits
AX-152
A- Tank Farm
1954-55
6 @
1,000,000 gal
Valve
Pits
242-A
Evaporator
Valve
Pits
Grout
Equip.
PUREX
A-151
Vault
Field
AW-Tank Farm
1978-80
6 @ 1,160,000 gal
AP-Tank Farm
1963-86
8 @ 1,160,000 gal
29104056.3C

Ventilation Rates in DSTs

- Aging Waste Tanks - 600 cfm
  - new ventilation system - 100 cfm
- 241-SY-101 - 600 cfm
- 241-SY-102 - 400 cfm

All other DSTs approximately 100 cfm

PITS/Transfer Lines

- Diversion Boxes
  - drain to catch tanks
  - catch tanks not ventilated
- Valve Pits
  - drain to double-shell tanks or catch tanks
  - some transfers use A, AX valve pits
- Clean-out Boxes
  - flush slurry lines either direction
- Limited instrumentation - leak detectors
  - leak detectors being replaced

FUTURE DOUBLE-SHELL TANK OPERATIONS

Kent Hodgson

January 19, 1998

Gas Release Event Safety Analysis Workshop

Richland, Washington

Outline

- Waste Receipts
- Saltwell Pumping
- Evaporator Operation
- Feed Delivery for Disposal Vendors

Projected Miscellaneous Waste Generations

- 300 Area - 50 Kgal/year
- 400 Area - 7 Kgal/every third year
- S Plant - 25 Kgal/year
- T Plant - 17-32 Kgal/year
- Tank Farms - 120 Kgal/year
- PUREX - 5 Kgal/year

Projected Terminal Cleanout Waste

- B Plant - 200 Kgal (FY 1997-1998)
- PFP - 34 Kgal (FY 1997-2006)
- 100 N - 13.5 Kgal (FY 1997 on)
- 100 F & H - 240 Kgal (FY 2000-2005)
- 100 K - 350 Kgal (FY 2000-2001)

IMUST Wastes - 500 Kgal (FY 2011-2015)

Projected Saltwell Liquid Pumping Volumes (Kgal/Year) (Draft based on data received 9/97)

Fiscal Year	200 East Area		200 West Area		Total
	DN	DC	DN	DC	
1998	28	203	140	0	371
1999	324	277	318	0	919
2000	33	331	1084	37	1485
2001	0	85	1245	48	1378
2002	0	16	226	604	846
2003	0	0	0	158	158
Total	385	912	3013	847	5157

Projected Evaporator Operations:

- Dilute wastes evaporated to DSSF
- Evaporation Limit, Specific Gravity - 1.41
- Evaporator feed tank - Tank 102-AW
- Evaporator receiver tank - Tank 106-AW

Feed Delivery for Disposal Vendors

Privatization Approach

Competitive, fixed price procurement for delivering immobilized waste meeting DOE's performance specifications

- *Phase I*: Waste treatment and immobilization demonstration, ~6 - 13% of waste
  - Low-level fraction plus option for high-level waste fraction
  - Three preliminary design contracts; 2 vendors selected to design, construct, and operate two competitive facilities
  - Schedule:

- Select two vendors	1998
- Hot startup	2002
- Complete demonstration phase	2011
- Complete D&D/RCRA Closure	2013

BTF121092.20

Privatization Approach (cont)

- *Phase II*: Waste retrieval, treatment and immobilization production, ~87 - 94% of waste

  – All remaining tank waste plus potentially cesium and strontium capsules

  – Two vendors selected to design, construct, and operate two competitive facilities

  – Schedule:

- Select two vendors	2005
- Hot startup	2011
- Complete SST retrieval	2018
- Complete immobilization	2028

BTF121092.21

Privatization Concept

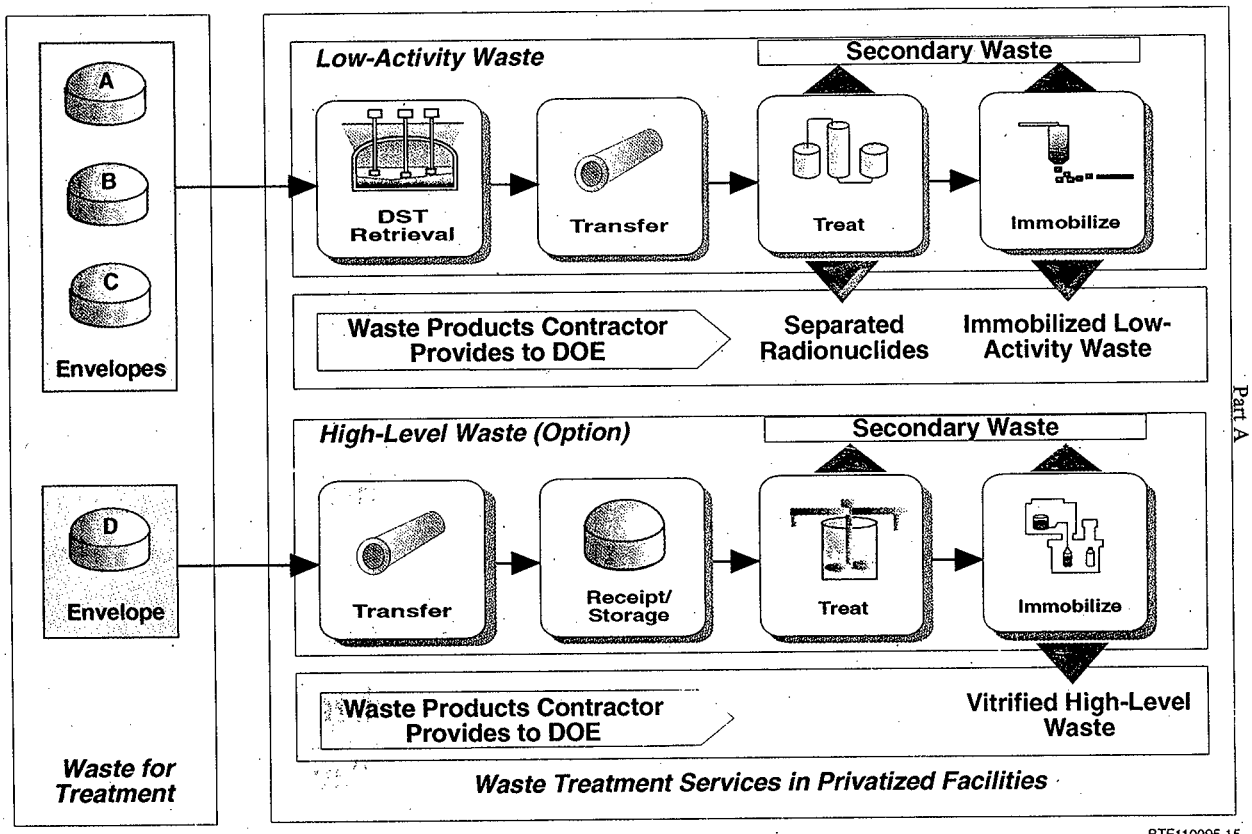

BTF110095.15

Privatization Waste Feed Envelopes

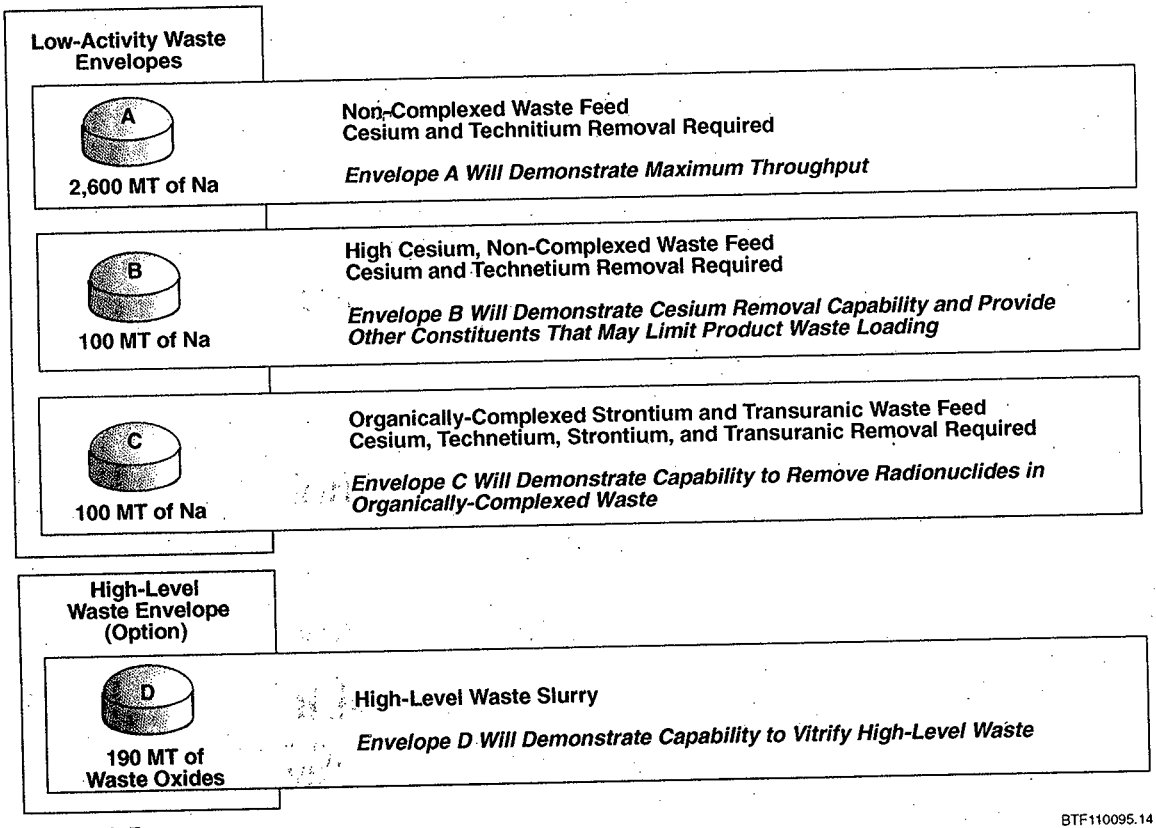

*MT - Metric Ton

BTF110095.14

Summary of Phase I Feed Delivery Schedule

Envelope	Feed Source	Batch Date
A	241-AN-105	12/2001
	241-AN-104	1/2003
	241-AW-101	10/2003
	241-AN-103	5/2004
	241-AP-101	3/2005
	241-AW-104	3/2005
B	241-AZ-101	3/2005
	241-AZ-102	
C	241-AN-107	1/2006
	241-AN-102	3/2006
	241-AN-106	8/2007
	241-SY-101	4/2007
	241-SY-103	11/2007

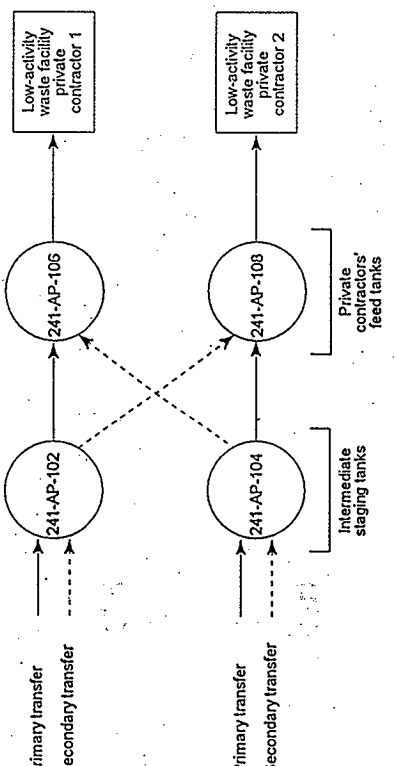

Figure 3.1-1. Feed Staging Strategy.

Figure A-4. Retrieval Model Configuration (2003 to 2007).

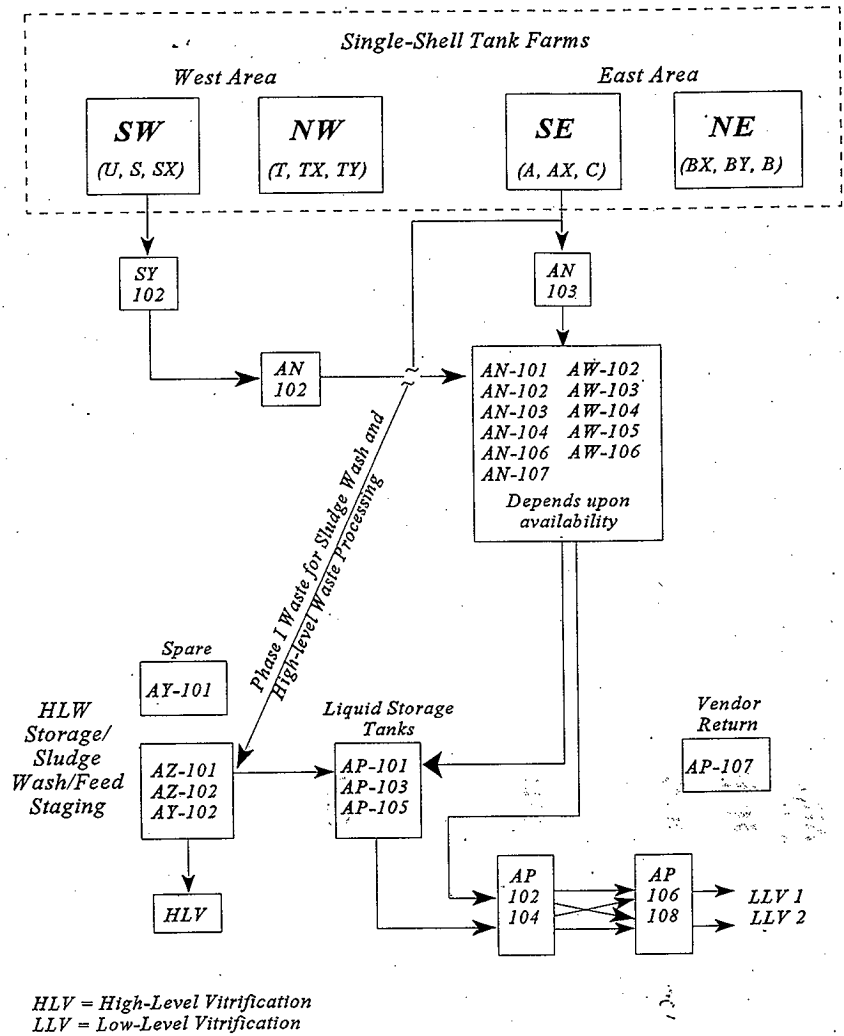

Figure A-3. Retrieval Model Configuration (2007 to end).

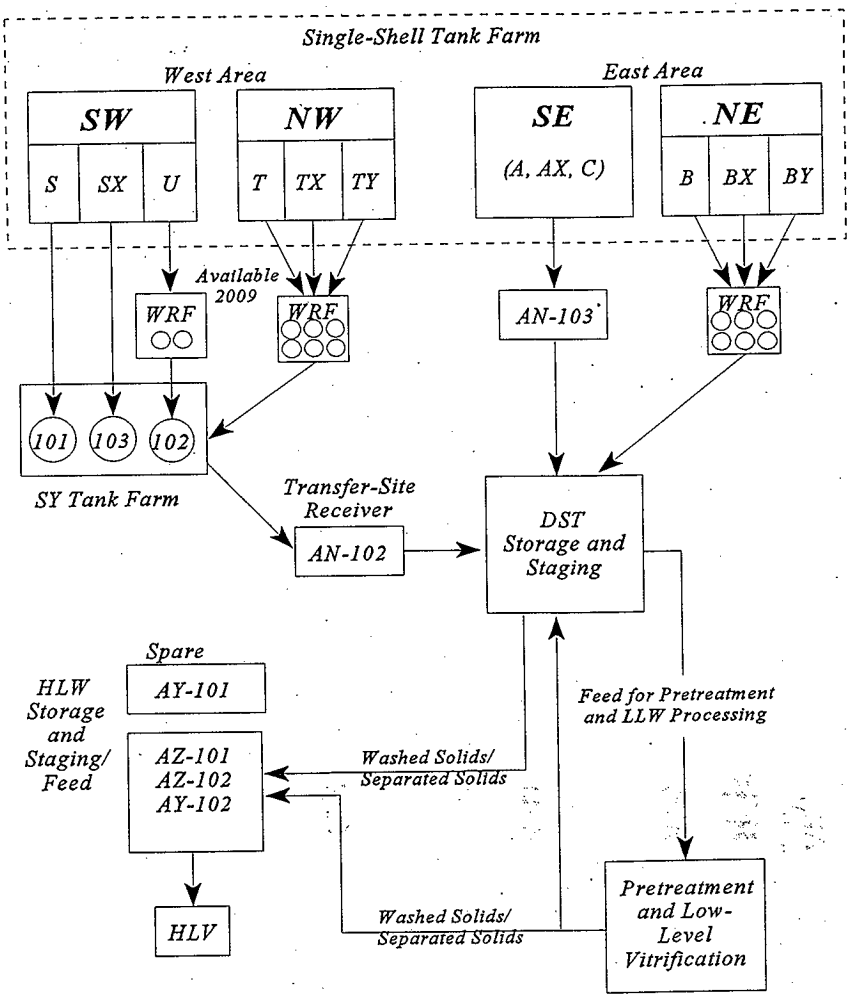

HLV = High-Level Vitrification
LLW = Low-Level Waste

Penwell\Phase 2.WPG

Key Feed Delivery Assumptions

- Resulting specific gravity must be $\leq$ 1.40
- Maximum of 5 volume % settled solids in feed transferred to private contractors
- Solids in LAW feed provided to vendors will be returned to Tank Farms (241-AP-107)
- LAW vendors will return separated radionuclides
- Prior to sludge pretreatment, the AZ Tank Farms tank are in-tank evaporated to 5M Na
- High level waste transfers maximum feed concentration 100g non volatile oxides/L

Key Feed Delivery Assumptions (cont.)

- Phase I high level waste settling and analytical time approximately 60 days
- Final high level waste sludge approximately 25 wt. %
- SST level waste retrieval by sluicing to achieve 5M Na or 10 wt. % solids
- Out-of-Tank sludge washing is assumed for Phase II processing
- Retrieved Phase II waste slurries are on the average 3 wt. % solids
- Retrieved SST slurries maybe stored in DST for up to 7 years
  - 5 M Na, 10 wt. % solids

Refined Safety Analysis Methodology for
Flammable Gas Risk Assessment in Hanford Site Tanks

Introduction to Proposed Analysis Framework for DSTs

January 19, 1998

Scott Slezak

WS1–SS–1/19/98-B
slide 1

Outline

- Additional analysis framework models.
- Conditioning cases for parameters previously quantified for SSTs.
- Additional parameters unique to buoyant displacement GRE analyses.
- Other items requiring panel decisions.

WS1–SS–1/19/98-B
slide 2

Key Assumptions

- Waste layers: buoyant "crust", convective liquid, potentially mobile "nonconvective" solids, stationary "hardpan".
- Large scale of tank, creep flow, weak tensile strength all contribute to make $\alpha_{crit} \approx \alpha_{nb}$.
- Crust is marginally buoyant, $\rho_{crust} \approx \rho_{liquid}$.
- When degassed, crust and nonconvective layer have same density, $\rho_{crust,ng} \approx \rho_{nc,ng}$.

WS1–SS–1/19/98-B
slide 3

Waste Configuration of Model

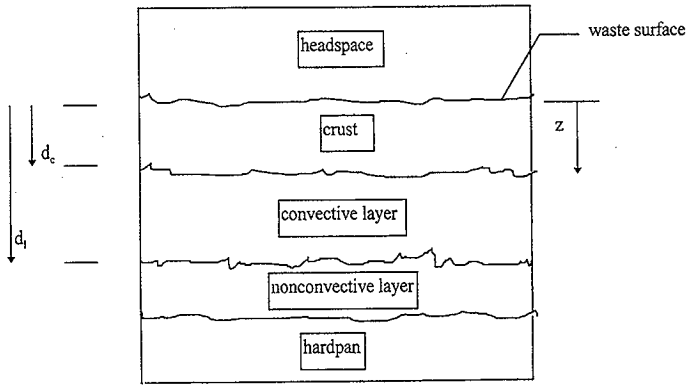

WS1–SS–1/19/98-B
slide 4

Analytical Frame of Reference

- Analytical expressions are derived in terms of masslength z, which is related to the physical length y by

$$y = \int (M_z/\rho_z)\, dz$$

- At fixed depth z the pressure is constant as the retained gas void fraction changes.
- As void fraction $\alpha \rightarrow 0$, $z \rightarrow y$.
- Deriving expressions in terms of masslength greatly simplifies mathematical expressions.

WS1–SS–1/19/98-B
slide 5

Governing Equation

$$\dot{g}_{uc,nc}(1 - \alpha_{t,z}) f_{ret} = \frac{\dot{\alpha}_{t,z}}{RT}(p_{c1} + \rho_{nc} g z) \qquad \text{(Eq. 40)}$$

- 1-D analysis (horizontally uniform waste).
- p_{c1} and $\dot{g}_{uc,nc}$ constant in time and position.
- p_{c1} is pressure contribution from atmosphere and weight of crust and convective layer.
- $\dot{g}_{uc,nc}$ is molar gas generation rate per unit volume of degassed nonconvective layer.
- f_{ret} is gas retention factor.

WS1–SS–1/19/98-B
slide 6

Governing Equation (2)

- f_{ret} is potentially a function of void fraction α, shear strength τ, viscosity μ, densities ρ_{nc}, ρ_l, pressure p, and other parameters.
- When a functional form for f_{ret} is specified, the governing equation can be numerically solved for void fraction as a function of time and depth.
- Conservative default is f_{ret} = 100% = constant.
- Simple example $f_{ret} = a + b\alpha$ in document because analytical solution possible; *Resolve!* to compute numerical solution for more complex forms.

WS1–SS–1/19/98-B
slide 7

Moles of Gas Released by BD GRE

- If waste only releases enough gas to return to neutral buoyancy at surface of waste:

$$N_{usg,roll} = \frac{A_{rel}\alpha_{nb}}{RT}\frac{\rho_l g}{2}(z^2 - d_l^2) \qquad \text{(Eq. 56)}$$

- Within assumptions, moles of gas released from 100% efficient BD GRE involving nonconvective layer to depth z is:

$$N_{usg,100\%} = \frac{A_{rel}\alpha_{nb}}{RT} p_h (z - d_l) + N_{usg,roll} \qquad (\approx \text{Eq. 53})$$

WS1–SS–1/19/98-B
slide 8

Moles of Gas Released by BD GRE (2)

- If nonconvective layer lifts straight vertically without rollover and releases just enough gas to return to neutral buoyancy:

$$N_{usg,lift} = \frac{A_{rel}\alpha_{nb}\rho_l g}{RT}\left(z(d_l - d_c) + d_l d_c - d_l^2\right) \quad \text{(Eq. 59)}$$

- Weighted average of rollover and lift results, with weighting factor n:

$$N_{usg,wavg} = \left[\frac{z - d_l}{z}\right]^n N_{usg,lift} + \left(1 - \left[\frac{z - d_l}{z}\right]^n\right) N_{usg,roll}$$

(≈Eq. 62)

WS1–SS–1/19/98-B
slide 9

Moles of Gas Released by BD GRE (3)

- In complete detail:

$$N_{usg,wavg} = \frac{A_{rel}\alpha_{nb}}{RT}\frac{\rho_l g}{2} G \quad \text{(Eq. 64)}$$

$$G = \left(z^2 - d_l^2 - \left[\frac{(z - d_l)}{z}\right]^n \left\{2z(d_l - d_c) + 2d_l d_c - z^2 - d_l^2\right\}\right)$$

- Group G is a release efficiency-type term between 0 and 1 that varies as the ratio of convective liquid to nonconvective solids changes.

WS1–SS–1/19/98-B
slide 10

Effect of Liquid Depth on N_{usg}

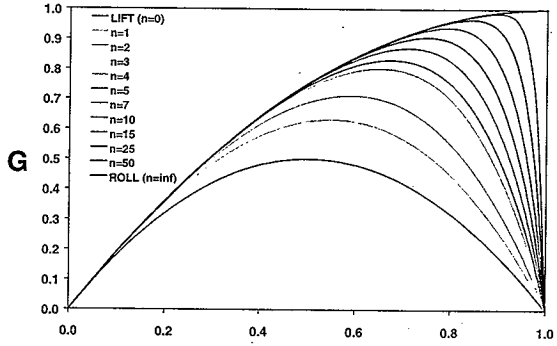

WS1–SS–1/19/98-B
slide 11

Observed BD GRE Trend

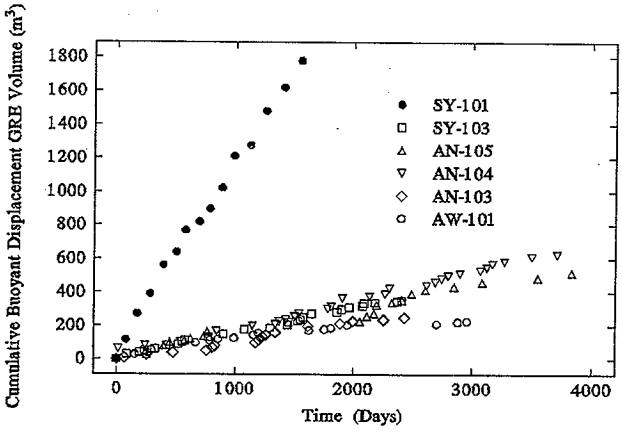

WS1–SS–1/19/98-B
slide 12

Spontaneous BD GRE Size

- From Rayleigh-Taylor stability analysis, characteristic size of nonconvective layer material involved in GRE is:

$$D_o = 5\sqrt{\frac{\mu_b^2}{\rho_l \bar{\tau}}}$$

μ_b is bulk viscosity of nc layer, ρ_l is liquid density, $\bar{\tau}$ is nc layer yield stress

- Depth of nc waste participating in GRE, z_{rel}, is minimum of $(d_l + D_o)$ and d_{nc}.

WS1–SS–1/19/98-B
slide 13

Spontaneous BD GRE Key Equations

- Number of moles of gas released:

$$N_{usg,rel} = \frac{\pi D_o^2 \alpha_{nb}}{4RT}\frac{\rho_l g}{2}\left(z_{rel}^2 - d_l^2 - \left[\frac{z_{rel}-d_l}{z_{rel}}\right]^n\left\{2z_{rel}(d_l - d_c) + 2d_l d_c - z_{rel}^2 - d_l^2\right\}\right)$$

(Eq. 70)

- Period between releases:

$$P_{rel} = \frac{(D_o/D_{tank})^2}{\dot{g}_{nc}(d_{nc}-d_l)}\frac{\alpha_{nb}}{RT}\frac{\rho_l g}{2}\left(z_{rel}^2 - d_l^2 - \left[\frac{z_{rel}-d_l}{z_{rel}}\right]^n\left\{2z_{rel}(d_l - d_c) + 2d_l d_c - z_{rel}^2 - d_l^2\right\}\right)$$

(Eq. 71)

- Shorthand notation:

$$N_{usg,rel} = \frac{\pi D_o^2 \alpha_{nb}}{4RT}\frac{\rho_l g}{2}G \qquad P_{rel} = \frac{(D_o/D_{tank})^2}{\dot{g}_{nc}(d_{nc}-d_l)}\frac{\alpha_{nb}}{RT}\frac{\rho_l g}{2}G$$

WS1–SS–1/19/98-B
slide 14

Computed Uncertainty Distributions

- Data from Meyer, et al. (1997) Table 4.2.2 used.
- Error estimates assumed $\pm 2\sigma$ values for normal error distribution.
- Crystal Ball® used to compute uncertainty distributions for $N_{usg,rel}$ and P_{rel} for FG1 tanks.
- n = 5 in all calculations; lowest value for good fit of available data; no data to know if a larger value is better description as $(z - d_l)/z \rightarrow 1$.
- Distributions are direct consequence of uncertainty in input data; no elicitation required.

WS1–SS–1/19/98-B

slide 15

Table 4.2.2. Properties and Parameters Used in Models

Property/Parameter	AN-103	AN-104	AN-105	AW-101	SY-101	SY-103
Densities (kg/m³)						
1. Convective Layer	1530 ± 50	1440 ± 30	1430 ± 30	1430 ± 30	1500 ± 70	1470 ± 30
2. Nonconvective Layer	1730 ± 110	1590 ± 60	1590 ± 40	1570 ± 30	1700 ± 50	1570 ± 50
Layer Thickness (cm)						
3. Waste Level	884 ± 5	979 ± 4	1041 ± 7	1040 ± 7	1054 ± 10	691 ± 3
4. Convective Layer	413 ± 16	524 ± 10	559 ± 11	693 ± 19	470 ± 8	337 ± 19
5. Nonconvective Layer	379 ± 9	415 ± 9	452 ± 11	283 ± 22	584 ± 40	334 ± 25
6. Stationary Layer	192 ± 35	69 ± 45	57 ± 55	57 ± 47	0	103 ± 20
7. Eff. Nonconvective Layer	187 ± 36	345 ± 10	395 ± 56	225 ± 52	584 ± 40	231 ± 25
Void Fractions (%)						
8. Neutral Buoyancy	12 ± 6	9 ± 4	10 ± 3	9 ± 3	12 ± 5	6 ± 4
9. Nonconvective Layer Avg.	10.7±1.0	6.2±0.9	4.2±0.8	3.8±0.6	~8	6±2
Pressure Ratio						
10. Nonconvective Layer	1.87±0.03	1.97±0.03	2.09±0.04	2.11±0.04	2.30±0.10	1.69±0.05
Nonconvective Layer Rheology						
11. Yield Stress (Pa) $\vec{\tau}$	142 ± 15	81 ± 11	129 ± 31	159 ± 37	225 ± 100	112 ± 40
12. Viscosity (Pa-s) μ_b	12,600 ± 1400	7,600 ± 650	11,600 ± 2,800	14,000 ± 3500	20,500 ± 10.000	10,400 ± 3900
Historical GRE Data						
13. Std. Rel. Volume (m³)	14 ± 4	23 ± 16	26 ± 11	14 ± 10	131 ± 47	13 ± 6
14. Period (days)	160 ± 120	120 ± 90	160 ± 130	190 ± 190	100 ± 24	90 ± 70
15. Level Rise (cm/day)	0.04±0.02	0.03±0.01	0.03±0.02	0.03±0.004	0.24±0.06	0.05±0.03

WS1–SS–1/19/98-B

slide 16

*****

Crystal Ball is a registered trademark of Decisioneering, Inc.

Table 3.
Buoyant displacement model parameters
for tanks with observed GRE behavior.

Input Values (± 2σ)						
Parameter	AN-103	AN-104	AN-105	AW-101	SY-101	SY-103
ρ_l, convective layer density, kg/m^3	1530 ± 50	1440 ± 30	1430 ± 30	1430 ± 30	1450 ± 70[1]	1400 ± 30[2]
ρ_b, nonconvective layer bulk (degassed) density, kg/m^3	1730 ± 110	1590 ± 60	1590 ± 40	1570 ± 30	1700 ± 50	1570 ± 50
H, total depth, m	8.84 ± 0.05	9.79 ± 0.04	10.41 ± 0.07	10.40 ± 0.07	10.54 ± 0.10	6.91 ± 0.03
d_c, crust thickness, m	0.92 ± 0.08[3]	0.00 ± 0.00[3]	0.75 ± 0.25[3]	0.63 ± 0.13[3]	1.27 ± 0.25[4]	0.0 ± 0.0[2]
d_l, depth to top of nc layer, m	5.05 ± 0.10	5.64 ± 0.10	5.89 ± 0.13	7.57 ± 0.23	4.70 ± 0.41	3.57 ± 0.25
d_{nc}, depth to top of hardpan, m	6.92 ± 0.35	9.10 ± 0.45	9.84 ± 0.55	9.83 ± 0.48	0.00 ± 0.00	5.88 ± 0.20
τ, yield stress, Pa	142 ± 15	81 ± 11	129 ± 31	159 ± 37	225 ± 100	112 ± 40
μ_b, absolute viscosity of nc layer, Pa-s[5]	970 ± 108	585 ± 50	893 ± 216	1078 ± 270	1579 ± 770	801 ± 300
$g_{nc,\,total}$, gas generation rate, mole/m^3-s	6.37E-8	6.71E-8	4.29E-8	5.88E-8	2.47E-7	7.98E-8

Slide 17

Frequency Distribution, V_{rel} for SY-101

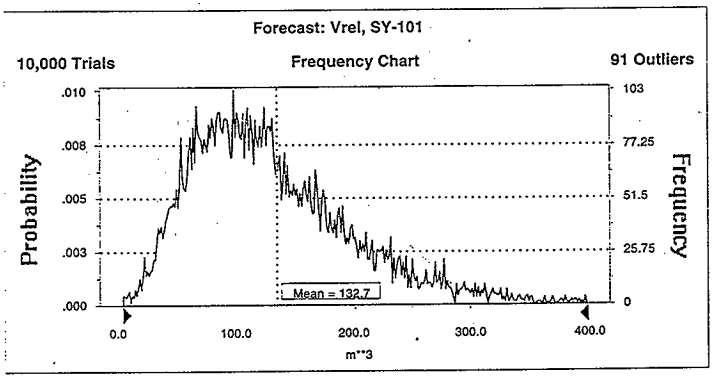

WS1–SS–1/19/98-B
slide 18

Frequency Distribution, P_{rel} for SY-101

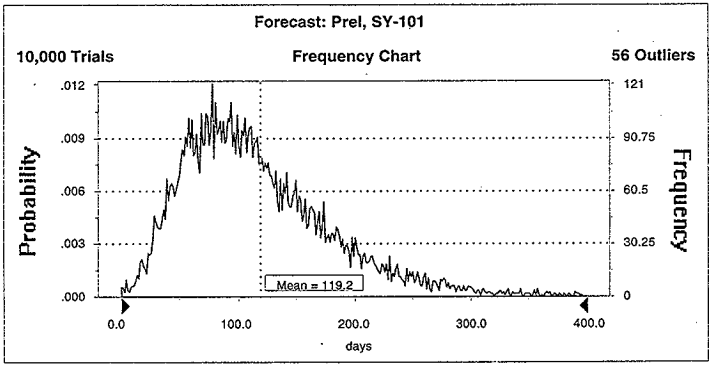

WS1–SS–1/19/98-B
slide 19

Cumulative Probability Distribution V_{rel} for SY-101

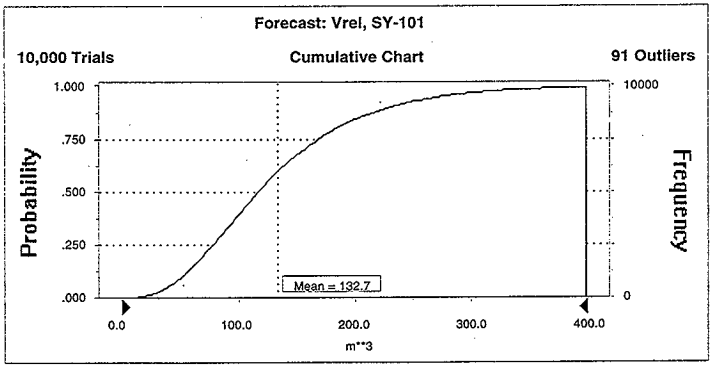

WS1–SS–1/19/98-B
slide 20

Cumulative Probability Distribution P_{rel} for SY-101

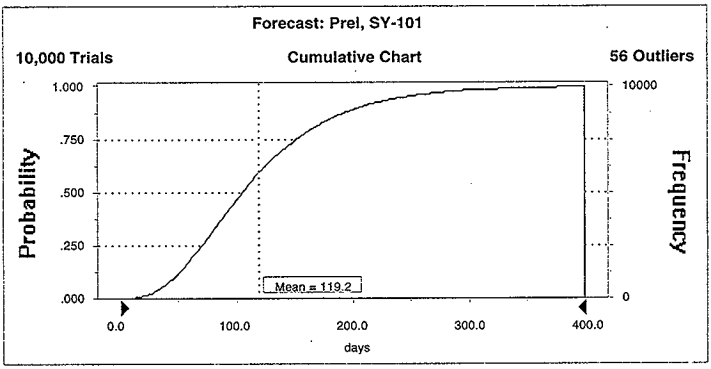

WS1–SS–1/19/98-B
slide 21

Cumulative Probability Distribution V_{rel} for AN-103

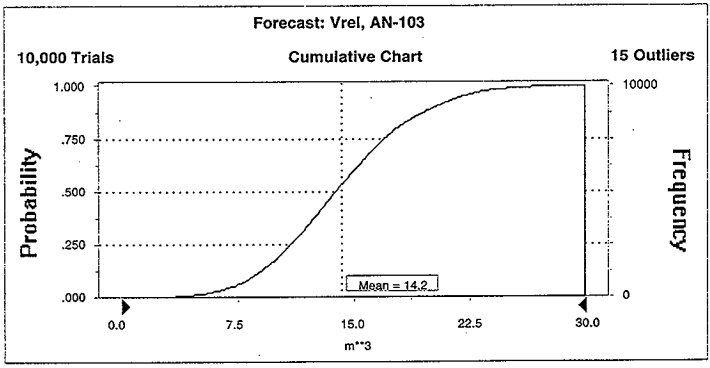

WS1–SS–1/19/98-B
slide 22

Cumulative Probability Distribution P_{rel} for AN-103

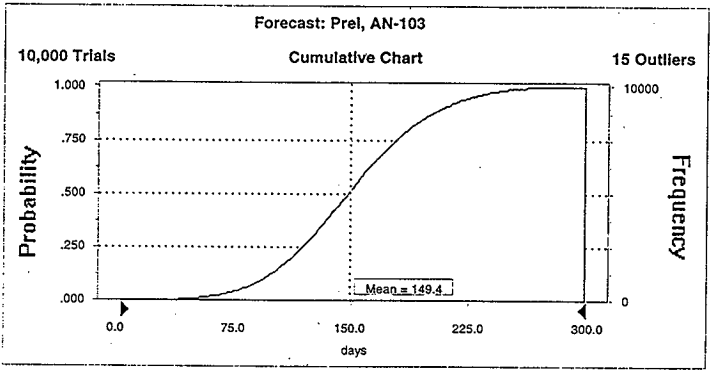

WS1–SS–1/19/98-B

slide 23

Output Values (± 1σ)						
Parameter	AN-103	AN-104	AN-105	AW-101	SY-101	SY-103
V_{rel}, median release volume, Eqn. (70), m^3	14.2	16.7	32.2	21.2	118.3	11.5
V_{rel}, mean release volume, m^3	14.2 ± 4.6	16.4 ± 4.6	31.6 ± 11	20.8 ± 8.0	133 ± 79	12.2 ± 5.6
$V_{rel, avg}$, historical, m^3	14 ± 4	23 ± 16	26 ± 11	14 ± 10	131 ± 47	13 ± 6
P_{rel}, median period between releases, Eqn. (71), days	149.7	90.4	238.8	200.5	106.3	77.7
P_{rel}, mean period, days	150 ± 46	90 ± 22	234 ± 77	205 ± 65	119 ± 70	83 ± 38
$P_{rel, avg}$, historical, days	160 ± 120	120 ± 90	160 ± 130	220 ± 230	100 ± 24	90 ± 70
$V_{rel, avg}/V_{head}$, %	1.01	1.66	4.28	2.80	16.90	0.52
~%LFL	16	20	66	22	122	7

1 - Value estimated from [Anantatmula, 1992]
2 - Value from [Shephard, et al., 1995]
3 - Value from [Shekarriz, et al., 1997]
4 - Value inferred from [Antoniak, 1993]
5 - Values reported in Table 4.2.2 of [Meyer, et al., 1997] are relative viscosity. On page 4.34 of that report it is noted that best estimate absolute values are determined by multiplying the relative viscosity values by 0.077.

Slide 24

Limit to Void Growth

- Waste cannot retain 100% of generated gas indefinitely; when α gets large enough, some gas can migrate out of nonconvective layer by mechanisms other than buoyant displacement.
- With conservative default of $f_{ret} = 1$, equations always predict non-zero values for period and amount released in BD GREs.
- BD GREs have never been observed in some tanks known to retain gas.
- A clear criteria is needed for when BD GREs are not significant contributors to risk.

WS1–SS–1/19/98-B
slide 25

Limit to Void Growth (2)

- Two methods proposed for determining when the void fraction remains too small for BD GREs.
  - Panel provides uncertainty distributions for maximum α. When $\alpha_{max} < \alpha_{nb}$, BD GREs precluded. Results used for default case of $f_{ret} = 1$.
  - Hanford team provides (and independently justifies) functional relation for f_{ret}. Solution to governing equation determines α_{max}, but uncertainty distribution for α_{max} may be used to establish exact form of f_{ret}.
- In DST AF paper, α_{max} included in example relation for f_{ret}.

WS1–SS–1/19/98-B
slide 26

Void Growth: f_{ret} linear in α vs. $f_{ret} = 1$

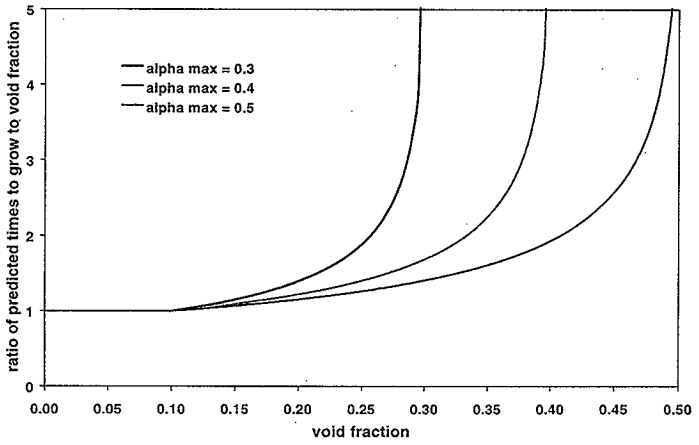

WS1–SS–1/19/98-B

slide 27

Determining Release Efficiency

- With f_{ret} specified, from governing equation compute value of α_o at depth z_{rel} such that the time to grow from α_o to α_{nb} is equal to P_{rel}.
- Local release efficiency is $(\alpha_{nb} - \alpha_o)/\alpha_{nb}$.
- Global average inventory of gas is:

$$N_{usg,nc} \cong \frac{A_{tank}(\alpha_{nb} + \alpha_{o,z_{rel}})}{2RT}\left(p_h(d_{nc} - d_l) + \frac{\rho_l g}{2}(d_{nc}^2 - d_l^2)\right)$$

- Global release efficiency is computed from $N_{usg,\,rel}$ / $N_{usg,\,nc}$; no elicitation required.

WS1–SS–1/19/98-B

slide 28

Void Fraction Change During Transfers

- As supernate pumped in/out of tank, hydrostatic pressure on retained gas increases/decreases.
- In receiver tank:
  - α decreases as liquid added, so probability of BD GRE decreases as transfer progresses.
  - at start of transfer, liquid addition is globally waste-disturbing event at maximum potential for BD GRE.
- In source tank α increases as liquid removed, so probability of BD GRE increases as transfer progresses.

WS1–SS–1/19/98-B
slide 29

Governing Equation for Transfers

$$\dot{g}_{uc,nc}(1-\alpha_{t,z})f_{ret} = C_6\alpha_{t,z} + (C_5 + C_6 t)\dot{\alpha}_{t,z}$$

(≈Eq. 85,89)

$$C_5 = \frac{p_h + \rho_l g d_{l,t=0} + \rho_{nc} g (z_{t=0} - d_{l,t=0})}{RT} \qquad \text{(Eq. 86)}$$

- For source tank: $C_{6,src} = -\frac{4\rho_l g R_p}{\pi R T D^2_{src\ tank}}$ (Eq. 87)
- For receiver tank: $C_{6,rcv} = \frac{4\rho_l g R_p}{\pi R T D^2_{rcv\ tank}}$ (Eq. 90)

WS1–SS–1/19/98-B
slide 30

Transfer-induced BD GREs

- For conservative case of $f_{ret} = 1$, α as function of time from start of pumping and initial depth z given by Eq. (92) with a = b = 0.
- From growth/shrinkage of α with time, can compute expected number of releases, and amount of gas in each, during pumping.
- As for spontaneous releases, uncertainty in ρ_l, ρ_{nc}, μ_b, $\bar{\tau}$, d_{nc}, etc. all contribute to generate uncertainty distribution for number and amount of BD releases induced by transfers; no elicitation required.

WS1–SS–1/19/98-B
slide 31

Local/Global Waste Disturbing Ops

- Probability that waste-disturbing activity initiates a BD GRE given by:

$$p_{rel} = p_{rel,last\ GRE}\ p_{dist\ last\ GRE} + p_{rel,rest}\ p_{dist\ rest}$$

  - $p_{rel,last\ GRE}$ = probability region of last GRE can undergo another GRE
  - $p_{dist\ last\ GRE}$ = probability that disturbed region was involved in last GRE
  - $p_{rel,rest}$ = probability that region not involved in last GRE can undergo another GRE
  - $p_{dist\ rest}$ = probability that disturbed region was not involved in last GRE

WS1–SS–1/19/98-B
slide 32

Local/Global Waste Disturbing Ops (2)

- Number of moles released by induced GRE is:

$$N_{rel,dist} = N_{rel,last\ GRE}\ p_{dist\ last\ GRE} + N_{rel,rest}\ p_{dist\ rest}$$

  - $N_{rel,last\ GRE}$ = number of moles expected to be released by waste involved in last GRE
  - $N_{rel,rest}$ = number of moles expected to be released by waste not involved in last GRE
- Probabilities and expected moles of release all computable from Eqns. 69, 70, 71 and solution to Eqn. 40.
- Uncertainty distributions computed based on uncertainty in data values; no elicitation required.

WS1–SS–1/19/98-B

slide 33

Steady-State Release Rate

- Volumetric gas generation rate specified in database or by software user is used to compute uncertainty distribution for frequency of BD GRE.
- Same data used to compute steady-state release rate from crust and convective liquid layers.
- Steady-state release rate and ventilation rates used to compute initial headspace concentration at start of BD GRE and change in headspace concentration with time if active ventilation stops.
- Could back-fit to SSTs to check that frequency x release amount does not exceed total generation.

WS1–SS–1/19/98-B

slide 34

Active Control of GREs

- Mixer pumps, gas or water lances, potential mixer paddles, ALCs, etc., all aim to control BD GREs by disrupting waste and "freeing" retained gas.
- From Eq. (40) can compute local void growth.
- Volume disrupted is engineering design criteria.
- Local efficiency of release is uncertain; initial void fraction after disrupting waste needed to evaluate efficacy of active control methods, time to next expected spontaneous BD GRE, amount of residual gas, etc. (I.e., uncertainty distributions for N_{rel} and P_{rel}.)

WS1–SS–1/19/98-B
slide 35

Ammonia Releases From BD GREs

- Ammonia is released from solution as well as from undissolved gas during a GRE.

$$q_{NH3} = h_l A (m_{NH3} - m^*_{NH3}) + N_{rel,GRE} X_{NH3} / \tau_{GRE} \qquad (\approx pg.\ 76)$$

- Mass transfer coefficient from liquid is function of diffusivity in liquid and surface renewal rate:

$$h_l = (D/\tau_{renew})^{0.5}$$

- Have data for dissolved NH_3 concentration, m_{NH3}.
- Effective area for release and surface renewal time are uncertain--panel to provide distributions or prescription for quantifying.

WS1–SS–1/19/98-B
slide 36

Outline

- Additional analysis framework models.
- **Conditioning cases for parameters previously quantified for SSTs.**
- Additional parameters unique to buoyant displacement GRE analyses.
- Other items requiring panel decisions.

WS1–SS–1/19/98-B
slide 37

Current Parameters for SST Analysis Framework			
No.	Parameter Description	Conditioning Factors	Changes from AF for SSTs required to apply parameter to DSTs
1	Void fraction of retained gases in waste	Facility Group, pumping status	none; not used for bd GREs in DSTs
2 & 5	Frequency of spontaneous GREs (by mechanisms other than buoyant displacement)	GRE release efficiency, Facility Group, pumping status	none; frequency of spontaneous bd GREs computed separately
3	Transition factor for plume to well-mixed burn behavior	no conditioning factors	none; applies to both SSTs & DSTs
4	Combustion efficiency ratio for stratified layer plume combustion	headspace inerted or with air	none; applies to both SSTs & DSTs
6	Probability of non-buoyant displacement GREs induced by locally waste-disturbing operations	GRE release efficiency, Facility Group	none; probability of bd GREs induced by locally waste-disturbing ops computed separately
7	Probability of GREs induced by globally waste-disturbing operations	GRE release efficiency, Facility Group	none; probability of bd GREs induced by globally waste-disturbing ops computed separately
8	Frequency of random ignition sources (unaffected by controls)	Lightning excluded	none; applies to both SSTs & DSTs

Slide 38

No.	Parameter Description	Conditioning Factors	Changes from AF for SSTs required to apply parameter to DSTs
9	Frequency of ignition sources during pumping operations	ignition control set 1, ignition control set 2, past practices	none; applies to both SSTs & DSTs
11	Probability of ignition source during equipment installation or removal	ignition control set 1, ignition control set 2, past practices	none; applies to both SSTs & DSTs
12	Probability of ignition source during short operation of general equipment	ignition control set 1, ignition control set 2, past practices	none; applies to both SSTs & DSTs
13	Probability of GRE-induced ignition source	Facility Group, GRE release efficiency	revisit; condition of bd GRE may be added
14	Mass of material aerosolized in the headspace by a headspace burn	Burn too weak to crack dome, dome cracks, dome collapses	revisit; condition of GRE w/o burn may be added
15	Fraction of parameter 14 that is respirable	Burn either too weak to crack dome, or dome cracks, or dome collapses	none; data to be used to quantify parameter for DST analyses
16	Duration of a GRE	GRE release efficiency	revisit; condition of bd GRE to be added
17	Frequency of salt well pumped-induced GREs	GRE release efficiency and FG	none; not applicable to DSTs

Slide 39

No.	Parameter Description	Conditioning Factors	Changes from AF for SSTs required to apply parameter to DSTs
18 a-d	salt well pumping-related parameters for undissolved and soluble gas release	no conditioning factors	none; not applicable to DSTs
19	Probability of an earthquake-induced GRE	GRE release efficiency, Facility Group, earthquake return frequency	revisit; may add conditions of liquid layer present, pumped vs unpumped
20	Probability of an earthquake-induced ignition source	earthquake return frequency	revisit; condition of liquid layer present may be added
21	Mole fraction of source gas in waste-intrusive equipment when opening access	purging with NFPA standards	none: DST data to be used instead of uncertainty distributions
22	Frequency of flammable gas mixtures in salt well pump pits	active/passive ventilation, Facility Group	none; not applicable to DSTs
23	Mass of waste ejected from a burn inside equipment	air or inerting, burn or detonation	none; applies to both SSTs & DSTs
24	Fraction of parameter 23 that is respirable	air or inerting, burn or detonation	revisit

Slide 40

New Cases for Current Parameters

- **Mass of material suspended in headspace by GRE mechanisms other than buoyant displacement if no combustion occurs or combustion is too weak to fail HEPA.**
  - Provides continuous dose consequence metric for evaluating SST controls.
  - Panel may choose to replace existing SST uncertainty distributions with those for mass of material *released*.
  - Uncertainty distributions for mass of respirable material suspended also needed.

WS1–SS–1/19/98-B
slide 41

New Cases for Current Parameters (2)

- **Probability of a GRE-induced ignition source.**
- **Duration of a GRE.**
- **For DST analysis, both parameters to be conditioned on small, medium, and large efficiency buoyant displacement GRE.**
- **Buoyant displacement GRE mechanisms not considered for SST analysis by many panel members.**

WS1–SS–1/19/98-B
slide 42

New Cases for Current Parameters (3)

- Probability of an earthquake-induced GRE
- Probability of an earthquake-induced ignition source.
- Both parameters conditioned on:
  - liquid layer present.
  - Salt well pump status.
  - Small, medium, large efficiency GRE (same as before).
  - 100-, 1,000- and 10,000-year return frequency seismic event (same as before).
  - Panel to decide if condition of Facility Group is applicable when conditioned on presence of liquid layer.

Outline

- Additional analysis framework models.
- Conditioning cases for parameters previously quantified for SSTs.
- Additional parameters unique to buoyant displacement GRE analyses.
- Other items requiring panel decisions.

New Parameters for DSTs

- **Maximum achievable void fraction in nonconvective layer waste.**
  - Provides finite limit to void growth.
  - Used to determine if α_{nb} can be reached and buoyant displacement GREs are possible in a given DST.
  - Conditioning factors, if any, to be determined by panel.
  - No conditioning factors are proposed as needed, other than sufficient liquid layer must be present to enable buoyant displacement GRE behavior.

WS1–SS–1/19/98-B
slide 45

New Parameters for DSTs (2)

- **Mass of material *released* by combustion event per unit volume of gas vented.**
  - Presence of dome liner in DST may change release behavior compared to SST--prevent falling debris, seal against cracks in concrete.
  - Splash and impact debris that falls back into tank or filtered by overburden does not contribute to source.
  - Propose conditioned on:
    - No combustion or combustion too weak to fail HEPA.
    - Deflagration fails HEPA but no gross dome failure occurs.
    - Detonation fails HEPA but no gross dome failure occurs.
    - Deflagration causes gross dome failure.
    - Detonation causes gross dome failure.

WS1–SS–1/19/98-B
slide 46

New Parameters for DSTs (3)

- **Local efficiency of gas release from nonconvective layer material when hydraulically, pneumatically or mechanically disrupted.**
  - Needed to evaluate the efficacy of equipment designed to release gas in a controlled manner.
  - No conditioning factors are proposed as needed, other than sufficient liquid layer must be present to enable buoyant displacement GRE behavior.
  - Volume of influence of equipment to be engineering design criteria.
  - Conditioning factors, if any, to be determined by panel.

WS1–SS–1/19/98-B
slide 47

New Parameters for DSTs (4)

- **Characteristic time for surface renewal.**
  - Used to compute NH_3 release rate.
  - Conditioning factors to be determined.
  - Potential conditioning factors are:
    - small, medium, large efficiency GRE
    - operation of gas release control equipment (e.g., mixer pump, lance) or other globally waste-disturbing operation.
  - Prescriptive methods for computing τ_{renew} may be specified by panel instead of using uncertainty distributions (e.g., relating to τ_{rel} or volumetric disturbance rate).

WS1–SS–1/19/98-B
slide 48

New Parameters for DSTs (4)

- Surface area disrupted for enhanced NH_3 release.
  - Used to compute NH_3 release rate.
  - Conditioning factors to be determined.
  - Potential conditioning factors are:
    - small, medium, large efficiency GRE
    - operation of gas release control equipment (e.g., mixer pump, lance) or other globally waste-disturbing operation.
  - Prescriptive methods for computing A_{dist} may be specified by panel instead of using uncertainty distributions (e.g., relating to D_o for BD GREs with crust, A_{tank} if no crust, radius of influence of equipment to be engineering design criteria, etc.)

WS1–SS–1/19/98-B
slide 49

Outline

- Additional analysis framework models.
- Conditioning cases for parameters previously quantified for SSTs.
- Additional parameters unique to buoyant displacement GRE analyses.
- Other items requiring panel decisions.

WS1–SS–1/19/98-B
slide 50

Panel Decisions / Actions

- Endorse spontaneous and induced BD GRE models as suitable for risk assessment or specify required changes if not suitable as presented.
- Provide criteria for when BD GREs are not risk significant and SST-type analysis is suitable.
- Specify how parameters are to be quantified if not by uncertainty distributions (e.g., τ_{renew}, A_{dist}).
- Specify if BD GRE risk is added to or replaces risk from GRE mechanisms other than BD.

WS1–SS–1/19/98-B
slide 51

Panel Decisions / Actions (2)

- Provide consensus basis for excluding subsurface burns or provide analysis method for evaluating their risk.
- Review and approve proposed application of previously quantified parameters to DST analysis; provide additional uncertainty distributions if current distributions are not valid.
- Endorse time at risk evaluation for ex-tank intrusive regions during active ventilation (propose 2 x duration of positive pressure).
- Document all consensus decisions in writing.

WS1–SS–1/19/98-B
slide 52

Time at Risk, Ex-Tank Intrusive Areas

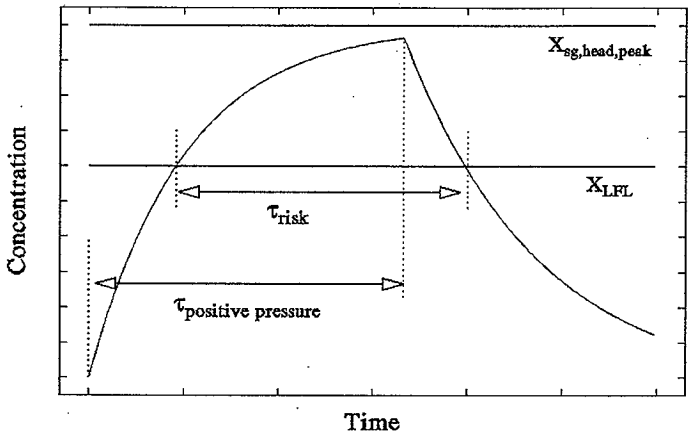

WS1–SS–1/19/98-B
slide 53

Summary

- DST analysis builds on SST groundwork.
- Proposed AF for DSTs contains mathematically complex models for BD behavior.
- Benefit from added complexity is key uncertainty distributions derived from data, not judgment.
- Panel's role for DST analysis is more peer review and approval and less data evaluation and uncertainty quantification as was for SSTs.

WS1–SS–1/19/98-B
slide 54

PNNL-SA-29606

Presentations by Chuck Stewart

Pacific Northwest National Laboratory

Stage II Experts' Panel Elicitation Workshop #1

January 19-23, 1998

Richland, Washington

Presentations

- **GRE History of Hanford DSTs (1/20/98)**
- **Overview of DST Field Data (1/20/98)**
- **Seismic Response of DST Waste (1/22/98)**

PNNL-SA-29606

Presentations by Chuck Stewart

Pacific Northwest National Laboratory

Stage II Experts' Panel Elicitation Workshop #1
January 19-23, 1998
Richland, Washington

Presentations

- **GRE History of Hanford DSTs (1/20/98)**
- **Overview of DST Field Data (1/20/98)**
- **Seismic Response of DST Waste (1/22/98)**

GRE History of Hanford DSTs

Chuck Stewart **PNNL**

In recent Hanford history only six tanks have exhibited evidence of relatively large sudden gas releases. These are the six double shell tanks (DSTs) on the Flammable Gas Watch List (FGWL). It is important to characterize the GRE behavior of these tanks in order to evaluate the hazard they present and rank them accordingly, to understand the mechanisms of these gas releases and develop models to predict them and, finally, to propose methods for mitigating these gas releases.

While there are many conceivable indications that GREs have occurred, there are only two practical methods to quantify gas releases. These are analysis of the waste surface level drop history and analysis of the tank headspace hydrogen concentration. Waste surface level drop is an indirect and imprecise indication of gas release, but it is the only method available prior to ~1994-95. Headspace hydrogen concentration measurements provide a positive and direct measurement of integral gas release that is extremely sensitive and precise, but it has been available only since ~1994-95 and covers relatively few events. Where possible, the two methods need to be used together to develop the most accurate representation of GRE behavior. The primary reference for the results of the level drop method is Meyer et al. (1997). This presentation represents the most complete reference for the headspace hydrogen analysis method, although the data are also discussed in Wilkins et al. (1997).

The surface level drop method simply assumes that a sudden waste surface level drop was the result of a corresponding release of retained gas from the nonconvective layer. The gas release volume is computed as the product of level drop, tank area and the estimated hydrostatic pressure at which the retained gas was held. This method works well with tanks that experience the largest gas releases, specifically SY-101 (prior to mixing), SY-103 and AN-105.

Small GREs are difficult to detect from the waste level history, and detecting a GRE signature is more "art" than science. The detection limit is on the order of 1 cm which corresponds to a minimum gas release of ~10 m^3. A small gas release often does not produce a "clean" level drop. Apparently some of the rising solids are temporarily trapped by the floating layer so that the entire "episode" may occur over weeks. These factors make determining gas release from level drop particularly difficult in AN-103, AN-104, and AW-101.

Level instrument problems can create indications that look like GREs. The most pervasive is the accumulation of a solid "stalactite". When this solid deposit is occasionally flushed off, it creates a sudden level drop that looks like a gas release. Instrument recalibration can cause a similar indication. The operations shift logs must be studied along with the data to sort this out.

There are typically at least two level instruments operating simultaneously. Which instrument (manual tape, FIC, Enraf) should be used to determine the level drop? The most accurate one in operation has been chosen in this study and indications of the others are ignored (Enraf®, FIC and manual tape in descending order).

The time period also needs to be considered. The time from the maximum to the minimum level in a single event may be 3-14 days, though most of the drop occurs over about one day. Meyer et al. (1997) use a one-day period as the basis for computing the level drop. This provides the best match with headspace hydrogen data in SY-101 and AN-105.

Determining gas release volume from headspace hydrogen data assumes a well-mixed headspace (this is a good assumption after ~ 1 hr) and a constant inlet ventilation flow rate (good

except for short periods during large releases from SY-101). A lower bound for the gas release volume can be computed as the product of the peak hydrogen concentration and the headspace volume divided by the estimated hydrogen fraction in the waste gas. A more accurate method models the gas release rate from the waste surface as an exponential function and adjusts the model parameters and ventilation rate to minimize the difference between predicted and measured hydrogen concentration. The total release is simply the integral of the release rate function divided by the hydrogen fraction in the waste.

The headspace hydrogen data are so sensitive that one must ask how small a gas release should be considered a GRE for the purposes of model development or hazard analysis? This same question applies to small secondary releases that often appear while the primary release decays. This study considers only the primary release as part of the GRE history unless succeeding releases are of similar size. Generally releases that raise the headspace concentration to less than 1000 ppm of hydrogen are ignored.

The best estimate of the GRE history derived from all sources is given. Generally the value based on hydrogen concentration is taken as the best estimate since: 1) headspace data cover the period for which we also have in-situ gas fraction and rheology data, and 2) it is the only positive and direct measure of gas release for several of the tanks. The values differ somewhat from those given in Meyer et al. (1997) and no estimate is provided at all for AN-103. The revised GRE histories will ultimately result in a revised gas release model.

Waste level and waste temperature histories are given for all six tanks (no temperatures are given for SY-101 - see Antoniak [1993]). The GRE's based on headspace hydrogen analysis are also listed separately for each tank.

References

Antoniak ZI. 1993. *Historical Trends in Tank 241-SY-101 Waste Temperatures and Levels.* PNL-8880, Pacific Northwest Laboratory, Richland, Washington.

Meyer PA, ME Brewster, SA Bryan, G Chen, LR Pedersen, CW Stewart and G Terrones. 1997. *Gas Retention and Release Behavior in Hanford Double-Shell Waste Tanks.* PNNL-11536, Rev. 1, Pacific Northwest National Laboratory, Richland, Washington.

Wilkins NE, RE Bauer, and DM Ogden. 1997. *Results of Vapor Space Monitoring of Flammable Gas Watch List Tanks.* HNF-SD-WM-TI-797, Rev. 2, Lockheed Martin Hanford Corporation, Richland, Washington.

GRE History of Hanford DSTs

SY-101 AN-103

SY-103 AN-104

AW-101 AN-105

Chuck Stewart

PNNL

Expert Panel Elicitation Workshop #1,

January 19-23, 1998,

Richland, Washington.

Why is GRE History Important?

- **Evaluate the hazard**
- **Rank the tanks**
- **Understand the GRE mechanisms**
- **Develop and validate predictive models**
- **Propose mitigation methods**

Methods to Quantify Gas Releases

- **Waste surface level drop analysis**
  - Indirect and imprecise indication of gas release
  - Detection limit ~10 m^3
  - BUT: only method available prior to ~1994-95
- **Headspace hydrogen concentration analysis**
  - Positive and direct measurement of integral gas release
  - Extremely sensitive
  - BUT: available only since ~1994-95 (few events)

Surface Level Drop Method

$$V_R = \Delta L A P_G$$

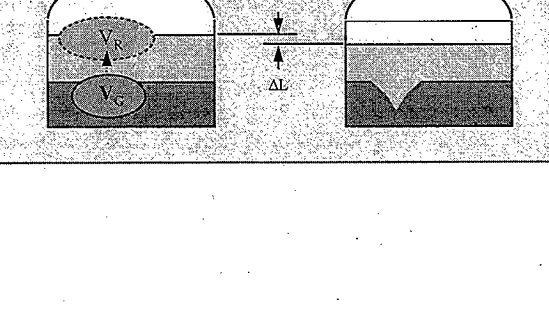

Waste Level Drop Example

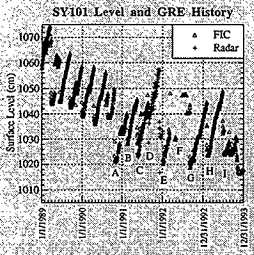

Surface Level Drop Method Caveats

- **Small GREs are difficult to detect**
  - detecting GRE signature more "art" than science
  - detection limit ~10 m^3
  - entire "episode" may occur over weeks
  - AN-103, AN-104, AW-101 marginal for level drop
- **Level instrument glitches can look like GREs**
  - flushes
  - recalibration
- **What determines the level drop?**
  - set period (i.e., single day)
  - maximum-to-minimum
  - which instrument (manual tape, FIC, Enraf)?

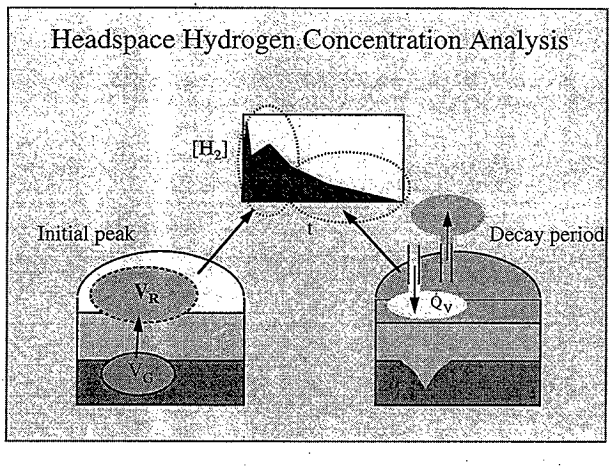
Headspace Hydrogen Concentration Analysis
[H2]
t
Initial peak
Decay period
VR
VG
QV

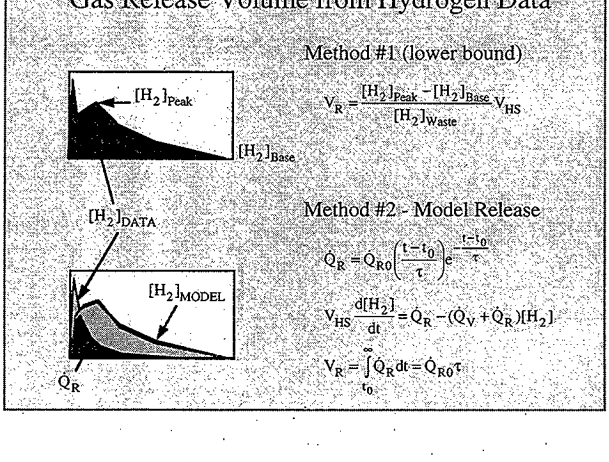
Gas Release Volume from Hydrogen Data
Method #1 (lower bound)
$V_R = \frac{[H_2]_{Peak} - [H_2]_{Base}}{[H_2]_{Waste}} V_{HS}$
[H2]Peak
[H2]Base
[H2]DATA
[H2]MODEL
QR
Method #2 - Model Release
$Q_R = Q_{R0}\left(\frac{t-t_0}{\tau}\right)e^{-\frac{t-t_0}{\tau}}$
$V_{HS}\frac{d[H_2]}{dt} = Q_R - (Q_V + Q_R)[H_2]$
$V_R = \int_{t_0}^{\infty} Q_R\,dt = Q_{R0}\tau$

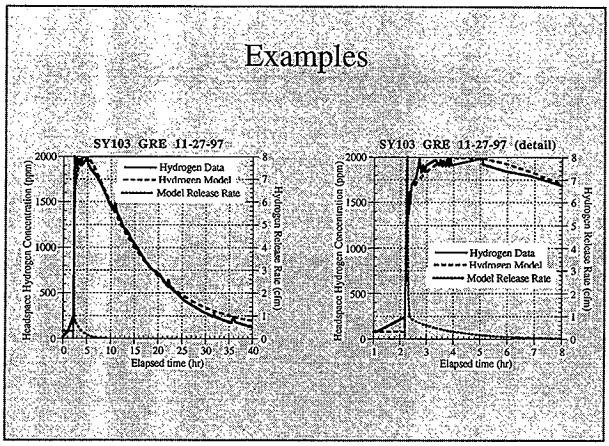
Examples
SY103 GRE 11-27-97
Hydrogen Data
Hydrogen Model
Model Release Rate
Headspace Hydrogen Concentration (ppm)
Hydrogen Release Rate (cfm)
Elapsed time (hr)
SY103 GRE 11-27-97 (detail)
Hydrogen Data
Hydrogen Model
Model Release Rate
Headspace Hydrogen Concentration (ppm)
Hydrogen Release Rate (cfm)
Elapsed time (hr)

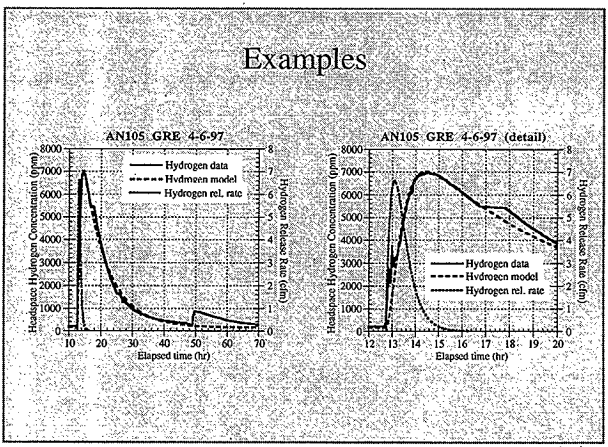
Examples
AN105 GRE 4-6-97
Hydrogen data
Hydrogen model
Hydrogen rel. rate
Headspace Hydrogen Concentration (ppm)
Hydrogen Release Rate (cfm)
Elapsed time (hr)
AN105 GRE 4-6-97 (detail)
Hydrogen data
Hydrogen model
Hydrogen rel. rate
Headspace Hydrogen Concentration (ppm)
Hydrogen Release Rate (cfm)
Elapsed time (hr)

Hydrogen Data Caveats

- **Hydrogen data available only since ~1994-95**
- **Analysis assumptions:**
  - **well-mixed headspace (good after ~ 1 hr)**
  - **constant ventilation rate (inlet)**
- **Total release requires $[H_2]_{Waste}$ value**
- **How should complex events be handled?**
  - **multiple major releases**
  - **secondary small releases**
- **How small a release should be considered a GRE?**

GRE History Summary

	AN-103	AN-104	AN-105	AW-101	SY-101	SY-103
From level drop (PNNL-11536 rev 1)						
first event date	05/02/89	02/28/86	05/21/85	11/17/86	03/25/89	12/08/89
last event date	02/11/96	05/05/96	04/06/97	12/22/94	06/26/93	07/14/96
number of events	19	30	21	37	15	28
Average gas release (scm)	14 ± 4	23 ± 16	26 ± 11	14 ± 10	131 ± 47	13 ± 6
From level drop (since 1993)						
first event date	07/11/93	04/28/93	01/25/93	04/10/94	12/04/91 (E)	07/01/94
last event date	02/11/96	05/05/96	04/05/97	12/20/95	06/26/93 (I)	11/27/97
number of events from 1993	7	12	6	9	5	18
Average gas release (scm)	15 ± 4	16 ± 5	21 ± 8	9 ± 4	151 ± 54	14 ± 9
From SHMS						
first event date	08/22/95	11/06/94	08/21/95	10/01/94	12/04/91 (E)	01/22/95
last event date	08/22/95	05/01/97	09/25/97	05/05/96	06/26/93 (I)	11/27/97
hydrogen fraction in waste	0.62 ± 0.07	0.47 ± 0.04	0.62 ± 0.04	0.32 ± 0.02	0.31 ± 0.03	0.58 ± 0.06
number of events	1	7	3	16	4	9
Average gas release (scm)						
Peak [H2] * headspace volume	5	8 ± 5	18 ± 9	11 ± 5	142 ± 44	9 ± 6
Integrate [H2] release model	4	10 ± 6	27 ± 12	19 ± 7		12 ± 9
BEST ESTIMATE GRE HISTORY		10 ± 6	27 ± 12	19 ± 7	142 ± 44	12 ± 9

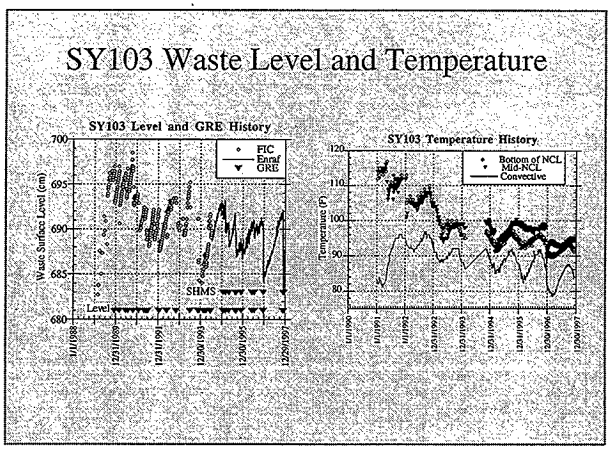
SY103 Waste Level and Temperature
SY103 Level and GRE History
Waste Surface Level (cm)
FIC
Enraf
GRE
SHMS
Level
SY103 Temperature History
Temperature (F)
Bottom of NCL
Mid-NCL
Convective

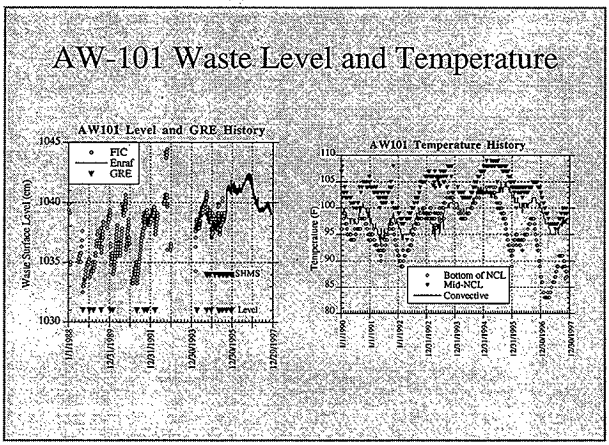
AW-101 Waste Level and Temperature
AW101 Level and GRE History
Waste Surface Level (cm)
FIC
Enraf
GRE
SHMS
Level
AW101 Temperature History
Temperature (F)
Bottom of NCL
Mid-NCL
Convective

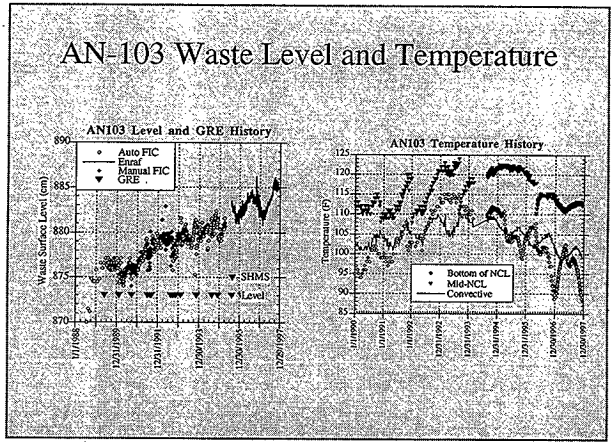
AN-103 Waste Level and Temperature
AN103 Level and GRE History
Auto FIC
Enraf
Manual FIC
GRE
SHMS
Level
Waste Surface Level (cm)
AN103 Temperature History
Bottom of NCL
Mid-NCL
Convective
Temperature (F)

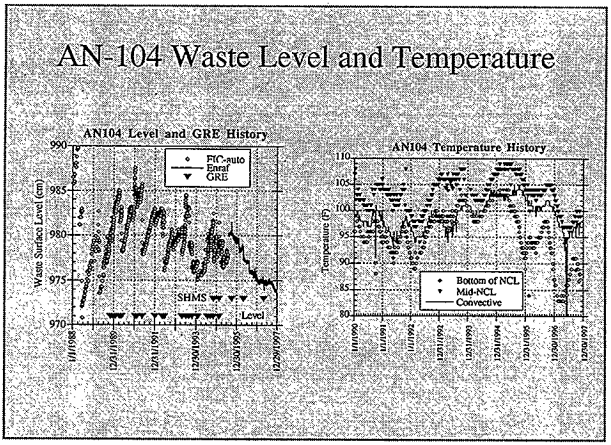
AN-104 Waste Level and Temperature
AN104 Level and GRE History
FIC-auto
Enraf
GRE
SHMS
Level
Waste Surface Level (cm)
AN104 Temperature History
Bottom of NCL
Mid-NCL
Convective
Temperature (F)

AN-105 Waste Level and Temperature

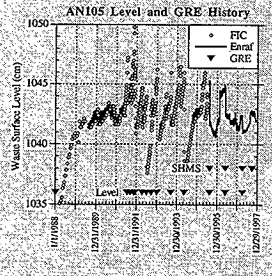

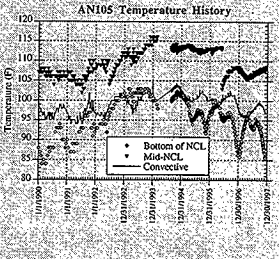

SY-103 GRE Summary

Date	Peak [H2] (ppm)	Level drop (cm)	Release (scm) (peak/headsp)	Release (scm) (level drop)	Release (scm) (integrate SHMS)	Vent rate (cfm)
1/23/95	1090	1.5	5	10	6	90
3/2/95	2210	2.1	10	15	11	59
5/3/95	*1430*	1.8	6	13	6	36
8/24/95	1280	1.3	6	9	4	40
9/7/95	1890	2.2	8	15	9	104
12/14/95	*740*	0.6		4		
6/7/96	1090	0.8	5	6	6	37
7/15/96	*2009*	1.1	9	8	27	62
12/21/96	5110	4.6	23	32	25	133
11/28/97	*1980*	5.8	9	41	11	124
Average	1969	2	9	16	12	
stdev	1275	2	6	12	9	

(concentration in *italics* indicates initial plume spike ignored)

AW-101 GRE Summary

Date	Peak [H2] (ppm)	Level drop (cm)	Release (scm) (peak/headsp)	Release (scm) (level drop)	Release (scm) (integrate SHMS)	Vent rate (cfm)
10/2/94	5500		19		22	26.6
10/5/94	*6200*	1.4	21	12	30	25
10/22/94	2980		10			
11/28/94	*4900*		17		27	29
2/23/95	*4600*		16		22	41
5/9/95	1800	1.3	6	11	19	67
5/18/95	1000	0.5	4	4		
7/9/95	2000	1.8	7	15		
7/13/95	900					
8/3/95	3300		11			
9/19/95	1930		7		15	18
9/25/95	4560	0.9	16	8	28	40
10/17/95	1750		6		9	19
12/13/95	2110	0.8	7	7		
12/30/95	6000	0.7	21	6	29	19
2/6/96	3200		11			
5/15/96	*7389*		5		13	105
6/6/96	2511		9		17	111
Average	2814	1.0	11	9	19	
stdev	1521	0.5	5	4	7	

AN GRE Summary

	Date	Peak [H2] (ppm)	Level drop (cm)	Release (scm) (peak/headsp)	Release (scm) (level drop)	Release (scm) (integrate SHMS)	Vent rate (cfm)
AN-103	8/23/95	*1600*	1.2	5	9	4	67
AN-104	11/7/94	3050	2.8	9	23	11	81
	2/17/95	2089	1.6	6	12	7	71
	8/4/95	480		1			
	10/3/95	3068	1.3	9	11	11	91
	10/6/95	1000					
	10/9/95	1800	0.7	5	6	5	55
	5/4/96	6109	1.5	18	12	20	79
	5/2/97	2250		6		5	192
	average	2399	0.6	8	10	10	
	stdev	1841	1.3	5	3	6	
AN-105	8/22/95	17000	3.6	29	31		
	5/31/96	14500	1.7	25	15	35	37
	4/6/97	6980	1.0	12	9	18	102
	9/28/97	770					45
	average	7417	1.4	18	12	27	
	stdev	6875	0.5	9	4	12	

SY-101 GRE SUMMARY

	Date	Peak [H2] (ppm)	Level drop (cm)	Release (scm) (peak/headsp)	Release (scm) (level drop)
	4/20/90	35000	23.8	120	213
	8/6/90	12000	13.2	-	119
A	10/25/90	47000	25.4	162	229
B	2/17/91	400	12.7	-	115
C	5/17/91	28000	18.3	96	165
D	8/28/91	3800	15.2	-	137
E	12/5/91	53000	33.0	182	298
F	4/21/92	14800	18.3	-	165
G	9/4/92	51200	33.5	176	302
H	2/3/93	27400	21.6	94	195
I	6/27/93	34000	24.8	117	224
	Average	36080	26	142	237
	stdev	16182	7	44	61

DST Field Data

Chuck Stewart **PNNL**

DST field data of interest to understanding and predicting gas release behavior include retained gas volume fraction, waste temperature, rheology, and waste layer thickness. Visual data such as photographs and video of core sample extrusions, waste surface video scans, and video of various waste disturbing operations are also valuable in understanding how the waste behaves. While the gas fraction and rheology were measured only once in 1995-96, the temperature and waste level are recorded continuously. This allows a rough extrapolation of the gas fraction and rheology to periods prior to and after actual measurements were made.

The retained gas volume fraction has been measured in all six FGWL DSTs with the Void Fraction Instrument (VFI) and in AW-101, AN-103, 104, and 105 with the Retained Gas Sampler (RGS). The VFI provides the most detailed data while the RGS provides a few additional data points under different risers. Gas fraction profiles show the highest gas fractions in the lower half of the nonconvective layer. The primary reference for gas fraction distribution in the DSTs is Meyer et al. (1997). See also Shekarriz et al. (1997) for background on RGS measurements. Other applicable references are Stewart et al. (1996), Shepard et al. (1995), Stewart et al. (1995), and Brewster et al. (1995).

Waste temperatures are typically measured with both the original thermocouple tree and the newer multi-function instrument tree (MIT). The former have 18 thermocouples, only 6-9 of which may be recorded. The MITs have 22 thermocouples and are typically recorded daily. A validation probe can be run inside the MITs that provides the most accurate and detailed temperature profile. MIT validation probe data is required to determine waste layering with acceptable accuracy. Validation probe temperature profiles for all but SY-101 are shown. Temperature data for all tanks can be accessed via the TWINS data base at http://twins.pnl.gov:8001/TCD/main.html. The temperature profiles are discussed in Stewart et al. (1996). Detailed temperature histories of SY-101 and SY-103 are given in Antoniak (1993) and Antoniak (1994), respectively.

Waste rheology has been measured in-situ in all six FGWL DSTs (SY-101 was post-mixer pump) with the ball rheometer. The waste rheology is derived from the correlation of ball speed, position and cable tension. The measurement of interest to gas release behavior is the low-speed data for the first pass through the waste. The waste viscosity and yield stress typically increase linearly with depth from essentially zero at the top of the nonconvective layer to 150-200 Pa. The ball data also very accurately defines the upper boundary of the nonconvective layer and detects a "stationary layer" that is sufficiently stiff to support the ball (yield stress > 900 Pa). Ex-situ rheology measurements on core samples have not been uniformly successful and the ball rheometer data should be used as the best indicator of waste properties (the often quoted 6700 Pa yield stress for SY-101 waste is erroneous - the correct value is 200-400 Pa). The primary reference for waste rheology is Meyer et al. (1997). Discussion of the ball rheometer system and theory are also given in Shepard et al. (1994) and Stewart et al. (1996). Ex-situ rheology measurements of SY-101 and SY-103 waste is discussed in Herting et al. (1992a,b), Reynolds (1993), Bredt et al. (1995), and Bredt and Tingey (1996).

Waste layering is inferred from a variety of measurements including the waste surface level, ball rheometer first pass, core sample extrusion. The primary measurement is derived from the MIT validation probe temperature profile. These data clearly define the floating layer, convective layer and nonconvective layer in each of the tanks such that the layer thickness can be determined to within 10-20 cm. The primary reference for waste layering is Meyer et al. (1997)

and a detailed discussion of the post-mixing configuration in SY-101 is given in Brewster et al. (1995).

DST field data summaries are provided for SY103, AW101, AN103, AN104 and AN105. The summaries each include a riser map, time line in-situ measurements with major GREs and waste level superimposed, the gas fraction profile and the viscosity and yield stress profile.

References

Antoniak ZI. 1993. *Historical Trends in Tank 241-SY-101 Waste Temperatures and Levels.* PNL-8880, Pacific Northwest Laboratory, Richland, Washington.

Antoniak ZI. 1994. *Historical Trends in Tank 241-SY-103 Waste Temperatures.* PNL-10058, Pacific Northwest Laboratory, Richland, Washington.

Bredt PR, JM Tingey and EH Shade. 1995. *The Effect of Dilution on the Gas-Retention Behavior of Tank 241-SY-101 Waste.* PNL-10781, Pacific Northwest National Laboratory, Richland, Washington.

Bredt PR, and JM Tingey. 1996. *The Effect of Dilution on the Gas Retention Behavior of Tank 241-SY-103 Waste.* PNNL-10893, Pacific Northwest National Laboratory, Richland, Washington.

Brewster ME, NB Gallagher, JD Hudson, and CW Stewart. 1995. *The Behavior, Quantity, and Location of Undissolved Gas in Tank 241-SY-101.* PNL-10681, Pacific Northwest Laboratory, Richland, Washington.

Herting, DL, DB Bechtold, BA Crawford, TL Welsh, and L Jensen. 1992a. *Laboratory Characterization of Samples Taken in May 1991 from Hanford Waste Tank 241-SY-101.* WHC-SD-WM-DTR-024 Rev. 0, Westinghouse Hanford Company, Richland, Washington.

Herting, DL, DB Bechtold, BE Hey, BD Keele, TL Welsh, and L Jensen. 1992b. *Laboratory Characterization of Samples Taken in December 1991 (Window E) from Hanford Waste Tank 241-SY-101.* WHC-SD-WM-DRT-026 Rev. 0, Westinghouse Hanford Company, Richland, Washington.

Meyer PA, ME Brewster, SA Bryan, G Chen, LR Pedersen, CW Stewart and G Terrones. 1997. *Gas Retention and Release Behavior in Hanford Double-Shell Waste Tanks.* PNNL-11536, Rev. 1, Pacific Northwest National Laboratory, Richland, Washington.

Reynolds DA. 1993. *Tank 101-SY Window E Core Sample: Interpretation of Results.* WHC-EP-0628, Westinghouse Hanford Company, Richland, Washington.

Shekarriz A, DR Rector, LA Mahoney, MA Chieda, JM Bates, RE Bauer, NS Cannon, BE Hey, CG Linschooten, FJ Reitz, and ER Siciliano. 1997. *Composition and Quantities of Retained Gas Measured in Hanford Waste Tanks 241-AW-101, 241-A-101, 241-AN-105, 241-AN-104, and 241-AN-103.* PNNL-11450, Rev. 1, Pacific Northwest National Laboratory, Richland, Washington.

Shepard CL, JB Colson, KO Pasamehmetoglu, C Unal, JN Edwards and J Abbott. 1994. *Theory of Operation for the Ball Rheometer.* PNL-10240, Pacific Northwest Laboratory, Richland, Washington.

Shepard, CL, CW Stewart, JM Alzheimer, G Terrones, G Chen, and NE Wilkins. 1995. *In Situ Determination of Rheological Properties and Void Fraction: Hanford Waste Tank 241-SY-103.*

PNL-10865, Pacific Northwest Laboratory, Richland, Washington.

Stewart CW, CL Shepard, JM Alzheimer, TI Stokes, and G Terrones. 1995. *In Situ Determination of Rheological Properties and Void Fraction in Hanford Waste Tank 241-SY-101*. PNL-10682, Pacific Northwest Laboratory, Richland, Washington.

Stewart CW, JM Alzheimer, ME Brewster, G Chen, RE Mendoza, HC Reid, CL Shepard, and G Terrones. 1996. *In Situ Rheology and Gas Volume in Hanford Double-Shell Waste Tanks*. PNNL-11296, Pacific Northwest National Laboratory, Richland, Washington.

DST Field Data

Chuck Stewart
PNNL

Expert Panel Elicitation Workshop #1,
January 19-23, 1998,
Richland, Washington.

DST Field Data

- **Gas volume fraction profiles**
- **Temperature profiles**
- **Rheology**
- **Waste layering**
- **Summary**

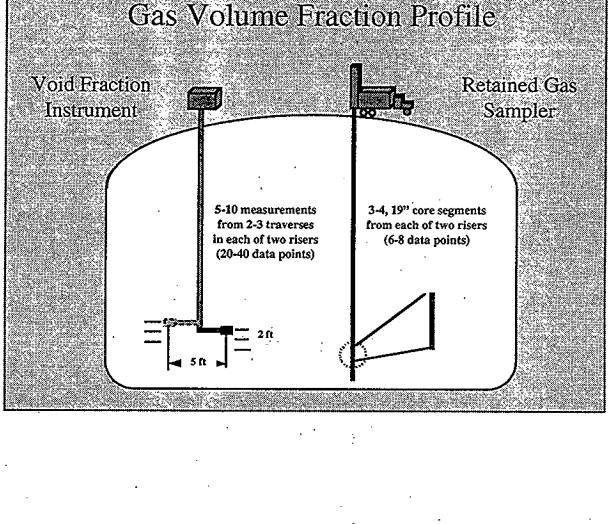
Gas Volume Fraction Profile
Void Fraction Instrument
Retained Gas Sampler
5-10 measurements from 2-3 traverses in each of two risers (20-40 data points)
3-4, 19" core segments from each of two risers (6-8 data points)
2 ft
5 ft

Gas Fraction Example
AW101 Gas Fraction
Convective Layer 283 - 976 cm
Top of Nonconvective Layer 13A (280 cm) 1C (259 cm)
13A - 1
13A - 2
13A - 3
1C - 1
1C - 2
1C - 3
RGS 24A
RGS 24B
Elevation (cm)
Elevation (in.)
Void Fraction

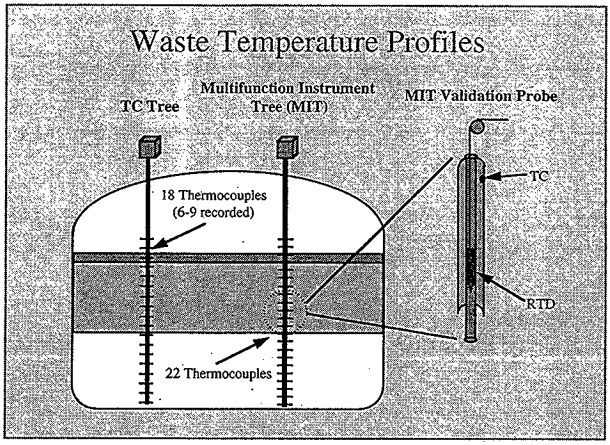
Waste Temperature Profiles
TC Tree
Multifunction Instrument Tree (MIT)
MIT Validation Probe
18 Thermocouples (6-9 recorded)
TC
RTD
22 Thermocouples

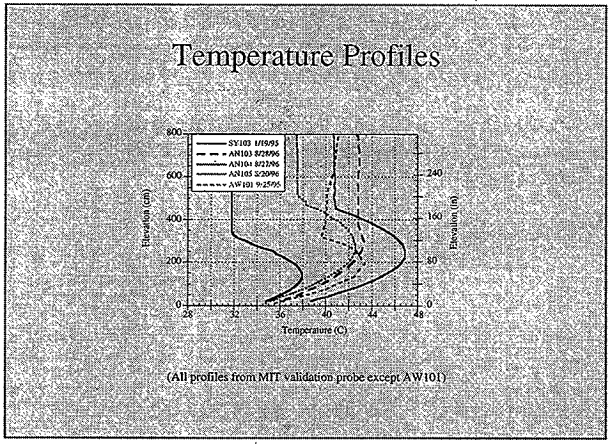
Temperature Profiles
SY103 1/19/95
AN103 8/29/96
AN104 8/23/96
AN105 8/20/96
AW101 9/25/95
Elevation (cm)
Elevation (in)
Temperature (C)
(All profiles from MIT validation probe except AW101)

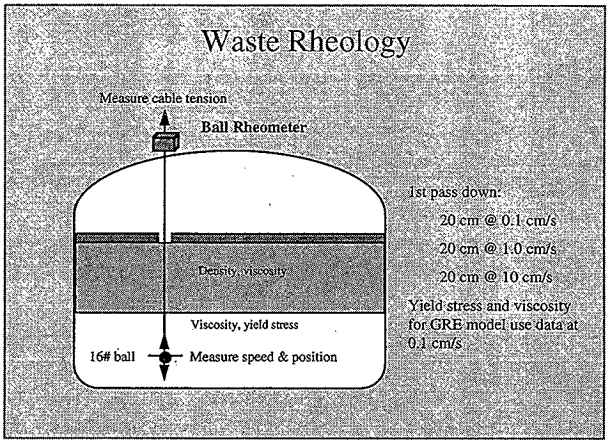
Waste Rheology
Measure cable tension
Ball Rheometer
Density, viscosity
Viscosity, yield stress
16# ball
Measure speed & position
1st pass down:
20 cm @ 0.1 cm/s
20 cm @ 1.0 cm/s
20 cm @ 10 cm/s
Yield stress and viscosity for GRB model use data at 0.1 cm/s

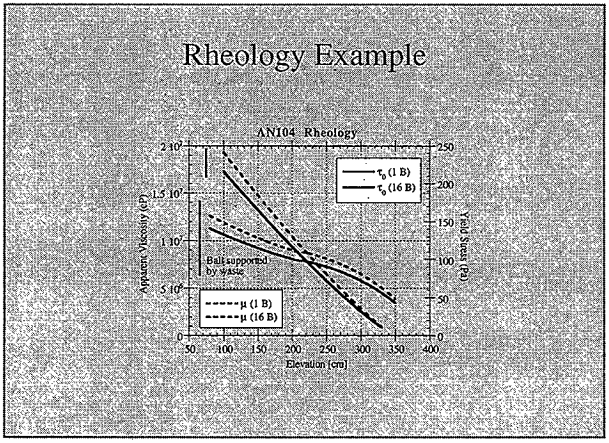
Rheology Example
AN104 Rheology
Apparent Viscosity (cP)
Yield Stress (Pa)
Elevation [cm]
τ0 (1 B)
τ0 (16 B)
μ (1 B)
μ (16 B)
Ball supported by waste

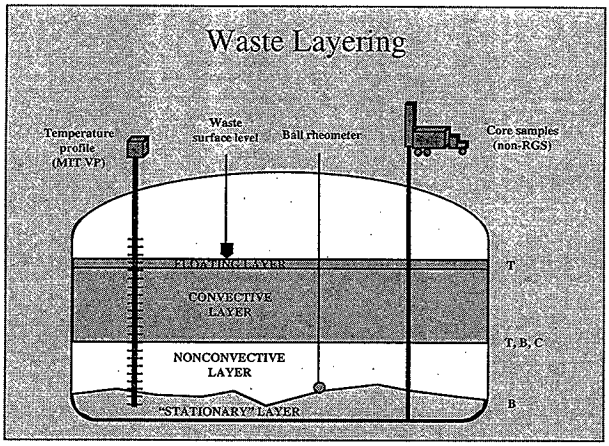
Waste Layering
Temperature profile (MIT VP)
Waste surface level
Ball rheometer
Core samples (non-RGS)
FLOATING LAYER
CONVECTIVE LAYER
NONCONVECTIVE LAYER
"STATIONARY" LAYER
T
T, B, C
B

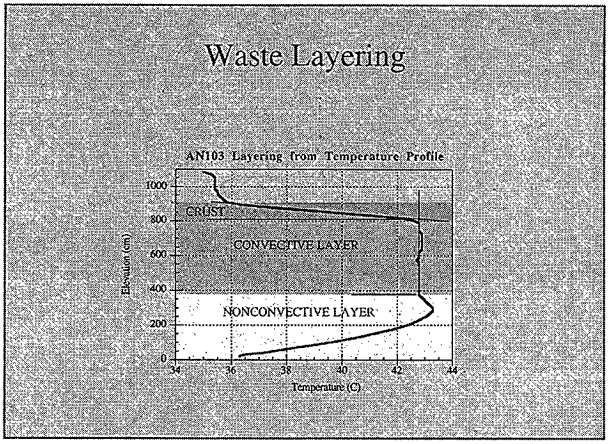
Waste Layering
AN103 Layering from Temperature Profile
CRUST
CONVECTIVE LAYER
NONCONVECTIVE LAYER
Elevation (cm)
1000
800
600
400
200
0
34
36
38
40
42
44
Temperature (C)

Waste Layering Summary

Layer (thickness in cm)	AN-103	AN-104	AN-105	AW-101	SY-101	SY-103
Total Waste	884 ± 5	979 ± 4	1041 ± 7	1040 ± 7	1054 ± 10	691 ± 3
Floating Layer	92 ± 20	40 ± 10	30 ± 10	64 ± 15	100 ± 30	20 ± 10
Convective Layer	413 ± 16	524 ± 10	559 ± 11	693 ± 19	470 ± 8	337 ± 19
Nonconvective Layer	379 ± 9	415 ± 9	452 ± 11	283 ± 22	584 ± 40	334 ± 25
"Stationary" Layer	192 ± 35	69 ± 45	57 ± 55	57 ± 47	0	103 ± 20

* SY101 values represent conditions prior to mixing

Elevations at which Ball Stopped

Tank	Riser #1	Min. Elevation (cm)	Riser #2	Min. Elevation (cm)
SY-101	11B	80	4A	0
SY-103	17C	102	22A	105
AW-101	13A	0	1C	94
AN-103	16B	227	1B	158
AN-104	16B	74	1B	65
AN-105	16B	0	1B	115

DST Field Data Summary

	AN-103	AN-104	AN-105	AW-101	SY-101	SY-103
Densities (kg/m³)						
Convective Layer	1530 ± 50	1440 ± 30	1430 ± 30	1430 ± 30	1500 ± 70	1470 ± 30
Nonconvective Layer	1730 ± 110	1590 ± 60	1590 ± 40	1570 ± 30	1700 ± 50	1570 ± 50
Layer Thickness (cm)						
Total Waste	884 ± 5	979 ± 4	1041 ± 7	1040 ± 7	1054 ± 10	691 ± 3
Convective Layer	413 ± 16	524 ± 10	559 ± 11	693 ± 19	470 ± 8	337 ± 19
Nonconvective Layer	379 ± 9	415 ± 9	452 ± 11	283 ± 22	584 ± 40	334 ± 25
"Stationary" Layer	192 ± 35	69 ± 45	57 ± 55	57 ± 47	0	103 ± 20
Void Fractions (%)						
Neutral Buoyancy	12 ± 6	9 ± 4	10 ± 3	9 ± 3	12 ± 5	6 ± 4
Nonconvective Layer Avg.	11 ± 1.0	6.2 ± 0.9	4.2 ± 0.8	3.8 ± 0.6	8	6 ± 2
Nonconvective Layer Rheology						
Yield Stress (Pa)	142 ± 15	81 ± 11	129 ± 31	159 ± 97	225 ± 100	112 ± 40
Viscosity (kPa-s)	12.6 ± 1.4	7.6 ± 0.7	12 ± 3	14 ± 4	21 ± 10	10 ± 4

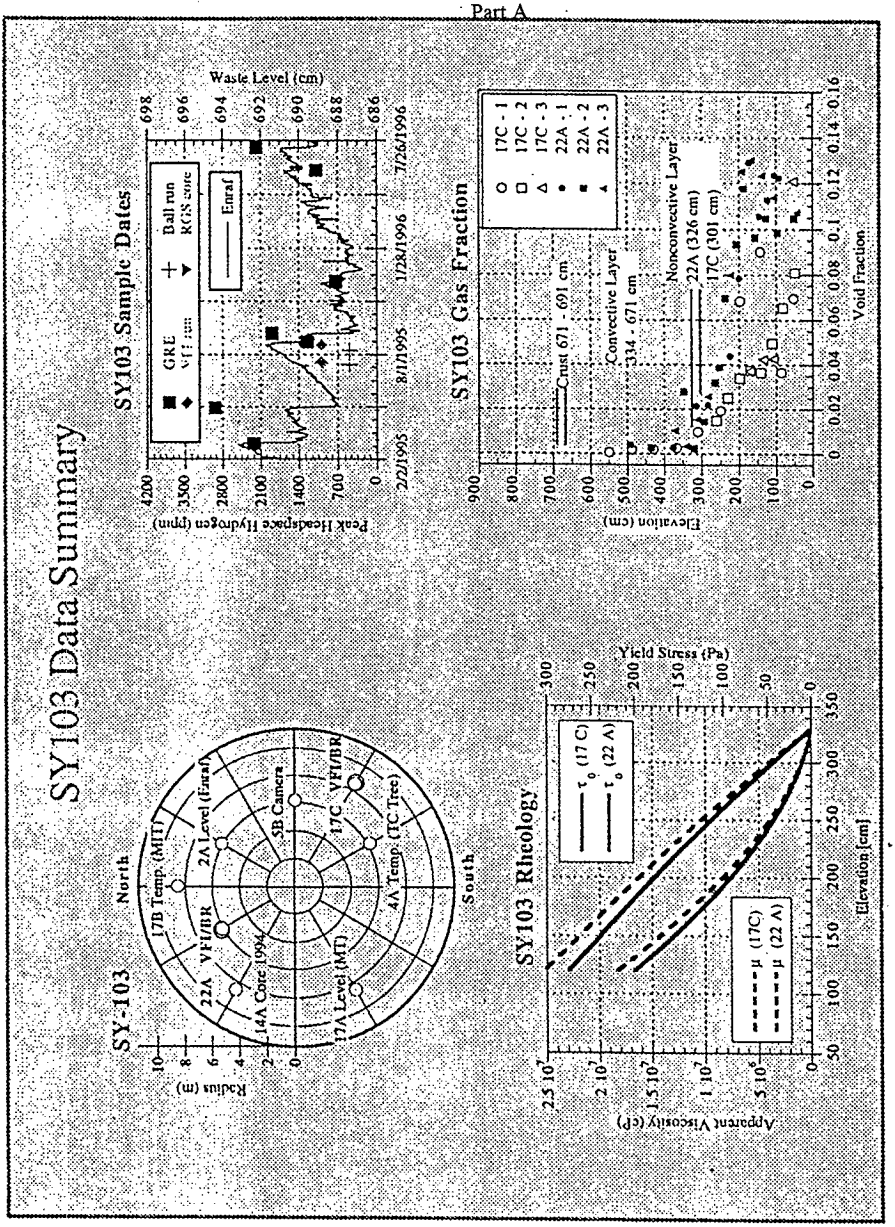
SY103 Data Summary
SY-103
North
South
Radius (m)
17B Temp. (MIT)
2A Level (Enraf)
SB Camera
VFI/BR
17C
22A
14A Core (1994)
17A Level (MIT)
4A Temp. (TC Tree)
SY103 Sample Dates
Waste Level (cm)
Peak Headspace Hydrogen (ppm)
GRE
Ball run
RGS core
Enraf
8/1/1995
1/28/1996
7/26/1996
SY103 Gas Fraction
Elevation (cm)
Void Fraction
17C - 1
17C - 2
17C - 3
22A - 1
22A - 2
22A - 3
Crust 671 - 691 cm
Convective Layer
334 - 671 cm
Nonconvective Layer
22A (326 cm)
17C (301 cm)
SY103 Rheology
Yield Stress (Pa)
Apparent Viscosity (cP)
Elevation [cm]
μ (17C)
μ (22 A)

AW101 Data Summary

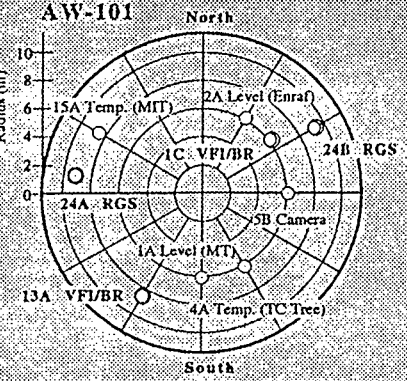

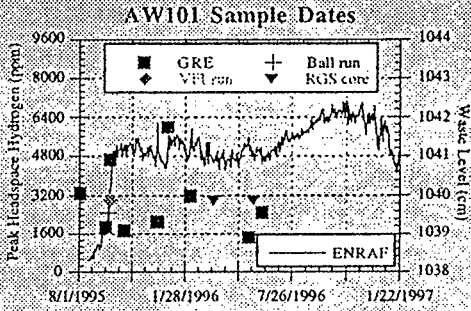

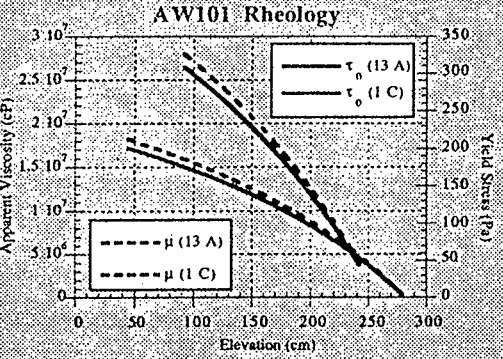

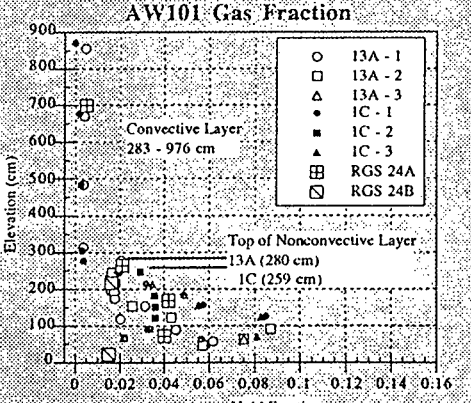

HNF-2193 Rev. 0
Part A

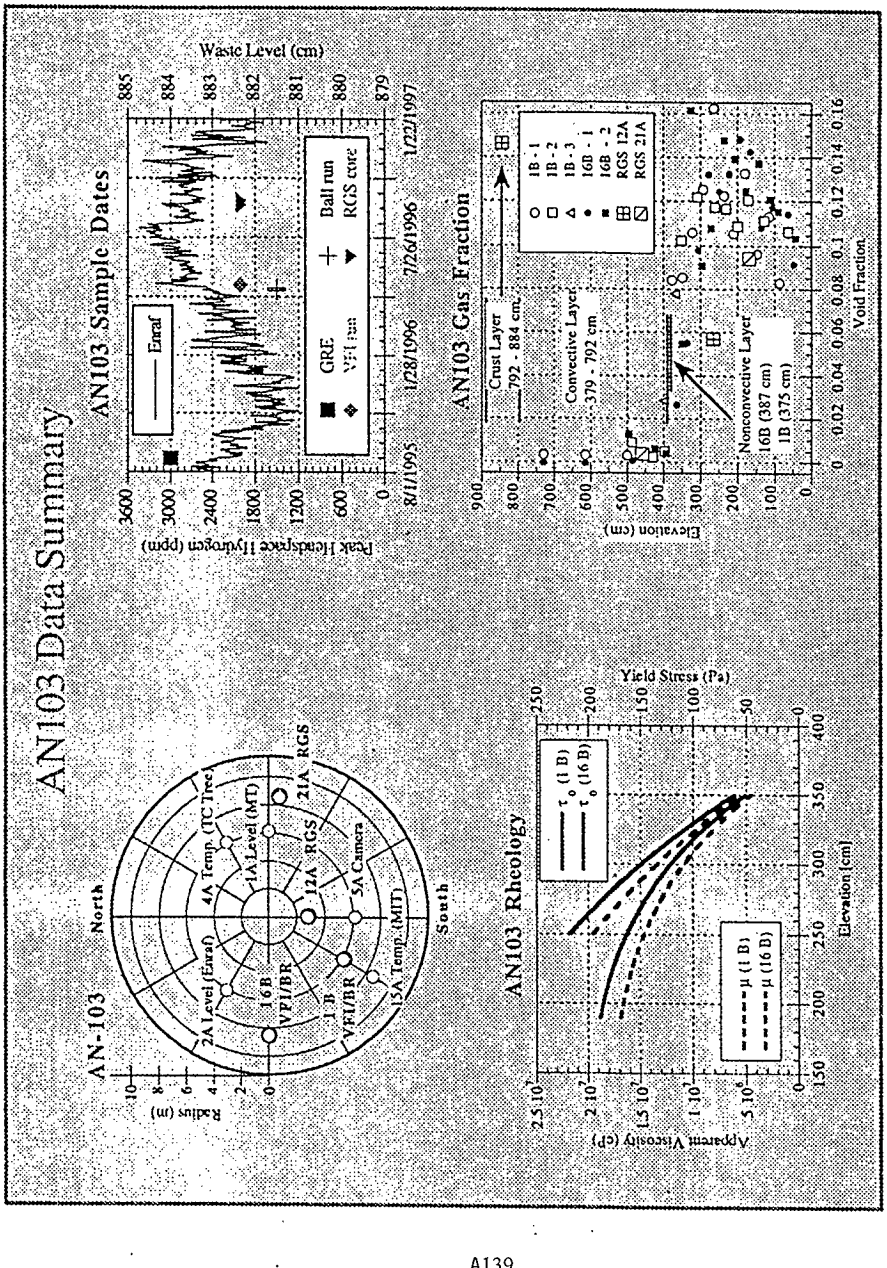
AN103 Data Summary
AN-103
North
South
Radius (m)
2A Level (Enraf)
16B
VF1/BR
1B
VF1/BR
1A Level (MT)
4A Temp. (TC Tree)
12A - RGS
21A - RGS
5A Camera
15A Temp. (MIT)
AN103 Sample Dates
Waste Level (cm)
Enraf
GRE
VF1 fan
Ball run
RGS core
Peak Headspace Hydrogen (ppm)
8/1/1995
1/28/1996
7/26/1996
1/22/1997
AN103 Gas Fraction
Crust Layer
792 - 884 cm
Convective Layer
379 - 792 cm
Nonconvective Layer
16B (387 cm)
1B (375 cm)
1B - 1
1B - 2
1B - 3
16B - 1
16B - 2
RGS 12A
RGS 21A
Elevation (cm)
Void Fraction
AN103 Rheology
Yield Stress (Pa)
Apparent Viscosity (cP)
Elevation (cm)
τ0 (1 B)
τ0 (16 B)
μ (1 B)
μ (16 B)

AN104 Data Summary

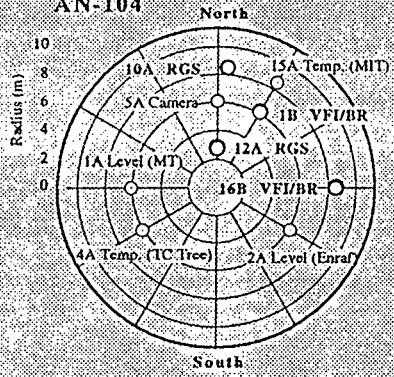

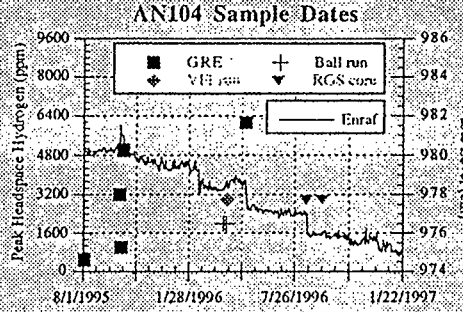

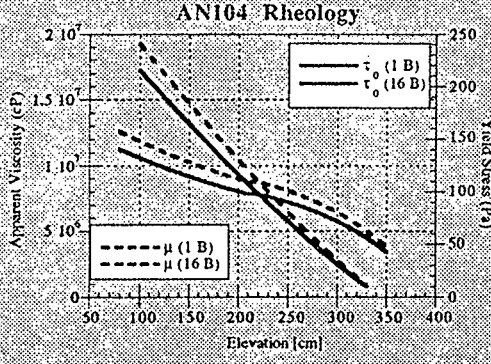

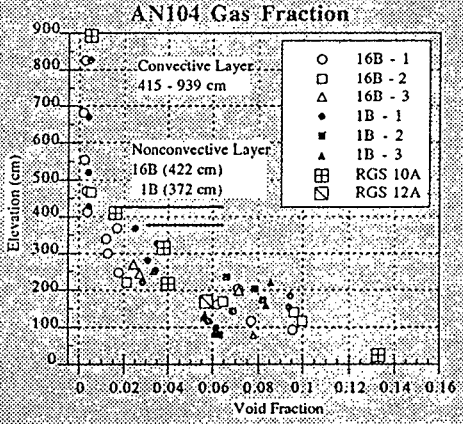

HNF-2193 Rev. 0
Part A

AN105 Data Summary

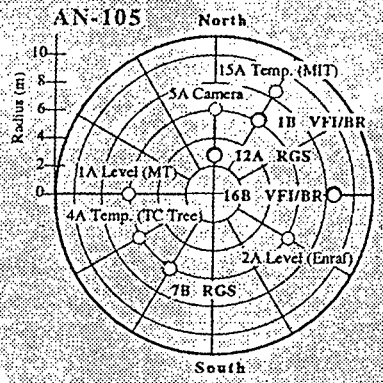

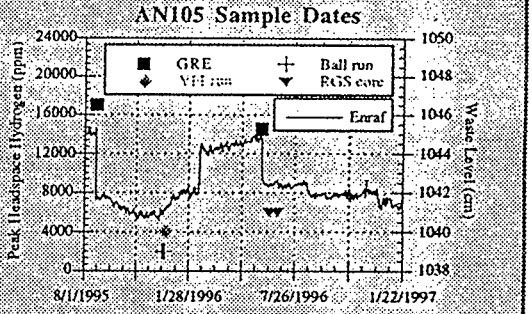

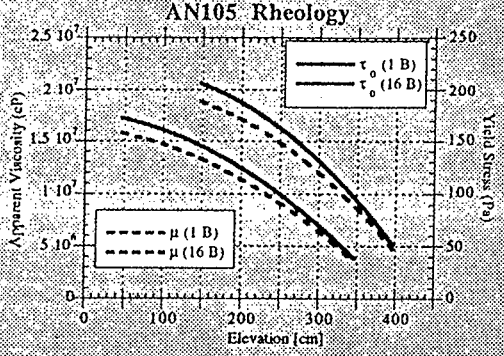

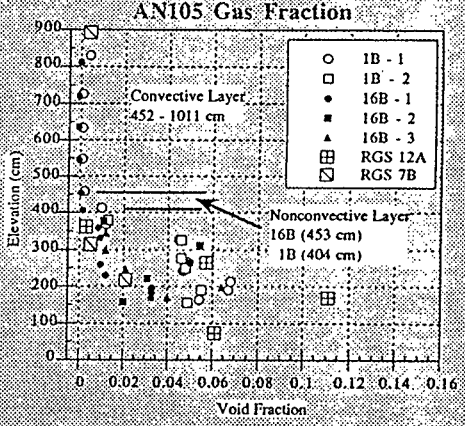

Seismic Response of DST Waste

Chuck Stewart **PNNL**

Part of the baseline risk of storing radioactive waste is the potential for retained gas to be released during the waste disturbance caused by a major earthquake. Waste mobilization during a 1000-year Design Basis Earthquake has been investigated via transient simulations with displacement boundary conditions using the ANSYS structural analysis code. Results are reported in Reid & Diebler (1997). Prior work is summarized in Stewart et al. (1996).

Four different waste configurations and several parametric cases were modeled to represent both single-shell tanks (SST) and double-shell tanks (DST). For SSTs a homogeneous solid waste with two depths and two yield stresses were modeled along with a special case representing the solid-over-liquid configuration of A-101. "Typical" DSTs were represented by a liquid-over-solid configuration with two depths and yield stresses. The total waste depth was divided equally between liquid and solid. A solid-over-liquid-over-solid waste was also modeled to represent tanks with a thick floating solids layer, specifically AN-103.

The simulations estimated the volume of the waste mobilized under the following assumptions:

- Waste is homogeneous except for distinction between liquid and solid layers
- Stress-strain behavior modeled as elastic to 5% strain then perfectly plastic (constant stress) to 100% strain at which point the material is considered "mobilized"
- Mobilized waste can release gas (though gas release was not specifically quantified)
- Perfect coupling assumed between soil and tank, effect of double-shell neglected

The details of finite element modeling and parameter values used are given in Reid & Deibler (1997). For a discussion of the seismicity of the Hanford area, refer to the presentation by Alan Rohay, PNNL, to the SCOPE Workshop #2, April 28-May 2, 1997.

All of the simulations quickly developed localized regions exceeding 100% strain. This stretched the capabilities of the ANSYS code. In hindsight, the phenomena might have been better modeled with fluid dynamics than with structural mechanics. However, the basic waste behavior revealed by the results gives some clear insights as to the potential effects of a severe earthquake. In summary:

- A large fraction of the seismic energy is dissipated in surface waves whose maximum amplitude is in the central region of the tank
- A liquid layer strongly amplifies the effect of the surface waves on the solids layer
- As a consequence, most of the solid waste in a DST is mobilized

Assuming 100% of the solids are mobilized and able to release gas, on the order of 50% of the total gas inventory might be released in the 1000-year earthquake studied. This release fraction is based on actual release fractions in the large, violent rollovers in SY-101 and from buoyancy considerations (see Meyer et al. 1997).

There is not sufficient data to extrapolate these results to more or less-severe earthquakes other than to say that a 10,000-year earthquake would probably not release much more than 50% of the gas and a 100-year earthquake would probably release somewhat less than 50% of the retained gas. Removing the liquid layer would tend to convert the DST waste to resemble an SST.

In the absence of the surface wave amplification caused by the liquid, relatively little of the total waste is mobilized and relatively little of the total gas is released (Reid & Diebler 1997).

References

Reid HC and JE Deibler. 1997. *Seismic Event-Induced Waste Response and Gas Mobilization Predictions for Typical Hanford Waste Tank Configurations.* PNNL-11668, Pacific Northwest National Laboratory, Richland, Washington.

Meyer PA, ME Brewster, SA Bryan, G Chen, LR Pedersen, CW Stewart and G Terrones. 1997. *Gas Retention and Release Behavior in Hanford Double-Shell Waste Tanks.* PNNL-11536, Rev. 1, Pacific Northwest National Laboratory, Richland, Washington.

Stewart CW, ME Brewster, PA Gauglitz, LA Mahoney, PA Meyer, KP Recknagle and HC Reid. 1996. *Gas Retention and Release Behavior in Hanford Single-Shell Waste Tanks.* PNNL-11391, Pacific Northwest National Laboratory, Richland, Washington.

Seismic Response of DST Waste

Chuck Stewart
PNNL

Expert Panel Elicitation Workshop #1,
January 19-23, 1998,
Richland, Washington

Seismic Response of DST Waste

- **Effect of 1000-year Design Basis Earthquake on SST and DST waste**
- **Based on transient simulations with displacements at tank walls (ANSYS)**
- **Elastic-perfectly plastic material**
- **"Mobilized" waste can release gas (based on strain energy density)**
- **Large gas releases can be expected from DSTs during severe earthquakes**

Historical Seismicity of Columbia Plateau
1850 – March 23, 1969

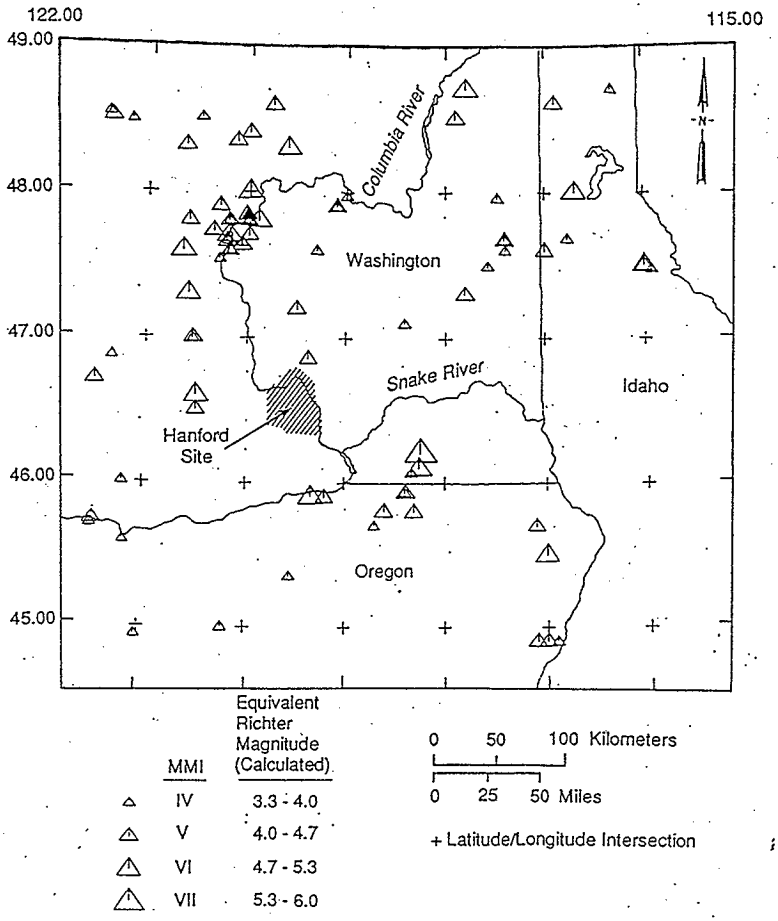

Recent Seismicity of the Columbia Platuea
March 23, 1969 - 1989

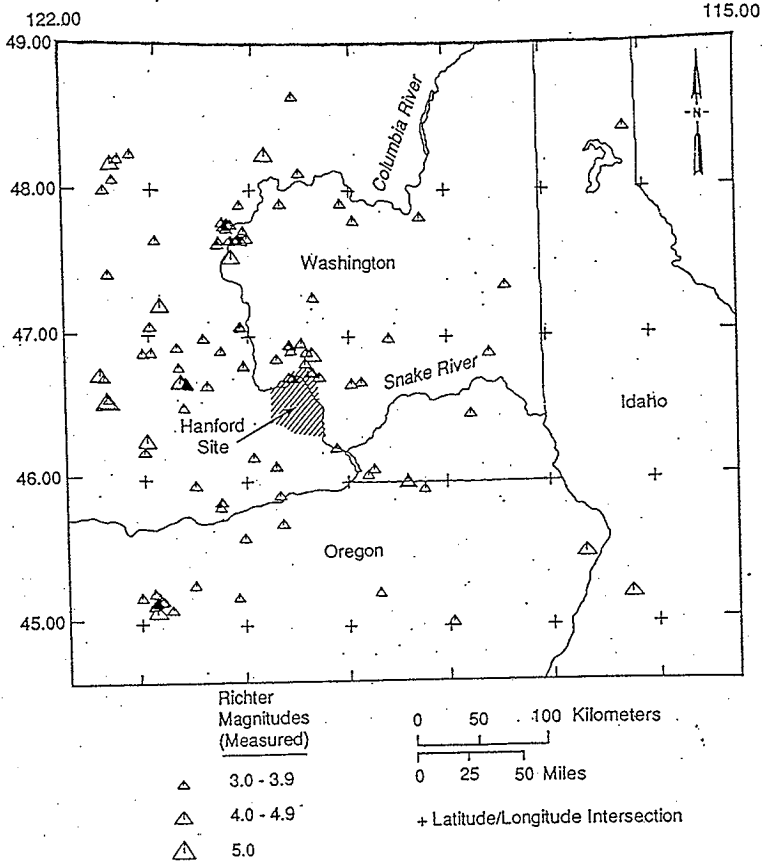

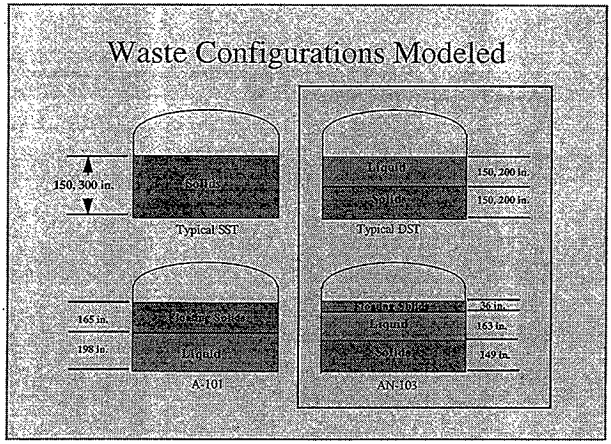
Waste Configurations Modeled
150, 300 in.
Solids
Typical SST
Liquid
150, 200 in.
Solids
150, 200 in.
Typical DST
165 in.
198 in.
Liquid
A-101
36 in.
163 in.
149 in.
AN-103

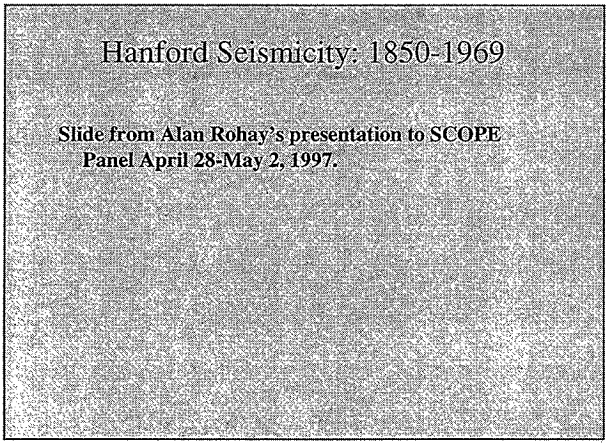
Hanford Seismicity: 1850-1969
Slide from Alan Rohay's presentation to SCOPE Panel April 28-May 2, 1997.

Hanford Seismicity: 1969-1989

Slide from Alan Rohay's presentation to SCOPE Panel April 28-May 2, 1997.

1000-Year Earthquake

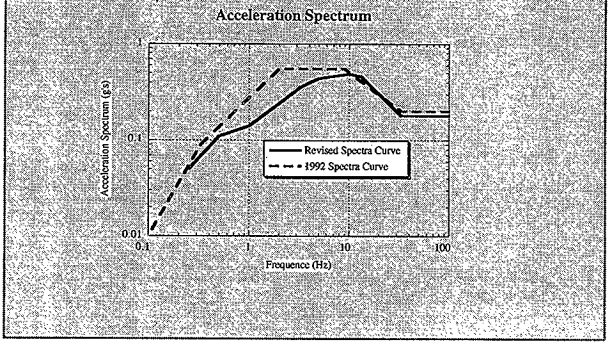

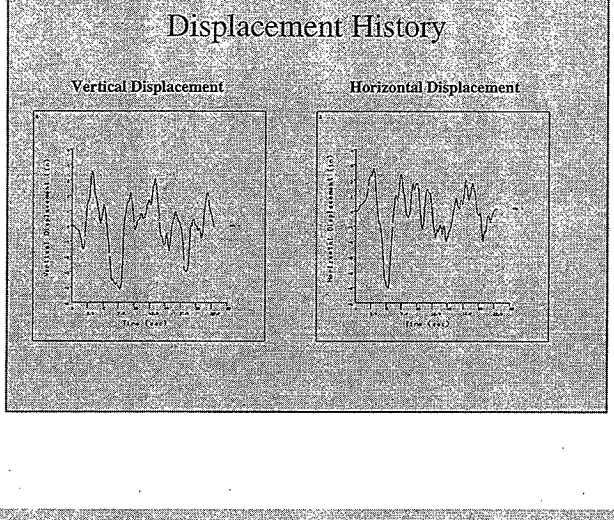
Displacement History
Vertical Displacement
Horizontal Displacement

Waste Material Properties
Plastic Region
Yield Stress
Stress
Mobilized Region
Elastic Region
Strain
100% Strain

Simulation Results

- A large portion of seismic energy is dissipated in surface waves
- The liquid layer amplifies the effect of waves on the solids layer
- Consequence: Most of the solid waste is mobilized

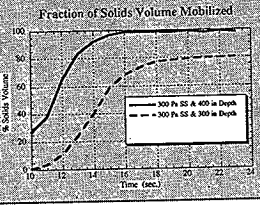

Strain Distribution in Solids

Map of Peak Strains

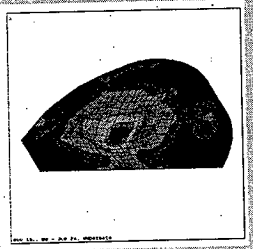

Map of Peak Strain Energy Density

(400-inch depth, 300 Pa yield stress)

Summary of Results

Waste Configuration	Solid Yield Stress (Pa)	Solids Depth (in.)	Liquid Depth (in.)	Total Waste Depth (in.)	Volume Mobilized (%)
Homogeneous (SST)	300	150	0	150	5
	300	300	0	300	13
(A-101)	300	165	198	363	68
Liquid-over-Solid (DST)	300	150	150	300	98
	300	200	200	400	80
(AN-103)	200	36;149	163	348	100

Gas releases ~50% of retained volume may be possible

Extrapolation?

- **Other earthquakes?**
  - 10,000-year: still ~50% gas release
  - 100-year: probably < 50% gas release
- **Removal of supernate?**
  - probably converts to SST pattern - little gas release

SY103

SY103	Headspace	2514 m3		[H2] =	0.57			ERROR MINIMIZATION SOLUTION			
	Peff	1.7 atm		number =	9						
	Date	Max H2 (ppm)	(peak/headsp) Release (m3)	Level drop (cm)	(level drop) Release (m3)	(integrate SHMS) Release (m3)	Calc. vent rate (cfm)	base rate (cfm)	time const. ~~(hours)~~ (MIN)	base rate #2 (cfm)	time const. #2 ~~(hours)~~ (MIN)
	01/22/1995	1090	5	1.5	10	6	90	0.7	84	10.9	6
	03/01/1995	2210	10	2.1	15	11	59	0.6	97	16.1	9.3
	05/02/1995	*1430*	6	1.8	13	6	36	1	34	18.8	4.5
	08/23/1995	1260	6	1.3	9	4	40	0.6	100	13.7	2.5
	09/06/1995	1890	8	2.2	15	9	104	2	39	25	4.6
	12/03/1995	740		0.6	4						
	06/06/1996	1090	5	0.8	6	6	37	0.1	550	0.8	80
	07/14/1996	*2009*	9	1.1	8	27	62	0.2	1762	0.4	487
	12/20/1996	5110	23	4.6	32	25	133	18.5	27.4		
	11/27/1997	*1980*	9	5.8	41	11	124	1	97	104	1.2
	Average	1969	9	2	16	12					
	stdev	1275	6	2	12	9					

AW101

AW-101	Headspace	1065 m3		[H2] =	0.31			ERROR MINIMIZATION SOLUTION			
	Peff	2.1 atm		number =	16						
	Date	Max H2 (ppm)	(peak/headsp) Release (m3)	Level drop (cm)	(level drop) Release (m3)	(integrate SHMS) Release (m3)	Calc. vent rate (cfm)	base rate (cfm)	time const. (hours) (MIN)	base rate #2 (cfm)	time const. #2 (hours) (MIN)
	10/01/1994	5500	19			22	26.6	1.5	161	9.7	1.8
	10/04/1994	*6200*	21	1.4	12	30	25	1.3	135	0.5	300
	10/21/1994	2980	10								
	11/27/1994	*4900*	17			27	29	1	191		
	02/22/1995	*4600*	16			22	41	6	42		
	05/08/1995	1800	6	1.3	11	19	67	0.5	435		
	05/17/1995	1000		0.5	4						
	07/08/1995	2000	7	1.8	15						
	07/12/1995	900									
	08/02/1995	3300	11								
	09/15/1995	1930	7			15	18	0.2	805		
	09/24/1995	4660	16	0.9	8	26	40	2	152		
	10/16/1995	1750	6			9	18	0.7	146		
	12/12/1995	2110	7	0.8	7						
	12/29/1995	6000	21	0.7	6	29	19	5	67		
	02/05/1996	3200	11								
	05/14/1996	*1383*	5			13	105	1	205		
	06/05/1996	2511	9			17	111	2	73		
	Average	2814	11	1.0	9	19					
	stdev	1521	5	0.5	4	7					

AN-103	Headspace Peff =	1717 m3 1.9 atm		[H2] = number =	0.6 1			ERROR MINIMIZATION SOLUTION			
	Date	Max H2 (ppm)	(peak/headsp) Release (m3)	Level drop (cm)	(level drop) Release (m3)	(integrate SHMS) Release (m3)	Calc. vent rate (cfm)	base rate (cfm)	time const. (hours) (MIN)	base rate #2 (cfm)	time const. #2 (hours)
	08/22/1995	*1600*	5	1.2	9	4	67	5	20		

AN-104	Headspace Peff =	1321 m3 2 atm		[H2]= number =	0.46 7			ERROR MINIMIZATION SOLUTION			
	Date	Max H2 (ppm)	(peak/headsp) Release (m3)	Level drop (cm)	(level drop) Release (m3)	(integrate SHMS) Release (m3)	Calc. vent rate (cfm)	base rate (cfm)	time const. (hours) (MIN)	base rate #2 (cfm)	time const. #2 (hours)
	11/06/1994	3050	9	2.8	23	11	81	4	45		
	02/16/1995	2089	6	1.6	13	7	71	4	31		
	08/03/1995	480	1								
	10/02/1995	*3068*	9	-1.3	11	11	91	6	29		
	10/05/1995	1000						48	2		
	10/08/1995	*1800*	5	0.7	6	5	55	78	1.7		
	05/03/1996	6109	18	1.5	12	20	79	26	12.5		
	05/01/1997	2250	6			8	132	6	20		
	average	2399	8	1	10	10					
	stdev	1841	5	1	3	6					

AN-105	Headspace	1024	m3	[H2] =	0.6						
	Peff =	2.09	atm	number =	3						
									ERROR MINIMIZATION SOLUTION		
	Date	Max H2 (ppm)	(peak/headsp) Release (m3)	Level drop (cm)	(level drop) Release (m3)	(integrate SHMS) Release (m3)	vent rate (cfm)	base rate (cfm)	time const. ~~(hours)~~ (MIN)	base rate #2 (cfm)	time const. #2 (hours)
	08/21/1995	17000	29	3.6	31						
	05/30/1996	14500	25	1.7	15	35	37	75	9.8		
	04/05/1997	6980	12	1	9	18	102	18	21.6		
	09/25/1997	770					45	1.4	22.7		
	average	7417	18	1	12	27					
	stdev	6875	9	0	4	12					

Predictive Models for Buoyant GRE's in Hanford Waste Tanks

Perry Meyer
PNNL

Stage II Experts' Panel Elicitation Workshop #1
January 19-23, 1998,
Richland, Washington

Predictive Models For Buoyant GREs

Perry Meyer **PNNL**

The large episodic gas release events (GREs) historically observed in the DSTs on the FGWL are believed to be caused by the *buoyant displacement* mechanism (Stewart 1996b). In a buoyant displacement, a portion, or "gob," of the nonconvective layer near the tank bottom accumulates gas until it becomes sufficiently buoyant to overcome the weight and strength of material restraining it. At that point it suddenly breaks away and rises through the supernatant liquid layer. The stored gas bubbles expand as the gob rises, failing the surrounding matrix, so a portion of the gas can escape from the gob into the head space.

Buoyancy tends to destabilize the nonconvective layer, while the material yield stress stabilizes it. A buoyant displacement can occur when local void fraction is high enough to produce a net upward buoyant force in the nonconvective layer. However, the yield stress of the bulk solids will keep the gob from rising until the buoyant force exceeds the strength of the layer. Therefore the void fraction must be significantly greater than the neutral buoyancy value before a buoyant displacement can begin. A simple relation is derived for the critical void fraction of a plane layer that agrees well with the results from scaled buoyant displacement experiments.

The magnitude of the effect of the yield stress depend on the shape of the gob as well as its size. The shape effect depends on the ratio of the surface area to volume. For large gobs, the effect of material strength is minimal, and the critical void fraction is approximately neutral buoyancy. However, small gobs have a higher surface-to-volume ratio and require a much higher void fraction. To first order, gobs with a diameter approximately equal to the nonconvective layer depth may be the most probable. Better estimates are obtained with a detailed stability analysis.

At the onset of a buoyant displacement, the yield stress of the nonconvective material is exceeded, and the material around the participating gob begins to flow. Assuming that at this point the entire nonconvective layer behaves as a viscous fluid, the length scale can be estimated from the Rayleigh-Taylor theory for superposed fluid layers of different densities and viscosities. This analysis allows both the size and critical void fraction of a gob to be determined and leads to a method to predict the gas release volume and frequency of buoyant displacements in the six FGWL DSTs. The estimates compare quite well with actual tank behavior as derived from the waste level history.

Basic energy conservation principles can be applied to the buoyant displacement process to determine the conditions required for it to release gas. A simple predictive model is derived that describes the energy requirements of buoyant displacement in terms of estimated or measurable parameters. The model establishes a criterion for gas release by a buoyant displacement. The total amount of energy stored in a gob of gas-bearing solids must exceed the energy required to yield the gas retaining matrix. The model is compared with data from scaled experiments and applied to the six DSTs on the FGWL. The conclusion is that a relatively deep layer of supernatant liquid is required for buoyant displacement to occur. This condition currently exists only in the DSTs.

The phenomenon of void growth leading up to buoyant displacement is being explored in an on-going study. The goal of this model is to predict under what circumastances sufficient void is retained in order to initiate a buoyant displacement.

The models discussed above, and the data on which they are based, allow us to evaluate these tanks' gas release potential. We now know how much gas they contain, its composition, and where it is stored; we also understand how the gas is released, and we can estimate how much gas will be released and how often. Though these models are not, and possibly cannot be, formally validated, they represent our best understanding and are consistent with the available knowledge base.

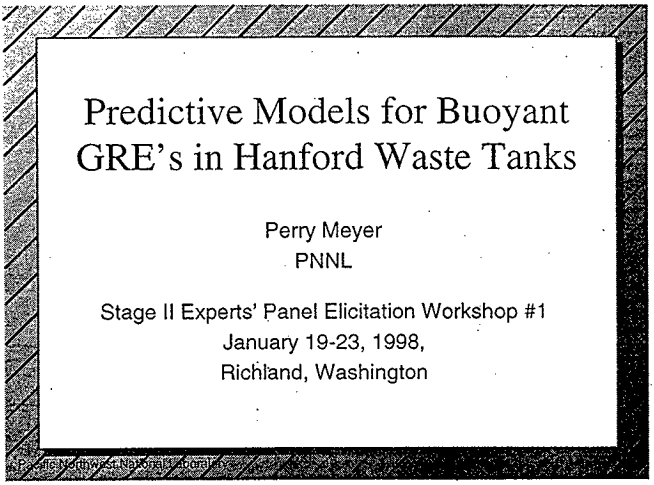
Predictive Models for Buoyant GRE's in Hanford Waste Tanks
Perry Meyer
PNNL
Stage II Experts' Panel Elicitation Workshop #1
January 19-23, 1998,
Richland, Washington
Pacific Northwest National Laboratory

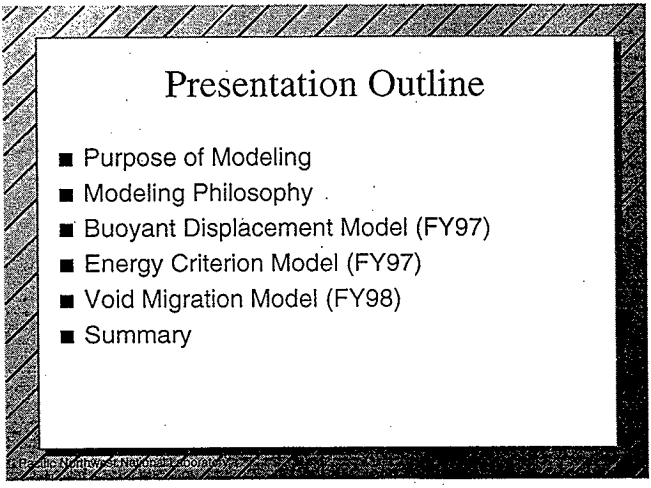
Presentation Outline
Purpose of Modeling
Modeling Philosophy
Buoyant Displacement Model (FY97)
Energy Criterion Model (FY97)
Void Migration Model (FY98)
Summary
Pacific Northwest National Laboratory

Purpose of Modeling

- Observation: Episodic GRE's occur in some tanks but not others. Both size and frequency of GRE's vary.
- Seek to predict under what circumstances, what size, and how often GRE's occur.
- Understand current tanks and predict/avoid future GRE situations.

Pacific Northwest National Laboratory

Modeling Philosophy

While waste tank behavior appears very complex, first order behavior may be dominated by simple physical law and basic scale

- Identify dominant physical processes.
- Simplify as much as possible.
- Use best available data as model inputs.
- Compare with historical data & tune.

Pacific Northwest National Laboratory

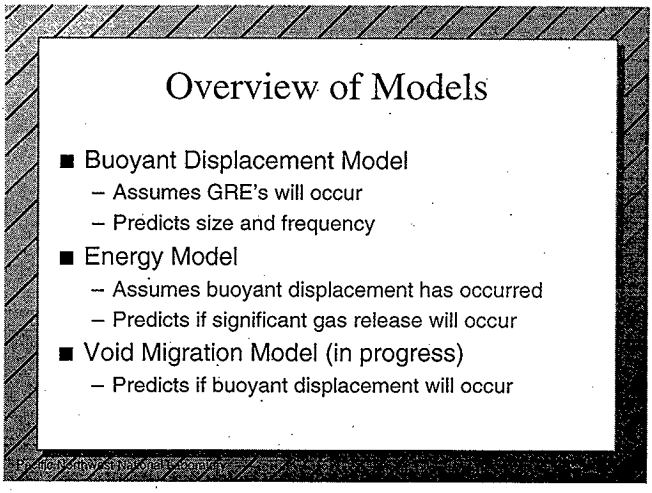
Overview of Models
Buoyant Displacement Model
– Assumes GRE's will occur
– Predicts size and frequency
Energy Model
– Assumes buoyant displacement has occurred
– Predicts if significant gas release will occur
Void Migration Model (in progress)
– Predicts if buoyant displacement will occur

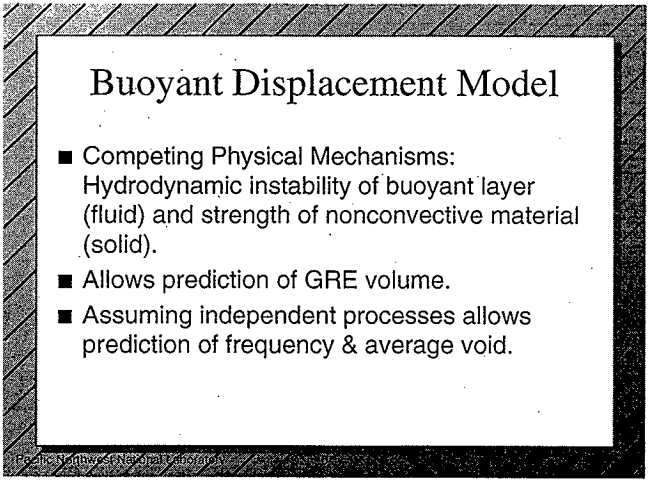
Buoyant Displacement Model
Competing Physical Mechanisms: Hydrodynamic instability of buoyant layer (fluid) and strength of nonconvective material (solid).
Allows prediction of GRE volume.
Assuming independent processes allows prediction of frequency & average void.

The Rayleigh-Taylor Instability

- Doubly infinite density-stratified layer of two Newtonian Fluids
- Analytic solution available for $\mu_L << \mu_B$ and $\Delta\rho/\rho << 1$
- $\lambda=2\pi[\mu_B^2/g(\rho_L^2-\rho_B^2)]^{1/3}$
- $D_0 \sim \lambda$

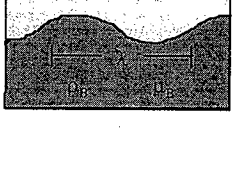

Material Strength Effects on Initial Buoyancy

- Buoyant Force:
  $F_B = (\rho_B-\rho_L)gV_0$
- Shear Force:
  $F_\tau = \tau S_0$
- Critical Void Fraction

$\alpha_c=\alpha_{NB}+(1-\alpha_{NB})(\tau S_0/\rho_L g V_0)$

$\alpha_{NB}=1-\rho_L/\rho_s$

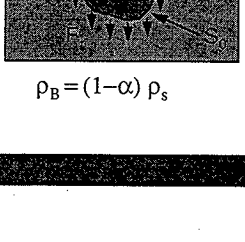

$\rho_B=(1-\alpha)\rho_s$

Evidence of Material Strength Effect on Critical Void

- Comparison with Scaled Experimental Data (Gauglitz)
- Gas generated in bentonite sludge until buoyant displacement occurs.
- Assume gob volume is plane layer.

h_s [cm]	ρ_s [Kg/m^3]	τ_y [Pa]	α_{KB} Eq. (4.2.7)	$\overline{\alpha}_C$ Measured	$\overline{\alpha}_C$ ($\beta = 1$)	$\overline{\alpha}_C$ ($\beta = \sqrt{3}$)
4.7	1087	67	0.08	0.25	0.21	0.31
4.8	1070	14	0.07	0.15	0.10	0.12
1.5	1070	14	0.07	0.19	0.15	0.22

Results for Cylindrical Gobs

Calculated Value	AN-103	AN-104	AN-105	AW-101	SY-101	SY-103
Gob Diameter (m) Eq. (4.3.26)	9 ± 2	8 ± 2	9 ± 2	8 ± 2	13 ± 3	9 ± 2
Number of gobs Eq. (4.4.9)	7 ± 4	8 ± 4	7 ± 3	8 ± 4	3 ± 1	7 ± 4
Critical Void (%) Eq. (4.3.16)	13 ± 6	10 ± 4	11 ± 3	10 ± 3	13 ± 5	7 ± 4
Release Fraction (%) Eq. (4.4.1)	52 ± 8	52 ± 5	54 ± 5	57 ± 6	60 ± 6	49 ± 8
GRE Std Vol. (m^3) (Historical) Eq. (4.4.4)	15±9 (14 ± 4)	21 ± 10 (23 ± 16)	28 ± 11 (26 ± 11)	15 ± 7 (14 ± 10)	128 ± 59 (131 ± 47)	7 ± 4 13 ± 6)
GRE Period (days) (Historical) Eq. (4.4.11)	100 ± 95 (160 ± 20)	180 ± 130 (120 ± 90)	210 ± 170 (160 ± 130)	120 ± 75 (190 ± 190)	110 ± 70 (100 ± 24)	40 ± 40 (90 ± 70)
NCL Avg. Void (%) Eq. (4.4.13) (VFI)	9 ± 5 (10.7 ± 1.0)	7 ± 3 (6.2 ± 0.9)	8 ± 2 (4.2 ± 0.8)	7 ± 2 (3.8 ± 0.6)	9 ± 3 (~8)	5 ± 5 (6.0 ± 2)

Simplified Model

- An approximate solution is obtained which demonstrates functional dependence

$$VREL \approx 750(\rho_s - 1)\alpha_{NB}H(\tau_y/\rho_L)$$

Standard Volume (m³)	AN-103	AN-104	AN-105	AW-101	SY-101	SY-103
Approximate Solution	14 ± 8	14 ± 6	29 ± 12	19 ± 8	100 ± 62	6 ±4
Full Solution	12 ± 7	17 ± 7	32 ± 13	17 ± 8	117 ± 76	7 ± 5
Historical Average	14 ± 4	23 ± 16	26 ± 11	14 ± 10	131 ± 47	13 ± 6
Revised Average	- ± -	10 ± 6	27 ± 12	19 ± 7	142 ± 44	12 ± 9

Energy Criterion Model

- Buoyant displacement model assumed gas release. Energy model determines if gas release will occur.
- Model compares potential buoyant energy with strain energy.
- Assumes gas will be released if NC material matrix yields
- Example: dropping an egg.

Buoyant Potential Energy

- Compressive work done on a gob by moving it from ambient to insitu.

$$E_b = \int_0^h F(z)dz \qquad F(z) = \Delta\rho g V = \alpha_0 \rho_L V_0 g\left(\frac{\gamma+1}{1+\gamma z/h} - k\right)$$

$$\gamma = \rho_L g h / P_A \qquad k = \frac{\alpha_{NB}(1-\alpha_0)}{\alpha_0(1-\alpha_{NB})}$$

$$\boxed{E_b = \alpha_0 V_0 P_A \gamma[(1+1/\gamma)\ln(1+\gamma) - k]}$$

Pacific Northwest National Laboratory

Strain Energy

- Energy required to strain a volume of material is the work done by an externally applied force.

$$E_y = V_s \int_0^{\varepsilon} \tau d\varepsilon$$

- $\tau(\varepsilon)$ = externally applied stress
- ε_τ = strain at at yield
- Elastic energy assumed small compared with strain energy

$$\boxed{E_y = V_0 \varepsilon_y \tau_y (1-\alpha_0)}$$

Pacific Northwest National Laboratory

Sludge Stress-Strain Behavior

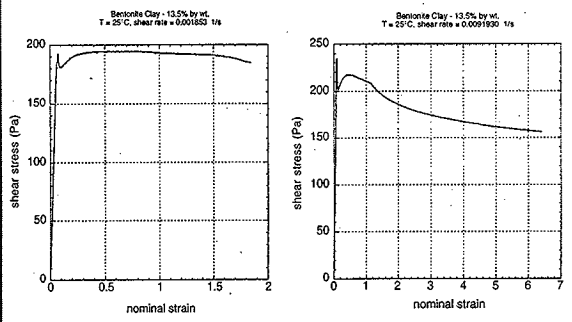

Pacific Northwest National Laboratory

The GRE Criterion

$$\frac{E_b}{E_y} = \frac{\alpha_0 P_A \gamma}{(1-\alpha_0)\varepsilon_y \tau_y}((1+1/\gamma)\ln(1+\gamma) - k)$$

- $E_b/E_y << 1$ expect no gas release
- $E_b/E_y >> 1$ expect large gas release

Pacific Northwest National Laboratory

Model Comparisons with Bentonite Simulant (Gauglitz)

ρ_s (kg/m^3)	α_0, α_{NB}	k	h_L (m)	γ	τ_y (Pa)	E_b/E_y	Energetic	Gas Release
1087	0.25, 0.087	0.286	0.105	0.010	67	2.6	Y	N
1087	0.25, 0.087	0.286	0.012	0.0012	67	0.30	N	N
1070	0.15, 0.07	0.426	0.101	0.0099	14	5.2	Y	Y
1070	0.20, 0.07	0.426	0.011	0.0011	14	0.81	N	Y

Energy Ratios for DST's

Gob Height h_g	AN-103	AN-104	AN-105	AW-101	SY-101	SY-103
Largest: $h_g = h_s/2$	26	49	52	44	24	13
Smallest: $h_g = 0$	18	29	31	35	11	8

- GRE Criterion:

  $E_b/E_y > 5$ for significant gas release during buoyant displacement

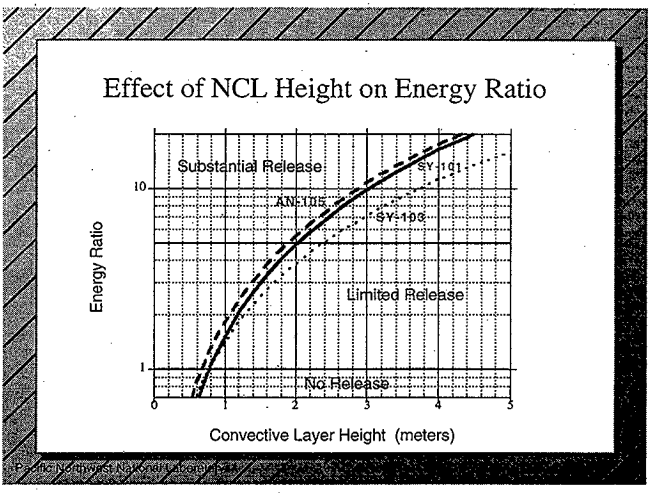
Effect of NCL Height on Energy Ratio
Substantial Release
SY-101
AN-105
SY-103
Limited Release
No Release
Energy Ratio
10
1
0
1
2
3
4
5
Convective Layer Height (meters)
Pacific Northwest National Laboratory

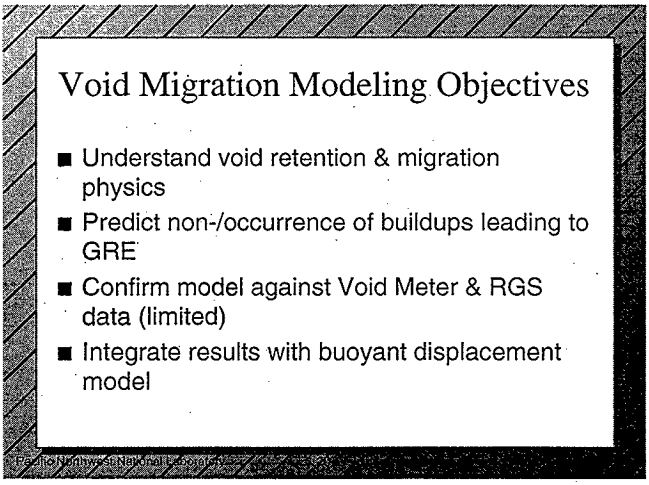
Void Migration Modeling Objectives
Understand void retention & migration physics
Predict non-/occurrence of buildups leading to GRE
Confirm model against Void Meter & RGS data (limited)
Integrate results with buoyant displacement model
Pacific Northwest National Laboratory

Key Physical Phenomenon

- Threshold for bubble motion
- Size-dependent bubble velocity
- Both size and number density as variables
- Variable viscosity

Summary

- We have two models with good qualitative and quantitative predictive capability for GRE's in DST's.
- They provide guidance for predicting and avoiding GRE's in new tanks.
- The key issue of void build up leading to GREs is presently being addressed.

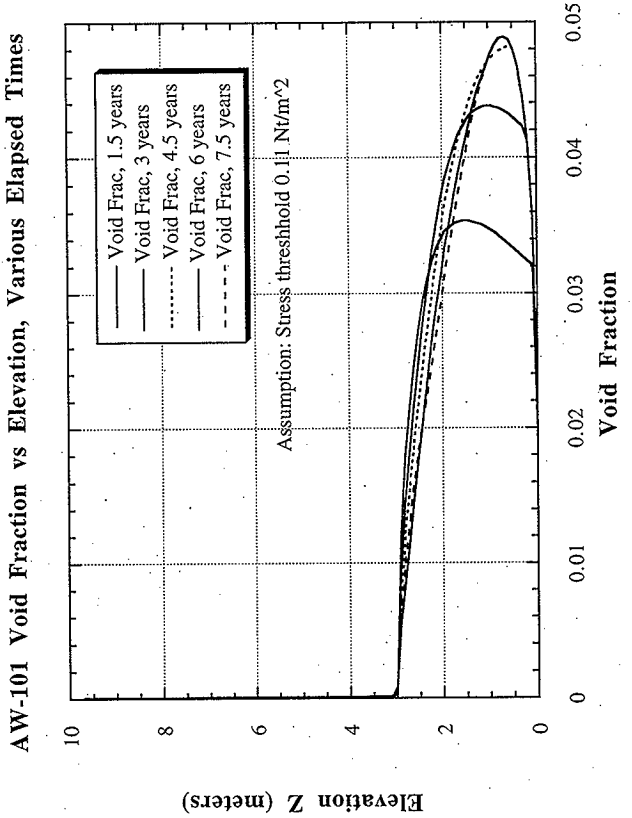
AW-101 Void Fraction vs Elevation, Various Elapsed Times
Void Frac, 1.5 years
Void Frac, 3 years
Void Frac, 4.5 years
Void Frac, 6 years
Void Frac, 7.5 years
Assumption: Stress threshhold 0.1|1 Nt/m^2
Elevation Z (meters)
Void Fraction
0
2
4
6
8
10
0
0.01
0.02
0.03
0.04
0.05

Properties & Parameters used in Models

Property/Parameter	AN-103	AN-104	AN-105	AW-101	SY-101	SY-103
1. CL Density (kg/m³)	1530 ± 50	1440 ± 30	1430 ± 30	1430 ± 30	1500 ± 70	1470 ± 3
2. Nonconvective Layer Density (kg/m³)	1730 ± 110	1590 ± 60	1590 ± 40	1570 ± 30	1700 ± 50	1570 ± 5
3. Waste Level (cm)	884 ± 5	979 ± 4	1041 ± 7	1040 ± 7	1054 ± 10	691 ± 3
4. CL Depth (cm)	413 ± 16	524 ± 10	559 ± 11	693 ± 19	470 ± 8	337 ± 19
5. Nonconvective Layer Depth (cm)	379 ± 9	415 ± 9	452 ± 11	283 ± 22	584 ± 40	334 ± 25
6. Stationary Layer (cm)	175 ± 25	33 ± 33	55 ± 55	55 ± 55	40 ± 40	128 ± 8
7. Eff. Nonconvective Layer Depth (cm)	204 ± 27	383 ± 34	397 ± 56	228 ± 59	544 ± 57	207 ± 26
8. NB Void Fraction (%)	12 ± 6	9 ± 4	10 ± 3	9 ± 3	12 ± 5	6 ± 4
9. Nonconvective Layer Void Fraction (%)	10.7±1.0	6.2±0.9	4.2±0.8	3.8±0.6	~8	6±2
10. Nonconvective Layer Pressure Ratio	1.87±0.03	1.97±0.03	2.09±0.04	2.11±0.04	2.30±0.10	1.69±0.0
11. Nonconvective Layer Yield Stress (Pa)	170 ± 85	100 ± 50	110 ± 55	140 ± 70	275 ± 130	140 ± 70
12. Nonconvective Layer Viscosity (Pa-s)	15,000	9,000	10,000	12,000	25,000	13,000
13. GRE Std. Volume (m³)	14 ± 4	23 ± 16	26 ± 11	14 ± 10	131 ± 47	13 ± 6
14. GRE Period (days)	160 ± 120	120 ± 90	160 ± 130	190 ± 190	100 ± 24	90 ± 70
15. Level Rise (cm/day)	0.04±0.02	0.03±0.01	0.03±0.02	0.03±0.004	0.24±0.06	0.05±0.0

Pacific Northwest National Laboratory

Mixer Pump Operations

Nick Kirch, LMHC

Mitigation of Tank 241-SY-101

- Mitigation by mixing selected as preferred concept for testing.
- Existing 150 horsepower submersible centrifugal pump with design flow of 2,800 gallons per minute and shutoff head of 120 feet modified for application.
- Pump uses 480 volt oil-cooled induction motor.
- Pump installed on July 3, 1993.

Mixer Pump Information

- Mixer Pump was installed in 241-SY-101 on July 3, 1993 to mitigate gas releases.
- Pump is 150 hp, 10,600 liter per minute with shut off head of 37 m.
- Discharge near bottom of tank.
- Suction about mid tank.

Tank 241-SY-101 Hydrogen Mitigation Test Pump

Testing

- Phase A was short term low speed operations. (Pump bump to keep nozzle unplugged more aggressive.)
- Phase B was 24 runs to attempt to slowly release gas. Completed December 17, 1993.
- Full-Scale Testing to test ability to control tank. Completed April 13, 1994.
- Normal operation since then.

Mitigation Testing

Phase A (July 14, 1993 to July 25, 1993)
Low speed (340 rpm) tests of increasing durations (up to 10 minutes) in a single nozzle direction. Nozzle velocity was 15 feet per second.

Phase B (October 12, 1993 to December 17, 1993)
24 runs of extended durations, phased velocities and varying nozzle directions. Nozzle velocities reached 60 feet per second. Pump nozzles were rotated in 30 degree increments to cover entire tank. Pump run durations reached 3 hours.

Mitigation Testing (continued)

Full-Scale Testing

- Directional Pump Bumps (December 18, 1993 to February 2, 1994) - 3 pump bumps per week.
- Sequence 1 (February 4, 1994 to February 25, 1994) - 1 hour, 750 rpm runs varying nozzle orientation 30°, 3 times per week.
- Regrowth Test (February 28, 1994 to March 25, 1994) - 3 pump bumps per week.
- Knockdown Test (March 28, 1994 to March 30, 1994) - 6 pump runs of 30 minutes at 750 rpm in nozzle orientations 30° apart.
- Jet Penetration Test (April 6, 1994 to April 13, 1994) - 4 high speed tests (920 and 1000 rpm) directed Riser 17B multifunction tree.

Parameters Influenced by Mitigation

- Gas Release
  - — Release as monitored with gas measurements
  - — Release influenced by pump conditions
- Temperature Profile
  - — Temperature response shows that jet reaches MIT
  - — Pumping keeps temperature nearly uniform

Mixer Pump Profile

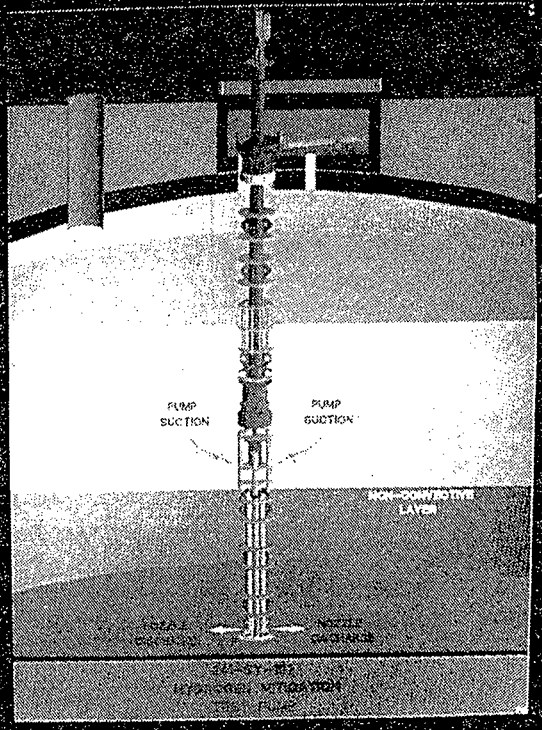

29408046.8

Mixer Pump on Crane

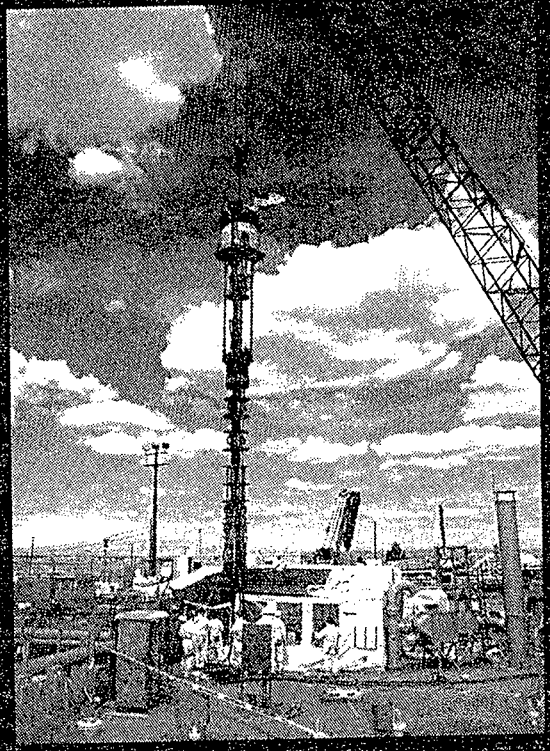

29408046. 7

Tank 241-SY-101
Gas Chromatograph 3 Hydrogen

Part A

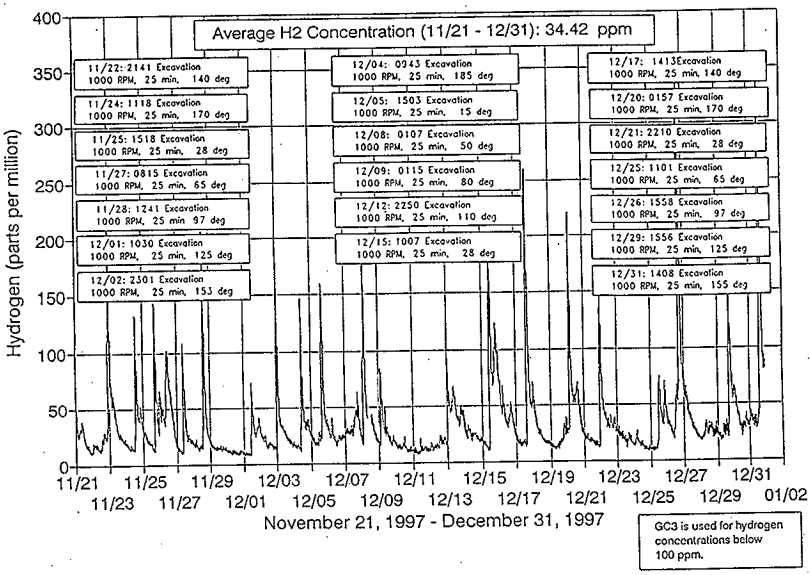

Tank 241-SY-101
FTIR Gas Compositions

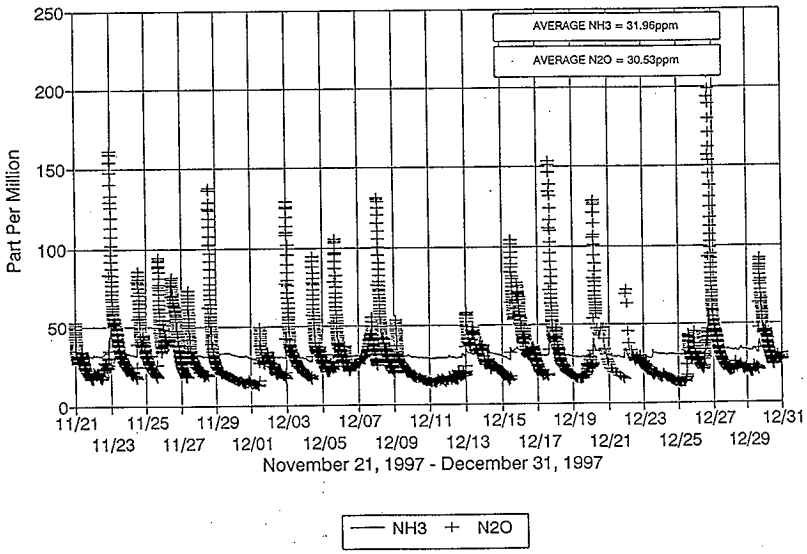

Pump Testing

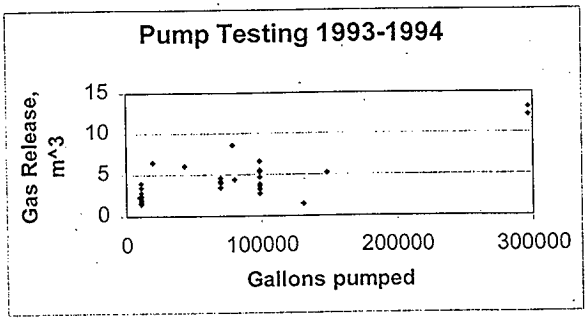

Nick-sy101.10 1/19/98

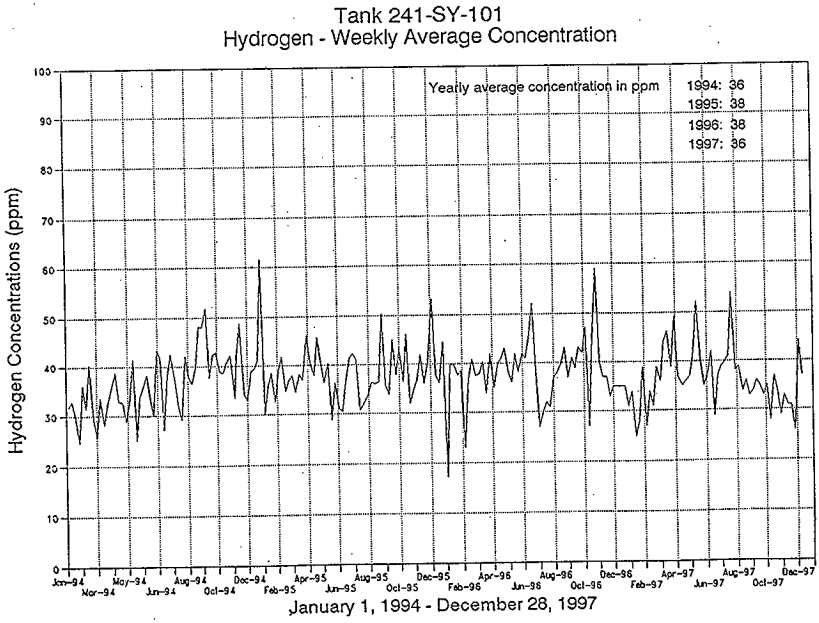

Tank 241-SY-101
N2O - Weekly Average Concentrations

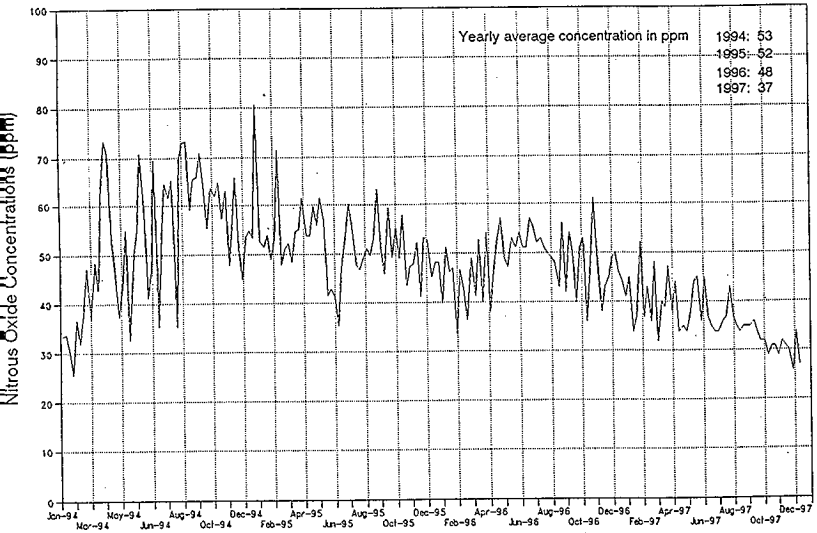

January 1, 1994 - December 28, 1997

Tank 241-SY-101
Ammonia - Weekly Average Concentration

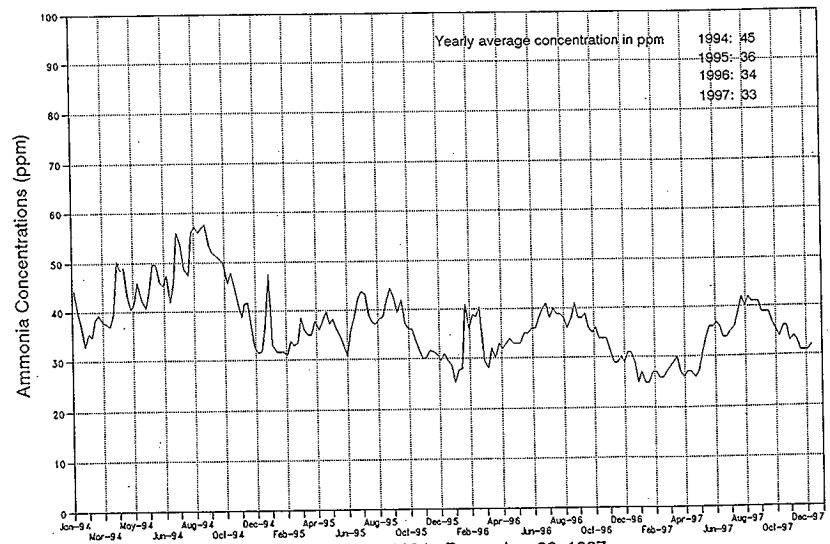

January 1, 1994 - December 28, 1997

241-SY-101
MIT 17C Validation Probes

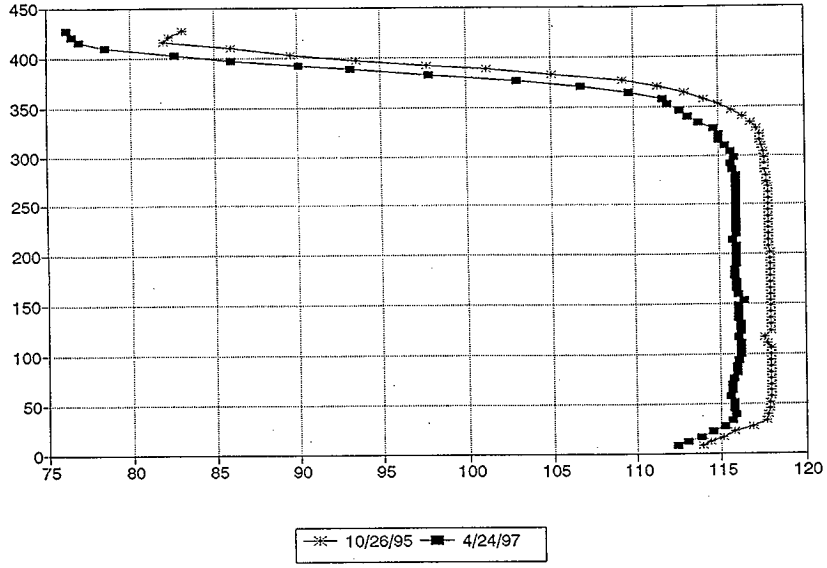

241-SY-101
MIT 17B Validation Probes

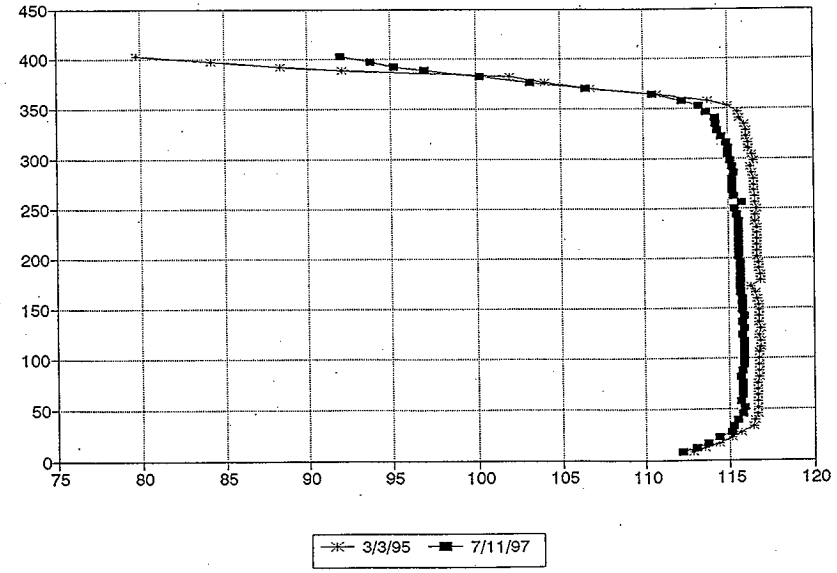

MIT-17B Bottom Temperatures Part A

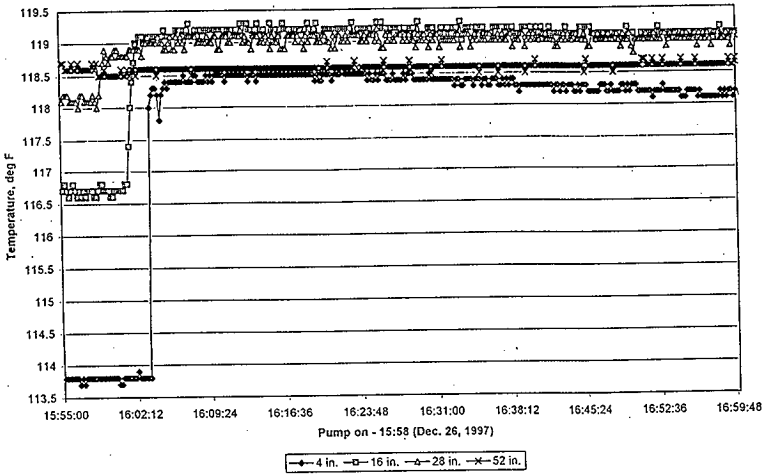

MIT 17C Bottom Temperatures

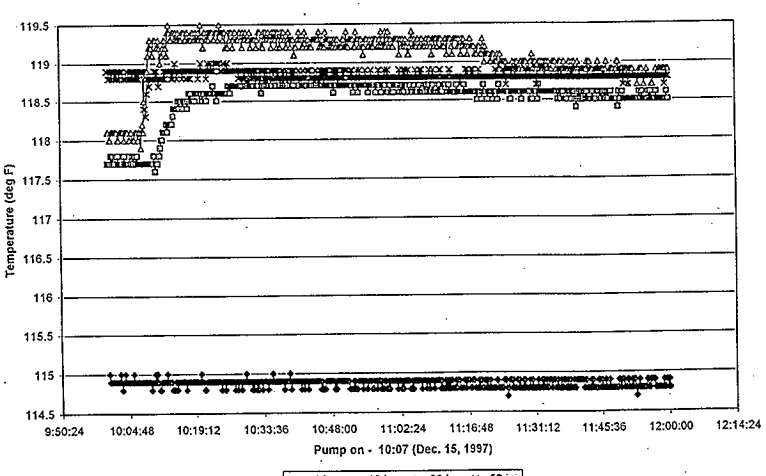

Waste Influenced by Pumping

- PNNL Models
- Temperature probe observations

Conclusions

- The mixer pump has worked as planned.
- The waste is influenced enough to cause gas to be released.
- This tank has been mitigated and removed from off USQ.

Part A

Pump Induced Flow Field

Pump operated at 5°/185°

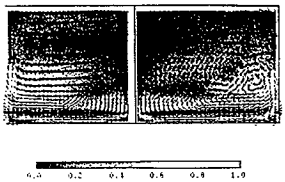

Side view in plane of jet

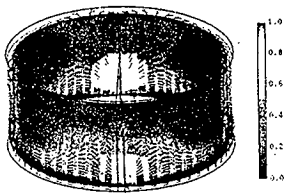

Near-wall flow field

Pump-Induced Flow Field

Pump operated at 5°/185°

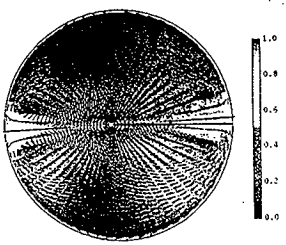

Plan view 2' above jet

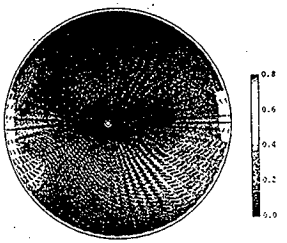

Plan view 7.5' above jet

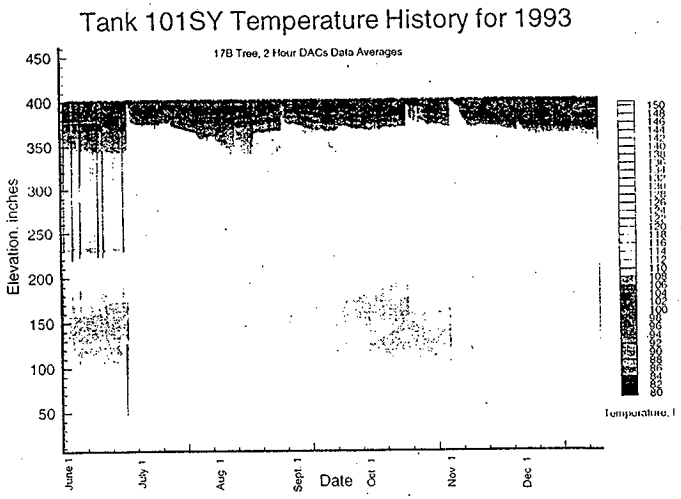

Figure 4.1. Full Temperature History at the 17B MIT (June 23-mid-January 1994)

Gas Generation Rates, Retained Gas Composition Data and Modeling

Daniel A. Reynolds, LMHC
T. Albert Hu, LMHC
David C. Hedengren, MACTEC-Meier

Stage II Experts' Panel Elicitation Workshop #1
Tuesday, January 20, 1998

Gas Generation Equations

- There have been a few experiments which measure rates.
- Will look at various forms.
- Will focus on hydrogen generation rates.
- Break down into thermal models and radioanalysis models.
- Ignore corrosion contribution.

Thermal Models

- Will look at two types.
- Will discuss which one is preferred and how to apply it.

Type I Thermal Model

$$Rate_{hydrogen} = Rate_{bl} * M * \frac{[TOC]*[Al]}{[TOC]_{bl}*[Al]_{bl}} * \exp[(\frac{-Ea}{R}*(\frac{1}{T}-\frac{1}{T_{bl}})]$$

M = total mass of liquid in tank
TOC = total organic carbon expressed as percent
Al = aluminum concentration expressed as percent
Ea = activation energy, 91 KJ
bl = base line - baseline tank is SY-103

Type I Thermal Model

- Ratios TOC, Al, and temperature to tank SY-103
- Implies that doubling the aluminum concentration doubles the rate.

Type II Thermal Model

$$Rate_{\ i} = A_i * e^{\frac{-Ea_i}{R*T}}$$

Ai = Rate Constant
Ea = Activation Energy
R = gas constant, 8.314 J/mol/K
T = temperature, Kelvin
i = hydrogen or nitrogen or nitrous oxide

Activation Energy, Ea

Source	H_2	N_2O	N_2
Bryan SY-103	91.3	116.7	83.7
PERSON SY-101	94	95	91
King S-102	91	79	127

Rate Constant, A

Source	H_2	N_2O	N_2
Bryan SY-103	1.4E+09	5.5E+12	1.1E+08
PERSON SY-101	1.58E+09	4.14E+09	7.27E+08
King S-102	2.1E+08	5.6E+05	5E+12

Thermal Model Summary

- The second type is preferred.
- Use for hydrogen only.
- The other gases will be derived by observed distributions discussed later.

Radioalysis

- This is added to the rate from thermal model.
- Radioalysis is predominate at tank temperatures.
- Several G values from different experiments.
- Nitrate and nitrite lower the G value for water.

G Values

Source	H_2	N_2O	N_2
Bryan SY-103	0.14	0.033	0.011 0.533
King S-102	0.017	0.009	0.01
Meisel Synthetic for H_2O	0.031		

Radioalysis Summary

- Use the G value from Bryan.
- Use the Cs-137 and Sr-90 for radiation rate.

Rate Summary

- Radiation induced gas generation dominates at tank temperatures.
- Perhaps multiple pathways for gases other than hydrogen.
- Other gases will be based on distributions.

Gas Composition

- Two methods of looking at the data:
  - — Retained Gas Sampler/Drill String Correlation
  - — Ratios based on RGS, SHMS Grab samples, Vapor samples

RGS Correlation

- "Best" Gas Composition
- Limited Data Set
- 4 DSTs and 5 SSTs
- Set too small for correlation on tank average
- Additional data from drill string analysis
- There are 39 data sets on a segment basis

"Best" Correlation

- The "best" correlation stated that about 65% of the variability in the N_2/H_2 ratio is related to chromium concentration, nitrite concentration, total organic carbon, and carbonate concentration.

N_2/H_2 Ratio, Carbonate

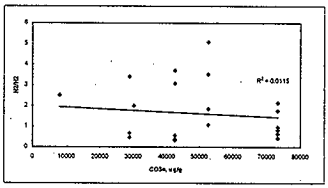

N2/H2 Ratio, Nitrate

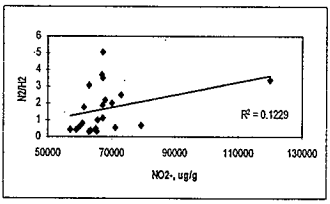

N2/H2 Ratio, TOC

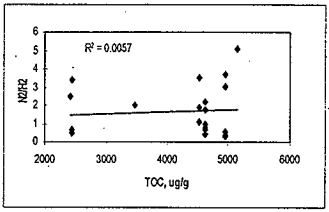

N2/H2 Ratio, Chromium

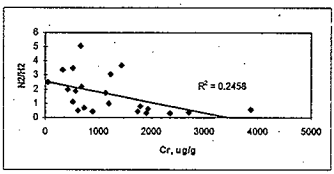

RGS Conclusions

- Data set too small for meaningful correlation.
- Does not look promising at this time.

Composition Distribution

- Use hydrogen from generation rate.
- Other gases use a ratio to hydrogen.
- Three sets of data:
  - RGS/Drill String
  - SHMS Grab Samples
  - Dome Vapor Samples

Composition Results

- N_2/H_2 ratios distribution based only on RGS
- N_2O/H_2 and CH_4/H_2 based on all three
- Use in a Monte Carlo type analysis
- Tri-Modal Distribution
  - Deconvolute?

N_2/H_2 Ratio Distribution

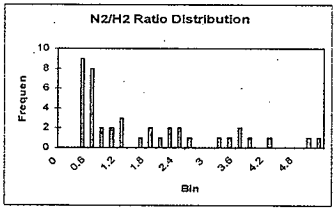

N_2O/H_2 Ratio Distribution

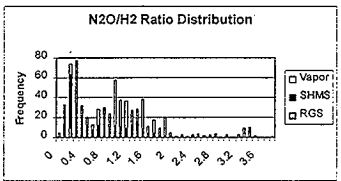

CH_4/H_2 Ratio

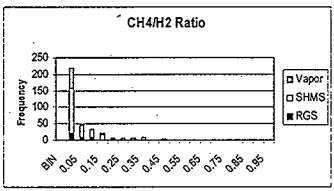

Composition Conclusions

- RGS/DRILL string not sufficient.
- Gas composition based on distribution is the method of choice for non-hydrogen gases.

Overall Conclusions

- Hydrogen volume will be based on the thermal rate equation and radiolytic G value.
- Other gas volumes will be based on distribution of gas-to-hydrogen ratios.
- Outcome will be a distribution of gas volume and composition.

DST Intrusive Data

- Five tanks representing 16.5 tank years of operations
- Locally waste disturbing operations include MIT installation, core sampling, liquid grab sampling, Void Fraction Instrument deployment, and viscometer deployment
- Only observed event during VFI deployment in AW-101

DST Intrusive Data

Tank	Start date	Dome Intrusive	Waste Intrusive	GREs
SY-103	Jan-96	1	1	0
AN-103	Sep-94	6	2	0
AN-104	Sep-94	5	2	0
AN-106	Sep-94	5	4	0
AW-101	Aug-94	4	6	1
Totals		21	15	1

Specific Examples of Releases

- Mixer Pump
  - ~800 Pump runs
  - All have shown releases
  - Small "natural" releases between pump runs

Double Shell Tank Intrusive Activity History

W. B. (Blaine) Barton
Lockheed Martin Hanford Co.
January 21, 1998

Agenda

- Observations on sources of data
- DST intrusive data
- Specific examples of activities and releases
- Conclusions

Observations on Sources of Data

- Must be able to detect the release
  - Level change
  - Pressure change
  - SHMS
- None of these systems is capable of detecting small GREs ~10 Ft^3
- SHMS can detect smaller releases than level or pressure
- Only 6 of the 28 DSTs have observed GREs by level or pressure
- SHMS are only installed on tanks with observed GREs
- Three tank farms have SHMS on the exhaust stack
  - SY; AW; AN.

Tank 241-SY-101
Gas Chromatograph 1 Hydrogen
November 21, 1997 - December 31, 1997

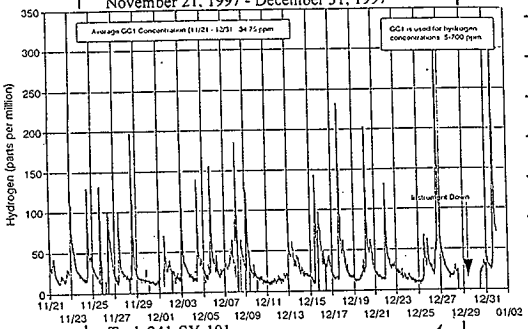

Tank 241-SY-101
Gas Chromatograph 1 Hydrogen
January 01, 1998 - January 15, 1998

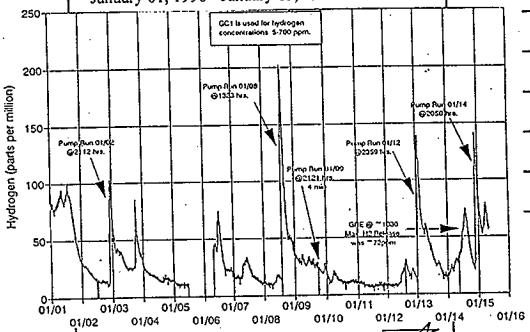

Transfer of Waste

- November 1997 transfer from Catch Tank A-417 to AN-101
- Observed small increase in the tank farm stack to ~100 ppm

January 21, 1998 12 Name-hnf.ppt

1

Waste Level History - October 1994 to October 1995

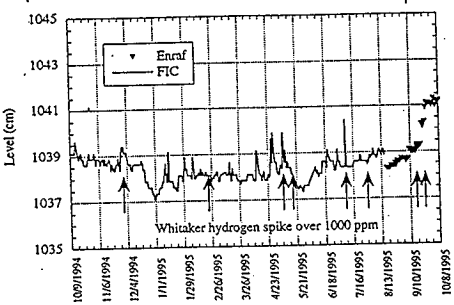

Hydrogen Concentration History During Deployment

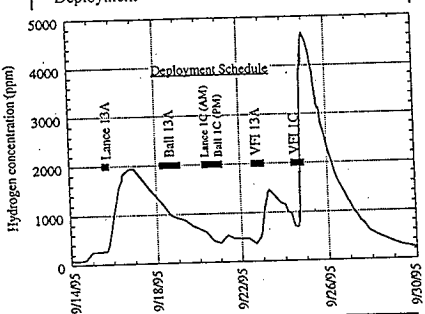

Sequence of Gas Release Compared with VFI Deployment

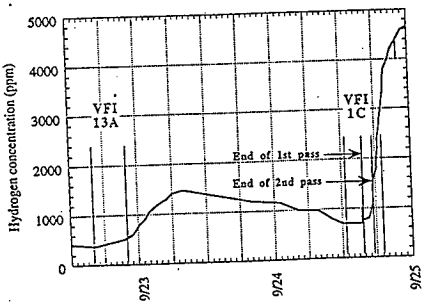

AN Stack SHMS Hydrogen
November 16, 1997 - November 29, 1997

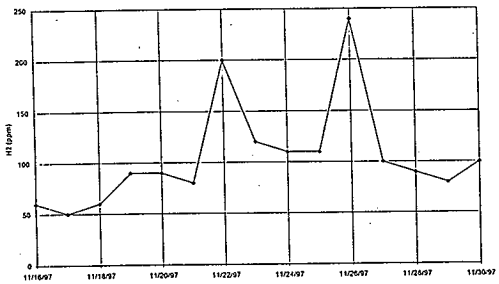

Air Lift Circulator Operation

- On January 11, 1998 the air lift circulators in AY-102 were turned on
- The SHMS showed an increase from 20 to 107 ppmv H_2

Tank 241-AY-102
Gas Chromatograph hydrogen
January 10, 1998 - January 12, 1998

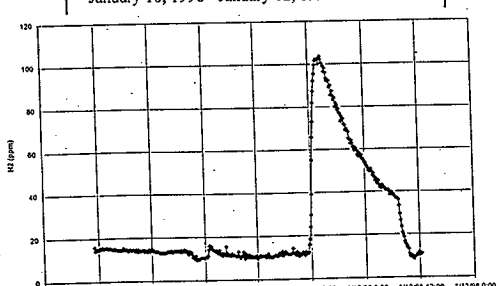

Conclusion

- Locally waste disturbing activities do not trigger BD-GREs unless tank is near conditions for a spontaneous BD-GRE
- Global waste disturbance releases gas held in disturbed areas.

Westinghouse Hanford Company

Documentation of Induced BD-GRE

Internal Memo

74A10-96-015

From: Waste Tanks Process Engineering
Phone: 373-5154
Date: January 23, 1996
Subject: RECENT GAS RELEASES IN TANK 241-AW-101

To: G. D. Johnson S7-15

cc:

W. B. Barton	R2-11	J. P. Sloughter	R2-54
D. B. Engelman	R1-49	R. J. Van Vleet	A3-34
B. M. Hanlon	R1-80	K. A. White	R2-70
G. R. Sawtelle	A3-37	S. U. Zaman	R3-08
E. R. Siciliano	H0-31	NEW File/LB	

Reference: PNL-MIT-110195, "In Situ Determination of Rheological Properties and Void Fraction: Hanford Waste Tank 241-AW-101," dated October 1995.

Waste tank 241-AW-101 (101-AW) is on the Flammable Gas Watch List. Gas release events (GREs) occurred in this tank on September 15, 22, 24, October 16, December 12 and 29, 1995. The September GREs are related to instrument deployments within the tank's waste. Gas release events occur in this tank every one or two months.

Hydrogen levels in the tank's vent header are monitored with two Whittaker cells. One cell has a range of 0-1 percent, and the other has a range of 0 - 10 percent. Attachment 1 shows the response of the narrow range Whittaker cell since September 1994. The hydrogen concentration began to rise at about 5 p.m. on September 15, 1995, from a 100 ppm baseline. It reached a maximum of 1930 ppm at about 8 p.m. on September 16 (see Attachment 2). Attachment 3 shows the waste surface level since September 1994. The surface level rose 0.1 inches between September 15 and 16 and remained at that level. This gas release occurred soon after water lancing was completed prior to insertion of a ball rheometer (a viscosity measurement device) in Riser 13A. The water did not penetrate past the sludge layer; therefore, the gas released must have originated from just below the crust. Integrating under the hydrogen curve (assuming a 15 cfm vent flow rate) totals a release of 150 ft^3 of hydrogen (see Reference). No changes were noted in the waste temperature profile.

Another gas release began on September 22 at about 9 p.m. The hydrogen concentration rose from 400 ppm to 1400 ppm within ten hours (see Attachment 2). It began to increase again on September 24, rising from 700 ppm to 4660 ppm within seven hours. These releases correspond with two deployments of a void fraction instrument into the tank waste. This instrument did penetrate the sludge layer. Integrating under the hydrogen curve from September 22 through 29 (assuming a 15 cfm vent flow rate) totals about 220 ft^3 of released hydrogen (see reference). Hydrogen levels had returned to 100 ppm by October 1. The surface level rose 0.75 inches between September 21 and 27. No changes were noted in the waste temperature profile.

A third gas release began on October 16, 1995, at about midnight. Hydrogen rose from a baseline concentration of 100 ppm to a 1750 ppm peak within 12 hours (see Attachment 4). The concentration had decayed to 200 ppm by October 24. The surface level fell 0.12 inches. No changes were noted in the waste temperature profile. The dome pressure stripchart showed a slight increase from -2.25 to -1.95 in. w.g. that began about 8 a.m. on October 16. The pressure remained elevated at -1.95 in. w.g. for about eight hours between 12 and 8 p.m. before returning to its earlier level.

Another gas release began on December 12, 1995, at about 6 a.m. The hydrogen concentration rose from a 800 ppm baseline and peaked 25 hours later at 2100 ppm. There were no sudden spikes in the hydrogen concentration (see Attachment 5). The surface level rose 0.23 inches between December 11 and 12 and then fell 0.27 inches between December 12 and 13, according to the ENRAF level gauge in riser 2A. According to the manual tape in riser 1A, the surface level rose 0.5 inches between December 11 and 12 and then fell 1.25 inches between December 12 and 13. No changes were noted in the waste temperature profile.

On December 29, beginning about noon, the hydrogen concentration began rising from a 400 ppm baseline, reaching 6000 ppm five hours later. The increase was steady (see Attachment 6). The concentration remained at about 6000 ppm for about six hours and then began to slowly decay. The surface level increased 0.3 inches between December 28 and 30. It fell back to its initial level by January 2, 1996. No significant temperature changes were seen near the thermocouple tree or the MIT. No dome pressure changes occurred at the time of the gas release.

An in-tank video was recorded on September 19, and still pictures were taken on November 15 and January 4, 1996. These pictures were compared with photos taken on September 7. Some crust changes occurred underneath the ENRAF level gauge between September 7 and 19. Otherwise, no crust changes were noted near the supernate pump or the ENRAF.

N. E. Wilkins

N. E. Wilkins, Engineer
Waste Tanks Process Engineering

Attachments (6)

74A10-95-015

ATTACHMENT
Recent Gas Releases in Tank 241-AW-101

Consisting of 6 Pages

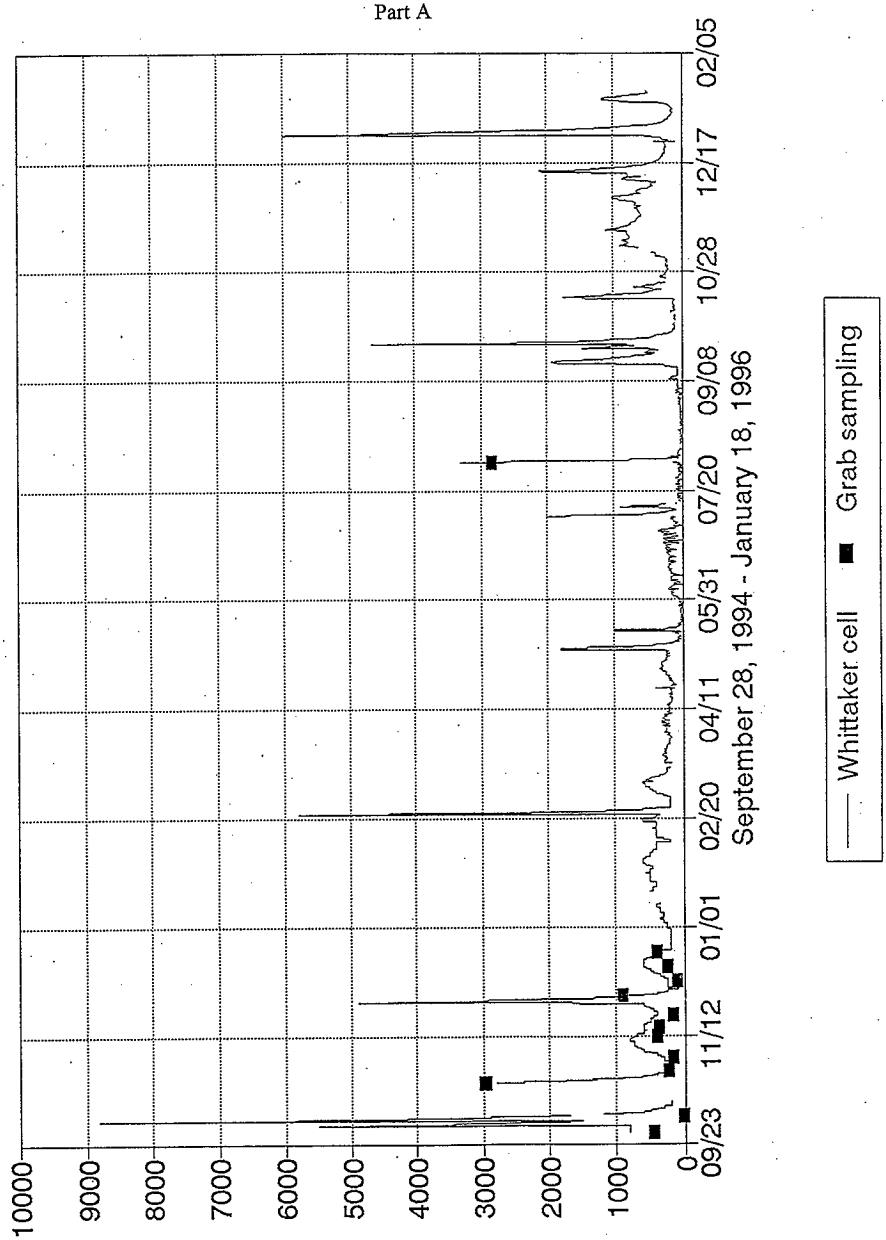
Tank 241-AW-101
Hydrogen Concentration
H2 (ppm)
10000
9000
8000
7000
6000
5000
4000
3000
2000
1000
0
09/23
11/12
01/01
02/20
04/11
05/31
07/20
09/08
10/28
12/17
02/05
September 28, 1994 - January 18, 1996
Whittaker cell
Grab sampling

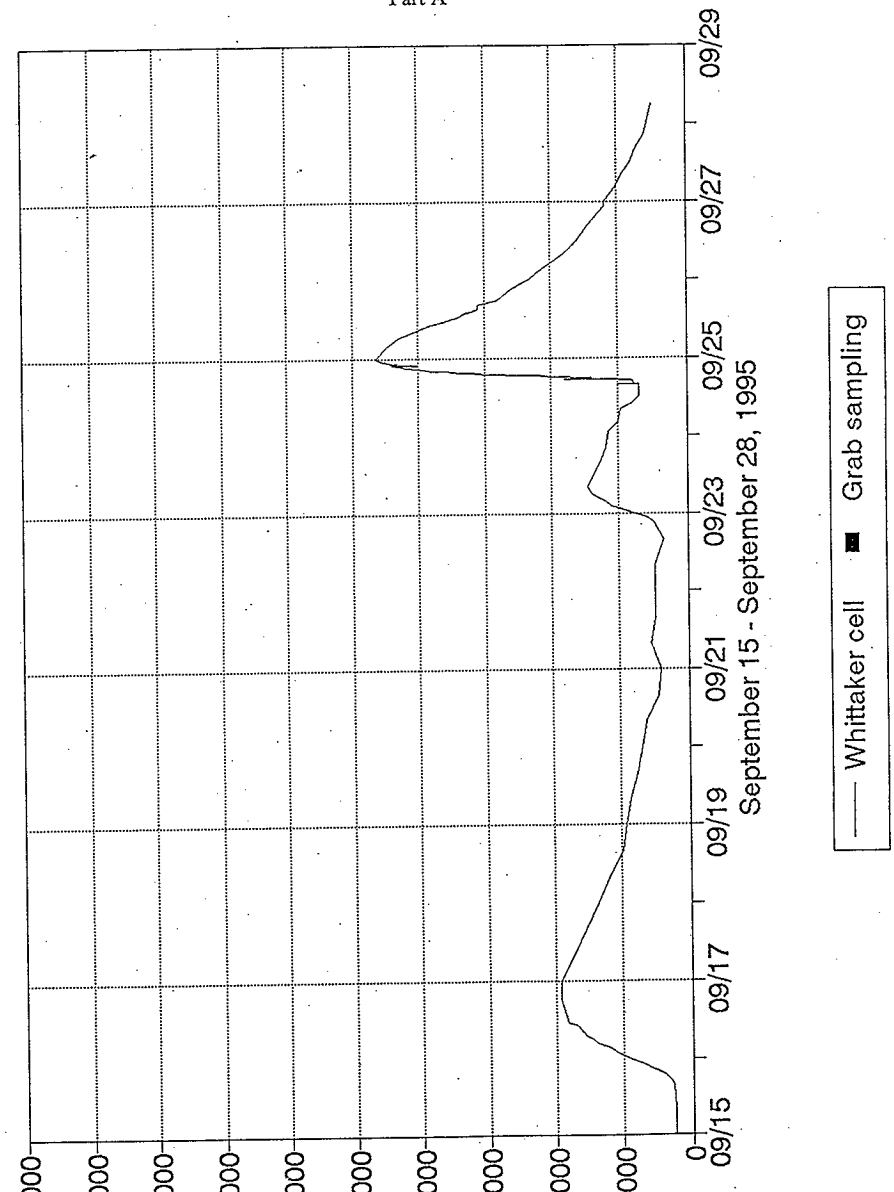
Tank 241-AW-101
Hydrogen Concentration
H2 (ppm)
10000
9000
8000
7000
6000
5000
4000
3000
2000
1000
0
09/15
09/17
09/19
09/21
09/23
09/25
09/27
09/29
September 15 - September 28, 1995
Whittaker cell
Grab sampling

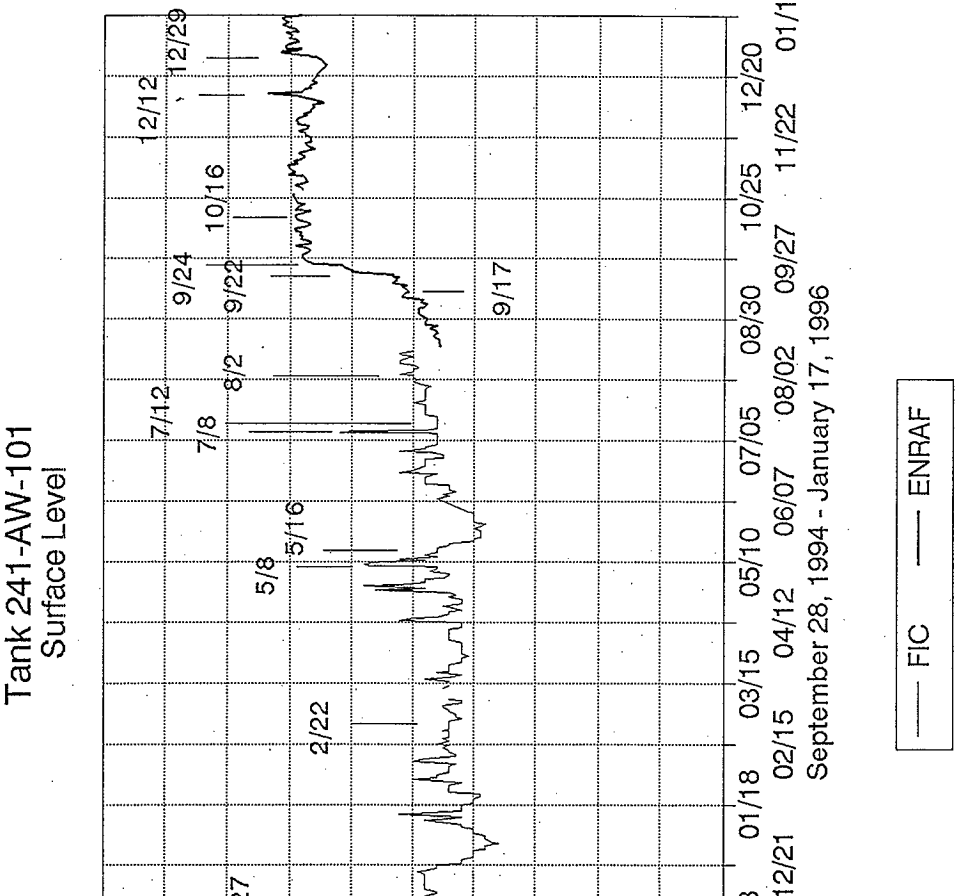
Tank 241-AW-101
Surface Level
Waste Height (in.)
411.5
411
410.5
410
409.5
409
408.5
408
407.5
407
406.5
09/28
10/26
11/23
12/21
01/18
02/15
03/15
04/12
05/10
06/07
07/05
08/02
08/30
09/27
10/25
11/22
12/20
01/17
September 28, 1994 - January 17, 1996
10/1
11/27
2/22
5/8
5/16
7/8
7/12
8/2
9/17
9/22
9/24
10/16
12/12
12/29
FIC
ENRAF

Tank 241-AW-101
Hydrogen Concentration

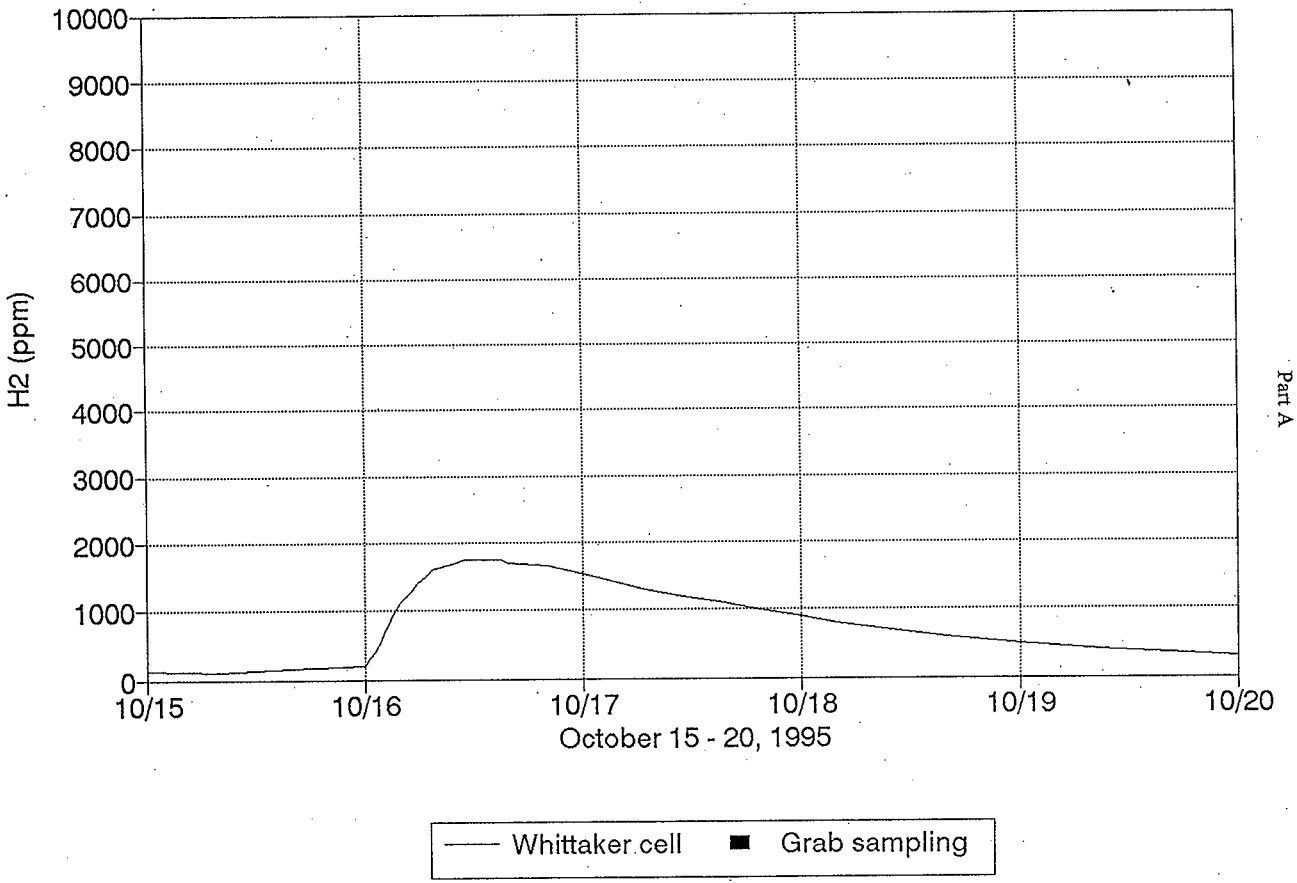

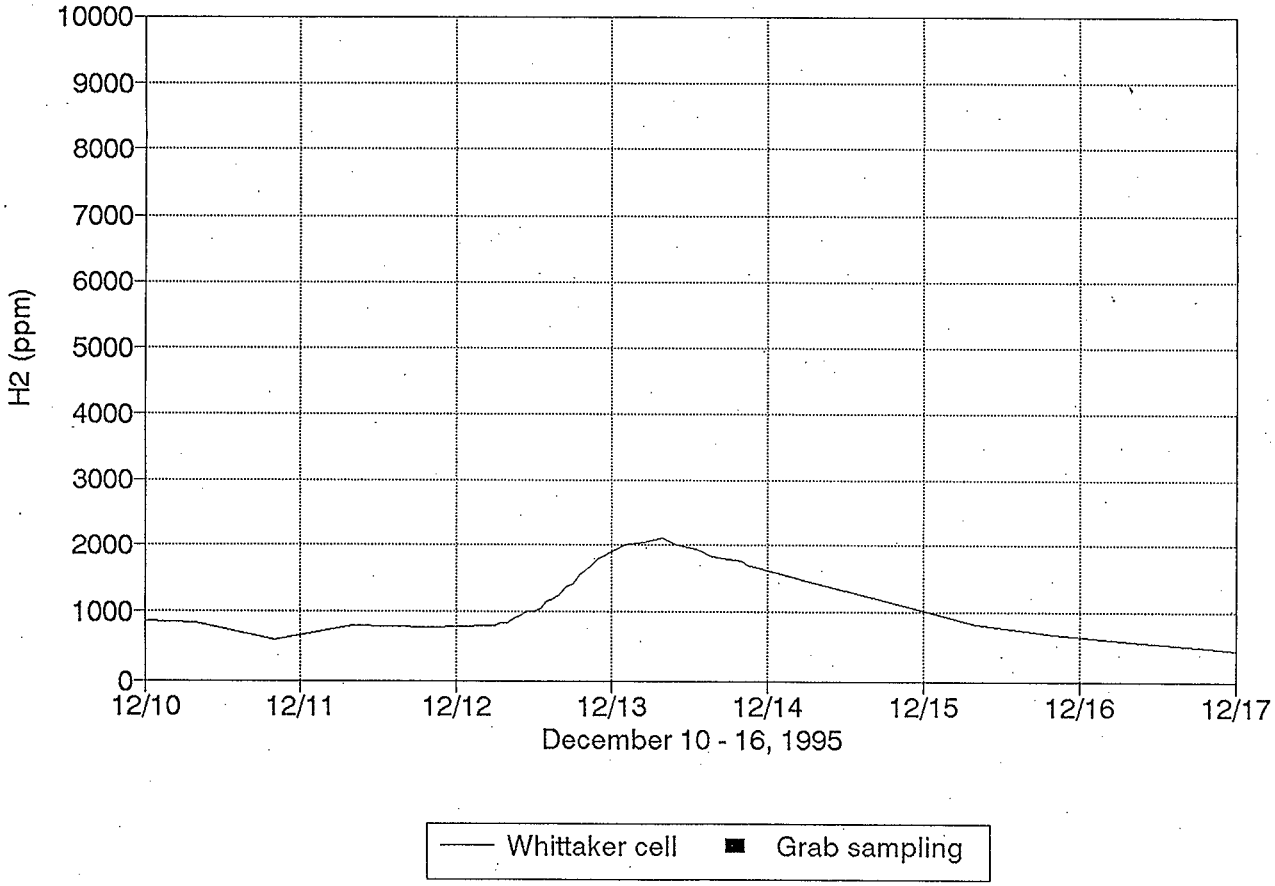
Tank 241-AW-101
Hydrogen Concentration
H2 (ppm)
10000
9000
8000
7000
6000
5000
4000
3000
2000
1000
0
12/10
12/11
12/12
12/13
12/14
12/15
12/16
12/17
December 10 - 16, 1995
Whittaker cell
Grab sampling

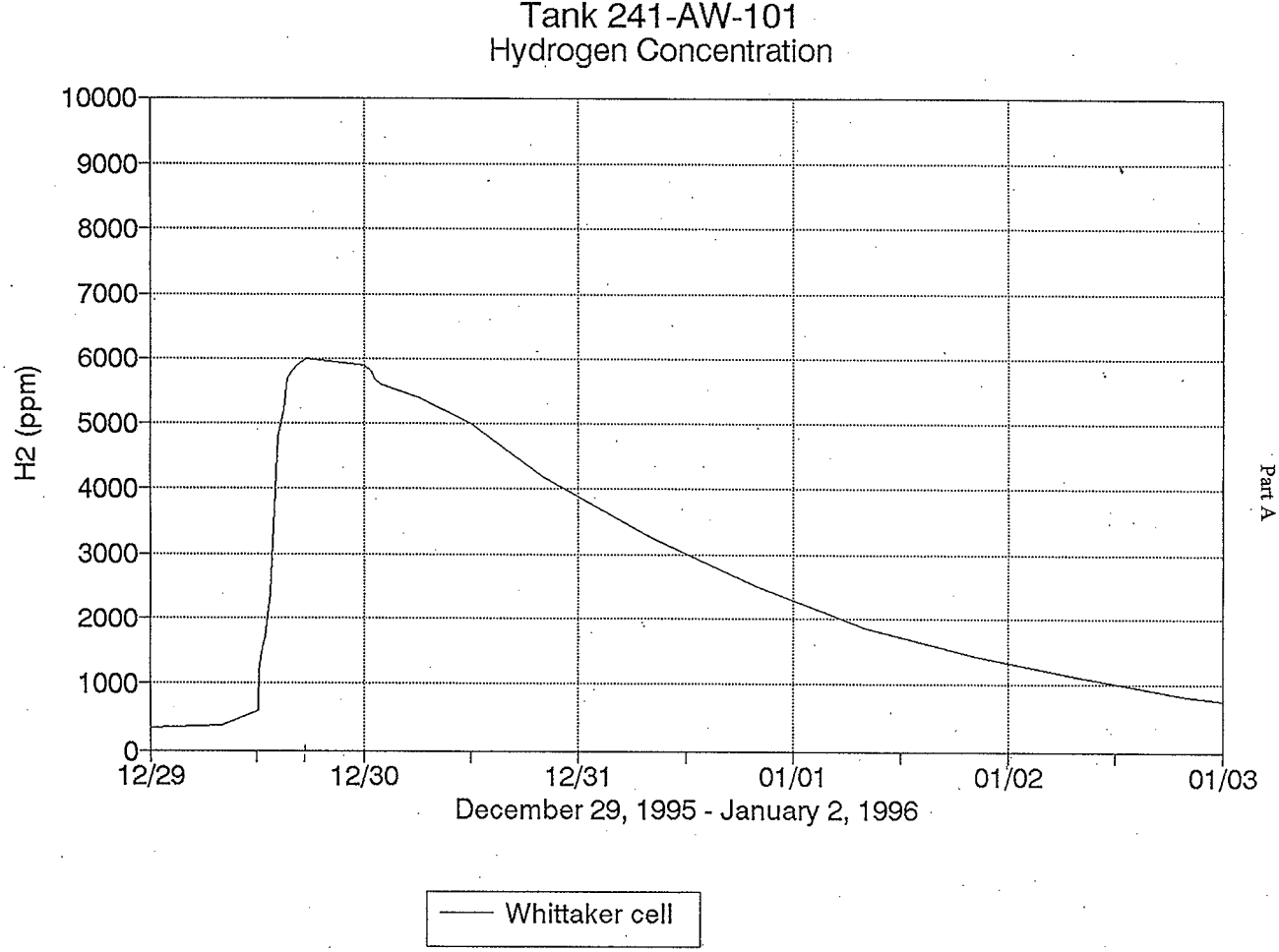
Tank 241-AW-101
Hydrogen Concentration
H2 (ppm)
10000
9000
8000
7000
6000
5000
4000
3000
2000
1000
0
12/29
12/30
12/31
01/01
01/02
01/03
December 29, 1995 - January 2, 1996
Whittaker cell

Ammonia Release Data

W. B. (Blaine) Barton
Lockheed Martin Hanford Co.
January 21, 1998

Topics of Discussion

- Where does ammonia come from?
- Present ammonia release data associated with GRE's
- Mechanism of release of ammonia
- Implications on transfers

Where Does Ammonia Come From?

- Small amounts introduced from Plant Operations
  — AN-103, AN-105
- Majority from reactions within the waste

Sources of Data

- Three tanks have ammonia monitors
  - SY-101; AN-105; AW-101
- Data on SY-103 can be obtained from stack monitoring
- Waste samples

Measured Ammonia Concentration in Dome Space During GREs

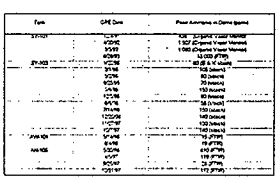

Historical Maximum Ammonia Concentrations in DST Liquid Waste

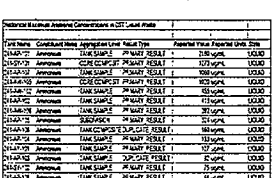

241-AN-105 HYDROGEN and AMMONIA

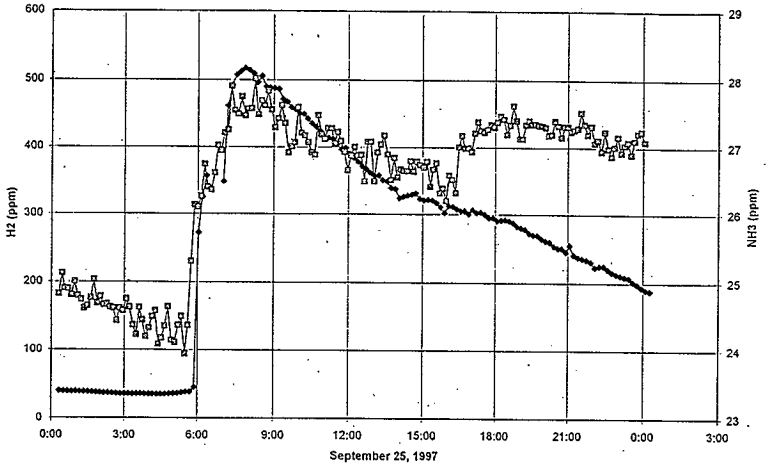

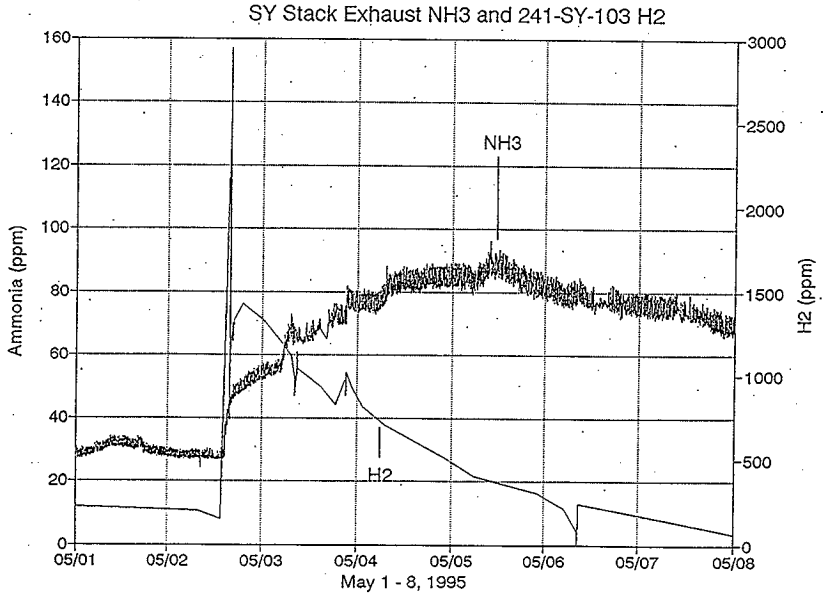

241-AN-105

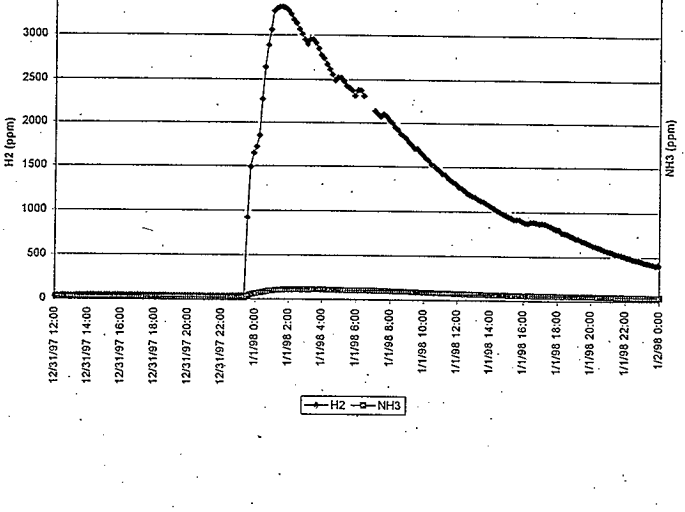

241-AN-105

Historical Maximum Ammonia Concentrations in SST Liquid Waste

Historical Maximum Ammonia Concentrations in SST Liquid Waste

Tank Name	Constituent Name	Analyte Value Level	Result Type	Reported Value	Reported Units	Basis
241-AX-101	Ammonium	TANK SAMPLE	DUPLICATE RESULT	2200	ug/mL	LIQUID
241-SX-103	Ammonium	TANK SAMPLE	DUPLICATE RESULT	1600	ug/mL	LIQUID
241-A-101	Ammonium	TANK SAMPLE	DUPLICATE RESULT	531	ug/mL	LIQUID
241-T-105	Ammonium	SEGMENT	DUPLICATE RESULT	400	ug/mL	LIQUID
241-T-107	Ammonium	CORE COMPOSITE	DUPLICATE RESULT	225	ug/mL	LIQUID
241-S-110	Ammonium	TANK COMPOSITE	PRIMARY RESULT	58	ug/mL	LIQUID
241-SX-104	Ammonium	TANK SAMPLE	PRIMARY RESULT	80	ug/mL	LIQUID
241-S-111	Ammonium	SUBDIVISION	PRIMARY RESULT	64	ug/mL	LIQUID
241-S-104	Ammonium	SEGMENT	PRIMARY RESULT	40	ug/mL	LIQUID
241-BY-103	Ammonium	TANK SAMPLE	DUPLICATE RESULT	10	ug/mL	LIQUID
241-C-108	Ammonium	TANK SAMPLE	DUPLICATE RESULT	3	ug/mL	LIQUID

Note: 1 Results may be high because of precipitation of solids.

Mechanism for Ammonia Release

- Vapor/liquid equilibrium
  - — Schumpe Model
- Sensitive to temperature and salt content
- Controlled by liquid phase mass transfer to the surface
- Crust limits response to GREs

Typical Double Shell Tank Subject to GRE

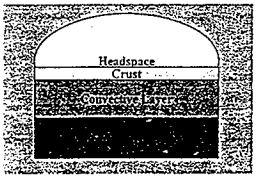

Transfers

- Tank to tank transfers are at rates of 60-300 GPM
- Ventilation required during transfers; rate ~100 CFM
- High temperature in some source tanks
- Relatively high ammonia concentrations in SST waste

Transfers

- Equilibrium considerations suggest high NH3 releases
  - — Worst case >100,000 ppmv
- Little evidence of actual NH3 release from tank farm stacks
  - — Stacks are 10-40 feet tall, exhaust ~1000 CFM

What this means

- Ammonia releases are generally small
- Ammonia releases last longer then hydrogen releases

G.2 Determination of NH_3 Composition

Besides hydrogen, the gas that presents the most hazard is the soluble gas ammonia. Ammonia gas measurements in the waste tanks and the evaluation of safety hazard associated with this gas are discussed in this section.

G.2.1 Recent Estimates

In the previous revision of this document, the volume of ammonia released into the dome space in a GRE has been assumed to be 22% of the total volume of insoluble flammable gas released (Hopkins 1996). It was assumed that the majority of the ammonia is released into the dome space by evaporation from the waste brought to the surface by rollover in a GRE. VanVleet (1996) assumes that the quantity of ammonia released in a GRE is only 15% of the released insoluble gas, the majority of which is again assumed to evaporate from the waste surface after a significant disturbance caused by a large rollover in a DST or a major earthquake.

Results from the more recent RGS measurements on ammonia (Shekarriz et al. 1997) indicate that the amount of gaseous ammonia in the waste gas is very small (see Table G-3). These measurements estimate a maximum value for the average mole % ammonia to be 2.4±1.3%. This maximum was observed for the SST A-101. Preliminary calculations by Shekarriz et al. (1997) indicate that the actual ammonia concentration may be 2 to 3 times this value or up to about 8%. These estimates are at room temperature.

TABLE G-3
Summary of RGS Data for Nonconvective Layers

	AW-101	A-101 (Upper Layer)	AN-105	AN-104	AN-103
%H_2 in Free Gas	32±2.4	75±3.8	62±3.6	47±3.8	62±6.6
%N_2 in Free Gas	56±4.6	16±0.9	24±2	31±2.9	33±3.7
%NH_3 in Free Gas	0.06±0.05	2.4±1.3	0.02±0.02	0.02±0.01	0.06±0.03
Total NH_3 in Layer (STP m^3)	59±32	280±120	54±46	89±76	92±59

G.2.2 Mechanism of Release in a GRE

Ammonia is highly soluble in aqueous solutions and has a significant vapor pressure even at room temperature. The release of ammonia into dome space under steady-state conditions is by evaporation from the waste surface. This process is severely limited by the rate at which ammonia can be brought to the surface by diffusion through the liquid. The slow diffusion in conjunction with the tank ventilation keeps the concentration of ammonia in the tank head space at a much

lower level than the equilibrium concentration corresponding to the vapor pressure of dissolved ammonia in the liquid. The headspace concentration of ammonia is further reduced by dilution in tanks (including all the DSTs) that are actively ventilated.

A large release of ammonia into the dome space is possible if fresh liquid is brought to the surface by some severe waste disturbance. When the waste is disturbed suddenly, ammonia release is greatly accelerated by evaporation from the fresh liquid surface until the surface layer is depleted and transport again becomes diffusion-limited. Regardless of how much liquid surface is exposed, the maximum ammonia concentration in the headspace is bounded by vapor/liquid equilibrium value corresponding to the concentration of ammonia dissolved in the liquid.

Events that might significantly disturb the waste include rollovers and severe earthquakes. Buoyant displacement rollovers can only occur in tanks with a deep layer of supernatant liquid (Stewart et al. 1996). This condition currently exists only in the DSTs. Severe earthquakes are the only mechanism capable of such a disturbance in SSTs. Dissolved ammonia release can be accelerated if its solubility were reduced by raising the waste temperature or increasing the solution pH (if the starting pH is less than 9). Neither of these events is likely to occur spontaneously.

G.2.3 Recommended Default Distribution

We will now proceed with the description of a default ammonia distribution expected in the tank headspace following a GRE for a generic tank for which no ammonia data are available. Table G-4 gives the ammonia concentration data obtained during GREs from tanks SY-101 (prior to mixer pump installation), AN-105 and AW-101 (Wilkins 1997).

Although the RGS data indicate an ammonia concentration of 2.4±1.3% in the flammable gas of tank A-101, the tank is not expected to have a measurable buoyant displacement. These estimates were made by Shekarriz et al. (1997) at 25°C (standard temperature and pressure, STP, conditions), while the actual temperature of tank A-101 is approximately 60°C. At this higher temperature, the partial pressure of ammonia will be higher than at STP conditions and, therefore, the concentration of ammonia in the dome space will be higher. Furthermore, Shekarriz et al. (1997) indicate that the RGS measurements can only account for one-third to one-half of the actual ammonia in the tank contents. By back-calculating through the data, it is possible to estimate a maximum value of 15% of ammonia in the vapor space for equilibrium conditions. Therefore, this value will be used as the limiting case for a generic tank when there is a large scale movement of liquids to the waste surface.

TABLE G-4

Measured Ammonia Concentration in Dome Space During GREs

Tank	GRE Date	Peak Ammonia in Dome (ppmv)
SY-101	12/4/91	438 (Organic Vapor Monitor)
	4/20/92	1,507 (Organic Vapor Monitor)

	9/3/92	1,060 (Organic Vapor Monitor)
	6/26/93	13,000 (FTIR[1])
AW-101	5/14/96	15 (FTIR)
	6/4/96	19 (FTIR)
AN-105	5/30/96	610 (FTIR)
	4/5/97	119 (FTIR)

Based on the foregoing, a relationship for ammonia concentration in the dome space with the frequency of occurrence can be obtained that includes all the possible events that can lead to the presence of ammonia in the vapor space, for tanks experiencing rollovers (some DSTs) as well as those that are non-rollover tanks (all SSTs and some DSTs).

The data for tanks not exhibiting rollover capabilities found in Table G-5 are plotted in Figure G-3. Figure G-3 shows a logarithmic relationship between ammonia concentration and event frequency. The following equations are derived by best curve fit of data to describe the frequency distribution of the ammonia concentration.

For ammonia concentrations between 800 and 150,000 ppmv, the frequency is described by:

$$\text{Frequency} = e^{(9.627 - 1.607 \ln([NH3]))} \qquad \text{[Eq. G-3]}$$

where Frequency = event frequency (events/year)

$[NH_3]$ = the ammonia concentration (ppm)

The data for tanks exhibiting rollover capabilities found in Table G-6 are plotted in Figure G-4 expressing a logarithmic relationship between ammonia concentration and event frequency. The following equations are derived to describe the frequency distribution of the ammonia concentration.

For ammonia concentrations between 50 and 15,000 ppmv, the frequency is described by:

$$\text{Frequency} = -0.215 - 0.123 \ln([NH_3]) \qquad \text{[Eq. G-4]}$$

where $[NH_3]$ = the ammonia concentration (mass fraction)

For ammonia concentrations between 15,000 and 150,000 ppmv, the frequency is described by:

$$\text{Frequency} = -0.245 - 0.130 \ln([NH_3]) \qquad \text{[Eq. G-5]}$$

where $[NH_3]$ = the ammonia concentration (mass fraction)

[1] Fourier Transform Infra-red Spectrometer

Equations G-4 and G-5 were combined and an overall cumulative frequency distribution (the fraction of values less than or equal to a given concentration) was determined, which in turn was used to create an equivalent custom probability distribution function (the individual probability of a given concentration occurring) for the Monte Carlo analysis within "Crystal Ball"[2].

TABLE G-5
Ammonia Concentration in Dome Space Versus Event Frequency for Non-rollover Tanks

Frequency (event/year)	Concentration (ppm)	Basis
1	800	High end of measured steady-state values in SSTs
10^{-1}	1,200	Maximum measured in SST headspace
10^{-2}	4,000	Estimate
10^{-4}	150,000	Large (10,000-yr) earthquake and A-101 bounding NH_3 concentration

TABLE G-6
Ammonia Concentration in Dome Space Versus Event Frequency for Rollover Tanks

Frequency (event/year)	Concentration (ppm)	Basis
1	50	Steady-state levels in actively ventilated tanks
$3x10^{-1}$	15,000	Maximum seen in SY-101
10^{-3}	150,000	1,000-yr earthquake and A-101 bounding NH_3 concentration

[2] Crystall Ball is a trademark of Decisioneering, Inc., Denver, CO.

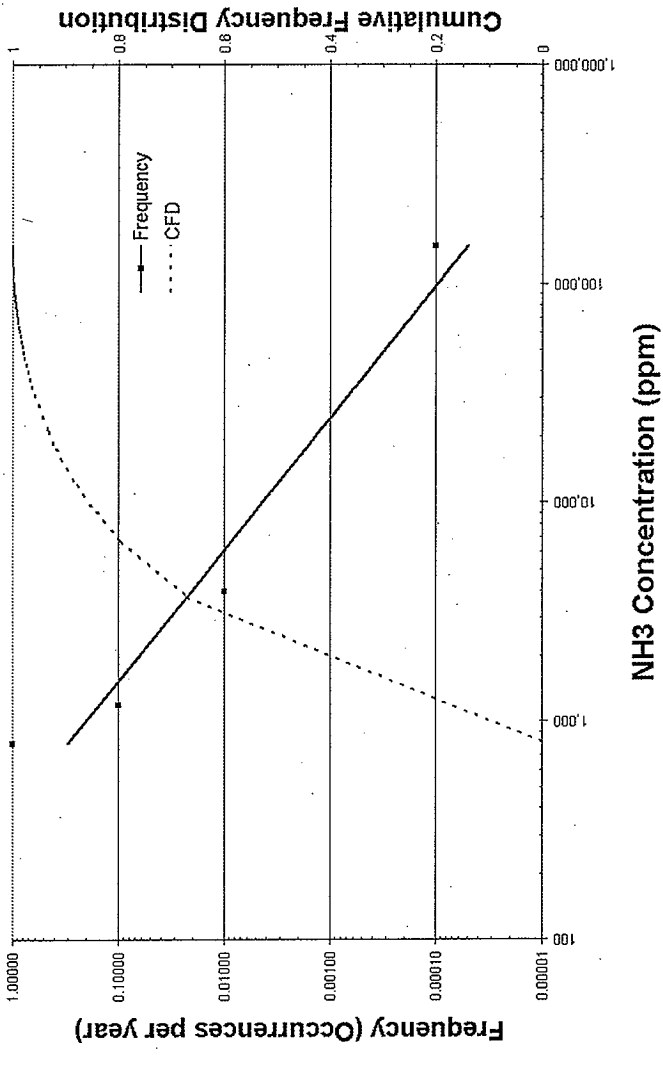

Figure G-3. Ammonia Concentration Versus Frequency for Non-Rollover Tanks.

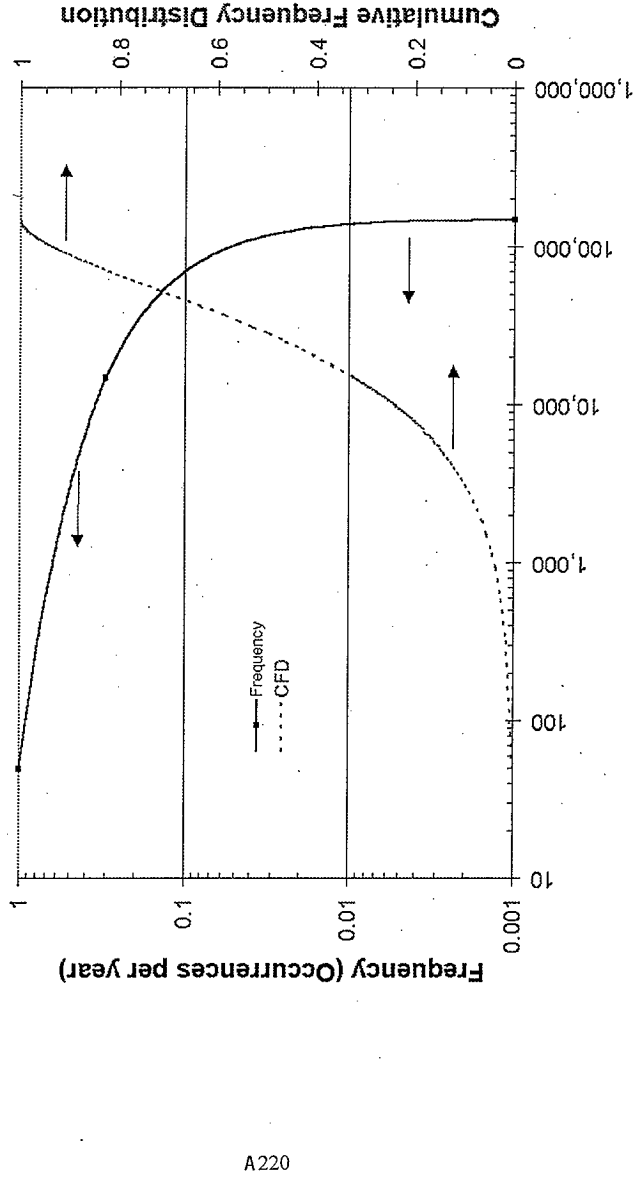

FIGURE G-4. Ammonia Concentration Versus Frequency for Rollover Tanks.

G.3 References

Hopkins, J. D., 1996, *Methodology for Flammable Gas Evaluations*, WHC-SD-WM-TI-724, Westinghouse Hanford Company, Richland, Washington.

Mahoney, L. A., Z. I. Antoniak, J. M. Bates, and A. Shekarriz, 1997a, *Preliminary Retained Gas Sampler Measurement Results for Hanford Waste Tank 241-S-106*, TWSFG97.47, Pacific Northwest National Laboratory, Richland, Washington.

Mahoney, L. A., Z. I. Antoniak, J. M. Bates, and A. Shekarriz, 1997b, *Preliminary Retained Gas Sampler Measurement Results for Hanford Waste Tank 241-U-103*, TWSFG97.40, Pacific Northwest National Laboratory, Richland, Washington.

Mahoney, L. A., Z. I. Antoniak, J. M. Bates, and A. Shekarriz, 1997c, *Preliminary Retained Gas Sampler Measurement Results for Hanford Waste Tank 241-BY-109*, TWSFG97.62, Pacific Northwest National Laboratory, Richland, Washington.

Shekarriz, A., D. R. Rector, L. A. Mahoney, M. A. Chieda, J. M. Bates, R. E. Bauer, N. S. Cannon, B. E. Hey, C. G. Linschooten, F. J. Reitz, and E. R. Siciliano, 1997, *Composition and Quantities of Retained Gas Measured in Hanford Waste Tanks 241-AW-101, A-101, AN-105, AN-104, and AN-103*, PNNL-11450 Rev. 1, Pacific Northwest National Laboratory, Richland, Washington.

Stewart, C. W., M. E. Brewster, P. A. Gauglitz, L. A. Mahoney, P. A. Meyer, K. P. Recknagle, and H. C. Reid, 1996, *Gas Retention and Release Behavior in Hanford Single-Shell Waste Tanks*, PNNL-11391, Pacific Northwest National Laboratory, Richland, Washington.

Wilkins, N. E., R. E. Bauer, and D. M. Ogden, 1997, *Results of Vapor Space Monitoring of Flammable Gas Watch List Tanks*, HNF-SD-WM-TI-797, Rev. 1, Lockheed Martin Hanford Corporation, Richland, Washington.

Refined Safety Analysis Methodology for Flammable Gas Risk Assessment in Hanford Site Tanks

Proposed Analysis Framework for Ammonia Release During Buoyant Displacement GREs and Waste Intrusive Activities

January 21, 1998

Wu-Ching Cheng

wrkshp1-wcc-1/98
slide 1

Outline

- Introduction
- Ammonia Release Model
  - Model concepts
  - Important parameters
  - Comparisons with monitoring data
- Application of Model to Waste Intrusive Activities
  - Parameters requiring quantification
  - Comparison of sample calculation with lancing data
- Summary - What We Need from Panel
  - Endorsement of model
  - Decide which parameters can be calculated vs. elicited

wrkshp1-wcc-1/98
slide 2

Introduction

Importance of Ammonia Issue

- IDLH - 300 ppmv
- LFL - 150,000 ppmv
- Monitoring Data

Tank	Steady-State, ppmv	Peak, ppmv
SY-101	40	13,000
SY-103	25 (SY Stack)	1200
AN-105	15	610
AW-101	7	19

wrkshp1–wcc–1/98
slide 3

Dissolved Ammonia Release Model

- Probability of Limnic Eruption Low (Palmer 1996)
- Model: Concentration Driven, Transport Limited
  $q = h_l A (m - m^*)$ Liquid Phase Limiting
- Use Schumpe Equilibrium Model to Determine m*
  $K_H = m^*_{NH3}/P_{NH3}$ K_H is Temp. and ion conc. dependent
- Use Surface Renewal Theory for h_l When Surface is Disturbed - *(Like Cooling Oatmeal)*
  - $h_l = (D/\tau_{renew})^{0.5}$ $D\mu/T$ = Constant
  - τ_{renew} is small during violent roll-over, larger during bubbling (2 min. vs. 20 min. for SY-101)

wrkshp1–wcc–1/98
slide 4

Ammonia Release Model (Continued)

- **Use Film Theory After Surface Stops Moving**
  - $h_l = D/\delta$ $\delta = (4Dt/\phi)^{0.5}$ Time Dependent
- **Use PreviousFeed and Bleed Mass Balance to Obtain Concentration as Function of Time**
  - Release term is mass transfer plus NH_3 released from retained gas
- **Important Parameters**
  - m - ammonia conc. in waste - known to factor of 2 or 3
  - τ_{renew} and A - must have a method to quantify
  - τ_{renew} should be relatable to τ_{GRE}
  - A should be dependent on GRE volume

wrkshp1–wcc–1/98
slide 5

Growth of Mass Transfer Film With Time

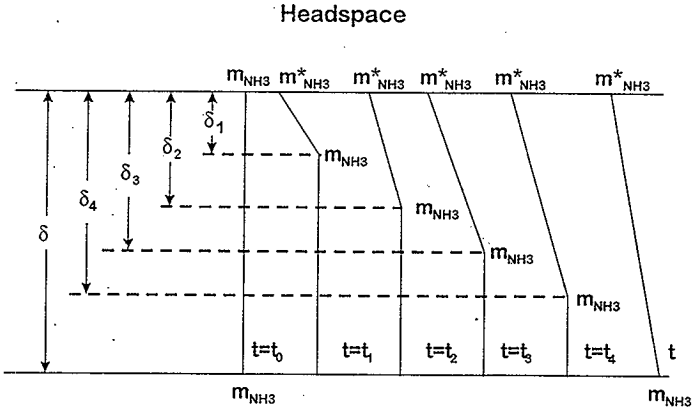

wrkshp1–wcc–1/98
slide 6

Ammonia Model - Comparison with Data
AN-105 Release in April 1997

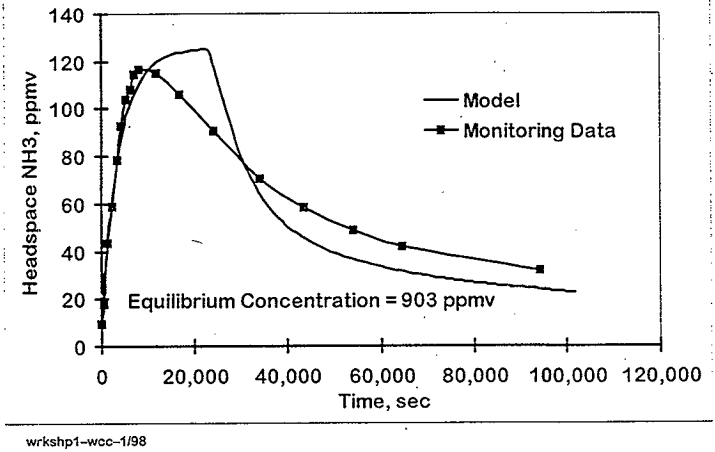

wrkshp1–wcc–1/98
slide 9

Ammonia Model - Comparison with Data
AN-105 Release in May 1996

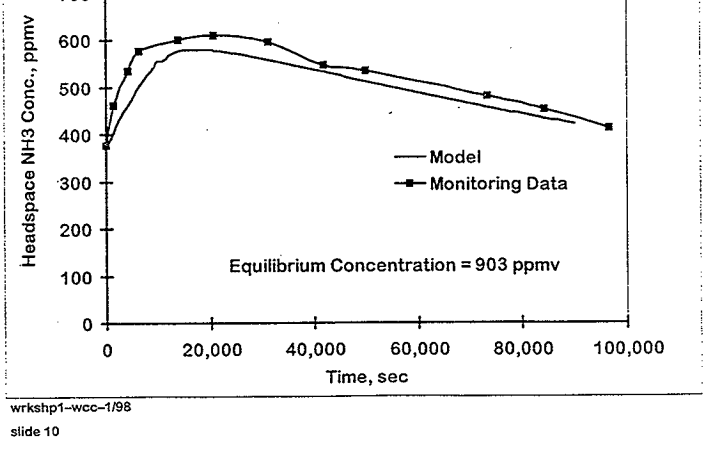

wrkshp1–wcc–1/98
slide 10

Ammonia Model - Comparison With Data
SY-103 Release in Nov. 97 (A=100 m^2 Assumed)

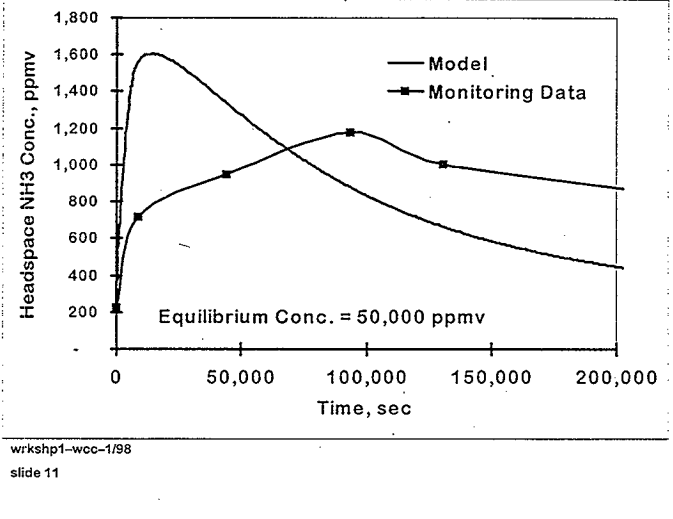

wrkshp1–wcc–1/98
slide 11

Parameters Used in Model Calculations

Tank	τ_{renew} (1), sec	τ_{renew} (2), sec	τ_{GRE}, sec	A, m^2
SY-101	120	1,200	1,200	410
AN-105	1,000 2,000	1,000 2,000	10,000 20,000	410 410
SY-103	540	5,400	5,400	100

wrkshp1–wcc–1/98
slide 12

Fig A101

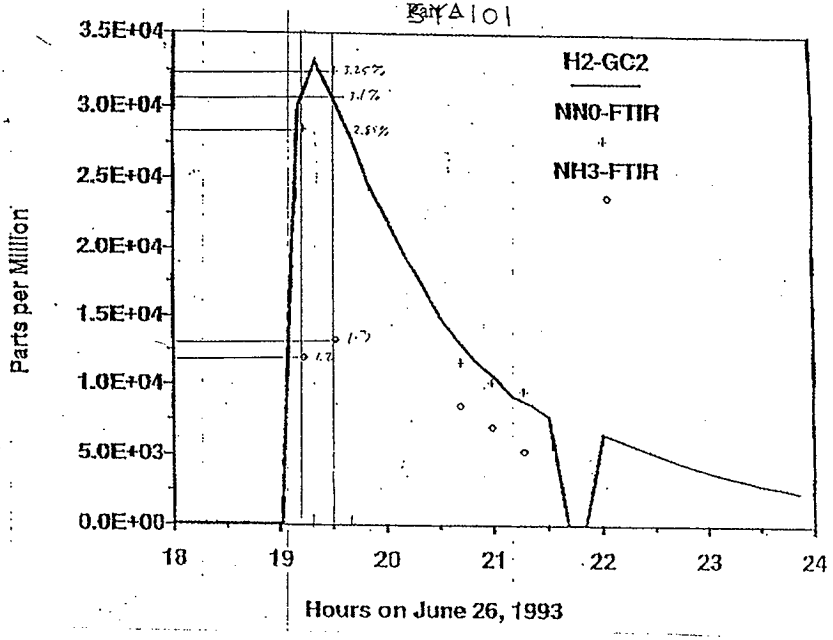

241-AN-105
12/31/97

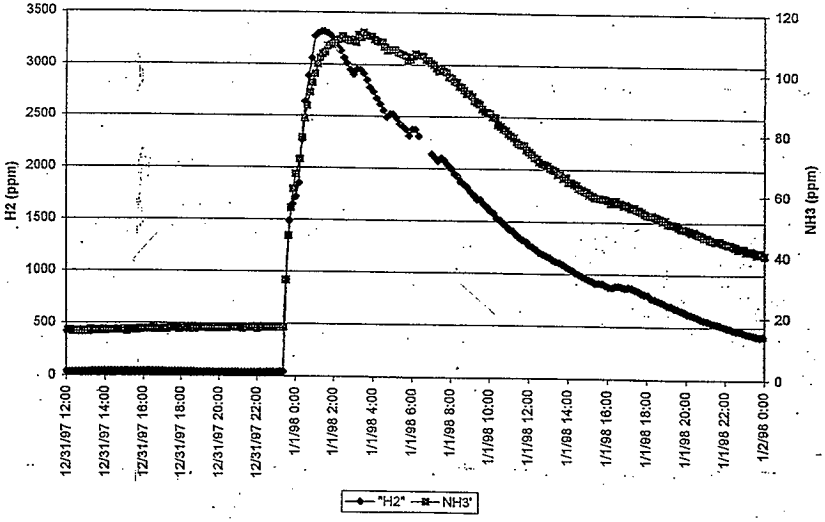

Application to Waste Intrusive Activities

- Waste Intrusive Activities Include Mixer Pumping and Lancing
- The Important Parameters are τ_{renew} and A
- One possibility is
  - $1/\tau_{renew} = 1/\tau_{circ} + 1/\tau_{bubbling}$
  - $\tau_{circ} = AH/nQ$
    - Q = pump rate, n = entrainment factor
  - $\tau_{bubbling} = AH_{stagnant}/(V_{GRE}/\tau_{GRE})$
  - $A = \pi R^2_{influence}$

wrkshp1–wcc–1/98
slide 13

Sample Calculation for Comparison with SY-101 Lancing July 3, 1993

- Factors Requiring Quantification

  $R_{influence} = 5$ ft n = 5

- Tank Data

  H = 30 ft $m_{NH3} = 400$ mole/m^3

  $H_{stagnant} = 3$ ft mole fract. NH_3 in retained gas = 0.06

- Data From Operating Experience

  Q = 17.4 gpm $C_0 = 80$ ppmv

  $\tau_{bubbling} = \tau_{GRE} = 3800$ s $V_{GRE} = 4.6$ m^3

- Calculated Parameters

  $\tau_{circ} = 6300$ s $\tau_{renew} = 2378$ s

wrkshp1–wcc–1/98
slide 14

Comparison of Model with Monitoring Data SY-101 Lancing on 7/3/93

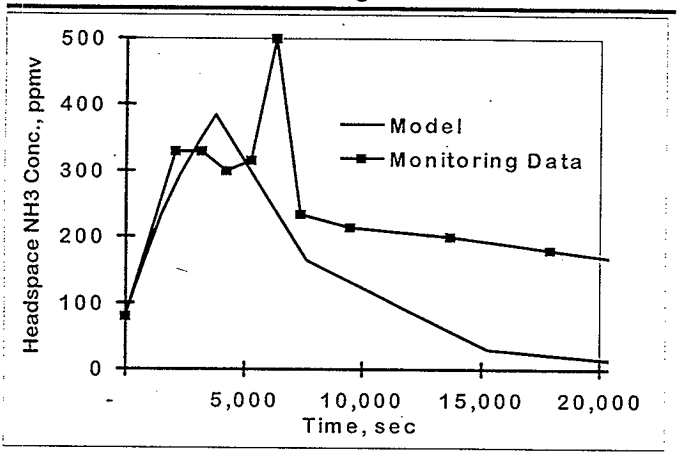

wrkshp1–wcc–1/98
slide 15

Summary - What We Need From the Experts

- Formally endorse model for ammonia release during GREs and intrusive activities or stipulate modifications required
- Stipulate methods for quantifying τ_{renew} and A, either by prescriptive method or by elicitation, for both GRE and intrusive activities
  - Perhaps n and $R_{influence}$ can be obtained from PNNL work to obtain τ_{renew} and A for intrusive activities

wrkshp1–wcc–1/98
slide 16

Definition of Terms

- A - surface area for mass transfer
- D - diffusivity of ammonia in waste liquid
- h_l - mass transfer coefficient in liquid phase
- H - depth of waste
- $H_{stagnant}$ - depth of crust
- K_H - Henry's constant
- m - concentration of ammonia in waste
- m* - equil. conc. of ammonia in waste corresponding to conc. in headspace
- n - entrainment factor
- P_{NH3} - partial pressure of ammonia
- q - ammonia release rate from waste into headspace
- Q - ventilation rate, waste circulation pump rate

δ - thickness of mass transfer film

ϕ - tortuosity factor

ν - specific molar volume of gas

τ_{circ} - characteristic circulation time

$\tau_{bubbling}$ - characteristic time for bubbles to renew surface

τ_{renew} - characteristic surface renewal time

			Comparison of Ammonia Release Terms					
Term 1 = hl*A*m			g-mole/sec					
Term 2 = VGRE*XNH3/(v tGRE)			g-mole/sec					
	Stage 1		Stage 2		Stage 3		Diffusion Through Crust	
Tank	t renew, s	Term1/Term2	t renew, s	Term1/Term2	t, s	Term1/Term2	delta, m	Term1/Term2
AN-105	1500	302.4	15000	95.6	15000	27.6	0.15	1.4E+00
SY-101	120	1.1	1200	0.4	1200	0.1	1.00	2.2E-04
SY-103	500	5.6	5400	1.7	5400	0.5	0.30	7.0E-03

AN-105 Chart 5

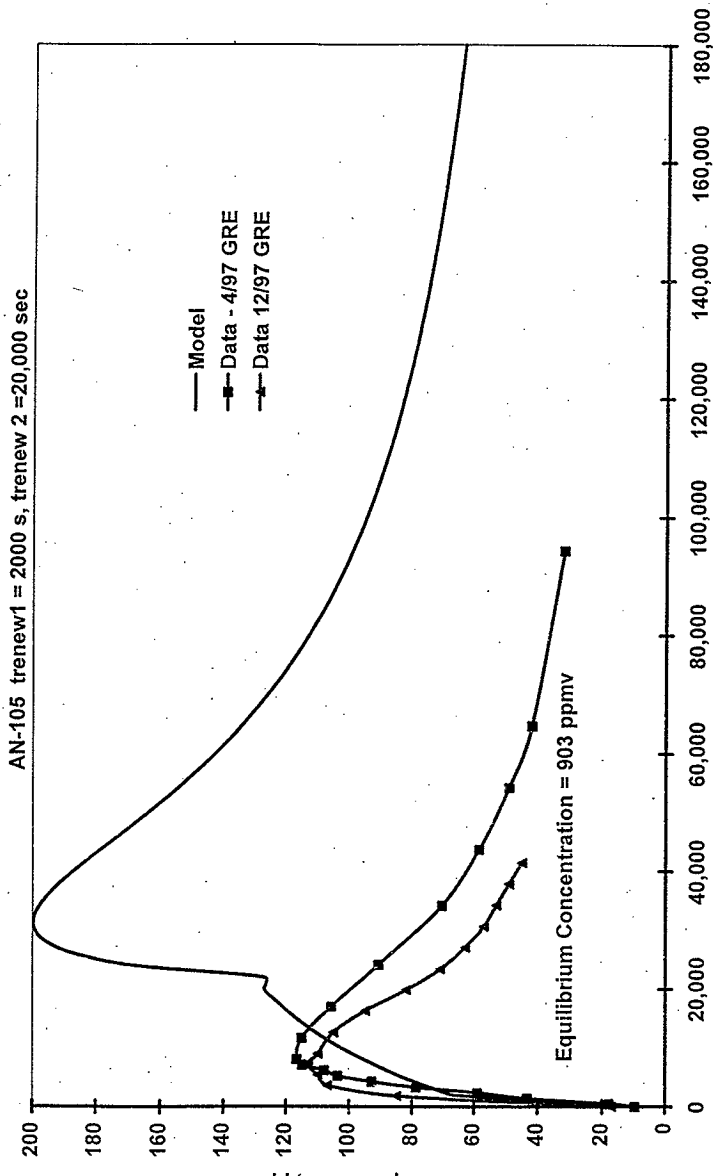

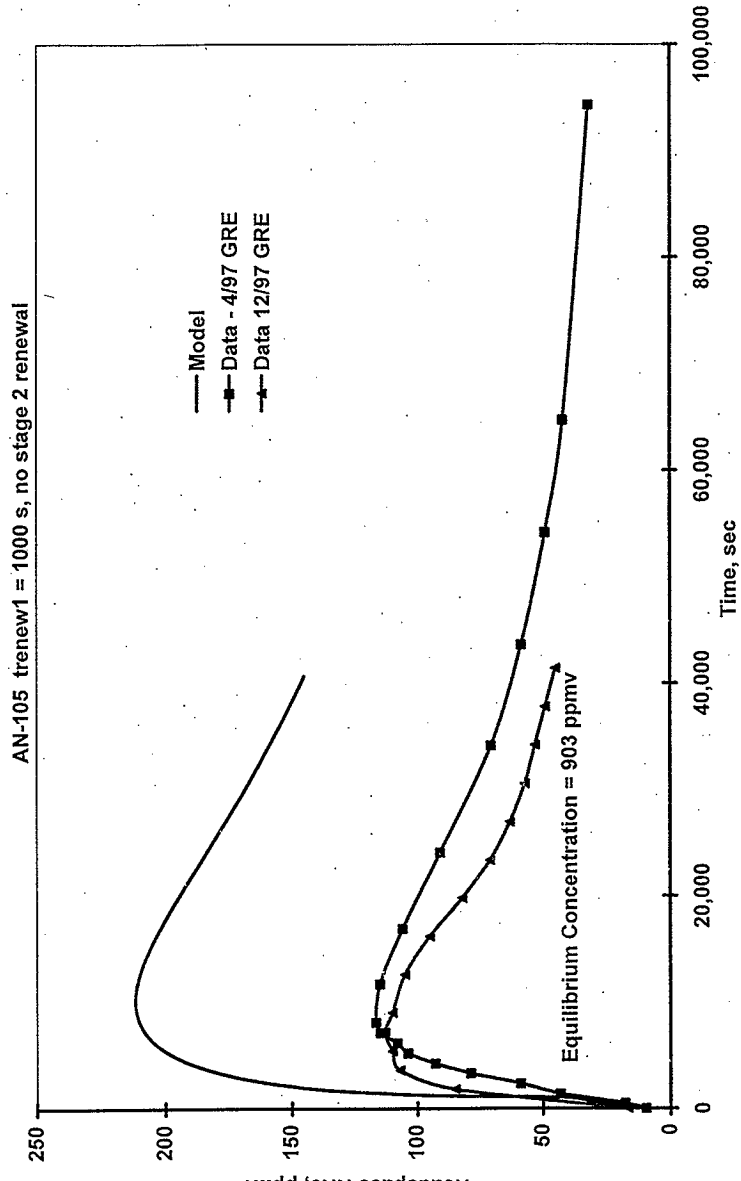

AN-105 Chart 5

AN-105 Chart 5

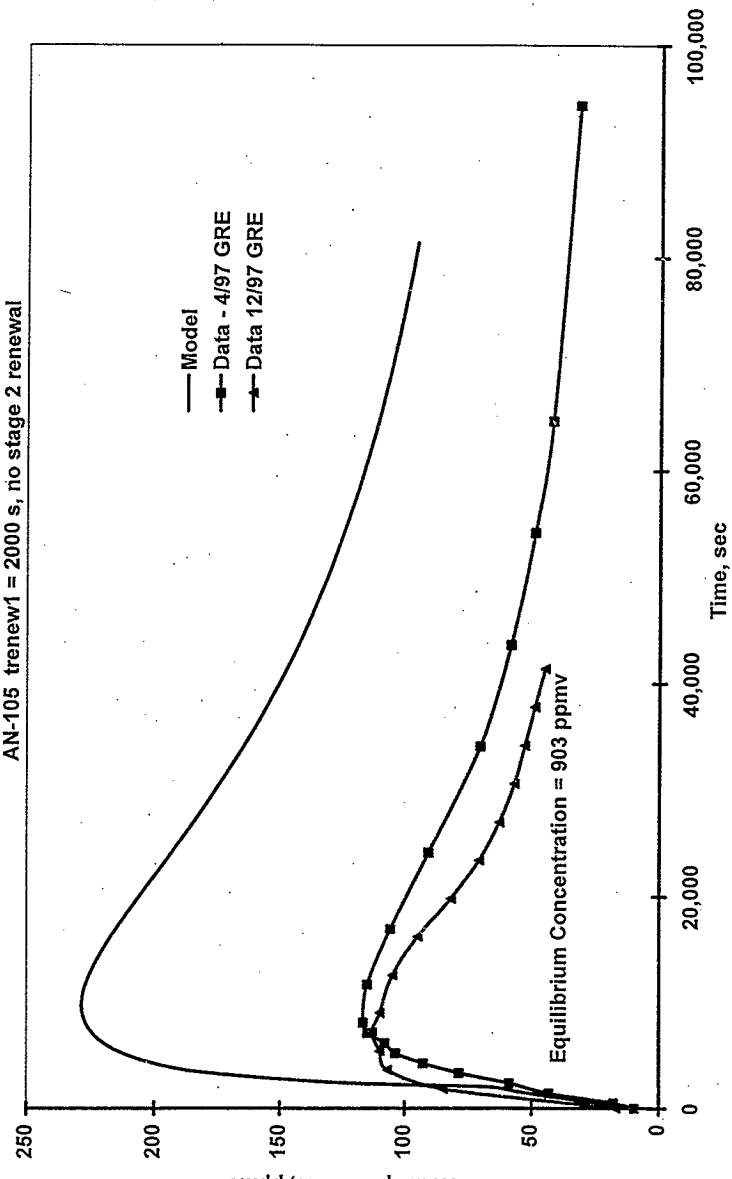

Page 1

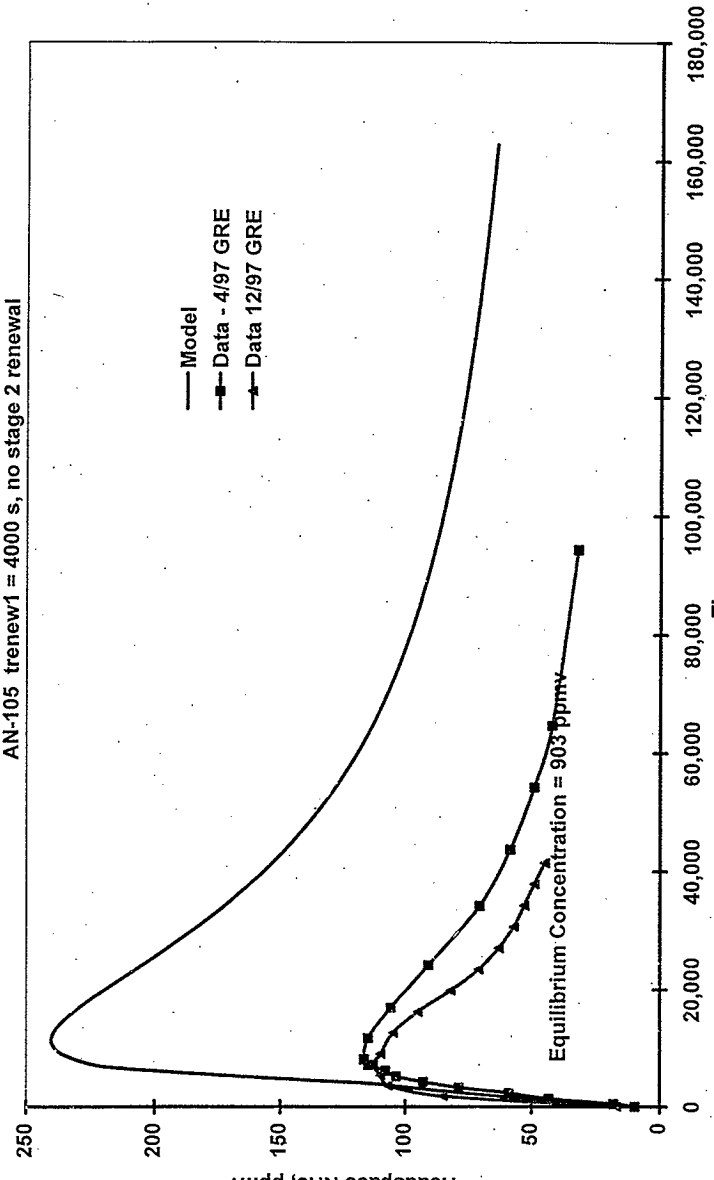

AN-105 Chart 5

Page 1

AN-105 Chart 5

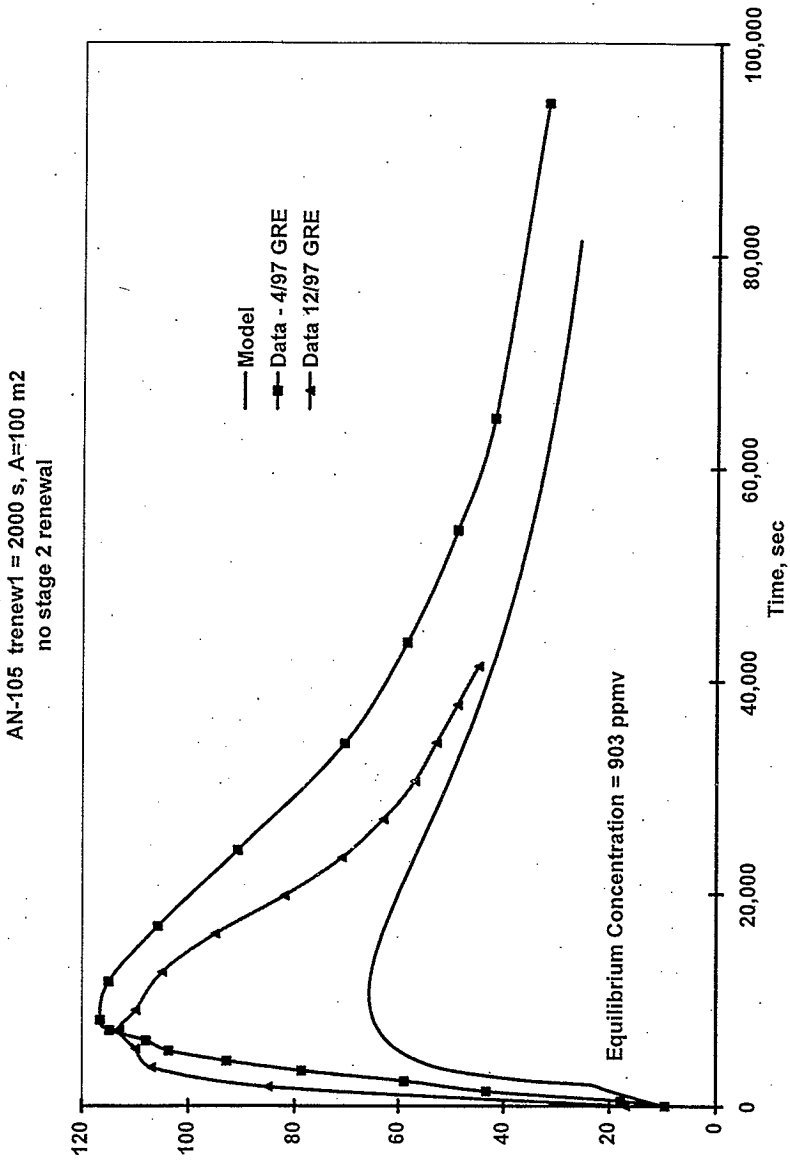

Page 1

AN-105 Chart 5

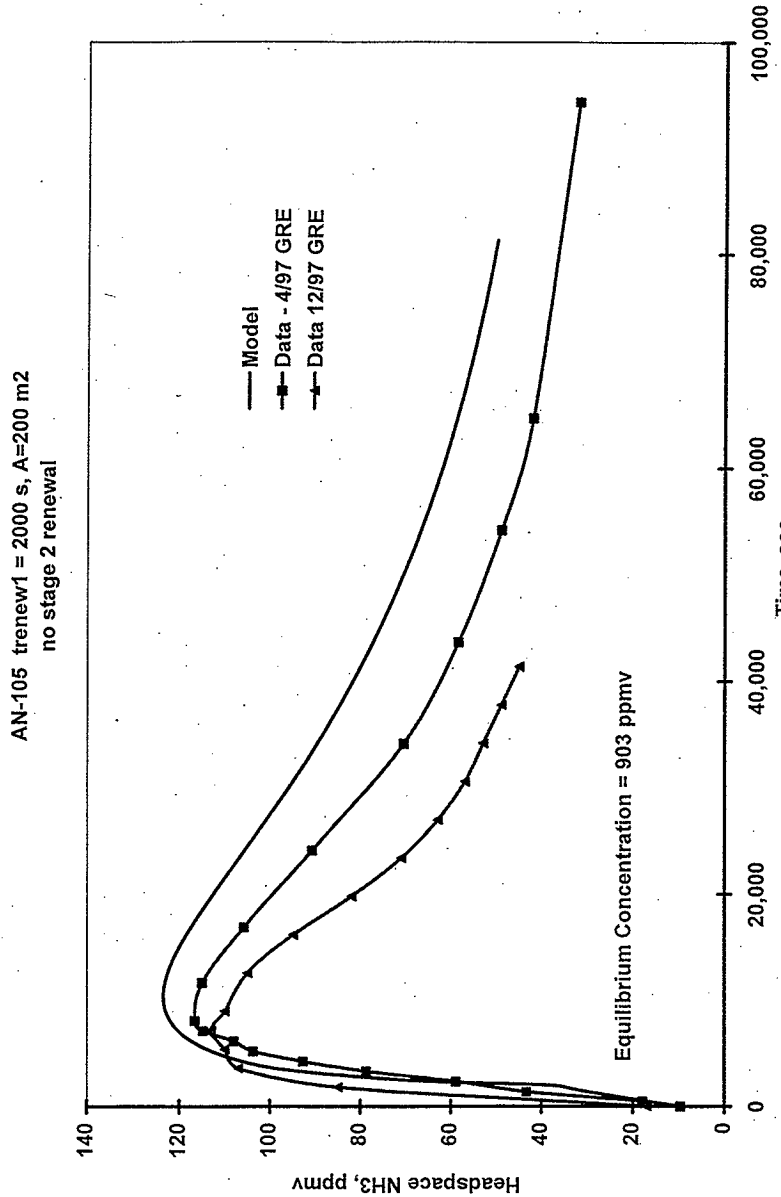

AN-105 Chart 5

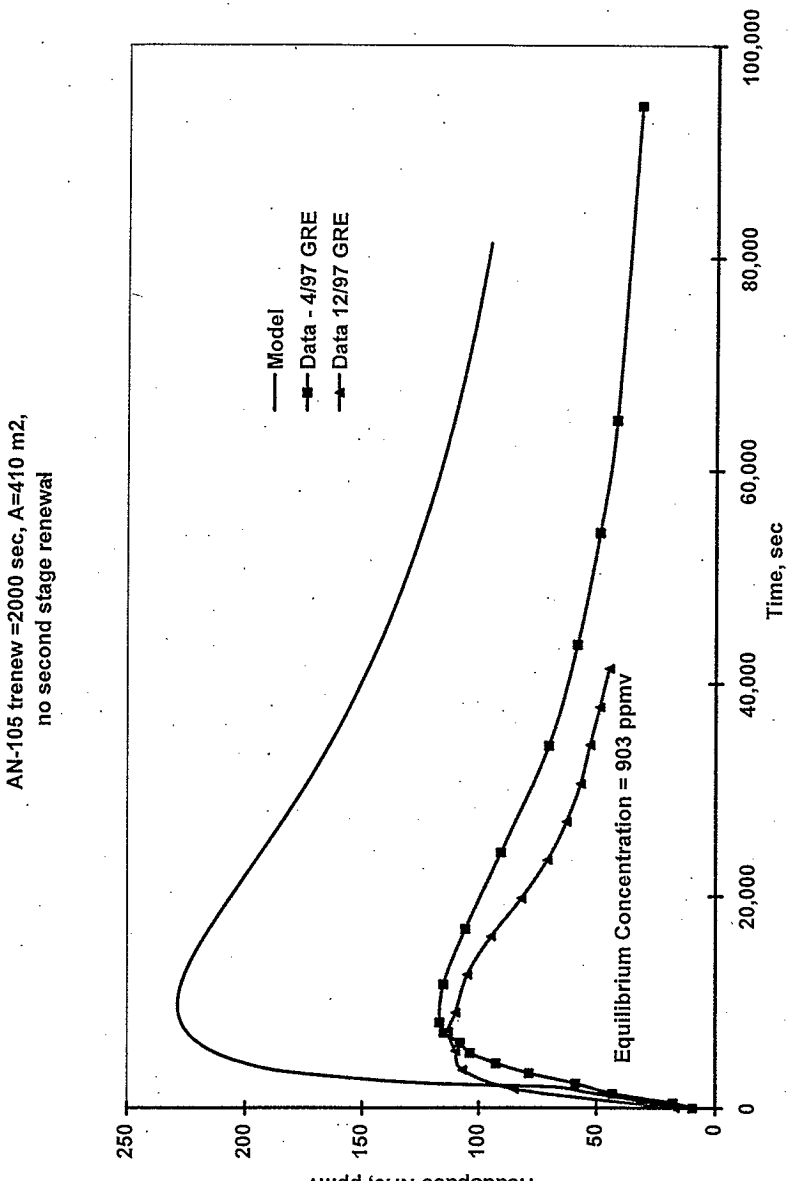

AN-105 Chart 6

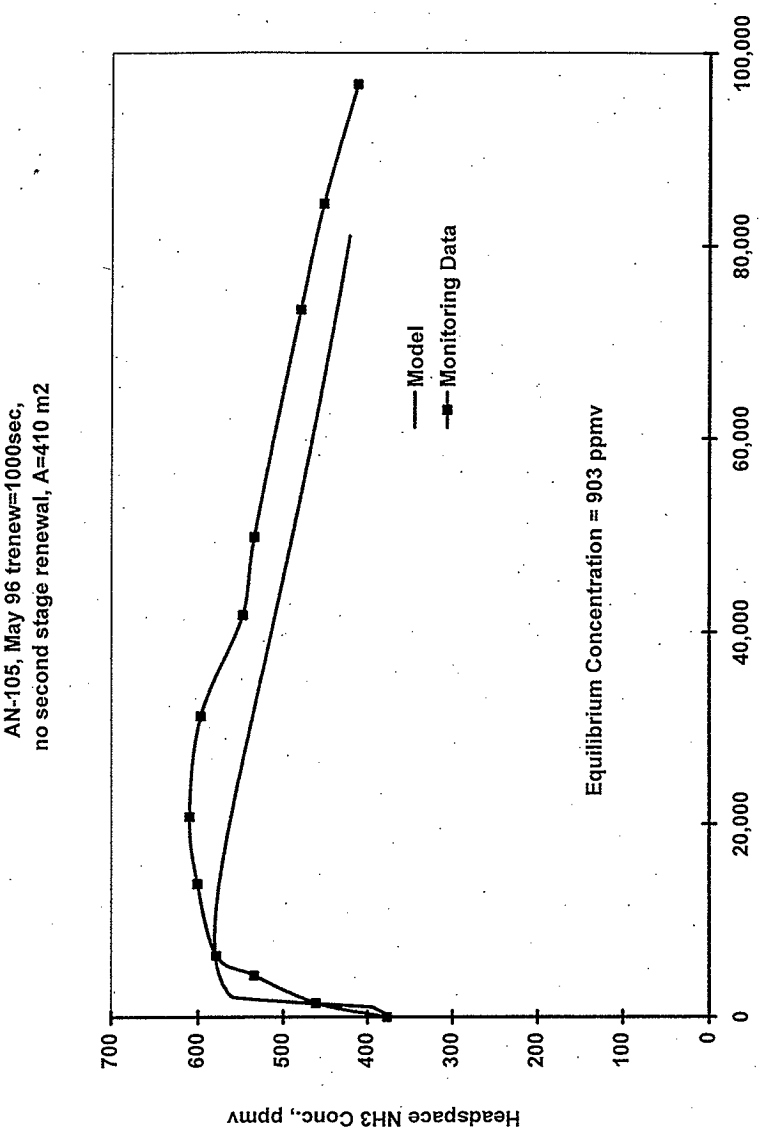

Page 1

Determination of Maximum Ammonia Concentrations by Ratioing Key Parameters to SY-101 Values

Cmax = Cmax(SY-101) * m/m(SY-101) * Q(SY-101)/Q * VGRE/VGRE (SY-101)

Tank	Date	m, moles/m3	Q, cfm	VGRE, m3	Cmax by Ratio	Cmax by Model	Cmax, Data
SY-101	Jun-93	300	500	180	13,000	12,000	13,000
SY-103	Nov-97	300	100	17.5	6,319	1,600	1,200
AN-105	May-96	2.8	25	19.4	262	580	610
AN-105	Apr-97	2.8	125	19.4	52	225	120

GRE CONTROL STRATEGIES

Mike Grigsby

for

TWRS Safety & Licensing

Safety Analysis Process

- GRE AT is used in the safety analysis process
- The goal is to:
  - determine the proper level of control and
  - determine the optimum control strategy
- The GRE AF must focus on overall risk and control effectiveness to support the control selection process

Control Selection Process

Process same as used in BIO/FSAR/TSR efforts

Process Involves:

- TWRS Engineering
- TWRS Operations
- TWRS Safety & Licensing

Input to Process:

- Impact on risk (safety analysis with GRE AT and others)
- Engineering feasibility (engineering studies)
- Impact on Operations

Control Selection Process (Cont)

Process Steps:

- Define postulated accidents - GREs and SS releases
- Define tank groups and representative tanks
- Calculate uncontrolled risk - AB "without controls" case
- Calculate controlled risk for various candidate control options
- Factor-in engineering and operations feasibility
- Optimize risk reduction vs costs and ops impacts
- Calculate risk with final control selection - AB "with controls" case

GRE AT - Uses in Control Selection

I. Assess risk:

- Uncontrolled risk determines rigor of control implementation
- Controlled risk to target TWRS REGs
- No control may be warranted if risk << REGs
- Prudent controls can be implemented as defense-in-depth rather than TSRs

GRE AT - Uses in Control Selection (cont.)

II. Assess risk impact of control candidates:

- Controls represented by key AF parameters
- AF must be focused towards assessing control impacts
  - frequency of GREs
  - frequency of flammable conditions given a GRE,
  - ignition frequency,
  - tank damage,
  - material release
- Controls with high risk impact favored in selection

PLL1197.1. 6 (11/11/97)

Control Option Candidates for DSTs

Leading Candidates:

- Ignition Source Controls
- Head Space Inerting
- Ventilation
- GRE Mitigation (equipment, waste treatment, waste management)

Others Suggested:

- hydrogen ignitors/recombiners
- combustion suppression or mitigation
- containment or robust confinement
- limiting operations

Ignition Source Controls

Controls to prevent ignition sources:

- mechanical sparks
- electrostatic
- electrical circuits
- limit temperature of hot surfaces

Controls for ignition prevention:

- explosion proof equipment
- purged equipment

Monitoring and safe shutdown

Ignition Source Controls (cont.)

- Controls for DSTs are same as for SSTs
- Three levels of control:
  - IC Set 1 - no single point failure
  - IC Set 2 - non-sparking under normal operation
  - Past Practices - no formal controls
- Meet intent of industry standards - not code compliance
- FGEAB chartered to interpret application
- Some DOE approved exceptions are needed

Ignition Source Controls (cont.)

Implementation in AF:

- Ignition frequencies are elicited conditioned on control level
  - spark frequency for installed equipment
  - spark probability during installation or removal of equipment
  - spark probability for equipment used for a short duration
- Uncontrolled ignition sources are included in AF

Ignition Source Controls (cont.)

Implementation Status and Insights:

- Ignition Controls are implemented in the field via BIO/TSRs
  - equipment modified
  - procedures revised
  - monitoring being performed for manned activities
  - each work package evaluated for compliance
- Biggest cost is for equipment and activities in ex-tank locations (pits and outside open risers)

Head Space Inerting

- Reduces oxygen in head space
  - prevents flammable conditions when N_2O is not in sufficient concentration
  - fuel rich burns limited by available oxidizer
  - reduces combustion efficiency for stratified layer burns
- N_2, CO_2, and Ar considered for inerting in AF

Head Space Inerting (cont.)

Engineering study of inerting systems is in progress:

- N_2 is gas of choice (least costly yet effective)
- Control point of 1-2 % oxygen in dome space
- System requirements differ from tank to tank
  - — passively ventilated SSTs - purged
  - — actively ventilated SSTs - inerted inlet
  - — DSTs (actively ventilated) - inerted inlet
- Nitrogen demand may favor onsite production plant

Ventilation

- DSTs are all actively ventilated (75 to 600 cfm)
- Increased flow rates to be investigated
- Reduces time at risk (above LFL)
  - stratified layer
  - well mixed headspace
- Tank vacuum reduces flow of GRE gases to pits or out open risers

GRE Mitigation

- Reduce gas retention
- Reduce GRE frequency and/or magnitude

- LANL is evaluating many possible options:
  - Pump mixing
  - Low -frequency sonic probe
  - Supernatant liquid removal
  - Heating
  - Cooling
  - Dilution

GRE Mitigation (cont.)

- LANL evaluation based on effectiveness and feasibility - focus AF on leading candidates

- Incorporation in AF can be explicit or implicit (AF input parameters varied based on effect of mitigation scheme)
  - size and/or density of CL and NC layer
  - rheology of NC layer
  - mixing of NC layer (radius of influence, release effectiveness)
  - gas generation rate

Control Strategies for GREs

Mike Grigsby for TWRS Safety & Licensing

The primary goal of the safety analysis of gas release events (GREs) is to determine the appropriate level of control and the optimum control strategy to manage risk from this hazard to acceptable levels.

Control Selection Process - A control selection process has been developed for use at TWRS to determine safety controls for all hazards and possible accidents. The results of the control selection are reflected in the TWRS Safety and Authorization Basis (Basis for Interim Operation - BIO, Final Safety Analysis Report - FSAR, and Technical Safety Requirements - TSRs). The control selection process uses safety analysis information as well as engineering feasibility and operations impact information to determine the appropriate safety controls. The process involves defining representative accidents and tanks for key hazards. For flammable gas hazards, the representative accidents are deflagrations/detonations of gases generated by the wastes that are (1) retained within the waste, (2) are released to the headspace in a steady, chronic manner and which may accumulate to flammable concentrations, and (3) gases which are released to the tank headspace in a rapid, episodic manner (gas release events - GREs). The focus of the GRE safety analysis effort (GRE SA analysis framework and supporting workshops) is accident scenarios 1 and 3.

The control selection process first compares accident risk with no controls to TWRS risk evaluation guidelines (REGs). If risk is well below guidelines, no safety controls may be warranted. If risk is above guidelines, control strategies are evaluated to determine if risk can be reduced to below guideline values by use of reasonable control measures. The control selection process thus, involves and evaluation of unmitigated and mitigated risk as well as engineering feasibility and operations impacts.

GRE SA Framework Supports Control Selection - To support the control selection process, the GRE safety analysis must evaluate both the magnitude of risk without controls and with controls, as well as the relative risk impact of various candidate control options. To accomplish these goals, the analysis framework must represent safety control impacts in its key parameters and models. Impacts may be manifested as changes to (1) the frequency that flammable conditions may develop in the tank, (2) the frequency that ignition occurs, (3) the severity of the combustion event, or (4) the consequences of the combustion event (tank damage and waste material release).

Candidate control options for GREs in double shell tanks (DSTs) include ignition source controls, headspace inerting, ventilation, and GRE mitigation (that is the reduction of gas retention or the size and frequency of GREs). GRE mitigation may involve use of equipment (e.g., mixer pump), waste treatment (e.g., dilution), or waste management (e.g., reduce waste volume).

Ignition Source Controls - The ignition source controls used in TWRS are based on industry standards and experience. Controls include measures to prevent ignition sources including mechanical sparks (impact, friction, thermite reactions), electrostatic sparks, sparks from electrical equipment, and ignition from hot equipment surfaces. In addition, controls allow the use of explosion proof equipment and purged equipment to prevent ignition of waste generated gases. A companion control is gas monitoring with shutdown of activities and operations if gas concentrations exceed 25% of the LFL.

Ignition source controls are graded into three levels: Set 1 which is based on preventing a single point failure from creating an ignition source, Set 2 which prevents use of equipment that sparks under normal use, and "past practice" which requires no formal control of ignition sources.

The ignition source control's impact in the analysis frame work is implemented by including different ignition source frequencies under the different control levels (Set 1, Set 2, past practice). Ignition sources affected by these controls include those arising from installed equipment (ignition source frequency), arising during equipment installation and removal (ignition source probability per activity), and those occurring during short duration use of equipment (ignition source probability per activity). Several ignition sources included in the AF are not affected by these controls including random sources, lightning, those caused by seismic events and those caused by a GRE.

Implementation of ignition source controls at TWRS has identified that the control requirements in ex-tank locations (i.e., in pits and outside open risers) are most costly as much of the equipment and activities involve these locations. It is, therefore, useful for the AF to be able to evaluate the risk impacts of ignition sources and controls in ex-tank locations independent from those in the tank dome space.

Head Space Inerting - Inerting would be used to reduce the oxygen available in the tank dome space to act as an oxidizer. Because waste generated gases include nitrous oxide, which is also an oxidizer, complete prevention of flammable conditions may not be possible through headspace inerting. However, flammable conditions may be limited to very infrequent GREs and may be limited to short durations as mixing and dilution below flammable concentrations under inerted conditions may occur more rapidly than with air.

The AF represents the impacts of inerting by tracking gas compositions and concentrations in the dome space, including inert gases and oxygen. The AF determines if GRE gases are flammable when mixed with the dome space gases (during plume formation and under well mixed conditions), fuel-rich burns are limited by available oxidizer, and the combustion efficiency for stratified layers is reduced under inerted conditions.

The AF considers nitrogen , carbon dioxide, and argon as possible inerting gases. However, a preliminary conclusion of the engineering study is that nitrogen is the preferred gas for use in the tank farms.

Ventilation - DSTs are all actively ventilated with flow rates ranging from about 75 to 400 cfm. Ventilation can reduce the peak concentration for the well mixed headspace, but primarily reduces the time at risk (time above LFL) for both a stratified layer as well as the well mixed condition. The risk impact of varying ventilation flow rates is to be evaluated by the AF.

GRE Mitigation - GRE mitigation, as used here, is application of equipment (e.g., mixer pumps, sonic probes), waste treatment (e.g., heating, cooling, dilution, chemical adjustment), or waste management schemes (e.g., removal of supernatant liquid, reduce waste volume) to reduce the size and or frequency of GREs. Many possible scheme are available. To reduce the options to those most promising, LANL is performing an assessment of candidate schemes based on effectiveness and feasibility. Leading candidates need to be reflected in the AF.

Key characteristics of the mitigation schemes might include impacts on waste properties (e.g., the size and or density of the convective and non-convective layers of waste, the viscosity and strength of the non-convective layer, the maximum retained gas void fraction), gas generation rates, gas release mechanisms (e.g., prevent buoyant displacement GREs), ga retention (e.g., release gases by mixing or agitation). The AF may incorporate GRE mitigation affects directly such as reducing waste volume or supernate volume, or indirectly by modifying key AF parameters as a result of off-line calculations (e.g., AF parameters of supernatant density, NC layer volume and rheology may be adjusted based on the results of off-line dilution calculations or the retained gas void fraction may be adjusted based on an off-line assessment of the effects of a sonic probe).

WASTE TANK SYSTEM MODELS

William L. Kubic, Jr.
Cetin Unal
Pratap Sadasivan
J. Robert White

Nuclear Systems Design and Analysis Group
Los Alamos National Laboratory
Los Alamos, New Mexico 87545

January 22, 1998

ACKNOWLEDGMENTS

Our current understanding of waste tank behavior and flammable gas issues is the culmination of at least five years of work at Los Alamos National Laboratory that involved many technical staff members. We would like to acknowledge former members of our team and others who have made significant contributions to our conceptual models of the waste tanks.

Kemal Pasamehmetoglu

Steve Eisenhawer

Steve Agnew

Bill Bohl

INTRODUCTION

Since 1992, the Waste Tank Safety Team at Los Alamos National Laboratory has prepared several safety assessments to address flammable gas issues at the Hanford Site and has been involved in other support activities for the flammable gas program.

Los Alamos Perspective - Analysis of Waste Tank Operations

- Changes to the Waste
- Long-Term Effects

Los Alamos Approach - Waste Tank Systems Model

- Need to consider interactions in the system
- Need to model the entire system and not separate effects
- Need a realistic, not optimistic, treatment of uncertainty
- Need to avoid speculation

Los Alamos
Los Alamos National Laboratory

PURPOSE AND OUTLINE

Purpose of This Presentation

- Review of pertinent LANL models
- Summary of current LANL model for estimating the impact of changes to the waste

Topics to Be Discussed

- Summary of LANL data reconciliation studies
- Review of select data from Facility-Group-1 Tanks
- Summary of other models developed by LANL
- Summary of current system model of the tank

SUMMARY OF LANL DATA RECONCILIATION STUDIES

Los Alamos
Los Alamos National Laboratory

WHAT IS DATA RECONCILIATION?

Data reconciliation is an integrated, model-based approach to data analysis.

- Considers ALL data from a global point of view
- Emphasizes resolution of inconsistencies in the data

A data reconciliation study exploits:

- Redundancies in the data
- Physical dependencies
- Prior knowledge
- Physical constraints

TOOLS FOR DATA RECONCILIATION

CONCEPTUAL MODEL

- Model of the system (i.e., waste tank)
- Parts of the model can be qualitative
- Can include inequalities

MAXIMUM LIKELIHOOD METHOD

- Statistical method that combines data and models to exploit redundancies, physical dependencies in the data, and prior knowledge.
- Considers uncertainty in the data.
- Can be used to determine if the model is consistent with the data.
- Can be used to obtain consistent estimates of model parameters.

INVENTORY AS A UNIFYING FACTOR

The waste tank inventory is characterized by:

- Total mass or volume of solids, liquid, and gas
- Composition of the solids, liquid, and gas
- Distribution of solids, liquid, and gas in the tank

Waste behavior depends on the inventory:

- Physical properties are a function of waste inventory
- Gas generation is a function of waste inventory
- Gas retention is a function of the physical properties, gas generation, and waste inventory
- Gas releases are a function of the physical properties, gas generation, and waste inventory

WASTE TANK DATARELATIONSHIPS

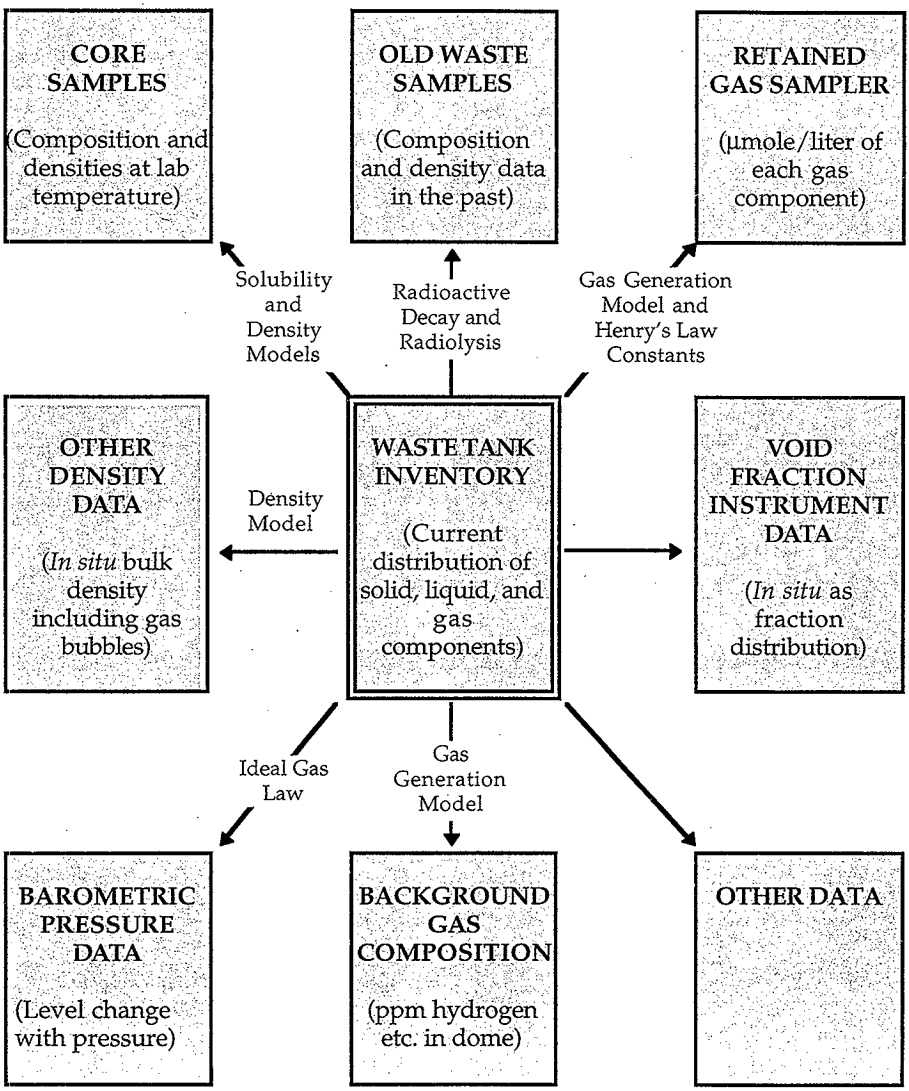

Los Alamos
Los Alamos National Laboratory

MAXIMUM LIKELIHOOD ANALYSIS

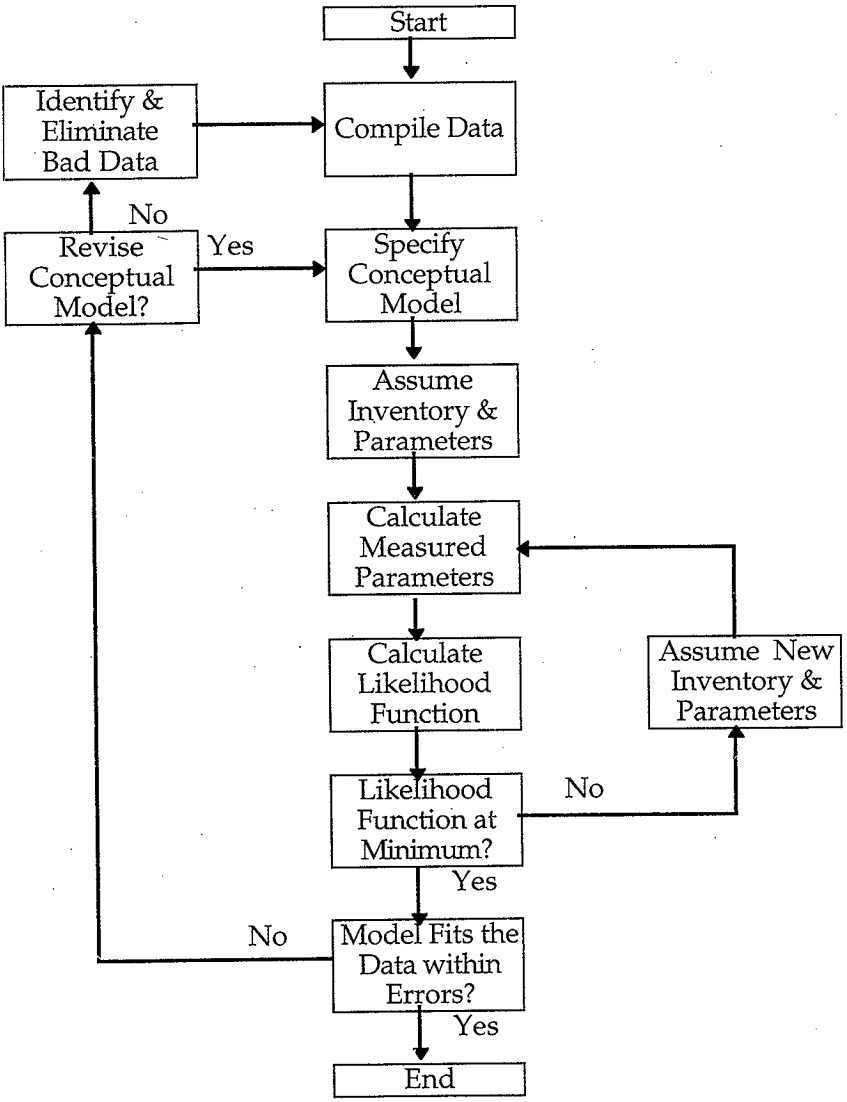

Los Alamos
Los Alamos National Laboratory

LIST OF MODELS USED FOR DATA RECONCILIATION

INVENTORY-RELATED MODELS

- Representation of the waste (layers, solids fractions in the layers, etc.)
- Charge balance
- Density models
- Solids solubility model
- Stability conditions
- Radioactive decay
- Radiolysis of nitrate and nitrite
- Volume balances
- Waste compressibility

GAS-GENERATION-RELATED MODELS

- Gas generation model
- Ammonia generation model
- Gas material balances
- Gas solubility
- Mass transfer to the dome

REPRESENTATION OF THE WASTE

- Assume three uniform layers exist in the waste:

  1. Nonconvective layer
  2. Convective layer
  3. Crust

- Use a simplified representation of the waste composition.

DENSITY

LIQUID DENSITY

- Use correlation for density as a function of concentration based on the mixing rule of Patwardhan and Kumar (1993).

AVERAGE SOLIDS AND BULK DENSITY

- Average solids density and bulk density are simply the weighted average of the densities of the individual phases.

SOLIDS SOLUBILITY MODEL

AQUEOUS PHASE (LIQUID ACTIVITY COEFFICIENTS)

- Problems developing a liquid activity coefficient model:
  - o No suitable activity coefficient model for the waste.
  - o Little reliable data available for evaluating parameters.
- We use Meissner's method with a quadratic mixing rule for estimating activity coefficients.

SOLID PHASES

- Assume sodium hydroxide, soluble organic acid salts, and ammonia are completely dissolved in the aqueous phase.
- Assume that insoluble organic acid salts and heavy salts have negligible solubility.

STABILITY CONDITIONS

- Crust must be less dense than the C layer.
- Bulk density of the NC layer must be greater than the density of the C layer.
- Average density of the solids plus gas in the C layer must be greater than the liquid density.

RADIOLYSIS OF NITRATE AND NITRITE

- Nitrate and nitrite ion concentrations change as a result of radiolytic reduction.

$$NO_3^- \rightarrow NO_2^- \rightarrow OH^- + N_2, N_2O, NH_3, \text{ etc.}$$

WASTE COMPRESSIBILITY

- The waste compressibility is the change in waste level as a result of a change in dome pressure (i.e., barometric pressure).

GAS GENERATION MODEL

- We lack the data and understanding of gas generation to develop a mechanistic model.
- We can summarize our understanding of gas generation in a simple, empirical model.
- Two general mechanisms of gas generation are: radiolytic and thermal reactions:

$$r_{total} = r_{rad} + r_{thermal}$$

- For radiolytic gas generation:

$$r_{rad,H_2} = (G_o + G_1 \cdot C_{TOC}) \cdot E$$

$$r_{rad,N_2O} = G_{N_2O} \cdot C_{TOC} \cdot E$$

- For thermal reactions:

$$r_{thermal,H_2} = k_{H_2} \cdot \exp\left(\frac{E_{H_2}}{R \cdot T}\right) \cdot C_{TOC} \cdot C_{Al}$$

$$r_{thermal,Other} = k_{Other} \cdot \exp\left(\frac{E_{Other}}{R \cdot T}\right) \cdot C_{TOC}^2 \cdot C_{Al}$$

- Because of differences in composition, model parameters vary from tank to tank.

AMMONIA GENERATION RATE AND MATERIAL BALANCE

- There are two sources of ammonia generation:

  o Radiolytic decomposition of nitrite
  o Reaction involving organic complexants

- The reactions involving organic complexants are only important in SY-101 because of the high TOC concentration.

- The rate of ammonia production is:

$$r_{NH_3} = G(+NH_3)\, E\, C_{nitrite}$$

- An ammonia material balance is used to estimate the ammonia concentration from the waste history.

GAS SOLUBILITY

- Use Henry's law to estimate gas solubility.
- Developed correlations for salt cake wastes from literature data to estimate effect of changes in waste composition and temperature.

HYDROGEN BALANCES

- Hydrogen material balances are used to reconcile dome space hydrogen concentrations in the dome with generation and release rates.

RATE OF LEVEL RISE

- The rate-of-level-rise model is a bubble material balance used to reconcile the observed rate of level rise with the gas generation rate.

MASS TRANSFER CONSTRAINT

- The mass transfer constraint is used to ensure consistency between the release rates and mass transfer rates through the crust.

SUMMARY OF SOME DATA RECONCILIATION RESULTS

- The available data are reasonably consistent
  - o Problematic data are typically limited to a few components in the waste composition data.
- The retained gas composition may not have reached a steady-state value.
- Dissolved hydrogen cannot be neglected in some tanks.
- Solids composition varies significantly.

Salt	Composition (wt %)				
	AN-103	AN-104	AN-105	AW-101	SY-101
$NaNO_3$	0	0	0	87	24
$NaNO_2$	18	0	0	0	13
$NaAlO_2$	56	0	0	0	19
Na_2CO_3	13	48	71	10	30
Na_2SO_4	2	18	7	1	2
$Na_2C_2O_4$	2	5	8	1	8
Other	10	29	14	<1	3

REVIEW OF SELECT DATA FROM FACILITY-GROUP-1 TANKS

REVIEW OF GAS RELEASE EVENTS IN SY-101

- Description of GREs in SY-101
  - o There are three layers in the waste: NC layer, C layer, and crust.
  - o Gas accumulation in NC layer creates a density instability, which cause the tank to roll over.
- Observed behavior during GREs.
  - o Large level drop
  - o Increase in hydrogen concentration
  - o Increase in dome pressure
  - o Temperature data indicate mixing
- GRE statistics for SY-101
  - o Average level drop is ~8 in.
  - o The maximum level drop was ~13 in.
  - o Average period between GREs is ~100 days.
  - o GREs are a stochastic process.
- Thermal balance calculations indicate that the size of a release is proportional to the volume of NC layer that participates in the rollover.

GAS RELEASE EVENTS IN OTHER FACILITY-GROUP-1 TANKS

- SHMS data indicate that GREs occur in AN-103, AN-104, AN-105, AW-101, and SY-103.
- Peak hydrogen concentrations are much less than observed in SY-101.
- Large level drops have not been observed in these tanks.

Los Alamos
Los Alamos National Laboratory

REVIEW OF LEVEL DATA

- Level drop alone is not sufficient to identify GREs because of the uncertainty in level measurement.

- We did a statistical analysis of level changes to determine if and when significant level changes have occurred.

  AN-103.....No significant level drops
  AN-104.....Significant level drops occurred but we could not distinguish real level drops from noise
  AN-105.....Significant level drops occurred and we identified the drops
  AW-101 .....No significant drops occurred
  SY-101.....Significant level drops occurred and we identified the drops
  SY-103.....Not analyzed

SHMS DATA

- In SY-103, there is some correlation between hydrogen concentration and level drop.
- In AW-101 and AN-104, there is little correlation between hydrogen concentration and level drop.
- Based on SHMS data, GREs occur in AW-101 without a corresponding level drop.
- There is insufficient data from AN-103 and AN-105 to determine whether there is a correlation between hydrogen concentration and level drop.

TEMPERATURE DATA

- In AN-103 and AW-101, GREs produce no significant changes in the measured temperature profile.
- In AN-104, AN-105, and SY-103, some GREs produce significant changes in the measured temperature profile.
- Thermal balance calculations for AN-104 and AN-105 indicate that the entire NC layer does not participate in GREs.

CHANGES IN THE NC LAYER THICKNESS AS A RESULT OF COOLING

- All Facility-Group-1 tanks have cooled.
- We examined temperature profile data to determine the effect of cooling on NC layer thickness.
  - o AN-103 - The NC layer thickness increased, but gas accumulation can account for the increase.
  - o AN-104 - There has been no significant change in the NC layer thickness.
  - o AN-105 - There has been no significant change in the NC layer thickness.
  - o AW-101 - There has been a significant increase in NC layer thickness that can not be accounted for by gas accumulation.
  - o SY-101 - There has been an increase in NC layer thickness as a result of cooling.
  - o SY-103 - There is insufficient temperature data to evaluate NC layer changes.

SOME OBSERVATIONS CONCERNING GREs

- Different gas release behavior is observed in the Facility-Group-1 tanks
  - o Complete rollovers - SY-101 and SY-103
  - o Partial rollovers - AN-104 and AN-105
  - o No rollovers - AN-103 and AW-101
- Differences in gas release behavior are related to waste composition
  - o High TOC concentration favors high gas generation rates, which favor large GREs

    Example - SY-101
  - o Solid sodium aluminate and sodium nitrite favor significant gas retention

    Examples - AN-103 and SY-101
  - o Significant amounts of solid sodium carbonate (>25 wt. %) favor rollovers

    Examples - AN-104, AN-105, SY-101, SY-103

SUMMARY OF OTHER MODELS DEVELOPED BY LANL

RAYLEIGH-TAYLOR MODEL

- Criterion for determining if rollovers occur.
- A spontaneous rollover occurs when gas accumulation in the NC layer creates a density instability.
- Neglecting strength, the criterion for an instability is:

$$\alpha_{nc} \geq 1 - \frac{\rho_c}{\rho_{nc}}$$

INDUCED ROLLOVERS

- The waste may be in a meta-stable condition.
- A large disturbance may trigger a rollover.

  Model calculation shows induced rollovers
  Pump-induced rollovers occurred in SY-101

- An induced rollover cannot occur if:

$$\alpha_{nc} \cdot \frac{P_{nc}}{P_{atm}} < 1 - \frac{\rho_c}{\rho_{nc}}$$

MODEL OF SY-101 GAS RELEASES FROM MIXER PUMP SAFETY ASSESSMENT

- A large rollover cannot release more gas than is released as a result of aggressive mixer pump operation.
  - o Minimum waste level after a rollover can be determined from mixer pump data.
- Amount of releasable gas as a function of level can be determined from a volume balance.

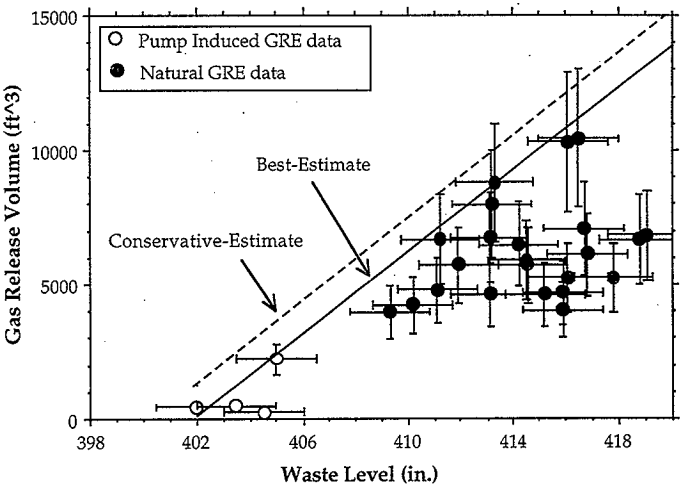

Los Alamos
Los Alamos National Laboratory

UNRELEASABLE GAS IN SY-101

There is unreleasable gas in SY-101 that can not be released as a result of a rollover or normal mixer pump operation.

- The level observed after a GRE varies from 402.0 in. after the October 1990 GRE to 414.2 in. after the December 1988 GRE. This variability can be attributed only to retained gas.

- Based on fill history, the waste level without gas is ~386 in. The data reconciliation study of SY-101 gives a degassed waste level of ~377 in. The minimum waste level as a result of mixer pump operation was ~400 in. This difference indicates that there is significant retained gas in the waste.

- Experiments with waste simulants suggest that organic compounds and their decomposition products make the solids hydrophobic. Bubbles will attach to hydrophobic solids.

SY-101 RELEASE MODEL

- Model Assumptions
  - o Gas bound to solids
  - o Uniform gas fraction profile in the NC layer
  - o Release gas until slurry neutrally buoyant at waste surface
- Gas Release Volumes

$$V_{release} = V_{nc} \cdot \left(\alpha_{nc} \cdot \frac{P_{nc}}{P_{atm}} - 1 + \frac{\rho_c}{\rho_{nc}} \right)$$

- Comparison to Data

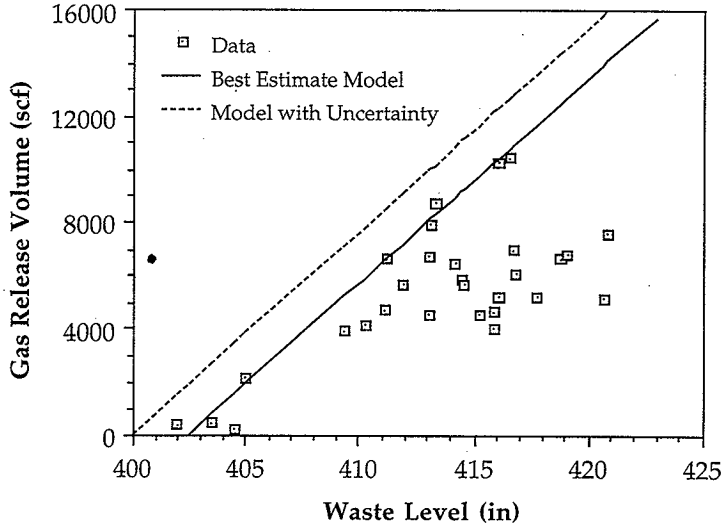

Los Alamos
Los Alamos National Laboratory

NC-LAYER BUBBLE TRANSPORT MODEL

- The time-dependent transport equation for bubbles in the NC layer is based on a material balance.
- The one-dimensional, time-dependent transport equation for gas fraction is:

$$\frac{\partial[\alpha(i+m_{s,a}+m_{s,w})]}{\partial t}=\left[i\alpha'_{G,o}\right](1-\alpha)-\left[\frac{\partial F_i}{\partial z}+\frac{\partial F_a}{\partial z}+\frac{\partial F_w}{\partial z}\right]+E_a+E_w$$

α	=	$\alpha(z,t)$
$m_{s,a}$	=	Saturation density of ammonia vapor
$m_{s,w}$	=	Saturation density of water vapor
$i\alpha'_{G,o}$	=	Gas generation rate
F_i	=	Total flux of insoluble gas
F_a	=	Ammonia bubble flux
F_w	=	Water vapor flux
E_a	=	Ammonia source from liquid to bubbles
E_w	=	Source of water vapor from liquid to bubbles
i	=	$(P-P_a-P_w)/(RT)$

- This is the first bubble retention model:
  - o To consider the effect of viscosity and gas generation rate on gas retention.
  - o To consider the dynamic behavior of gas accumulation.
  - o To predict the axial void fraction profile that agrees qualitatively with the data.

APPLICATION AND EXTENSIONS OF THE MODELS FOR ANALYSIS OF MITIGATION SCHEMES

METHOD OF EVALUATION

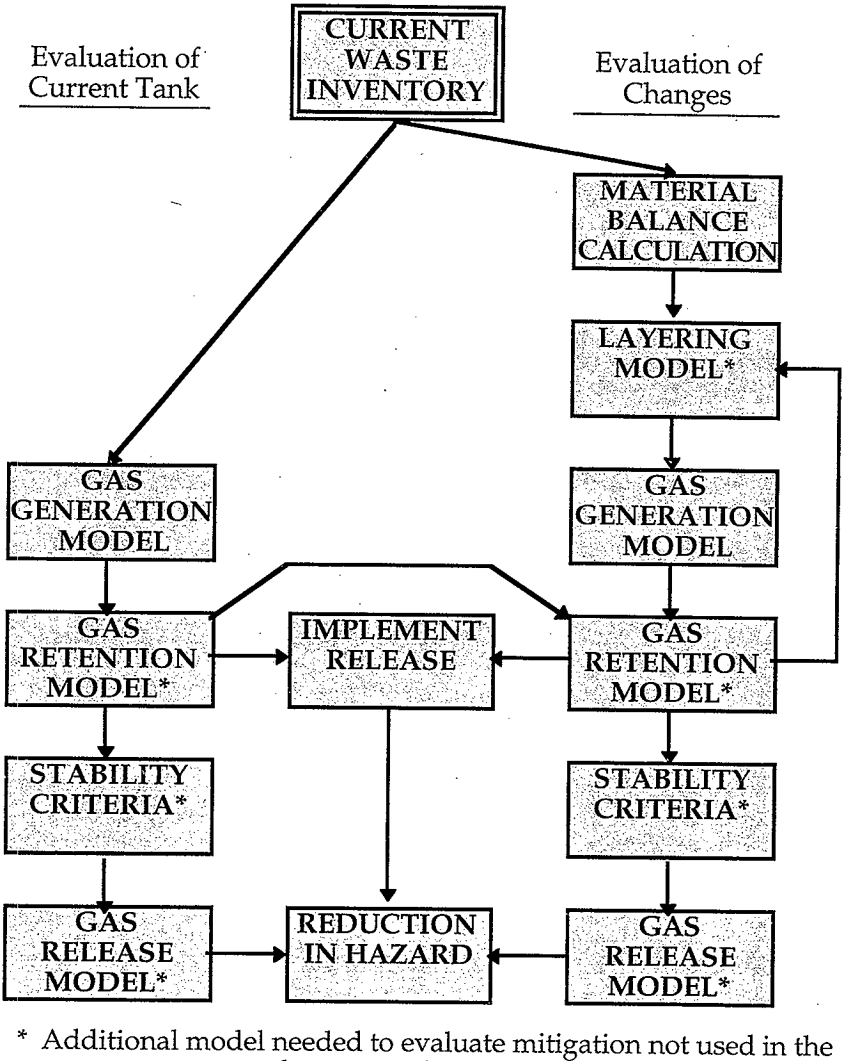

* Additional model needed to evaluate mitigation not used in the data reconciliation studies.

Los Alamos
Los Alamos National Laboratory

SETTLING AND LAYERING

NC LAYER

- No model exists for predicting solids fraction in the NC layer.
- We consider two cases in our analysis: constant solids fraction and constant NC-layer thickness.
  - o Data indicate that heating AW-101 corresponds to the constant solids fraction case.
  - o Data indicate that heating AN-103 corresponds to the constant thickness case.

CRUST

- We assume that mitigation does not affect the crust thickness or solids fraction.
  - o Data indicate that heating does not change the crust thickness

GAS RETENTION MODEL

- The transport equation can be used to obtain a scaling law for the steady-state value of average gas fraction:

Diffusion Limited: $$\alpha_{ave} \propto \frac{\alpha_G \cdot Z_{nc}^2}{D_e}$$

Creep Limited: $$\alpha_{ave} \propto \sqrt{\frac{\mu \cdot \alpha_G \cdot Z_{nc}^2}{\rho_s}}$$

Stokes Flow Limited: $$\alpha_{ave} \propto \frac{\mu \cdot \alpha_G \cdot Z_{nc}}{\rho_s}$$

- Use the Stokes flow limit in the analysis:
  - o Diffusion is not important at steady state. Stokes flow is conservative for evaluating several mitigation schemes.
- Determine a tank-specific proportionality constant from current tank data.
- Also consider the maximum possible gas retention obtained from the Rayleigh-Taylor limit.

STABILITY CRITERIA

- Analysis of SY-101 based on a uniform gas fraction distribution.
  - o Void fraction instrument data indicate that this assumption is not valid for other Facility-Group-1 tanks.
- A stability criterion based on average gas fraction does not explain the data.
  - o Average gas fraction in AN-105 is less than the Rayleigh-Taylor limit.
  - o Temperature data indicate rollovers occur in AN-105.
- The criteria for spontaneous and induced rollovers will be based on the maximum gas fraction.

GAS FRACTION DISTRIBUTION MODEL

- The scaling law gives average gas fraction, but we also need maximum gas fraction.
- The limiting cases of the transport equation gives values of $\alpha_{max}/\alpha_{ave}$ between 1.3 and 2.0.
- From the void fraction instrument, $\alpha_{max}/\alpha_{ave} = 2.0 \pm 0.6$.
- We assume the best-estimate value of α_{max} is α_{ave}.

Los Alamos
Los Alamos National Laboratory

GAS RELEASE VOLUME

ROLLOVERS

- Need to estimate gas release volumes for the gas of nonuniform gas fraction.
- Model Assumptions
  - o Gas bound to solids
  - o Linear gas fraction profile in the NC layer
  - o Gas fraction is zero at the top of the NC layer
  - o Release gas until slurry neutrally buoyant at waste surface
  - o Entire NC layer participates in the rollover
- The total gas release volume is determined by integrating.

$$V_{release} = A \cdot Z_{nc} \cdot \frac{P_{nc}}{P_{atm}} \cdot \alpha_{ave} \cdot \left(1 - \left(1 - \frac{\rho_c}{\rho_{nc}}\right) \cdot \frac{P_{atm}}{2 \cdot \alpha_{ave} \cdot P_{nc}}\right)^2$$

- Model implies that no gas is released from the top portion of the NC layer.

IMPLEMENTATION RELEASES

- Implementation of the mitigation scheme will either induce a rollover or release gas as a result of an inventory change.

FACTORS NOT CONSIDERED IN THE ANALYSIS

- The effect of changes in waste composition and temperature on strength and slurry viscosity is not considered.
- The effect of changes in waste composition and temperature on settled solids fraction is not considered directly.
- The effect of changes in waste composition and temperature on the crust is not considered.
- The effect of strength on the stability of the waste is not considered.
- Factors that limit the extent of a rollover are not considered.
- The effects of surface forces and changes in surface forces are not considered.

SUMMARY

- The LANL Waste Tank Safety Team uses a systems model to evaluate the impact of changes on flammable gas hazards.
- The approach used by the LANL Waste Tank Safety Team is:
  - o Recognize the importance of waste inventory
  - o Use an integrated model of the waste
  - o Calibrate models to actual waste tank data whenever possible

EVALUATION OF MITIGATION STRATEGIES IN FACILITY-GROUP-1 DOUBLE-SHELL FLAMMABLE-GAS TANKS AT THE HANFORD SITE

by

C. Unal, P. Sadasivan, W. Kubic, and J. R. White

Presented to the Expert Elicitation Panel
January 22, 1998

Los Alamos National Laboratory
Technology and Safety Assessment Division
Nuclear Systems and Design Group, TSA-10
Los Alamos, NM 87545

Los Alamos
NATIONAL LABORATORY

OUTLINE

- Scope of Work and Objectives
- Analysis of Framework and Performance Criteria
- Identification of Mitigation Strategies
- Key Parameters—Gas Generation, Retention, and Release
- Ranking Methodology and Results
- Mixing by Horizontal Jets
- Supernatant Liquid Removal, Inerting, and Burn Mitigation
- Heating and Dilution

Los Alamos
NATIONAL LABORATORY

SCOPE OF WORK AND OBJECTIVES

- Closure of FG safety issue may require mitigation of gas generation, retention, or release.
- Babad et al. (1992) evaluated mitigation strategies.
- Significant new data and analysis tools are available.
- **The overall objective of work** is to reevaluate mitigation strategies.
- The emphasis is on generation, retention, and release in FG-1 DSTs (AW-101, SY-013, AN-103, AN-104, AN-105)
- **This presentation** is an overview of mitigation strategies.

ANALYSIS FRAMEWORK

- Ignition---> **Fuel + Oxidizer + Ignition Source**

- No ignition--->mitigate/eliminate fuel, oxidizer, or ignition source

- Fuel---> hydrogen and ammonia
- Oxidizer---> air and nitrous oxide
- Ignition sources---> electrical, mechanical, static, lightning, etc.

- The methodology is based on best-estimate data and models.
- No attempt was made to estimate the uncertainty.
- GREs occurring as a result of seismic events or plume releases are not considered.
- Flammability limits are provided for ignition energies <100 J.

Los Alamos
NATIONAL LABORATORY

KEY PERFORMANCE CRITERIA

- The primary goal of a proposed mitigation strategy is to prevent FG concentrations from exceeding 25% of the LFL in the tank dome or at the ventilation header.
- The FG hazard during implementation of the mitigation strategy is also a concern.
- We try to answer two key questions:
  - Does the mitigation strategy eliminate the FG hazard at the final steady-state conditions after its implementation?
  - Is an FG hazard possible during implementation of the mitigation strategy until the final steady-state conditions are obtained?

KEY PARAMETERS AFFECTING GAS RETENTION

Strength of Waste (NC Layer)

- The strength of the waste overcomes the buoyancy force.

Apparent Viscosity of Waste (NC Layer)

- High viscosity values result in a low terminal velocity.

Presence of Solid Aluminum

- Sodium aluminate tends to retain more gas.

Waste Type

- Noncomplexed waste has little tendency to retain gas.
- DSS and DSSF wastes tend to retain more gas.

NC-Layer Volume

- Large NC-layer volumes allow for larger accumulations of gas.

NC- and C-Layer Density and Density Ratio (ρ_C/ρ_{NC})

- A low ρ_C/ρ_{NC} gives higher neutral-buoyancy retention.

Solid Fraction (ϕ)

- A high ϕ yields a higher yield stress and viscosity.
- A low ϕ favors less stable bubbles and enhances bubble coalescence, which results in larger bubble sizes.

Settling

- Settling of salt crystals with different sizes and shapes produces a salt matrix with a higher solid fractions and strength.
- Strong interparticle forces may enhance the shear strength.

Henry's Law Constants

- Low Henry's Law Constants result in more dissolved hydrogen.
- High Henry's Law Constants result in greater ammonia partial pressures.

Surface Forces

- A high liquid-gas surface tension increases the capillary pressure, which favors bubble coalescence (easier liquid film thinning).
- Hydrophobic surfaces tend to retain more gas.

Ionic Strength

- Low ionic strength favors bubble coalescence.
- High ionic strength lowers the solids solubility and increases the ammonia partial pressure.

KEY PARAMETERS FOR GAS GENERATION

- Low levels of total organic carbon (TOC) decrease the gas generation rate.
- Low ^{137}Cs and ^{90}Sr concentrations decrease the hydrogen generation rate.
- A low T_{WASTE} decreases the gas generation rate but increases the hydrogen concentration.
- High concentrations of nitrate and other scavengers decrease the radiolytic hydrogen generation rate.
- Low levels of dissolved aluminate ions decrease the gas generation rate.

KEY PARAMETERS FOR GAS RELEASE

- A lower ρ_C/ρ_{NC} increases the neutral-buoyancy point.
- A low L_{NC} results in low gas releases.
- A low waste strength yields small gas releases.
- A low L_C results in less likelihood of a GRE occurring.
- Tanks rich in sodium carbonates tend to roll over.
- Higher gas generation rates increase the frequency of GREs.

IDENTIFICATION OF MITIGATION STRATEGIES

- A small review team
- Previous work
- A total of 38 mitigation strategies were identified:
  - 23 previously proposed
  - 15 new

TWO-STEP RANKING METHODOLOGY

- First, identify strategies with sound and proven principles using judgment factors.

    1. Sound principle
    2. Proof of principle
    3. New data
    4. New analysis
    5. Technology status
    6. Preclude retrieval

- Second, consider the cost and schedule.
- **Eliminate nonachievable mitigation strategies as soon as possible.**
- Ranked 0 to 4, where 0 = least favorable, 4 = most favorable.

Los Alamos
NATIONAL LABORATORY

RESULTS OF PRELIMINARY RANKING

1. Horizontal Jet Mixing
2. Using Inert Gas in the Dome Space
3. Supernatant Liquid Removal
4. Burn Mitigation [Multiport Risers (MPRs)]
5. Heating
6. Dilution
7. Vertical Jet Mixing
8. Past-Practice Sluicing
9. Organics Destruction by Heating
10. Retrieval
11. Removal of Radioactive Isotopes
12. Removal of Aluminate
13. Spark Control
14. Low-Frequency Sonic Probe
15. Cooling the Waste
16. NC-Layer Recirculation

Horizontal Jet Mixing

- Mobilizes NC layer by jet mixing
- Mitigates gas retention and release
  - Prevents sedimentation and formation of NC layer
  - Reduces NC-layer volume, solids fraction, yield strength, and viscosity
  - Controls the volume of the gas release and its frequency
- Successfully provided a constant waste level in Tank SY-101
- Adversely affects the long-term pump mixing operations
- Mixing is costly

Mitigation of Burn

- Prevents explosion
- Mitigates consequences of FG ignition
  - Adequate venting
  - Damaging pressures prevented
- Does not prevent material release
- Is a low-cost, fast-schedule concept; reduces consequences

Heating

- Controls temperature
- Mitigates retention and release
  - Reduces NC-layer volume by dissolving solids
  - Increases gas generation (higher temperatures)
  - Affects density ratio, solids fraction, strength, viscosity, Henry's Law Constants, surface tension, and particle-to-particle attractive forces
- Changes gas composition
- May require mixing
- Could be relatively costly

Inerting Dome Space

- Controls the oxidizer
- Eliminates FG hazard by removing the oxidizer
- Prevents FG hazard during installation
- Could be low in cost

Supernatant Liquid Removal

- Controls dome volume
- Mitigates gas generation, retention and release, and FG concentration
  - Eliminates episodic GREs (no C layer)
  - Decreases FG concentration
  - Reduces gas inventory, creates low pressure in NC layer
  - Affects temperature and gas generation
- Requires simple equipment and a storage tank; medium cost

Dilution

- Causes dissolution of solids
- Mitigates gas retention and release
  - Reduces NC-layer volume and solids fraction
  - Affects the strength, viscosity, chemical composition and solubility, density ratio, solids fraction, Henry's Law Constant, ionic strength, composition of gas, and gas generation rate
- Studied extensively; medium cost

Los Alamos
NATIONAL LABORATORY

MIXING BY HORIZONTAL JETS

- Tank SY-101 mixer pump performance evaluation
- Sludge mobilization studies—review/conclusions
- Mobilization of waste in FG-1 DSTs
- Gas releases

Los Alamos
NATIONAL LABORATORY

TANK SY-101 MIXER PUMP PERFORMANCE

- In <100 hours, the mixer pump broke the gas release cycle.
- No episodic releases occurred with a H_2 con. >25% of the LFL.
- Quasi-steady waste level is 400 to 402 in.
- Waste fully mixed except at the top and bottom 30 to 40 in.
- Induced gas release is <1000 ppm, $\leq$2200 ft^3 (level-dependent).
- 12 episodic GREs with H_2 >25% of the LFL would occur if they were not mitigated.

Los Alamos
NATIONAL LABORATORY

MOBILIZATION FRACTION

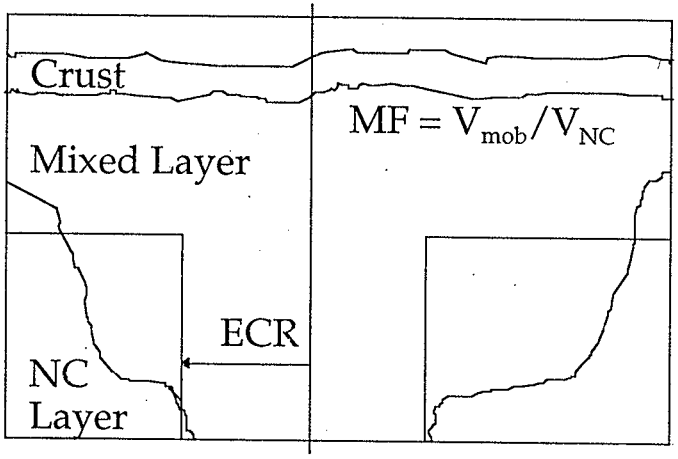

- $ECR_{40\text{-hour}}$ <20 ft (void data)
- $ECR_{67\text{-hour}}$ <28 ft (temperature data)
- Exact value of the ECR is unknown

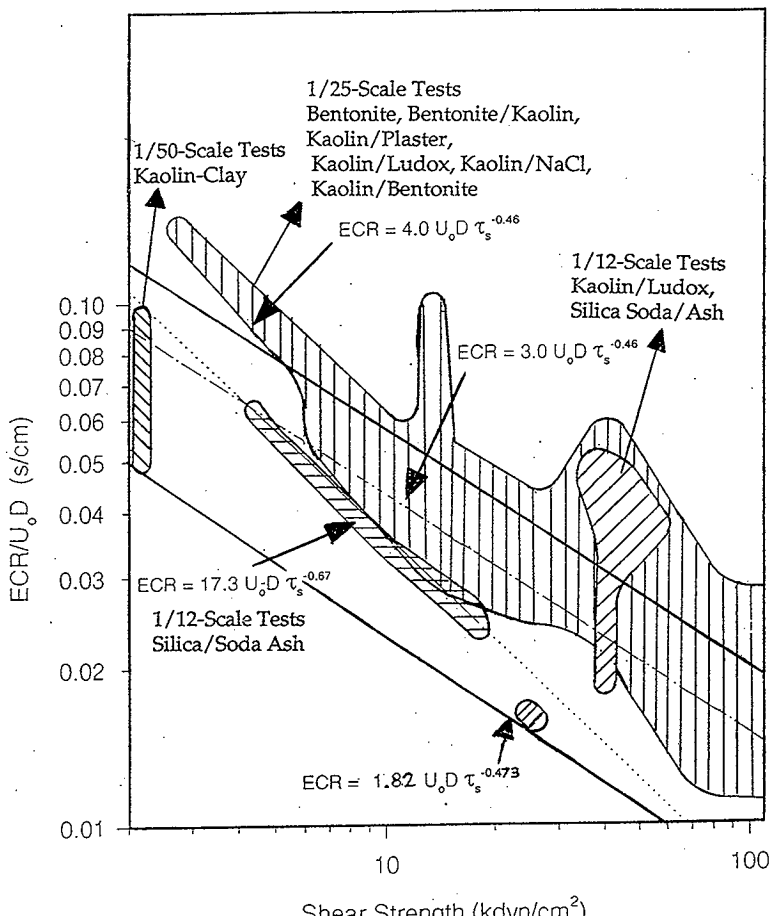
1/25-Scale Tests
Bentonite, Bentonite/Kaolin,
Kaolin/Plaster,
Kaolin/Ludox, Kaolin/NaCl,
Kaolin/Bentonite
1/50-Scale Tests
Kaolin-Clay
ECR = 4.0 U0D τs-0.46
1/12-Scale Tests
Kaolin/Ludox,
Silica Soda/Ash
ECR = 3.0 U0D τs-0.46
ECR = 17.3 U0D τs-0.67
1/12-Scale Tests
Silica/Soda Ash
ECR = 1.82 U0D τs-0.473
ECR/U0D (s/cm)
0.10
0.09
0.08
0.07
0.06
0.05
0.04
0.03
0.02
0.01
10
100
Shear Strength (kdyn/cm2)

STRENGTH OF THE NC LAYER

Tank	Risers	Viscometer-Ball Stop—Elevations (cm)	Maximum Void—Elevation (cm)	Yield Stress (Pa)
SY-101	11B, 4A	80, 0		225 (±100)
SY-103	17C, 22A	102, 105	100–200	112 (±40)
AW-101	13A, 1C	0, 94	100	159 (±37)
AN-103	16B, 1B	227, 158	200	142 (±15)
AN-104	16B, 1B	74, 65	100	81 (±11)

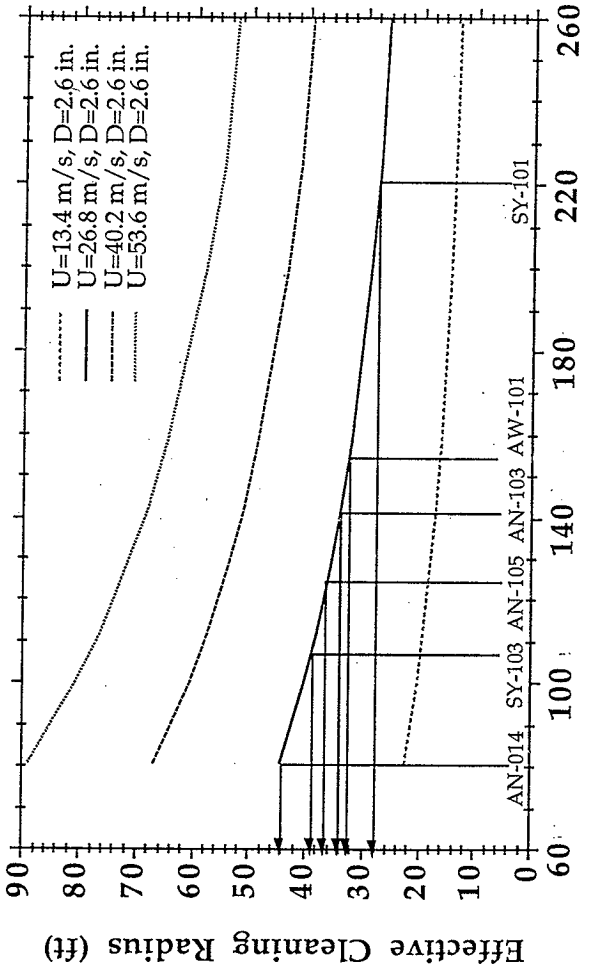

Los Alamos
NATIONAL LABORATORY

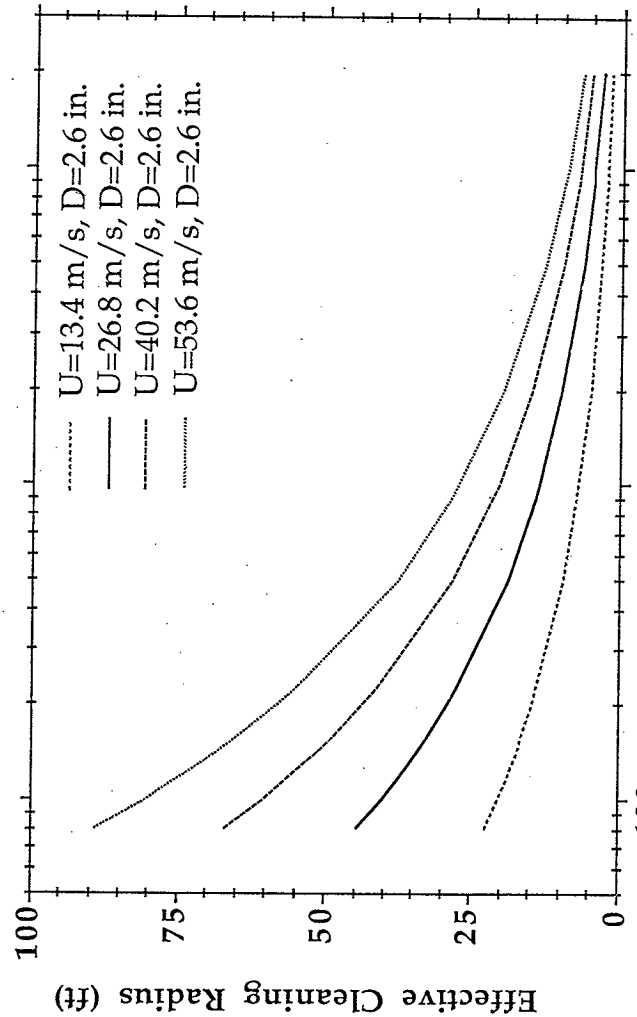

Los Alamos
NATIONAL LABORATORY

Yield parameter for Bingham plastics

$$Y = \tau_s / gd(\rho_p - \rho) = 0.04\text{-}0.22$$

- τ_s --->900 to 3000 Pa or higher
- ECR ---> <5 ft for U= 13 to 57 m/s if τ_s ---> 10000 Pa
- Pump needs more power to provide higher jet velocities
- Water addition or dilution can be used

GAS RELEASES

- **Installation causes a**
  - rollover (induced rollover)
  - local gas release
  - Local gas releases during installation do not pose a FG hazard
- **Operation causes a**
  - rollover (induced rollover)
  - local gas release
  - Local gas releases caused by operation are found to not pose an FG hazard

Los Alamos
NATIONAL LABORATORY

BEST-ESTIMATE GAS RELEASE VOLUMES FOR INDUCED ROLLOVERS

$$V_{release} = A \cdot Z_{nc} \cdot \frac{P_{nc}}{P_{atm}} \cdot \alpha_{ave} \cdot \left(1 - \left(1 - \frac{\rho_c}{\rho_{nc}}\right) \cdot \frac{P_{atm}}{2 \cdot \alpha_{ave} \cdot P_{nc}}\right)^2$$

PARAMETER	AW-101	AN-103	AN-104	AN-105	SY-103
Gas bubbles in NC layer (scf)	3035	10,210	7288	5399	5400
Gas bubble inventory (scf)	5279	11,671	7483	5535	5750
Soluble gas inventory (scf)	245,420	298,030	286,905	308,450	-
Releasable gas bubbles (scf)	38	4760	2530	602	2700
Releasable dis. gas (scf)	1005	1381	1637	1658	520
Max. H_2 con. (ppm)	5674	50,564	36,373	12,418	12,000
Max. FG con. (%)	**22**	**139**	**102**	**43**	**35**

Los Alamos
NATIONAL LABORATORY

SUMMARY AND CONCLUSIONS

- The horizontal jet mixing concept would mitigate the gas retention and release by preventing the formation of the NC layer.
- The horizontal jet mixing concept provides a means to keep the waste level or FG inventory at a safe level, as demonstrated in Tank SY-101.
- Possible long-term adverse effects of the mixer pump operations on the gas retention currently are being investigated.
- Waste mobilization depends on the yield stress of the waste and is time-dependent.
- Waste in the FG-1 tanks can be mobilized with pump capacities up to 2 m^2/s (SY-101 mixer pump) if $\tau_y < 1000$ Pa.

SUMMARY AND CONCLUSIONS

- For $\tau_y > 1000$ (the bottom layer), higher pump capacities and water addition during mixing would be needed.
- Local gas releases during the installation and operation of a mixer pump do not pose an FG hazard.
- If the installation and operation of a mixer pump cause an induced rollover in the FG-1 tanks, only Tanks AN-103 and AN-104 would release FG in excess of the LFL.
- All FG-1 tanks, except Tank AW-101, would release FG >25% of the LFL during a possible induced rollover.

SCHEMES THAT ARE NOT WASTE INTRUSIVE

- SUPERNATANT REMOVAL
- INERTING
- MITIGATION OF BURNS

Pratap Sadasivan
TSA-10, Los Alamos National Laboratory

January 22, 1998

Los Alamos
NATIONAL LABORATORY

SUPERNATANT LIQUID REMOVAL

- Increases dome volume
- Reduces likelihood of spontaneous GREs
- Increases retained gas void fraction
- Reduces gas release fraction during GRE
- Changes waste temperature
- Changes solids fraction
- Changes gas generation, retention

Los Alamos
NATIONAL LABORATORY

THERMAL MODEL

- Lumped models for C and NC layers
- Heat losses to annulus and dome space
- Effective conductances

Results

- NC layer cools when supernatant is removed
- Maximum cooling <8°C
- No significant effect on solids fraction expected

Los Alamos
NATIONAL LABORATORY

ANALYSIS

- Is a spontaneous GRE likely during removal? (Will void fraction exceed neutral-buoyancy void during removal?)
- Will the retention behavior change? (What is the void fraction in the NC layer?)
- Consequences of a spontaneous GRE?
- Consequences of steady release during removal?

Los Alamos
NATIONAL LABORATORY

SUPERNATANT LIQUID REMOVAL—SUMMARY

Issue	AN-103	AN-104	AN-105	AW-101	SY-103
DURING REMOVAL					
Will average NC-layer void exceed NB void during removal?	Yes	No	No	No	Yes
Consequences of a GRE when $\alpha = \alpha_{NB}$ during removal?	<50% LFL	N/A	N/A	N/A	>LFL
Consequences of steady releases?	<25% LFL	<25% LFL	<25% LFL	<25% LFL	<25% LFL
STEADY STATE (AFTER REMOVAL)					
Consequences of a GRE based on current retained gas?*	<LFL	<50% LFL	<25% LFL	<25% LFL	<50% LFL
Consequences of a Rayleigh-Taylor GRE?*	<LFL	<50% LFL	<50% LFL	<50% LFL	<50% LFL

* If some or all supernatant is removed.

Los Alamos
NATIONAL LABORATORY

INERTING

- Eliminates oxidizer
- Not waste intrusive
- Inert gas flow rate depends on ventilation flow rate
- Pressure drop depends on air inleakage paths
- Nitrogen as inert gas

Los Alamos
NATIONAL LABORATORY

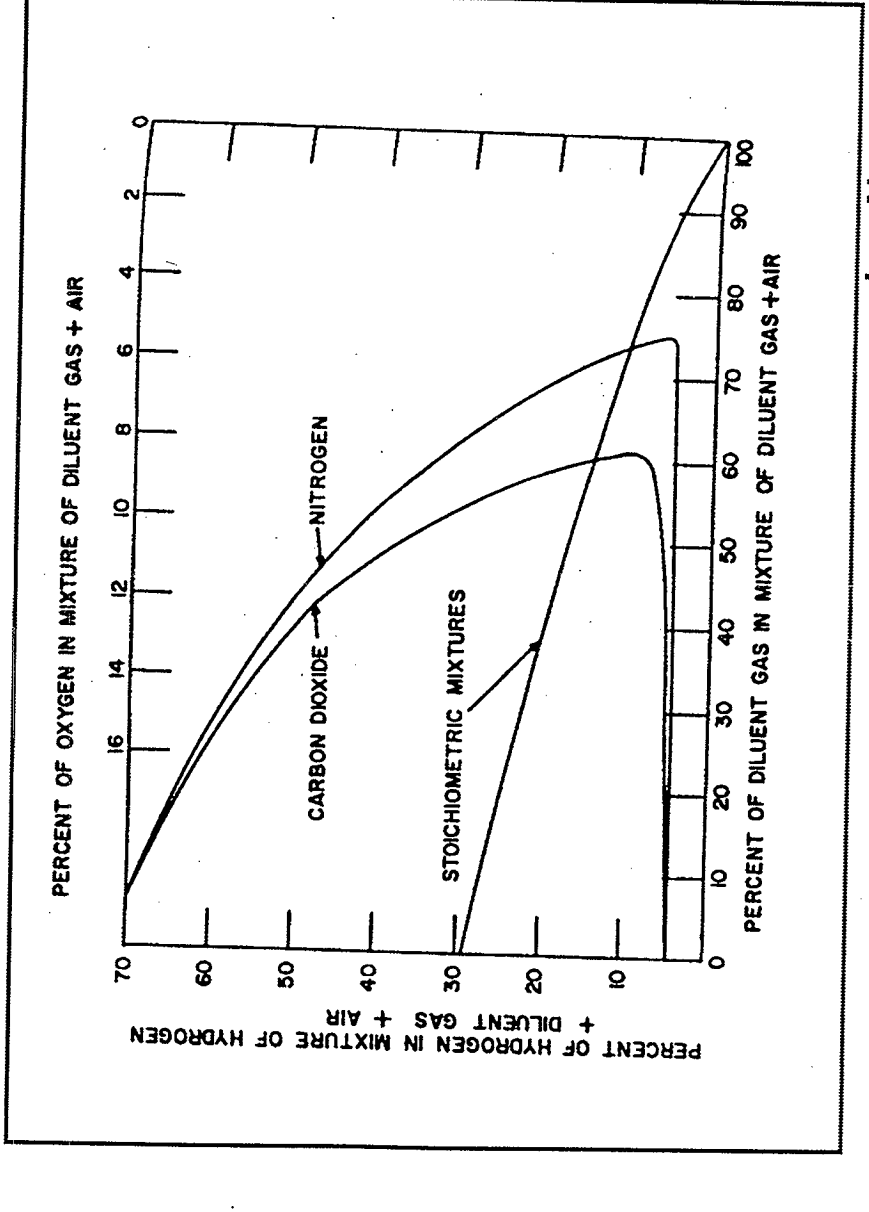

Los Alamos
NATIONAL LABORATORY

ANALYSIS

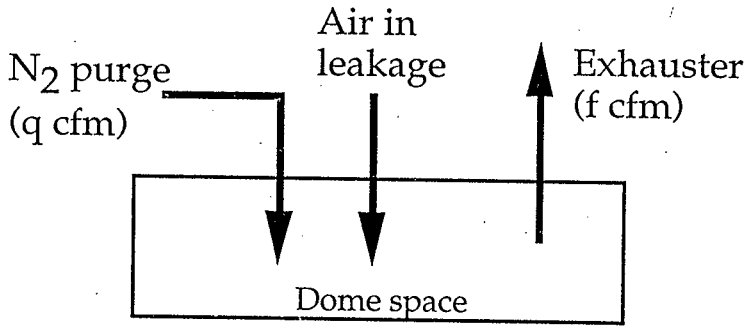

- $q > 0.7619\ f$

- $\Delta p = 7.19101 \times 10^{-5} \dfrac{K_{loss}\ f^2}{A^2_{sq.in.}}$

Los Alamos
NATIONAL LABORATORY

Los Alamos
NATIONAL LABORATORY

INERTING—SUMMARY

- Air leakage areas have to be <10 $in.^2$
- N_2 purge rates: 200–300 cfm
- Estimated costs: <$1 M per year
- Backup systems required
- N_2O fraction needs to be considered
- Possible dryout of crust needs to be considered
- Feasible for all FG-1 tanks

Los Alamos
NATIONAL LABORATORY

MITIGATION OF BURNS

- Assume burn occurs
- Mitigate pressures below safe limits
- Provide pressure relief by venting
- Peak pressure and rate of pressure rise
- Multiport risers (MPRs)

Los Alamos
NATIONAL LABORATORY

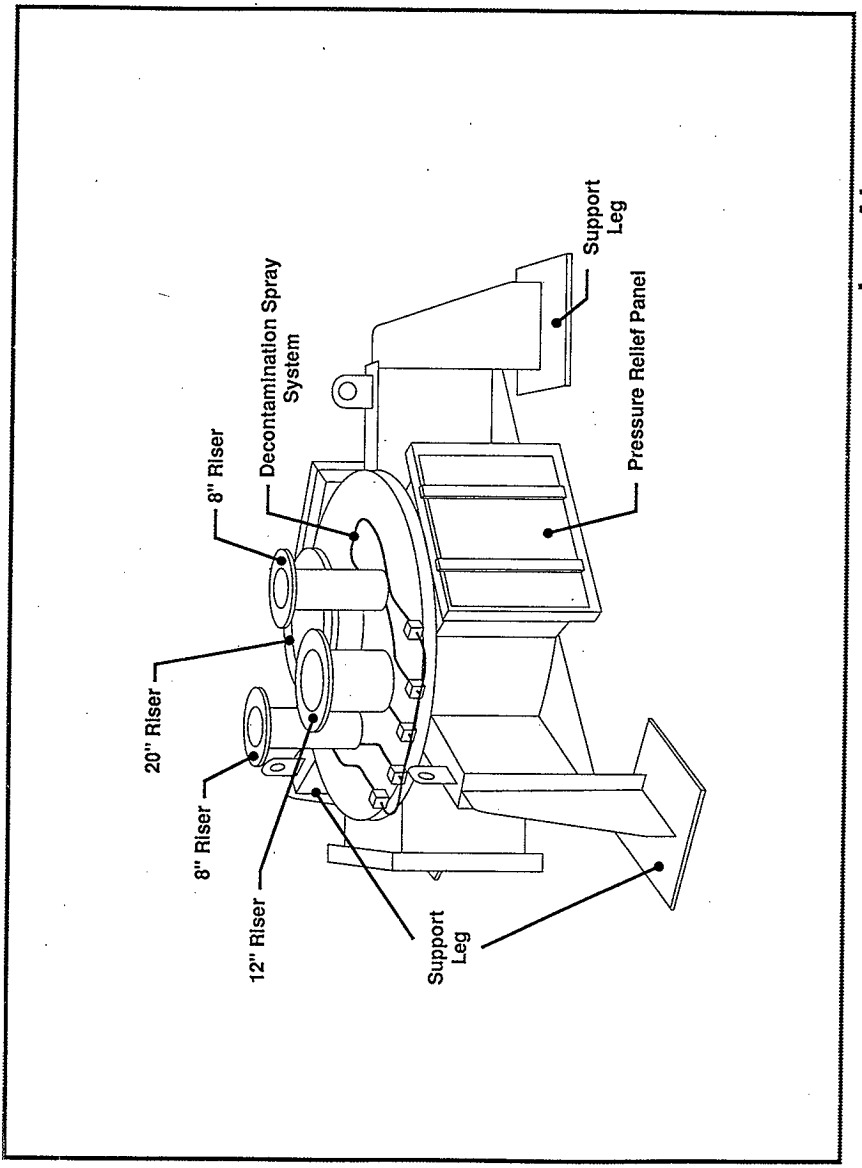
Support Leg
Pressure Relief Panel
Decontamination Spray System
8" Riser
20" Riser
8" Riser
12" Riser
Support Leg
Los Alamos
NATIONAL LABORATORY

ANALYSIS

- Burn calculations
- With and without venting
- Vent areas
- BE gas composition and release volumes
- Flame speeds specified

Los Alamos
NATIONAL LABORATORY

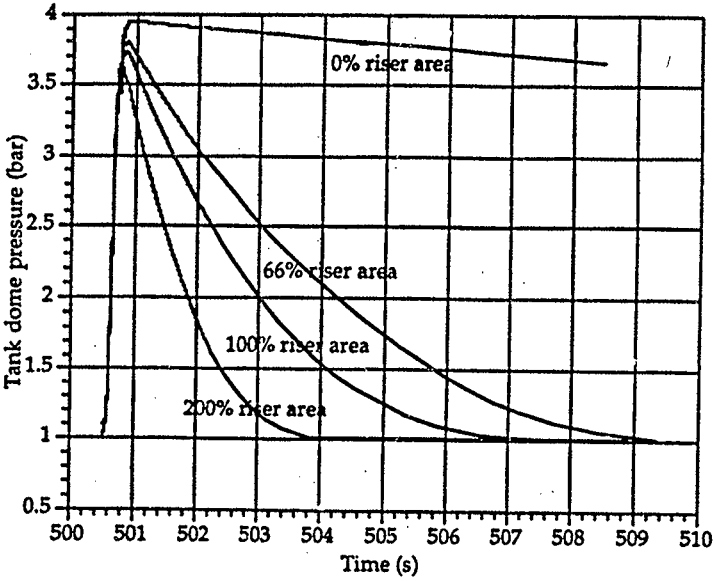

CALCULATIONS FOR TANK SY-101 (1994)

Los Alamos
NATIONAL LABORATORY

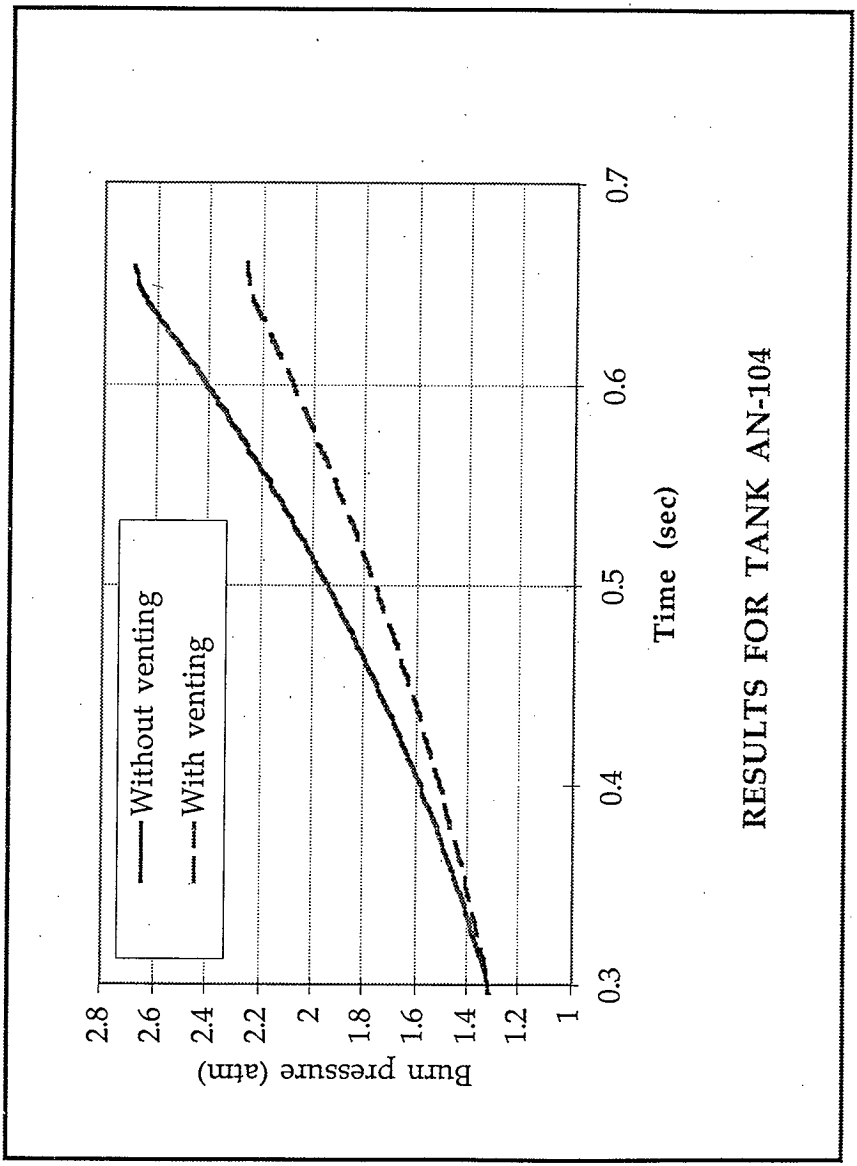
Without venting
With venting
Burn pressure (atm)
2.8
2.6
2.4
2.2
2
1.8
1.6
1.4
1.2
1
0.3
0.4
0.5
0.6
0.7
Time (sec)
RESULTS FOR TANK AN-104
Los Alamos
NATIONAL LABORATORY

MPRs—SUMMARY

- Relatively small reduction in peak pressure
- Reduction in rate of pressurization
- Much larger vent areas may be required
- Limited potential use for mitigation

Los Alamos
NATIONAL LABORATORY

SUMMARY

Scheme	AN-103	AN-104	AN-105	AW-101	SY-103
Removal of supernatant liquid	X	√	√	√	X
Inerting	√	√	√	√	√
Burn mitigation by MPRs	X	X	X	X	X

Los Alamos
NATIONAL LABORATORY

ANALYSIS OF MITIGATION OF FACILITY-GROUP-1 TANKS BY HEATING AND DILUTION

William L. Kubic, Jr.

Nuclear Systems Design and Analysis Group
Los Alamos National Laboratory
Los Alamos, New Mexico 87545

January 22, 1998

BASIC PRINCIPLE

- Gas retention and release increase with total solids inventory.
  - o The Rayleigh-Taylor model predicts that the retained-gas volume increases with the mass of settled solids.
  - o The bubble retention model predicts that the gas fraction in the NC layer should be an increasing function of NC-layer thickness and viscosity.
- Reducing the mass of settled solids will reduce the total inventory of retained gas and the size of GREs.
  - o The solubility of most electrolytes increases with temperature.
  - o Adding water or dilute sodium hydroxide solution dissolves many of the major solids components in the waste.

FACTORS THAT LIMIT THE EFFECTIVENESS OF HEATING

- Insoluble Solids—Sodium oxalate and salts of alkaline earth metals and transition metals are relatively insoluble in the waste at all reasonable temperatures.
- Sodium Carbonate and Sodium Sulfate—The solubility of forms of sodium carbonate and sodium sulfate in the waste decrease with increasing temperature.
- Gas Generation Rate—The gas generation rate increases with increasing temperature. Gas retention increases with the gas generation rate.
- Ammonia—The vapor pressure of dissolved ammonia and ammonia releases increases with increasing temperature.

ADDITIONAL BENEFITS OF DILUTION

- Reducing the concentrations of soluble organic compounds, aluminate, and radionuclides in the liquid will reduce the gas generation rate per unit volume.
- Dilution reduces the ammonia concentration.

FACTORS THAT LIMIT THE EFFECTIVENESS OF DILUTION

Insoluble Solids—Salts of alkaline earth and transition metals are relatively insoluble and can not be dissolved by dilution.

Aluminum Hydroxide Precipitation—Water addition may cause aluminum hydroxide to precipitate.

Density Ratio—Dilution increases the ratio of solid to liquid density, which increases the gas fraction obtained from the Rayleigh-Taylor limit.

Cooling—Dilution may cause cooling, which may cause additional salts to precipitate and may increase the hydrogen concentration.

Available Tank Space—Dilution may require the removal of supernatant liquid. There is limited tank space to receive supernatant liquid.

Dissolved Hydrogen—The reduction in ionic strength as a result of dilution will increase the amount of dissolved hydrogen.

Reduction in Free Radical Scavengers—Dilution will reduce the concentration of free radical scavengers, which may increase radiolytic hydrogen production.

EVALUATION CRITERIA FOR HEATING AND DILUTION

Objective: Reduce maximum flammable gas concentration in the dome to <25% of LFL.

Considerations: Best-estimate retained gas volume.

Rayleigh-Taylor limit as a measure of potential gas retention capacity.

Criteria: Best estimate >25% of LFL—Not acceptable.

Best estimate <25% of LFL and Rayleigh-Taylor limit >100% of LFL—Not acceptable because of large uncertainty.

Best estimate <25% of LFL and Rayleigh-Taylor limit <100% of LFL—May be a viable mitigation scheme.

Los Alamos
Los Alamos National Laboratory

RESULTS FOR HEATING AN-103

- Heating dissolves the sodium nitrite and sodium aluminate in the waste, reducing the total solids inventory by ~70%.
- Heating reduces the flammable gas concentration in the dome, but not to an acceptable level.

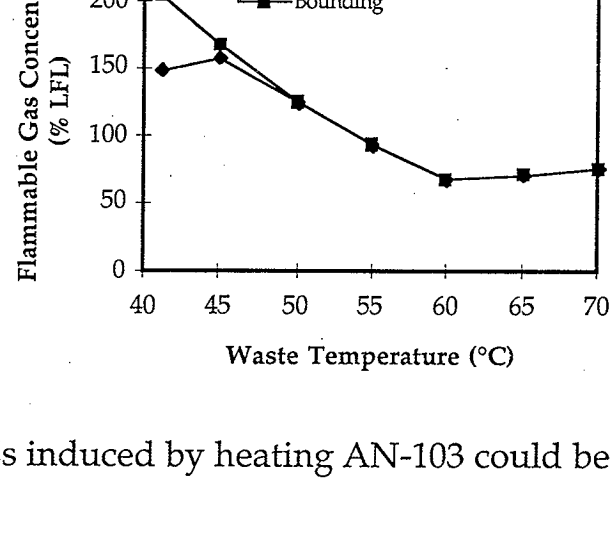

- GREs induced by heating AN-103 could be large.

Los Alamos
Los Alamos National Laboratory

RESULTS FOR HEATING AN-104 AND AN-105

- The solids in AN-104 and AN-105 are predominantly sodium carbonate, sodium sulfate, and insoluble solids. Heating increases solids inventory slightly.
- Heating increases the gas generation rate, which increases gas retention and the magnitude of the flammable gas hazard.

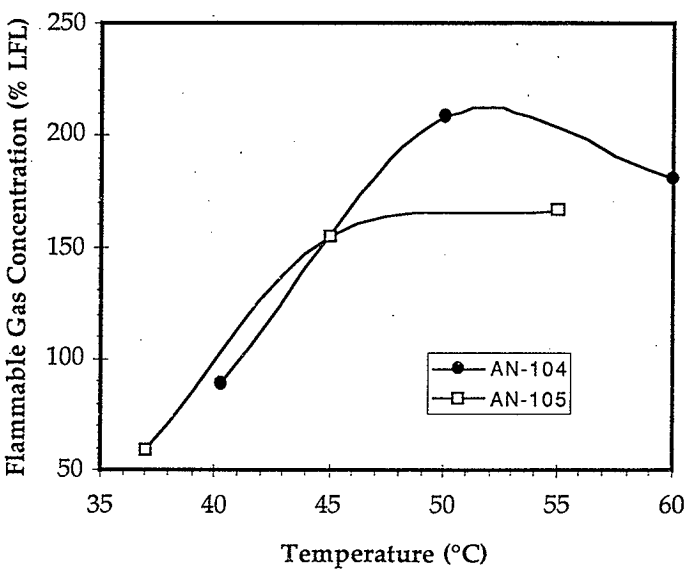

Los Alamos
Los Alamos National Laboratory

RESULTS FOR HEATING AW-101

- Based on our best-estimate analysis, GREs in AW-101 will not produce flammable gas concentrations >25% of LFL.
- Heating the waste to ~60°C can reduce the Rayleigh-Taylor limit to <25% of LFL.

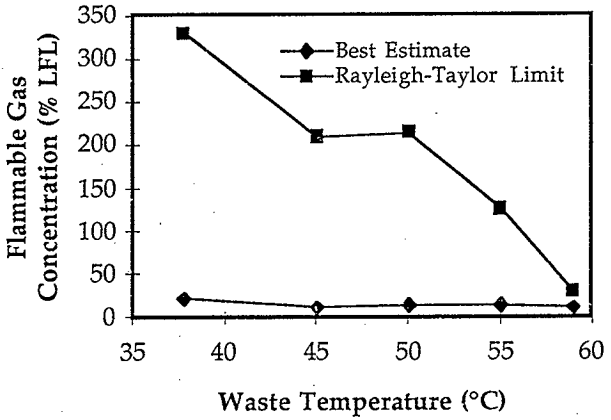

Los Alamos
Los Alamos National Laboratory

RESULTS FOR HEATING SY-103

- We have not performed a data reconciliation study on SY-103; thus, we do not have a model for quantitative analysis.
- Based on a qualitative evaluation, we conclude that:
  - heating the waste to 60°C will reduce the solids inventory by 35 to 50%;
  - heating the waste to 60°C will reduce the maximum flammable gas concentration to between 18 and 32% of LFL.
- Heating may reduce the GREs to an acceptable level, but there is a great deal of uncertainty in analysis.

IMPLEMENTATION OF HEATING

- Methods of heating the waste:
  - Reduce vent flow rate in the annulus
  - Heat the inlet air to the vent systems
  - Install an in-tank heater
- Reducing annulus vent flow rate not attractive:
  - May not increase the temperature enough
  - Large time constant
- In-tank heaters not attractive:
  - Waste-intrusive operations required
  - Mixer pump required to prevent boiling
- Heating the inlet air is the most attractive option
  - Heating the inlet air by ~20°C would maintain the steady-state temperature at the required level.
  - Heating the inlet air to ~85°C would reduce the heating time to ~3 months without boiling the waste.

PRELIMINARY EVALUATION OF MITIGATION BY HEATING

- Heating is not an attractive mitigation option:
  - It increases the flammable gas hazard in AN-104 and AN-105.
  - We cannot demonstrate that heating will reduce the best-estimate GRE to an acceptable level in AN-103 and SY-103.
  - We can demonstrate that heating will reduce the gas retention capacity in AW-101 to an acceptable level, but mitigation may not be needed unless an adverse change occurs.
- We do not recommend additional consideration of heating as a mitigation option.

DESIGN CONSIDERATIONS FOR DILUTION

- Dilution will be done with water or a hydroxide solution.
- There are three design parameters to consider for dilution:
  - Amount of diluant added.
  - Amount of supernatant liquid removed.
  - Hydroxide concentration in the diluant.
- Desire to minimize all three parameters.
  - Remove supernatant liquid if diluant addition increases waste level to >410 in.
  - Add diluant after removing the supernatant liquid to maximize the effectiveness of dilution.
  - Add sodium hydroxide if needed to prevent aluminum hydroxide precipitation.

DILUTION vs RECOVERY

- We do not consider removal of the NC-layer solids in our evaluation of dilution.
- We consider dilution with the removal of NC-layer solids to be waste recovery, which is a separate mitigation option.

RESULTS FOR DILUTION OF AN-103

- Supernatant liquid removal not required.
- Sodium hydroxide addition not required.
- Adding 220,000 gal. of pure water dissolves ~80% of the solids.
- Dilution with pure water can reduce the best-estimate gas release to <25% of LFL and the Rayleigh-Taylor limit to <100% of LFL.

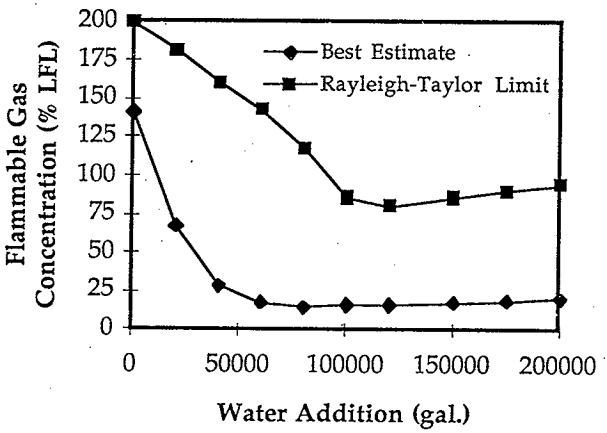

- Waste may cool, but it is not a problem.

Los Alamos
Los Alamos National Laboratory

RESULTS FOR DILUTION OF AN-104

- Supernatant liquid removal required.
- Sodium hydroxide addition not required.
- Adding 700,000 gal. of water dissolves ~60% of the solids.
- Dilution does not reduce the maximum flammable gas concentration to <25% of LFL.
  - o Dilution does not dissolve sufficient solids.
  - o Dilution increases hydrogen concentration.
  - o Water addition reduces dome volume.

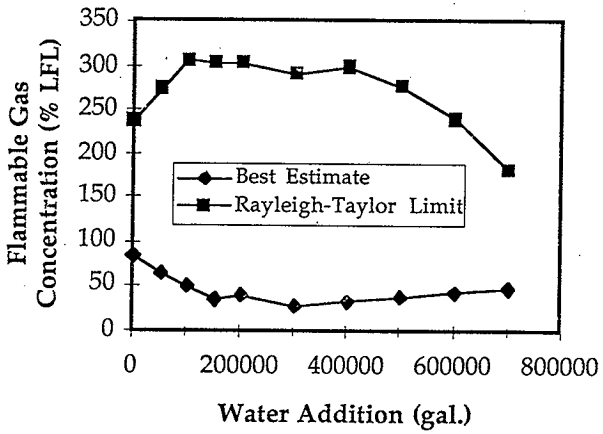

Los Alamos
Los Alamos National Laboratory

RESULTS FOR DILUTION OF AN-105

- Supernatant liquid removal required.
- Sodium hydroxide addition not required.
- Dilution does not reduce the maximum
- Flammable gas concentration to <25% of LFL.
  - o Dilution does not dissolve sufficient solids.
  - o Dilution increases hydrogen concentration.

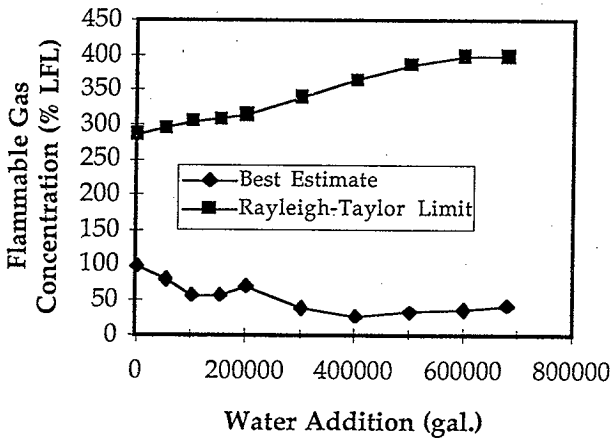

Los Alamos
Los Alamos National Laboratory

RESULTS FOR DILUTION OF AW-101

- Supernatant liquid removal not required.
- Sodium hydroxide addition not required.
- Adding 250,000 gal. of pure water dissolves a significant fraction of the solids.
- Dilution reduces the Rayleigh-Taylor limit significantly.

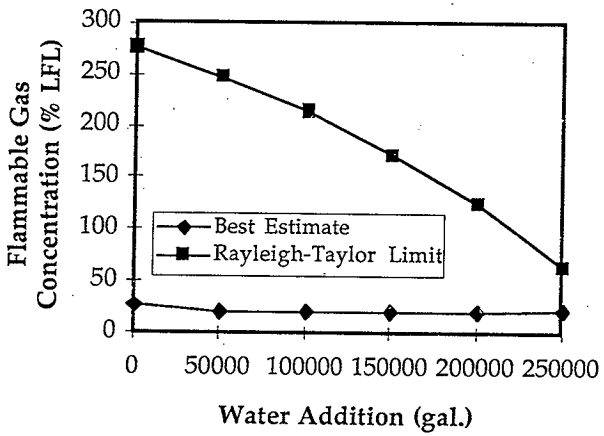

Los Alamos
Los Alamos National Laboratory

RESULTS FOR DILUTION OF SY-103

- No data reconciliation study for SY-103.
- Supernatant liquid removal required.
- Sodium hydroxide addition not required.
- Estimate that addition of ~100,000 gal. of water reduces the solids inventory by ~65%.
- Adding ~100,000 gal. of water reduces the flammable gas concentration to ~25% of LFL, but additional dilution increases the flammable concentration as a result of decreasing the dome volume.

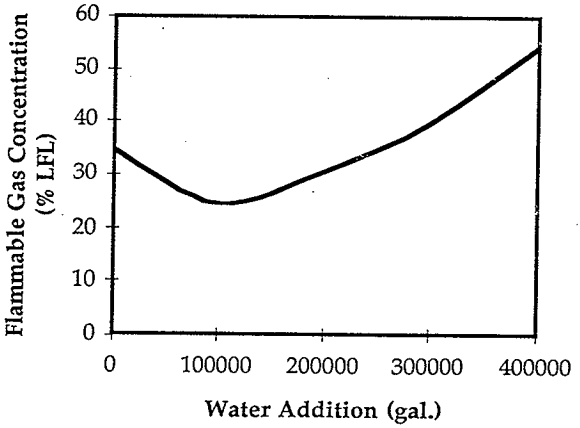

Los Alamos
Los Alamos National Laboratory

IMPLEMENTATION OF DILUTION

- Operations needed to implement dilution:
  - Supernatant liquid removal required in AN-104, AN-105, and AW-101.
  - Water addition.
  - Mixing is required in all tanks to minimize dissolution time.
- Procedure and equipment for supernatant liquid removal for dilution is the same as for mitigation by supernatant liquid removal.
- Possible methods for mixing are:
  - Installation of a mixer pump.
  - Adding water directly to the NC layer with water lances
- Large GREs expected during the dilution process.

EVALUATION OF MITIGATION BY DILUTION

- The effectiveness of dilution depends on the tank being considered.
  - o In AN-103, dilution reduces the best-estimate flammable gas concentration to acceptable levels without removing supernatant liquid.
  - o In AN-104 and AN-105, dilution does not reduce flammable gas concentration to <25% of LFL.
  - o In AW-101, dilution reduces the Rayleigh-Taylor limit in AW-101 to <<100% of LFL.
  - o Dilution may reduce the Raleigh-Taylor limit in SY-103 to 25% of LFL.
- Dilution is a viable option for AN-103.
- Dilution is a viable option for AW-101 if required.
- Dilution may be a good option for SY-103, but additional study is required.

Refined Safety Analysis Methodology for
Flammable Gas Risk Assessment in Hanford Site Tanks

Modeling Controls Implementation in the Analysis Framework

January 22, 1998

Scott E. Slezak

WS1–SS–1/22/98-A
slide 1

Objective: Evaluate Adequacy of DST AF Methodology for Assessing Impact of Controls

- The potential number of controls in DSTs for mitigating flammable gas is large.
  - Some strategies ranked high by LANL include multi-port risers, inerting, spark controls, low frequency sonic probes, mixer pumps, cooling, supernate liquid removal, heating, dilution, past practice sluicing
- The number of physical parameters potentially effected by control strategies is large.
- Question: Does the proposed AF for DSTs have sufficient capability to assess the wide range of potential controls?

WS1–SS–1/22/98-A
slide 2

Physical Parameters in AF for DSTs

- **Physical parameters in the DST AF are:**
  - ρ_l = density of supernate liquid
  - ρ_{nc} = bulk density of degassed nonconvective layer
  - τ = yield stress of nonconvective layer material
  - μ_b = bulk viscosity of nonconvective layer material
  - T_{waste} = Temperature of (nc) waste material
  - d_c = thickness of crust
  - $d_l - d_c$ = thickness of convective layer
  - $d_{nc} - d_l$ = thickness of nonconvective layer
  - ϕ = porosity of nonconvective layer material
  - g_s, g_l, g_{nc} = gas generation rate in solid, liquid, bulk nonconvective layer material

WS1–SS–1/22/98-A
slide 3

Specified Parameters in AF for DSTs

- **User/database specified parameters in DST AF:**
  - R_p = volumetric transfer pump rate
  - N_{vent} = molar ventilation rate in headspace
  - $X_{O2,head}$ = initial headspace O_2 concentration
  - inerting gas specie (N_2, CO_2, Ar)
  - f_{ops} = frequency of operations (pumping, sampling, etc).
  - Ignition Control set 1, IC set 2, or past practices
  - location of IC level (in-tank vs. ex-tank)
  - radius & volume of influence for equipment to disrupt waste hydraulically, pneumatically or mechanically
  - HEPA failure pressure

WS1–SS–1/22/98-A
slide 4

Control Evaluation Approach

- Detailed models for effects of most controls not explicitly in analysis framework.
- Approach is for users to perform side evaluations of effect of control on parameters in AF and input expected post-control parameter values.
- Approach allows users to update side calculation methods as new data and models are available.
- Approach requires users to justify basis for their assessment of the impact of controls on specific *parameters*, but AF still governs assessment of impact of controls on *risk*.

WS1–SS–1/22/98-A

slide 5

Example Evaluations

- Heating and cooling.
  - Directly effects viscosity, shear strength, retained gas temperature, thermolytic gas generation rate.
  - Indirectly may change thickness of layers due to temperature effects on solubility.
- Inerting, spark controls, supernate liquid removal
  - These controls are explicitly included in AF.
- Dilution.
  - Directly effects μ_b, τ, ρ_l, volumetric gas generation rate, thickness of layers.
  - May have indirect effects due to solubility changes.

WS1–SS–1/22/98-A

slide 6

Example Evaluations (2)

- **Mixer pump, ALCs, lancing, sluicing, mechanical stirring.**
  - These controls are included in the AF via efficiency of release when mechanically, hydraulically or pneumatically disrupted.
  - Engineering design evaluation required to determine characteristics of equipment: volume of waste disrupted, rate of disruption, radius of influence.
  - Water, steam or other liquid lancing or sluicing has further impact similar to dilution.

WS1–SS–1/22/98-A
slide 7

MPRs: Not Evaluated in AF

- **LANL rates multi-port risers (MPRs) high on list of potential mitigation strategies; AF does not have capability to evaluate impact of MPRs.**
- **MPRs purely mitigation (vs. prevention) strategy.**
- **Vents designed to protect equipment, not people.**
- **NFPA 68 *Guide for Venting of Deflagrations* calls for ~50 m^2 vent area (>10% of dome area); total riser area <5 m^2.**

WS1–SS–1/22/98-A
slide 8

NFPA Recommendation on Venting

- NFPA 68 (1994) states in Section 3-6.10:
  - "Situations can occur in which it is not possible to provide adequate deflagration venting as described in Chapters 4 through 7 of this guide. This is not justification for providing no venting at all. It is suggested that the 'maximum practical' amount of venting be provided, since some venting may reduce the resulting damage to a limited degree. In addition, consideration should be given to other protection and prevention methods. (*See NFPA 69, Standard on Explosion Prevention Systems.)*"

WS1–SS–1/22/98-A
slide 9

Impact of MPRs on AF

- Decision for panel: Is the inability to evaluate MPRs a serious inadequacy of the AF?
  - MPRs may be installed in combination with other controls equipment (e.g. integral to riser coupler for mixer pump), but not likely as the only flammable gas control without simultaneous prevention controls.
  - MPRs would provide added assurance that AF assessment of the prevention controls was conservative and MPRs would make expected consequences and/or frequencies smaller.

WS1–SS–1/22/98-A
slide 10

Summary

- AF evaluation of many potential controls requires "user intelligence" of the impact of the controls on parameters integral to AF.
- Approach allows evaluation of new data and models on impact of controls on parameters.
- Panel decision: Are the physical and user-specified parameters in the AF suitable for evaluating those controls that could reasonably be implemented if risk is determined to otherwise be unacceptably high?

WS1–SS–1/22/98-A
slide 11

Refined Flammable Gas Analysis

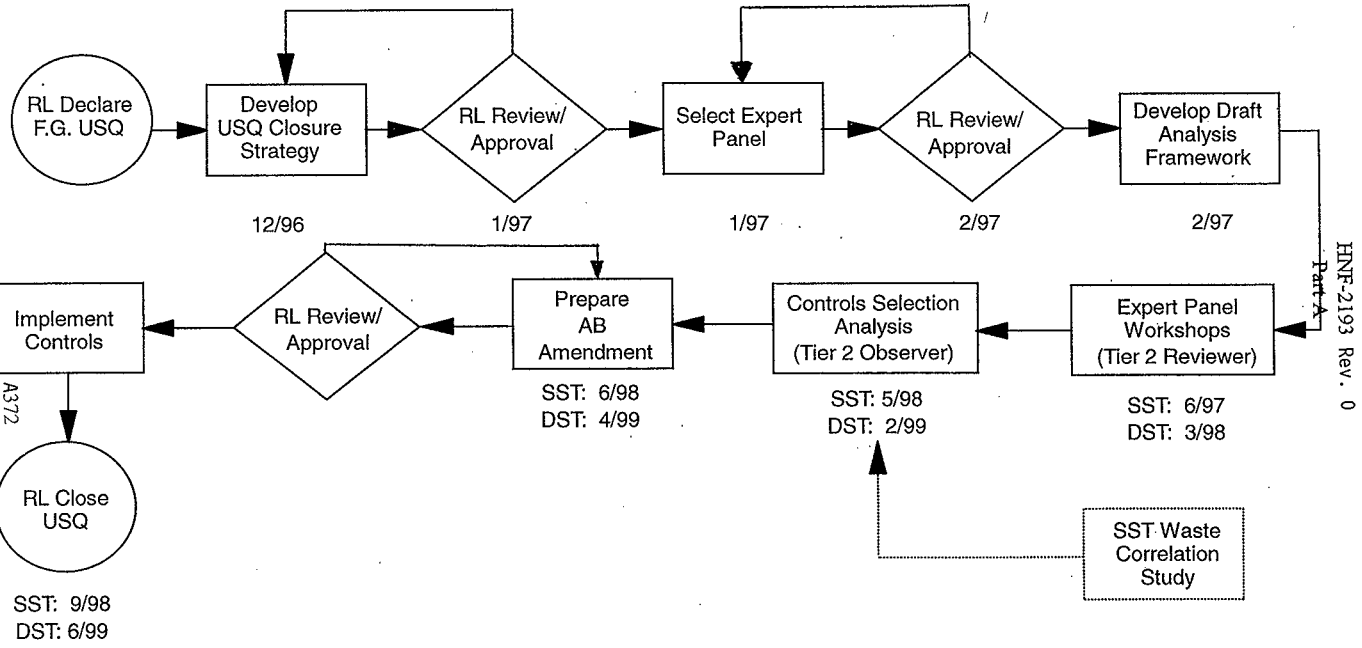

WASTE TANK IGNITION SOURCES AND CONTROLS

D. B. Smet/R. L. Schlosser
Lockheed Martin Hanford Corporation
January 22, 1998

BACKGROUND

- Ignition source control is the primary approach used to mitigate flammable gas combustion in the waste storage tanks.

- The site NFPA Interpretive Authority has determined that the current flammable gas generation data does not meet NFPA criteria for classifying tank regions as hazardous locations, but because of insufficient data, recommends that a conservative approach be taken. The adopted approach is more conservative than the codes require!

- Ignition Source Control (ISC) Set 1 is primarily based upon NFPA 70 (NEC) electrical and heat source requirements for a Class 1 Division 1 Group B hazardous location and uses a `no single point failure' approach. For mechanical , electrostatic and chemical ignition sources, appropriate industry practice is used as the basis. ISC 1 requirements are applied to all waste-intrusive ignition sources.

BACKGROUND (continued)

- Ignition Source Control Set 2 is based upon NFPA 70 electrical and heat source requirements for a Class Division 2 Group B hazardous location and uses a `non-sparking under normal operation' approach. Again, for mechanical, electrostatic and chemical ignition sources, appropriate industry recommendations are the basis for the requirements. ISC 2 requirements are applied to vapor (dome) space ignition sources within the tank and to specific regions around openings to the tanks (ex-tank) depending upon the risk-based facility groupings of the tanks as well as on the specific equipment activity being performed.

DISCUSSION

- All SST's are either Facility Group 2 or 3.
- Numbers and types of ignition sources in SST's are widely variable.
- Permanently installed active ignition sources in SST's are much fewer than in DST's.
- Primary activities involving ignition sources in SST's are temporary applications.
- Many of the ignition sources in DST's are in ex-tank vs. in-tank regions.

Item #	Authorized Activities
1	Personal Protection Equipment (i.e., raingear, airline respirator hoses, rubber/plastic and canvas gloves, respirator masks, rubber/plastic boots, masking tape, Tyvek® coveralls) are authorized for use in ex-tank locations, but may be used in a minimally dome intrusive location (e.g., at the plane of a riser).
2	Wearing of plastic badges, badge holders, and dosimeters.
3	Installation of, removal of, working on, or extended presence of nonconductive lead blankets in ex-tank (global waste disturbing) regions. Lead blankets shall not be used in a vapor trapping configuration
4	Installation, removal, or extended presence of nonconductive adhesive tape (e.g., green tape, white tape) in ex-tank regions, Dome Intrusive regions, and in Waste Intruding Equipment.
5	Use of Portable Alpha Monitor (PAM) in ex-tank regions, Dome Intrusive regions, and in Waste Intruding Equipment.
6	Use of nonconductive poly bottles in ex-tank and Dome Intrusive regions.
7	Use of zip cords in ex-tank regions, Dome Intrusive regions, and in Waste Intruding Equipment (e.g., inside failed Liquid Observation Wells [LOWs]).
8	Use of nonconductive plastic ropes in ex-tank regions.
9	Use of nonconductive plastic tubing in ex-tank regions and Dome Intrusive regions (e.g., aerosol testing). Nonconductive plastic tubing shall not be used below the plane of a riser.
10	Installation and removal of Garlock gaskets in ex-tank regions.
11	Use of nonconductive plastic garden type sprayer (approximately 5 gallons, hand pump pressurizer and brass spray wand) in ex-tank regions.
12	Use of grab sample cap, sampling and sludge weight retrieval device and coated steel cable in ex-tank and Dome Intrusive regions.
13	Installation and removal of PVC riser liners in Dome Intrusive regions.

*****
Tyvek is a trademark of E. I. du Pont de Nemours & Company, Wilmington, DE.

Part A

Item #	Authorized Activities
14	Presence of PVC liners for manual tapes, FICs, flushing, ICS 1 compliant equipment, and authorized activities in Dome Intrusive regions.
15	Presence of manual tapes in ex-tank and Dome Intrusive regions.
16	Installation and removal of manual tapes in ex-tank and Dome Intrusive regions.
17	Installation of, removal of, working with, or extended presence of the pipe wiper (Frisbee) during push mode core sampling (PMCS) with Truck 1, 2, and 3, in ex-tank and Dome Intrusive regions.
18	Installation of, removal of, or extended presence of plastic Kamlock caps during push mode core sampling with Trucks 1, 2, or 3 in ex-tank and Dome Intrusive regions.
19	The presence of extension cords in ex-tank regions. Power strips (and outlet strips) are not allowed in these regions. Energized lines shall not be connected or disconnected in an ex-tank region.
20	Installation, removal, and use of low and high pressure spray whirlie and operation of valve handles in ex-tank and Dome Intrusive regions.
21	Electrical bonding is not required for removal or installation of fittings on openings less than or equal to 2.54 cm (1 in.) inside diameter during intrusive location entry.
22	Use of Type 4 vapor sampling head in ex-tank and Dome Intrusive regions. Conductive plastic sleeving shall be used during Type 4 vapor sampling.
23	Use of electric impact wrench in ex-tank regions.
24	Use of Type 4 vapor cart in ex-tank and Dome Intrusive regions.
25	Open pit work related equipment (e.g. Pike Poles, T-Bars, Sockets, Chokers, Shackles, and Bull Hooks) in ex-tank regions. Installation and removal of process blanks, vapor seals, jumpers, and leak detectors in ex-tank regions. Continuous monitoring in the tank dome and the pit is required during use of this exception.
26	Installation and removal of valve handles in ex-tank regions. This activity is performed in closed pits when no global waste disturbing activities are in progress.

Item #	Authorized Activities
27	Installation, removal, presence of, or movement of cover blocks, riser flanges, shield plugs, tank installed waste and non waste intrusive equipment items (e.g. TC trees, steel LOWs, pumps, manual tapes, FICs, ENRAFs, radar gauges, heated vapor probes, MITs, corrosion probes, VDTTs, water lances, void fraction meter, core sampling drill string, saltwell screens, dip-tubes, cameras/lights, viscometer, auger, sampler) each as used in ex-tank or dome intrusive or waste intrusive regions. Work packages and procedures will include practical measures to reduce the likelihood of a mechanical spark when equipment movement performed as part of an operation or activity can create mechanical sparks. Such measures may include: limiting insertion speeds, water bathing of equipment, prevention of contact with other non-spark resistent materials by use of collars or bumpers, use of critical lift procedures where appropriate. This exception does not cover the operation of large mixer pumps that might cause significant motion of installed equipment. Any other ignition source hazards (other than mechanical spark source potential) must comply with this JCO's requirements for ignition source controls.
28	Use of pressure switches, limit switches, and leak detector for the saltwell pumping system for 241-T-104. Continuous monitoring of the pump pit is required during pumping with automatic shutoff at 10% of LFL.
29	Use of pressure switches, limit switches and leak detectors for the saltwell pumping system for 241-BY-109 after it is re-categorized to a Facility Group 3 tank. Continuous monitoring of the pump pit required during pumping with automatic shutoff at 10% of the LFL.
30	Presence of intact fiberglass and Tefzel[1] LOWs in Facility Group 2 or 3 tanks or presence of failed fiberglass LOWs as waste-intruding equipment. (Work in a known failed LOW shall meet IC Set 1 controls).
31	Use of Continuous Air Samplers in ex-tank regions. CAS shall be shutdown if 10% of the LFL is exceeded in the ex-tank area. Motor shall be placed outside the ex-tank region. Continuous monitoring in the tank dome and the pit is required during use of this exception.

*****

Tefzel is a trademark of E. I. du Pont de Nemours & Company, Wilmington, DE.

WASTE TANK IGNITION SOURCES

The following are examples of typical ignition sources in both DST's and SST's . Included within are ignition sources associated with temporary and permanently installed equipment and/or activities (reference accompanying tank graphic):

1) Waste transfer pumps - typically 480V AC Induction type (motor located in ex-tank area).

2) Saltwell transfer pumps - 480V AC Induction type (motor located in ex-tank area, temporary application, SST's only.

3) Video camera/light systems - Permanently installed in approximately 10 DST's, temporary applications in other DST's and all SST's (dome space - electrical, heat source).

4) Leak detectors - located in ex-tank or dome space, electrical.

WASTE TANK IGNITION SOURCES (continued)

5) High level probes - dome space, DST's only, electrical.

6) Various switches e.g., pressure, valve position limit - ex-tank, electrical.

7) Portable tools, equipment - ex-tank, mechanical, electrical, electrostatic - temporary manned activities.

8) Waste/vapor sampling systems - ex-tank, dome space, waste - electrical, mechanical, electrostatic.

9) Thermocouple trees - ex-tank, dome space, waste - mechanical.

10) Waste level detectors - ex-tank, dome space, waste - electrical, mechanical.

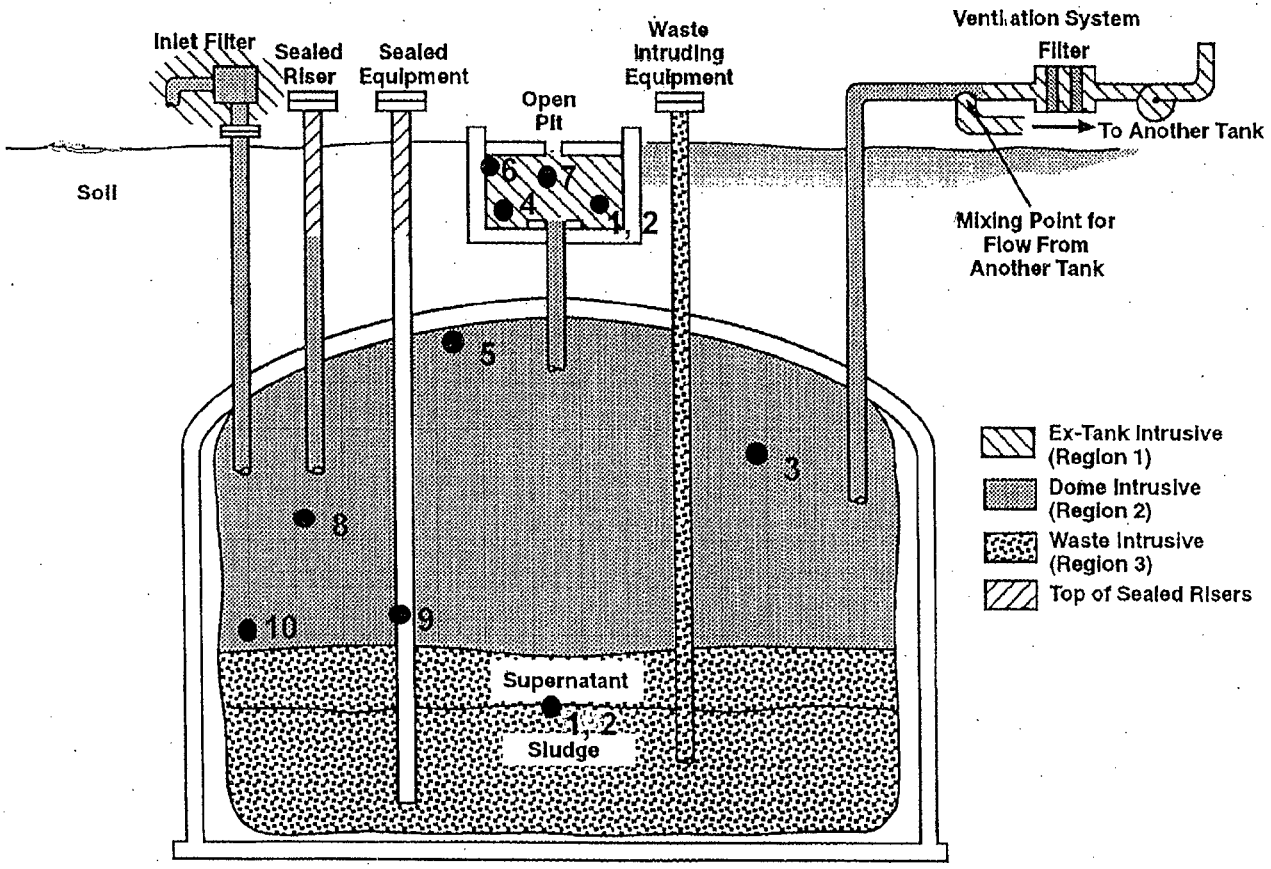

Actively Ventilated Tank
(Ventilation Off)

RG96050264.2

SUMMARY

The majority of SST activities that employ ignition source equipment are temporary manned activities. Much of the permanently installed ignition source equipment associated with SST's has been de-energized and/or isolated. By contrast, most of the examples referred to, as well as others, are active in and around the DST's.

Los Alamos National Laboratory (LANL) Preliminary Flammable Gas Mitigation Engineering Analysis Overview

BASIC PRINCIPLE

- Gas retention and release increase with total solids inventory.
  - The Rayleigh-Taylor model predicts that the retained-gas volume increases with the mass of settled solids.
  - The bubble retention model predicts that the gas fraction in the NC layer should be an increasing function of NC-layer thickness and viscosity.
- Reducing the mass of settled solids will reduce the total inventory of retained gas and the size of GREs.
  - The solubility of most electrolytes increases with temperature.
  - Adding water or dilute sodium hydroxide solution dissolves many of the major solids components in the waste.

FACTORS THAT LIMIT THE EFFECTIVENESS OF HEATING

- Insoluble Solids—Sodium oxalate and salts of alkaline earth metals and transition metals are relatively insoluble in the waste at all reasonable temperatures.
- Sodium Carbonate and Sodium Sulfate—The solubility of forms of sodium carbonate and sodium sulfate in the waste decrease with increasing temperature.
- Gas Generation Rate—The gas generation rate increases with increasing temperature. Gas retention increases with the gas generation rate.
- Ammonia—The vapor pressure of dissolved ammonia and ammonia releases increases with increasing temperature.

Los Alamos
Los Alamos National Laboratory

ADDITIONAL BENEFITS OF DILUTION

- Reducing the concentrations of soluble organic compounds, aluminate, and radionuclides in the liquid will reduce the gas generation rate per unit volume.
- Dilution reduces the ammonia concentration.

FACTORS THAT LIMIT THE EFFECTIVENESS OF DILUTION

Insoluble Solids—Salts of alkaline earth and transition metals are relatively insoluble and can not be dissolved by dilution.

Aluminum Hydroxide Precipitation—Water addition may cause aluminum hydroxide to precipitate.

Density Ratio—Dilution increases the ratio of solid to liquid density, which increases the gas fraction obtained from the Rayleigh-Taylor limit.

Cooling—Dilution may cause cooling, which may cause additional salts to precipitate and may increase the hydrogen concentration.

Available Tank Space—Dilution may require the removal of supernatant liquid. There is limited tank space to receive supernatant liquid.

Dissolved Hydrogen—The reduction in ionic strength as a result of dilution will increase the amount of dissolved hydrogen.

Reduction in Free Radical Scavengers—Dilution will reduce the concentration of free radical scavengers, which may increase radiolytic hydrogen production.

EVALUATION CRITERIA FOR HEATING AND DILUTION

Objective: Reduce maximum flammable gas concentration in the dome to <25% of LFL.

Considerations: Best-estimate retained gas volume.

Rayleigh-Taylor limit as a measure of potential gas retention capacity.

Criteria: Best estimate >25% of LFL—Not acceptable.

Best estimate <25% of LFL and Rayleigh-Taylor limit >100% of LFL—Not acceptable because of large uncertainty.

Best estimate <25% of LFL and Rayleigh-Taylor limit <100% of LFL—May be a viable mitigation scheme.

Los Alamos
Los Alamos National Laboratory

RESULTS FOR HEATING AN-103

- Heating dissolves the sodium nitrite and sodium aluminate in the waste, reducing the total solids inventory by ~70%.
- Heating reduces the flammable gas concentration in the dome, but not to an acceptable level.

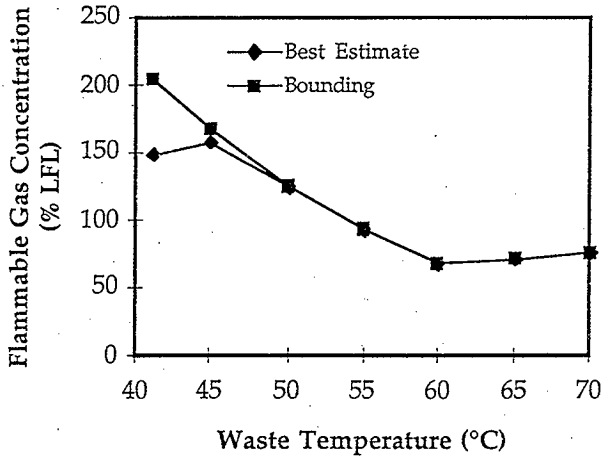

- GREs induced by heating AN-103 could be large.

RESULTS FOR HEATING AN-104 AND AN-105

- The solids in AN-104 and AN-105 are predominantly sodium carbonate, sodium sulfate, and insoluble solids. Heating increases solids inventory slightly.
- Heating increases the gas generation rate, which increases gas retention and the magnitude of the flammable gas hazard.

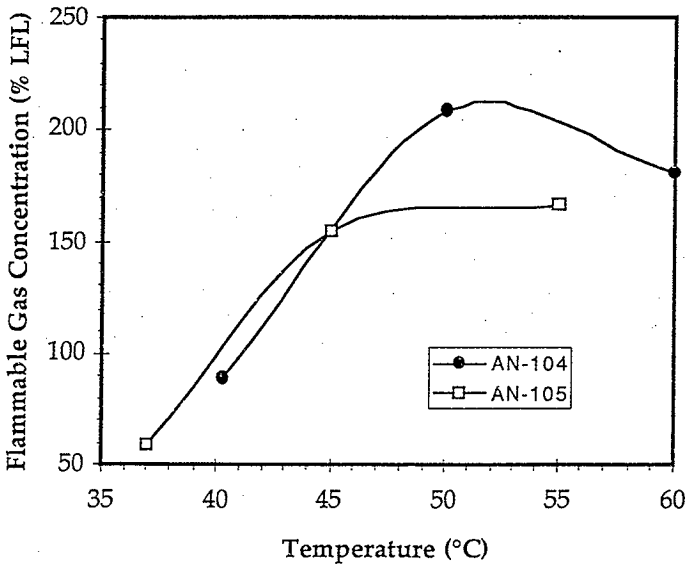

Los Alamos
Los Alamos National Laboratory

RESULTS FOR HEATING AW-101

- Based on our best-estimate analysis, GREs in AW-101 will not produce flammable gas concentrations >25% of LFL.
- Heating the waste to ~60°C can reduce the Rayleigh-Taylor limit to <25% of LFL.

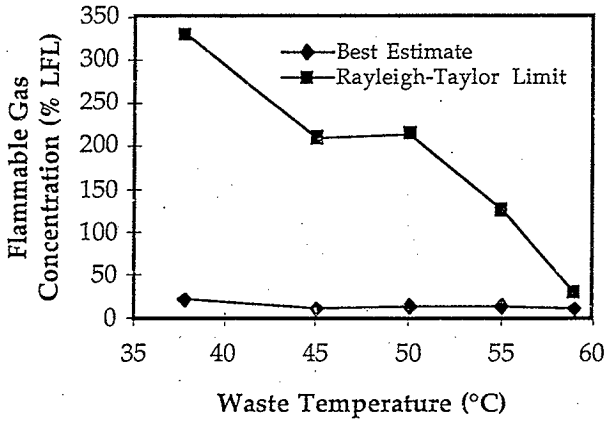

Los Alamos
Los Alamos National Laboratory

RESULTS FOR HEATING SY-103

- We have not performed a data reconciliation study on SY-103; thus, we do not have a model for quantitative analysis.
- Based on a qualitative evaluation, we conclude that:
  - heating the waste to 60°C will reduce the solids inventory by 35 to 50%;
  - heating the waste to 60°C will reduce the maximum flammable gas concentration to between 18 and 32% of LFL.
- Heating may reduce the GREs to an acceptable level, but there is a great deal of uncertainty in analysis.

IMPLEMENTATION OF HEATING

- Methods of heating the waste:
  - Reduce vent flow rate in the annulus
  - Heat the inlet air to the vent systems
  - Install an in-tank heater
- Reducing annulus vent flow rate not attractive:
  - May not increase the temperature enough
  - Large time constant
- In-tank heaters not attractive:
  - Waste-intrusive operations required
  - Mixer pump required to prevent boiling
- Heating the inlet air is the most attractive option
  - Heating the inlet air by ~20°C would maintain the steady-state temperature at the required level.
  - Heating the inlet air to ~85°C would reduce the heating time to ~3 months without boiling the waste.

PRELIMINARY EVALUATION OF MITIGATION BY HEATING

- Heating is not an attractive mitigation option:
  - It increases the flammable gas hazard in AN-104 and AN-105.
  - We cannot demonstrate that heating will reduce the best-estimate GRE to an acceptable level in AN-103 and SY-103.
  - We can demonstrate that heating will reduce the gas retention capacity in AW-101 to an acceptable level, but mitigation may not be needed unless an adverse change occurs.
- We do not recommend additional consideration of heating as a mitigation option.

DESIGN CONSIDERATIONS FOR DILUTION

- Dilution will be done with water or a hydroxide solution.
- There are three design parameters to consider for dilution:
  - Amount of diluant added.
  - Amount of supernatant liquid removed.
  - Hydroxide concentration in the diluant.
- Desire to minimize all three parameters.
  - Remove supernatant liquid if diluant addition increases waste level to >410 in.
  - Add diluant after removing the supernatant liquid to maximize the effectiveness of dilution.
  - Add sodium hydroxide if needed to prevent aluminum hydroxide precipitation.

DILUTION vs RECOVERY

- We do not consider removal of the NC-layer solids in our evaluation of dilution.

- We consider dilution with the removal of NC-layer solids to be waste recovery, which is a separate mitigation option.

RESULTS FOR DILUTION OF AN-103

- Supernatant liquid removal not required.
- Sodium hydroxide addition not required.
- Adding 220,000 gal. of pure water dissolves ~80% of the solids.
- Dilution with pure water can reduce the best-estimate gas release to <25% of LFL and the Rayleigh-Taylor limit to <100% of LFL.

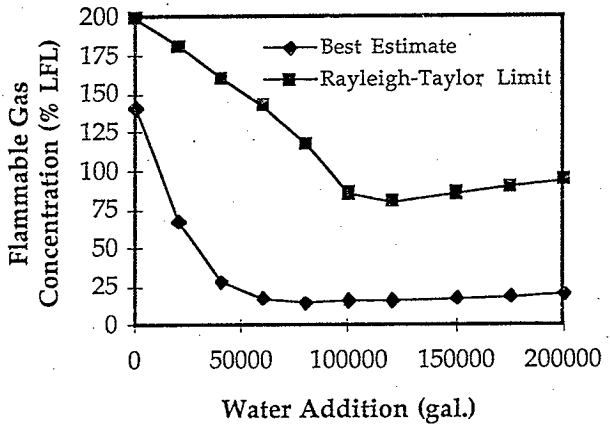

- Waste may cool, but it is not a problem.

Los Alamos
Los Alamos National Laboratory

RESULTS FOR DILUTION OF AN-104

- Supernatant liquid removal required.
- Sodium hydroxide addition not required.
- Adding 700,000 gal. of water dissolves ~60% of the solids.
- Dilution does not reduce the maximum flammable gas concentration to <25% of LFL.
  - o Dilution does not dissolve sufficient solids.
  - o Dilution increases hydrogen concentration.
  - o Water addition reduces dome volume.

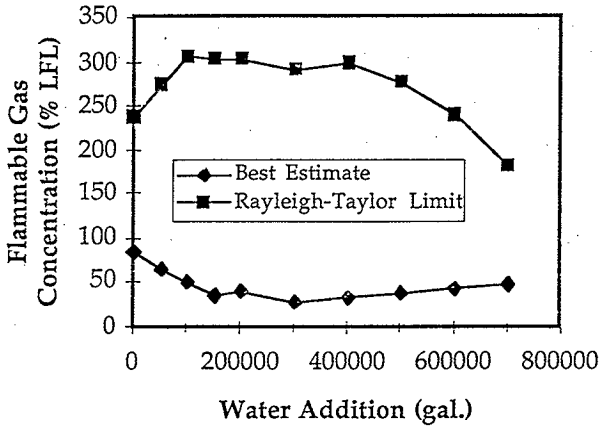

Los Alamos
Los Alamos National Laboratory

RESULTS FOR DILUTION OF AN-105

- Supernatant liquid removal required.
- Sodium hydroxide addition not required.
- Dilution does not reduce the maximum
- Flammable gas concentration to <25% of LFL.
  - o Dilution does not dissolve sufficient solids.
  - o Dilution increases hydrogen concentration.

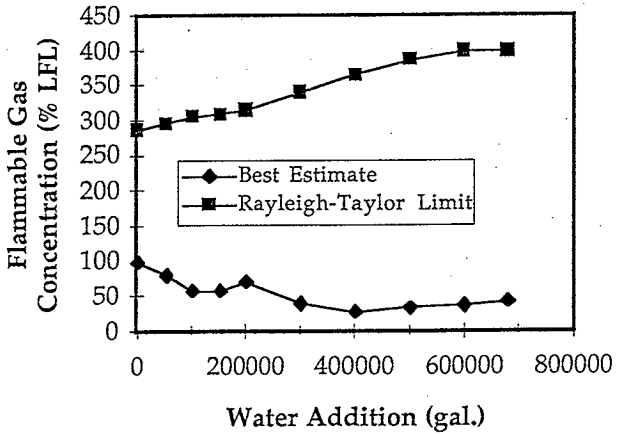

Los Alamos
Los Alamos National Laboratory

RESULTS FOR DILUTION OF AW-101

- Supernatant liquid removal not required.
- Sodium hydroxide addition not required.
- Adding 250,000 gal. of pure water dissolves a significant fraction of the solids.
- Dilution reduces the Rayleigh-Taylor limit significantly.

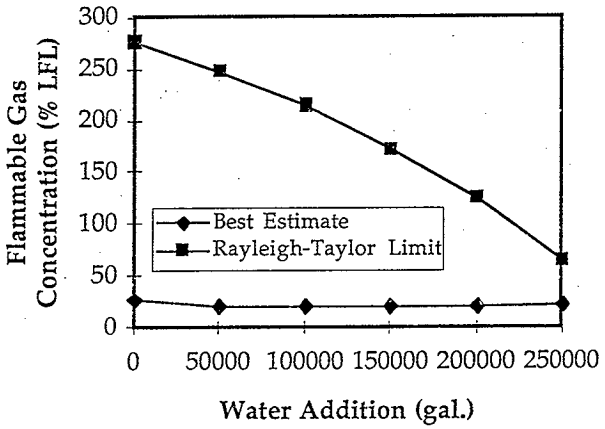

Los Alamos
Los Alamos National Laboratory

RESULTS FOR DILUTION OF SY-103

- No data reconciliation study for SY-103.
- Supernatant liquid removal required.
- Sodium hydroxide addition not required.
- Estimate that addition of ~100,000 gal. of water reduces the solids inventory by ~65%.
- Adding ~100,000 gal. of water reduces the flammable gas concentration to ~25% of LFL, but additional dilution increases the flammable concentration as a result of decreasing the dome volume.

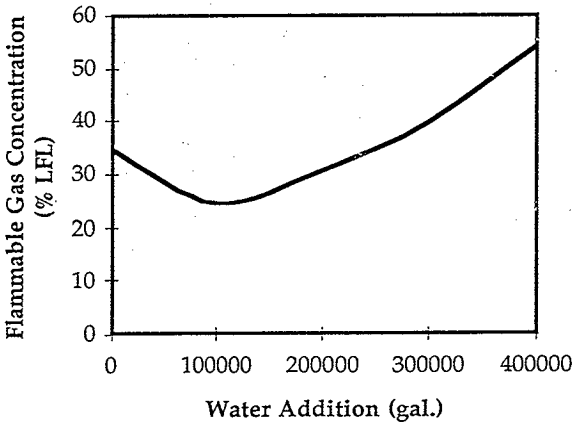

Los Alamos
Los Alamos National Laboratory

IMPLEMENTATION OF DILUTION

- Operations needed to implement dilution:
  - Supernatant liquid removal required in AN-104, AN-105, and AW-101.
  - Water addition.
  - Mixing is required in all tanks to minimize dissolution time.
- Procedure and equipment for supernatant liquid removal for dilution is the same as for mitigation by supernatant liquid removal.
- Possible methods for mixing are:
  - Installation of a mixer pump.
  - Adding water directly to the NC layer with water lances
- Large GREs expected during the dilution process.

EVALUATION OF MITIGATION BY DILUTION

- The effectiveness of dilution depends on the tank being considered.
  - o In AN-103, dilution reduces the best-estimate flammable gas concentration to acceptable levels without removing supernatant liquid.
  - o In AN-104 and AN-105, dilution does not reduce flammable gas concentration to <25% of LFL.
  - o In AW-101, dilution reduces the Rayleigh-Taylor limit in AW-101 to <<100% of LFL.
  - o Dilution may reduce the Raleigh-Taylor limit in SY-103 to 25% of LFL.
- Dilution is a viable option for AN-103.
- Dilution is a viable option for AW-101 if required.
- Dilution may be a good option for SY-103, but additional study is required.

Typical Double-Shell Tank

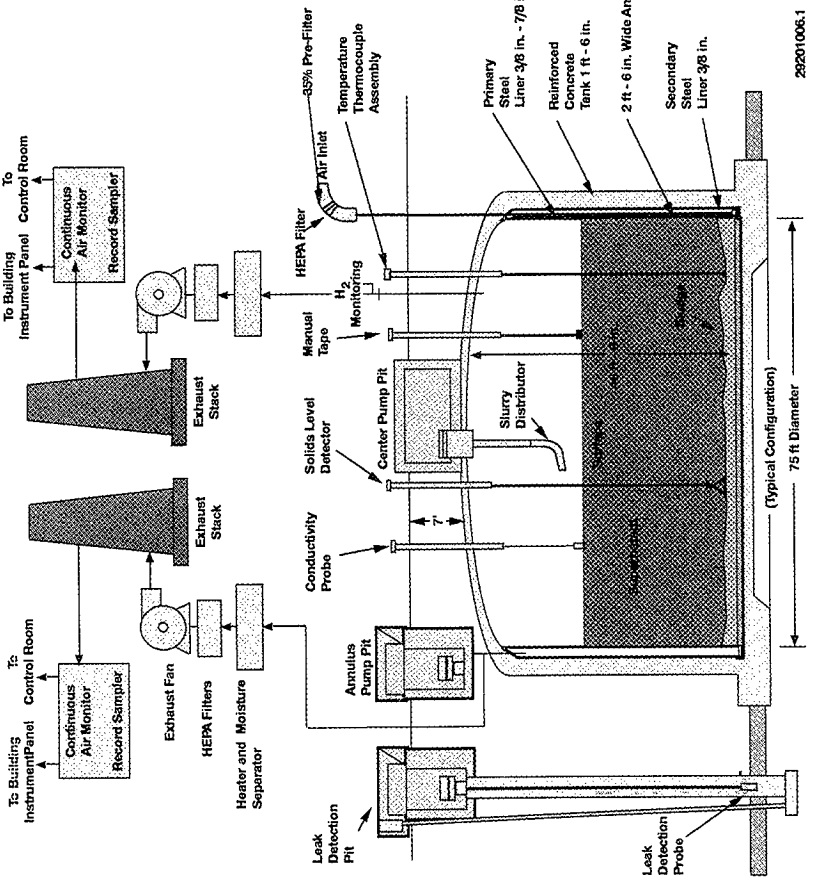

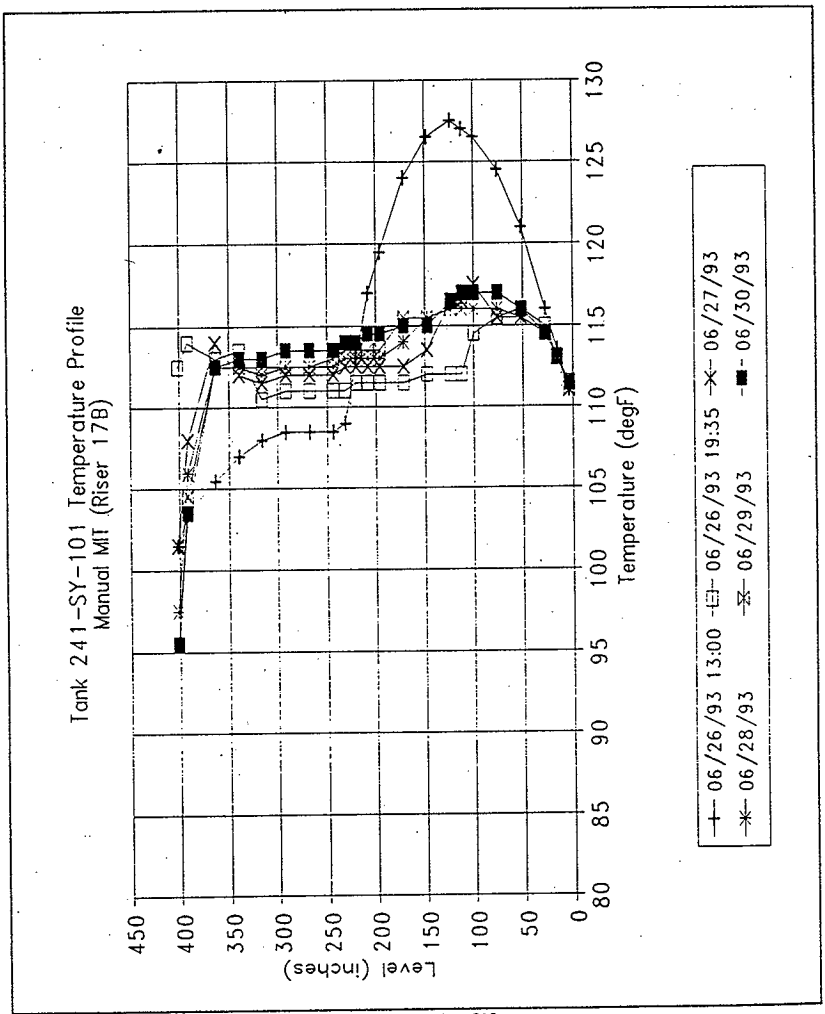

Figure 6-4. Tank 241-SY-101 Temperature Profiles

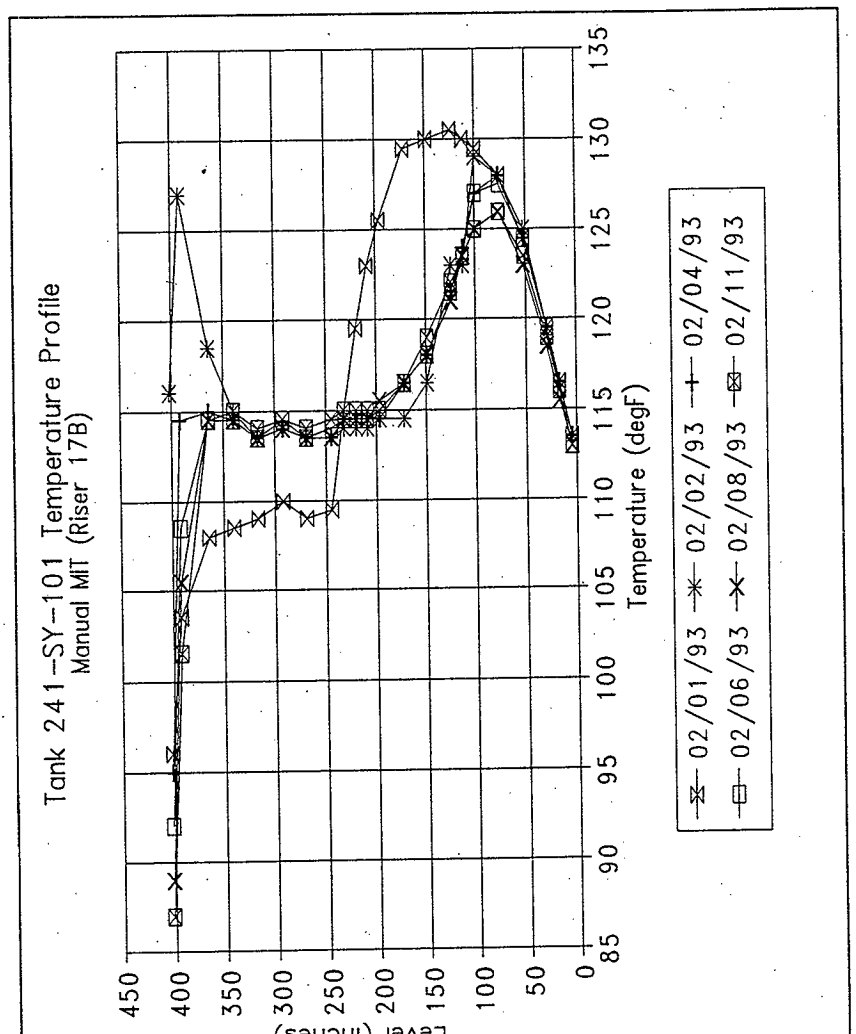

Figure 6-4. Tank 101-SY Temperature Profile.

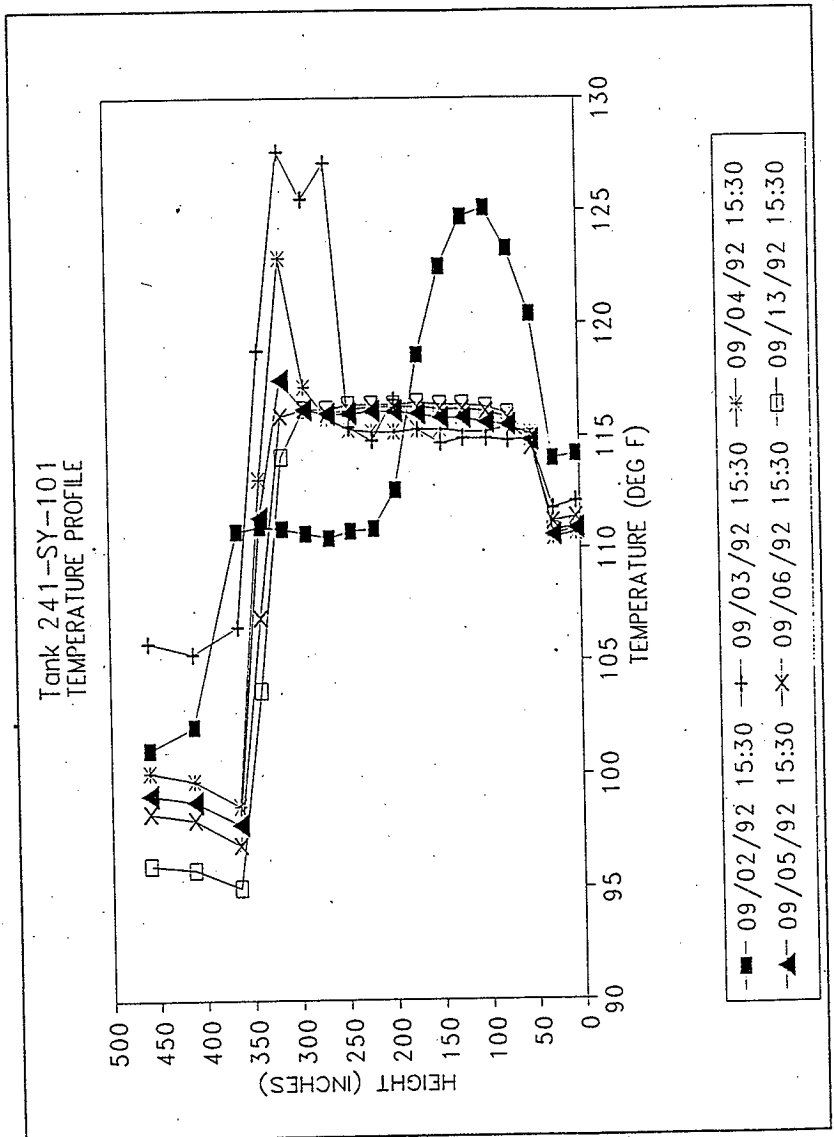

Figure 6-4. Tank 241-SY-101 Temperature Profile.

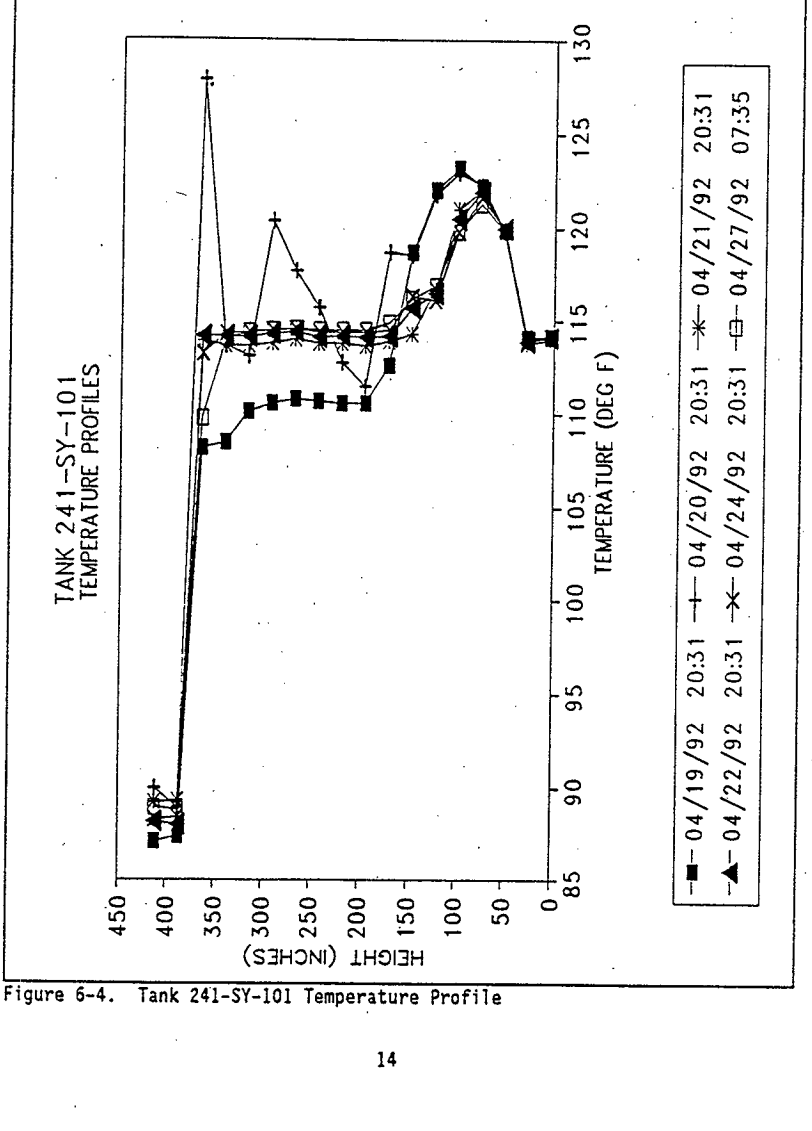

Figure 6-4. Tank 241-SY-101 Temperature Profile

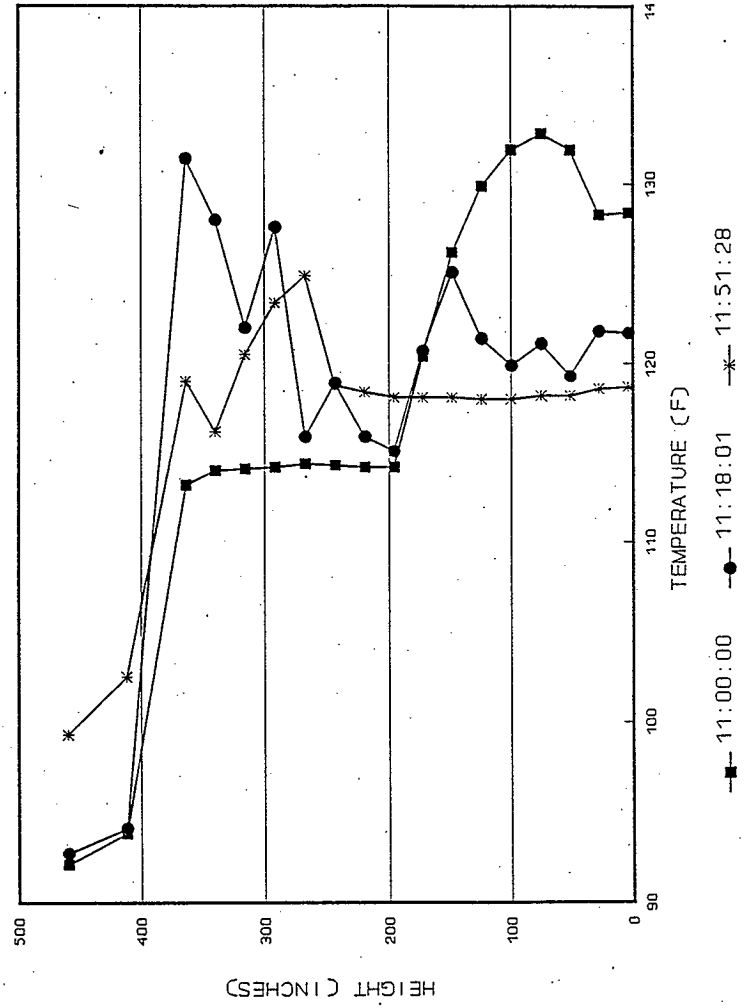

Figure 6-3 Thermocouple Temperature Comparison Before, During, and After Event.

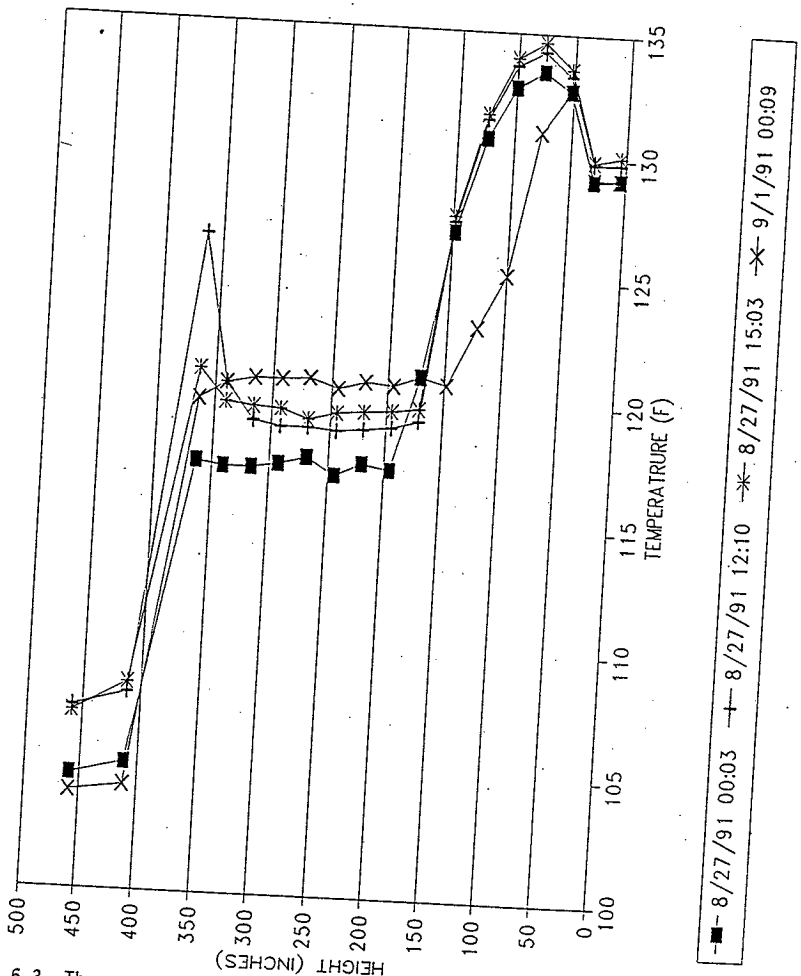

Figure 6-3 Thermocouple Temperature Comparison Before, During, and After Event.

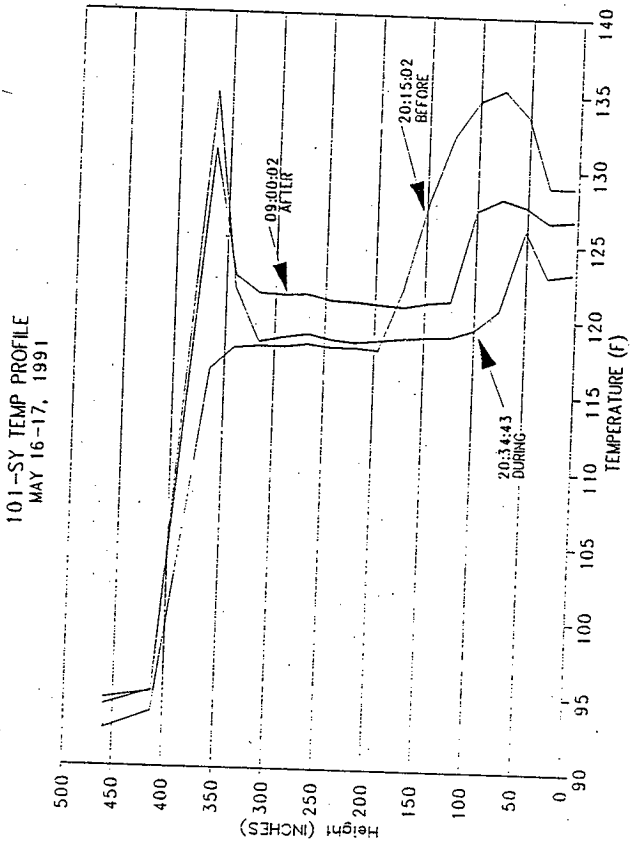

Figure 6-3 Thermocouple Temperature Comparison Before, During, and After Event.

Figure 6-3. Thermocouple Temperature Comparison Before, During, and After Event.

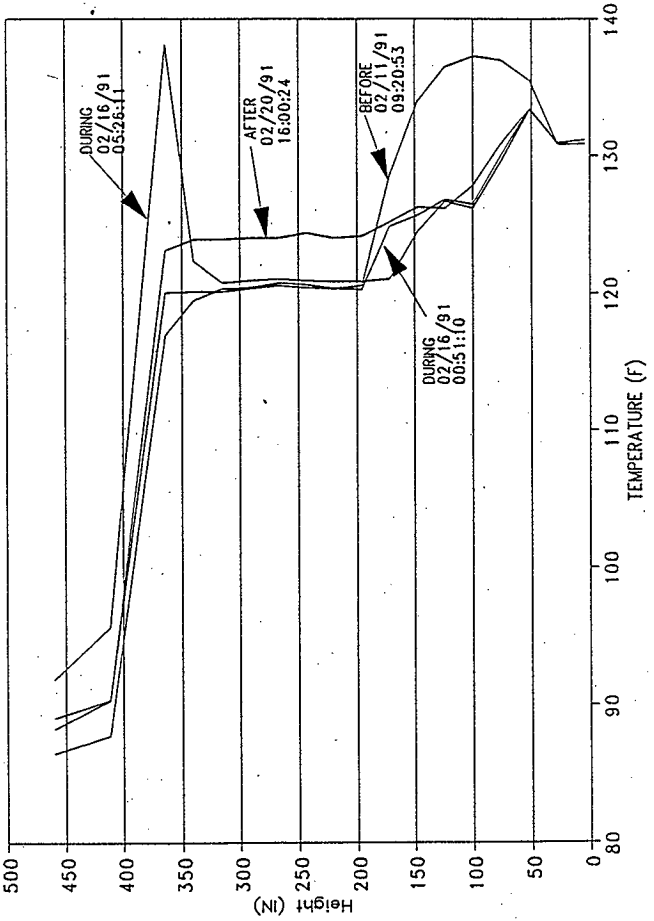

GAS RELEASE EVENT SAFETY ANALYSIS TOOL LIBRARY

1. Risk Analysis, Vol. 14, Nov. 5, 1994 — Workshop Proceedings: When and How Your Specify A probability Distribution When you Don't Know Much.

2. 9655781 Lockheed Martin — Flammable Gas Project: Memorandum of Understanding on the Strategy for Closure of the Flammable Gas Unreviewed Safety Question to meet Performance Agreements TWR1.3.2 and 1.3.6

3. American Institute of Chemical Engineers: — Symposium Series, Heat Transfer -- Pittsburgh 1987.

4. ANL-RE-92/2 — Effect of Viscosity on Seismic Response of Waste Storage Tanks, June 1992

5. CONF-660904, Volume 1 — Proceedings of the Ninth AEC Air Cleaning Conference - held in Boston, Massachusetts - 13 - 15, September 1966.

6. COO-4442-4 — Compilation and Analysis of Hydrogen Accident Reports, Final Technical Report, by Robert G. Zalosh and Thomas P. Short., October 1978

7. Guidelines for Safe Storage and Handling of Reactive Materials, American Inst. of Chemical Engineers

8. HNF-EP-0182-103 — Waste Tank Summary Report for Month Ending October 31, 1996

9. HNF-EP-0182-107 — Waste Tank Summary Report for Month Ending February, 28, 1997

10. HNF-EP-0182-113 — Waste Tank Summary Report for Month Ending August 31, 1997.

11. HNF-EP-0899-2 — The Solubilities of Significant Organic Compounds in HLW Tank Supernate Solutions - FY 1997 Progress Report

12. HNF-SD-WM-CN-116 — Calculaton Note: Hydrogen Generation Rates at Steady-State Flammable Gas Concentrations for Single Shell Tanks, September 1997.

GAS RELEASE EVENT SAFETY ANALYSIS TOOL
LIBRARY

13. HNF-SD.CN-116, Rev. 0-A Calculation Note: Hydrogen Generation Rates at Steady-State Flammable Gas Concentrations for Single Shell Tanks, September 1997.

14. HNF-SD-WM-CN-117, Rev.0 Calculations of Hydrogen Release Rate at Steady State for Double-Shell Tanks, September 1997.

15. HNF-SD-WM-ES-410, Rev. 0 Safety Controls Optimization by Performance Evaluation (SCOPE) Analysis Framework, August 1997

16. HNF-SD-WM-JCO-007, Rev. 1 Flammable Gas/Slurry Growth Unreviewed Safety Question: Justification for Continued Operation for the Tank Farms at the Hanford Site.

17. WHC-SD-WM-TI-724, Rev. 0 Methodology for Flammable Gas Evaluations, December 1995.

18. WHC-SD-WM-TI-724, Rev. 1 Methodology for Flammable Gas Evaluations, June 1996

19. HNF-SD-WM-TI-797, Rev. 0 Results of Vapor Space Monitoring of Flammable Gas Watch List Tanks, January 1997.

20. HNF-SD-WM-TI-806, Rev. 0 Safety Controls Optimization by Performance Evaluation - Analysis Tool (SCOPE-AT) Pedigree Database for Hanford Tanks, September 1997

21. HNF-SP-1193, Rev. 2 Flammable Gas Project Topical Report, January 1997.

22. HNF-SD-WM-ES-412, Rev. 0 Safety Controls Optimization By Performance Evaluation (SCOPE) Expert Elicitation Results for Hanford Site Single-Shell Tanks - August 1997

23. IN TANK PHOTO COLLAGES of the 177 Waste Storage Tanks for the Hanford 200 Areas.

24. LA-UR-92-3196 A Safety Assessment for Proposed Pump Mixing Operations to Mitigate Espsodic Gas Releases in Tank 241-SY-101: Hanford Site, Richland, Washington

GAS RELEASE EVENT SAFETY ANALYSIS TOOL
LIBRARY

25. LA-UR-94-1323-TSA-6-94-R142 Bounding Gas Release Calculations of Flammable Gas Watch List Single-Shell Tanks.

26. LA-UR-94-2088-TSA-694-R120 Double-Shell Tank Bounding Analysis

27. LA-UR-95-1900, TSA-11-94-R110 Probabilistic Safety Assessment for Hanford High-Level Waste Tanks

28. LA-UR-95-4038 The Eleventh Workshop on Mathematical Problems in Industry, June 12-16, 1995.

29. LA-UR-97-2214 Data Reconcililiation Study of Tank 241-AW-101 at the Hanford Site, Los Alamos National Laboratory, Los Alamos, New Mexico

30. LA-UR-97-3916 Data Reconciliation Study of Tank 241-AN-105 at the Hanford Site, Los Alamos National Laboratory, Los Alamons, New Mexico

31. LA-UR-97-3954 Data Reconciliation Study of Tank 241-AN-104 at the Hanford Site, Los Alamos National Laboratory, Los Alamos, New Mexico

32. LA-UR-97-3955 Data Reconciliation Study of Tank 241-AN-103 at the Hanford Site, Los Alamos National Laboratory, Los Alamos, New Mexico

33. LA-UR-97-4021 Parameters to Consider Before Mixing Waste From Different Hanford Waste Tanks From A Flammable Gas Perspective, Fluor Daniel Northwest & Los Alamos National Laboratory, September 1997.

34. Los Alamos National Laboratory Interim Report: Flame Speed Scaling for Turbulent Reacting Flow

35. March 6, 1997, Rev. 1 Sandia National Laboratories
Safety Controls Optimization by Performance Evaluation (SCOPE) Proposed Analysis Framework for Scope Expert Panel Deliberations on Suitable Uncertainty Distribution Parameters

36. NUREG/CR-178 SAND80-0200 RX, AN Handbook of Human Reliability Analysis with Emphasis on Nuclear Power Plant Operations - Final Report

GAS RELEASE EVENT SAFETY ANALYSIS TOOL
LIBRARY

37. NUREG 1150 Methodology: Eliciting Expert Judgements to Predict the Outcomes of the FARO L-21 Experiment: by Thomas Eppel and Detlof von Winterfeldt. Final Report (Revised) January 29, 1997.

38. PNL-10091, UC-2030 Some Theories of Dissolved Gas Release from Tank 241-SY-101, September 1994.

39. PNL-10120, UC-510 Mechanisms of Gas Bubble Retention, September 1994.

40. PNL-10173 Ammonia in Simulated Hanford Double-Shell Tank Wastes: Solubility and Effects on Surface Tension, September 1994.

41. PNL-10198 The Effects of Heating and Dilution on the Rheological and Physical Properties of Tank 241-SY-101 Waste, Pacific National Laboratory, Richland, Washington

42. PNL-10417 An Assessment of the Dilution Required to Mitigate Hanford Tank 241-SY-101, February 1995

43. PNL-10681 The Behavior, Quantity, and Location of Undissolved Gas in Tank 241-SY-101, October 1995.

44. PNL-10682 In Situ Determination of Rheological Properties and Void Fraction in Hanford Waste Tank 241-SY-101, August 1995.

45. PNL-10740 Gas Bubble Retention and Its Effects on Waste Properties: Retention Mechanisms, Viscosity, and Tensile and Shear Strengths, August 1995

46. PNL-10773 Hanford Tank Clean up: A Guide to Understanding the Technical Issues, TWRS Technology Program Office, October 1994.

47. PNL-10821 Screening the Hanford Tanks for Trapped Gas, October 1995.

48. PNL-10865 In Situ Determination of Rheological Properties and Void Fraction: Hanford Waste Tank 241-SY-103, November 1995

49. PNL-8124, AD-940 Gas Generation and Retention in Tank 101-SY-101: A Summary of Laboratory Studies, Tank Data, and Information Needs, June 1992.

GAS RELEASE EVENT SAFETY ANALYSIS TOOL
LIBRARY

50. PNL-8880 Historical Trends in Tank 241-SY-101 Waste Temperatures and Levels, September 1993.

51. PNL-9423 Mitigation of Tank 241-SY-101 by Pump Mixing: Results of Testing Phases A and B, March 1994.

52. PNL-9959 Mitigation of Tank 241-SY-101 by Pump Mixing: Results of Full-Scale Testing, June 1994.

53. PNNL-11237 Evaluation of the Potential for Significant Ammonia Releases from Hanford Waste Tanks, July 1996.

54. PNNL-11296 In Situ Rheology and Gas Volume in Hanford Double-Shell Waste Tanks, September 1996.

55. PNNL-11297 Status and Integration of Studies of Gas Generation in Hanford Wastes, October 1996.

56. PNNL-11298 Mechanisms of Gas Bubble Retention and Release: Results for Hanford Waste Tanks 241-S-102 and 241-SY-103 and Single-Shell Tank Simulants, September 1996

57. PNNL-11310 Gas Release During Salt Well Pumping: Model Predictions and Comparisons to Laboratory Experiments, September 1996.

58. PNNL-11335 Summary of Tank Information Relating Salt Well Pumping to Flammable Gas Safety Issues, September 1996.

59. PNNL-11373 Flammable Gas Data Evaluation Progress Report, October 1996.

60. PNNL-11391 Gas Retention and Release Behavior in Hanford Single-Shell Waste Tanks, December 1996.

61. PNNL-11416 Mechanisms of Stability of Armored Bubbles: FY 1996 Final Report, December 1996

62. PNNL-11450, Rev. 1 Composition and Quantities of Retained Gas Measured in Hanford Waste Tanks 241-AW-101, A-101, AN-105, AN-104, and AN-103, March 1997.

GAS RELEASE EVENT SAFETY ANALYSIS TOOL
LIBRARY

63. PNNL-11536, Rev. 1 Gas Retention and Release Behavior in Hanford Double-Shell Waste Tanks, May 1997

64. PNNL-11600 Thermal and Radiolytic Gas Generation from Tank 241-S-102 Waste, July 1997.

65. PNNL-11621 Gas Release During Salt-Well Pumping: Model Predictions and Laboratory Validation Studies for Soluble and Insoluble Gases, August 1997.

66. PNNL-11639 Initial Parametric Study of the Flammability of Plume Releases in Hanford Waste Tanks, August 1997

67. PNNL-11642 Mechanisms of Gas Retention and Release: Experimental Results for Hanford Waste Tanks 241-AW-101 and 241-AN-103

68. PNNL-11668 Seismic Event-Induced Waste Response and Gas Mobilization Predictions for Typical Hanford Waste Tank Configurations

69. PNNL-11674 Ammonia Concentration Modeling Based on Retained Gas Sampler Data

70. PNNL-11693 Estimating Retained Gas Volumes in the Hanford Tanks using Waste Level Measurements, September 1997.

71. LA-UR-96-989 History of Organic Carbon in Hanford HLW Tanks: HDW Model Rev. 3.

72. PNNL-11737 Evaluation of Scaling Correlations for Mobilization of Double-Shell Tank Waste, September 1997.

73. Presentations - SCOPE II Conference, Book 1

74. Presentations - SCOPE II Conference, Book 2

75. Presentations - SCOPE I Conference, Book 1

76. Presentations - SCOPE I Conference, Book 2

77. SNL-SCOPE Project -- PQAP, Rev. 1 Safety-Controls Optimization by Performance Evaluation (SCOPE) Project, Project Quality Assurance Plan (PQAP) Sandia National Laboratories, October 1997.

GAS RELEASE EVENT SAFETY ANALYSIS TOOL
LIBRARY

78. Safety Controls Optimization by Performance Evaluation (SCOPE) Flammable Gas Expert Elicitation Results for Hanford Site Single-Shell Tanks - July 1997

Sandia National Laboratories Safety-Controls Optimization by Performance Evaluation (SCOPE) Project, October 1997

79. Scope Concept Paper — Safety-Controls Optimization by Performance Evaluation: A Systematic Approach for Safety-Related Decisions at the Hanford Tank Waste Remediation System. CONCEPT PAPER, August 1996.

80. Software Requirements Specification (SRS) (SCOPE-AT VERSION 1.0)

81. Summary of CRS Comments on Flammable Gas (First 25 Meetings, December 1993 - February 1997), 1st CRS Meeting (December 7 - 9, 1993)

82. TSA10-CN-WT-SA-TH-108, Dome Collapse Accident for Single-Shell Flammable Watch List Tanks

83. TWS96.3 Analysis of Visual Waste Observations for Single Shell Tanks, May 3, 1996.

84. TWSFG97.40 Preliminary Retained Gas Sampler Measurement Results for Hanford Waste Tank

85. Westinghouse Memo 12110PCL92-068 To. J.W. Lentsch, from J.C. Person, , Gas Retention Tests on 101-SY Tank Waste After Mixing, Westinghouse Hanford Company, Richland, Washington

86. Westinghouse Internal Memo 75210-906-006 Evidence of Release Events During Waste Intrusive Activities in Flammable Gas Watch List (FGWL) and Proposed FGWL Tanks.

87. WHC-EP-0182-102 Waste Tank Summary Report for Month Ending September 30, 1996.

88. WHC-EP-0628 Tank 101-SY Window E Core Sample: Interpretation of Results, January 26, 1993, Westinghouse Hanford Hompany, Richland, Washington

GAS RELEASE EVENT SAFETY ANALYSIS TOOL
LIBRARY

89. WHC-EP-0734, Rev. 1 Tank 241-C-103 Headspace Flammability, May 1994.

90. WHC-SD-TWR-RPT-002, Rev. 0 Structural Integrity & Potential Failure Modes of the Hanford HLW Tanks, September 1996.

91. WHC-SD-WM-CN-041, Rev. 0 Tank Farm Deflagration Rates Due to Various Ignition Sources

92. WHC-SD-WM-CN-116, Rev. 0 Calculation Note: Hydrogen Generation Rates at Steady-State Flammable Gas Concentrations for Single ShellTanks, June, 1997

93. WHC-SD-WM-DTR-045, Rev. 0 Effects of NaOH Dilution on Solution Concentrations in Tank 241-SY-101 Waste, January 1997

94. WHC-SD-WM-ER-411, Rev. 0A Tank Characterization Report for Double-Shell Tank 241-AZ-102, December 1995.

95. WHC-SD-WM-ER-515, Rev. 0 Waste Tank 241-SY-101 Dome Airspace & Ventilation System Response to a Flammable Gas Plume Burn, November 1995.

96. WHC-SD-WM-ER-526, Rev. 1 Evaluation of Hanford Tanks for Trapped Gas., March 1996

97. WHC-SD-WM-ER-526, Rev. 1 Evaluation of Hanford Tanks Trapped Gas, December 1996.

98. WHC-SD-WM-ER-526, Rev. 1A Evaluation of Hanford Tanks for Trapped Gas, March 1996 and January 1997.

99. WHC-SD-WM-ER-526, Rev. 1C Evaluation of Hanford Tanks for Trapped Gas, April 1997

100. WHC-SD-WM-ER-571, Rev. 0 Evaluation of Hydrogen Release During Saltwell Pumping for Tanks T107 & S110 & S108, April 1996.

101. WHC-SD-WM-ER-576, Rev. 0 Compilation of Hydrogen Data for 22 Single Shell Flammable Gas Watch List Tanks, May 1996.

GAS RELEASE EVENT SAFETY ANALYSIS TOOL
LIBRARY

102. WHC-SD-WM-ER-594, Rev. 0	Evaluation of Recommendation for Addition of Tanks to the Flammable Gas Watch List, June 1996.
103. WHC-SD-WM-ES-219, Rev. 0	Lab Flammability Studies of Mixtures of Hydrogen & Nitrous Oxide & Air, September 1992.
104. WHC-SD-WM-ES-362, Rev. 1	Tank Farm Potential Ignition Sources, January 1996.
105. WHC-SD-WM-ES-387, Rev. 1	Probability, Consequences, and Mitigation for Lightning Strikes to Hanford Site High-Level Waste Tanks, August 1996.
106. WHC-SD-WM-FHA-020, Rev. 0	Fire Hazard Analysis for Tank Farms
107. WHC-SD-WM-PE-046, Rev. 0	Evaluation of December 1991 TANK 101-SY Gas Release Event, April 1992.
108. WHC-SD-WM-RPT-281, Rev. 0	Deflgration and Detonation Hazards in Hanford Tank Farm Facilities.
109. WHC-SD-WM-SAD-033, Rev. 2-A, Section I	Safety Assessment for Proposed Pump Mixing Operations to Mitigate Episodic Gas Releases in Tank 241-SY-101, Hanford Site, Richland, Washington
110. WHC-SD-WM-SAD-033, Rev. 2-A, Section II	Safety Assessment for Proposed Pump Mixing Operations to Mitigate Episodic Gas Releases in Tank 241-SY-101, Hanford Site, Richland, Washington
111. WHC-SD-WM-SAD-033, Rev. 2	Tank 241-SY-101 Mitigation Program, July 1996.
112. WHC-SD-WM-SAD-035, Rev. 0-A	A Safety Assessment for Rotary Mode Core Sampling in Flammable Gas Single Shell Tanks, Hanford Site, Richland, Washington
113. WHC-SD-WM-SAD-035, Rev. 0	A Safety Assessment for Saltwell Jet Pumping Operations in Tank 241-A-101: Hanford Site,

GAS RELEASE EVENT SAFETY ANALYSIS TOOL
LIBRARY

Richland, Washington

114a. WHC-SD-WM-SAD-036, Rev. 0	Tank Farm Transition Projects (TFTP), November 1996.
114b. WHC-SD-WM-SAD-036,	A Safety Assessment forSalt-Well Pumping Operations in Tank 241-A-101: Hanford Site, Richland, WA.
115. WHC-SD-WM-SAR-061, Rev. 0	Tank 241-SY-103 Hazard Assessment, October 1993.
116. WHC-SD-WM-SARR-004, Rev. 1	Safety Basis for Activities in SST with Flammable Gas Concerns
117. WHC-SD-WM-SARR-016, Rev. 2	Tank Waste Compositions & Atmospheric Dispersion Coefficients for use in Safety Analysis Consequence Assessments, July 1996.
118. WHC-SD-WM-TI-513, Rev. 0	101-SY Window "C" Core Sample-Evaluation of the Chemical and Physical Properties, April 1992.
119. WHC-SD-WM-TI-724, Rev. 1	Methodology for Flammable Gas Evaluations, April 1996.
120. WHC-SD-WM-TI-753, Rev. 0	Summary of Flammable Gas Hazards and Potential Consequences in Tank Waste Remediation System Facilities at the Hanford Site, December
121. WHC-SD-WM-TRP-256, Rev. 0	Test Evaluation of Industrial Hygiene Hand Held Combustible Gas Monitor, May 1996
122. WHC-SP-1193, Rev. 0	Flammable Gas Program Topical Report, October 1996.
123. WHC-SP-1193, Rev. 1	Flammable Gas Program Topical Report
124. WHC-IP-0842, Rev. 0b	Authorization Basis Amendments and Annual Updates
125. Sandia Nat'l Lab	Software System Test Plan (SSTP) Gas Release

GAS RELEASE EVENT SAFETY ANALYSIS TOOL
LIBRARY

Event Safety Analysis Tool (Resolve! Version 1)

126. HNF-SD-WM-ES-412, Rev. 0 — Safety Controls Optimization By Performance Evaluation (SCOPE) Expert Elicitation Results for Hanford Site Single-Shell Tanks

127. FDH-9761360A R1 — Contract Number DE-ACO6-96RL13200; Flammable Gas Project: Revised Review Comment Records for Closure of the Flammable Gas Unreveiwed Safety Questions for Single-Shell Tanks

128. FDH-9761064 — Contract Number DE-ACO6-96RL13200; Flammable Gas Project: Revision of the Expert Elicitation Results for Hanford Site Single-Shell Tanks

129. FDS-9761360A R2 — Contract Number DE-ACO6-96RL13200; Flammable Gas Project: Directed to Perform Data Correlation on Available Void Fraction Data with Respect to Tank Wastes Types

130. HNF-SD-WM-ES-410 — Enhanced Safety Analysis methodology For Flammable Gas Risk Assessment In Hanford Site Tanks

131. PNL-10198 — The Effects of Heating and Dilution On The Rheological and Physical Properties of Tank 241-SY-101 Waste

132. PNL-9062 — Flammable Gas Safety Program Analytical Methods Development: FY 1993 Progress Report

133. PNL-10776 — Flammable Gas Safety Program Organic Analysis and Analytical Methods Development: FY 1995 Progress Report

134. PNL-11307 — Flammable Gas Safety Program: Actual Waste Organic Analysis: FY 1996 Progress Report

135. PNNL-11312 — Organic Tanks Safety Program: FY 96 Waste Aging Studies

GAS RELEASE EVENT SAFETY ANALYSIS TOOL
LIBRARY

136. PNNL-11309	Organic Tanks Safety Program Advanced Organic Analysis: FY 1996 Progress Report
137. PNNL-11480	Speciation of Organic Carbon in Hanford Waste Tanks: Part I
138. Letter from Dan Meisel	Environmental Management Science Program (EMSP) Report FY-1997
139. PNNL-11640	Homogeneity of Passively Ventilated Waste Tanks
140. PNNL-11702 Rev. 1	Chemical Pathways for the Formation of Ammonia in Hanford Wastes.
141. PNL-11670	Organic Tanks Safety Program FY 97 Waste Aging Studies.
142. WHC-SD-TWR-RPT-003	DELPHI Expert Panel Evaluation of Hanford High Level Waste Tank Failure Modes and Release Quantities.
143. Presentation	Illustrative Examples from SST Elicitation Rationale Reports.
144. Information	Explosive Fragmentation.
145. 97-SCD-031	Flammable Gas Project - Safety Controls Optimization by Performance Evaluation (SCOPE) Flammable Gas Expert Elicitation Results for Hanford Site Single-Shell Tanks to Meet Performance Agreement TWR 1.3.2.
146. LMHC-9761360 R3	Subcontract Number 80232764-9-K001, Flammable Gas Project, Data Correlation Analysis Results.
147. Information	Solving the "Small-Medium-Larg" Problem.
148. Empty	

GAS RELEASE EVENT SAFETY ANALYSIS TOOL
LIBRARY

149. HNF-SD-WM-TI-797	Results of Vapor Space Monitoring of Flammable Gas Watch List Tanks.
150. LA-UR-97-3955	Data Reconciliation Study of Tank 241-AN-103 at the Hanford Site.

This page intentionally left blank.